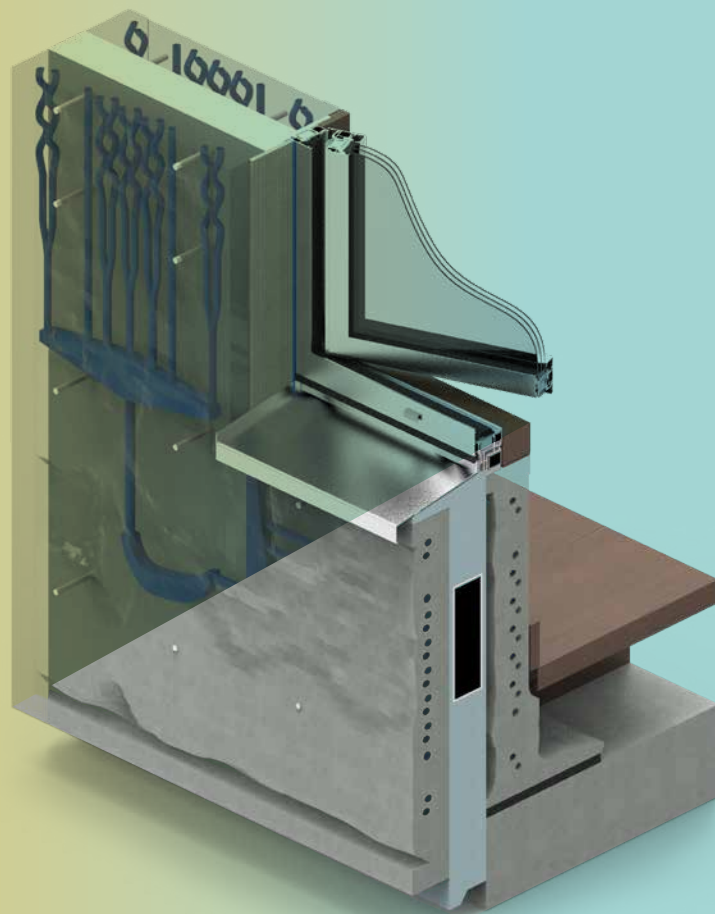


# THERM VENTATION

Active Thermal Façade Venation



# **THERM\_VENATION:** Active Thermal Façade Venation

**Fabricating a concrete twin-wall façade panel optimised for integrated heat exchange system**

Project by:

**Subhranshu Panda | 4727606**

[spandaindia@gmail.com](mailto:spandaindia@gmail.com)

Guided by:

**Dr. Michela Turrin**

Architectural Engineering +Technology

Design Informatics

**Prof.de.ing Ulrich Knaack**

Architectural Engineering +Technology

Design of Construction

**THERM:** *The therm (symbol, thm) is a non-SI unit of heat energy. (wikipedia, 2019)*

**VENATION:** *an arrangement or system of veins, as in the tissue of a leaf or the wing of an insect. (merriam-webster, 2019)*

10<sup>th</sup> July 2019



MSc Architecture, Urbanism and Building Sciences  
Building Technology Track

Faculty of Architecture and the Built Environment  
Delft University of Technology  
Julianalaan 134, 2628 BL Delft, The Netherlands

# ACKNOWLEDGEMENT

*This thesis is dedicated to Mankind.*

This graduation project marks the end of masters academic journey at TU Delft. The journey from August 2017 to 2019 has been memorable with a great bunch of people and their unparalleled support to guide me up as an evolved personality in the span of these 2 years. The exchange of knowledge and critical understanding of the personalities with varied culture, experience and background, was something to be acclaimed for.

First of all I would like to thank my Mama- Reena Panda and Baba- Simanchala Panda and sister Sudeekshya Panda for your belief in me and selfless support throughout my life. I will always be by your side. Loads of love.

This project does compliment the effort and support of my mentors Dr. Michela Turrin and Prof. Ulrich Knaack for believing in my vision and guiding me throughout the project. I would like to specially thank Dr. Mark Alston, Assistant Professor in Environmental Design, University of Nottingham for his ideas and support for helping me design and analyse the aspects of fluid flow. With guidance from specific departments that are dealt in this project, I am also very grateful for the insights and guidance by Peter Eigenraam and Prof. Fred Veer (Structural design & mechanics, TU Delft), Prof. Martin Tenpierik (Building physics, TU Delft) and Marcel Bilow (Building product innovation).

The prototyping of this project would not have been feasible without the support and help of Vedula Nitisha and Jochem de Langen from Schüco, personnels from Solidian GmbH, Schöck Nederland b.v., Technogrip GmbH and machinablewax.com. I am hertily obliged to them for providing me with samples and materials to realise the project in rits physical form.

Last but not the least I would like to thank all my dear friends in India and in Netherlands for their constant cheer. Especially the bunch of North & South; Ammar Taher, Ivneet Singh Bhatia, Krittika Agarwal, Natchai Suwannapruk, Premith Satish, Prethvi Raj Manoharan, Priya Nanda and Yamuna Sakthivel a big shout out to you guys for being a family to me away home.

# PREFACE

Cities and its buildings are evolving, and so is the energy demand. The move towards highly sustainable building measures by exploring the critical nodes in the field of architecture is mandatory and needs to be explored and put forward an idea that may evolve and serve the greater purpose in the future.

**THERM\_VENATION- Active Thermal Façade Venation** is a project dealing with designing and fabrication of a twin-wall concrete façade panel with heat exchange tubular network embedded within it inspired by the leaf venation, which by actively exchanging fluid between the two panels conditions the indoor temperature.

Passive measures to tackle increasing energy demands of modern buildings are aimed to generate energy from the roof or the ground beneath and by improving insulation to isolate indoors and outdoors. This project targets the opaque facade sections of a building to develop an active panel to exchange solar thermal energy with the indoor space and vice-versa. It helps to capture the solar heat and keep the indoors warm during winters while capturing the excess heat from indoors and releases to the environment during summers. The location chosen in this project is Delhi because of its composite climate that tests the designed capacity of to extremes. This research will examine and challenge the possibilities of designing and fabricating a highly complex tubular network geometry based on the venation of a leaf, cascaded within a concrete twin-wall façade panel with reduced volume in comparison to an elementary concrete façade panel and a maximised capacity of capturing and exchanging heat.

This project follows a design through research methodology with computation tools, boundary conditions, material properties and the method of fabrication guiding the design and its result. The different constraints for the research performed, and production feasibility may guide for change in design considerations. The two primary topics dealt in this project are the use of computation tools to design for higher efficiency and method of fabrication. The third aspect of thermal analysis of the facade was performed abstractly only to evaluate the considered design methodology and capacity of the proposed facade system..

This report is divided into two sections. The first part deals with the introduction to the scientific framework of the project and literature study to absorb the needed information and filter them to be considered for the second part of this project. The second part details the design and performed evaluations, which are guided primarily by four elements: the system- **Façade**; the material- **Concrete**; the process- **Computation**; the target- **Fabrication**.

# CHAPTERS

## 1. Introduction 07

1.1 Context	10
1.2 Concrete façade systems	11
1.3 Facade integrated system	11
1.4 Optimisation and fabrication	12
1.5 Problem statement	12
1.6 Focus and restrictions	13
1.7 Research questions	14
1.8 Aims and objectives	16
1.9 Research overview	16

## 2. Study 17

2.1 Façade: A system	10
2.2 Concrete: The material	10
2.3 Computation: The process	10
2.4 Fabrication: The target	10
2.5 Projects: The references	10
2.6 Design framework	10
2.7 Conclusion	10

## 3. Conceptual design 101

3.1 Heat exchange system	102
3.2 Work cycle	105
3.3 Design elements	107
3.4 Concept of network geometry	108
3.5 Concept network geometry	114
3.6 Conclusion	116

## 4. Design considerations 117

4.1 General boundary conditions	118
4.2 Fabrication criteria	124
4.3 Design criteria	127
4.4 Conclusion	133

## 5. Digital methodology 135

5.1 Target based strategy	136
5.2 Design strategy 01	138
5.2 Design strategy 02	148
5.3 Performance	157
5.4 Conclusion	163

## 6. Fabrication criteria 165

6.1 Structural system	166
4.2 Fabrication	182
4.3 Base network geometry	192
4.4 Conclusion	195

## **7. Design criteria** **197**

7.1 Medium of fluid	198
7.2 Type of flow	198
7.3 Flow resistance	199
7.4 Volume variance	209
7.5 Pressure drop	216
7.6 Shape modification	225
7.7 Heat transfer - Geometry	233
7.8 Heat transfer - Insulation	248
7.9 Heat transfer - Performance	257
7.10 Conclusion	262

## **8. Results** **263**

8.1 Final results	264
8.2 Path dependency analysis	279

## **9. Details and prototype** **283**

9.1 Schematic drawings	284
9.2 Details	288
9.3 Physical prototypes	291
9.4 Exploded view	294
9.5 Assembly sequence	295
9.6 Options per use type	296

## **10. Closure** **299**

10.1 Conclusion	300
-----------------	-----

10.2 Critical reflection	301
10.3 Future scope	302

## **11. Bibliography** **305**

## **12. Appendix** **315**

*"Architecture is an art of pure invention. Unlike the other arts, [it] does not find its patterns in nature, they are unencumbered creations of the human imagination and reason. In consideration of this, architecture could be considered the freest of all arts were it not also dependent on the laws of nature in general, and the mechanical laws of material in particular. For, regardless of which artistic creation of architecture we look upon, it was primarily and originally always conceived to satisfy particular material need, primarily that of shelter and protection from the onslaught of climate and the elements or other hostile forces. And since we can gain such protection only through combining the materials nature offers us into solid structures, we are always forced to adhere closely to the structural and mechanical laws."*

*Gottfried Semper, 1854 (Müller & Vogel, 1982)*

# 1. INTRODUCTION

## CHAPTER OVERVIEW

*This chapter introduces the research framework with its scope and restrictions. This introduces the facade system and use of concrete in it and also introduces the optimisation and fabrication methods for this project. At the end of this chapter a detailed overview of the research has been briefed.*

## 1.1 CONTEXT

An architecture project does rely on the performance and aesthetics of the facade amongst all its other factors, which in turn decides the market value and comfort of the users and the investor. The economic viability of the construction is always the key deciding factor of any project in developing countries such as in the Indian subcontinent and other south-east Asian countries. Universal availability, traditional production methods, design flexibility, availability of a high level of expertise and craftsmanship, durability, aesthetics, low maintenance and economical cost in comparison to other materials, etc., has made concrete the confident building material. It was proven to be an economical and versatile solution for most facade constructions worldwide in the past, until the fancy blue and green glass skin and other technologies did sprawl over the industry as the standard facade implementation, at least in high-rise structures. But recently, this trend is flipping back to introduce more opaque materials combined with glass panes. The responsibility to drastically reduce the exploitation of materials for construction drives the need of optimisation and derive an expression to ornament the material with the tool while establishing a conversation with its users and admirers.

*“To gain some kind of foothold in the broad field of the architecture of our age, where the confusion or complete lack of principles in relation to style is on the increase and criticism of its application is very severe among the infinite mass of structures that have been built on this Earth in various eras, I would like to express one main principle: architecture is construction! I derive a second main principle for good architecture from the following observation: every completed construction in a certain material has its very particular character and could not sensibly be built in the same way using any other material.”*

Karl Friedrich Schinkel

## 1.2 CONCRETE FACADE PANEL

As per Maslow's hierarchy of needs, building is an elementary human need. It corresponds to mankind's need to shape the environment sensibly for its own benefit. Architecture is the result of the synthesis of different utilisation requirements, constructional options and artistic concepts. With a wide variety of material, fixtures, market strategies for designing a building facade, the possibilities are endless. The advantages of concrete as a material in the building industry and for facade needs to be taken a step further with the help of current available digital tools. The economical and robust behaviour of this material dominates a significant market share of the construction industry in comparison to other building materials in the rapidly developing economies. Using this material in the facade of a building has further benefits and has to be explored further in a rather responsible manner considering its ecology. A facade that acts as a skin to the building needs to qualify its basic function of providing comfort to its users inside in relation to the external climatic condition while being committed to safety, upgradation, production, maintenance, high service life and sustainable development.

## 1.3 FACADE INTEGRATED SYSTEM

The development of energy efficient facade panels did start during the crisis of Arab oil embargo (History of Insulation with Masonry), and since then a number of different methods of insulating the facade panels to segregate the internal and external environment have been developed and succeeded. But the concern here is not targeted towards the insulating behaviour and the physical properties that the materials do carry which accounts for the insulating behaviour of the panel. Rather, the participation of the mass of the internal and the external panels in contributing towards the sustainable behaviour of the designed building and the facade panel as one of its element was considered.

The implementation of functional measures to these inactive concrete mass of the façades to translate them into energy manipulating systems could help in infusing sustainable design means which in turn delivers an integrated facade system that accounts for the reduced energy consumption of the whole building. The current measures implemented are limited mostly to that of heat sink methods that capture the heat and store it for future use. This thesis targets for an active measure that reflects the environment through out the year everyday and proposes an active heat exchange system embedded within the concrete mass of the external and internal facade panel.

## 1.4 OPTIMISATION AND FABRICATION

Exploitation of non renewable energy resources along with the building materials and hence the environment for the construction and functioning of buildings has been since ages. The material is the prime necessity for construction, and the optimal use of these materials along with the energy needed to ensure comfort of the users, are what need to be addressed in order to reduce the environmental burdens and develop a sustainable society. Optimisation of efficient functioning and material use in this ever-developing digital age has been much efficient and faster than compared to yesteryear. Using the state of the art tools to optimise the most efficient and versatile material concrete is need of exploration.

Design and production are inter-dependent. The modern state-of-the-art fabrication methods do imply their respective constraints and shortcomings in comparison to others. The identification of the appropriate fabrication method for complex shapes and geometry with concrete is necessary for production and designed performance of the element. The expression and function of a building and its elements are specific to the built era. The appearance of these elements, subjected to minimalist detail or the language of enhancing it which symbolises the current advancement in the field of architecture is subjective and necessary.

## 1.5 PROBLEM STATEMENT

Building infrastructures do demand energy resources and materials from different available sources, ex: extracted minerals, biologically grown, etc. The efficient use of the renewable energy resources and the minimum possible use of the building materials that can help in improving the performance of a building element and reduce the energy need of a building, could be an alternate sustainable measure for today's construction industry.

Non-optimised exploitation of non renewable energy resources and available materials to satisfy the demands of the architectural industry and comfort of the user are the prime contributors towards an unsustainable development. Most of the biologically grown materials like wood etc., are usually processed with chemicals to render them as a viable building material replacement that does loose the sustainable aspect of the modified material, while being argued as one of the feasible alternatives. Optimised geometries for efficient performance of building elements tend to develop a complicated geometry as the best feasible solution and efficient renewable methods of fabrication need to be considered or developed in order to embrace the

complexities that drive efficiency and not render them out while compromising the designed solution.

*This project deals and establishes the predicament with the fabrication of a complex concrete facade panel with an integrated heat exchange system derived from the method of optimisation for its efficient performance.*

## 1.6 FOCUS AND RESTRICTIONS

All architectural construction consists of a facade element and depending on multiple different factors there are a set of feasible options for the particular architecture. Facade as a building element primarily deals with a material, and the properties and moulding of the article are reflected to be the aesthetics of the building. This project focuses primarily on three different aspects. Firstly concrete as the material developed into facade panel which derives the purpose based on various different comparative study and comparative analysis. Secondly, optimising the integrated function within the facade panel to maximise its efficiency based on various different parameters and lastly, analysing the geometry and proposing a feasible method of manufacturing the facade panel. Concrete in itself consists of various compositions, and the most effective amongst them that complies with the chosen method of optimisation and method of fabrication is considered. A building has façades that connect the internal and external environment and also façades that are opaque monolithic and are usually neglected with aesthetics and attention. This proposal aims at developing a method that would be applicable to different facade typologies of the building with minor modifications.

The design and validation of this project needed to consider a specific climatic condition and building typology to base the research on while studying the behaviour and aesthetic of the desired facade. The construction industry is shifting from the developed countries in the west to the rapidly evolving and progressing nations in the middle-east and south-east Asia like India, UAE, etc (Geleff, 2018). The composite climate was the focus condition considered for this project and its research so as to analyse the effect of the extremities of the climatic conditions. The project also focuses on optimisation of the facade panel with the aim of maximising the efficiency of the integrated function within the facade panel and also minimising the material used in it while discussing the factors of structural stability, fabrication, maintenance and the architectural expression thus derived as a result. The expression here refers to the tool of optimisation being able to express its procedure and generate a conversation with its user and admirer.

This project is currently restricted to flat fragment facade panel without tapered edges and could be modified

further to complex shaped panels. Even though the climatic aspect of the facade is considered for the selection of material and specific locations for its justified application, the climatic behaviour analysis of the designed facade panel to that of the indoor comfort and energy consumption analysis is restricted in the scope of this project. All the designed products need to take into consideration the method of its fabrication and the restrictions to be considered based on the selected production method. While the modern computer-aided production methods do open up a broad scope of fabricating complex shapes, the limits and constraints of these methods and their capabilities coupled up with that of the material properties, structural behaviour and fixtures are considered in combination for the design.

## 1.7 RESEARCH QUESTION

### 1.7.1 Main research question

This research contemplates the hypothesis of designing the integrated heat exchange system embedded within the mass of the facade panels, the combination of which is optimised for improved performance of the system. The design methodology used is considered to embrace various constraints for its structural viability and manufacturability.

*How to design and fabricate a concrete façade panel with integrated heat exchange system and optimise geometry to increase efficiency ?*

### 1.7.2 Sub research question

Considering the material selection as concrete, the following sub-research question is formulated;

*Why is concrete a viable material choice for facade in today's scenario?*

The consideration of an office building typology based in the composite climate of rapidly developing countries like India, UAE and other South and South-east Asian countries generates the interest of following sub-question will be addressed;

*Which parameters and constraints need to be addressed considering the application typology of an office or mixed-use building for a specific location?*

The method of designing the geometry of the function integrated facade panels for the purpose of heat exchange and optimising the geometry of the facade panel and the tubular network to maximise its efficiency needs to be addressed in concern to the CAD tools used and the parameters used to achieve the envisaged design idea. This leads to the following sub-research question;

*What method, tool and parameters of optimisation needs to be considered for deriving the geometry and maximising the efficiency of the heat exchange system ?*

In this developing era of technology assisted fabrication, new considerations and opportunities have paved their way and hence the following ;

*How does the constraint of the manufacturing process affect the method of design?*

The hypothesis also tries to justify that the endless alternative possibilities and efficiency of using digital tools in design and fabrication can generate a new expression of architecture, and address the following;

*How do the digital tools and manufacturing process boast their purpose in façades and ornamentation?*

## 1.8 AIMS AND OBJECTIVES

The primary aim of this study and research is to implement a active system within the mass of the facade panels in a sense to sustainably harvest renewable energy to benefit in reducing the energy demands of the buildings. This research also aims at delivering an idea of enabling building technologies to dialogue with its user and establish a value of design. This study also allows the architecture fraternity to get knowledge of the effective use of available conventional building materials employing different optimisation tools.

The first objective of this research is to analyse and justify the use of concrete as the chosen material for the facade panel and the type of facade panel chosen, in the sense of practical sustainable aspects that respond to the locality of the proposed design.

The second objective is to analyse the type of active function to be integrated within the facade to minimise the energy load of the building. This also concerns about how the designed geometry would be optimised to deliver the maximum efficiency for the designed function and in the designed context while complying with the constraints of concrete as a material, the structural system of the facade, the method of fabrication and fixtures. This objective will also enable in determining the economical aspect and effectiveness of the research in saving a significant amount of material for façades as per current practices.

The last objective is aimed to analyse the most suitable fabrication method to develop a prototype of the facade panel using computation and technology-assisted tools. This will also accredit the possibilities of the specific production method and a workaround for its limitations and scopes will be developed.

While not a primary objective, this thesis also envisions to communicate the idea of the optimised building element as a language for architectural expression using concrete as the material for facade in comparison to that of a standard and traditional building facade practices.

## 1.9 RESEARCH OVERVIEW

This project will adopt a design through research methodology with formulated tools and design boundaries guiding the research. The constraints researched and production feasibility may guide for change in design considerations. Figure 1.1 shows the detailed research framework in a flowchart.

**Literature study:** This project will deal with three primary aspects of research and designing,

1. Concrete as a material for facade panels
2. The process of optimisation minimise volume with fabrication constraints
3. To fabricate the designed facade panel

The aspects of ornamentation and facade design will scrutinise along all the above elements.

**Design Framework:** The boundary conditions and focus area for the research of the optimisation method and design of the facade panel and fabrication method will be made. Different algorithms and software with different design and fabrication considerations will be explored and analysed to establish the tools to be used.

**Design and Optimisation:** Within the brackets of tools and methods analysed previously, the final design element and the optimised geometry will be determined. The method of fabrication and the material configuration selected along with their related constraints will be outlined and a continuous method to update the optimisation parameters will be established.

**Prototyping:** With the final design and considerations the prototyping of the design element and the method of fabrication will be made. The type of materials to be used for the final design and fabrication method will be identified and the needed modifications to the design will then be considered learning from the experiments.

**Validation and Detailing:** The validation of the designed element will be carried out by analysing the efficiency and change in performance of the final facade panel to that of the initial concept design and the derived change at every stage of the defined design parameters will also be stated. The detailing and visualisation of components within the panel and its fixture will be carried out.

**Production:** The optimal design will be fabricated and analysed on a feasible scale depending on the fabrication method and available resources. The functioning of the fluid flow for the designed geometry will be mocked up within the limitation of production method, to verify with the envisaged idea.

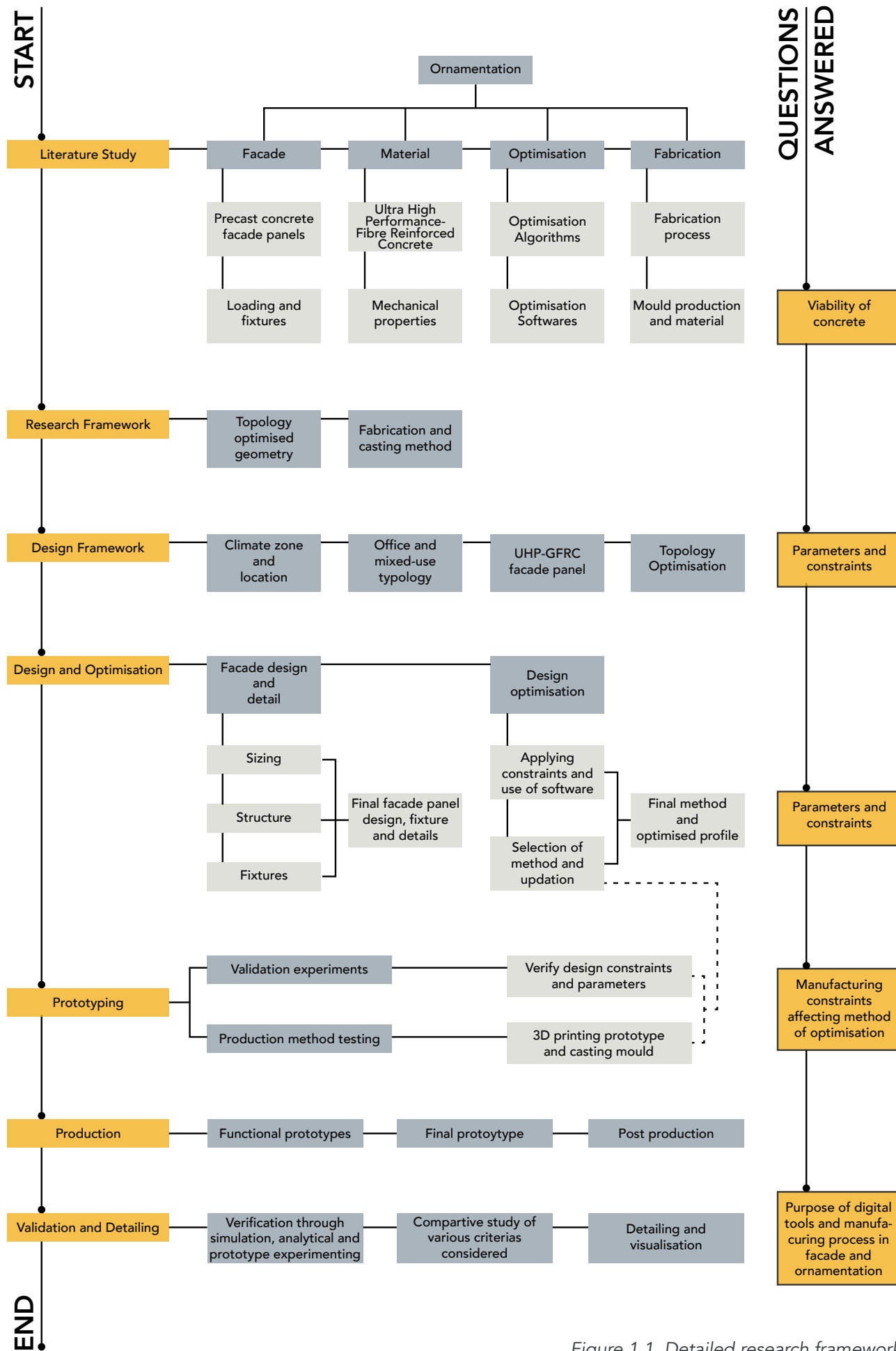


Figure 1.1. Detailed research framework

# 2. STUDY

## CHAPTER OVERVIEW

This chapter forms the background literature study for conducting the thesis. The four different aspects of this project have been studied and justified about its consideration. At the end realised projects that are relevant to the author's ideation have been referred and design inferences are drawn for the further elaboration of the thesis.

## 2.1 FAÇADE: A SYSTEM

Within the boundaries of maintaining the technological, aesthetical, climatic, economic and cultural aspects, the primary goal of architecture is to develop a comfortable shelter. This is aimed at protecting people from the external climatic conditions viz., solar radiation, temperature fluctuations, rainfall and wind along with other natural calamities like earthquake and weathering. The building skin is the preliminary element that can be a condition to be influenced and adapt to the external conditions of the building and develop comfort for the occupants on the interior of the building. The building skin or façade can be analysed on the basis of its three prior tasks to be fulfilled. (Schittich, 2008)

1. **Function:** This defines the practical purpose and impact of the building/ the building skin.
  2. **Construction:** This outlines the elements/components used to fabricate the building skin and the assembly of these elements individually and in relation to the building.
  3. **Form:** This describes the visual and aesthetic perception of the building skin.
- Over-lining these another factor that is considered in analysing the facade. The 4. **Ecology of the facade** in response to the sustainable development of the specific building element. The inter-relation between these factors is shown in Figure 2.1.

The function of the facade is governed by various external and internal conditions of the building. These specific functions are related to different functional components of the facade. The combination of these functional components describes the efficiency and performance of the facade. these various functions and facade components are depicted in Figure 2.2.

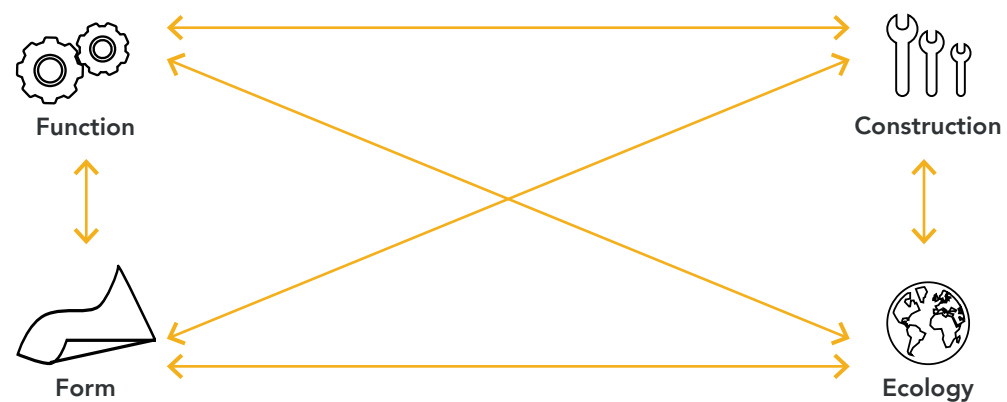


Figure 2.1. Connectivity diagram between different aspects of building envelope (Schittich, 2008).

There are multiple options to express the way an architecture looks and is perceived by the users and public, and also the way it behaves with the context and environment. These variations may be dependent on the geographical location, orientation, use type, context, economic viability and various different situations viz, structural stability, new or refurbishment, availability of materials and quantity etc. and are normal to any specific project.

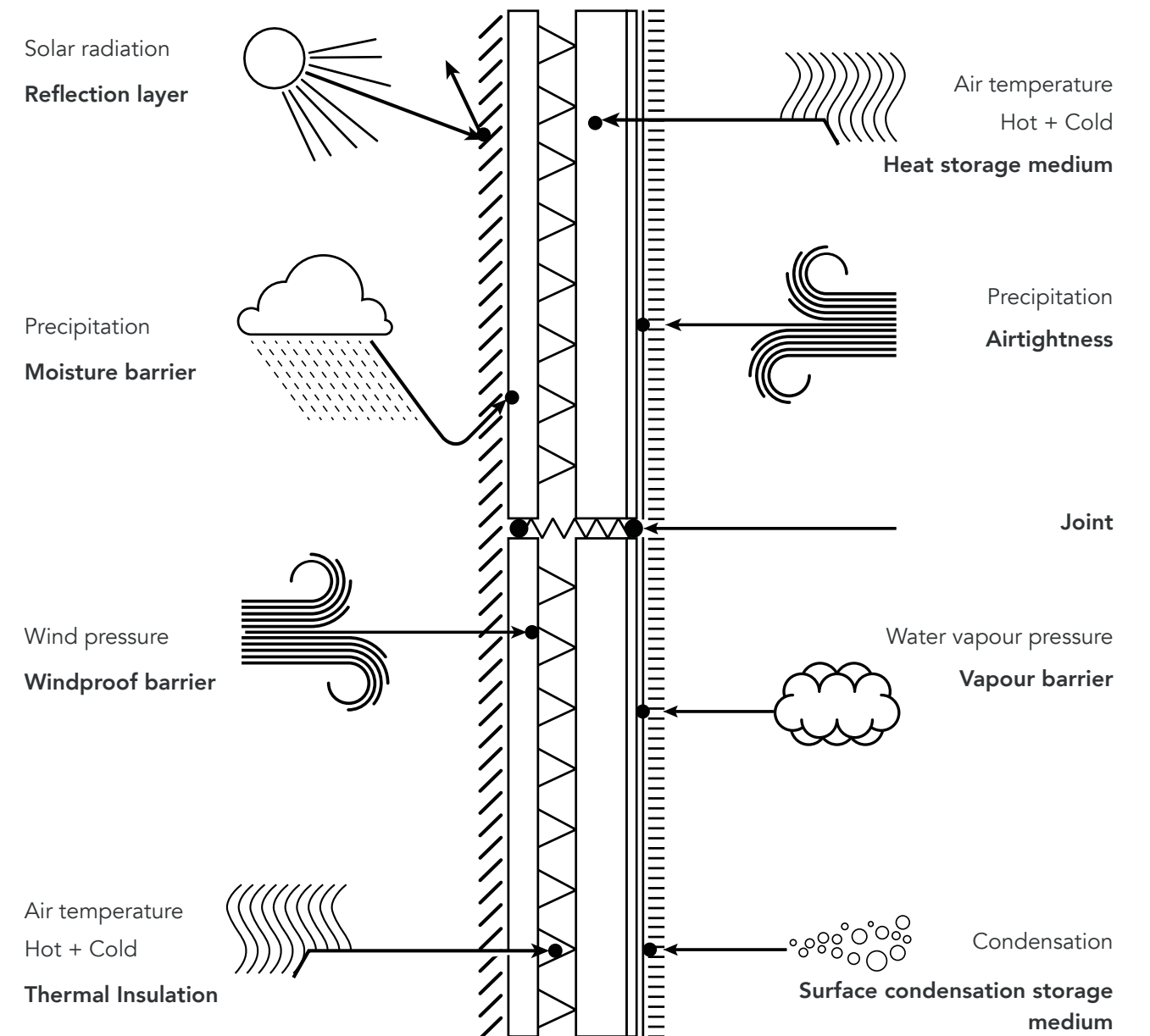


Figure 2.2. Influences on external components and their function in a building facade (Friedbert, Kauhsen, Polonyi, & Brandt, 2013).

## 2.1.1 Structural aspects of a facade panel

In consideration to the comfort and energy requirements, the building skin as a part of the space making also needs to contemplate other specifics that concern the structural function. These functions as stated by Schittich (2008) are:

- Transfer of vertical loads, which concerns the dead weight and superimposed loads
- Transfer of horizontal loads, from the wind pressure and suction forces of impact loads
- Structural safety and prevention of mechanical damage
- Qualify the structural integration of facade components to harness the direct and indirect use of solar energy or sun and also protect the inner space from heat.
- Qualify the structural integration of the dynamic transformation of the building skin to adapt the functional and user-oriented requirements.

There are two different methods for supporting the precast panel on to the building's load bearing structure. These are when: (Kjcerbye & Sai, 2001)

- The façade panel is supported on the main load bearing walls and is designed to carry its own weight between supports.
- The façade panel is connected to the floor slab or beam, which is then designed and reinforced to provide support to the wall.

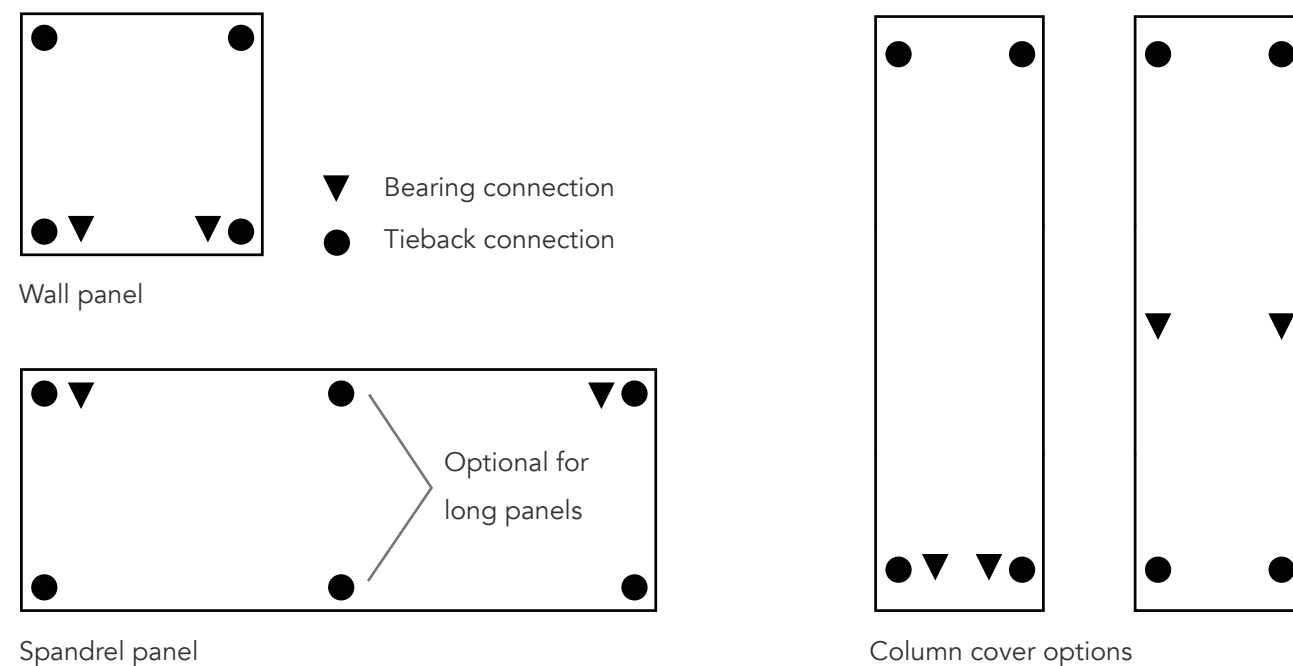


Figure 2.3. Location of typical cladding panel connectors (DN-32 Connections for Architectural Precast Concrete).

## 2.1.2 Classification of building façades

In general building façades can be broadly classified under 2 categories

- Load-bearing: The load-bearing facade elements are designed and reinforced to be compression and buckling resistant. The type of walls are usually made up of wood, clay, masonry, steel, reinforced concrete and glass.
- Non load-bearing facade structures: The non load bearing facade elements are designed to self support their weight and the components attached to them while able to withstand wind and other external forces. In this the load transfer is done via integrated support components that eventually transfer the loads to the main structure. These types of walls are made or clad with wood, glass, metal, polymers, fabric, clay, stone and concrete.

### Classifying the building facade with regard to constructional criteria

Considering all the different factors of construction and properties of the material for building facade, the building façades are classified into the following mentioned criteria with sub divisions (Figure 2.4) within them.(Schittich, 2008)

- Load transfer (bearing/non-bearing)
- Structure of external wall in terms of shell arrangement (single-skin or multi-layered)
- Structure of external wall in terms of sequence of layers
- Radiation transmission (transparent, translucent, or opaque)

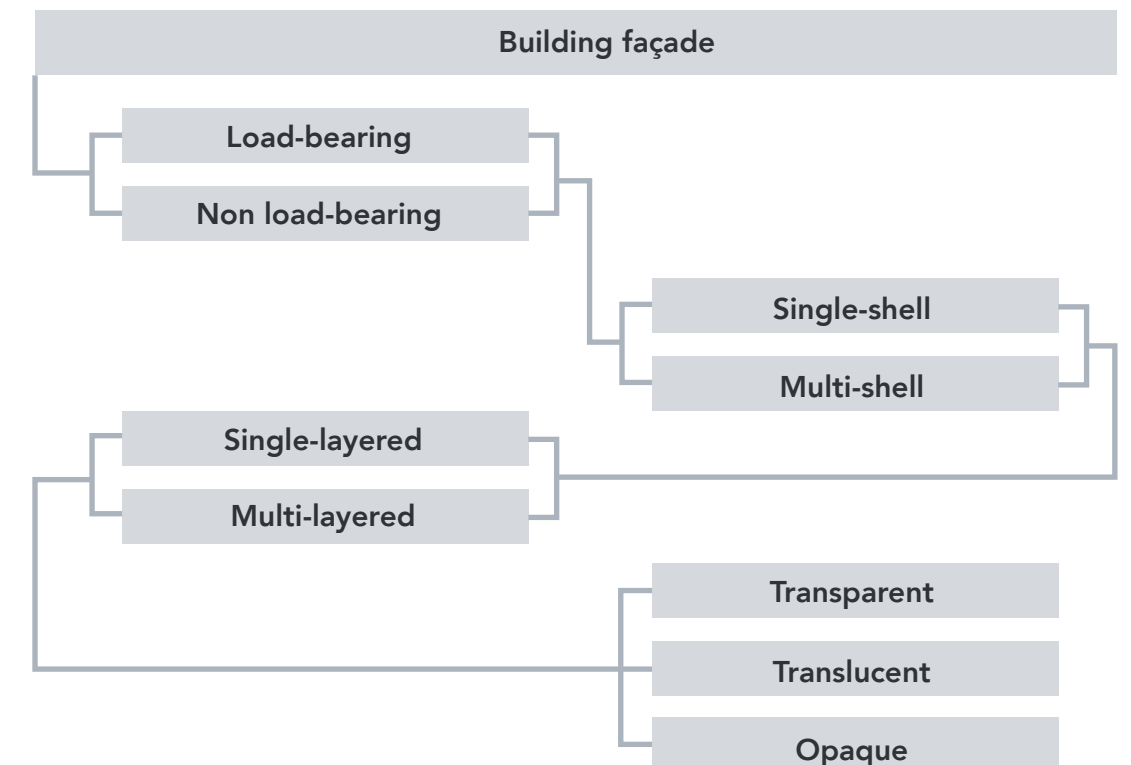


Figure 2.4. Diagram showing the different types and hierarchy in building skins (Schittich, 2008).

In consideration to the above mentioned criteria, the building façade can also be classified depending on the placement and distance of the building skin in relation to load-bearing and bracing components such as girders, floors / ceilings and walls.

## 2.1.1 Concrete for façade

There are a galore of facade material used in the past and in the current times while more innovative materials being researched. Since the invention of Portland concrete in the 19th century, concrete has been used in buildings and their façades. During this same period of time glass façades were also being developed and used in the façades. The rapid advancement in the field of glass started to replace other heavy opaque material for facade and has since then been a standard skin for highrise buildings (Geleff, 2018). But the obvious benefits of concrete as a mass in comparison to its durability, climatic behaviour, appearance, maintenance ,etc. still make concrete as a superior material for facade in the current scenario. The expression of architecture using concrete for facade has been long proven since the period of modernism till contemporary and after. The versatility of concrete as a material has led to its innovative use in every age of architecture and there is no denial of its continuation further.

The introduction of self supported endoskeletons of steel and reinforced concrete for buildings, lead to rise in the implementation and innovation of thin facade buildings made up of lightweight facade panels (usually spandrel panels). This also led to the support of large span windows on the building façades. Improvements in the field of technology and inflow of wealth and investment after the second world war encouraged the development of this trend. The post war movement led to the innovation and extensive use of precast concrete panels from high-rise commercial construction to almost all industrialized buildings.

One of the first use of reinforced concrete in a skyscraper was in that of Ingalls Building built in the year 1903 in Cincinnati by Elzner & Anderson, *Figure 2.5*. This building did made the use of cast-in-situ concrete facade as shown in the detail, *Figure 2.6*.

Concrete as a material for facade can be used in 2 categories depending on its type of fabrication (Friedbert , Kauhsen, Polonyi, & Brandt, 2013).

- In-situ concrete structures
- Precast concrete panels

## 2.1.2 Precast concrete façade panels

Precast concrete is a building element produced by casting concrete off-site in a reusable mould or 'form' and cured in a controlled environment. This is then transported to the construction site and lifted up to the place. In contrary, standard concrete is poured into site-specific form-work and cured on-site. In conjunction with concrete, expanded polystyrene and other insulating materials are used in the core forming a sandwich to develop a lightweight and highly insulated precast panel. Precast facade panel can be classified into further two different types depending on its load bearing behaviour (Watts, 2013).

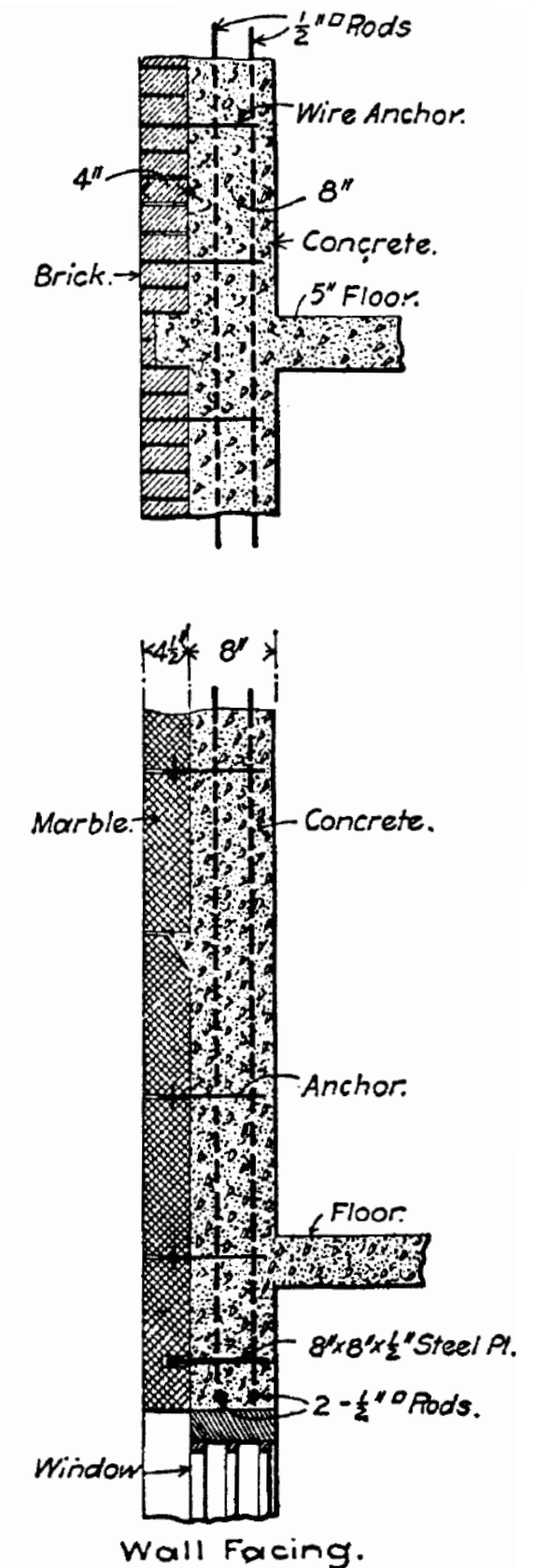


Figure 2.5. Ingalls Building, 1903, Cincinnati; Elzner & Anderson; First steel reinforced concrete skyscraper (Condit, 1968).

Figure 2.6. Vertical section of concrete facade, Ingalls Building (Condit, 1968).

- **Load bearing pre-cast concrete facade panel-** These panels double as an agent of load transfer and a part of the structural system of the building as well as act as a facade element. These panels have three layers to them. The first being inner load bearing concrete panel that is designed and reinforced to carry the structure as well the load of the self sandwich panel system, while the outer being the concrete fascia panel with aesthetic behaviour interacting the outer climate. These two panels are filled with an insulating material in between to reduce the weight and improve the performance of the panel. These panels usually span from floor to floor and may contain an opening for windows, etc. within them, Figure 2.7.

- **Non-load bearing pre-cast concrete facade panel-** These panels may be a single leaf or multi-leaf as the load bearing counterpart. Usually, the concrete wythes at both the external and internal elevations are non-load bearing facade elements. Such panels are analysed and designed to carry their self-weight and then transfer the weight to the structural system of the building viz., beams, floor slabs and roofs. These panels also do usually span from floor to floor and may contain an opening for windows, etc. within them, Figure 2.8. There are also small and modular non-load bearing concrete panels for the facade. One of the prominent examples could be the Proximity Hotel located in Greensboro, North Carolina built in the year 2007 built with non-load bearing concrete facade panels and is the first Platinum LEED certified green hotel in the United States Figure 2.9 and Figure 2.10.

The Non-load bearing pre-cast concrete facade panel can also be divided into three different types depending on its fixture. (Friedbert, Kauhsen, Polonyi, & Brandt, 2013)

- **Non-loadbearing facade, precast concrete cladding**
- **Non-loadbearing facade between loadbearing in-situ concrete construction**
- **Non-loadbearing facade, load-bearing in-situ concrete construction**

#### Reason for selecting non-load bearing pre-cast concrete facade panel

Architecture as a language does evolve at every instance and discipline. With the changing trend, regulatory system and climate change globally, the building needs to adapt itself within its service life. The adaptation of a building here may refer to upgrading itself to meet the new building norms made effective in a given locality, change the user group and function of the building or make use of more efficient building elements to comply with the structural system or the comfort level of its occupant. This can also be factored with the design language and relevant market trend of the locality at a given point of time in future. Adaptation of a building is necessary in the aspect of the aesthetic and function of the building but also in terms of building the economy. An outdated structure may not be preferred to be occupied or is vacated due to some circumstances and needs to thrive through its investors or owners or due to demand of the local authority or insurance company while upgrading the building is the only choice.

Upgrading a building is not feasible for all the built architecture. Constructing a building with the load-bearing

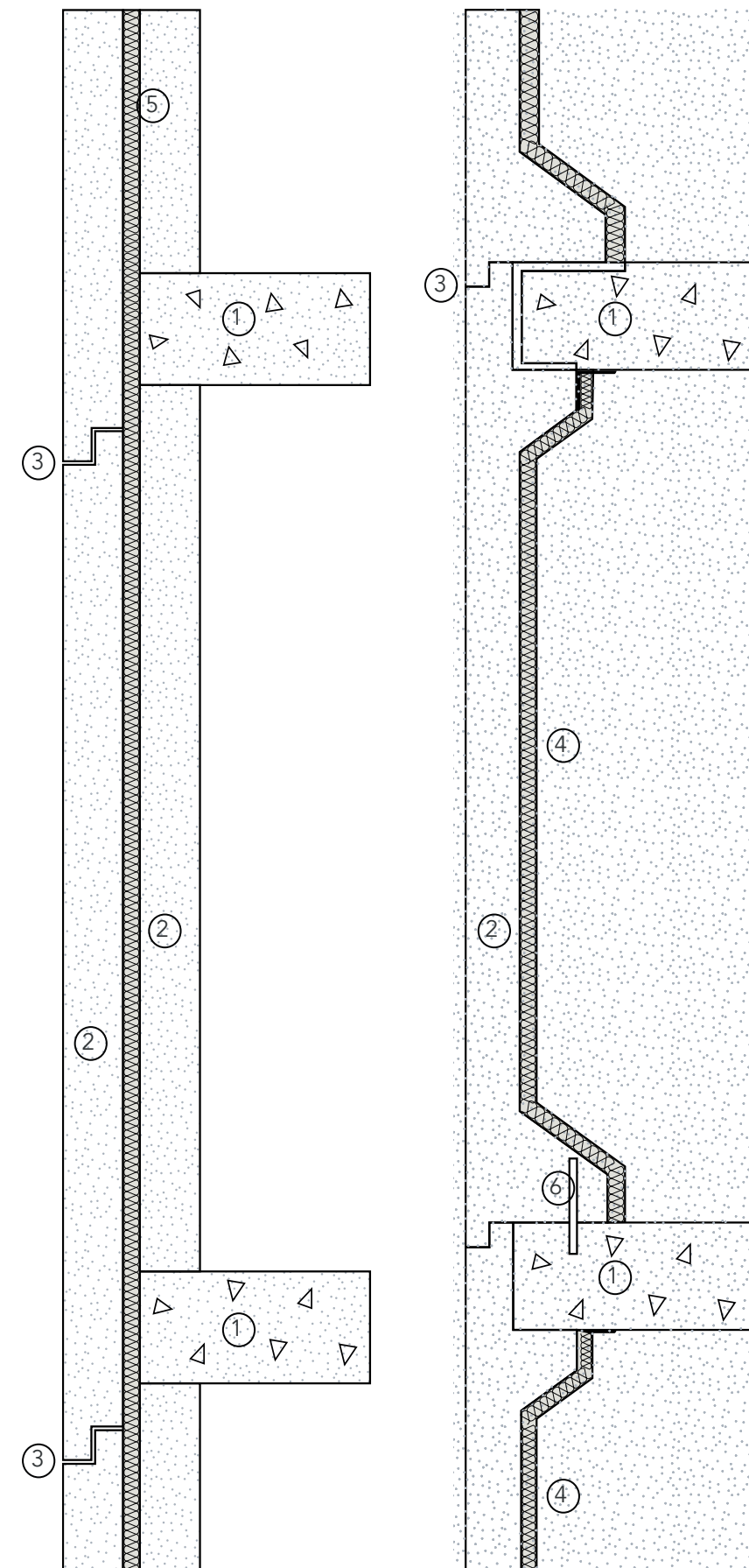


Figure 2.7. Typical vertical section of a load bearing precast concrete facade panel (Watts, 2013)

Figure 2.8. Typical vertical section of a non-load bearing precast concrete facade panel (Watts, 2013)

1. Concrete Floor Deck
2. Precast concrete panel
3. Horizontal joint
4. Drywall/ Dery lining
5. Thermal insulation
6. Steel dowel

structural elements included in the facade makes it practically impossible to improve the building, as the upgrading a building primarily depends on its facade. The need for frequent upgrade bought in the trend of non-load bearing facade systems into the market betting on its long-term feasibility and return of investment. Load bearing facade structure unable to keep up with the market economy and needs of the user are usually demolished and reconstructed, which renders the high unsustainable aspect of the building (Panda, 2017).

### 2.1.3 Considerations and constraints for facade panels

The precast facade panels are constrained on different factors depending on the primary material of the facade, its joints and various other components. The basic considerations for the connection joints of the facade panels are dependent on their location on the panels and needed to be selected considering the following criteria (Kjcerbye & Sai, 2001),

- Structural Considerations
- Aesthetics
- Panel Weight
- Transport Limitations
- Internal Crack Control

The precast facade panels are designed to carry vertical loads of self weight and a share for floor loads. An additional loads for external wind pressure is also carried by these panels. Depending on these strength factors, the typical thickness of the facade panel is considered to be 120 mm and to accommodate window profiles and fixtures along its perimeter of opening (Kjcerbye & Sai, 2001). The consideration of accommodating other



Figure 2.9. Fixing the non-load bearing concrete facade panel under construction, Proximity Hotel (Pearce & Ahn, 2013)



Figure 2.10. Elevation of Proximity Hotel (Pearce & Ahn, 2013)

facade components of hoods, sills, ledges, lighting, conduits, air vents, shading devices ,etc is needed in calculating the load carrying capacity, function and detail of the facade panel.

The consideration of some other fundamental aspects for a feasible facade panel are also equally important as its aesthetic and functional behaviour. Some of these factors as outline by (DN-32 Connections for Architectural Precast Concrete) are:

- Façade and connection hardware and materials
- Strength of connections
- Durability and corrosion protection of connections and fillers
- Fire Protection of Connections
- Ductility of connection component
- Volume change accommodation
- Fire resistance.
- Wind considerations
- Seismic considerations
- Blast resistance
- Cladding/Structure Interaction
- Tolerances and Clearances
- Fabrication and economy
- Supply of local hardware

### 2.1.3 SYSTEM INTEGRATION IN FACADE

Facade as an building element has been one of the most crucial aspect of the building performance. Since the very first evolution of human shelters, building elements have evolved to solve specific purpose, but the facade remained to solve its core purpose of being a barrier between the external environment and the internal space with points of access. These access points were then evolved into windows to let the natural lights in the space and the combination of such system with the structural element of the external walls were considered to be the façades of the building (Hafez, 2016). The purpose of letting light in while segregating the internal environment to that of external intended for more comfort marks the start of integration of systems into the facade. With years and advancement of human knowledge, discovery and study of materials and techniques, the facade element started to evolve and became the prime aspect of expression of architecture.

With stages of evolving forms of facade from being massive from classical period to being decorated and expressive at different intermediate eras to that of simple expression in modernism to the current era of technology loaded sustainable approach, the functions of the facade have evolved in parallel (Fraser, 2019). The year of 1973 did experience the Arab oil embargo crisis, and an urgent need of to minimise the energy needs of the buildings did rise up along with stricter building codes. High performance facade started to

develop and since then high efficient building façades were an emergent segment of the market (History of Insulation with Masonry, n.d). While energy crisis as well as global warming due to exploitation of energy use are at alarming state, the purpose of designing an energy efficient functional facade in this environmentally responsible age is highly crucial and potentially rich and hence needs to be researched further to make building less energy demanding and relying over renewable forms of energy sources.

According to classification of intergrated facade systems stated by Hoces (2018) in refernce to many other researches that dealt with similar topics, the following diagram was derived. Since it is decided on the grounds of maintenace and upgradability that the facade panels needs to be modular and non-load bearing, the intergrated facade with a building service within classifies as shown in figure 2.11.

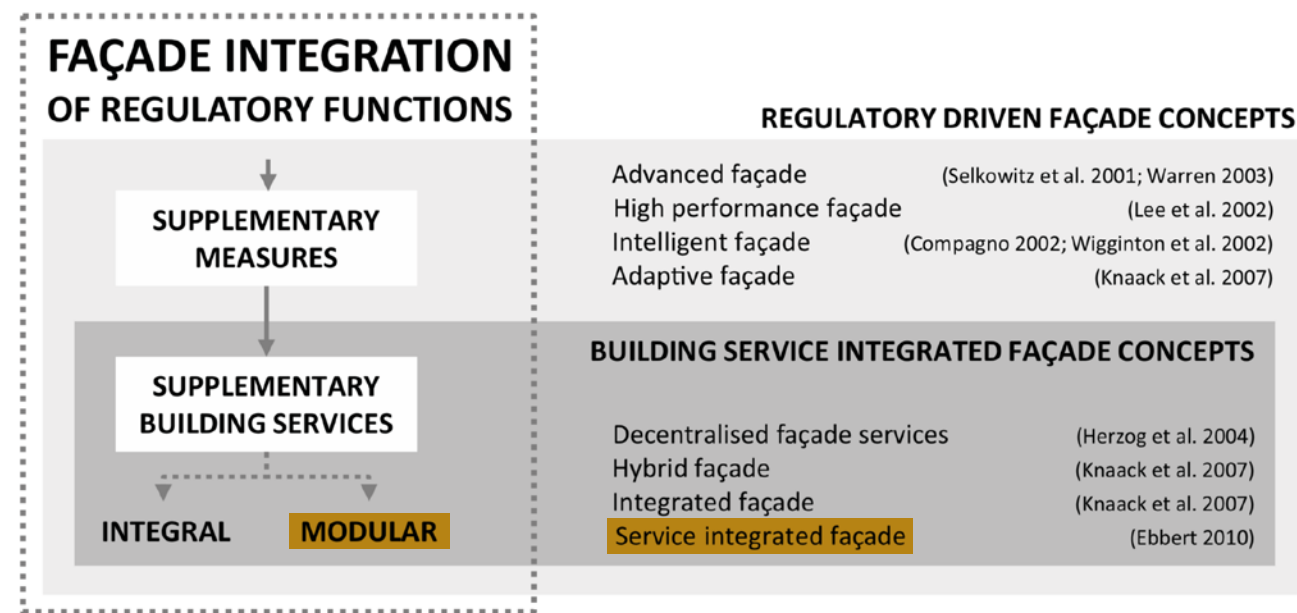


Figure 2.11. Diagram showing the scheme for facade integration of regulatory functions (Hoces, 2018).

## 2.1.4 Ornamentation in façade

Past the aesthetic homogeneity of all-glass horizons which refers the now most common format of building blueish green tint of facade with glass, there is developing suspicion and discussion in regards to the general advantages of this sort of architectural development. This sort of language of glass skin facade is embraced by some some architects who believe in implementing state of the art technologies incorporated within them and leveraging the potential use of sustainability, many other well known architects and firms are refraining from this practice and break the monotonous trend. As a result some of the new proposals and built projects in particular in New York City, are both stunning and stimulating, and offer an appreciated relief from the usual belief. (Geleff, 2018) This slow shift of trend does also express a shift in use of material and ornamentation.

For nearly one hundred years, academic principles stated that architecture did not require ornamentation. Modernism had abolished it, or at least tried to abolish it. Mies van Rohe's steel sections – superfluous from a structural perspective – are ultimately no more and no less than a kind of tectonic ornamentation. With its disdain for ornamentation, Modernism, which dedicated itself wholly to “the plastic effect of the building volume in light” instead of decoration, broke with a tradition that had endured for millennia. For people in all cultures around the world have decorated their homes since the beginning of time. This is true for monumental or public buildings and for residential buildings. And such ornamentation ranges from simple reliefs, to carvings, coloured tiles and elaborate frescoes, from the Greek or Chinese temple to the Arabic mosque, from the vernacular fresco painting in the European Alps to the azulejos, the coloured tiles used in Portugal. Jacques Herzog and Pierre de Meuron are true pioneers in using the building skin as an image carrier. (Schittich, 2008)

### The facade as an information carrier

One very effective example of this is without doubt the Gothic cathedral and its rich sculptural programme on the portals and stained-glass windows, Figure 2.12 which tells entire stories. Today's architecture can hardly match such deep meaning, restricting itself instead to individual, sometimes superficial references which the uninitiated observer finds hard to interpret (Schittich, 2008). The modern developments have an different approach of implementing the capabilities of glass in facade, as in the Chanel boutique in Amsterdam made with glass bricks Figure 2.13.



Figure 2.12. Stained window of lancet pointed arch, St. Vitus Cathedral, Prague (EKCEAB www.alamy.com, 2018)



Figure 2.13. Chanel Boutique, Amsterdam by MVRDV (Stamkot, 2016)

### Light and drama – architecture at day and night

Ever since it was discovered, electric light has been used to add drama to buildings. Kazuyo Sejima's Flagship Store for Christian Dior on Tokyo's fashionable Omotesando is an impressive demonstration of this trend, Figure 2.14, 2.15. By day a simple, almost reserved glass cube, the building at night turns into a beaming lantern, with colours changing subtly from floor to floor, an effect created by using different curtains and partition walls behind the glass facade.

A similar concept of decoration, although carried out on a somewhat more modest scale, is seen in Wiel Arets' new university library in Utrecht Figure 2.16. He, too, joins the different materials of glass and concrete together, by covering them with the same pattern. Printed willow branches, which also have a role in screening the sun, lend the glass a delicate veil-like appearance; on the adjacent visual concrete surfaces they appear in the form of relief. In addition the architect uses the abstract plant motif to communicate a hidden message by referencing the green swathe that was originally planned for in front of the windows. (Schittich, 2008)

Ornamentation and decoration differ in the terms of the added value of ornament that relates it to the functional aspect of element. The pattern of concrete in Figure 2.16 are merely aesthetic than functional and may be termed as decoration and not ornamentation.

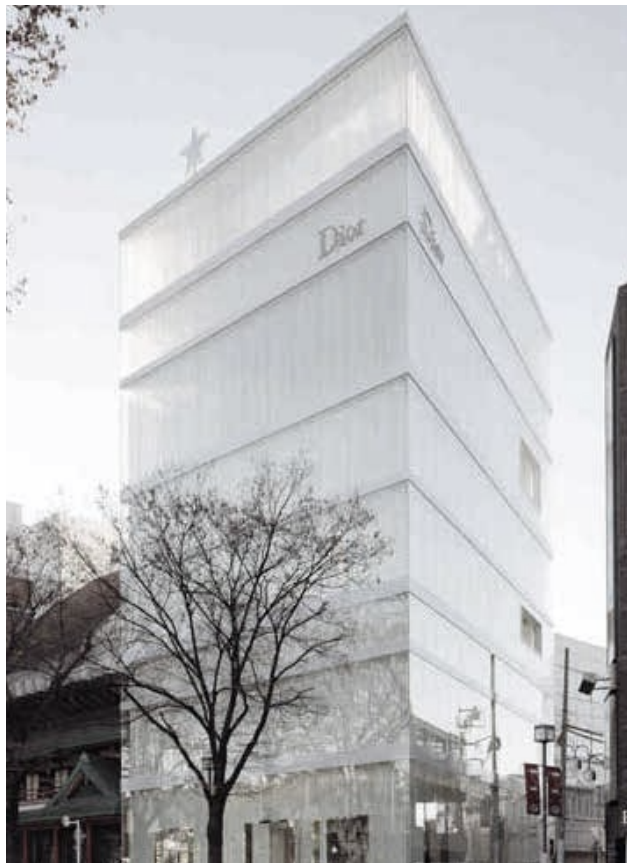


Figure 2.14. Dior Omotesando during day, Tokyo by SAANA, (StudiInternational, 2004)



Figure 2.15. Dior Omotesando during night, Tokyo by SAANA, (Phaidon, 2018)

Facade is an element of the building that expresses and communicates with the user and admirer of the building with its form, colour and texture. The inclusion of these elements may be dependent and related to the material, manufacture and detailing of the facade element. Expression of the building can also be regulated as an idea of the architect's vision and formulation of the technologies needed to achieve the desired facade panel. As humans, the facade of every building is what derives the unique identity of its architecture which may or may not be governed by a same set of constraints and ideology. The expression of the buildings may differ by the nature of implementation of the facade in terms of being repetitive or dynamic. The overall element expression in macro and the micro scale does depict the necessity of ornamentation of the facade.



Figure 2.16. Concrete and glass facade, University library, Utrecht by Wiel Arets Architects (Schittich, 2008)



Figure 2.17. Precast concrete facade, 11 Hoyt, Brooklyn by Studio Gang, (Geleff, 2018)

## 2.2 CONCRETE: THE MATERIAL

Concrete in the built environment, has been one of the most versatile material proven by its existence in ancient times while its validity makes sense to be studied and implemented for the built environment at present. This material has a notable events in its timeline traced back to the Great pyramids of Giza to that of sensor embedded self-healing smart concrete systems. Romans were the first to widely use this material in their constructions and the dome of Pantheon in Rome constructed during 600 BC, Figure 2.18 is one of the greatest example of the early use of concrete with tuff fragments and clay chippings made up of lime mortar. After the fall of the Roman empire in 476 AD, the technology of making Pozzolan cement was lost, until John Smeaton reformulated it and used concrete for rebuilding of the Eddystone Lighthouse in Cornwall, England (Auburn, 2018).

After the invention of Portland cement in 1824, concrete during the 19th century was mostly used for industrial buildings but started to make its shift towards home construction after the addition of steel rods prevented the exterior walls from spreading. This was a breakthrough in the material for façades of buildings because of its high performance and durability only after the clay bricks as the modern material. Since then the advancement in the use of concrete has been significant with the ability of precise calculation, behaviour tests and alternative additives. The development of pre-stressed concrete have rendered the unseen possibilities of the material and hence the ever grown demand of concrete in the infrastructure market developed (Friedbert et al., 2013). The art of fusing computing tools and crafting the extreme possibilities out of concrete, has pushed the boundaries even further, and this project contributes in the lines of exploring concrete in a more



Figure 2.18. Interior of the Pantheon dome, seen from beneath. The concrete for the coffered dome was laid on moulds, mounted on temporary scaffolding. (Kabel, 2008)

sustainable manner while celebrating the structural properties of the material as a form of art and expression for the field of architecture.

### 2.2.1 Composition

In ancient times, Roman concrete for example was made from volcanic ash (pozzolana), and hydrated lime. Modern concrete or most commonly known as the Portland cement concrete is a composite material comprising of fine (sand) and coarse aggregate (gravels) bonded together with a fluid cement paste that develops its strength over time with a benchmark of 28 days of curing (Friedbert et al., 2013). Water is one of the main component in the concrete that is responsible for the chemical reaction between the cement and binds them with others. While this is a general composition of concrete, the composition of the concrete can vary significantly depending on the use type. While ratios of the material is one of the factor, the components, admixtures and supplements could be added for specific performance and appearance of the concrete.

Concrete in modern times have developed to address the common problems with concrete. While concrete lacks in tensile strength, the addition of steel reinforcements and most recently steel fibres and glass fibres have taken their way into the composition making it an even more viable material for extreme loading and climatic conditions. The replacement of aggregates with reused concrete, waste glass, chipped woods, industrial wastes or other materials addresses the after life of concrete in the built environment and significantly reduces the environmental impact. Replacement of cement with polymer based materials has developed ultra high performance concrete which are aimed at specific use conditions. The introduction of metal silicates helps in development of very light weight aerated concrete which has comparative advantages in use for partition walls and mass concrete use regions along with many other compositions of concrete that contain their justification over others.

The demand of concrete has been varyingly distributed in the infrastructure industry and the dependency on the type of concrete used for a project mostly depends on the performance expected out of the concrete.

### 2.2.2 Classification

Generally concrete has hundreds of different types of its composition, but depending on different terms of classification, there are few ways to segregate typologies of the material.

The most commonly used classification of concrete are according to Friedbert et al. (2013) and Serbia (2018).

**Grades of concrete:** The concrete grade (M) is denominated by the compressive strength of the concrete composition in MPa, based on the characteristic strength of concrete at the age of 28 days. For the

construction of concrete blocks the following grades (M) are used: 10, 15, 20, 25, 30, 35, 40..... 75 etc It is not permissible to use concrete grade of M15 or lower for reinforced concrete.

**Bulk density of the concrete:** Lightweight concrete: composition of concrete whose bulk density doesn't exceed 1900 kg/m<sup>3</sup> with special condition with 2100 kg/m<sup>3</sup> with high mechanical behaviour.

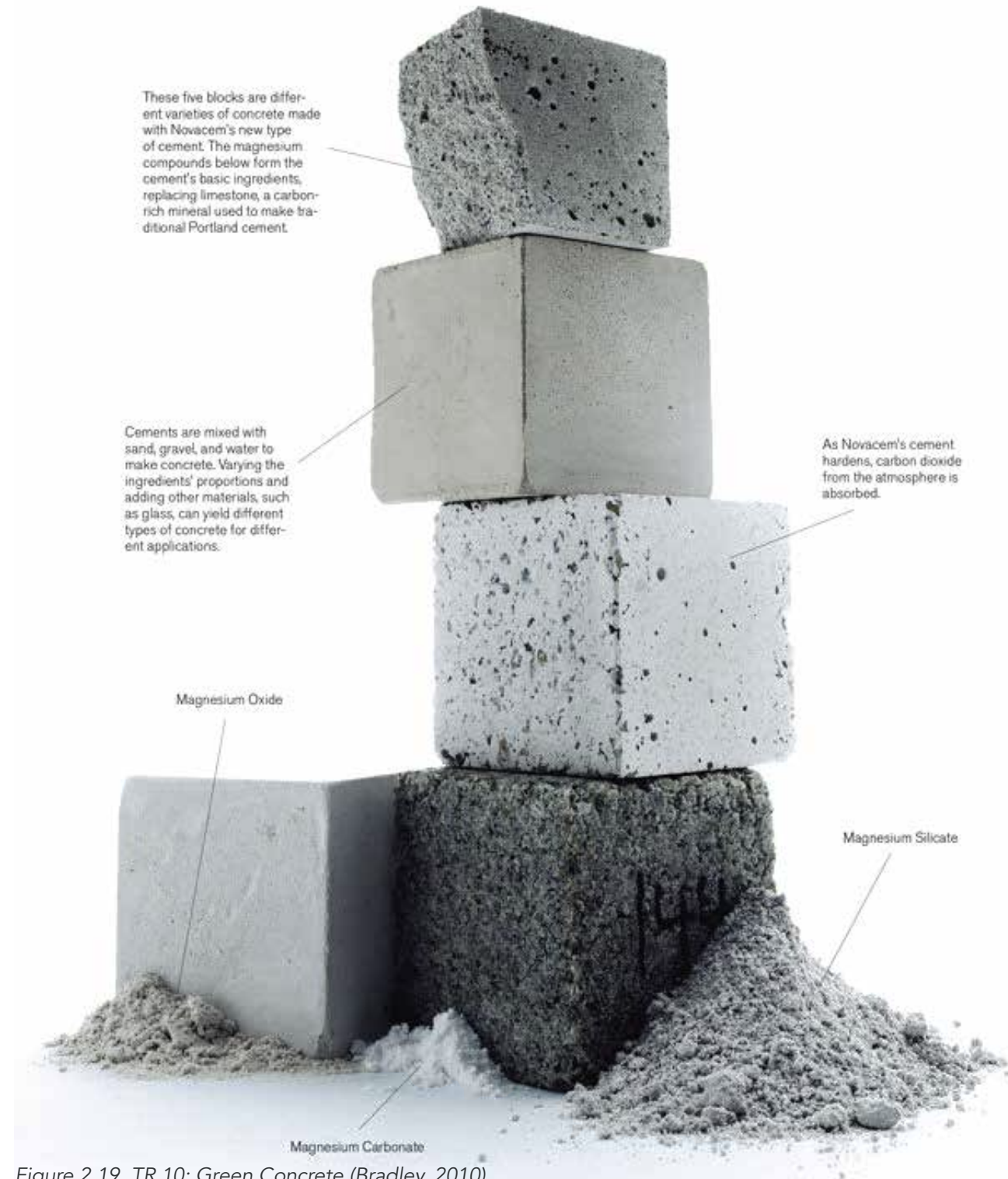


Figure 2.19. TR 10: Green Concrete (Bradley, 2010)

Ordinary concrete: with bulk density ranging between 1900 kg/m<sup>3</sup> to 2500 kg/m<sup>3</sup>

Heavy-weight concrete: with bulk density of higher than 2500 kg/m<sup>3</sup>.

It is to be considered that the density of the concrete is irrelevant to its compressive or tensile strength.

**The type of binder material:** Depending on the type of binder used for preparing concrete there are:

Cement-concretes: where the binder is used Portland cement or similar cementitious binder material

Asphalt-concretes: which uses bitumen as a binder. These types of concrete are mostly used in roads and streets, considering their low wearability.

Polymer concretes: replace cement with polymers. This concrete is also known as Polymer modified concrete (PMC).

**The agility of fresh concrete:** Depending on the consistency of the concrete used to pour in place, it has been divided into solid, low-plastic, plastic and liquid. This classification is considered in terms of workability and process-ability of the composition. Concrete consistency can also be termed as the degree of stiffness or agility of fresh concrete.

**The purpose of concrete and others:** Depending on the designated use type of concrete, it can be classified into some of following examples of concrete (Serbia, 2018),

- Hydro-technical concrete
- Concretes for pavement structure
- Prestressed concretes
- Precast concretes
- Concrete for decorative purposes
- Concretes for radiation protection (heavy-weight concrete)
- Thermal insulating concretes (lightweight concretes)
- Waterproofing concretes
- Soundproofing concretes (lightweight concretes)
- Fire proof concrete
- Concrete and mortar for repairing or restoration, etc.

Above the mentioned classification on concrete, there are some other special types of concrete

that have unique composition that lend them high performance and reduce material use and weight. The Ultra High Performance Concrete (UHPC) classified under Fiber Reinforced Concrete (FRC) and Textile reinforced concrete (TRC) are among the promising category of concrete that are considered to study for this project and are discussed in detail below.

### 2.2.3 Fiber Reinforced Concrete (FRC)

Fiber reinforced concrete is a concrete by composition with added fibers in it that act as reinforcement. The idea of using glass fibers in concrete has been around since 1970s (Horsley, 2001). Fibre reinforce concrete does consider all different possible fibres that may be mixed with concrete that include alkali glass, synthetic, organic and metal fibres. While the use of glass fibre is widely familiar in the construction industry, the recent developments related to natural fibre reinforced concrete (Chockalingam, Sethunaryanan, & Ramanathanan, 1989) may prove more efficient and sustainable way of composite concrete. The role of fibres used in the concrete are to arrest the growth of crack Figure 2.20. The random orientation of thousands of micro fibres enhances the performance of the concrete (Parameswaran, 1991).

One of the earliest use of GFRC (spray-up form) was back in 1974 ( Iskender & Karasu, 2018). The GFRC is used in architecture under different forms, the thin walled GFRC cladding being the most commonly known such as in 30 Cannon Street building, London. There has been a shift in the perspective of use type of GFRC for example one of the first complex geometry thin-walled GFRC was introduced for façade of the Heydar Aliyev Center in Baku designed by ZHA (Studinka & Joseph, 1986).

### Ultra-High Performance Concrete (UHPC)

UHPC is a cementitious, concrete material that has a minimum specified compressive strength range of 130 -150 MPa (Azmeem & Shafiq, 2018). Fibers are usually added to the concrete mixture to achieve specified requirements of UPHC. UHPC strengthened with fibers is considered to be a combination of three different types of concrete technologies viz. self-compacting concrete (SCC), fiber reinforced concrete (FRC) and high-performance concrete (HPC) (Torregrosa, 2013).

UHPC, is also known as reactive powder concrete (RPC) because of the inclusion of the reactive powder in

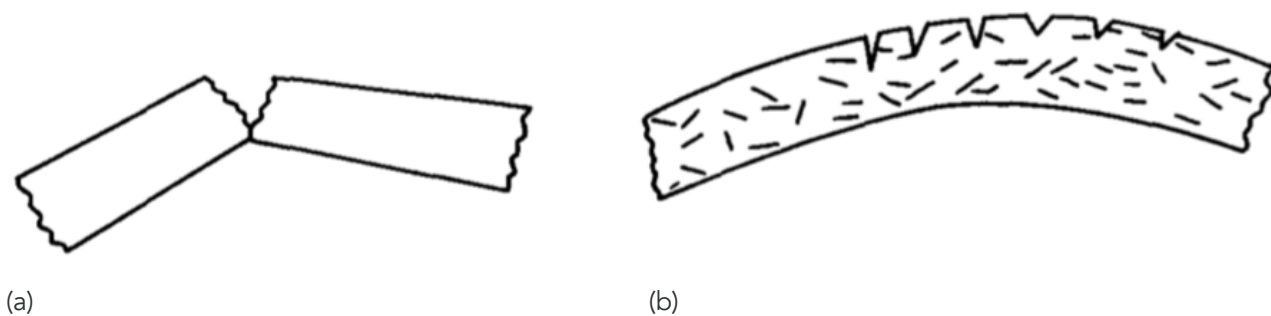


Figure 2.20. Crack arresting mechanism of fibres (a) Failure of plain concrete prism without fibres. (b) Failure of prism with fibres act as "crack arresters" (Parameswaran, 1991).

the composition. This material is typically formulated by the combination of portland cement, additional cementitious materials, reactive powders, limestone and or quartz flour, fine sand, high-range water reducers, and water (Richard & Cheyrezy, 1995). This material can be modified to formulate an UHPC with a compressive strength of about 200 MPa. Using different types of fine materials only for the mixture results in a highly compacted, smooth surfaced external appearance with high aesthetic value.

UHPC mixture while combined with different types of fiber viz., metal, synthetic or organic fibres can result in a flexural strength of 48 MPa or higher. The different types of fibres used in UPHC are high carbon steel, PVA, carbon or combination of these. The high cost of carbon based fibres makes the alkali glass fibres a viable selection for the mixture. By the elimination of reinforcing steel members in most applications, the material behaves to be high flow behaviour and self compacting resulting in a simplified construction process of UHPC (Association, 2018). The mould-ability of concrete and added strength and weight reduction by the fibres make the FRC the most flexible building materials. This combined with the complex solution solving capabilities of modern computing and manufacturing process paves way for development of highly efficient architectural components, which is explored in this project.

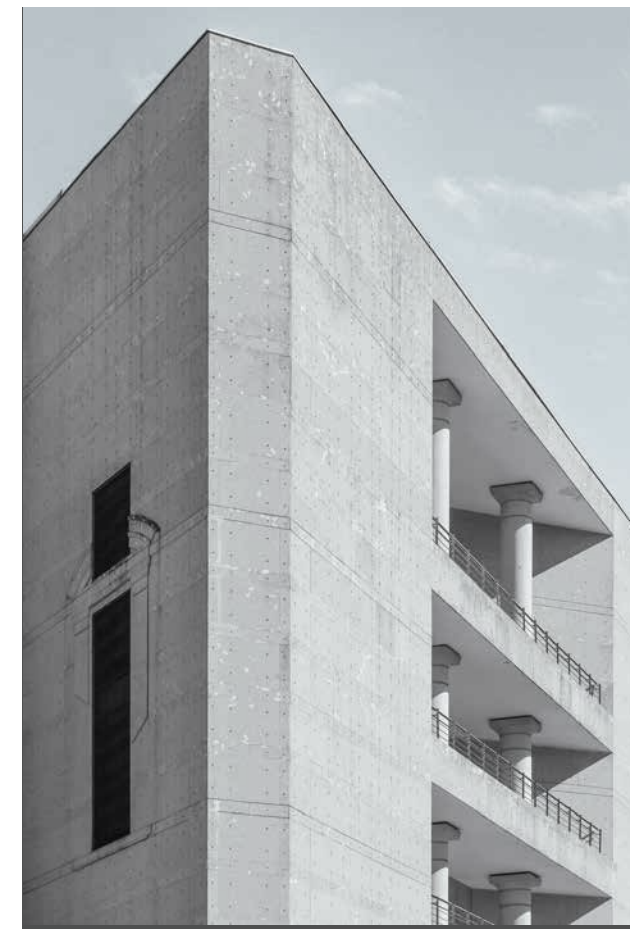


Figure 2.21. Load bearing cast-in-situ common concrete facade



Figure 2.22. Non-load bearing GFRC facade panels, Broad Museum, Los Angeles by Diller Scofidio + Renfro (WillisConstruction, 2015)

## 2.2.4 Textile Reinforced Concrete (TRC)

TRC is newly developed technique of reinforcing concrete for high performance applications. It is a cementitious composite based material that involves the engineered fabrics as the reinforcing material. This material depends on the proper bonding between the reinforce textile and the concrete. Usually RPC is used for textile reinforced concrete. Usually the steel reinforcement is a factor for the high thickness of a concrete

Constituent	Units	RPC 200	RPC 800
Portland cement		955	1000
Fine sand	150-600 $\mu$ m	1051	500
Ground quartz	d <sub>50</sub> =10 $\mu$ m	—	390
Silica fume		239	230
Superplasticizer(Polyacrylate)		15	19
Steel fibres		168	630
Total water		162	190
Compacting pressure		—	50MPa
Heat treatment		20°C/90°C	250°C-400°C

Table 2.1. Typical composition and mechanical properties of UHPC (Azme & Shafiq, 2018).



Figure 2.23. Glass fibres for concrete mixture (alibaba.com)

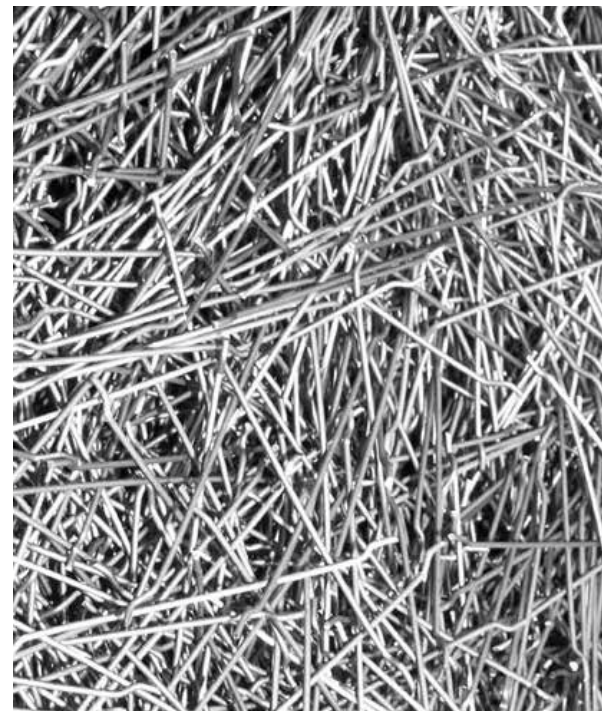


Figure 2.24. Steel fibres for concrete mixture (bautech.eu)

sandwich facade panel and replacing the steel bars with thin textile mesh that can result in fabrication of significantly thinner and lighter concrete sandwich facade panels similar mechanical properties as shown in figure 2.25 (Malaga, Flansbjer, Blanksvärd, & Petersson, 2012).

The application of TRC has currently been confined to that of facade panels and footbridges only with further scopes of exploration. As a reference large scale implementation of TRC facade panels have been realised on the new building of ROC Leiden Community College in the Netherlands with an area of more than 10,000 m<sup>2</sup> of facade panels. Some other examples of application of TRC facade panels are the Faculty of TU Dresden and RWTH Aachen (Novotná, Kostecká, Hodková, & Vokáč, 2014).

Potential alternatives of concrete as a material for a building facade are considered to be terracotta for its potential equivalent mechanical property and mould-ability to that of solid concrete, natural wood in response to its natural material behaviour and carbon negative footprint, glass for its transparency and aesthetics. The criteria of selecting concrete as a material for the facade in a Hot and humid climate region of India, ex-Mumbai, over the other possibilities has been briefly analysed in the following section.

## 2.2.5 Selecting concrete as the material

'It's almost impossible to find out the optimal material for a particular structure is what regarded by the chemistryworld.org. Concrete as a material has proven itself to be one of the most versatile material since the early ages of construction and at current times with further scopes into future development. Concrete is the second most consumed material in the world after water. Concrete as a material accounts to double that of the other materials in combination used for the building industry. This tends to the uncertain fact of concrete living up as a material for future (Gagg, 2014).

Concrete has been the most preferred choice of building material currently and its benefits in the sector of building façades have been recognised previously and also today in comparison to other building materials. Especially Glass Fiber Reinforced Concrete has been an effective replacement option, with the known advantages of concrete, versatile to an architect's vision and compared aspects of performance and sustainability.



Figure 2.25. Glass fibre woven textile reinforcement for concrete casting (Malaga et al., 2012)

### 1. Comparison of concrete to conventional facade cladding materials

A research journal by Plummer et al. (2016) established a comparative analysis of seven different exterior wall types with different cladding materials (table 2.2, figure 2.26), in which the thermal performance, heat transfer and energy consumption of the space behind was investigated, along with their behaviour in different climate zones specific to the United States. Considering the future impact due to climate change on the energy consumption referring to years 2050 and 2080 was investigated and studied. This study was conducted by modelling heat transfer wall sections of seven different wall configurations that considered conventional systems like brick cavity wall with metal framing, rain-screen facade with terracotta cladding, rainscreen

Effect of Orientation on Total Energy Use(GJ) Heating-Cooling-Lighting-Fans													
Climate Zone	Wall Type	Orientation											
		0	30	60	90	120	150	180	210	240	270	300	330
1A	Type 1, 0% WWR	5.46	5.52	5.61	5.67	5.69	5.66	5.63	5.64	5.64	5.56	5.50	5.49
1A	Type 2-6-7, 0%WWR	5.40	5.41	5.45	5.47	5.48	5.47	5.46	5.47	5.50	5.50	5.47	5.43
1A	Type 3, 0% WWR	5.45	5.47	5.53	5.56	5.58	5.57	5.56	5.59	5.61	5.61	5.56	5.51
1A	Type 1, 20%WWR	5.20	5.90	6.84	7.30	7.05	5.99	5.70	6.04	6.89	7.22	6.75	5.88
1A	Type 2-6-7, 20%WWR	5.20	5.85	6.63	7.06	6.83	5.97	5.63	5.84	6.56	6.87	6.43	5.64
1A	Type 3, 20%WWR	5.18	5.81	6.58	7.00	6.76	5.91	5.63	5.77	6.46	6.77	6.34	5.56
1A	Type 1, 40%WWR	5.26	7.36	9.45	10.48	9.98	8.02	7.04	8.00	9.81	10.32	9.34	7.45
1A	Type 2-6-7, 40%WWR	5.28	7.27	9.30	10.32	9.82	7.87	6.71	7.81	9.57	10.08	9.12	7.27
1A	Type 3, 40% WWR	5.26	7.26	9.26	10.27	9.77	7.83	6.69	7.75	9.50	10.00	9.05	7.22
1A	Type 4	6.40	8.33	10.70	11.91	11.12	8.76	7.62	8.80	11.11	11.89	10.81	8.49
1A	Type 5	6.40	8.33	10.70	11.91	11.12	8.76	7.62	8.80	11.11	11.89	10.81	8.49

Table 2.2. Total annual energy use for different analysed wall systems and orientation in the hot and humid climatic zone 1A (Miami) (Plummer, Aburas, Nikas, Santi, & Velasquez, 2016).

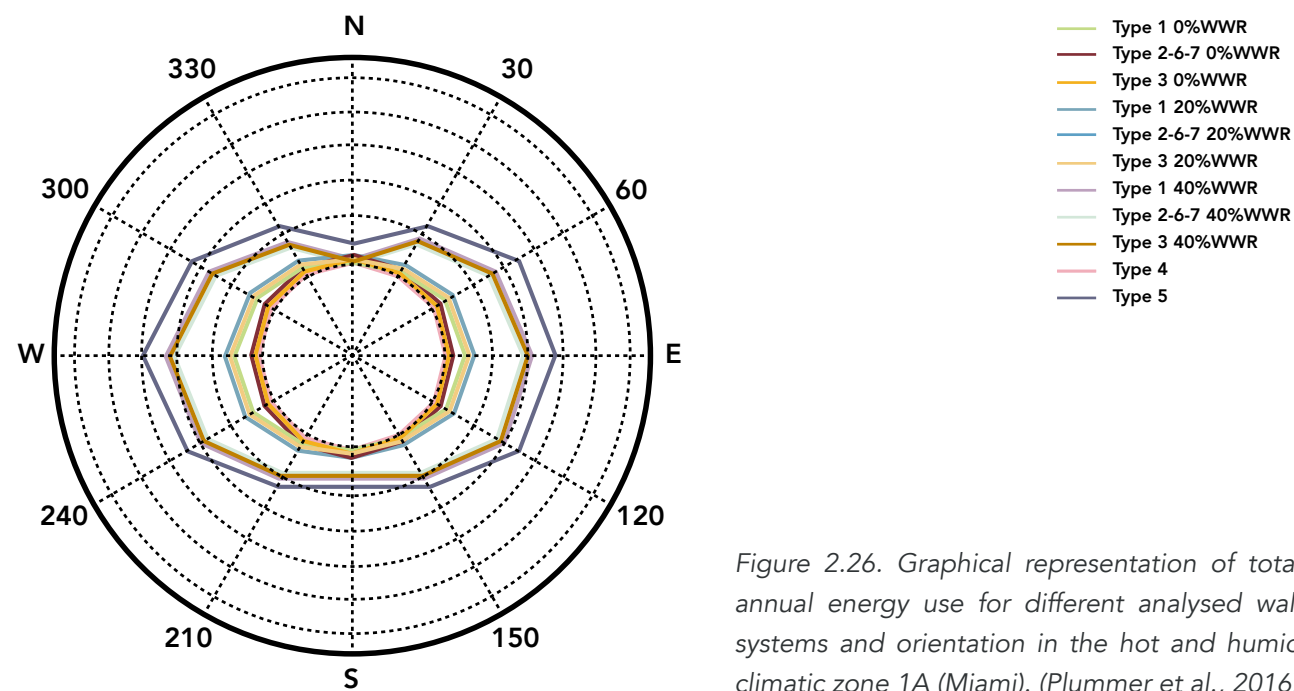


Figure 2.26. Graphical representation of total annual energy use for different analysed wall systems and orientation in the hot and humid climatic zone 1A (Miami). (Plummer et al., 2016)

facade with glass-fiber reinforced concrete cladding, standard glass curtain wall and also thermally improved assemblies. The thermal gradients of the seven different finishes of exterior walls were modelled and their respective U-values were calculated to perform the analysis.

The performance of GFRC wall (Type 3) was particularly referred for this project in comparison with other materials. The simulation were carried out using THERM software with a setup to mimic different extremities of climate types with exterior and interior temperatures of 90° F & 72° F, 60° F & 72° F, 30° F & 72° F and 0° F & 72° F. The Climate Zone 1A of Miami, U.S has resemblance with that of Mumbai, India with hot and humid type of climate and is considered to be closest study in relation to the proposal of this project.

The above analysis by Perkins + Will did realise that façades that act as an envelope to any building do significantly impact the energy consumption and the comfort of the users inside. Climate based approach considering the specific climatic conditions of the project location, to design different elements of a building is the key for high performance building façades. Results of the analysis of the different types of facade assemblies depict that the curtain wall is the worst performing facade system followed by the brick cavity wall. The terracotta cladding facade system had the highest U-values and was considered superior to the GFRC facade system with a small margin (Plummer et al., 2016). Although the terracotta as a material was better performing system, but the problem related to this material in comparison to that of the mechanical behaviour and properties of GFRC, renders it as not a preferable option in consideration for this project. The limited size of manufacturability of terracotta, high distress value, constant repairing and replacement issues, low compressive strength in comparison to concrete, water absorption of 6 - 14 % by weight, etc. make GFRC a preferred option above terracotta (Gerns & Freedland, 2006). These reasons tend terracotta to be

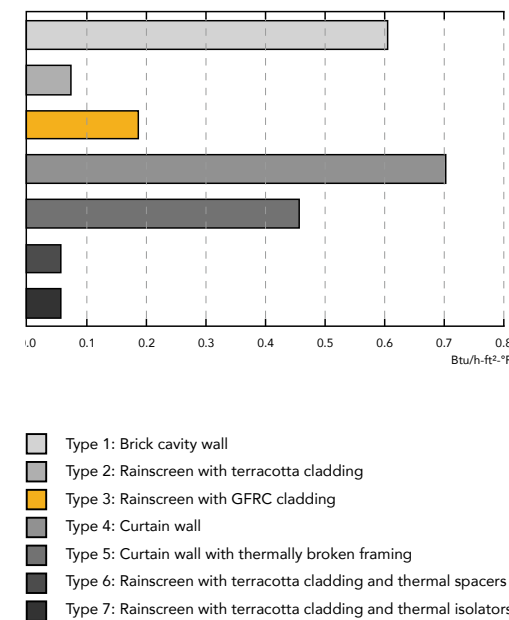


Figure 2.27. Total annual energy use for different analysed climatic zones. (Plummer et al., 2016)

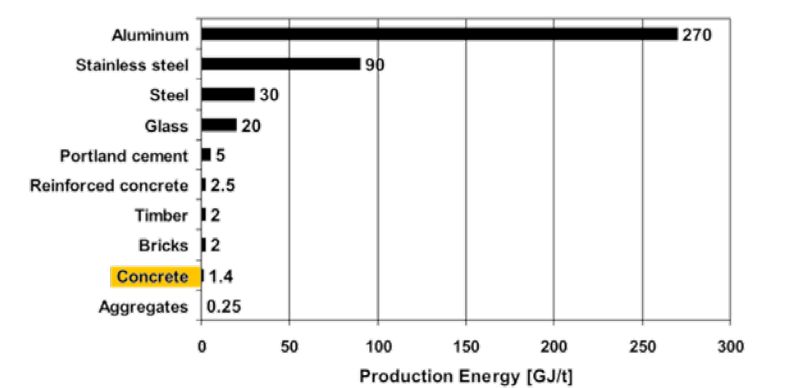


Figure 2.28. Production energy of various building construction materials.(Alsamsam, Lemay & VanGeem, 2008)

used only in limited size flat panels to be used in building façades. The marginal difference in building energy performance as analysed in the above study can be overcome by UHPC with glass fibers and in long term of life expectancy of concrete.

In another study done by Alsamsam, Lemay & VanGeem (2008) as shown in figure 2.28, it is mentioned that concrete as a material in itself that considers the non inclusion of any steel/ metal reinforcement which segregates it from Reinforced concrete, has a very low production or embodied energy even lower than that of timber (engineered wood). On the counter part the reinforced concrete or the cement in itself are higher on the bar. While cement only comprises of 5-12% of the composition, concrete tends to sit lower on the charts.

## 2. Comparison of concrete to engineered wood or Cross Laminated Timber (CLT)

Wood is unarguably the most green building product that can be used as it has a carbon negative footprint and can deliver certain required structural, climatic and aesthetic behaviour in its natural form and for certain consideration of use type. Its regrowth property makes it abundantly available in the nature and decomposable making it the most sustainable building product. But the building industry is not responsible for the only material being used in it. The final product made up from the material, economy around it, the politics of the locality, the service life & performance and the after life are also related to assess the feasibility of a building product.

Cross Laminated Timber is a composite form of solid lumbers laid in alternating direction of the fibre grains and pressure glued using synthetic binders. Use of organic binders have not yet been successful enough to a satisfactory building regulatory safety structural standards (Smyth, 2018). Although the current commercially available CLT are although a viable solution for the building industry claiming to replace other materials 15-story building and also 30 stories via some proposals, there are some serious considerations that are still in debate and uncertain some of which are discussed below (DESIGN, 2012) .

'Mechanically ventilating a CLT building will eventually cancel out the carbon negativity that made it worthwhile in the first place' (Astbury, 2017). Even though timber is considered to have a very high thermal mass, it has a marginal difference of about 2.5 times than compared to the higher thermal mass of concrete, that reduces the thermal comfort of the occupant without mechanical solutions. The high very low light reflectivity reflects back on the artificial solution than that compared to white or grey finish of concrete. The constant maintenance of exposed timber construction is a menace and need to be addressed unless and until covered with a cladding material, which is a discussion out of the scope of this project. The most important aspect of considering CLT constructions is the after life of the material. Usually the solution in degraded reuse or burning fuel and supplying it back to the grid as it cannot be disposed in the open refill grounds like natural wood as CLT releases methane to the environment in its decomposition. The current business model and market does not satisfy the closing cycle of building with CLT and maintaining thermal grid based on its after life. The possible viable solution of degraded reuse also do produce a significant amount of waste (Smyth, 2018).

Amongst other major drawbacks of using CLT as a building material are unpredictable standardised or modifiable compressive strength of the material determining its effective use (Oh, Lee, & Hong, 2014), the high moisture and damping decay in critical places of the wood construction leading to failures, very poor and uncertain fire resistance and rating of CLT, lack of mortgage and insurance for CLT building because of uncertain safety behaviour that in majority hits the economic viability of the property in current times, high mass construction leading to loss of floor and height space in comparison to traditional concrete construction, high cost because of very few manufacturing companies and unavailability of quality wood uniformly around all the regions of world, lack of standardisation, legal building regulatory barriers, uniform skill management in terms of production and built quality across the globe, etc (Smyth, 2018; Astbury, 2017).

The alternatives to concrete can be proven to be more environmentally sustainable in the future and so can be concrete with recent developments of binder that would have minimal CO<sub>2</sub> emissions and perform carbon negative by absorbing them (Bradley, 2010). The use of glass for its obvious reasons of transparency cannot be replaced and will continue to hold its position of its absolute need. In general the Window-to-Wall Ratio (WWR) for a typical 2 story high office building in a hot and dry climate of India holds to be around 30-40% (Didwania, Garg, & Mathur, 2011), with most of the facade being dead or opaque.

## 2.2.6 Recycling concrete

As recorded by the UNEP-SBCI (United Nation's Environment Program's Sustainable Building and Climate Initiative) (2009), the infrastructure industry is accountable for approximately 40% of the total energy, 25% of water and 40% of resources consumption. It is also environmentally responsible for generating about one-third of CO<sub>2</sub> emissions (Novotná, Kostecká, Hodková, & Vokáč, 2014). The important contributor to that is the concrete industry. The reason that concrete has such a big carbon footprint is because of use of the material in such huge quantities worldwide.

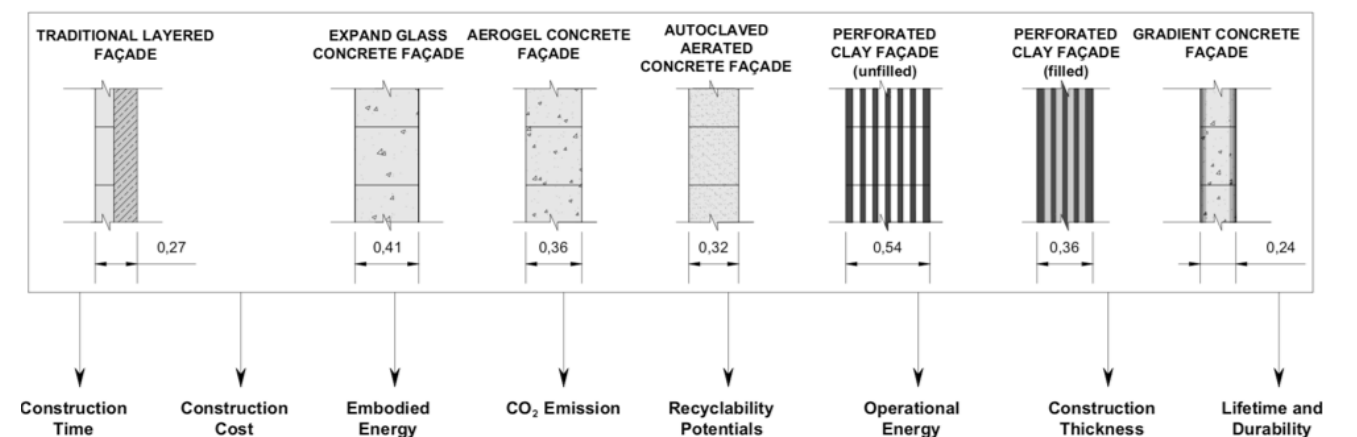


Figure 2.29. Different wall design and performance parameters (Hafez, 2016).

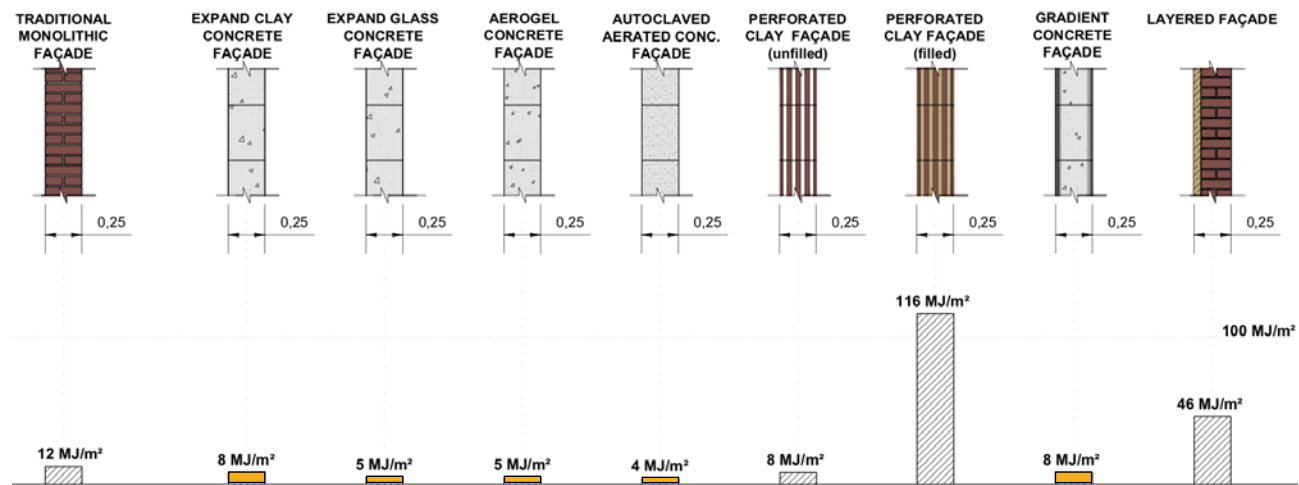
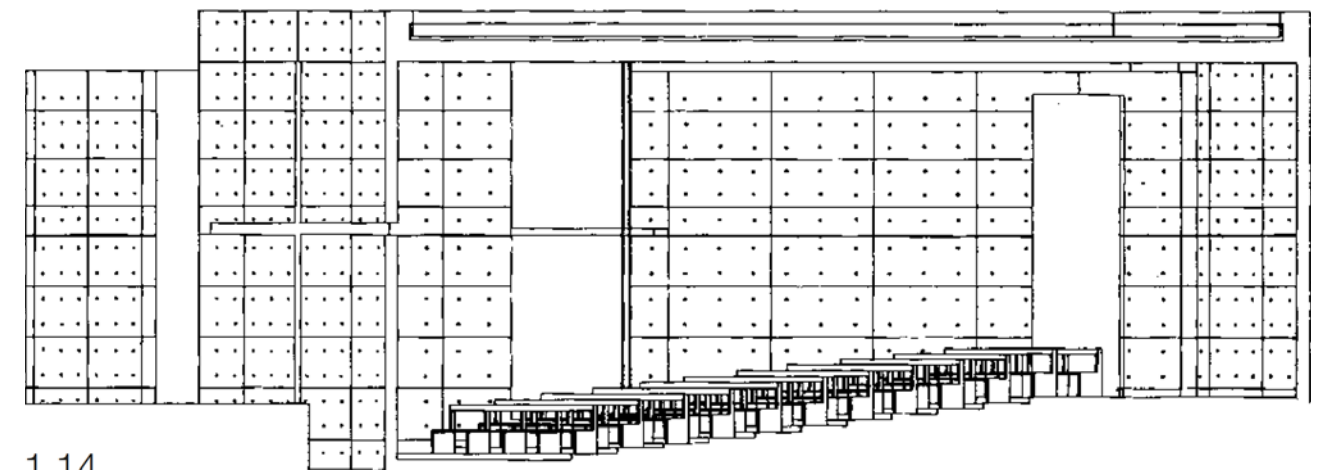


Figure 2.29. Recyclability potentials for different external walls in Egypt (Hafez, 2016).

While most of the materials used in concrete are naturally derived, the most unsustainable ingredient is the commonly used cement which comprises only 7-20% (may vary depending on the use type) of the concrete volume. The active replacement research for cement as the binding material of concrete may lead to a more sustainable concrete than at present times.

But all the above discussions doesn't mean that concrete is not recyclable. Although cement cannot be viably separated from concrete but the after life of concrete could be reusing and recycling the material in the form of aggregates for the new concrete without exploiting any virgin materials. Because of the huge demand of concrete construction since many decades the demolition rate of the material is also high. According to the World Business Council for Sustainable Development, an approximated 30 billion tonnes of concrete as a material were used for infrastructure globally in 2006, while the generation of construction and demolition waste (C&DW) is estimated at 900 million tonnes every year only in Europe, the US and Japan (Concrete Recycling, 2009). China being the highest consumer in the world with a significantly higher margin of difference than any other country while India joining in as second (Statista, 2018) that also depicts the shift of market in the sector of infrastructure. There are a lot of misconceptions and constraints related to recycling of concrete and using it back in the building industry and it has been studied and detailed out by Panda (2017) and in Concrete Recycling (2009).

By an extensive research done by Hafez (2016) by considering a wide variety of aspects contributing towards the assessment of performance of different composition of concrete against wall configurations with other materials like clay, figure 2.28, 2.29. It is seen that some specific concrete configurations tend to low or similar to that of perforated clay facade, but considering the fact of developing large single high strength mono block cast of clay is very tough giving the edge of advantage to concrete.



1.14

Figure 2.30. Patterns of concrete formwork, Church with Light; Ibaraki, Japan by Tadao Ando (Schittich, 2008).



Figure 2.31. Glazed and concrete facade, 152 Elizabeth Street, New York by Tadao Ando (Howarth, 2017).

Based on research journal by the Royal Society of Chemistry (Crow, 2008) they do state the possibility of eliminating 20 % of cement content while maintaining the durability of concrete and also that reducing the cement levels in concrete the durability is improved in the final results. Ravindra Dhir, director of the concrete technology group at the University of Dundee, UK does mention that more than the short term saving of green house emissions, the ultimate strength and the service life of the concrete is equally important. Concrete could be design for performance within the bounds of engineering requirements and being responsible to the environment. The reduction in the use of concrete and exploitation of virgin materials can prove marginal differences in CO<sub>2</sub> emissions and highly sustainable concrete construction might be established.



Figure 2.32. Ench Mendelsohn, Einstein Tower, observatory and astrophysical institute; Potsdam, 1920-21 (Friedbert et al., 2013)

## 2.2.7 Ornamentation of concrete

Ornamentation with concrete is flexible to be expressed in a wide disciplines and varieties than any other building materials. The ease of moulding concrete into any desired shape and form subjective to its stability and concerned behaviour, is what made exploration of modern building forms and ornamenting them a norm of practice during the post modern era.

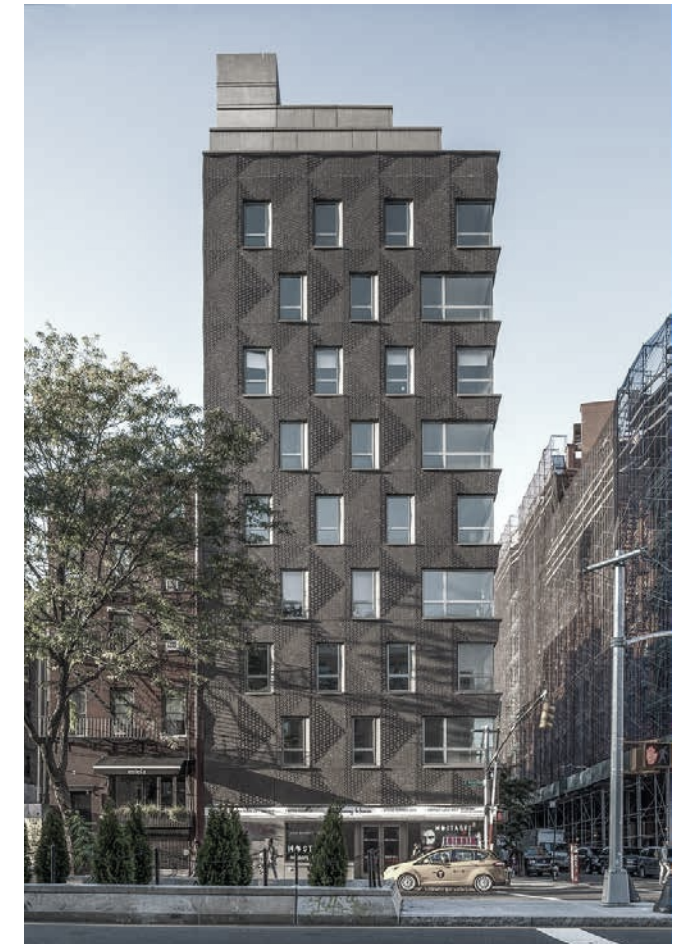
In the junction of Modernism and Post-modernism era of architecture, the architects of the Expressionist Period recognised the sculptural potential of concrete and at first tried to employ this in their structures as an artistic element. At the outset, they did meet with various problems, large and small. For example, the irregularly curved surfaces of Erich Mendelsohn's Einstein Tower, Figure 2.32. in Potsdam led to problems in developing the formwork, because of which the upper part of the structure was built in traditional masonry and later clad with a thin layer of



Figure 2.33. Rudolf Steiner; Goetheanum Dornach. 1928 (Friedbert et al., 2013)

shaped concrete. Rudolf Steiner's Goetheanum in Dornach, Figure 2.33 near Basel was built between 1925 and 1928 after the previous timber building burned down. Here Steiner managed here to create a graceful moulded, monolithic concrete construction, which could not have been built with such a power of expression in any other material than concrete.

The ability to express and ornament a built structure from the load bearing concrete façades of pre-eras to current modern times of flexible and non-load bearing concrete façades have been explored by many architects and one of the example being that of the Mulberry House built in 2013 by SHoP Architects Figure 2.34, constructed using precast folded concrete panels clad with brick patterns, an expression that acts to be an ornament of the facade. The precast GFRC panels of the Broad Museum, Los Angeles by Diller Scofidio + Renfro, Figure 2.34 and 2.35 also delivers an expression with ornamentation while acting as a functional element to the building.



Top: Figure 2.34. Ornamented brick texture and chamfering, Front elevation; 290 Mulberry, New York by SHoP Architects (Zimmerman, 2015)

Bottom: Figure 2.35. A unit of brick on concrete non-load bearing facade panel; 290 Mulberry, New York by SHoP Architects (Basulto, 2008)

## 2.3 COMPUTATION: THE PROCESS

Optimisation is a method that deals with finding the extremes of numbers (minima and maxima), functions or systems. The foundations of optimisation are traced back to the great ancient philosophers and mathematicians who defined the optimum over several basic factors viz., numbers, geometrical shapes, optics, physics, astronomy, the quality of human life and government, etc. This era dates back to the Pythagoras of Samos (569 BC to 475 BC) a Greek philosopher, with his noted developments in the fields of astronomy, mathematics and the theory of music (Kiranyaz, Ince, & Gabbouj, 2013).

In other terms, optimisation is a method to achieve the best possible result under a given set of conditions. In every sector of innovation and development in the discipline of architecture and engineering, the goals of an optimised decision making are to minimise or to maximise the desired benefit within a limited boundary. Currently with the advancement of technology, the method of optimisation has progressed well beyond the mathematical solving towards nature-inspired and artificial intelligence based algorithms.

According to Merriam-webster dictionary, Optimisation is defined as an 'act, process, or methodology of making something (such as a design, system, or decision) as fully perfect, functional, or effective as possible.'

### 2.3.1 Structural Optimisation

Optimisation related to the structures is aimed at finding the best material allocation and distribution within the domain of physical volume while satisfying the applied loading condition(s) in supporting and transmitting the load safely. This method of optimisation deals with one or more of the four elements that formulate the mathematical expression it: objective function (including fitness and constraint), design variables, state variable or the algorithm, and the resulting output. These four elements have been described in the section 2.2.2 in relation to the general expression of this optimisation method. The constraints by the manufacturing methods and its ultimate use should also be taken into consideration. (Victoria, Alonso, Ansola, & Marti, 2017)

### 2.3.2 General mathematical expression for structural optimisation

- **Objective function (f):** A function used to classify designs. For every possible design,  $f$  returns a number which indicates the goodness of the design. Usually we choose  $f$  such that a small value is better than a large one (a minimization problem). Frequently  $f$  measures weight, displacement in a given direction, effective stress or even cost of production.
- **Variable (x):** A function or vector that describes the design, and which can be changed during optimization.

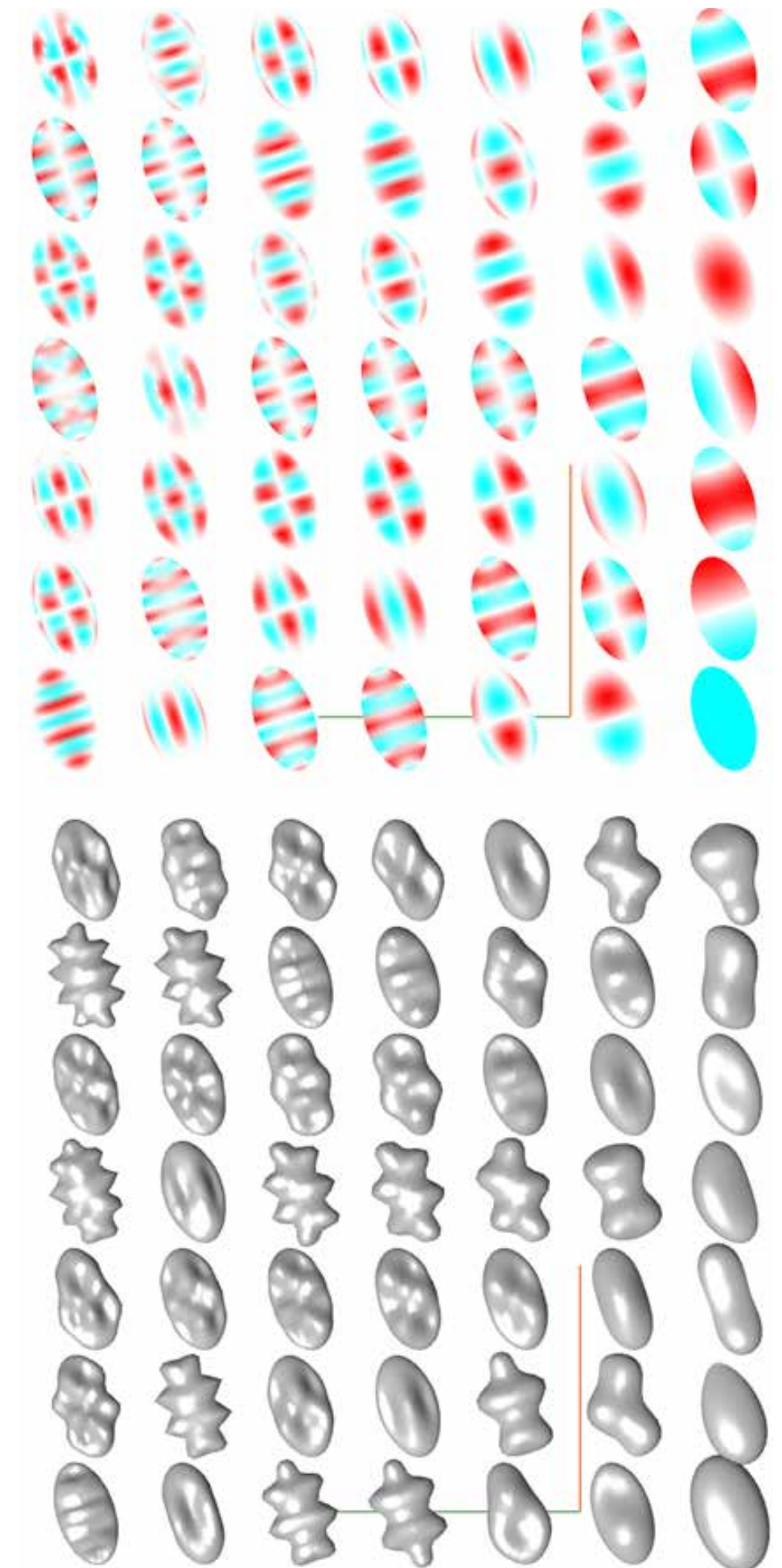


Figure 2.36. Alternate iterations of topology optimisation using Milipede plugin for grasshopper (Milipede, 2014).

It may represent geometry or choice of material. When it describes geometry, it may relate to a sophisticated interpolation of shape or it may simply be the area of a bar, or the thickness of a sheet.

• **State variable (y):** For a given structure, i.e., for a given design  $x$ ,  $y$  is a function or vector that represents the response of the structure. For a mechanical structure, response means displacement, stress, strain or force.

A general structural optimization problem takes the form (Slobbe, 2015):

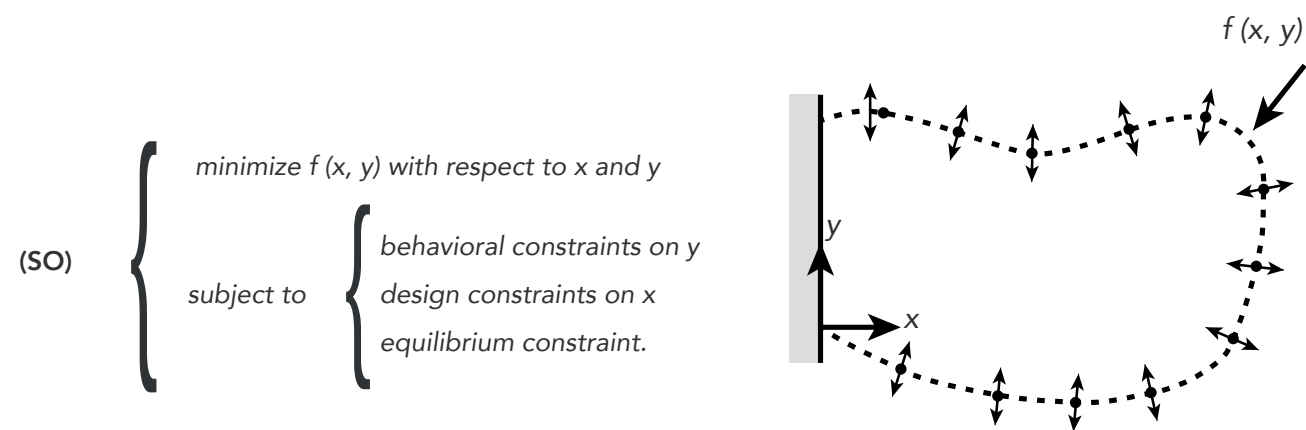


Figure 2.37. Structural design domain with the boundary represented as either an equation  $f(x,y)$  or as control points which can move perpendicularly (or otherwise) to the boundary. (Querin et al., 2017)

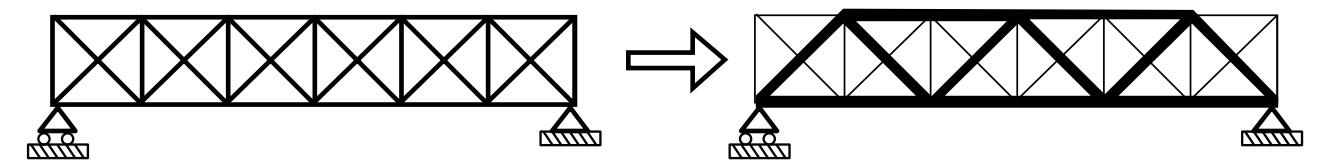
It is imagined as a problem with several objective functions, a so-called multiple criteria, or vector optimization problem:

$$\text{minimize } (f_1(x,y), f_2(x,y), \dots, f_l(x,y)),$$

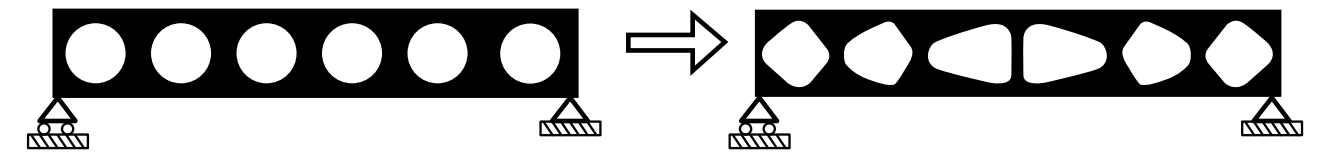
where  $l$  is the number of objective functions, and the constraints are the same as for (SO). This is not a standard optimization problem since all  $f_i$  in general are not minimized for the same  $x$  and  $y$ . Instead, it is recommended to achieve so-called Pareto optimality: a design is Pareto optimal if there does not exist any other design that satisfies all of the objectives better. (Slobbe, 2015)

### 2.3.3 Types of structural optimisation

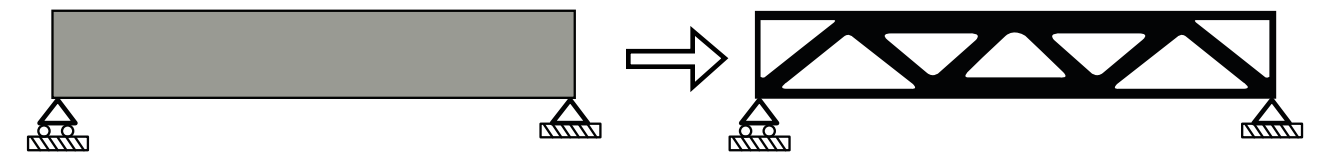
Structural optimisation is broadly divided into direct and indirect methods and categorised under three different methods of optimisation. These are: (1) size, (2) shape, and (3) topology optimization (Querin, Victoria, Alonso, Ansoala, & Marti, 2017; Beghini, Katz, Baker, & Paulino, 2014) with a fourth category considered to be multi-material optimisation.



Size optimisation



Shape optimisation



Topology optimisation

Figure 2.38. Comparative illustration of size, shape and topology optimization (Gebisa & Lemu, 2017).

• **Size optimisation:** This method of optimisation is usually used to determine the optimal cross-section area of elements of a beam in a frame or determining the optimal thickness of items in a plate, while the design criteria are satisfied.

• **Shape optimisation:** This method of optimisation is usually used to formulate an optimal solution by considering the shape of the initial material layout confined within a design domain and providing alternatives to the shape boundaries.

• **Topology optimisation:** TO is a mathematical method which may or may not be gradient based which aims at determining the allocation of material within a given domain of design based on the loading condition and boundary constraints of the given object. The alternate solutions can possess any shape, size or connectivity.

The complexity of the different types of known optimisation methods have been studied and simplified in a simple to understand flowchart shown in Figure 2.40 and Figure 2.41.

## 2.3.4 Topology Optimisation

Topology optimisation is one of the structural optimisation techniques that deals with optimizing the distribution or allocation of material confined within a given domain of design subjected to a loading condition and given boundary, while in concern with that of the criteria satisfaction of the given structure. Most of the topology optimisation methods do work in conjunction with that of a conceptual CAD design and Finite Element Analysis and considering one of the various different optimisation algorithms or in combination while contemplating the manufacture process and its constraints. The CAD model forms the base design to be considered as the design boundary in the optimisation program with given degrees of freedom while the FEA is to analyse the distribution of stresses of the elements in the structure.

Based on the nature of the design problem requirement and the end result, distinct optimization algorithm or combination of algorithms are considered remove material in the elements of the structure, which tend to be invalid in supporting any load for the given situation and / or add around the areas which are highly stressed (Gebisa & Lemu, 2017). Usually topology optimisation is solved using a gradient based mathematical programming but also by the non gradient method of heuristic methods involving genetic algorithms or in combination of both (Ahmed, Deb, & Bhattacharya, 2018).

The Topology optimisation generally follows the following workflow;

- Finds optimal distribution of material in a prescribed design domain given boundary conditions and external loads.
- Optimises the design of a structure by minimising an objective function and satisfying certain constraints.
- Discretization of the design domain by finite elements.

A schematic diagram of the work-flow has been shown in the *Figure 2.39*.

## 2.3.5 Methods of Topology Optimisation

**1. Homogenization Method:** The topology optimisation using homogenization involves a method of solving a batch of shape optimization problem where the topology of the shape is derived from infinite number of micro-scale voids which produce a porous like structure. The process of optimization then determines the optimum (global optima) for the geometry parameters of the voids that are determined to be the variables of the design. The regions of the geometry that carry only the voids, it corresponds to no material placed in that region which can be considered to be a cavity of that region. Contrarily, if the region of the geometry does not consist of any porosity, then it is considered to be a solid material. Because the topology optimization

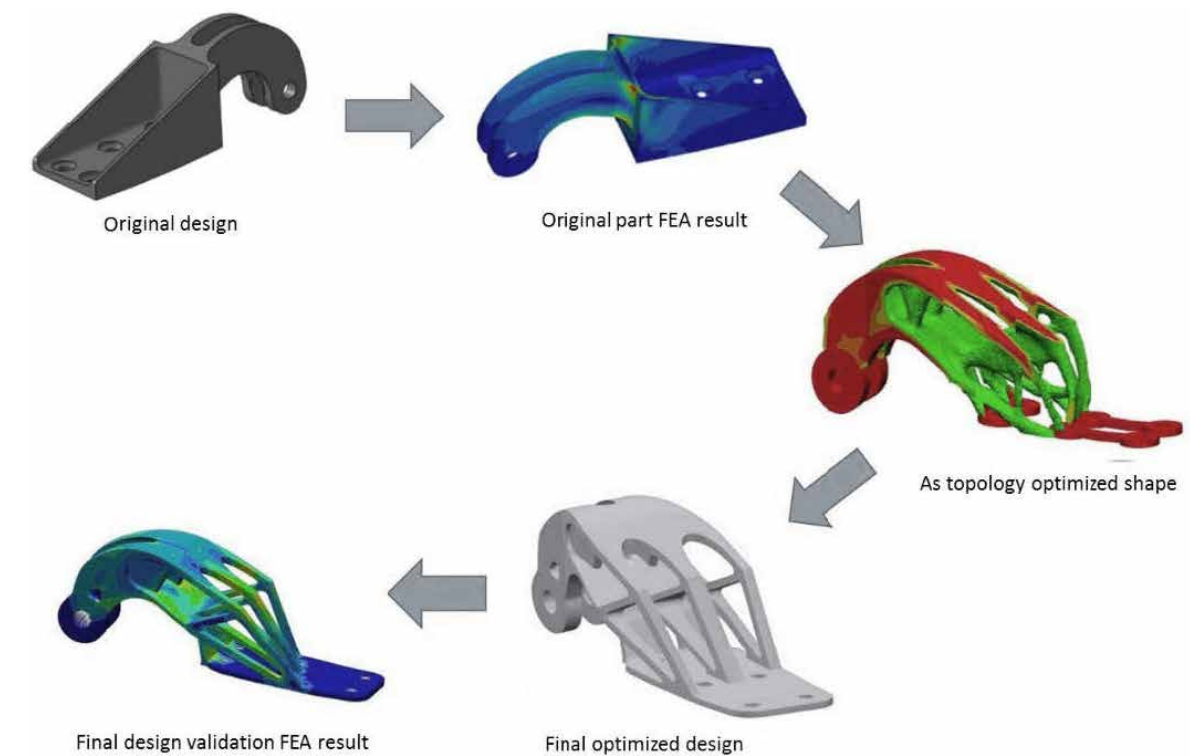


Figure 2.39. Topology optimization workflow (Gebisa & Lemu, 2017).

methods are simulated to continuous design domains, the effectiveness of the design or structure needs to be verified effectively using Finite Element Analysis. (Victoria, Alonso, Ansola, & Marti, 2017)

**2. MMA:** The Method of Moving Asymptotes is a method of non linear programming in structural optimisation characterized by an iterative process where a newly strict convex s-b=problem is generated and solved per each iteration. It is based on an approximation of convex sub-problem that is generated and solved. The moving asymptotes are the controller for the generation of the sub-problems. These sub-problems are responsible for the stabilization and acceleration of the process.

**3. Solid Isotropic Material with Penalization (SIMP):** SIMP is based on the principle of Finite Element Analysis and is one of the most efficient and commonly used methods of structural optimisation in the industry. The SIMP method was a optimisation method developed from culmination the Homogenization method. In this method a pseudo density represented by shades of grey is allocated to each pixel or cell of the finite element mesh. This principle idea is called the ersatz material approach. The pseudo density is visualised a value between 0 and 1 ranging from black to white with intermediate shades of grey. The factor of penalization is then implied to the method which derives solutions rounding off to 0 and 1 material distribution. This method is capable of solving optimisation problems that usually comprise of thousands of different design variables. (Bendsoe & Sigmund, 2003)

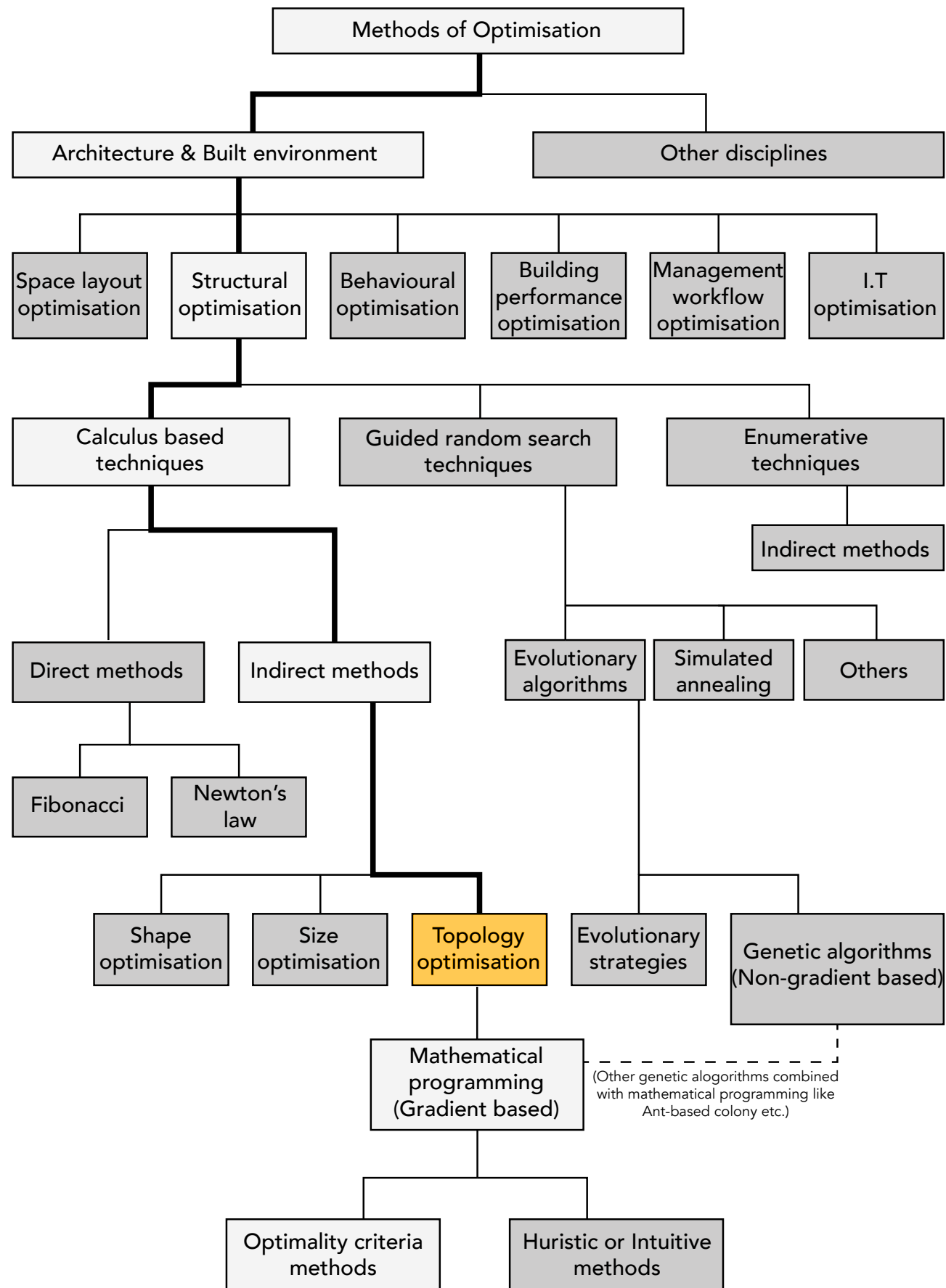


Figure 2.40. Family tree diagram of different types of optimisation methods (author; modified from Querin, et al., 2017; Chen & Chiou, 2013; Peña, 2006).

**4. Fully Stressed Design (FSD):** The fully stressed Design method for optimisation combines two methods viz. size and topology. This method is applied to structures which are subjected to constraints of stress and minimum gauge. The optimisation criteria of this method processes the material to be removed from regions of the structure which are not stressed out completely, unless it is overruled by the constraint of minimum gauge. This also considers the assumption that by addition or subtraction of material it only modifies their stresses without affecting or with insignificant effect on the rest of the structure (Victoria et al.,2017).

**5. Computer-Aided Shape Optimization (CAO):** CAO method of optimisation is inspired by the process of biological growth. The simulation process for this method takes place by inflating regions of the structure in correspondence to their stress allocation. The method of inflation corresponds to the addition of material in the structure while the deflation process is related to that of subtraction of material from the structure. The inflation in the structure is achieved by finite element analysis which uses the pseudo-thermal stress distribution method. (Design Considerations for a Precast Prestressed Apartment Building, 1975; Horsley, 2001) This is an iterative process that analyzes and modifies the structure (Victoria et al.,2017).

**6. Soft Kill Option (SKO):** This optimisation method is also inspired by nature as it removes inefficient materials and computes an optimal topology design which is very similar to that of nature's method. This is not a conventional method of optimisation as it simulates the method of adaptive bone mineralisation. This is done by differing the elastic modulus of the pixels or cells of the structure in correspondence to their stress distribution which is subjected to a loading condition (Victoria et al.,2017).

**7. Evolutionary Structural Optimization (ESO):** This is a hard-kill optimisation method according to (Christensen & Klarbring, 2009). This method follows the gradual omission of low stress elements of the structure

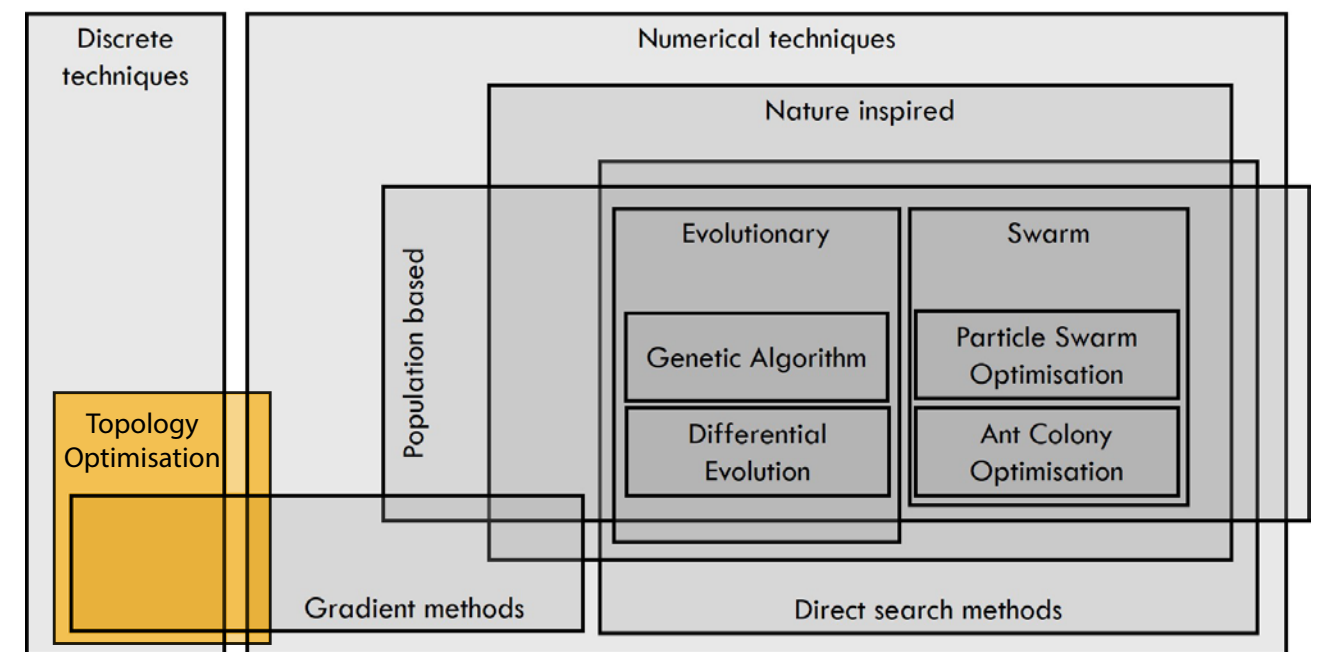


Figure 2.41. Relation of algorithms to other optimisation techniques (Slobbe, 2015).

that eventually leads to an optimised design solution. This method is formulated on the basic ideology of how a designer removes excessive materials from a design. The disadvantage of ESO is its immanent unidirectional approach. This kind of method is suggested to be used limited to optimisation method that intend an end result based on unidirectional approach (Victoria et al.,2017).

**8. Bidirectional ESO (BESO):** This method of optimisation is very similar to that of ESO with an exception of elimination the shortcoming of the later. ESO follows a unidirectional optimisation method which means that once the material is eliminated from the structure, it cannot be re introduced back into the design. To address this issue, BESO reintroduces material and allows it to be added back into the design domain. Around the elements which are highly stressed, the addition of material to the design is introduced. This method of addition of material makes it bidirectional and capable of generating higher number of iterations than that of ESO (Victoria et al.,2017).

In trend with modern manufacturing methods like Additive Manufacturing and in demand to retain the efficiency of traditional batch production process, the following methods of topology optimisation were developed. These various methods take into consideration the constraints of the manufacturing methods to evaluate the best possible effective iteration of the optimisation process.

**9. Overhang-free topology optimization:** The additive manufacturing process holds back at regions where the overhang of the material is too steep and would demand the need of additional support members. This method tries to address this manufacturing issue by developing a overhang free topologically optimised design member. The overhang free term indicates that all the overhang angles of the optimised design are larger than the minimum self-supporting angle. This is done by post treatment and adding materials (Leary, Merli, Torti, Mazur, & Brandt , 2014) to the topologically optimised design and eliminate the overhang criteria. by this there is a compromise to the process of optimisation but acceptable by the manufacturing aspect. (Liu, et al., 2018)

**10. Multi-material topology optimization and Nonlinear (multi-material) topology optimization:** These methods are based on Level Set optimisation framework. Advancing the level set method (LSM) proposed the 'colour' level set method (CLSM) (Wang, Chen, Wang, & Mei, 2005; Wang & Wang, 2004). This has allowed for multi-material based topology optimization. In the CLSM, the different materials are indexed separately by using varied sign combinations of n level set functions. This method is used to topologically optimise a design to be compatible for the Additive Manufacturing process. The complexity and unpredictable failures due to the layering in the AM process, non linear optimisation approach proves to be promising as per (Liu, et al., 2018).

Mesh distortions are another reason for the unpredictable failure of AM process. The low density elements deform unduly and are responsible for this issue. Mesh deformation is the main drawback of topology optimisation with geometric linearity. Addressing the issue of mesh deformation with the non linear multi

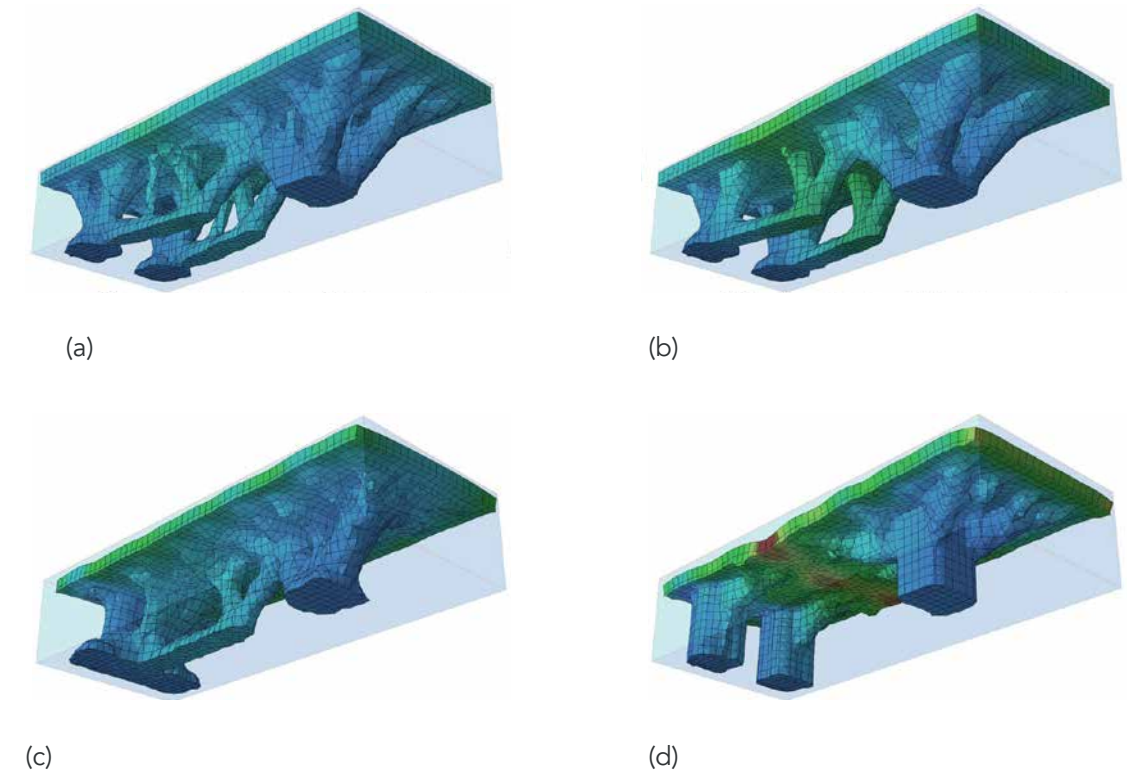


Figure 2.42. Topology optimization with fabrication constraints for different processes: (a) no fabrication constraints (for reference); (b) 3D printing; (c) casting and demoulding; (d) three-axis milling. Unlike the other case studies, 3D-printing constraints have a minor impact on the reference topology (Jipa et al., 2016).

material topology optimisation by various different methods, one of them being internal nodal forces exclusion scheme by Buhl et al. (2000) and Pedersen et al. (2001) ,etc resulted in much improved results that that of the linear optimisation and reliable performance under large deformations as shown in figure 2.42. (Liu, et al., 2018).

### 2.3.6 Comparison of different algorithms and inferences

The different algorithms that use different solving method than other, reproduces different result based on its no. of iteration, time consumed, errors solved, checkerboard corrections, efficiency etc. Based on the comparison of different algorithms stated by (Slobbe, 2015) in the Table 2.3 opens up an insight to decide the best effective method of topology optimisation feasible for this project .

- Gradient based methods (GBM) are much faster in comparison to other algorithms. Stochastic methods are very slow in finding the global optima until all the possible options are analysed as compared to other algorithms even though the method is robust in comparison (Chen & Chiou, 2013; Slobbe, 2015).
- The ability of GBM to identify checker-board effect and calculate possibility of manufacturing depending on the production method (Dominguez, Claver, & Sebastian, 2017).

- Genetic Algorithms (GA) use a huge population and do demand a high cost parallel computing to reach the global optima. (Slobbe, 2015) Usually is it very difficult to determine when to end the search. This does count for the complexity, time consumption, necessity of high computing power and cost (Chapman, Saitou, & Jakiela, 1994).
- The use of GBM for commercial structural analysis and optimisation because of its very high reliability. GA are usually unpredictable in comparison to other algorithms and hence possess a very low reliability for commercial applications (Chen & Chiou, 2013).
- GBM are although based on complex calculation and parameters than GA, are easy to use depending on the user interface of the software. This does exclude the modification of binary programming (Choi et al., 2015; Dominguez, Claver, & Sebastian, 2017; Choi, Kim, & Park, 2016).
- GA costs more than GBM even then both have a comparable achievement of pareto curve (Zingg, Nemeč, & Pulliam, 2008).
- GA and GBM can run in parallel to each other eliminating the disadvantages of each other but may require much higher computing power and hence cost. (Wang, Wang, & Tai, 2005)

Algorithms	Primary Type	Solution Space	Population based	Stability	Efficiency	Reliability
Brute Force	Stochastic	Discontinuous	No	Very robust	$n < 10$	Low
Simulated Annealing	Stochastic	Discontinuous	No	Very robust	$n < 10$	Low
Cyclic coordinate search	Direct search	Continuous	No	Local optima	$10 < n < 50$	Medium
Nelder-Mead simplex method	Direct search	Continuous	No	Local optima	$10 < n < 50$	Medium
Genetic Algorithm	Nature inspired	Discontinuous	Yes	Robust	$50 < n < 500$	Low
Particle Swarm Optimisation	Nature inspired	Discontinuous	Yes	Robust	$50 < n < 500$	Low
Ant Colony Optimisation	Nature inspired	Discontinuous	Yes	Robust	$50 < n < 500$	Low
First order methods	Gradient based	Continuous	No	Not robust	$n > 1000$	Very high
Second order methods	Gradient based	Continuous	No	Not robust	$n > 1000$	Very high

Table 2.3. Comparison of different optimisation algorithms, modified by Author from (Slobbe, 2015).

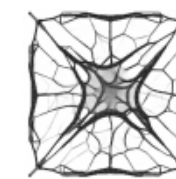
## 2.3.7 Computer solvers for Topology Optimisation



**1. Altair Optistruct:** This software is widely used in industrial application and analysis of state-of-the-art structural analysis solver which relies on the linear and no linear methods of optimisation under both the static and dynamic loading conditions. The Optistruct software is based on the density method of optimisation process or the SIMP method. This software analyses material density depending on the allocated value of either 0 or 1 corresponding to either void or solid. Optistruct allows for Topology concept alternatives and design and free-size optimisation for desired end results. It also incorporates constraints for manufacturing the optimised structure viz. member size control, draw direction control, extrusion constraints etc. Optistruct is limited to 30 iteration sample to find the best possible solution. (Altair OptiStruct™ Overview; Practical aspects of structural optimisation- A study guide, 2018)



**2. Millipede:** Millipede is a grasshopper component that analyses different structural designs and provides an optimised solution. The scripting of this component is a library based on very fast structural analysis algorithms for linear elastic systems. The library consists of proprietary topology optimisation algorithms. This plugin could also be coupled with Galapagos for form finding processes because of its high speed solving capability. (Millipede, 2014)



**3. tOpos:** tOpos is a 3D Topology Optimisation plugin which is using GPU for computation acceleration. It is based on CUDA technology provided by NVIDIA. Generally speaking, tOpos is based on SIMP methodology. As a BLAS solver, iterative Conjugate Gradient Method is applied. User has choice to use MatrixFree or Pre-assembled version of solver. tOpos claims to be almost 100X faster than competitive TO plugins for Grasshopper (Archiseb, 2018).



**4. Ameba:** Ameba is a topology optimization tool based on the BESO method, which provides optimization for 2D and 3D geometrical models. Users may, according to design requirements, apply different loading and boundary conditions to the initial design domain. During the computational process by the software, the design domain will evolve into various shapes, and eventually reach an organic form that is structurally efficient. (Ameba, 2018)

## Top3d

**5. Top3d:** This software is based on a 169-line MATLAB program that includes efficient approach for three-dimensional topology optimization. It is an updated MATLAB program of the '99-line program' by Sigmund (2001) and the 177-line program by Zhou and Wang (as cited in Liu & Tovar, 2014). This software is based on density method where the distribution of the material is parametrized by the density factor of the material distribution and follows the SIMP approach.



**6. Simulia Abaqus by Dessault systems:** This is a proprietary SIMP based topology optimisation algorithm used commercially for structural analysis. Abaqus Unified FEA is helpful in consolidated analysis of the processes and tools while reducing costs and inefficiencies. This program can be used to apply manufacturing constraints imposed by the specific methods with elimination of undercuts, minimum size for structural integrity of material, unconsolidated void, etc. (Jipa, Bernhard, Meibodi, & Dillenburger, 2016; Simulia, 2018).



**7. Autodesk Fusion 360 / Nastran in-CAD:** Autodesk Nastran is a general-purpose finite element analysis (FEA) solver and this topology optimization technology is currently incorporated with Autodesk Nastran stand-alone, Fusion 360 software, and Inventor Simulation software. This is based on the SIMP method of topology optimisation and allows restrictions and consideration for various different manufacturing process and processing the design for production. It has some advanced features that empower designers to create better designs and modify existing ones, making them lighter and more efficient.

Some other known topology optimisation software are Topostruct, ToOptix etc with an updated list of other software found on the website <http://www.topology-opt.com/software-list/>

Studies based on different commercially and open source available softwares are done by (Choi et al., 2015; Dominguez, Claver, & Sebastian, 2017; Choi, Kim, & Park, 2016; Jipa et al., 2016). Based on their conclusions and outcomes, millipede serves to be a best and reliable option to use for topology optimisation with additive manufacturing constraint (Dominguez, Claver, & Sebastian, 2017), Optistruct for highly reliable and faster than others (Choi et al., 2015; Choi, Kim, & Park, 2016) and Simulia Abaqus to be proven for its high reliability in simplifying the optimised result to comply with complex production methods and casting process (Jipa et al., 2016).

All logos are trademark copyrighted by the respective companies.

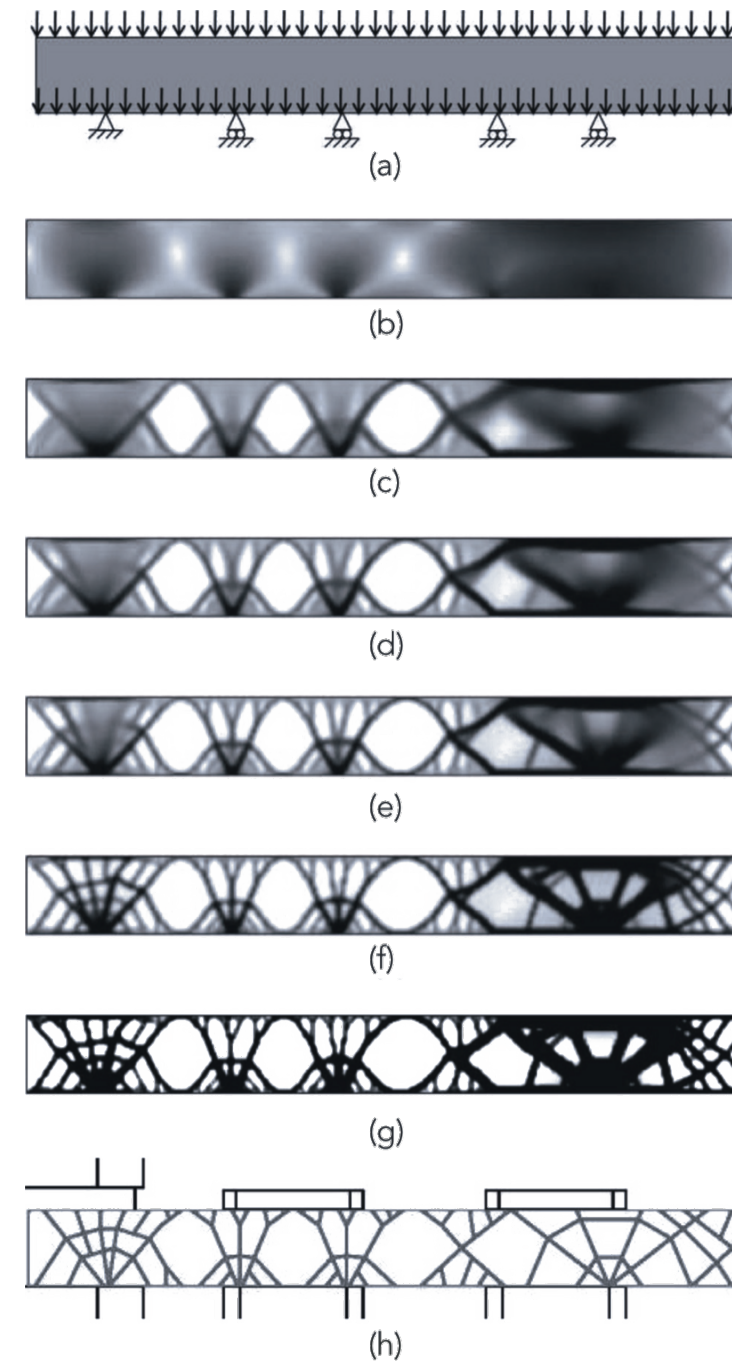


Figure 2.43. Topology optimization for design of the upper "beam" spanning several towers for the Zendai competition: Iteration (a) 0, (b) 1, (c) 10, (d) 15, (e) 20, (f) 40, (g) 100 (final design). (h) Resulting engineering interpretation. (Jipa et al., 2016)

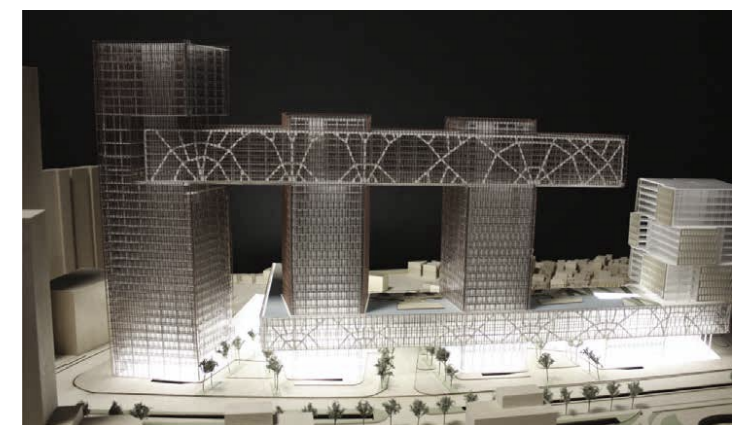


Figure 2.44. Picture of the physical model for the concept design of the Zendai competition using topology optimization results. (Jipa et al., 2016)

### 2.3.8 Ornamentation through Optimisation

Ornamenting has been around with architecture since ages with inscriptions on caves, stucco art, stone carvings, glass stains to the modern expressions with concrete and other modern materials. Ornament is a medium of language that establishes a communication between the architecture and the broader public. Concrete as a material is comfortable to be moulded into any desired shape and ornamentation complying with the expected outcome. Ornamentation as per English lexicons are defined as 'decorative elements added to something to enhance its appearance'. This can be true and specific to particular situations but can also be applied to the expressions derived by subtracting elements to enhance its appearance.

"Topology optimization allows us to really explore our creativity. Traditional methods of structural engineering are mostly associated with buildings that look like boxes. With topology optimization, we can address unique designs—for example green buildings and organic designs such as buildings that might be bio-inspired by an animal shape—and functionality" (Paulino, Topology optimization connects architecture and engineering, 2013). A concrete slab optimised using topology method by ETH Zurich delivers a unique expression to a regular structural element and depicts the possibilities of modern tool in expressing ornamentation, Figure 2.45. As another example the structure of the spanning beam for the Zendai competition was developed by topology optimisation, Figure 2.43. and 2.44.

As in the stone age, the mark of chisel carving delivered an expression of construction technology of that era, the method of construction of ornamentation through optimisation, develops a language of architecture celebrating technology of the current.

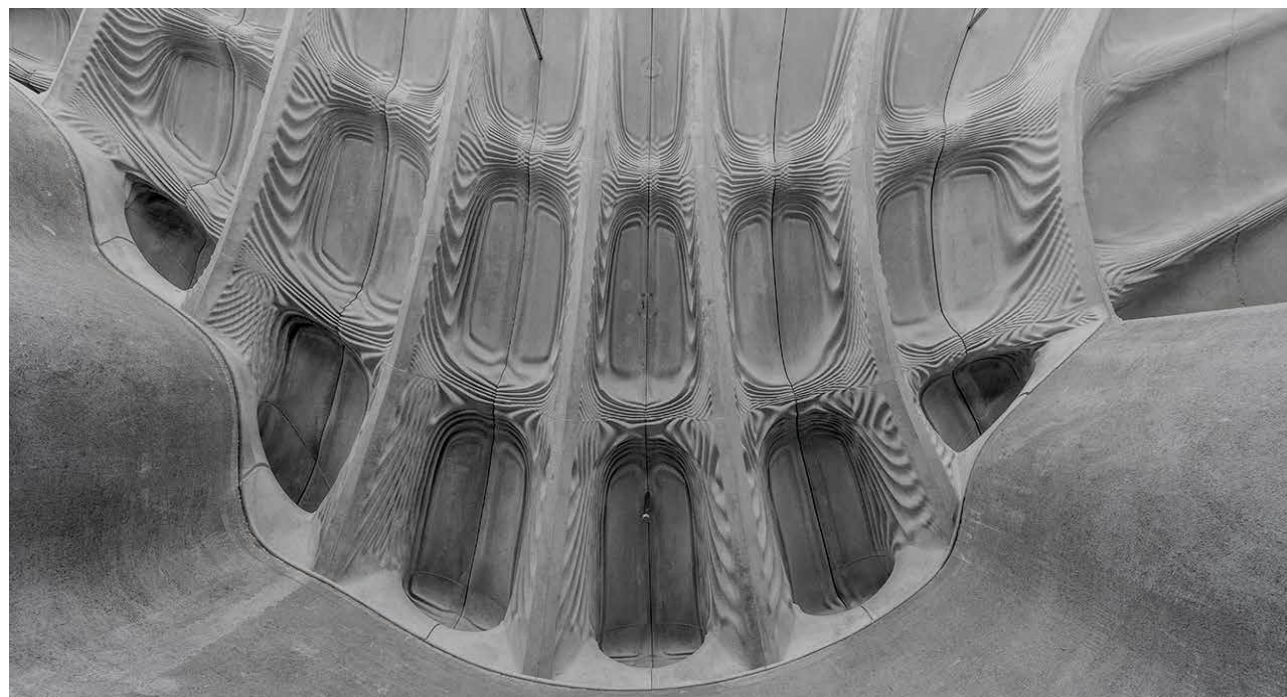


Figure 2.45. Smart Slab, ETH Zurich (Lyrenmann, 2018)

## 2.4. FABRICATION: THE TARGET

The liquidity and easy mouldability of concrete makes it favourable across a wide range of manufacture possibilities. While form work casting of concrete is the widely used method, the new and advanced digital tools and their ability to achieve design complexities does open up possibilities for new fabrication method or combination of traditional and digital fabrication methods. The fabrication methods that are feasible in the scope of this project and concrete (UHP-GFRC) as the material are described and analysed below.

### 2.4.1 Types of fabrication methods suitable for concrete

In the present scenario there are multiple fabrication methods that would comply for the fabrication of the concrete. The tradeoff between the benefits and the drawbacks between these various methods alone could alone be a criteria for selection. Along with the comparative analysis of these production method, the aspect of sustainable method of manufacturing, in the sense of low embodied energy, waste of material and reusability of the moulds need to be prioritised over other factors. Some of these compatible fabrication methods for the concrete along with their purpose, examples and their features are explained herewith.



Figure 2.46. Casting of UHPFRC into the binder jet 3D printed formwork, ETH Zurich (Jipa et al., 2016).

**1. Additive manufacturing (Material extrusion)**

Additive manufacturing is the process of fabricating a three dimensional object by fusing multiple layers . It was initially referred to as rapid prototyping and most commonly known as 3D printing. Additive manufacturing method can be used in seven different types Vat photo-polymerisation, Material Extrusion, Material Jetting, Binder Jetting, Powder bed fusion, Direct energy deposition and Sheet lamination (engineeringproductdesign, 2018).

Concrete as a material is used with material extrusion AM process which basically uses temperature or pressure (in case of concrete) to deposit layer over layer which may or may not need additional support depending on the support angle (the 45 ° rule) of the material and design.



Figure 2.47. Test 3D printing of a segment for a bridge, Project Milestone by TU/e (Mlot, 2018).

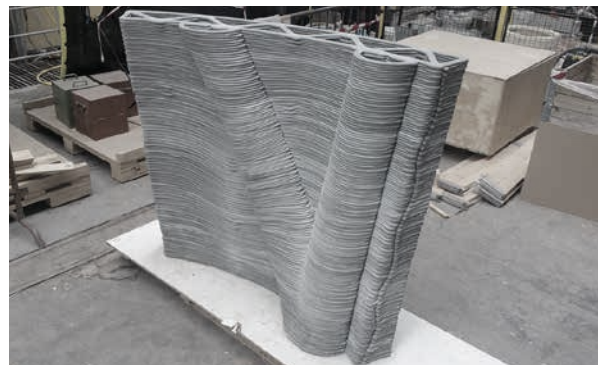


Figure 2.48. Large scale 3D printed concrete wall by XtreeE (Gaudilliere, 2015)

Benefits	Drawbacks
Complex shape can be achieved	Layering effect with visible layer lines
Zero investment on form work	Low resolution finish and low level of detailing
Reduced waste	Unavailability of tools
Versatile with wide range of materials	High initial tooling cost
	Slow production rate
	Unpredictable and high rate of failures along printed z-axis
	Effective mostly for compression loaded structures
	Interlaced support structures
	Limitation of print size

Table 2.4. Benefits and drawbacks of material extrusion- additive manufacturing production method (Author).

**2. CNC Milling and casting**

Computer Numerical Controlled (CNC) milling is a commonly used computer controlled method of subtractive machining and could be use to develop moulds that can be used for casting concrete. Usually the moulds are made in two or more halves (preferably without undercuts) to perform easy removal of the cast material. The facade panels for the Broad museum was made by CNC milling the mould of high density foam and casting with GFRC (WillisConstruction, 2015), Figure 2.49.

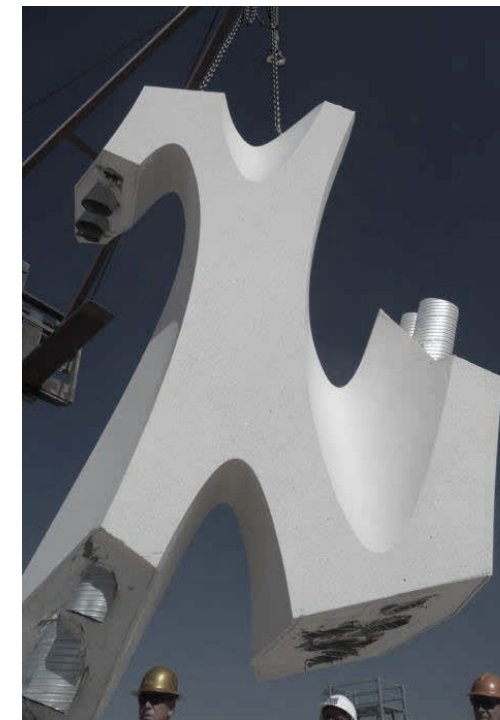


Figure 2.49. Prefabricated GFRC facade panel unit used in Broad Museum, Los Angles by Diller Scofidio + Renfro (NYA, 2015)

Benefits	Drawbacks
High level of detail	Cant handle undercuts
Superior finish	Hard to remove mould for complex shapes
Low cost tooling	Limitation of print size
Faster production rate	
Feasible for batch production	
Compatible with wide range of material	
Familiarity and global availability	

Table 2.5. Benefits and drawbacks of CNC milling and casting production method (Author).

### 3. Vaccumatic form work

Based on the principles of V-process sand casting method, this process uses vacuum stabilization of sand to generate free-form structures in concrete. This process is based on reverse engineering technique in which the final form is made by additive manufacturing methods or CNC milling and sand is vacuum compacted over to form the mould. The concrete is then poured into the reusable sand mould. This process has been used by abt to cast complex shaped concrete panels at the International Association for Shell and Spatial Structures (IASS) (Magan, 2016), Figure 2.50.

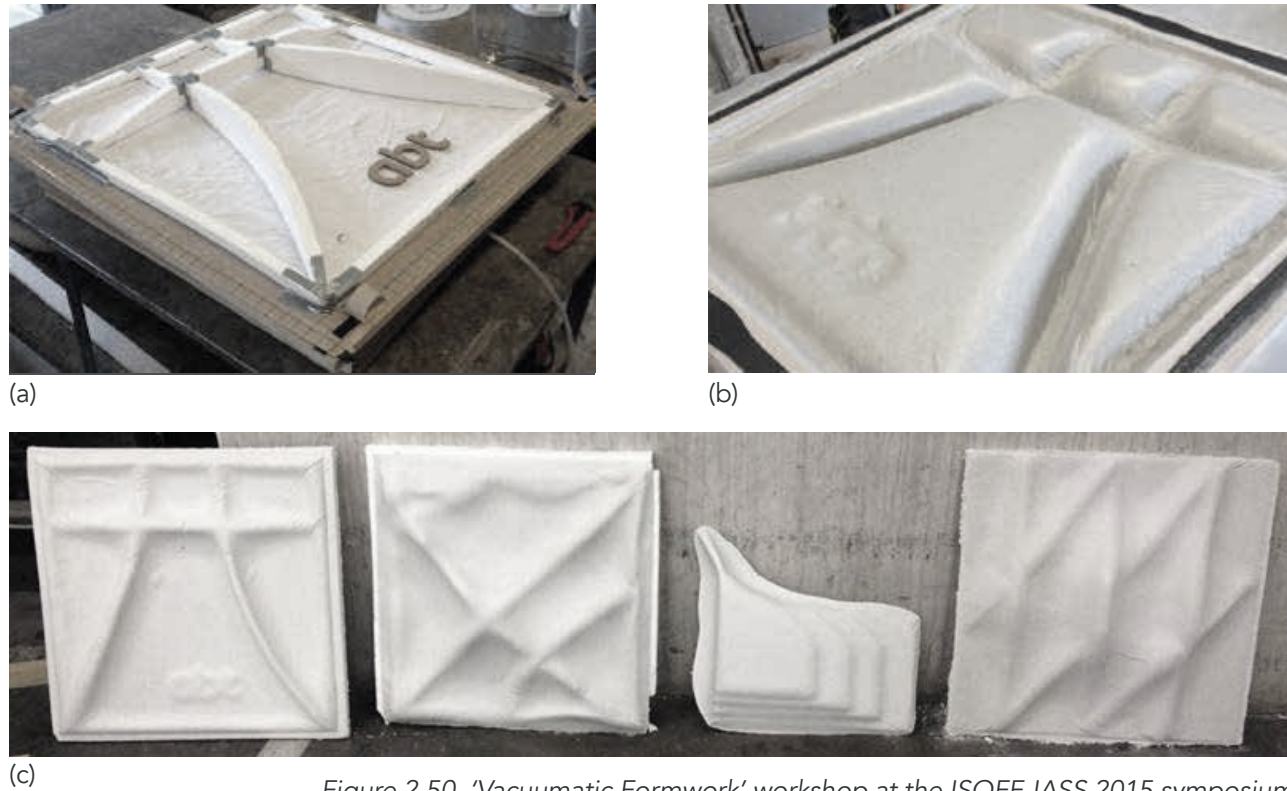


Figure 2.50. 'Vaccumatic Formwork' workshop at the ISOFF-IASS 2015 symposium (a)Base formwork (b) Vaccumised mould (c) Final concrete casting (Magan, 2016).

Benefits	Drawbacks
High level of detail	Multiple stages incurred
Superior finish	Cant handle undercuts
Low cost tooling	Hard to remove mould for complex shapes
Faster production rate	Only possible for single sided shape casting
Feasible for batch production	Wastage produced by primary formwork for pattern
Compatible with wide range of material	Non-recyclable
Familiarity and global availability	
Suitable for prototyping	

Table 2.6. Benefits and drawbacks of vaccumatic formwork production method (Author).

### 4. Wax moulding and casting

With recent development 3D printing, casting or CNC milling wax has been effective in producing complex structure to support the casting of concrete. This methods used a wax mould to cast concrete and later be dissolved saving on form work material. This process has been applied by Crossrail in its station that used 36,000 concrete panels and 1400 unique moulds, Figure 2.51. The method of 3D printing wax moulds manufactured by an Australian company FreeFab did decrease the casting time from 16 hours to 2.5 hours compare to plywood mould by eliminating the tooling paste (ianVisits, 2017).

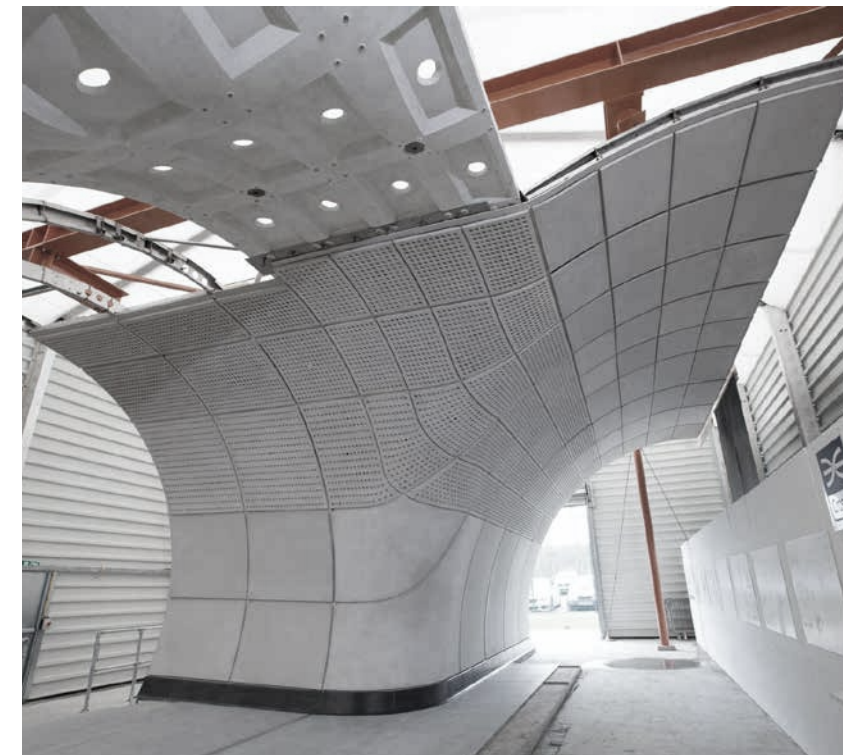


Figure 2.51. Cast GFRC panels with wax moulds by Crossrail (ianVisits, 2017)

Benefits	Drawbacks
High level of detail	High cost tooling
Superior finish	Limited resource availability
Can handle undercuts	Undercuts may need to break the mould
Faster production rate	
Feasible for batch production	
Compatible with wide range of material	
Recyclable	

Table 2.7. Benefits and drawbacks of wax molding and casting production method (Author).

### 5. Binder jetting and casting

The process of binder jetting is a type of Additive Manufacturing methods which incorporates two different material bonded together. First is a powder material that forms the mass of the print and a binding liquid that is selectively deposited to join the layers of powder together.

This method of AM differs from the other as it does not incur heat in printing. Compared to others this method is very expensive because of its slow speed and limited availability. 3D printed stay in place form work to cast concrete slabs by ETH Zurich used binder jetting to create moulds for the UHP-GFRC (Jipa et al., 2016), Figure 2.52.



Figure 2.52. Post processing of the fabricated concrete slab by binder jetting by ETH Zurich (Jipa et al., 2016).

Benefits	Drawbacks
Intricate and complex detailing	Very high cost tooling
Superior finish	Limited resource availability
Can handle undercuts and critical shapes	Undercuts may need to break the mould
Compatible with wide range of casting material	Faster production rate
Suitable for prototyping	Waste of moulding material
Can be used as stay in place formwork	No need of release agent
Recyclable	

Table 2.8. Benefits and drawbacks of binder jetting and casting production method (Author).

### 6. Investment casting

Investment casting is a very old method used to cast metal. It is a multifold production method which incorporates 3 steps of casting. At first the actual shape to be casted in either printed or milled from wax or a suitable polymer. Secondly, this object is then coated by submerging into a refractory material slurry. After the hardening of the first coating occurs, the process is then repeated to form a hard coating thickness and strength. This composite mould is then heated to melt the wax or burn the polymer (with rapid heating method to eliminate cracks) to develop a hollow mould ready to cast in. Finally, the material (UHP-GFRC) is then poured (by the premixed method) into the mould and rest to set. After the material is cure the mould is removed by breaking the refractory mould (engineeringproductdesign, 2018).



Figure 2.53. Production steps from MDF mould to final glass model (Bristogianni, Oikonomopoulou, Veer, Snijder, & Nijse, 2017).

Benefits	Drawbacks
Intricate and complex detailing	Very high cost tooling
Superior finish	Limited resource availability
Can handle undercuts and critical shapes	Undercuts may need to break the mould
Compatible with wide range of casting material	Faster production rate
Suitable for prototyping	Waste of moulding material
Can be used as stay in place form work	No need of release agent
Recyclable	

Table 2.9. Comparative analysis of different production methods (Author)

## 2.4.2 Feasibility study between different production methods

Considering the different factors that are relevant to this project and concrete as the material and the known complex surface derived by the topology optimisation, the different methods of production are compared to various different factors and constraints that they possess in the Table 2.10. Depending on these factors and constraints the investment moulding method of production does seem to be feasible for prototyping a topologically optimised concrete facade panel.

	Material Extrusion	CNC milling and casting	Vaccumatic form work	Wax moulding and casting	Binder jetting and casting	Investment casting
Lateral load handling	NO	YES	YES	YES	YES	YES
Complex shape moulding	High	Low	Medium	High	Very High	Very High
Resolution and finish	Low	High	Medium	Very High	Very High	Very High
Undercuts and critical details	YES	NO	NO	YES	YES	YES
Production speed	Slow	Medium	Medium	High	Very slow	Medium
Batch production	NO	YES	YES	YES	NO	YES
Tooling cost	Medium	Low	Low	Very High	Very High	Medium
Resource availability	Scarce	Abundant	Abundant	Very Scarce	Scarce	Abundant
Prototype feasibility	YES	YES	YES	NO	YES	YES
Labour effort (set up and /or demoulding)	Low	Low	High	Medium	High	High
Release agent	NA	YES	YES	NO	YES	Depends on material
Waste	NO	YES	YES	NO	NO	YES
Recyclable	NO	NO	Depends on material	YES	YES	Depends on material

Table 2.10. Comparative analysis of different production methods (Author)

## 2.4.3 Casting of UHP-GFRC

The feeding process of GFRC to a mould is done by 2 basic methods for usually developing thin walled structures for flat facade panels, the sprayed method and the premixed method. The third method is a hybrid method.

In the sprayed method, the shredded glass fibres are mixed with the cement slurry in a specific proportion which are pre loaded onto a spray gun which in turn sprays a continuous spool under air pressure. This method is carried out periodically in alternating perpendicular direction to increase the bonding between layers and each layer is compressed with hard rollers to ensure the fibers embedded into the slurry, eliminate air pockets and maintain a consistent thickness. This method is feasible with surface casting for one face only and cannot be used for closed complex shapes.

While in the premixed method, the fibres are mixed with the cement slurry only during the mixing process. The mixed slurry is then poured into a mould and set using vibrating floor plates to eliminate air pockets. The lack of pressure in this method usually tends to make this method low on the mechanical properties than compare to that of the sprayed method. (Henriksen, 2017; CCI, 2018)

In the hybrid method , a hopper gun is used to spray the face coating and a poured backer mix. A thin face of without the fibers is sprayed into the moulds and then the backer mix packed by hand is poured in. The cheap hopper gun and the method used in this process makes it economical in comparison to other methods. The creation of the face mix and baker mix with uniform consistency and layup is critical and needs attention (CCI, 2018).

	UNITS	SPRAYED GFRC	PREMIX GFRC	PREMIXED GF-UHPC
Density	kN/m <sup>3</sup>	19-21	19-21	24-25.5
Compression strength	MPa	50-80	40-60	170
Elasticity modulus	GPa	10-20	13-18	45
Impact strength	MPa	10-15	8-14	
Poission ratio		0.24	0.24	
Limit of proportionality(fy)	MPa	7-11	5-8	20(34 Mpa-steam cured)
Thermal expansion coefficient	10 <sup>-6</sup> /K	7-12	7-12	10-12
Moment of rupture(fu)	Mpa	21-31	10-14	23
Tensile strength	Mpa	8-11	4-7	11

Table 2.11. Relative performance of sprayed, premixed, and premixed UHP GFRC (modified by Author from Henriksen, 2017).

It is evident that the premixed UHP-GFRC performs better in terms of mechanical behaviour as compared to the spray up GFRC and premixed GFRC (Henriksen, 2017). This method is also preferable in consideration of casting complex closed moulds as the spray up is not feasible for the process.

The method used to fabricate the mould and the material that GFRC is cast on, decides the production cost and the feasibility of the casting process. Based on the feasibility material of the mould, Table 2.12 provides a comparative analysis (Henriksen, 2017).

MOULD TYPE	LABOUR INTENSITY	MATERIAL COST AND LABOUR COSTS *	MOULD PRODUCTION TIME	REUSABILITY **	COMMENTS
Wooden moulds (limited to single curved and large radii ( $r > 0.5\text{m}$ ) double curvature)	Medium	Material 25€/m <sup>2</sup> ; Labour 40€/h	2-4h/m <sup>2</sup>	1-20 times	Sometimes a structural calc. for a timber mould is also required (concrete-pressure and weight). This adds additional cost.
Rubber moulds	High	Material 80-200€/m <sup>2</sup>	3-5h	10-50 times	Must be applied to a timber mould. Limited sizes.
Polystyrene foam moulds, wire cut	Low	Material will be calc. in m <sup>3</sup> foam. approx. € 30,-/m <sup>3</sup>	1 h	5-30 times	Standard Polystyrene foam-block is 120x120x500cm, Significant waste
3D computer numerical controlled (CNC) milled moulds (Foam, Plastic)	Low	300-400€/m <sup>2</sup>	5-10 h	5-10 times	Made from foam or plastic, timber or metal. The quality of the mould depends of the quality of the foam or plastic. Limited sizes
Binder jet 3D printed (sand)	High	Approx 500€ - 210x210 x 5 cm	12 h (depends on complexity of geometry)	1 time	No waste

Table 2.12. Existing mould system to produce then walled GFRC (\*Prices are 2016 estimates, \*\*Depends on the mould geometry) (modified by Author from Henriksen, 2017)

## 2.4.4 Method of manufacturing or casting

Although there is a 7 step method proposed for the additive manufacturing, the following mentioned steps have been modified to mention the combination and relation between the above mentioned production methods and explained with the help of a diagram in Figure 2.54.

**Step 1 – 3D model creation:** Generation of a 3D model of the object to be printed is done using any CAD software or a 3D object scanner. This has to be a close polygon which or else may not be identified by some software for print processing.

**Step 2 – Export to a compatible file format:** CAD models can be converted to either .stl, .obj, .amf or .3mf format file to tessellate the 3D geometry and convert it into digital pixelling or layering for the manufacturing machine to process. While .3mf is the most advanced and promising format that carries a lot of information related to the model in comparison to other formats, .stl and .obj are the most commonly used file formats for additive or subtractive manufacturing.

**Step 3 – File transfer and m-code manipulation:** The formatted file is then directed to the custom software by the machine manufacturer or generic available software. The further modifications or tweekings if needed are done using the G-code of the file before it is sent to the machine to initiate the process.

**Step 4 – Machine set up:** Consumables or materials are then loaded onto the machine. The parameters to be considered by the manufacturing machine are then modified depending on the type of end product needed and the properties of the material to be printed.

**Step 5 – Build:** Printer builds the model by depositing / sintering material layer by layer or CNC mills it by subtracting from a block of material. This process is completely handled by the machine and need human intervention only in case of errors or failure.

**Step 6 – Part Removal:** The machined or printed part is then removed from the build platform and its support structure. This step needs manual attention and special considerations.

**Step 7 – Post processing:** Finally, post processing, such as cleaning, polishing, painting or applying of release agent might be required on to the product.

**Step 8 – Casting for mould:** The printed element is then covered with sand and compacted or coated multiple times with by submerging into a refractory material slurry until a thick layer of coating is formed. This is then set to settle until it gains strength.

**Step 9– Melting the filler:** The printed filler element used to cast the mould is then melted or burnt depending on the material used. This forms a hollow mould to cast the material in.

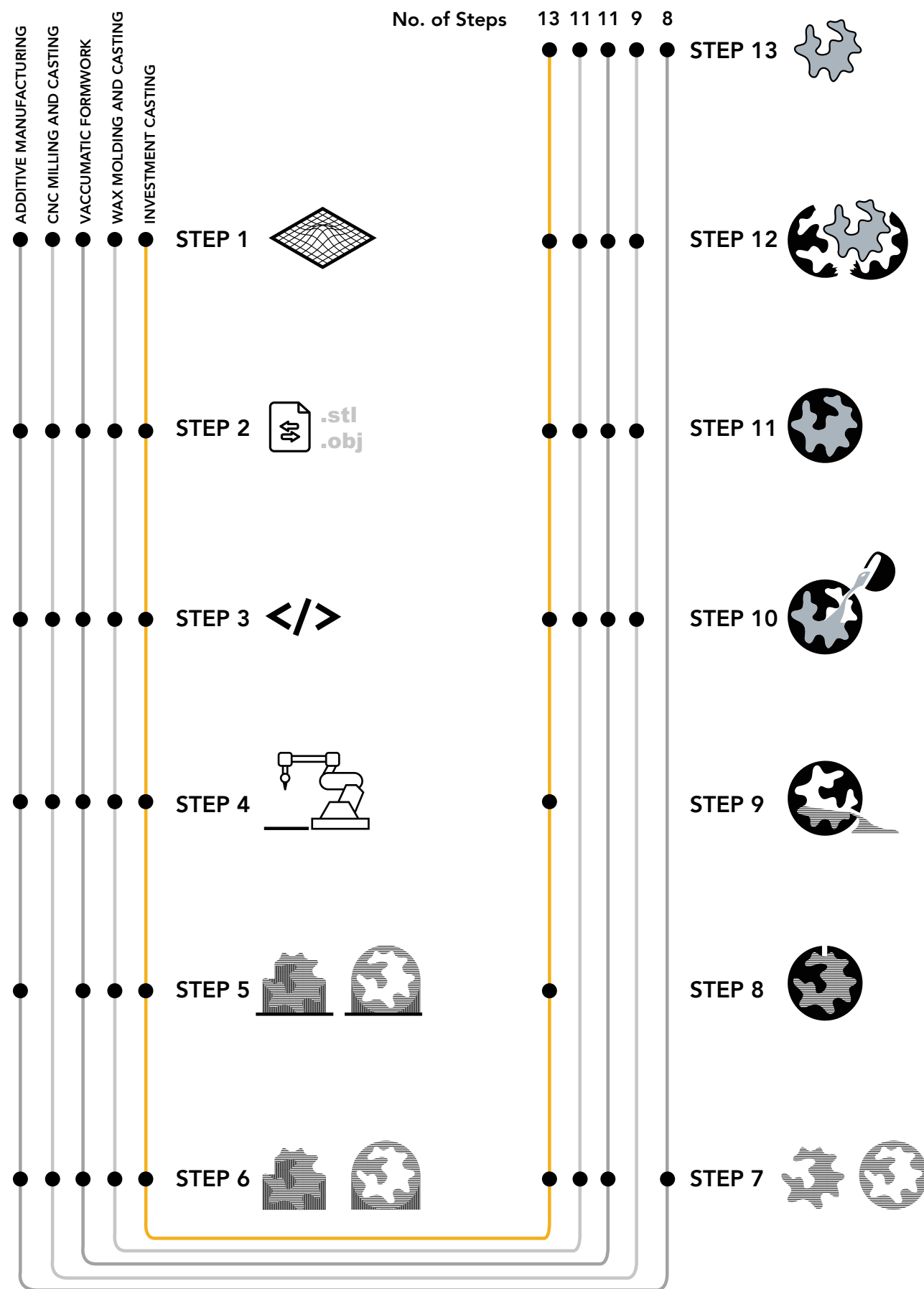


Figure 2.54. Diagram depicting different steps undertaken by various methods of fabrication (author).

**Step 10 – Casting and setting:** Pouring of material (UHP-GFRC) into the mould is done. Depending on the type of mould developed, the composition of material and speed of this process may vary. For materials like GFRC, constant vibration may be needed to eliminate air bubbles and flow of material to the complex junctions.

**Step 11- Curing:** The casted material needs attention of curing by water or heating for the next couples of minutes or hours (in case of GFRC) until the casted material gains its complete strength. This is a labour intensive process.

**Step 12- Demoulding, melting or breaking:** The removal of the mould is a very high labour intensive and time consuming process. Depending on the type of material and mould method used, the mould needs to be forcefully removed with care (in case of vacuumatic form work, or melt with high temperature (in case of wax moulding) or break the support material (in case of binder jetting) to release the final product out.

**Step 13- Final processing:** The final cleaning of material for extra material, lumping, support of damaged parts may be taken care in this process to generate the final designed element.

### 2.4.5 Considerations for fabrication of concrete facade panels

Concrete facade panels to be used on a building facade need to have a batch of repetitive patterns. In regard to the same, the optimised panels need to be fabricated in batch with a process that eliminates the need of molds viz. additive manufacturing or by making reusable moulds without the need of repetitive iteration in the manufacturing process. The low availability and familiarity of the manufacturing method may be considered unsuitable for producing these panels. The complexity of Topologically optimised panels may tend to consider the manufacturing methods that can produce undercuts with high levels of finish and resolution so as not to affect the optimised and designed structural topology. The recyclability of the moulds and producing minimum waste for the production of the facade panel or a prototype must be considered.

### 2.4.6 Behaviour and constraints of concrete (GFRC) fabrication

Concrete as a composite material is quite familiar in the building construction industry and has been familiar since centuries, but even then there are unexpected behaviours and eventually failures experienced in the recent times. Most of them may be primarily dealt with structural calculations and design criteria, but largely depends on how the material behaves independently. Construction of a concrete structure deals with the following mentioned behaviours classified by the stages of concrete construction and constraints related to them. (Friedbert et al, 2013)

**1. Mixture:** The composite material highly depends on the appropriate mixing ratio of its constituents and addition of fibres and admixtures for its improved performance. Deviation from this may result in unexpected behaviour in the later stage of the construction, viz its workability, compaction, curing and service life. The desired configuration of the concrete to be used in a project depends on the loading condition, architectural expression and other specific behaviour expected in the use type viz, size, thickness, water proofing, climate specific region, etc. The variations in the type of composition act as a design constraint depending on the delivered mechanical and climatic behaviour and also a constraint to the possible manufactured outcome of an architect's vision.

**2. Workability:** Fresh concrete is always used as a fluid material that needs to be taken into account of the versatility and complexities related to it. Normal concrete can act brittle in thin and tender section and may require only UHPC along with additives to satisfy the design considerations. The moulds for precasting or in-situ casting needs to take into consideration the behaviour of the specific composition used in the given condition to be able to withstand the critical elements of the design. The proper layout of the reinforcement with the needed design cover (may not be considered for FRC) and the temporary support systems are needed for the concrete to behave in the designed combination. The finish, behaviour and reaction of the moulding material with that of the concrete used also is a constraint specific to the type of manufacturing method.

**3. Compaction:** The fine setting of the material to deliver its designed properties is must. The fibre size, agility of the concrete composition, method of setting the designed formwork or mould, the shrinkage ratio, flow rate, lumping, etc., which also act as constraints to the design and manufacturing process should be taken into consideration.

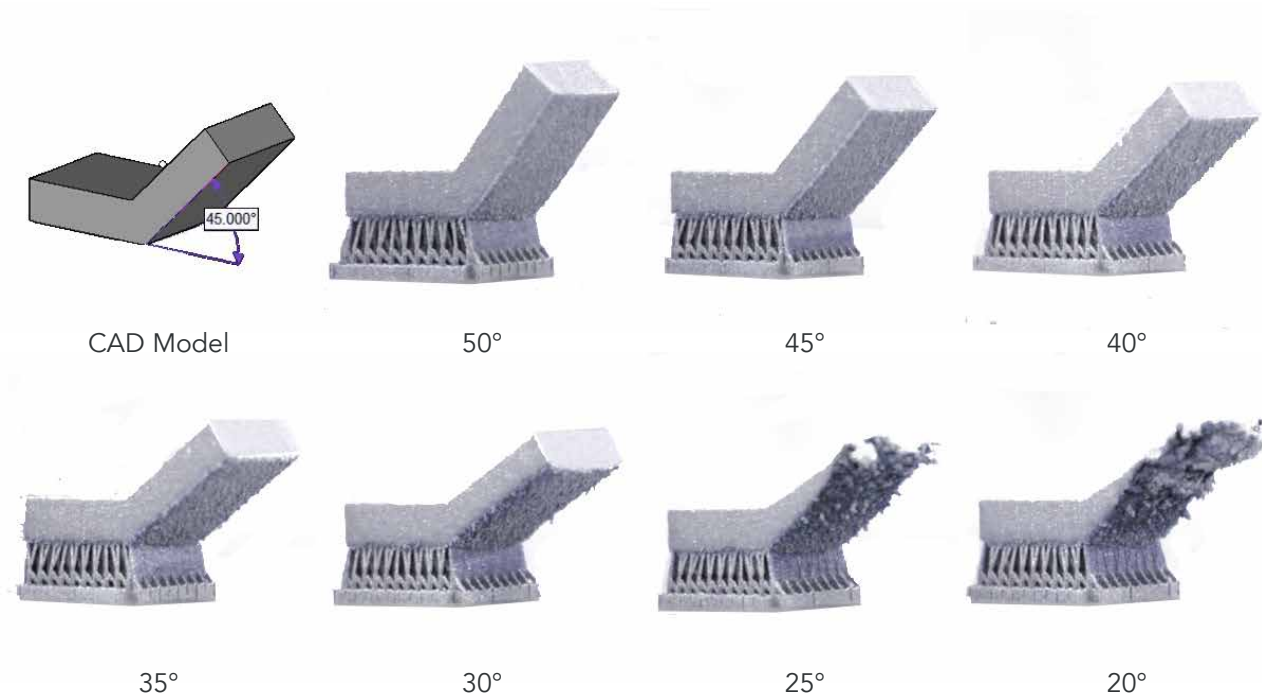


Figure 2.55. Overhang as a constraint to material extrusion printing method, experiment with metal 3D printing (Utley, 2017)

**4. Curing:** The final stage of the production is that of curing the material which is dependent on the final behaviour and expression after the specified time of curing for the composition of concrete. GFRP and special concrete with admixtures can be cured and handled within 24 hours whereas normal precast concrete can take weeks to attain strength. The over or under treatment during the curing process of the material may deter from the expected behaviour. Depending on the manufacturing process, demoulding and designing temporary support systems (in case of Additive manufacturing) of concrete is another constraint that needs to be considered while designing.

Along with the above mentioned constraints, there are some others that should be taken into consideration as well for fabrication with GFRP. They are material composition, agility of the mixture, cost, availability of resources, undercuts and voids, minimum size for structural integrity of material (0.20 mm for concrete), unconsolidated void, etc.

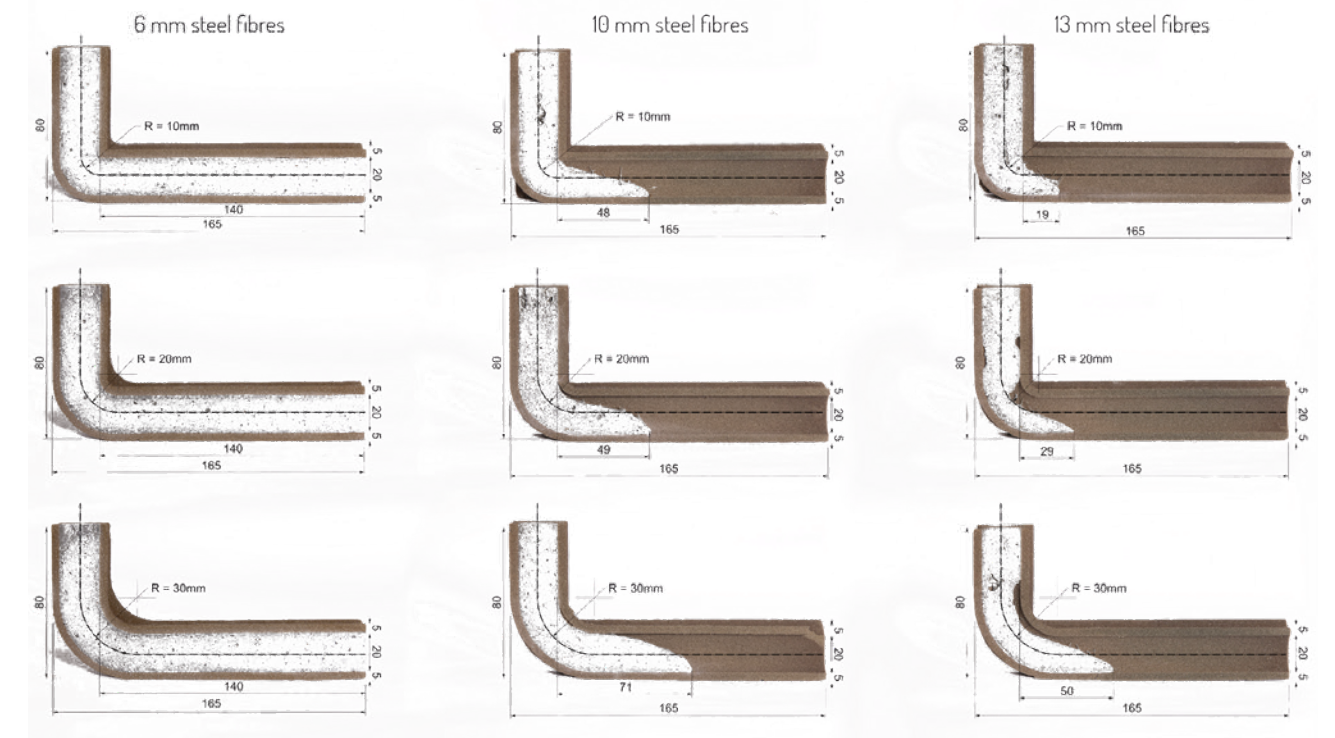


Figure 2.56. Rheology studies investigating the relation between fibre reinforcement and geometric features (Jipa et al., 2016).

## 2.4.7 Ornamentation by Fabrication

Ornamentation with concrete can be related to the surface finish, components of the concrete type used, finish colour of cured raw concrete, effects by the release agents, texture of the formwork, manual or mechanical or technical treatments, rushing and washing, the use of different coatings and the weathering effect Figure 2.58. The effect of depth to express an ornament in an artistic manner can also be an expression as shown in Figure 2.57.

With the use of modern design and fabrication tools and the ease of realising an designers thought, advanced materials with complex geometries can be fabricated. The freedom of developing any complex geometry with additive manufacturing coupled with various different materials does contribute in a large sector of advanced digital architecture. A such example of advanced complex design and fabrication was demonstrated with the 3D printed chair using concrete and manipulating the path by altering movement by Studio 7.5, Figure 2.59.

The effect of the formwork panels used to cast concrete as by Tadao Ando while using the bolting holes and the joints between two panels as the groove is an expression with ornamentation, Figure 2.29. and 2.30.

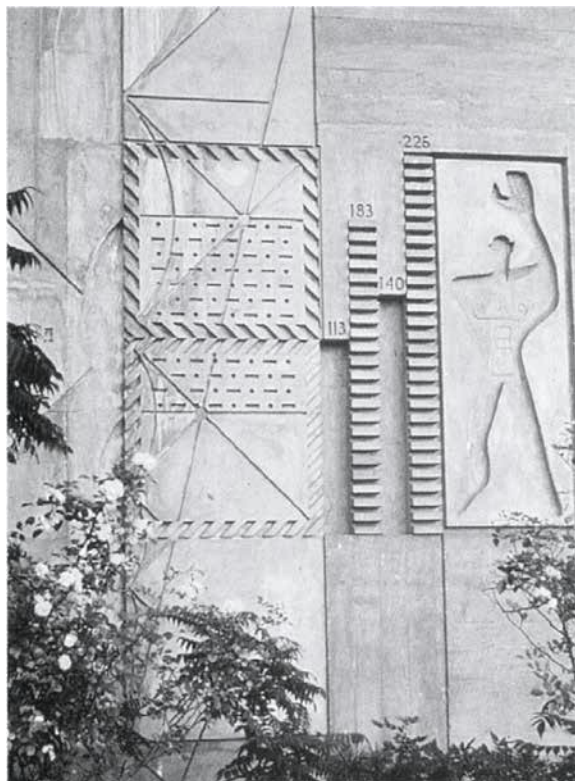


Figure 2.57. Joints, ornamentation and relief used to decorate a surface by fabrication moulds (Friedbert et al., 2013).



Figure 2.58. 3D printed chair using concrete by Studio 7.5 ([www.seven5make.com](http://www.seven5make.com)).

## 2.5 PROJECTS: THE REFERENCES

In consideration to the previously discussed system, material, tool and method that concern this project, a handful built and realised projects have been studied in brief and outlined below. The conclusions from these projects will be inferred for the further research and design of this project.

### 2.5.1 Case study 01: 3D-Printed Stay-in Place Formwork for Topologically Optimized Concrete Slabs

**Project by:** ETH Zurich

**Project year:** 2016

**Function:** Concrete slab

**Goal (Prototype A) :** Reduce material to a 0.2 set fraction of the initial amount while minimizing deformations of the slab under uniform surface load.

**Goal (Prototype B) :** Reduce material to a 0.18 set fraction of the initial volume while minimizing the stress of the slab under uniform surface load

**Boundary conditions (Prototype A) :** Three fixed supports.

**Boundary conditions (Prototype B) :** Four simple supports located close to the corners.

**Software used (Prototype A) :** Millipede, a free add-on for McNeal Rhinoceros; Catmull-Clark and loop subdivision algorithms. Design space was discretized into 135,000 nodes and the algorithm was run for 500 cycles

**Software used (Prototype B) :** Simulia ABAQUS (SIMP topology optimization algorithm). 1.8 x 1 x 0.15 m<sup>3</sup> design domain was discretized into 83,072 nodes with a volume of approximately 3.4 cm<sup>3</sup> each.

**Material used:** UHPFRC consisting 2.75 vol. % steel fibres 10 mm long and 0.16 mm in diameter.

**Fabrication Method:** Binder Jet 3D Printing with Phenolic binder (PDB) or Furanic binder

**Machine used:** Binder jet printer- Ex-One S-MAX 3D printer bed , full size 1.8 x 1 m<sup>2</sup>

**Considerations:**

- The properties of 3D-printed formwork in relation to concrete—how the porosity, sorptivity, and capillary absorption of the sandstone influenced the setting of concrete;

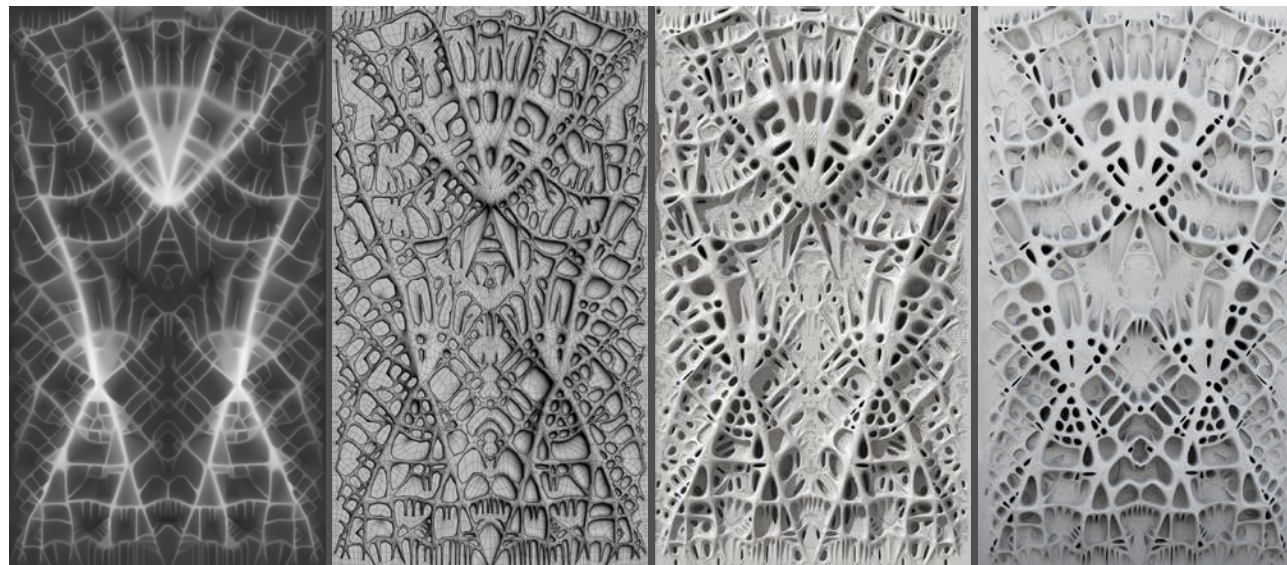


Figure 2.59. Design process for prototype "A": From left to right: greyscale bitmap resulting from Millipede, where each pixel represents an optimization node; vectorization with hierarchical differentiation of ribs and fields; three-dimensional mesh with depth based on greyscale values of underlying pixels; selective subdivision algorithms to achieve desired aesthetics. (Jipa et al., 2016)



Figure 2.60. Prototype A: Topology optimisation of a concrete slab with three point support (Jipa et al., 2016).

- New ultra-high performance fibre-reinforced concrete mixes with ductile behaviour;
- The rheological properties of these new mixes as a relation between fibre content and geometric features—inner radii, bending radii, and channel length to diameter ratios
- The properties of the sandstone to concrete bond;

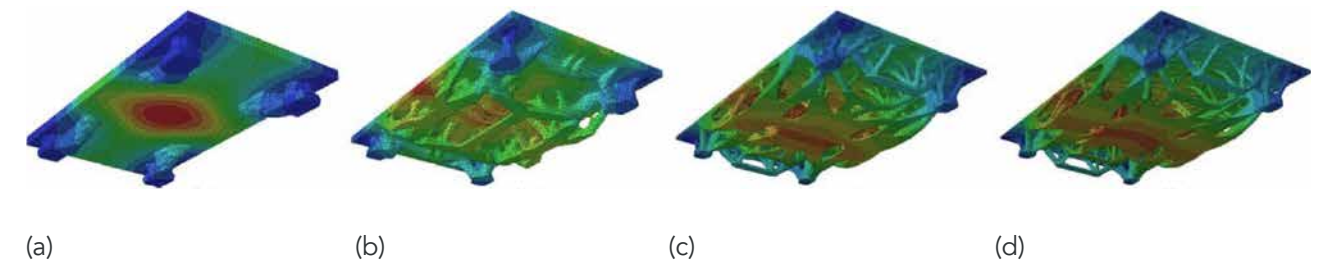


Figure 2.61. Topology optimization of Prototype "B" with different numbers of nodes (a) voxel count: 33,792, voxel size: 1.5cm<sup>3</sup>, Optimisation cycle: 51 (b) voxel count: 83,072, voxel size: 3.4cm<sup>3</sup>, Optimisation cycle: 51 (c) voxel count: 270,336, voxel size: 1.0 cm<sup>3</sup>, Optimisation cycle: 59 (d) voxel count: 2,162,688, voxel size: 0.12cm<sup>3</sup>, Optimisation cycle: 72 (Jipa et al., 2016)

#### Constraints:

- Smoothen under-sampling and correct artefacts resulting from the discretized nature of the topology
- Filtering out geometric features that were too fragile to be 3D printed
- Filtering out geometric features that were too narrow to permit 3D printing post-processing (unconsolidated sand removal and surface infiltration)
- Filtering out geometric features that were too narrow to permit the flow of concrete because of local fibre clogs;

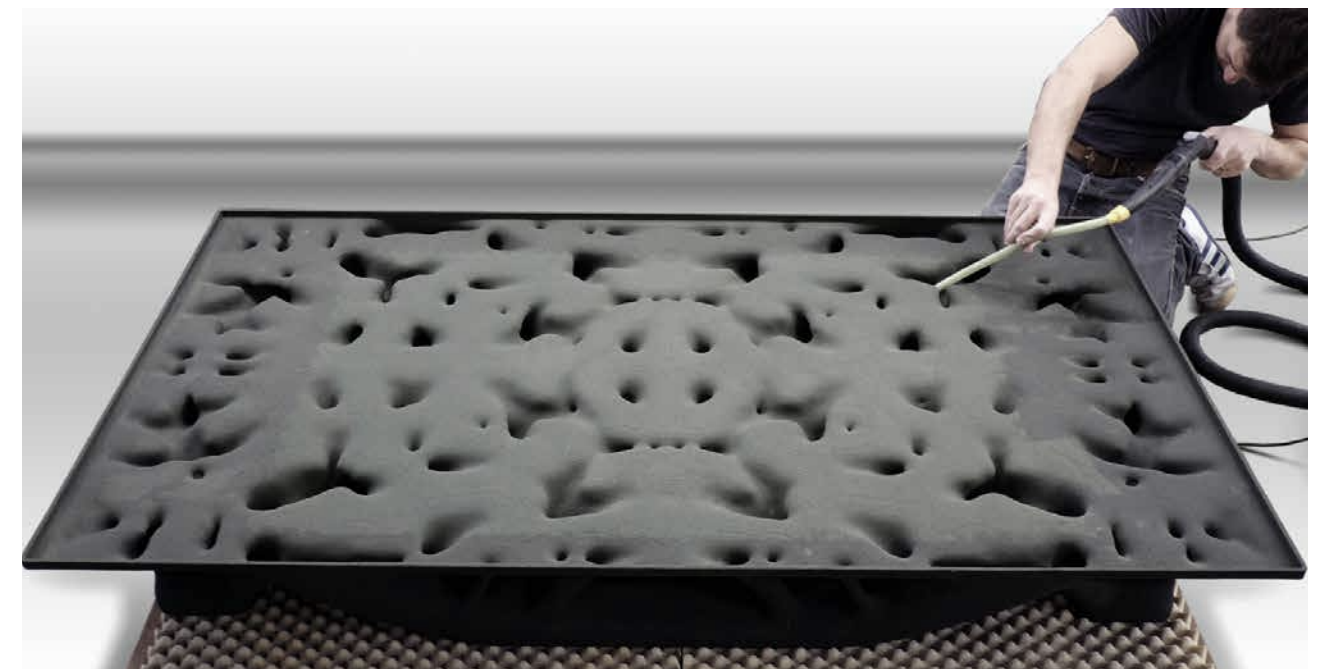


Figure 2.62. Binder jet 3D printed casting formwork for concrete (Jipa et al., 2016)

**Conclusions:**

- 3D-printed sandstone has reasonably good resistance to compression, but is brittle when exposed to bending forces.
- Geometric features become problematic at a scale of around 20 mm. Such fabrication constraints are close to the material limitations of concrete
- Steel-fibre reinforcement was sufficient for the prototypes,
- The average concrete thickness achieved, 30 mm, indicates that weight reductions of up to 70% are possible. The initial structural tests performed so far by applying a 2,500 KN/m<sup>2</sup> distributed load on Prototype "B"
- Mechanically removing a nine-millimetre-thick layer of 3D-printed sand completely requires pressures greater than 3,000 atm. with a water jet.
- UHPFRC mixes work well with 3D-printed channels with diameters as low as 20 mm and bending radii of 10 mm.

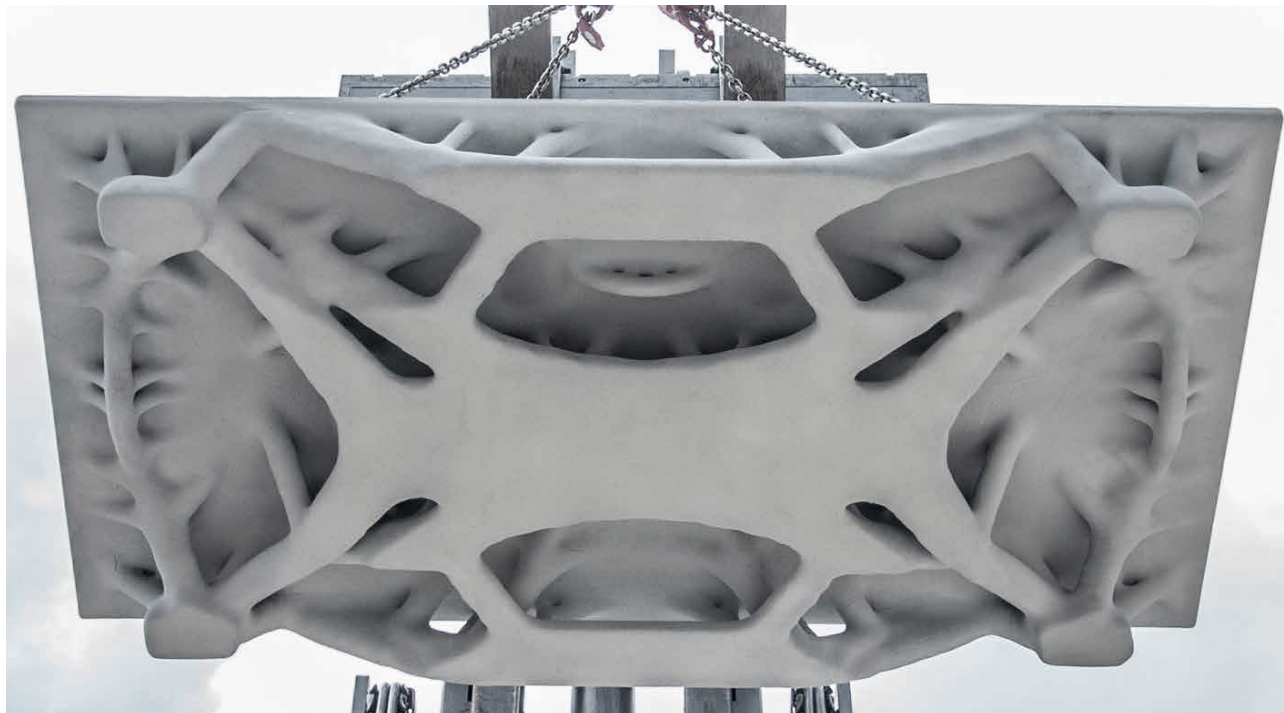


Figure 2.63. Prototype B: Prototype of concrete cast slab with four point support (Jipa et al., 2016)

## 2.5.2 Case study 02: St. Regis Hotel & Residences

**Architect:** WATG

**Project year:** 2005

**Function:** Non load bearing Façade

**Boundary conditions :** Punched window openings

**Software used :** Traditional construction

**Material used:** Concrete

**Fabrication Method:** Mould precast

**Facade fixture:** Metal members fixed to GFRC panels

**Goals:**

- Create relief in the tower's facade, maximizing the possibilities of light and shadow while minimizing materials.
- Minimize the joinery size between precast concrete sections.

**Considerations:**

- Fixing of window frames and glass before installation reducing the labour cost and facilities by a high margin.
- Design of facade as a woven fabric, distinguished by different colours of the element of the panel.
- Designed to minimize additional seismic mass of the superstructure while accommodating elastic and inelastic drift movements due to extreme seismic ground motion.
- The upturned beam approach was selected to allow the perimeter beam to serve as a window seat and to allow a continuous ceiling plane to the window head and precast concrete wall opening—without resulting in a beam projection into the line of the ceiling plane. This minimized the potential for architectural precast concrete anchorage interference with the post-tensioned concrete slab.
- For maintenance, in this system, as a window-cleaning platform



Figure 2.64. Street view of St. Regis Hotel & Residences (Boswell, Sarkisian, Clark, & Ball, 2006).

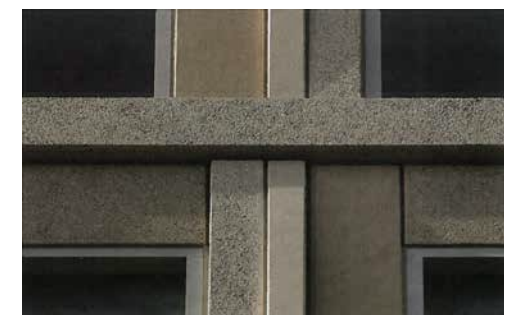


Figure 2.65. Use of two concrete colours and two sandblasted finishes created four distinct elements that are woven like threads across the "fabric" (Boswell et al., 2016).

is lowered by crane from top of the building The track was integrated into the precast concrete and glazing system serves to complement the sculpted geometry.

**Conclusions:**

The use of GFRC enabled the creation of complicated 3-D shapes out of concrete while keeping the weight of the facade to a minimum and construction cost. (Boswell, Sarkisian, Clark, & Ball, 2006; WillisConstruction, 2015)

**Constraints:**

- Seismic conditions demands for flexible joineries and high tolerances between the panels
- Chamfered corners posed critical fabrication and maintenance problems

**Awards received:**

- ACI 2004 Construction Award
- ACI 2004 Structural Award
- 2007 PCI Design Award



Figure 2.66. Erection of precast concrete facade wall with pre-installed windows using tower crane (Boswell et al., 2016).

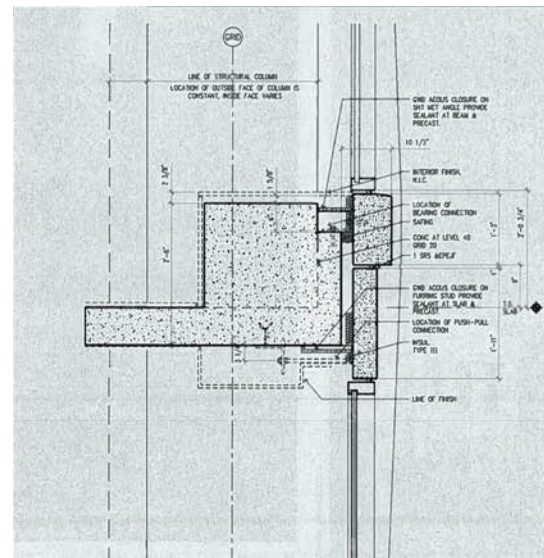


Figure 2.67. Drawing of typical precast concrete facade connection detail (Boswell et al., 2016).

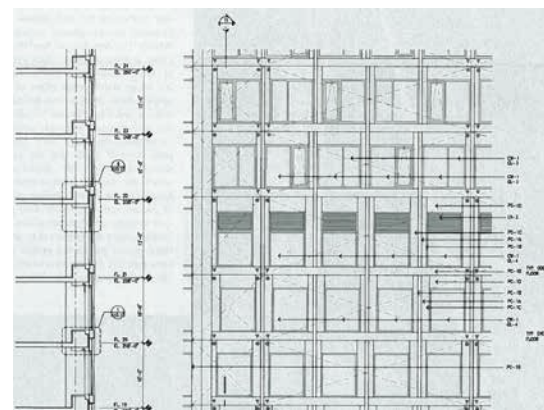


Figure 2.68. Typical precast concrete facade wall section and elevation (Boswell et al., 2016).

Element	Nos.	Dimension, Weight
Punched window panels	532	32x 10ft; 14,000 lb
Column cover panels	155	10x 6ft; 4000 lb
Spandrels	57	32 x 7 ft; 15,000 lb
Other	24	
Total panels	768	

Table 2.13. Detail of precast concrete elements (Boswell et al., 2016).

**2.5.3 Case study 03: The BROAD**

**Architect:** Diller Scofidio + Renfro

**Project year:** 2015

**Function:** Non load bearing Facade

**Boundary conditions :** Window openings

**Software used :** Generic tool path software (WillisConstruction, 2015)

**Material used:** GFRC

**Fabrication Method:** CNC milling mould and spray-up casting

**Mould:** Steel frame work

**Facade fixture:** Metal members fixed to GFRC panels

This building is LEED Gold rate certified. The use of GFRC enabled the creation of complicated 3-D shapes out of concrete while keeping the weight of the facade to a minimum. (WillisConstruction, 2015)



Figure 2.69. The Veil facade comprised of 2500 GFRC panels with window opening in each of them. (Bianchini, 2016).

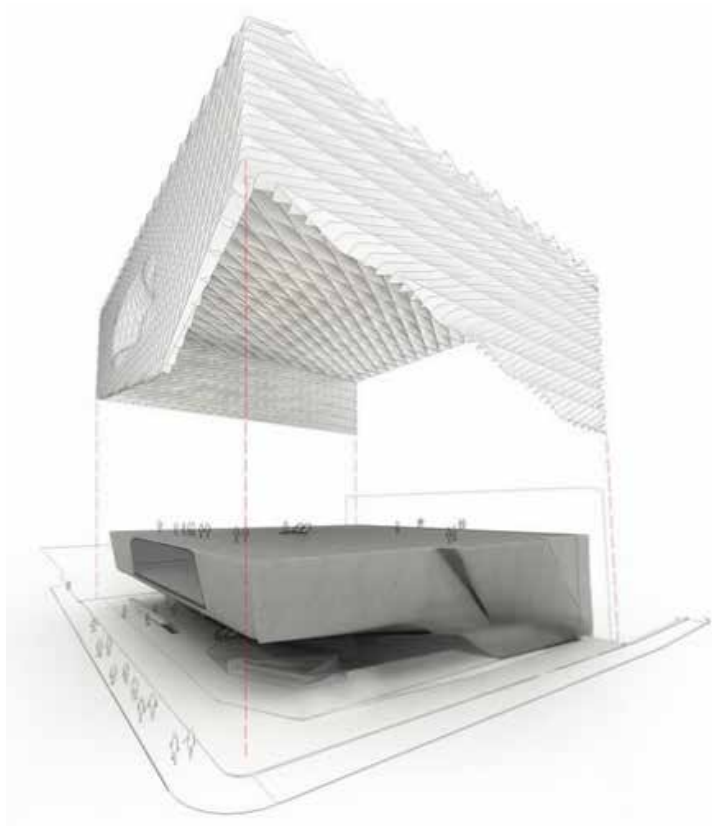


Figure 2.70. The facade as a skin to the museum (TheBroad, 2015).



Figure 2.71. Drying of GFRC casted facade panels (Gensler, 2015).



Figure 2.72. Spray up casted panels fixed to one module of steel member support (Lubell, 2014).

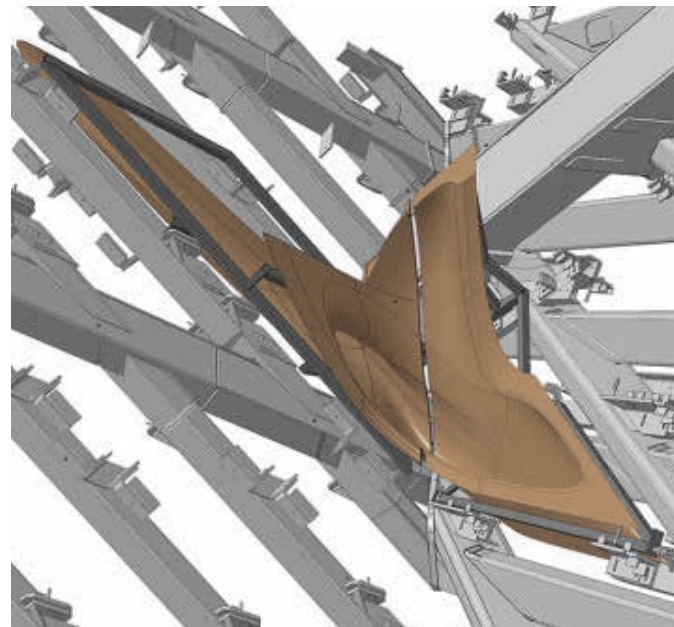


Figure 2.73. CAD model of fixing the facade panels to the steel frame structure (Stephens, 2016).

### 3.4.1 Case study 04: Spong3d

This is an adaptive facade system developed to enable heat exchange system between an external and internal tubular network separated by an insulated geometry, the combination of which was a unified panel 3D printed using PETG (Sarakinoti, Turrin, Konstantinou, & Tenpierik, 2018). This project did research upon 2 primary goals of increasing the thermal insulation capacity by designing the geometry of the insulation layer and secondly to maximising the heat storage capacity with studies for heat exchange performance of the panel in interaction to the specific surroundings and climatic condition (Klijn-Chevalerias, et al., 2017). This system was also designed and analysed in consideration for factors affected by 3D printing method of fabrication. Although this system did consider the inspirations from different natural fluid flow systems like leaf veins, human blood vessels and other bionic structures, the flow and pressure drop were not simulated and optimised for the best possible solution. This designed network has been demonstrated in the image below.

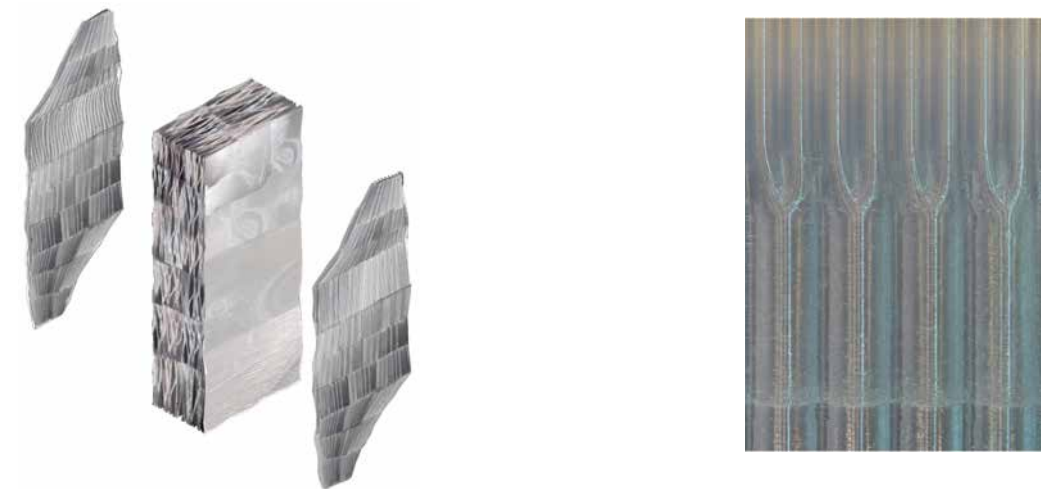


Figure 2.74. (Left) Image showing the external and internal tubular network with the intermediate insulation layer, (Right) Elevation of a section of the tubular network. Source: Sarakinoti, et al. (2017).

#### Referred design considerations

Functioning of the heat exchange system.

Collaboration of natural systems to the designed geometry to mimic the fluid flow.

Performance of tubes configuration for heat movements and insulation.

#### Factors not considered in the research

This research does not consider thermal mass heat trapping and heat transfer to the tube is assumed to be only by direct solar gain.

Optimising the tubular geometry for maximising the volume of the fluid volume in the network

Optimising the geometry for minimised pressure drop across the geometry

Long term serviceability of PETG as a material in a façade considering the degrading property of the material under UV radiation.

### 3.4.2 Case study 05: Leaf venation, as a resistor.

As stated by Alston & Barber (2016) his research deals with designing a switchable IR absorber using polymer which analyses the leaf venation as a resistor to the fluid flow and proposes circuit conduit optimisation for transport fluidic flow resistance. This research deals with a single two dimensional venation network only which develops an algorithm to design the width of the veins in determination to equalise the resistance of the fluidic flow in the network. This project has been inspired by the network of veins and their dimensions to which the flow resistance of these veins were unified are studied and calculated framework was designed to mimic the same using CFD analysis of fluid flow. The diagram below shows the designed 2D network and the equivalent resistance network below.

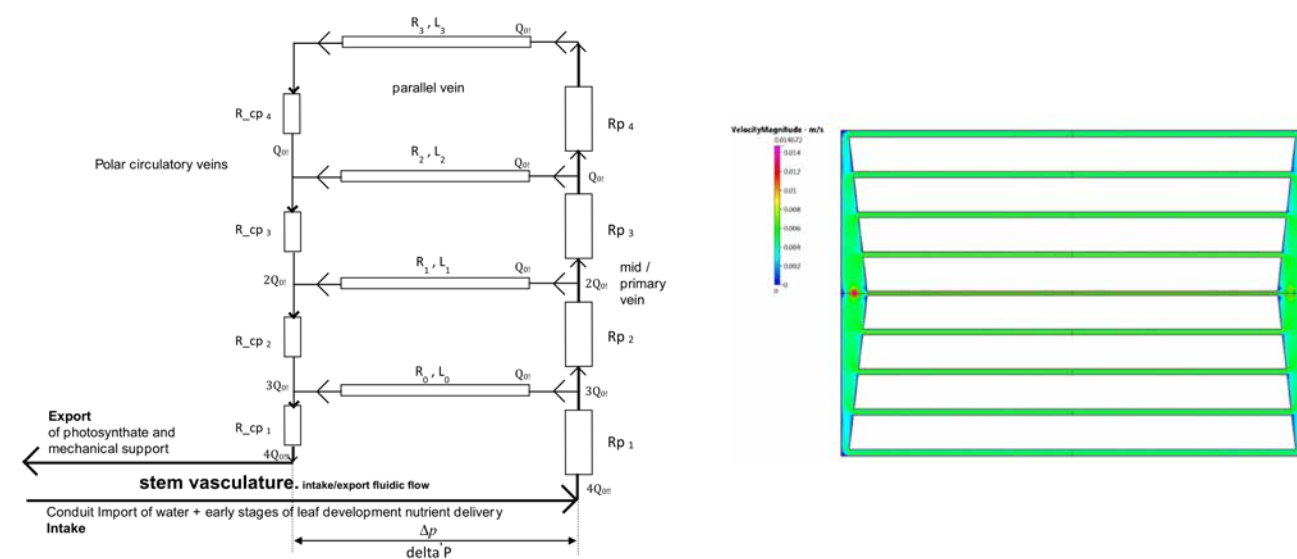


Figure 2.75. (Left) Fluidic resistor network, (Right) Velocity distribution of 2D designed network. Source: Alston & Barber (2016)

#### Referred design considerations

Issues related to fluid flow in small diameter tubes and related pressure drops.  
 Understanding of fluidic flow network and flow resistances.  
 Calculation of diameters of tube in networks to unify fluidic resistance.

#### Factors not considered in the research

Three dimensional venation network.  
 Consideration of different tube configurations to minimise pressure drop.  
 Optimisation of geometry through CFD simulation and shape optimisation.

### 3.4.3 Case study 06: A study of flow patterns for gas/ liquid flow in small diameter tubes.

This project deals with research of time resolved void fraction data and flow pattern of two- phase air/ water flow in small tubes diameter ranging to 5mm diameter with conductance probes As stated by Omebere-Iyari & Azzopardi (2007), mostly all heat exchanger designs do involve optimisation for heat transfer and pressure drop, both of which are affected by the various two-phase flow patterns. This research also states that depending on the flow type and transition of these flow types may develop blockages in the tubes.

Since the usual heat exchangers used in industrial purposed have high flow rate of fluid flow for efficiency of the machines, the flow is usually of turbulent nature. These problems of pressure drop and blockage due to the flow type transition could be eliminated if the flow type is restricted to laminar type only. The two medium flow type is considered for the design pf this thesis, so as if any part of the designed tubular network does experience leakage or loss of fluid due to evaporation, the fluid flow may invite gaps of air and convert the flow type into a dual medium developing problems as mention in this research.

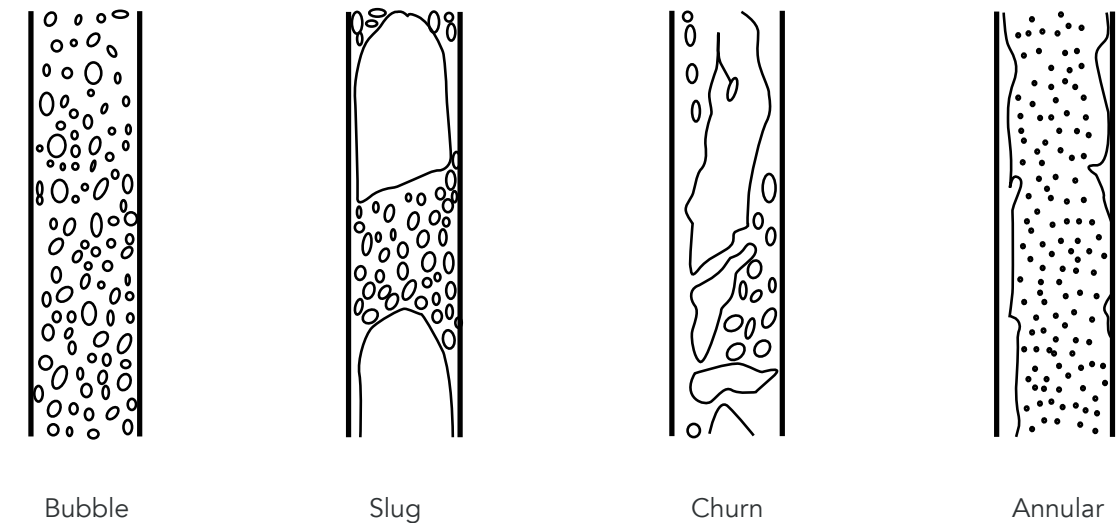


Figure 2.76. Different flow type patterns for a dual medium in small diameter tubes. Source: Omebere-Iyari & Azzopardi (2007)

#### Referred design considerations

Eliminate flow type transitions and problems related to pressure drop and blockages by limiting the flow of fluid to laminar type.

#### Factors not considered in the research

Change in flow pattern in complex tubular network geometry.

### 3.4.4 Case study 07: Convective concrete

The goal of the convective concrete research is to transfer the over heating generated during the summers in a residential space by active heat exchange between the structure and the outdoor air at night. This system did incorporate tubular networks on both sides cascaded within the concrete walls that dis circulate the air to exchange the heat between the indoor an outdoor environment. The concrete and tubes within were proposed to be 3D printed out of wax but were than cast with tubular moulds and poured with concrete due to various reasons as stated by Klijn-Chevalerias, et al., 2017. These wax cast tubes were then melted out to form hollow tubes within the concrete mass. A schematic diagram of the concept is shown below.

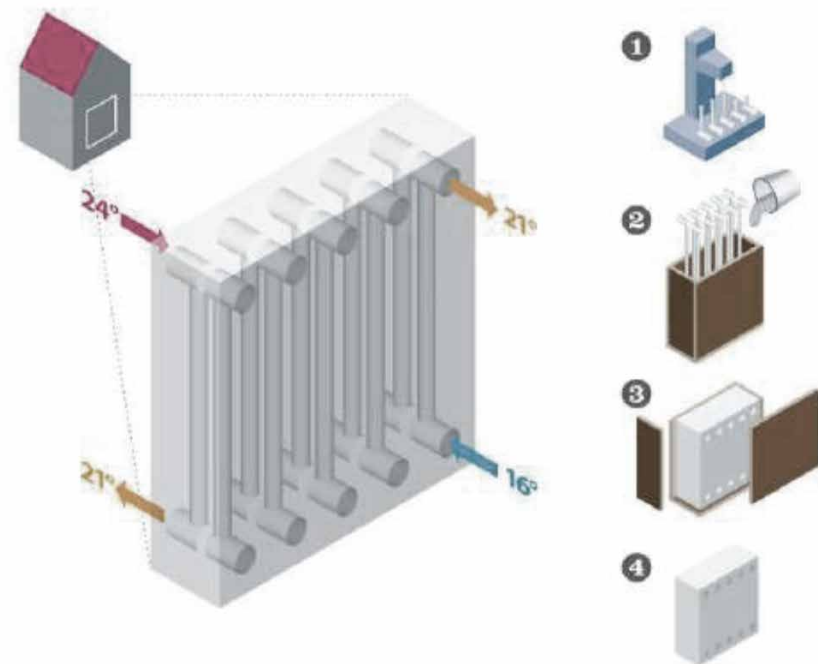


Figure 2.77. Conceptual diagram of convective concrete. Source: Klijn-Chevalerias, et al. (2017).

#### Referred design considerations

The method of tubes cast within concrete to absorb the thermal mass capture from the indoor environment to outdoor.

The method of investment casting using wax as an internal form work and melting out to form void tubes.

#### Factors not considered in the research

Casting of complex 3D tubes within the concrete with slimmer tube profiles.

Melting of wax for large size castings is not considered.

## 2.6 DESIGN FRAMEWORK

In consideration to the previously discussed system, material, tool and method that concern this project, a handful built and realised projects have been studied in brief and outlined below. The conclusions from these projects will be inferred for the further research and design of this project.

### 2.6.1 Facade segment

The basic type of a mix used and office buildings are laid out of the so-called bookshelf framework, Figure 2.78. A boom of building renovation projects was unavoidable at the beginning of the 1990s as a large number of blocks of flats had reached the age of 20–30 years. The problems were chiefly in facade panels and balconies. The load bearing facade were critical to upgrade because of structural issues. The non-load bearing façades on the other hand tend to be serviced and upgraded easily. The segments of the building with facade panels with window opening/s and the opaque exterior façades are considered in this project.

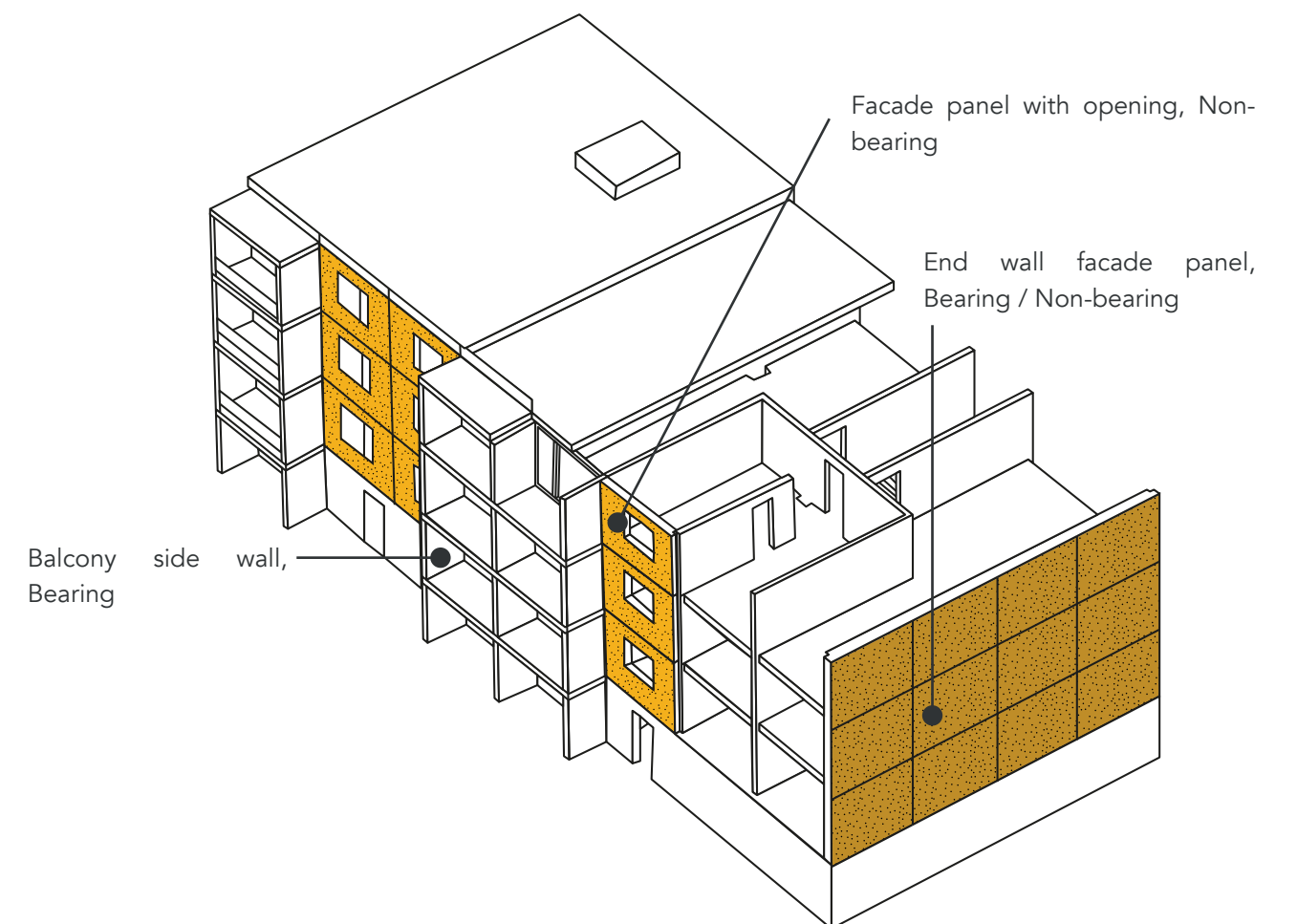


Figure 2.78. The bookshelf framework of a multi-storey building (modified from Koskiahde, 2004).

## 2.6.2 Typology

Depending on the study by The Skyscraper Center (2018), it is evident that India as a rapidly emerging market has about 22% of the total projects under-construction as compared to that of 7% of whole of Europe in the time frame of 2010-2025. More than 75% of the buildings under construction in India are about 1-49 stories while most of it under 30 floors. As per the graphs, it is also evident that the residential typology contributes to the highest number of construction in India between 2010-2025, with about 10-12% counting for the mixed use and office typologies. This gap is reducing slowly with the high rate of adoption in mixed use typology construction in India. Figure 2.79, 2.80 and 2.81

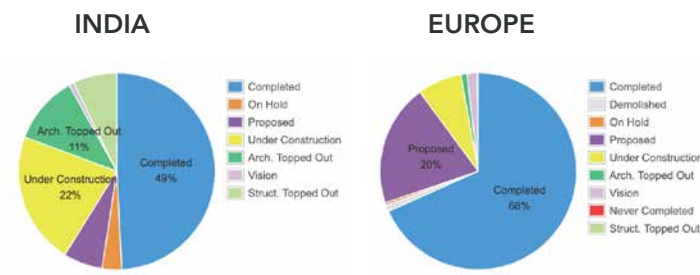


Figure 2.79. Comparative graph for construction status of buildings with height 0-150m bet. 2010-2025 in India and Europe

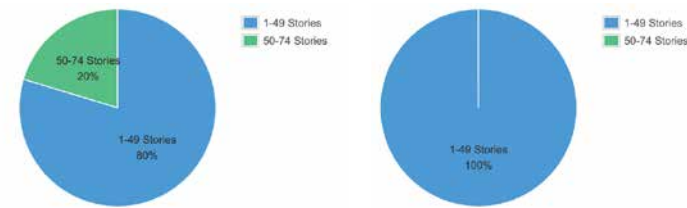


Figure 2.80. Comparative graph for no. of stories for buildings with height 0-150m constructed or under-construction bet. 2010-2025 in India and Europe

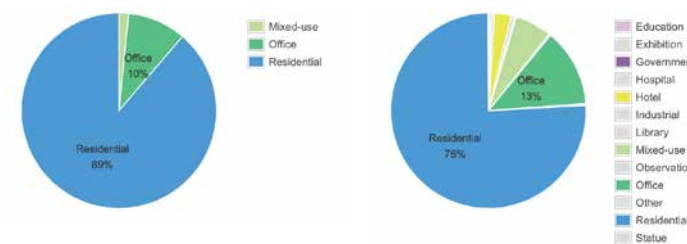


Figure 2.81. Comparative graph for building typologies in India and Europe for buildings with height 0-150m constructed or under-construction bet. 2010-2025.

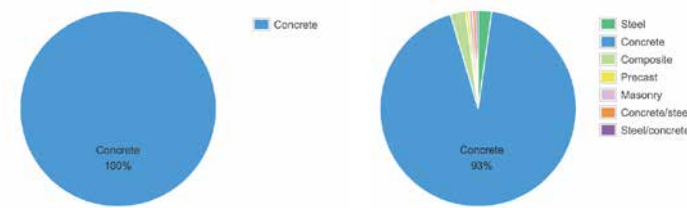


Figure 2.82. Comparative graph for structural material for construction in India and Europe for buildings with height 0-150m constructed or under-construction bet. 2010-2025.

Graphs from skyscrapercenter.com

## 2.6.3 Concrete in India

With rapid infrastructure development in India, the demand for concrete is ever rising. At about 1/10th the consumption of China (2400 million metric ton in 2007), India consumed about 280-290 million metric ton in the same period (Statista, 2018). As per the statistics of construction by The Skyscraper Center (2018), 100% of recorded construction in India (excl. small scale constructions) depends on concrete and needs to be addressed to decrease by optimal usage of it, Figure 2.82.

## 2.6.4 Location and climate zone

India has a diverse climate zones with the prevailing conditions being the hot & humid and composite climates. Most of the metropolitan cities viz., Mumbai, Ahmedabad, Chennai, Hyderabad, Kolkata, Bhubaneswar etc. lie in the hot and humid climatic zone, Figure 2.83. Delhi amongst all poses a composite climate with extremes of temperature during the summers and winters. Being the capital of India, exploding infrastructure development in Delhi and Delhi NCR marks it the favourable site for exploration of this project.

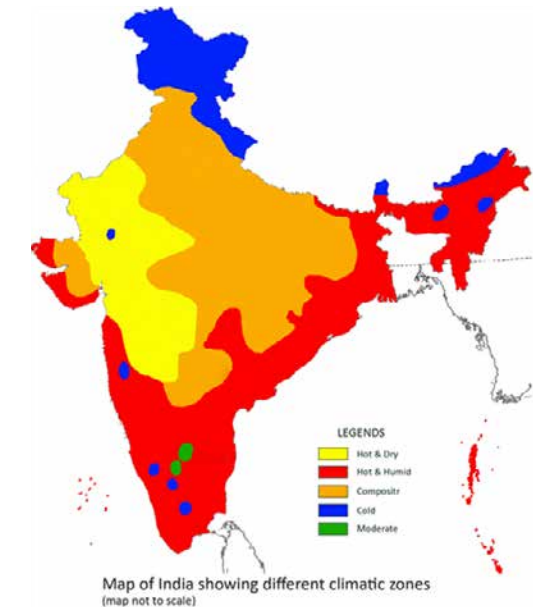


Figure 2.83. Map of India showing different climatic zones ((Das & Karakoti, 2014).

## 2.6.5 Wind

Based on the analysis by Kumar, Cini, & Sifton (2012), it is found that the estimated 50-year return period mean-hourly wind speed is 18.9 m/s and 22.5 m/s. As per the current study, the best estimate 50-year return period Basic Wind Speed (3-seconds gust) for Mumbai is 39 m/s. These estimates are based on measurement at a height of 10m above the ground level. Even though Delhi (site considered) experiences wind from 3-10 m/s, the maximum wind loading in the country was considered for safe loading. The gust to mean ratio graph for Mumbai at a level of 10 m from ground is shown in Figure 2.84.

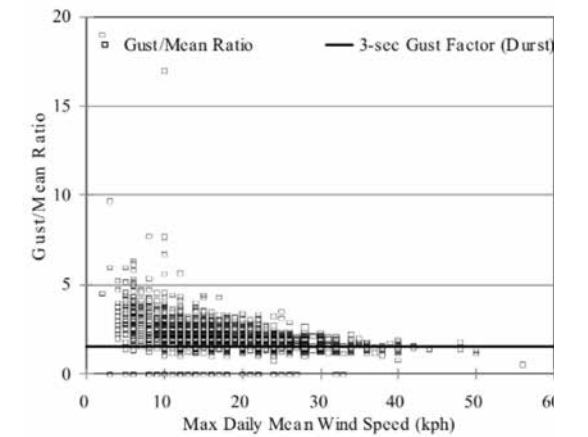


Figure 2.84. Gust to Mean Ratio – Mumbai (Kumar, Cini, & Sifton; 2012).

## 2.5.6 Window to wall ratio

As studied by Didwania, Garg, & Mathur (2011), the optimum WWR is prescribed to be 30-40%, 15%, 10%, and 10% on an average for north, east, west and south facade respectively for a advanced single glass pane. For double glass assembly the optimum value for WWR reached 40%-60% on north, 25% on east, 20% on west and 15% on south. This study has been done on a G+1 office typology set up in the city of Delhi with a composite climate.

## 2.6.6 Design reference database from literature study

**Location:** Delhi, India

**Climate:** Composite

**Wind speed:** 39 m/s @ 10m above ground

**Typology:** Office or Mixed-use

**Height of building:** 21-30 floors

**Approximate panel size:** Height 3.5 to 4m

**Optimisation type:** Topology Optimisation

**Goal:** Minimise volume of material

**Thickness of panel:** Min: 120mm Max: 350mm (including cavity for twin wall system)

**Type of panel:** Non-load bearing Precast

**WWR:** 40%, south oriented

**Fabrication (prototype):** Investment casting

**Material (prototype):** Ultra high performance Fibre Reinforced Concrete (UHPFRC) consisting 2.75 vol. % steel fibres 10 mm long and 0.16 mm in diameter.

**Handling:** 3 point lifted- Tilt-up crane handling system

**Fixtures:** Window sections, Facade brackets etc.

## 2.7 CONCLUSION

This chapter did explore and explain the criteria selected for this thesis. The four basic elements were described individually with justifications stated in comparison to other possibilities and the final selection made was stated.

The system- Facade discussed the different types of precast facade system and the reasoning over choosing non-load bearing twin wall facade system. This section also does introduce to the various different functions that are integrated within the facade. The material- Concrete was justified over its use in the context of developing countries, its physical behaviour with benefits and cumulative beneficiary aspects over other building materials used in the industry. The process- Computation does outline the benefits of using the computation tools especially optimisation and defines the methods of optimisation used with reasons for selecting topology optimisation over others. This section also underlines the possible digital tools to achieve the design goals. The target- Fabrication, being the ultimate goal of this project, was explored to determine the preferred method compatible with the complex geometry of this project. The various different aspects in terms of constraints applied by the chosen method of fabrication was understood and was taken into account from the very basic stage of designing which would be further described in the following chapters.

### Sub research question answered:

*Why is concrete a viable material choice for facade in today's scenario?*

and partly,

*What method, tool and parameters of optimisation needs to be considered for deriving the geometry and maximising the efficiency of the heat exchange system ?*

This page is intentionally left blank.

# 3. CONCEPTUAL DESIGN

## CHAPTER OVERVIEW

This basic concept of the function of the concrete facade panel and designing inspirations and criteria for the network geometry through which the fluid would flow has been discussed in this chapter. The basic method of deriving the design geometry is stated in relation to the inspired concepts.

## 3.1 HEAT EXCHANGE SYSTEM

Amongst all other building elements, façades are the most exposed to the environment. While this building element could although be considered as the crucial element to which the building defends itself to attain comfort for the living entities inside, it also holds true to be considered that façade of a building is the most potentially rich building element to harvest energy from the nature. In lieu of these concerns, the proposed system integration for the facade was chosen to be a solar heat exchange system for a twin wall facade panel cascaded within concrete. The specific reasoning over choosing concrete as a material and its sustainable aspects have been detailed out and discussed in contrary to other building materials in section 2.2.5.

Building in present times tend to harvest natural form of energy mostly by solar panels for harnessing the solar energy from the terraces and fenestrations, micro wind turbines for wind with external installation of structure or heat pump systems to drive energy from the ground beneath. But harvesting energy from the opaque sections of the facade has been seldom explored. One such example of harnessing energy from a facade is stated by O'Hegarty, Kinnane, & McCormack (2016) for thermal collector system within a facade. Façade of a building is the most exposed and in contact with the external environment and due to this reason, it was considered as the focus element for this thesis. The potential of harvesting and processing the solar heat through facade is much higher than any other building elements holds true but also depends largely on the height, context and the configuration of the building. The potential of harnessing solar energy through facade

### Current scenario

Target: Roof, ground and fenestrations sege

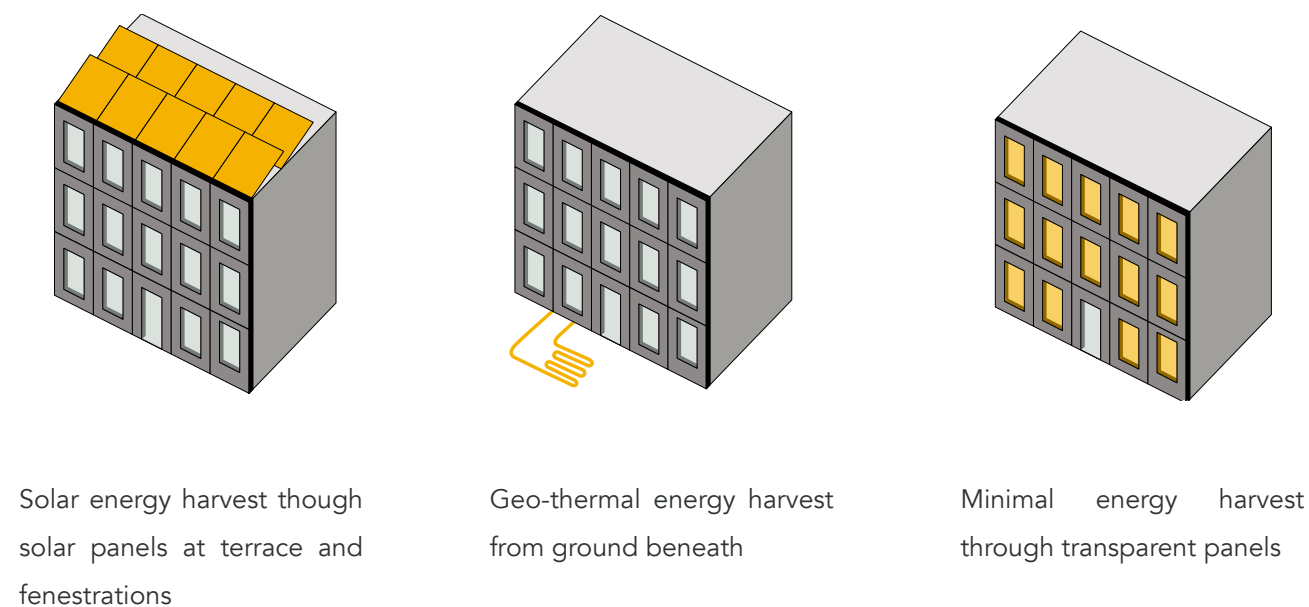


Figure 3.1. Typical methods of harvesting passive energy in a building.

in present time has been mostly limited to those of solar panels to generate electricity and do possess a very typical aesthetical expression of the system. Although new glass panes with transparent solar panels are commercially available, the yield rate of the same are very low as compared to conventional systems while or else are usually not preferred on the facade because of their generic look, maintenance and cost. By the mean time, architectural expressions are moving away from the glass curtain wall buildings currently and opaque facade panels are being main stream again. Systems for such opaque facade zones/ panels are still seldom used to harvest solar energy and process them for the benefit of the building. A schematic comparison of the focus zone of design in this thesis is shown below.

### Proposed scenario

Target: Opaque segments of facade

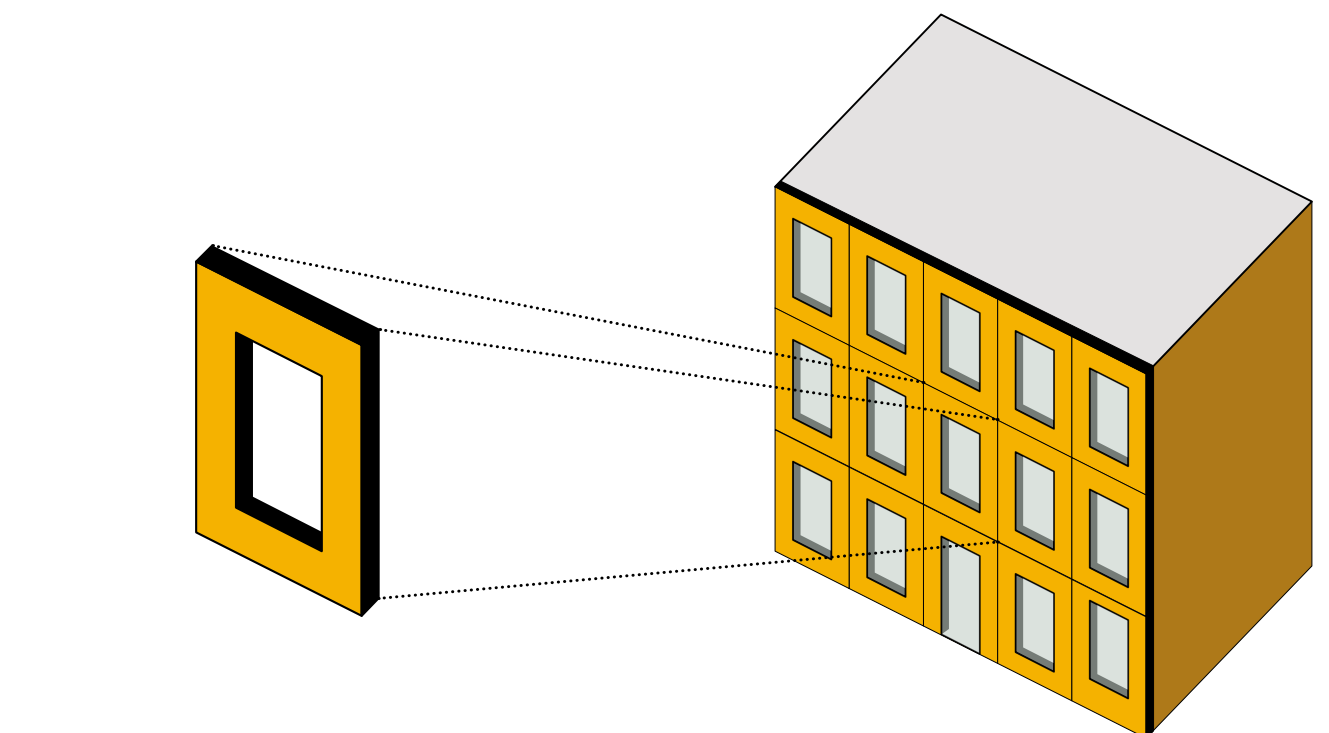
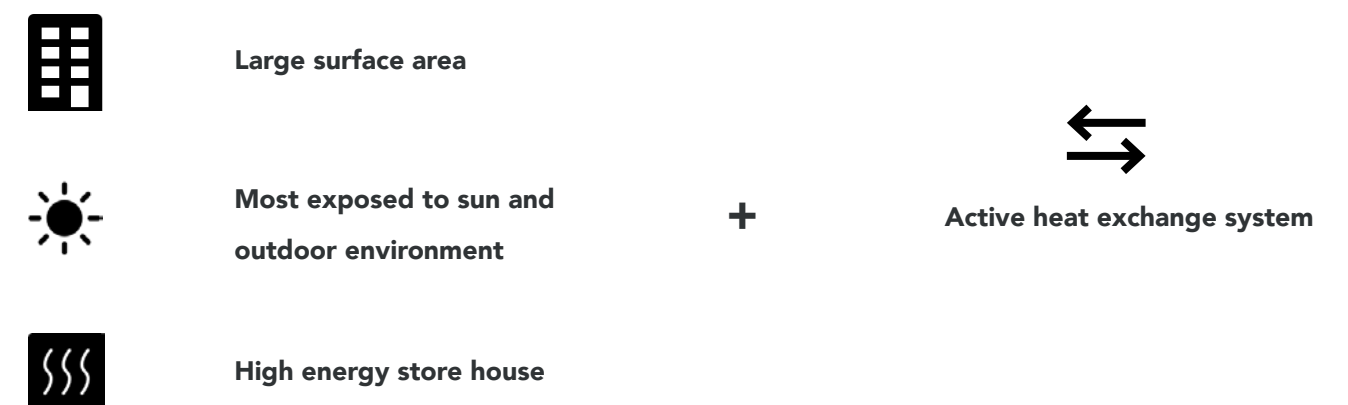


Figure 3.2. Opaque sections of facade to harvest solar energy.

A typical solar energy harvesting system used in present time incorporated with façades are to generate thermal energy through the cascaded tubes in facade and collect them for various different energy needs of the building (O'Hegarty, Kinnane, & McCormack, 2016). While such concepts hold true for a solar collector system, the proposed system for this thesis is an active system which interacts with the outer space to that of the immediate inner space and the response or efficiency is directly dependent on the capacity of thermal exchange between the internal and external facade panel. Usual twin wall facade panels are considered to be highly insulated for improving the performance of the building which is effective, but the external and internal panels in those facade systems are inactive and do not harvest energy actively. By cascading the tubes within concrete facade panels, the fluid within the tubes benefits from the high thermal mass of concrete as a material that captures high amount of thermal energy and transfers the same to the fluid. The proposed system integration of heat exchange system within the concrete facade panels targets these specific use type and regions, which can make sustainable development by using such products. Also that the economic viability of concrete over other building materials still makes it favourable for most commercial and residential construction, especially in developing countries like India. A schematic diagram of the basic functioning of the system within the facade panel is envisioned through figure 3.4.

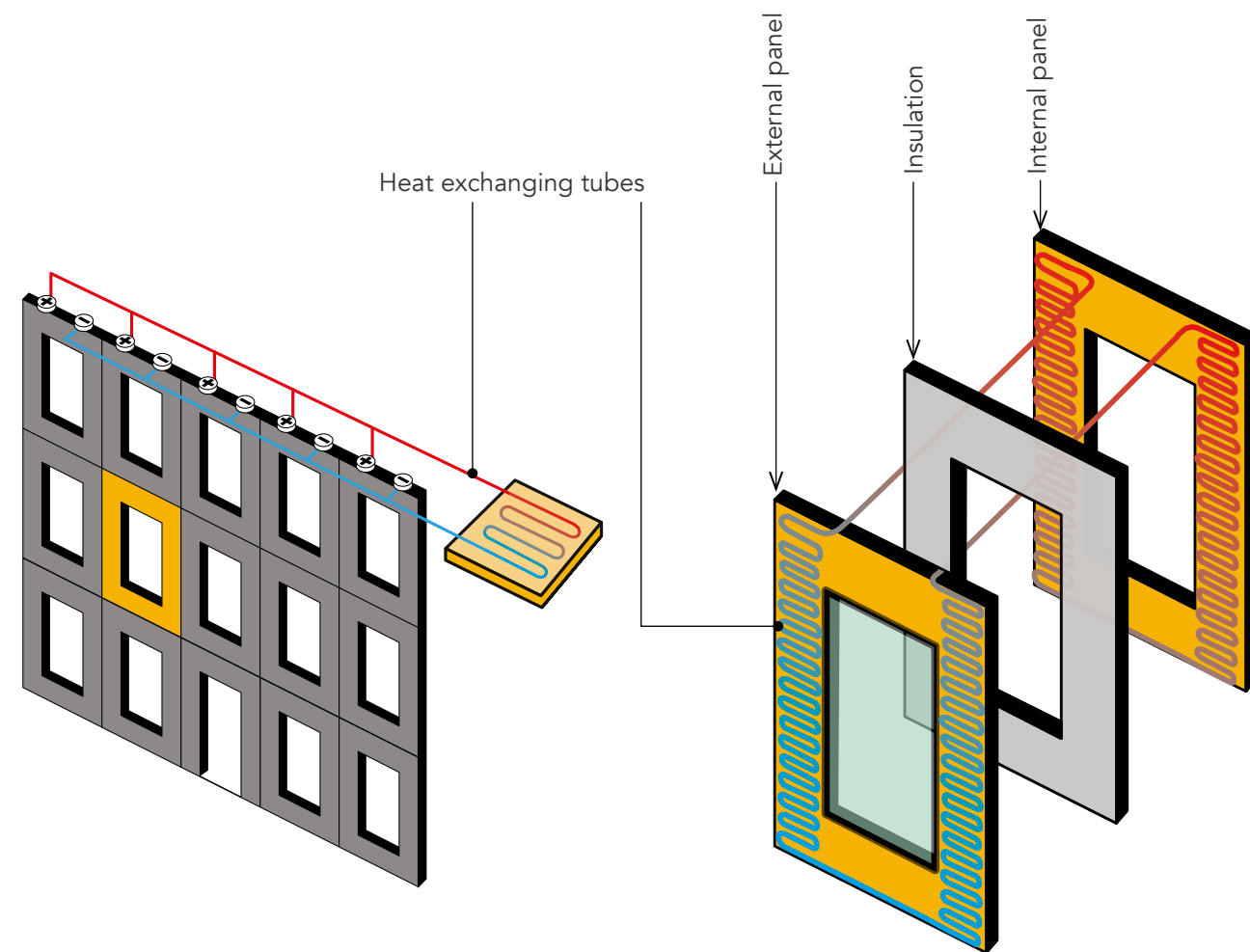


Figure 3.3. Generic solar collector system  
(Author)

Figure 3.4. Schematic proposed heat exchange system.

## 3.2 WORK CYCLE

The use of such heat exchange system does depend on the climatic condition of the locality/ region used in and the season of conduct. Even further, the selection of the cycle of conducting the heat exchange depends on the time of the day for corresponding climatic type or season. While this thesis does focus on the composite climate of Delhi, India which experiences high of summer of 40°C and lows of sub zero temperature during winters, this system could be deployed in relatively colder regions or hotter climate across the globe, with a specific set of purpose to conduct. A schematic diagram of performance of such system in a typical office space has been depicted in the following series of diagrams.

### 3.2.1 Work cycle type 01- Winters with cold nights and sunny days

In winters or in cooler regions, the system is designed to capture the solar heat from the external environment during the day and transfer the heat captured by the mass of external facade panel to the fluid in the tubes cascaded within the facade panel. The heated fluid is then transferred from the external panel to the tubes in the internal panel during the night and the thermal energy captured within the fluid is then transmitted through to the cooler internal space. A depiction of this cycle has been shown in figure 3.5.

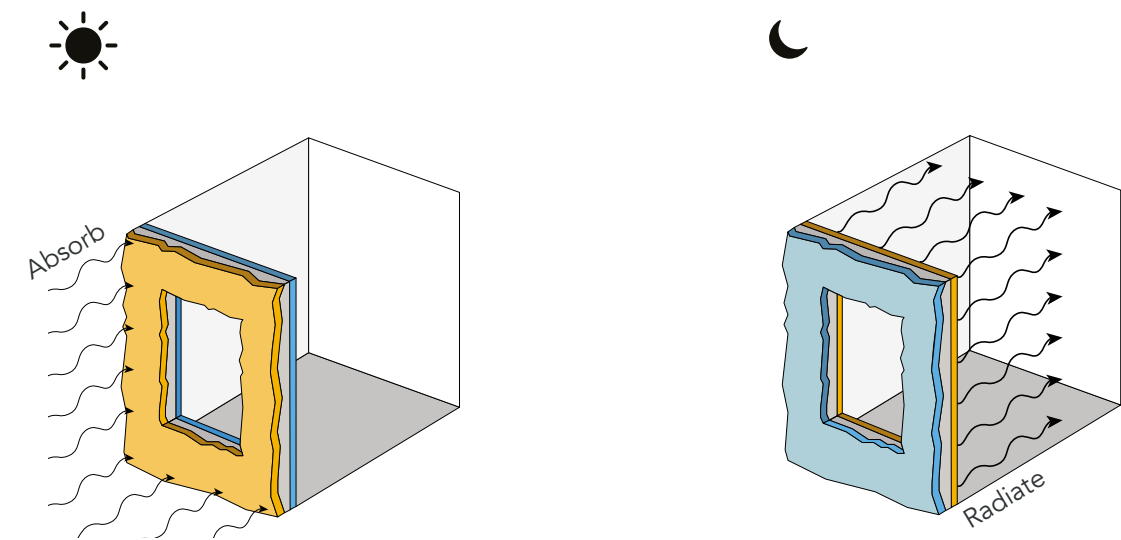


Figure 3.5. Schematic diagram showing the operation of heat exchange facade system during winters with cold nights and sunny days. (Author)

### 3.2.2 Work cycle type 02- Summer with hot days and cooler nights

During summers, the above cycle is flipped. The goal during the summer is to capture the maximum possible heat penetrated from the external environment to internal or generated by the occupancy within during the day time. This capture heat is then transferred from the internal panel to the external panel through the fluids in the connected network and radiated to the cooler outdoor environment at night. If the nights are much cooler than the days, the external panel can also be used to cool the fluid within and transferred back to the internal panel by the day time that would compensate in cooling loads indoor for the day time. A schematic depiction of the same has been shown below by figure 3.6.

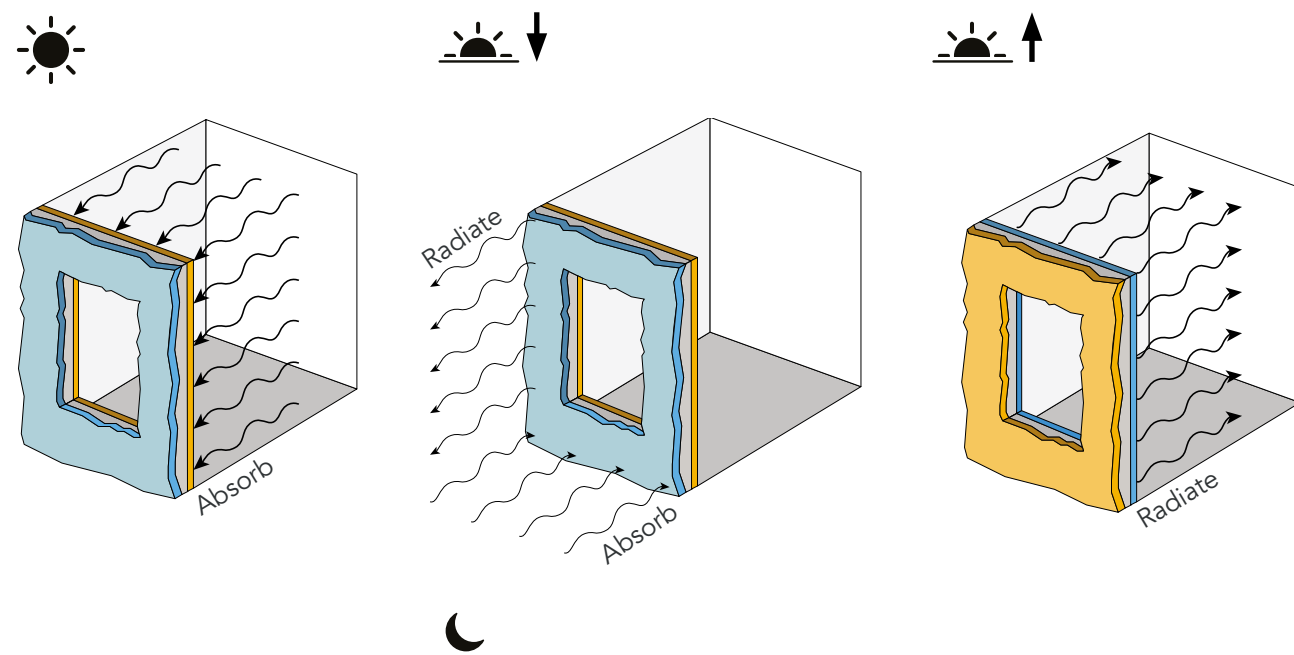


Figure 3.6. Schematic diagram showing the operation of heat exchange facade system during Summer with hot days and cooler nights. (Author)

### 3.2.3 Work cycle type 03- Summer with hot days and hot nights

There are certain regions which are hot during the days as well as during the nights. In such zones both the panels, the external as well as internal facade panels are used to capture the heat and make use of the same as a heat collector system and connect them separately to store the driven energy. This will help in capturing the heat from the sun as well as heat generated by the occupants within the space helping decrease the cooling load significantly. Such system does require extra processing for the heat exchange to cool down the heated fluids from the panel out and back and has been kept beyond the scope of this thesis. A schematic depiction of the same has been shown below by figure 3.7.

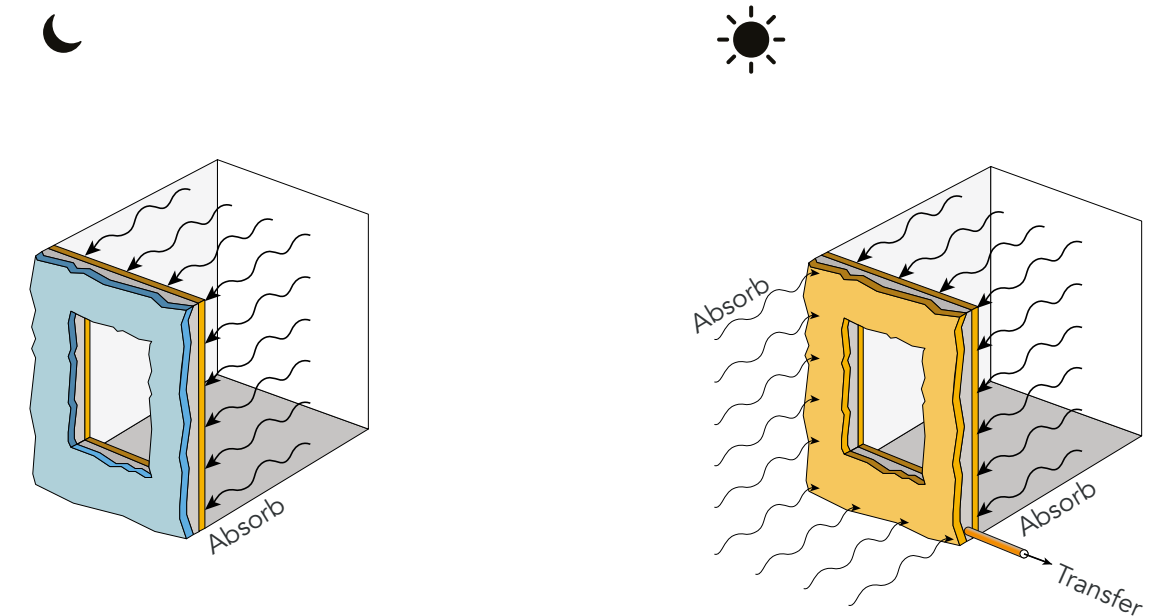


Figure 3.7. Schematic diagram showing the operation of heat exchange facade system during summer with hot days and hot nights. (Author)

It is to be taken into consideration that regions or seasons with cooler days and nights with no solar energy to harvest during the whole cycle of the day do not suffice the concept of heat exchange and fails the purpose of the proposed system. Such climatic zones are not considered to be served by the idea of this project. As mentioned previously, the consideration of the composite climate zone as in Delhi, India, does allow for the proposed facade system to experience the above mentioned work cycles as this region receives an extreme winter and summer and the temperature difference in days and nights are considerably distinguished.

## 3.3. DESIGN ELEMENTS

The envisaged design of the facade panel system with cascaded tubular network within the mass of concrete do form two different domains to consider and design. These two domains form the mass and the void of the facade panel. In terms of layering, the system comprises of three layers, the external panel, the internal panel and the layer of insulation in between the two panels. Structurally the internal panel will be fixed on both ends while the external panel will be loaded onto the internal panel with the help of reinforcement dowels. The designed facade concerns two environment to function: the exterior environment and the interior space to condition. A schematic section of these elements are shown in figure 3.7.

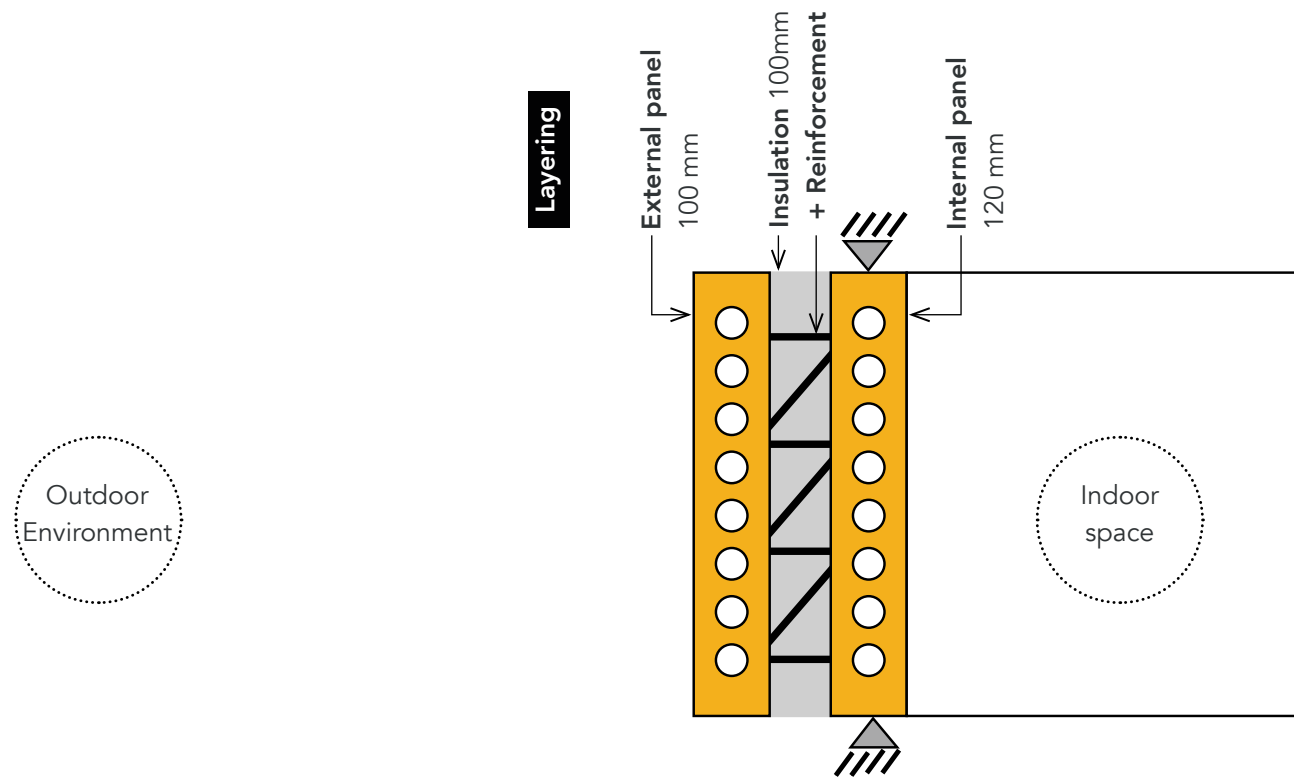
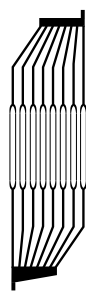


Figure 3.7. Nomenclature of basic proposed facade elements.

### 3.4. CONCEPT OF NETWORK GEOMETRY

To understand, derive and then design a facade system with embedded heat exchange system, studies of similar ideas in different fields were researched. To understand the possibility and feasibility of incorporating the idea and developing the same in the real world scenario, related projects were referred and sorted in terms of their implication for different aspects of designing and realising the project. The study of different cases in relation to understanding the behaviour of fluid in small diameter tubes, the designing of the tubes to minimise pressure drop in order to avoid blockages, possible methods of designing networks for heat exchange system and methods of fabricating them. The three case studies referred in designing the network of the facade are detailed in section 2.5 and mentioned herewith.



**Case study 04**  
Method of heat exchange by convection using water.

+



**Case study 05**  
Pressure management and geometry modification.

+



**Case study 06**  
Water flow in small diameter tubes and pressure management.

With two basic consideration for the design, first a single inlet and outlet to and from the facade panel that connects the outer and the inner facade panels in a loop for exchanging fluids among them and second designing the primary network considering the layout of the tubular network along a typical facade panel with a central opening for window. The first network geometry was inspired from the typical industrial heat exchange tube that does curl to maximise the surface area / length of the tube. The problem with such an design implementation would be a single long tube combined to form a network around the panel which would dramatically increase the pressure drop across the inlet and outlet. Also the single phased connection of the inlet and outlet without parallel branching would be prone to failure if the tube blocks at any segment of the network. A conceptual depiction of these ideas are shown in figure 3.8.

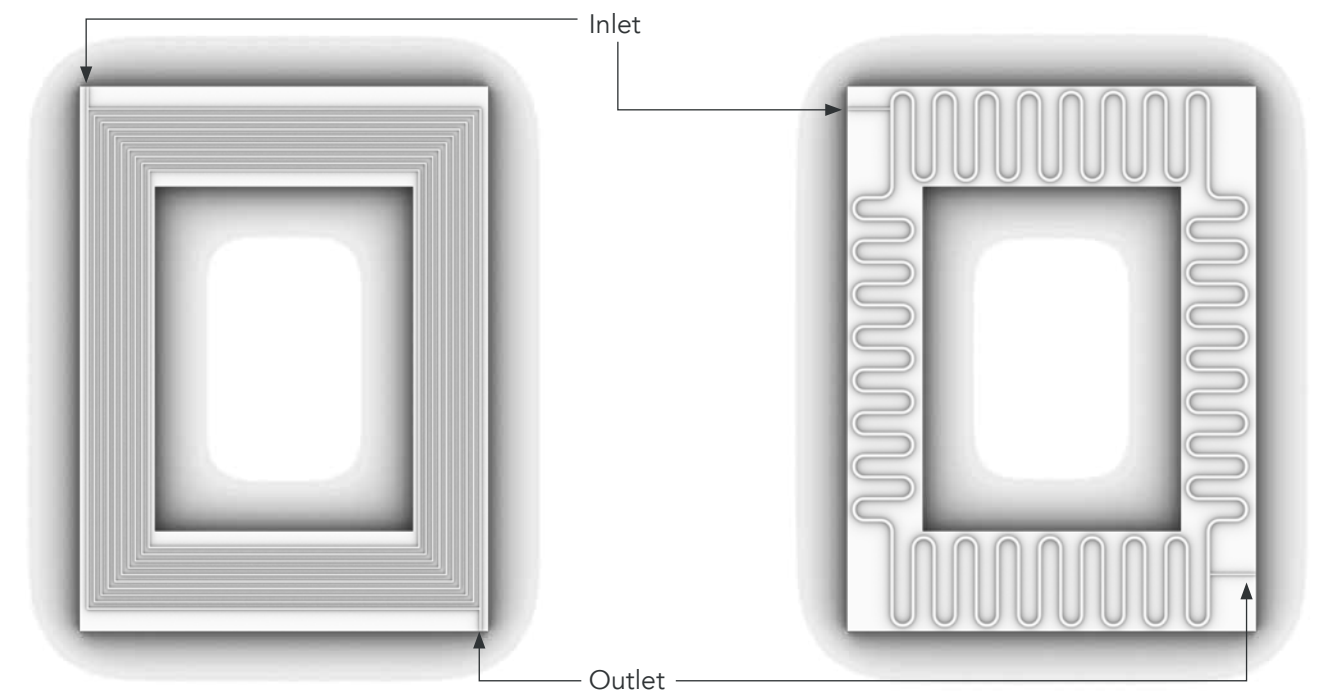


Figure 3.8. Conceptual network with curled tubes inspire by the industrial heat exchange tubes

Figure 3.9. Conceptual network with curled tubes inspire by the commercially available indoor heat radiators.

To overcome the demerits of the first concept, the second network idea was considered to be that of splitting the tubes to decrease the length of the tube and arrangement in a parallel connection similar to that of an heat radiators used in the residences and offices to radiate heat through supply of heated water. This geometry did occupy the very corners of the facade panel, leaving no room for the fixtures to bracket the panel to the main structure. This layout would also significantly compromise the structural integrity of the facade panel considering the structural systems for twin wall facade panel and concrete as a material. The idea of this concept is shown in figure 3.9.

Based on the previous case studies, the branching of the tubular pipes arranged in parallel to each other was referred from the case study 02 and derived to be a network geometry per span of the facade panel, viz, two vertical networks and two horizontal networks combined to form a complete network geometry.

The vascular network of the leaf is one of the most efficient form of fluid flow network in the nature. The pattern division of tertiary veins from the central vein and dimension of the tertiary vein inlets are precisely developed for equal flow of water at every section of the leaf. This ensures equal amount of water to reach at the very tip of the leaf so as the first branch of the tertiary veins (Katifori & Szollosi, 2010). An overlaid diagram of the veins of a leaf is shown in figure 3.10. It is to be noted that the branching of the tertiary veins are arranged in an parallel connection per half of the primary vein of the leaf. These two half along the central axis of the primary vein are connected in series. The network design of this geometry was also referred to that of the network arrangement of the veins of a leaf as done by Alston & Barber (2016).

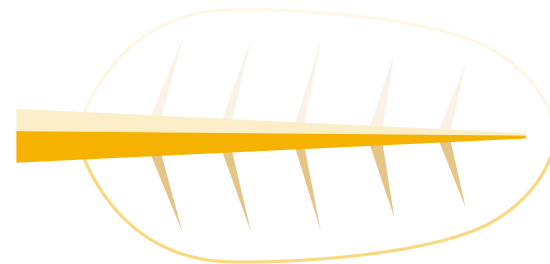


Figure 3.10. Vascular network of a typical leaf (collins dictionary)

The designing of the network along the facade panel with an central opening has been split into the following mentioned 6 steps that describes the evolving function of the network in relation to that of the behaviours of veins in a leaf. The diagram depicting the vasculature of the leaf is exaggerated for better understanding of the referred context.

### Step 01

To describe the derivation of the primary geometry, the leaf was split in half along its primary central vein. As in the figure, it is seen that the central vein does have a tapering geometry which ensures equal pressure distribution of water along the downstream of the network flow. This manifold geometry though which many tertiary tubes are initiated is considered to be one arm of the network which has multiple tubes arranged in parallel manner to each other.



### Step 02

The half split leaf or a single arm of the designed network was mirrored to form the second arm of a single network. At this point of the two parallel geometries are connected in series and configure the same as the network of a full leaf. The central node of the two arms is considered to be the inlet of the network



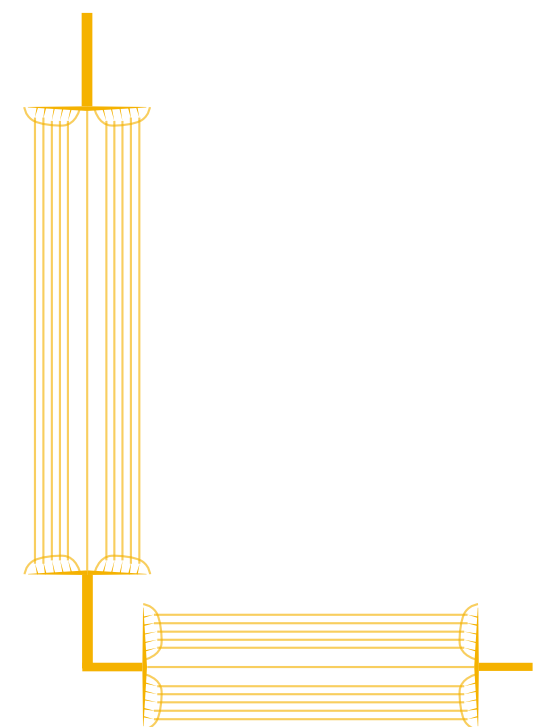
### Step 03

Since the geometry developed in the previous step was not in a closed loop as needed for the designing the tubular network of the facade, the configuration of the two parallel arms were extended and connected with another set of connected geometry with two sets of parallel geometry. This configuration marks the network set for the single span of facade panel which has a set of tubes connected in a parallel configuration with an inlet and an outlet.



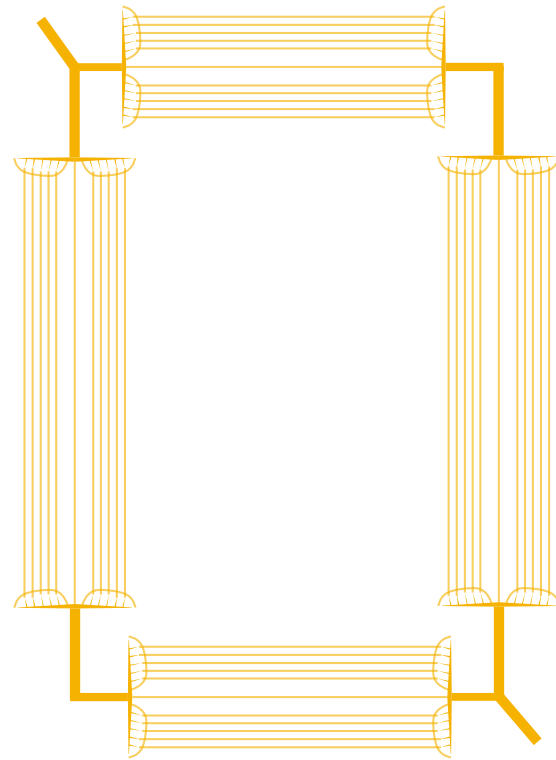
### Step 04

Since the adjacent spans of the facade panel are perpendicular to each other, the outlet of the geometry of step 03 was connected in series to the inlet of another similar geometry but with different tube lengths. By this point we have two parallel networks connected in a series to each other.



**Step 05**

To mark the completion of the network of a single panel, the two network geometries connected in series at two adjacent spans of the facade panel are repeated to form another network similar to the one in step 04 and connected in parallel to each other along the inlet and outlet, which is now a single combined inlet and a combined outlet of the whole network around a single facade panel. A depiction of the same is shown in figure adjacent.



An equivalent flow resistance network dependent on the flow of the fluid in the combination of the parallel tubes, which is referred to as Fluidic resistor network diagram by Alston & Barber (2016), is shown in figure 3.11.

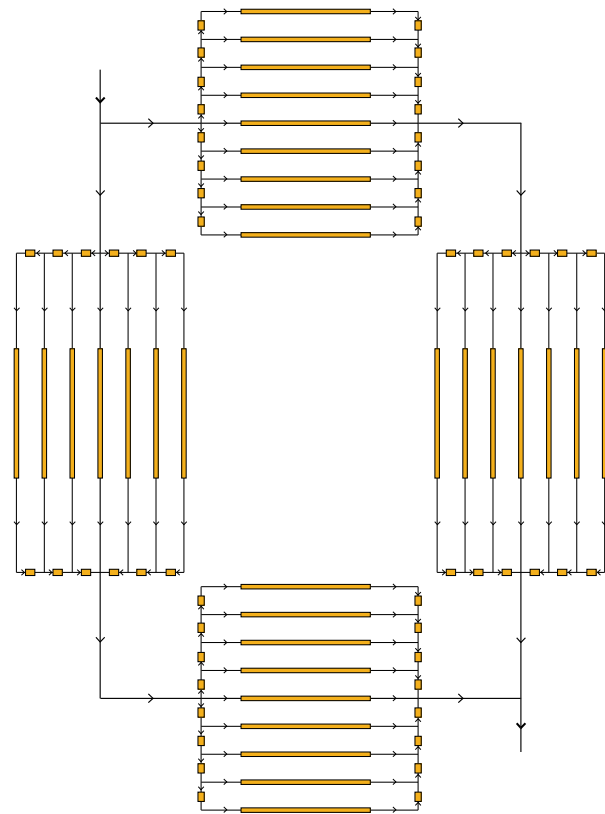


Figure 3.11. Fluidic resistor network of a single parallel system. (Author)

**Step 06**

Since the proposed facade system is that of a heat exchange system between the external and internal panels, the second panel was also replicated with the geometry of the first panel and connect from inlet to inlet and outlet to outlet through an intermediate tank for fluid transfer to develop a closed loop geometry which are in series to each other.

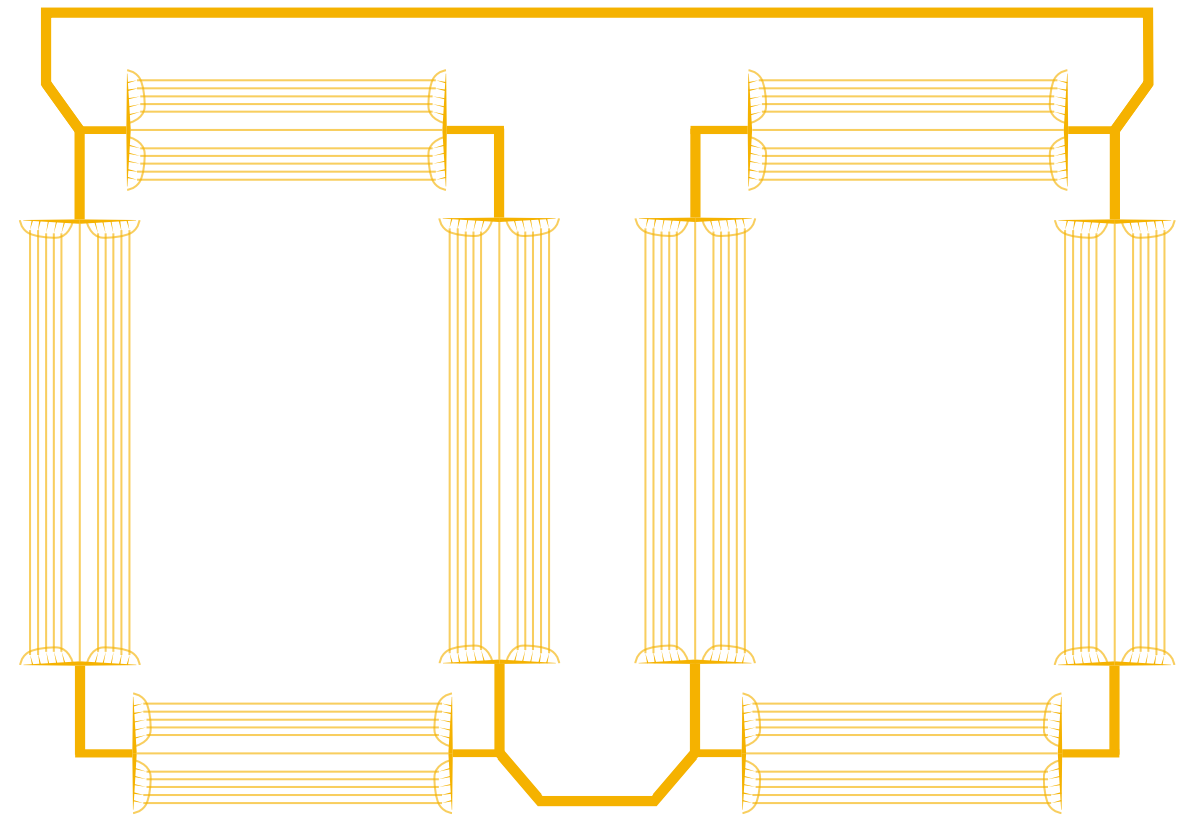


Figure 3.12. Fluidic tubular network layout for a combined facade panel (twin-wall facade panel). (Author)

While the overall layout of the basic tubular geometry of a single panel is designed and combined together to form a network around an opening of the facade panel, there are many different design considerations to be made to make the fluid flow feasible within the network designed, the efficiency of the facade panel in terms of fluid transfer and capturing the thermal energy, behaviour to the loading conditions and its feasibility to manufacture the complex geometry in combination. The successive chapters discuss and detail about these in detail.

## 3.5 CONCEPT NETWORK GEOMETRY

In consideration to the above mentioned criteria to design the panel, constraints from materials, fabrication methods and structural systems are also taken into account which are further discussed, elaborating their interference in the design and considered workarounds. A conceptual network geometry depending upon the discussed criteria was designed as shown in figure 3.13 and arranged in the design domain which would be refereed for the further stages of design and modification. The tubes in the network was designed to be spaced at 20 mm edge to edge as cover for the concrete in lieu of maximum coverage over the facade panel, which would be reconsidered in the following stages. The four nodes of the network were shaped in approximation for slope, depending on the direction of fluid flow with minimum obstruction.

The designed network geometry, although referred to the case studies and influenced for the basic form of a single sub-network, the complete network did consist of various different elements explained below.

### 1. Inlets and outlets:

The inlets and outlets are used to connect the two networks concealed within the mass internal and external facade panels. There would be an intermediate tank between the connections to manage the required flow rate and accomodate the expansion due to the thermal change.

### 2. Sub networks

In response to the typology of facade panel with a central window opening selected, the complete tubular network for a single panel was divided into 4 segments primarily to eliminate long length of tubes and develop joints for maintenance. There was also the consideration by the method of fabrication described in chapter 5, to provide multiple access points to be able to fabricate the facade.

### 3. Tubes and manifold

Each sub network is consisted of multiple tubes, joined by the manifolds. the shape of the manifold was approximated for a slope enough to direct the fluid within towards the nodes. The slopes and shape vary depending on the location of the manifold.

### 4. Nodes

The junction of the sub-networks between the inlet and the outlet is where the nodes are. The shape of these nodes are designed primarily with slopes to direct the fluid to connect the inlet and outlet and at points towards the maintenance outlets and outlets for fabrication.

### 3.5.1 Conceptual network geometry

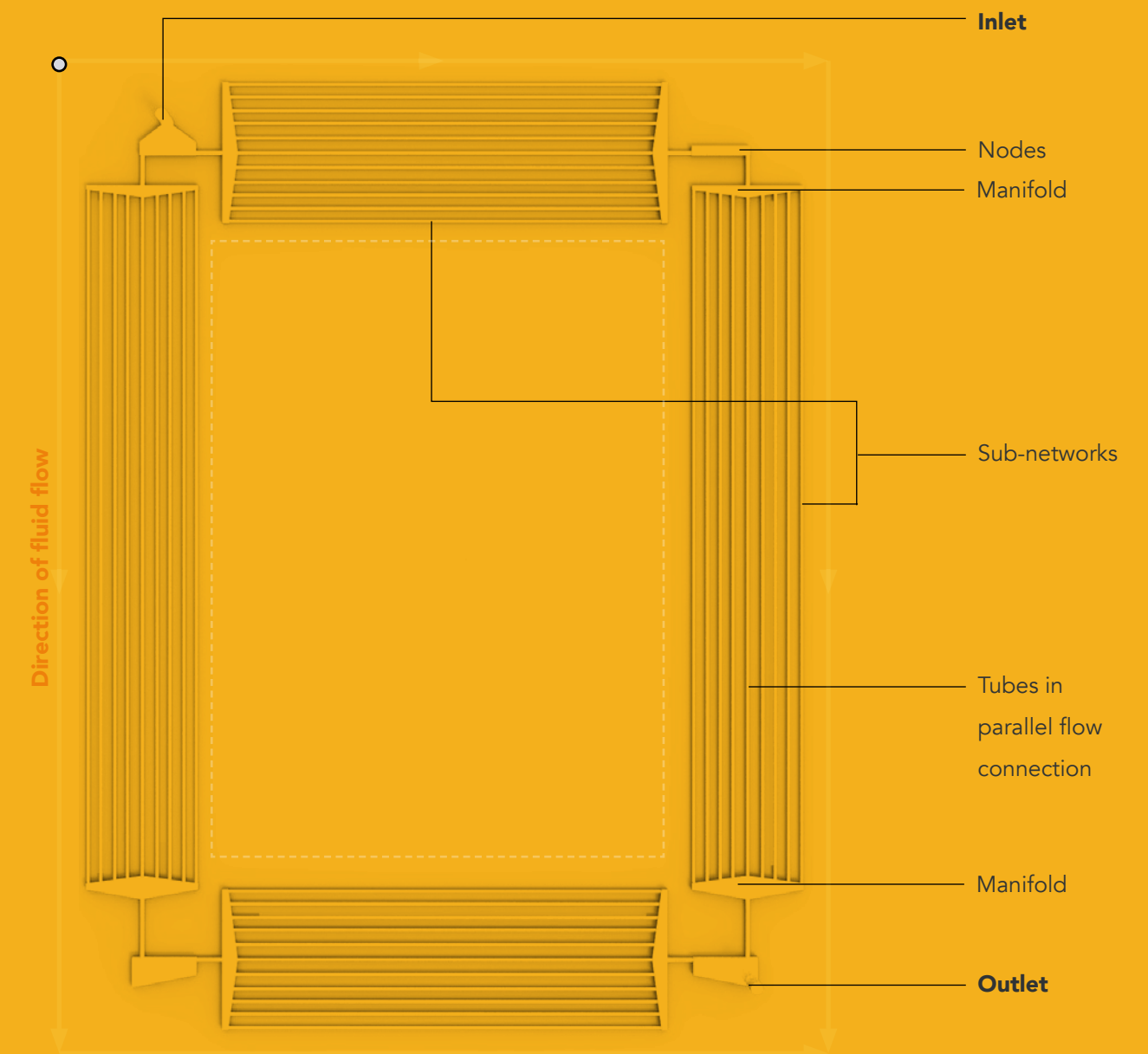


Figure 3.13. Conceptual network geometry considered for further modification.  
Source: author

Volume of network:

**26.3 litres**

## 3.6 CONCLUSION

The integration of a function within the facade panel was decided to be that of an heat exchange system that works in order to exchange fluids from the external to internal panel and vice versa with a layer of insulation in between. The geometry of the heat exchange tube would be inlaid within the mass of the concrete of the facade panels to ensure high thermal encapsulation through the thermal mass of the materials. The various different climatic condition and the corresponding behaviour and response of the designed facade were depicted and elaborated. The specific performance depending on the climatic condition a similar to Delhi around the world was highlighted with an assumption of similar response of the facade.

The design of the network of the tubular geometry was derived from various different case studies some of which were inspired from nature and designed for various different purposes. The amalgamation of the ideas and methods used were refereed from these case studies and developed for implementation in designing the network geometry for this thesis, and learnt from the various different issues and solving methods used to address some specific issues like the blockage of fluid, the pressure drops and problems with working around a method of fabrication specific geometries within a concrete mass.

# 4. DESIGN CONSIDERATIONS

## CHAPTER OVERVIEW

This chapter discusses the general boundary conditions upon which the design methodology of the facade depends upon for the purpose of design framework, simulation, analysis and performance derivation. This chapter also does outline the various design and fabrication criteria needed to be considered for designing the VOID- tubular network geometry as well as the MASS- concrete panel along with combination of these two elements.

## 4.1 GENERAL BOUNDARY CONDITIONS

With the design concept layout decided in the previous section, a number of design boundary conditions were needed to be laid up and analysed, before integrating the concept of heat exchange tubes within the mass of the facade panel. These design considerations started with the location and the behaviour of the proposed panel and integrated heat exchange system in different locations of the world, to that of the type and physical dimensions to accommodate the different fixtures of the facade panel followed by the considerations in fabrication and different design strategies for designing the tubular network and the facade panel for improved performance. These parameters are discussed below.

### 4.1.1 Location and climatic response of the proposed design

The selected location for the purpose and analysis of the design of the facade panel is selected to be in Delhi, India. The reason of selecting the city of Delhi is because of the composite climatic behaviour of the region, which experiences highs of 40 to 45°C during summers and an average of 33°C while lows of subzero to -3°C during winters with an average of 13°C. A dry-bulb temperature mapping by average per month for the city of Delhi is shown in figure 4.1.

#### 1. Temperature

According to the Köppen climate classification, the location of the city of Delhi lies under two sub categories. The first being the hot semi-arid climates (Bsh) with an average temperature of the zone being 18°C that consists of very highs of 38-40°C and lows of 4-25°C. The second climatic classification zone is the humid subtropical climate (Cfa and Cwa) which is experienced during the monsoon season. While the average high temperatures does decrease during the monsoon for Delhi, the climate shifts towards hot and humid. With such a condition, the designed system would have a varying range of temperature difference during the days and night per season and prove for the various possibilities of heat exchange that the system can suffice for. The regions that fall under the category of Bsh, Cfa and Cwa are shown in the figure 4.4, where the behaviour of the panel will be similar to the one simulated and designed for in the zone of Delhi with some minor variation in response to the local climatic context. The designed panel insulating performance would depend on the maximum average range of the outdoor temperature and assumed to be of 40°C.

#### 2. Solar radiation

To analyse the efficiency of the facade panel in response to the climatic condition of the locality, the solar radiation on the designed panels needs to be minimised during the scorching heat of summers to maintain an effective balance of heat exchange between the inner and exterior environment. In reference to the charts

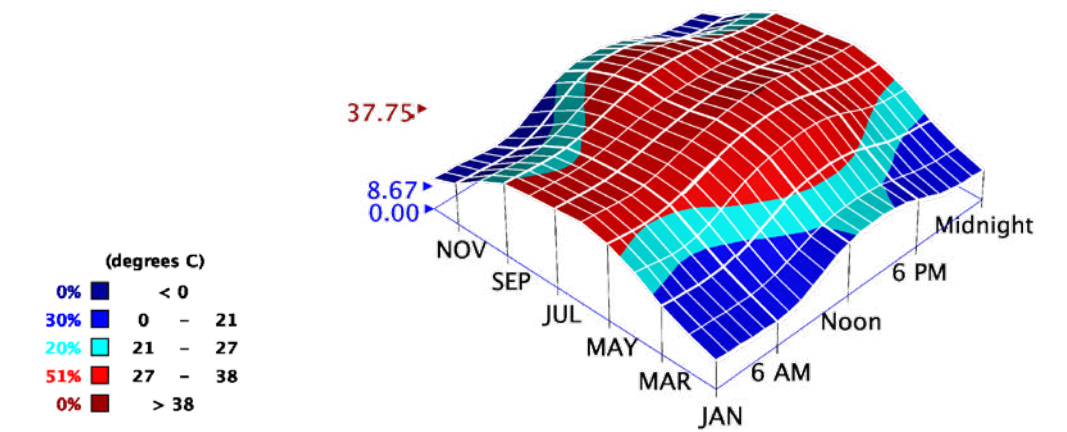


Figure 4.1. Dry bulb temperature by monthly average (author - climate consultant 6.0, Delhi weather file)

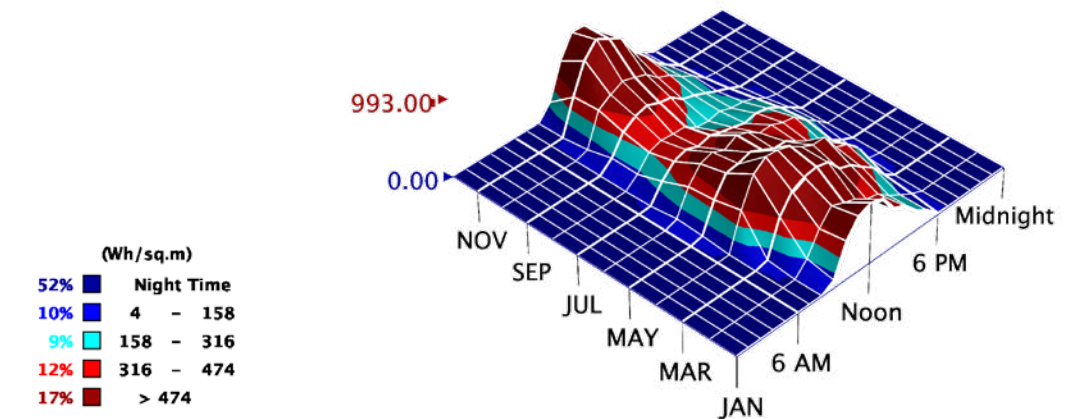


Figure 4.2. Direct normal radiation by monthly average (author - climate consultant 6.0, Delhi weather file)

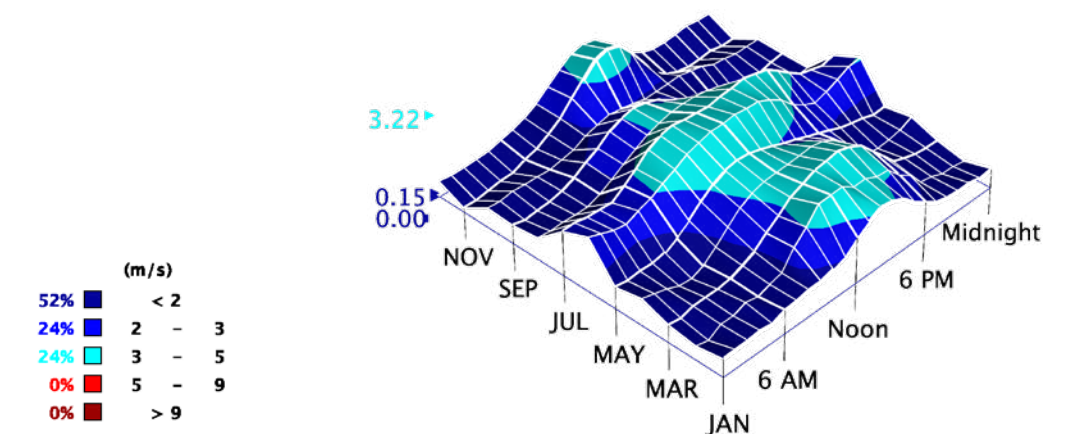


Figure 4.3. Wind speeds by monthly average (author - climate consultant 6.0, Delhi weather file)

plotted by the climate consultant, it is evident that the solar radiation of Delhi (figure 4.2) during the summer months of March to June are high and needs to be addressed in the design of the facade panel to eliminate the direct solar heat. While in winters this phenomenon needs to be complied for maximum radiation on the panel to absorb the solar heat and exchange the same to the inner space. As studied from the solar radiation graph of Delhi, the relatively high solar radiation during the winters from November to January can be taken advantage of orienting the geometry for the winter sun and maximising the surface area.

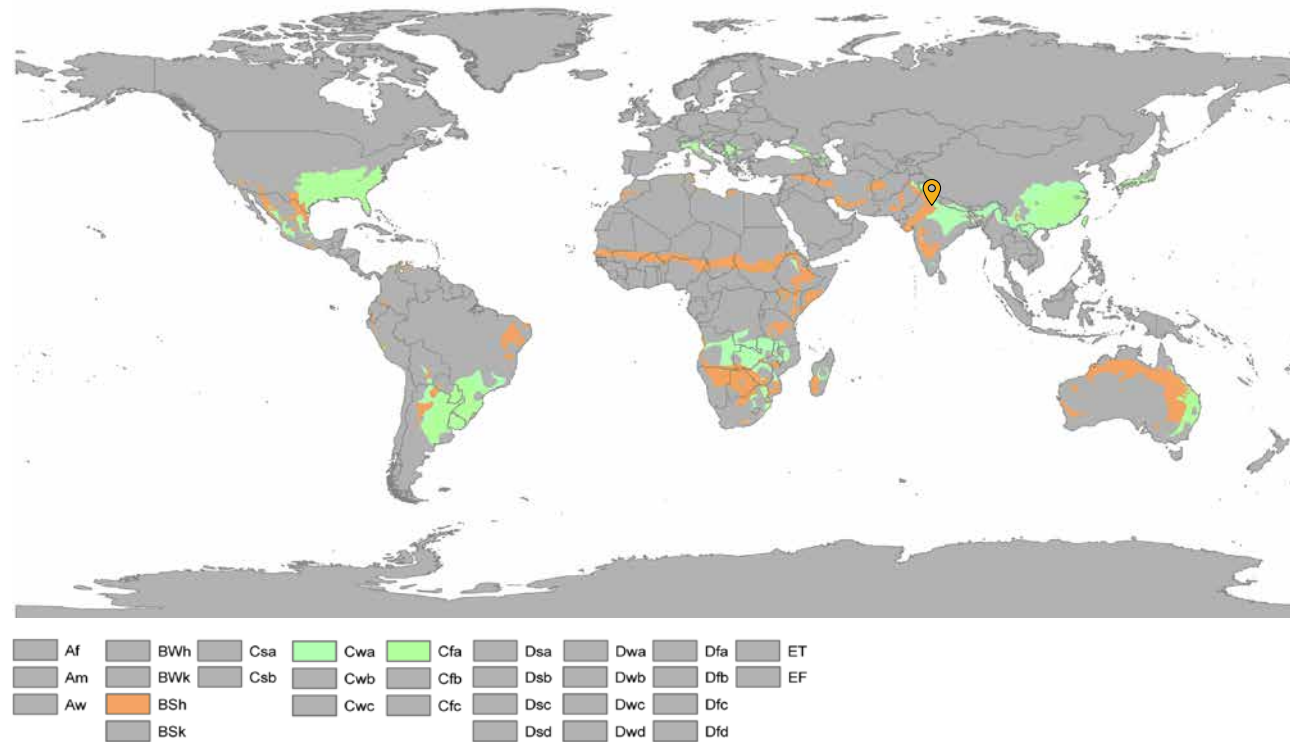


Figure 4.4. Bsh, Cfa and Cwa climatic zones under Köppen climate classification. Source: Wikipedia.

### 3. Wind

The average wind speed in Delhi as shown in image is well below 5 m/sec with highest wind gusts recorded to 10 m/sec by bluebus.net. But the fact of consideration that the acceptance of the design system could be done in places with high speed wind loads and needs to be designed for the same. The maximum wind speeds during a cyclone in a coastal region of India could be measured as high as 39 m/sec (Cini, & Sifton, 2012) and the facade panel designed in this thesis was done in consideration to the maximum possible wind loading for safety purpose and verify the possibility of designing of the panel for locations that experience such wind loads. Although this variation can be accommodated for facade panels customised for a very specific building project in a specific location and the parameters could be modified.

**Hypothesis:** South oriented facade, External temperature considered 40°C with the wind speed considered to be of 39 m/sec.

## 4.1.2 Facade typology

The various different types of facade panels and the needed preference has already been discussed in the section 2.1 of the second chapter. The priority of making the facade modular, future proof and segregated from the primary structure of the building for upgradation of the structure for long service period and to meet the future needs without rendering the complete building useless and need to be taken down solely because of the constraint by facade. These parameters lead to chose a non-load bearing facade panel. The need to segregate and insulate the internal and external facade panel to meet the stringent norms of the locality of India to be within 0.64 to 0.44 W/m<sup>2</sup>K and below that, a twin wall facade panel was selected, with an configuration of the fixation as shown below in figure 4.5 & 4.6. This will also ensure the maintenance of the facade if the system of the facade breaks down. In lieu of the same the fixation of the facade panel was then limited to a 4 point bracket system.

**Hypothesis:** Non load bearing twin wall facade panel with four point bracket system

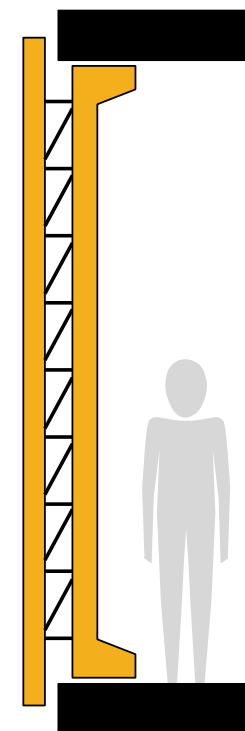


Figure 4.5. Typical section of twin wall system Source: author.

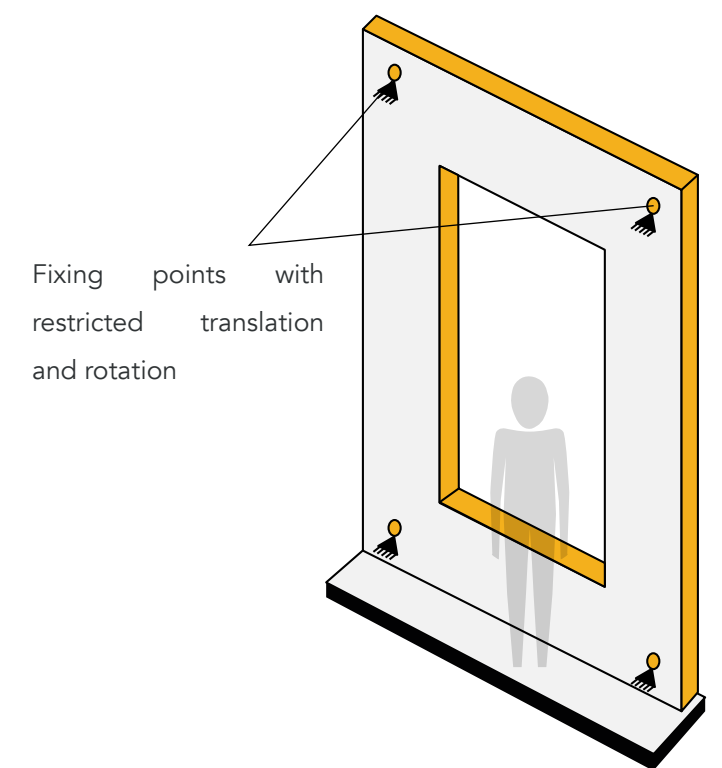


Figure 4.6. View of facade with 4 fixing points and constraints. Source: author.

### 4.1.3 Window to wall ratio

As studied by Didwania, Garg, & Mathur (2011) for above the ground floors in an office typology, the window to wall ratio has been agreed to be on average as following:

For single glass with an U-value of  
**5.6 to 6.1 W/m<sup>2</sup>K**

For double glass with an U-value of  
**3.3 W/m<sup>2</sup>K**

East **15%** | West **10%** | North **30-40%** | South **10%**

East **25%** | West **20%** | North **40-60%** | South **15%**

It was noted that the study done was in 2011 and the advancement and availability of higher thermal resistive glass in the market of India, the U-values and the performance of the openings will permit for higher WWR of the facade. While considering this fact, as an assumption, the WWR of the designed facade panel was assumed to be as 40%, but to be noted that on a South facade. As explained in the previous chapter, this was done on purpose to minimise the opaque region of facade and simulate for the solar radiation value and analyse the change in the final design, which or else would be more efficient in the real world scenario. It is also to be considered the end result of the dimensions fixed for the WWR may deviate depending on the fixtures and the final geometry simplification.

Figure 4.7 shows the dimensions of the facade panel that has been considered for the further stages of designing, simulating and modification to be considered for the fabrication.

**Hypothesis:** 40 % window to wall ratio with double glazing for south facade and U-value of glass considerably lower than 3.3 W/m<sup>2</sup>K.

### 4.1.4 Room size and energy requirement

The room size for the purpose of further consideration in determining the needed heat load was considered to be of width 3.00 m, depth 4.50 m (4.38 m clear) and a height of 4.00 m (without raised flooring and false ceiling) and 3.20 m (finished). This size was referred from the National Building of India (BIS, B. o., 2016) and considered for the minimum space occupancy of 11 m<sup>2</sup> by 1 to 2 person office space. While the simulations run are considered without radiation and convection to broadly classify the efficiency of the panel, the indoor heat flux was approximated to act as the heat generated by the occupants, appliances and the mechanical sources in the indoor space.

The energy required by a typical office space in India is mentioned by Singh, Sartor, & Ghatikar (2013), as the Energy Performance Index of an Indian office on average as 202 kWh/m<sup>2</sup> per annum (figure 4.8). This amounts to 55.3 W/m<sup>2</sup> per hour, in a shift of 10 hour operation. Of this a maximum of 40-60% accounts for HVAC.

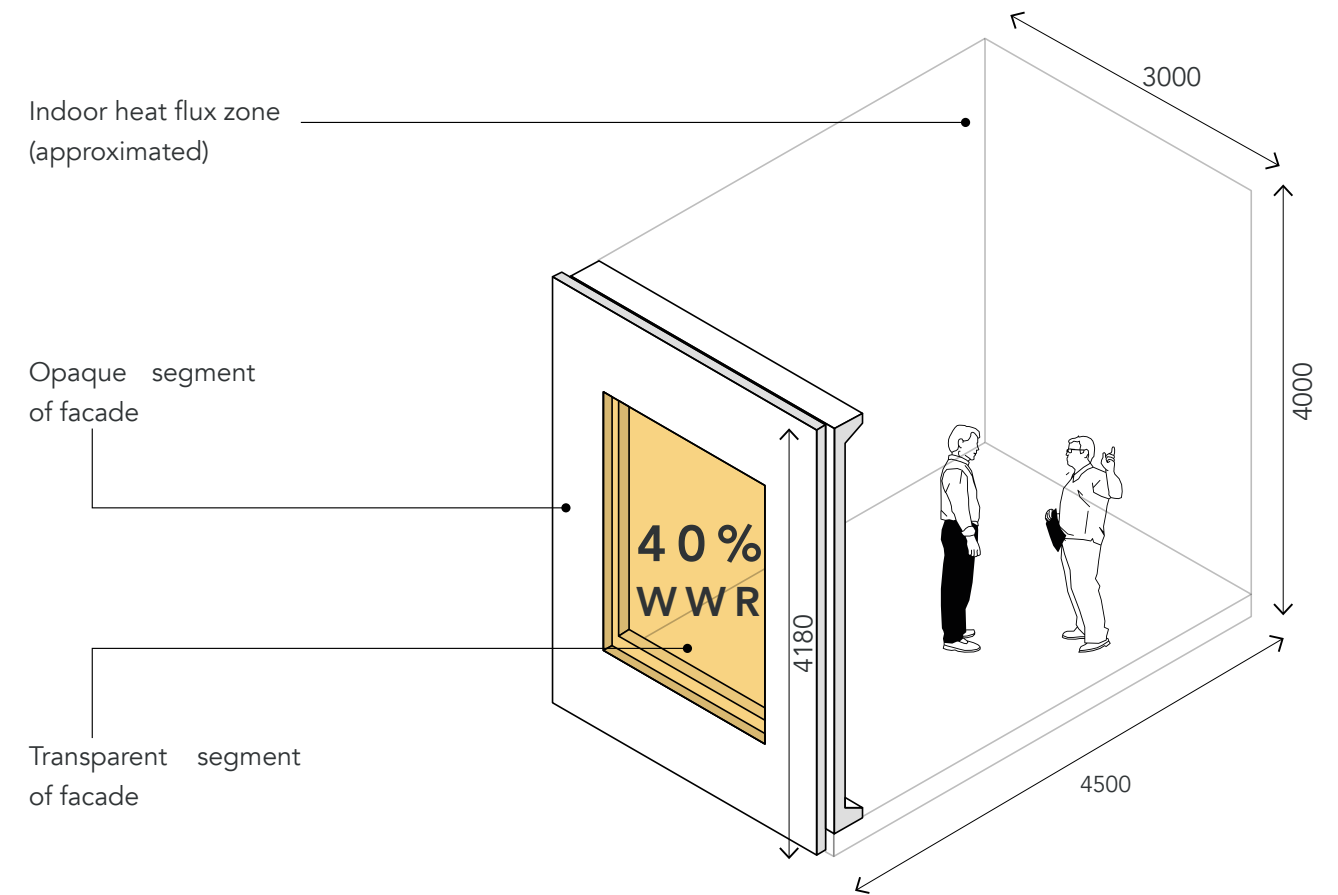


Figure 4.7. Dimensions of the facade and indoor space considered for design and evaluation.

Hence the designed system must compensate for the energy requirement of 33.18 W/m<sup>2</sup> per hour, in a shift of 10 hour operation.

**Hypothesis:** 3.00 m X 4.50 m x 4.00 m (ht) of room space considered for evaluating the effectiveness of the facade with Energy Performance Index of 33.18 W/m<sup>2</sup> per hour, in a shift of 10 hour operation.

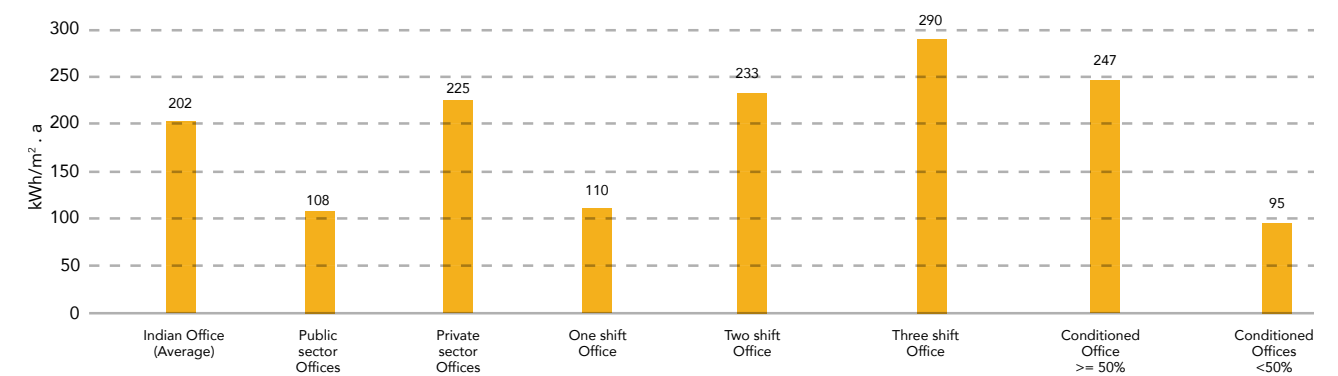


Figure 4.8. Energy Performance Index using site energy data for various commercial activities in India. (Singh, Sartor, & Ghatikar, 2013)

## 4.2 FABRICATION CRITERIA

In reference to the previously mentioned boundary conditions, the material and the fixtures used, the method of fabrication and the structural behaviour of the facade panel in combination do define the location and orientation of the tubular network to be embedded within the concrete facade panel. The considerations needed to be made for the cohesive behaviour of the facade panel as a mass and the tubular network as a void are described below and detailed in section 4.3.

### 4.2.1 Materials and fixtures

Depending on the material used as concrete, the specific mixture and composition of the material does matter in terms of its strength, workability and needed cover for designing and modifying the network within the facade panel. The type, load carrying capacity and fixture of the facade bracket also matters in defining the geometry of the internal facade panel. The geometry of the sill level of the external and the internal facade panel are determined by the type of window and the design of the fixing of the window (figure 4.9). To allow room for the external sill of the window to be able to be complaint for water runoff during the rain, accommodation of special fixtures like water pump and their accessibility, fixing and maintenance of the facade panel etc., the design needs to be informed by the mentioned entities and updated accordingly. The schematic image below shows the effect of different fixtures upon the primary design considerations.

**Hypothesis:** Considering constraints by material properties and behaviour of fixtures with design

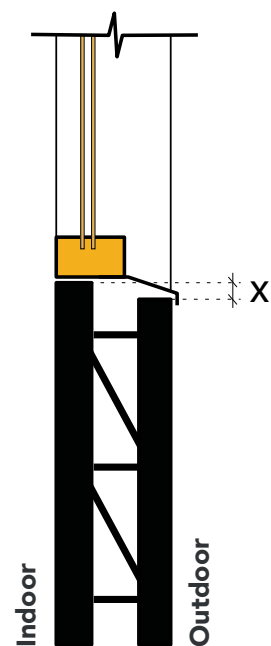


Figure 4.9. Section showing the shift in sill of the external panel in response to the window section (sill plate) fixture. (Author)

### 4.2.2 Structural system

In consideration to the material interaction with the design and addition of various different fixtures, the behaviour of the combined design keeps evolving along with the structural behaviour of the facade panel. The evolved design then needs to be complied for the dead loading of the facade as well as loading by the environmental behaviour as considered in the previous section 4.1.

To segregate the external facade panel from that being in contact of the main structure, reinforcement dowels are needed. The location of which is determined by the structural analysis of the facade system in combination and has been detailed out in section 6.1. The inclusion of these dowels in the facade system does demand for a room and redesign of the tubular network (figure 4.10 & 4.11). The facade panel would also require a reinforcement mesh for the integration of the material to the support type and loading on the panel. This mesh will also govern segments of the design of the network and limit the design. In consideration to a sustainable aspect and the combination of the ideas of the void network along with the slim profile of the facade system with complex detailing does demand for alternate materials for reinforcement rather than steel to be incorporated in the design. The structural system will also govern the domain allowed for modifying the geometry for maximum efficiency by modifying the external surface to comply for radiation requirement in summer and winter as mentioned in section 4.1, in response of the location and climatic condition considered for the design implementation.

**Hypothesis:** Consider constraints by reinforcement dowels and mesh along with the boundary conditions of loading and supports

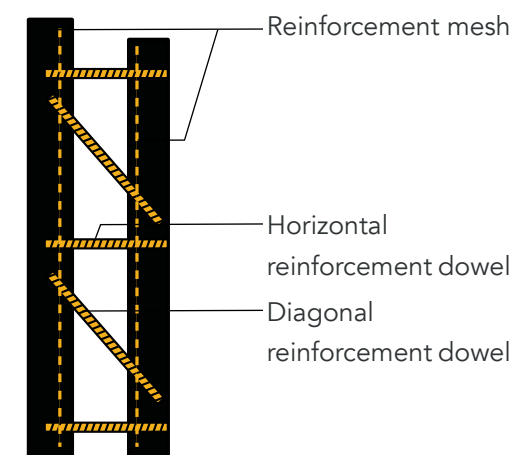


Figure 4.10. Section showing the connection of dowels between internal and external panel and domain of the mesh reinforcement in section

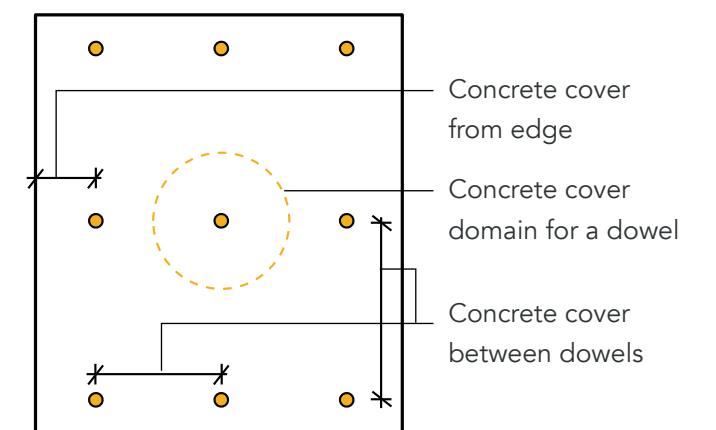


Figure 4.11. Elevation of zoomed in domain of constrained region around the dowels for concrete cover. (Author)

## 4.2.2 Method of fabrication

The method of fabrication has an upper hand to constrain the complete process of design, from the designing of voids comprising the tubular network geometry and other fixtures in collaboration to that of the appearance and feasibility of the facade panels. The limitations and behaviour of the materials used for the form work by the specific method of fabrication also govern the design and the final outcome. Since the complex nature of the void tubular network within the concrete panel is accessed by this junction of the project, a method of fabricating a form work that can be lost after casting the concrete around the same so as to have a void geometry built within the mass of facade was chose to be that of an lost wax fabrication method as already speculated as an proposal for the convective concrete project by Omebere-Iyari & Azzopardi (2007).

The method and specifications of fabricating the form work and casting of concrete has been detailed out in the section 5, after the various different constraints mentioned in the sections above are taken into account and informed for the network's geometry adaptation. The image below shows an conceptual representation of the proposed method of lost wax fabrication.

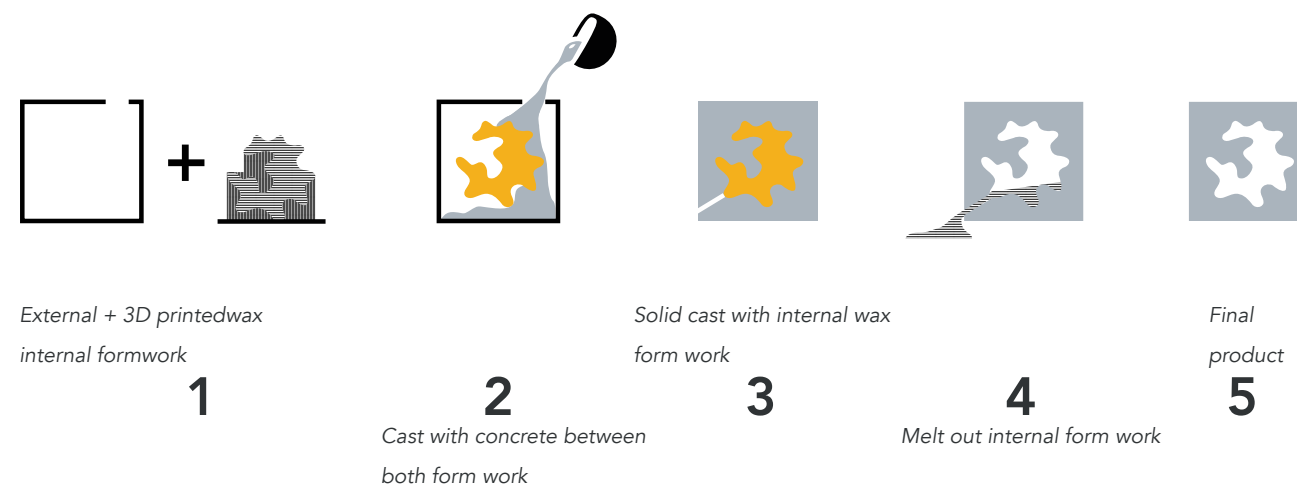


Figure 4.12. Conceptual manufacturing process for lost wax fabrication for complex inlay shapes. (Author)

## 4.3 DESIGN CRITERIA

Referring to the focus parameters defined, the design criteria to define and derive the geometry of the flow pattern and the panel in relation to different goals to achieve and constraints in the method are outlined in the following which are then further elaborated in the further stage of computation program.

### 4.3.1 Medium of fluid and concrete as the mass

The medium of fluid selected for this research was considered to be water. The abundance of the material coupled with the high thermal mass and thermal conductivity of water as a fluid in comparison to that of air was preferred. Water also has higher thermal mass in comparison to that of concrete the panel would be composed of and can hence help in absorbing and transferring the heat captured within (Table 4.1). The related simulations and property consideration for CFD are referred to the behaviour of water as a fluid unless specified. Water could be replaced with other high thermal fluids or phase changing materials in the future simulations and modification could be carried out in accordance.

**Hypothesis:** Water as the medium of fluid for heat exchange.

	Water	Air (250K)	Concrete	Brick	Aircrete
Specific heat capacity (J/kg K)	4200	716	1000	800	1000
Thermal conductivity (W/mK)	0.60	0.024	1.13	0.73	0.15

Table 4.1: Comparison of specific heat capacity and thermal conductivity of potential materials. Source: <http://www.greenspec.co.uk/building-design/thermal-mass/>

With a goal of maximising the solar heat capture, water serves as the best medium with very high specific heat capacity than air. Concrete as a mass has higher specific heat capacity than brick helping in trapping more heat and transferring it to the water. To conduct efficient transfer, the thermal conductivity of concrete is much higher than brick or aircrete as was hence a perfect match with water as a fluid for the facade panel

### 4.3.2 Type of Flow

Water within small diameter tubes could cause complex movements of the fluid coupled with the air within. The development of air pockets could also be a resultant of evaporation or developed wearing over time. Two phase flows are eminent in heat exchange systems which account for inefficient way of fluid flow and heat transfer. Two phase flow could develop different flow patterns that may increase the pressure difference and friction within the tubes (Omebere-Iyari & Azzopardi, 2007). These properties of flow patterns are usually

observed in the situations of turbulent flow of water. To eliminate the same, the water flow within the tubes are needed to be of laminar characteristics. The laminar flow of water is dependent on Reynold's number of the setup. The factors affecting the flow type of a setup are

$\rho$  = density of the fluid,

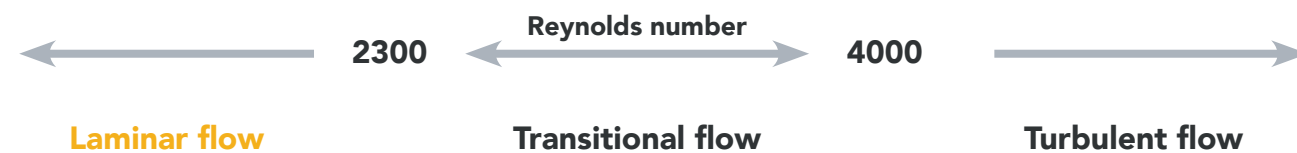
$v$  = velocity of the fluid,

$\mu$  = viscosity of fluid,

$L$  = diameter of the tube.

While the density and viscosity of water are fixed for the geometries to be analysed, the velocity and the diameter of the tubes do play a role in determining the flow type of the medium.

**Hypothesis:** Modify geometry for laminar flow of water.



### 4.3.3 Flow resistance

With the division of the tubes in the geometry, the addition of extra segments of tube transfer may result in varying resistance values of the tubes. The varying resistance will result in increased pressure drop across the tube segments of the network as the distance between the inlet and the outlet node varies. The water resistance of the tubes further away from the inlet are supposed to be equalised to that of the centre tube in direct line of the inlet and outlet to maintain an equal flow of water across the tubes of the network (Alston & Barber, 2016). The method of achieving the equal resistance across the tubes will be discussed in detail in section 7.3.

**Hypothesis:** Evaluate tube diameter to equalise flow resistance.

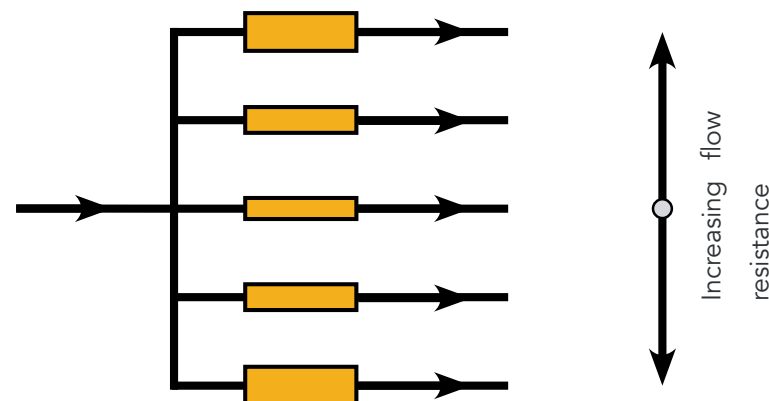


Figure 4.13. Diagram showing the effect of increasing flow in parallel connected branched tubes. (Author)

### 4.3.4 Volume variance

The exchange of fluid between the front and the back panel enables the heat exchange of the system. Higher the amount of water within the network of each panel, higher is the amount of heat exchange and increased efficiency of the system. To maximize the volume of water in the network the geometry needs to be altered within the panel while complying with the constraints of different domains, like the material used, the structural stability, the fixtures and the manufacturing methods. The strategies used to maximize the volume within the defined boundaries are discussed in detail in the section 7.4.

**Hypothesis:** Maximise volume of water within boundary conditions.

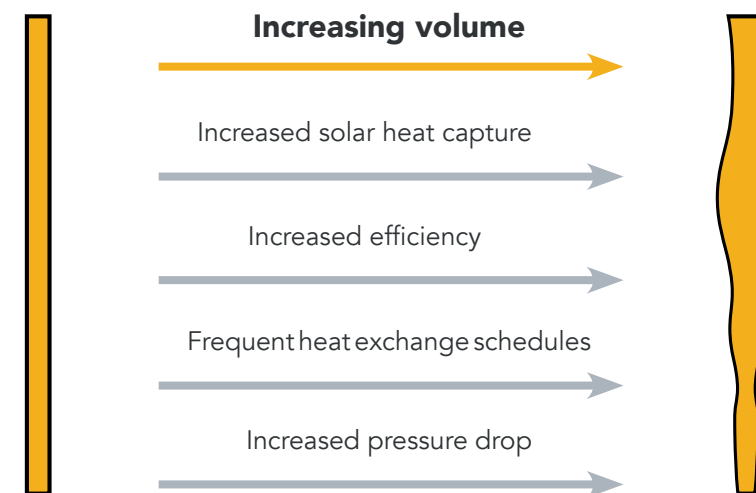


Figure 4.14. Effects of increasing the volume of the heat exchange network per panel. (Author)

### 4.3.5 Pressure drop

The pressure drop of a fluid in a specific geometry, circular tube in this case depends on the diameter, length of the tube and the velocity of the fluid in the tube. This also depends on the flow type of the liquid or the Reynold's number of the setup. With a higher pressure drop the volume of water at the inlet and outlet may vary developing blockages within the geometry. Also an increased pressure drop may tend to decrease the flow rate between the two panels increasing the transfer time and thermal loss in the process. This can also demand for higher amount of mechanical energy needed to conduct the transfer of the liquid. With the decrease in the pressure drop across the inlet and the outlet of the geometry, a uniform smooth and blockage free movement can be ensured between the panels. This will also ensure minimum amount of mechanical energy needed to pump the water if needed. The management of the pressure drop needs to be done at different segments of the geometry viz., tubes, nodes, inlet and outlet to achieve the needed decrease in the value. The pressure drop for a geometry may differ depending on the nature of the flow being downstream or upstream. To ensure the same different strategies are discussed in section 7.3 in detail for the different segments of the facade panel.

**Hypothesis:** Minimise pressure drop by modifying geometry

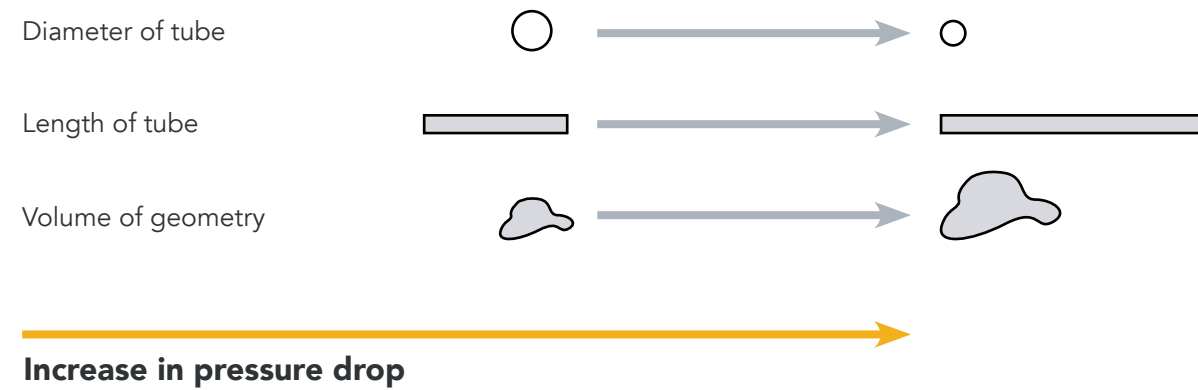


Figure 4.15. Effect of different factors on pressure drop. (Author)

### 4.3.6 Shape modification

Apart from the methods to minimise pressure drops in the tubes and unifying the geometry for minimum pressure drop, there are other complex geometries involved in the network which need to be manipulated for improved performance. In conjunction to the above mentioned strategy to minimise the pressure drop for the geometry/s, shape optimization of the nodes to further improve the geometry and hence the efficiency of the system. This can be done by analysing the pressure mapping and the velocity pattern of the geometries at different segments. The method of achieving the most optimum shapes is discussed in chapter x by a method of shape optimisation, with a goal to achieve the minimum possible pressure drop depending on the geometry and the flow of the medium while constrained with various different boundary conditions.

**Hypothesis:** Shape optimisation of nodes

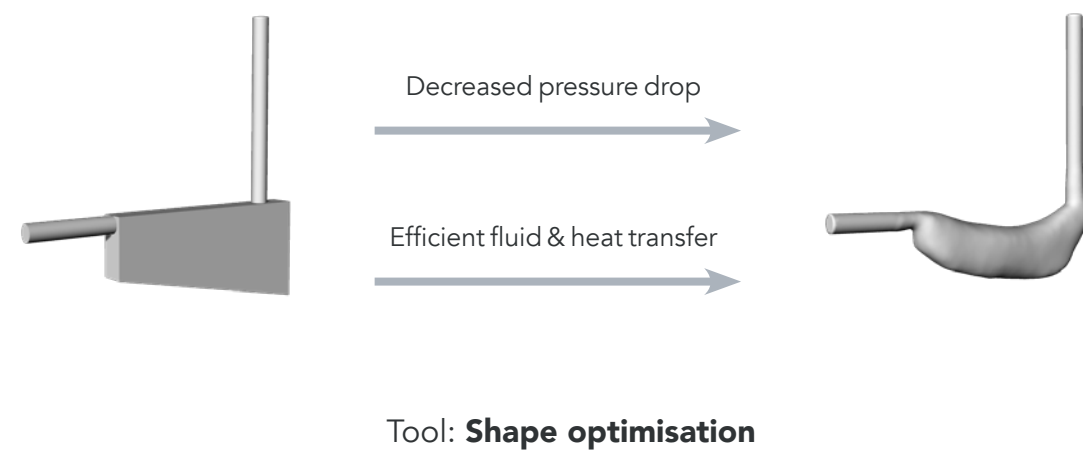


Figure 4.16. Effects of applying shape optimisation on pressure drop. (Author)

### 4.3.7 Heat transfer - Geometry

The conduction of heat from the outer environment to that of the concrete mass of the facade panel and further to the water in the tubes needs to be as high as possible during the winters and controlled during the summer to avoid over heating. This can also be considered in terms of the local climate conditions of a hotter or cooler region. Since conduction is directly proportional to the surface area of the material, increasing the surface area of the outer panel surface will ensure higher transfer of heat from the outer environment to the water tubes within during winter and vice versa from inner panel surface in the summer than conventional flat surface of the panels. This can be achieved by modifying a specific geometry at micro level that complies with high radiation in winter and self shading in summer and adding it on top of the panel which will increase the mass of the panel, or subtracting the geometries from the panel while compromising on its structural stability. To ensure the optimum solution to this, topology optimisation of the panels could prove a valid ground to increase the surface area as well as ensure structural stability of the panel. The method of topology optimisation and simulation for thermal performance of the panels can prove the stance of proving and benefiting both grounds with one method of solution and are discussed in detail at section 7.7.1.

**Hypothesis:** Maximise surface area with reducing mass by topology optimisation

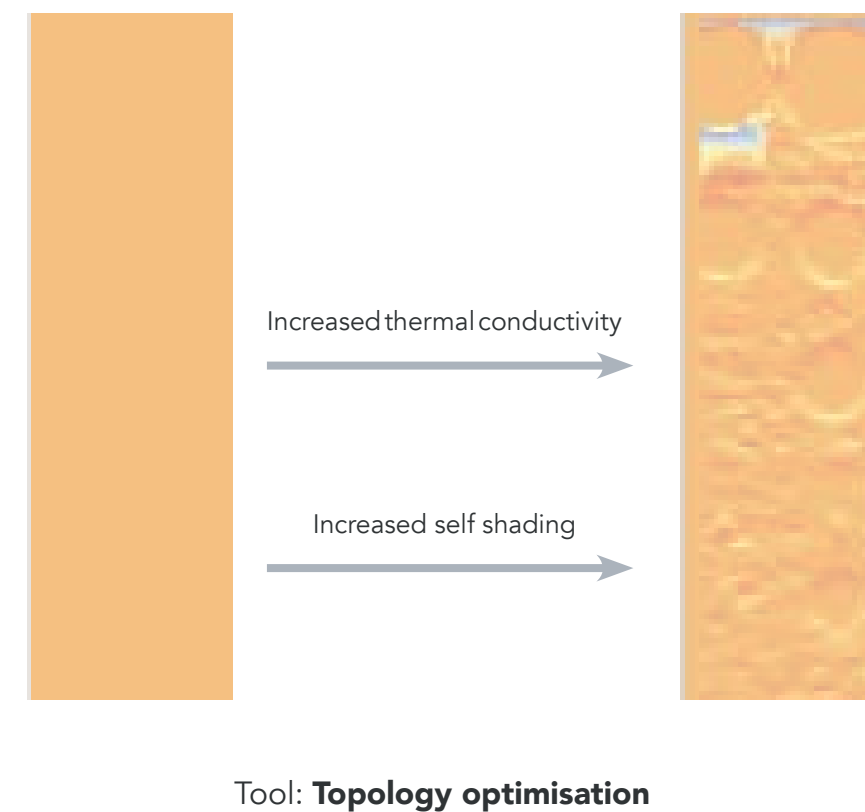


Figure 4.17. Segment of geometry showing effect of topology optimisation.(Author)

### 4.3.8 Heat transfer - Insulation

The energy performance of a building highly relies on the insulating behaviour of its skin. The evaluation of the behaviour of the skin/ facade can be divided into the fenestration and the opaque regions. The lower is the U-value of the system, higher is the thermal performance of the facade, and to ensure the same the focus was shifted onto the materials used in its construction. The elimination of steel from the whole composition of the panels does ensure minimised thermal bridges (figure 4.18) and low carbon footprint. This also does help in reducing the overall mass and the thickness of the panel. The comparative analysis of a traditional system of twin panel to that of the proposed twin panel with required modifications and materials are discussed in section 7.8. Higher insulating performance of the facade also ensures segregation of the outer and inner panel that minimises heat transfer in between them and increases performance of the heat exchange system by isolating the inner and the outer environment. The performance of the system also needs to be complied with the local building guidelines and green building laws to ensure quality, sustainable, responsible and future proof construction.

**Hypothesis:** Choose reinforcing materials with low U-value and high insulation filler.

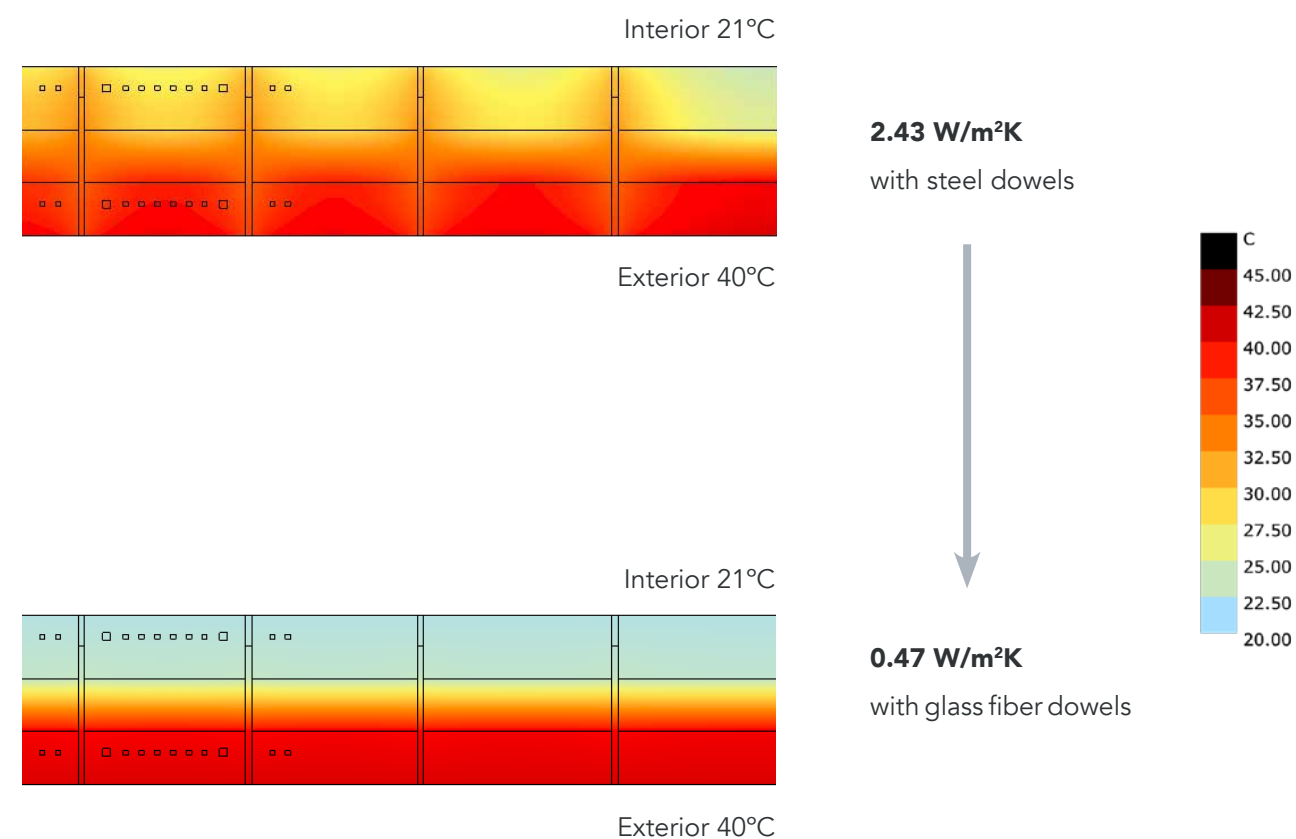


Figure 4.18. Thermal heat transmission analysis of a typical twin wall system with steel dowels (left) and non metallic resin based dowels (right). (Author, Therm 2D)

## 4.5 CONCLUSION

The location of the design was selected to be based in a composite climate and Delhi, India was selected. The wide range of climatic condition exhibited in the location of Delhi would expose the designed facade panel to deliver the behaviour under various different climatic condition and not only specific to a dominated climate type. The climatic loading conditions were considered to be the that of an extreme climate, through which the design would sustain for harsh climatic condition for any region it is deployed to.

Along with this the criteria to satisfy the method of fabrication and the design derivation of the tubular network with maximum possible performance of the facade panel in combination was laid out. These aspects are designed, analysed, evolved and simulated per part in the chapters ahead.

With the basic design parameter discussed at the start of this chapter, a sub research question was answered.

**Sub research question answered:**

*Which parameters and constraints need to be addressed considering the application typology of an office or mixed-use building for a specific location?*

This page is intentionally left blank.

# 5. DIGITAL TOOLS & METHODOLOGY

## *CHAPTER OVERVIEW*

This chapter discusses the various different software chosen to perform various different tasks, the constraints of the software, the setup used for the simulations and processing, the method of validation of the software and the followed work flow. This chapter also mentions the workarounds/ substitutions considered for the limitation incurred by the software.

This chapter elaborates upon the method used to digitally design and simulate the selected design to achieve the desired goal of the facade system. The method used for this project was a target-based strategy which can be broadly classified under three aspects viz., designing, optimising and performance. Each of the design goals were considered for designing with optimisation to maximise the possible result, independent of the other and the performance of the resulting design was analysed by simulations.

The used of digital tools to be assisted for the design does assist in the physical analysis of the setup and also does minimise the use of experimental resources maximising efficiency and probability of success. The use of digital methods can also help in analysing multiple different geometrical possibilities before filtering the best solution. The limitation of physical setup are also at times simulated and verified using the digital tools that can perform close the physical environment. Although these digital tools do come at a cost of their individual limitations which will be discussed further in this chapter.

## 5.1 TARGET BASED STRATEGY

With possibilities of various different geometries, combinations and strategies, the initial designs and considerations were based from the literature and case studies mentioned in chapter 2 and 3 respectively. The initial designs were then targeted towards achieving specific goals while modifying the geometry. These strategies used did define the methodology of digitally deriving the geometry of this project.

The designing of the heat exchange function integrated twin wall facade was basically targeted for two goals to maximise its efficiency. The first goal was targeted towards designing the void tubular network within the concrete facade panels for maximising the volume of water and minimising the pressure drop across the tubular network and secondly optimising and modifying the concrete mass to maximise the heat entrapment within, in order to maximise performance efficiency of the combined facade panel. After the designed goal were achieved in the form of an optimal geometry with maximum possible performance efficiency, the derived geometry was simulated for its performance value that concludes the design methodology.

Some design strategies were analysed with various options before the geometry did fulfil the target, while some were fixed to a goal that resulted to one optimal geometry only. For example applying the design boundary conditions to determine the most efficient geometry of the concrete mass to minimise material use by topology optimisation did result in one optimal result. While the strategies specified here are broadly classified into two types, these strategies are individually comprised of various considerations, viz., structural behaviours, material behaviour, fabrication method etc., and constraints viz., fabrication, software etc. While these all considerations and constraints will be elaborated in the further chapters, the following segments will elaborate upon the digital tools and the methodology, its constraints, workarounds and the setup used to achieve the target. A schematic diagram of the digital methodology has been depicted in figure 5.1.

The simulations carried out to design, optimise and verify the geometry of the facade panel was split in

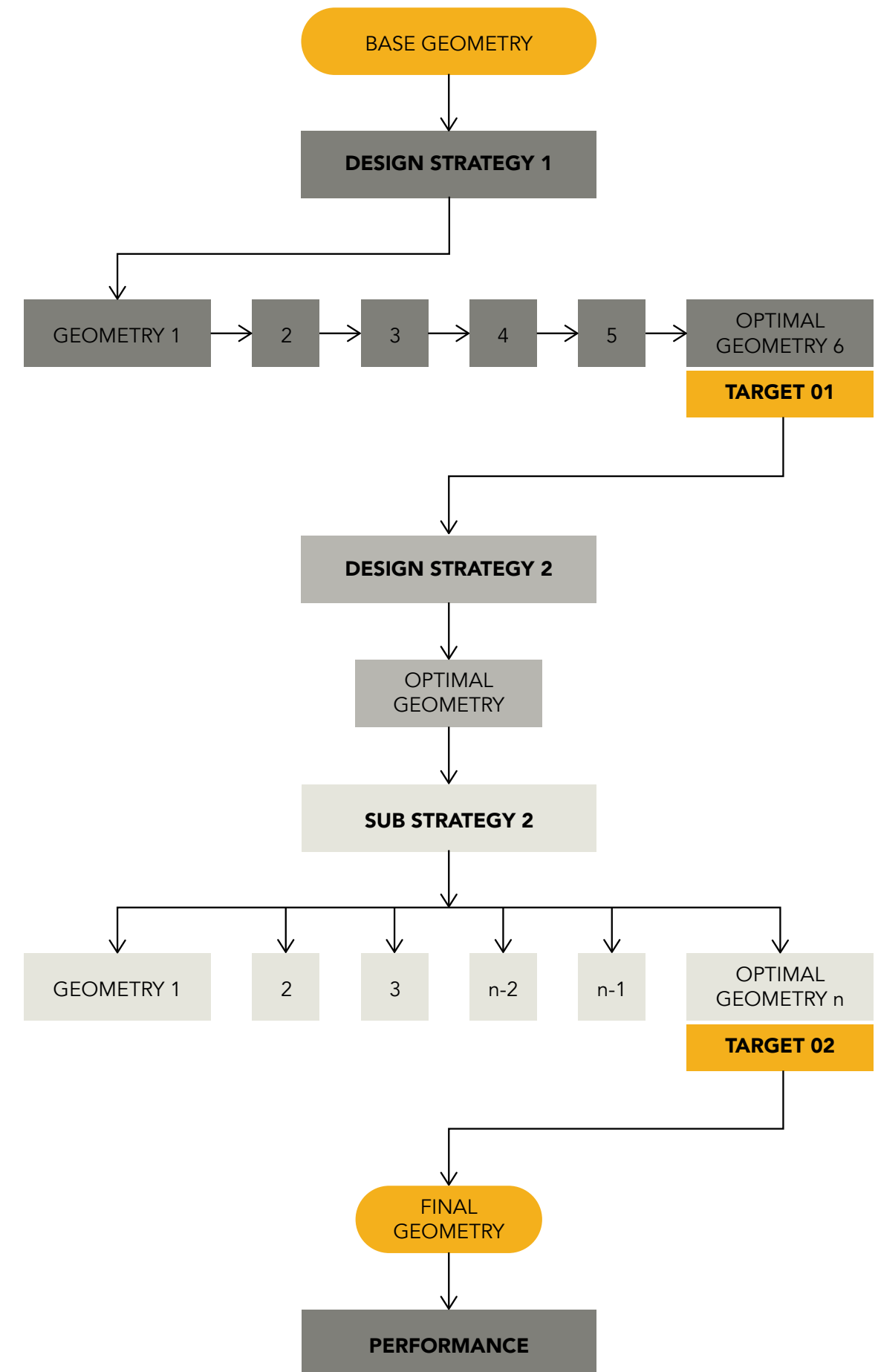


Figure 5.1. Target based methodology used to derive the mass and void geometries and accessing the design. (Author)

different steps depending on the method of operation needed to achieve each target. As mentioned in the strategic methodology in section 5.1, there were two targets to aim while designing the panel as described below:

1. **Target 01:** Void tubular network within the concrete panel
2. **Target 02:** Mass of concrete panel
3. **Performance check**

## 5.2 DESIGN STRATEGY 01 | TARGET 01

**Target geometry:** The void tubular network

**Design strategy:** Maximise volume of the tubular network + Minimise pressure drop across the tubular network

**Simulation software:** Ansys Fluent for pressure drop and fluid flow  
Ansys Fluent adjoint based solver for shape optimisation

Designing of the void tubular network did target to achieve the maximum volume while minimising the pressure drop. The prior target of maximising the volume was based on design ideologies and reference to various case studies as derived from section 3.4. The later target to minimise the pressure drop across the network was performed in parallel to designing for the prior.

The method involving the use of digital tools to minimise pressure drop was then divided into two parts, the first dealt with CFD simulation of water flow within the various designs of the designed tubular network while informing the geometry to be modified with necessary changes to maximise the target and the second to optimise the geometry to move further towards the target. A schematic flow diagram of the design strategy 01 is shown in figure 5.2.

### 5.2.1 Medium of fluid

To simulate the flow of fluids within the void tubular network, water was chosen as the material for the medium of fluid to analyse the pressure drop across the inlet and outlet and uniformity of velocity at the outlet. As the design is also governed by the method of fabrication, the final geometry was also simulated with molten wax to verify the flow out after casting. The properties used for the 2 materials in the fluid flow simulation is stated below.

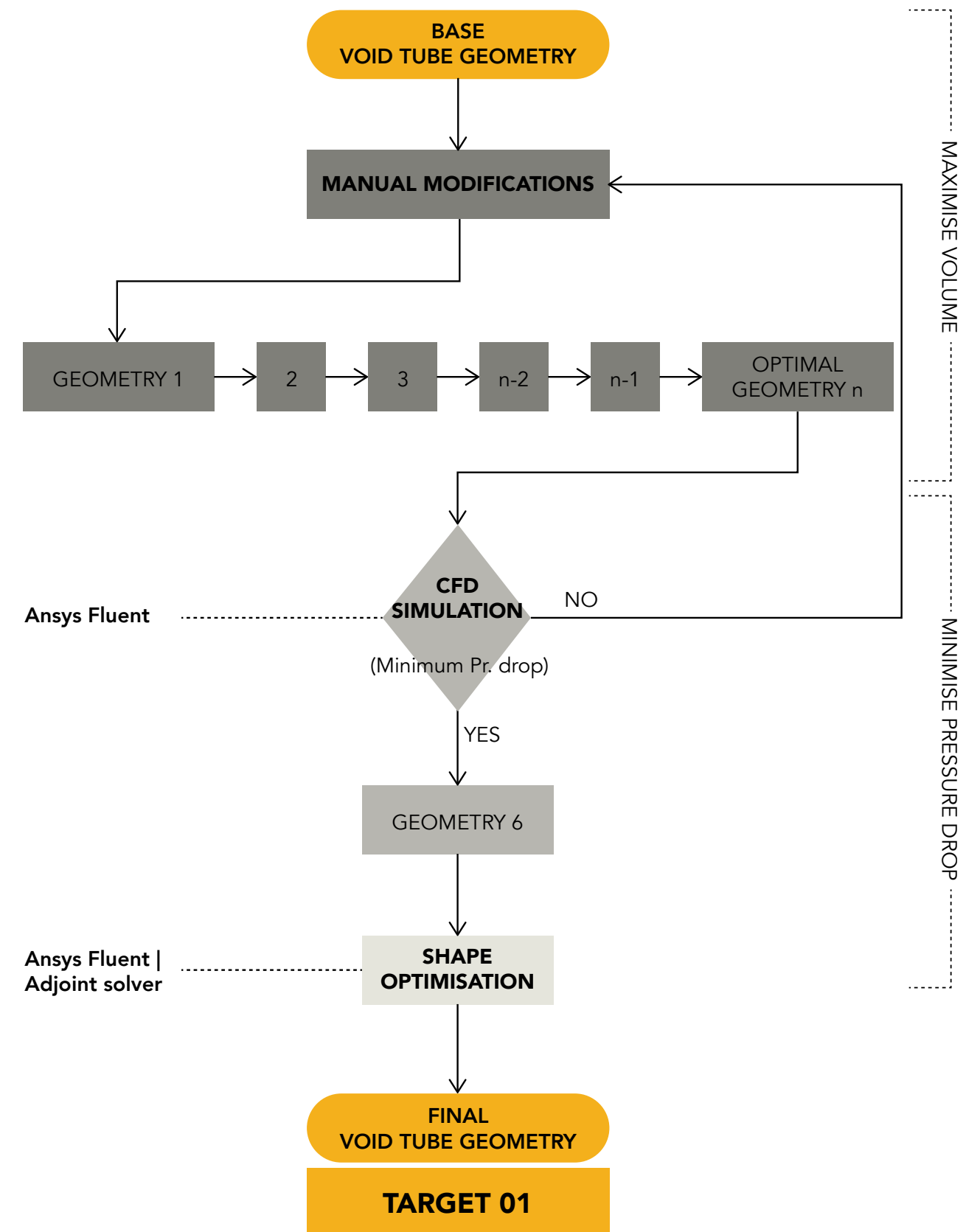


Figure 5.2. Flowchart showing the methodology used by design strategy 01 in order to achieve target 01.

**1. Water**Density: 998.2 kg/m<sup>3</sup>

Viscosity : 0.001003 kg/m-s

Temperature: 20° C

**2. Molten wax (MachinableWax, 2016)**Density: 912 kg/m<sup>3</sup>

Viscosity : 344 kg/m-s

Temperature: 120° C

**5.2.2 Meshing**

With a limitation of 512,000 nodes/ elements in the student version of Ansys Fluent, the meshing quality was highly determined by limitation from the software. The result of this limitation is a coarse meshing of the geometry, which may differ the simulation to a comparatively lower accuracy and also deter it from merging the solution of the solver equations. In relation to the same, the quality of the meshing for the different segments of the geometry needs to be in complaint for the simulation to be exact to the higher possible degree. The meshing tends to be coarser as the complexity of the geometry increases within the limitation.

In order to qualify the quality of the mesh to ensure the minimum requirements for the simulation to run, any given face of the geometry needs to be divided atleast into two nodes for the simulation to initiate. Figure 5.3 a&b show the wrong meshing in comparison to the one that qualifies the minimum meshing requirement for size of node. The different specifications, size and methods used to mesh the tubular geometries are mentioned next to the simulated geometries in the further chapters to adapt the specific geometry.

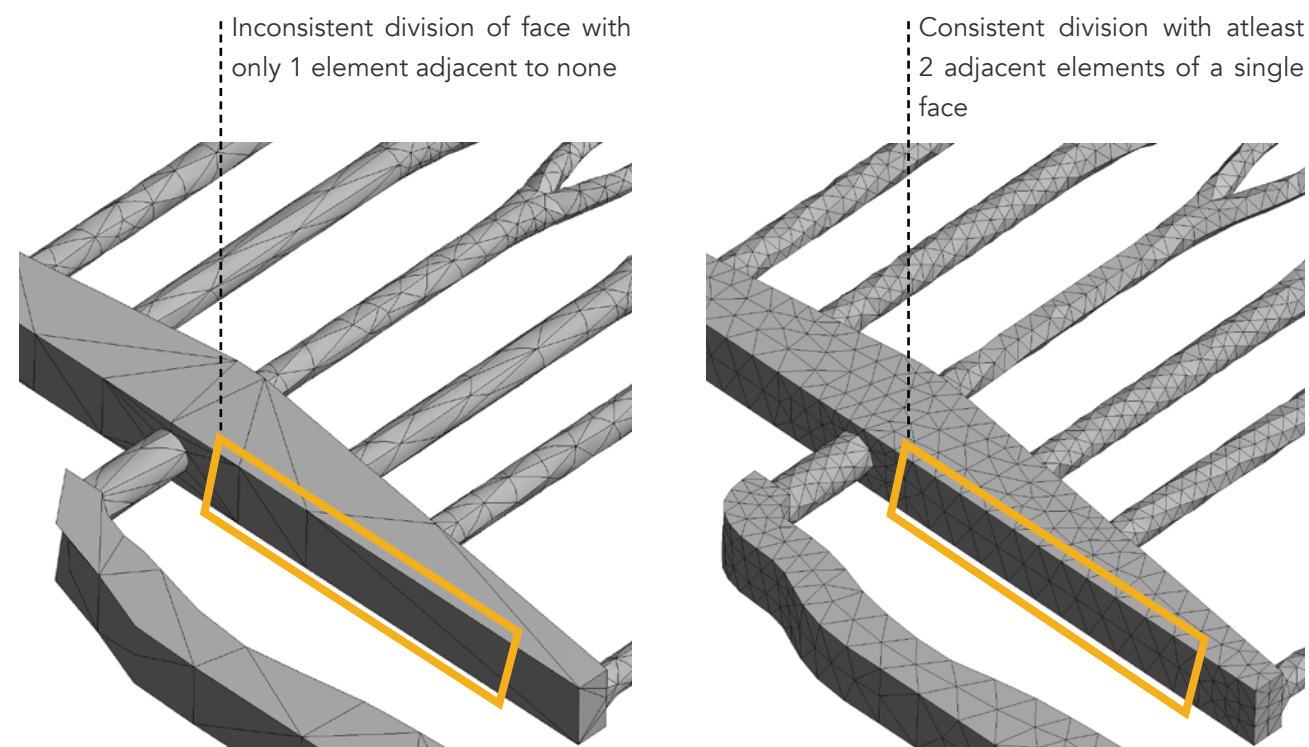


Figure 5.3a. Image showing a segment of geometry that does not qualify for simulation with less than 2 nodes per face. (Author- Ansys)

Figure 5.3b. Image showing a segment of geometry that qualifies for simulation with atleast 2 nodes per face. (Author- Ansys)

**5.2.3 Boundaries**

The boundaries set to analyse the pressure drop and flow behaviour of the fluids within the tubular network was limited to only three viz., inlet, outlet and boundary (wall). The surfaces corresponding to the respective boundaries were selected in the meshing counterpart of Ansys, with the inlet and outlet being two planar circular surfaces of the tubes while all others to boundary. The characteristics of these boundary conditions are shown below.

**1. Inlet**

Type: Velocity inlet

Velocity specification Method: Magnitude, Normal to Boundary

Velocity magnitude: 0.15 m/s (Refer section 7.2)

The other setup were selected as default.

**2. Outlet**

Type: Pressure Outlet. This is selected as outflow or other types are not supported for adjoint solver based optimisation.

Gauge pressure: 0 Pascals

Back-flow direction specification method: Normal to Boundary

The other setup were selected as default.

**3. Boundary**

Type: Wall

Wall motion: Stationary

Shear condition: No slip

The other setup were selected as default.

Note : For 2D simulations the Boundary conditions were set as same, with an alteration that the inlet and outlets were set to single line segments of the 2D geometry and the rest all as the boundary wall.

**5.2.4 Parameters for fluid flow calculation and simulation**

The other primary parameters for the fluid flow simulation are confined to models and methods used. While these two aspects were modified depending on the fluid flow simulation of the geometry type and complexity which was constrained by the limit of meshing nodes, the others were left to the default program selection.

The model used in the fluid flow simulation was confined to the viscous nature of the fluid. Since the behaviour of the fluid within the void tubular network is limited to the laminar behaviour of the fluid as explained in section 7.2, the model used was primarily laminar and checked for convergence because of the coarse nature

of the meshing. For simplified geometries like a straight tube, k-epsilon was used.

While the method used by default for higher grade of reliability is selected to be Least Squares Cell Based, this particular method is unsupported for the shape optimisation by adjoint solver. While the deviation of the resulting pressure difference using these method are very minimal and could be neglected, Green-Gauss Cell Based method is used for the simulations that are forwarded for the optimisation of the geometries through adjoint solver or else specified.

The choice of use of the models and methods are specified next to the simulated geometry further in the chapters. A basic setup of Ansys Fluent fluid flow is shown below in figure 5.4.

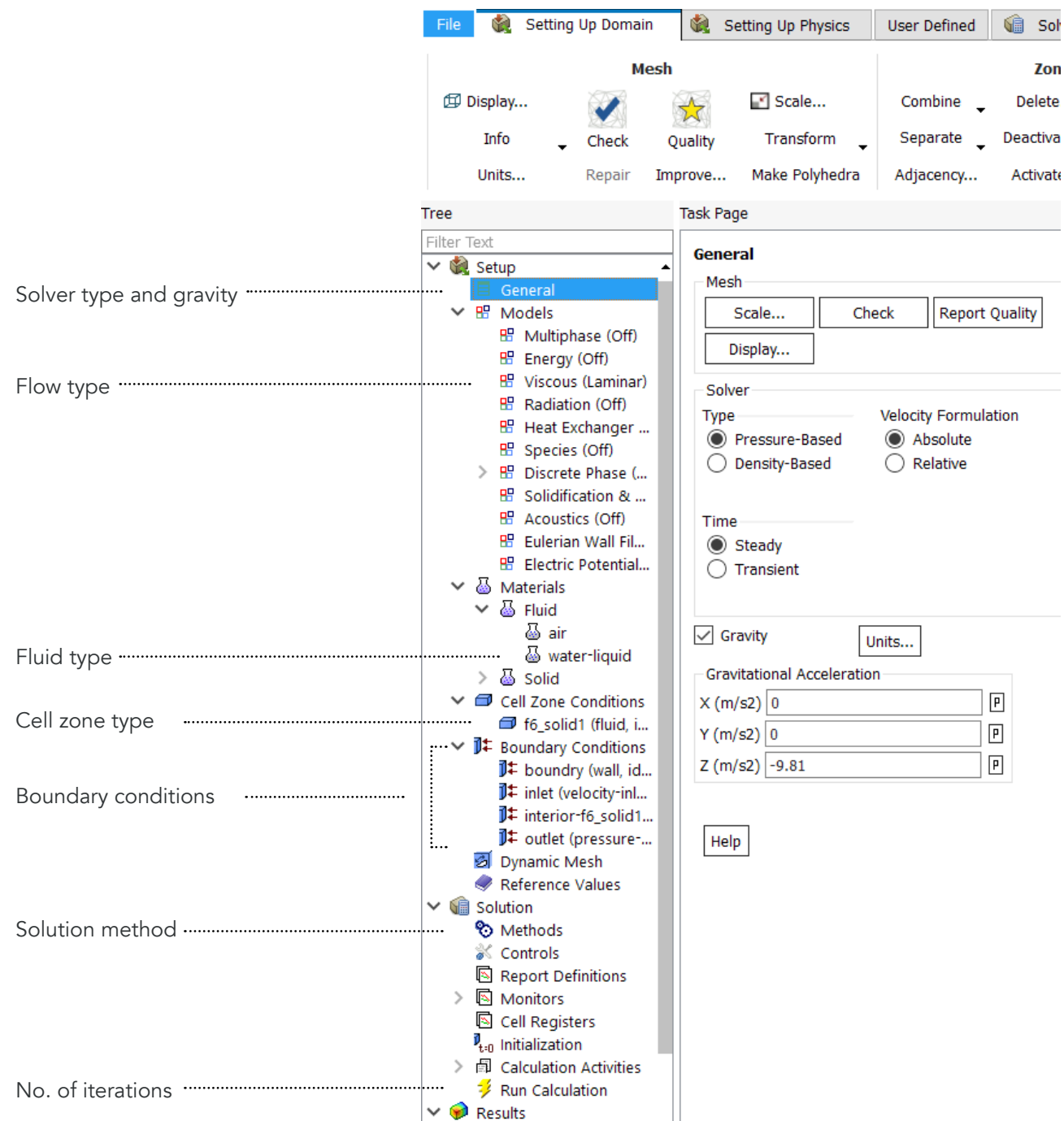


Figure 5.4. Image showing the setup used in Ansys Fluent fluid

## 5.2.5 Validation for fluid flow simulation

The validation for the pressure drop was made analytically to verify the method/ algorithm/ model used and that the input parameters used in the software do provide reliable results and simulation visualisations. The analytical pressure drop was considered for a circular tube with a vertical flow of fluid (water) arranged with the inlet at the top and outlet at the bottom. The exact same setup was also analysed in the CFD analysis software, Ansys Fluent. A schematic diagram of the setup used is shown in figure 5.5.

The analytical calculation for the pressure drop across the tube is shown below (<http://www.pressure-drop.com/Online-Calculator>),

<b>Element of pipe:</b>	Circular
<b>Dimensions of element:</b>	Diameter of pipe D: 15 mm Length of pipe L: 3.2 m
<b>Flow medium:</b>	Water 20 °C / liquid
<b>Volume flow:</b>	0.519 l/min
<b>Weight density:</b>	998.206 kg/m <sup>3</sup>
<b>Dynamic Viscosity:</b>	1001.61 10 <sup>-6</sup> kg/ms
<b>Velocity of flow:</b>	0.05 m/s
<b>Reynolds number:</b>	732
<b>Flow:</b>	laminar
<b>Absolute roughness:</b>	0.5 mm
<b>Pipe friction number:</b>	0.05
<b>Resistance coefficient:</b>	18.66
<b>Pressure drop:</b>	0.22 mbar

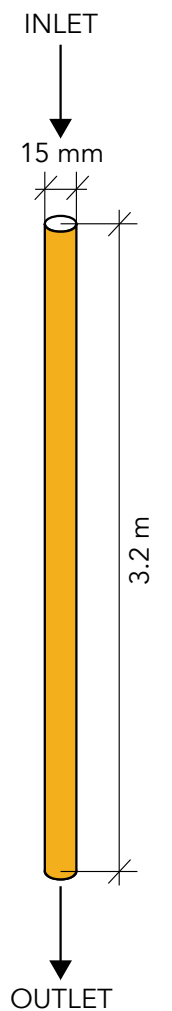


Figure 5.5. Schematic diagram of the setup used for validation of CFD done using Ansys Fluent. Source: author

As depicted in the next page, the geometry selected was a simple tube with relatively small size and no complexities and hence the meshing quality achieved was of very fine nature that ensures simulation close to the real world scenarios. The inlet and outlet contour mapping for pressure drop does provide an idea of the distribution of the pressure while the water enters to that while exits. A regular uniform distribution as shown in figure 5.6b does ensure a smooth water flow while a non-uniform contour may result in turbulent. The

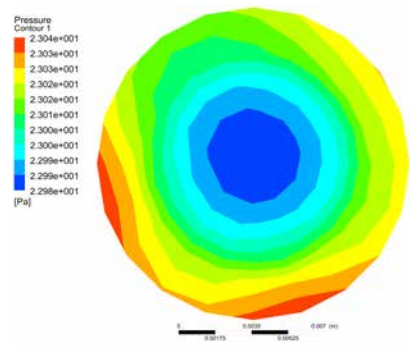


Figure 5.6a. Pressure contour inle (Author; Ansys fluent)

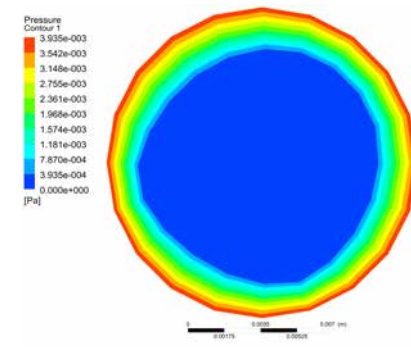


Figure 5.6b. Pressure contour outlet (Author; Ansys fluent)

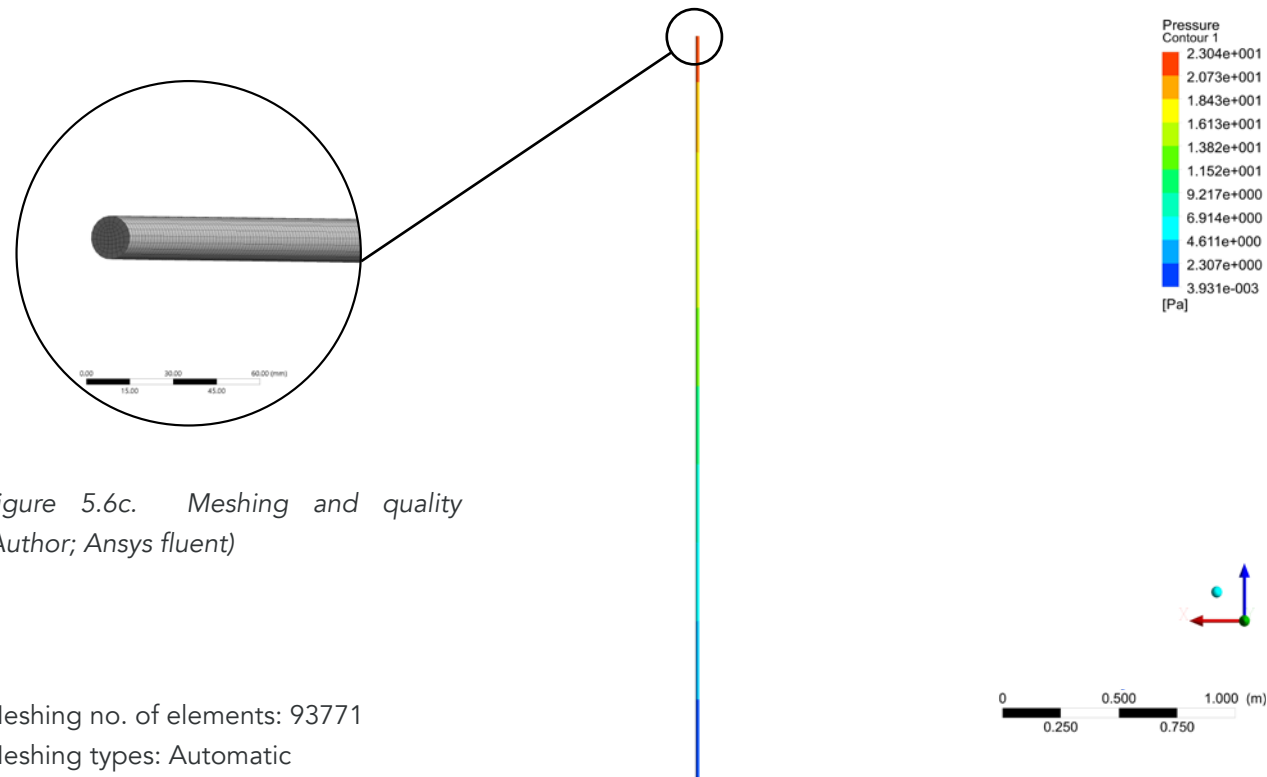


Figure 5.6c. Meshing and quality (Author; Ansys fluent)

Meshing no. of elements: 93771  
 Meshing types: Automatic  
 Quality: Medium  
 Min size: 1.6 mm  
 Max size: 160.00 mm

Viscous model: laminar  
 Method: Spatial Discretization-  
 Least Squares Cell Based

No.of iterations: 200  
 ΔP: 22.5 Pa

No.of iterations: 2000  
 ΔP: 23.03

Convergence iteration: NA  
 flat plate zone

Convergence exponential: e-03  
 Simulation time: 15 minutes

Figure 5.6d. Pressure of boundary domain (Author; Ansys fluent)

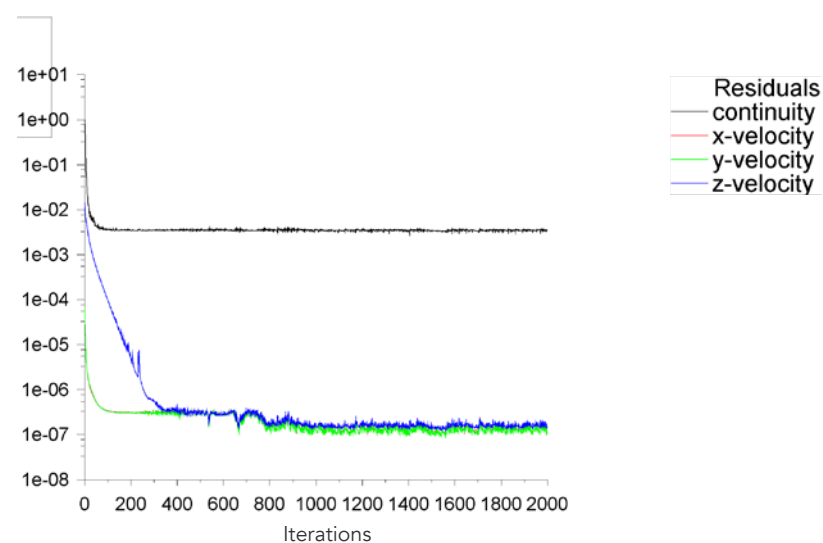


Figure 5.6e. Graph for 2000 iterations for CFD of validation geometry. (Author; Ansys fluent)

non-uniform contours could be a result of coarse meshing or of negligible difference in pressure and could be ignored. The continuity graph (figure 5.6e) shows the degree of error and should be resulted under e-03 for a complex shape while e-02 for simple shapes. The x,y,z velocity show the convergence of the solutions with the degree of error and if under e-03 could be considered as flat plate zone of converged simulation. As a substitute, the viscous model could be changed and/or run for higher number of iterations to determine convergence.

## 5.2.6 Parameters for shape optimisation by adjoint solver

To modify the shape of the tubular network geometry (specifically nodes), the adjoint solver was put into task that analyses the combination of pressure drop and velocity change across the inlet and outlet and modifies the geometry to minimise/ maximise the target. This works in conjunction to the calculation and simulation ran for the fluid flow and pressure drop as explained in the previous segments.

### 1. Observables

Pressure Drop: Between inlet and outlet

Velocity in x, y and z directions for volume integrity: Volume Integral set separately for all the three axis with the Field Variable as velocity and verifying the direction with integer 1 and rest 0.

Total velocity: A Linear combination of powers of 3 components with the volume integral of velocity combined with for all the three axis.

Total velocity with Pressure drop: A Linear combination of powers of 2 components with the total velocity and pressure drop combined for the final calculation. Figure 5.7 .

### 2. Adjoint Observables

Total velocity with Pressure drop set to minimise. Figure 5.7.

### 3. Methods, Solver controls and Monitors

Method: The default standard with first order upwind adjoint solver method was used for this calculation.

Solver control: Solution-based Controls Initialization and Auto-Adjust Controls were only selected.

Monitors: The monitors were set to default and could be customised for window view and no. of iterations.

### 4. Design Tool:

Design change: Boundary

Objective: Pressure drop - Subjective as the value of the calculation differs per calculation. Either decrease value or target change in value with a negative number in relation to the calculated and target pressure drop is set. The rest were set to default.

Region: The boundary to be modified is only set excluding the inlet and outlet. Bounding box dependent on the geometry and has been depicted in figure 7.27 of section 7.6.1.

Region conditions: 50 in x, y and z motions. It is dependent on the quality of the desired result, while others

were set to default.

Numerics: Preconditioning of the Freeform Motions was set to 10 to allow higher degree of mesh relaxation, while rest were set to default.

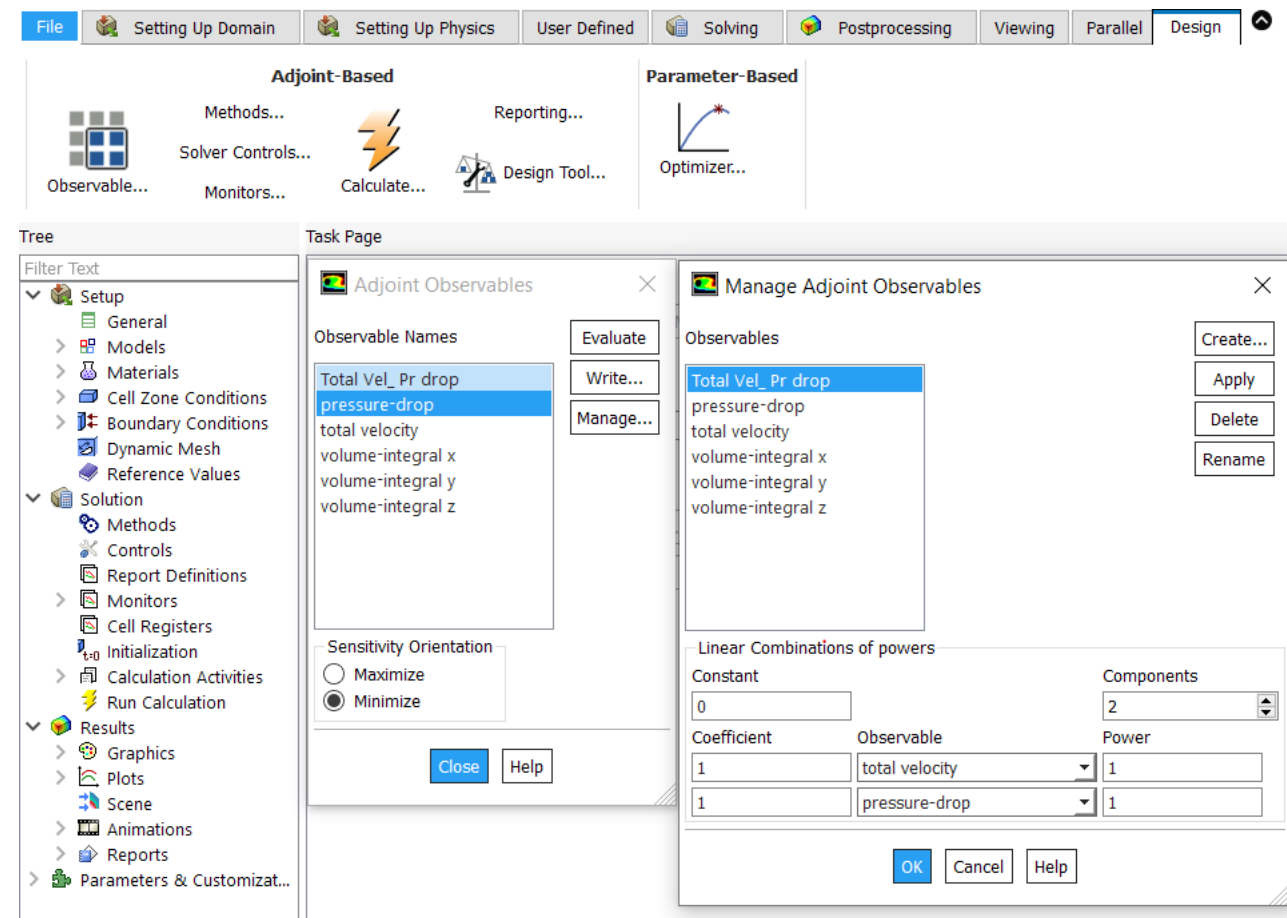


Figure 5.7. Image showing the setup used in adjoint solver of Ansys Fluent fluid flow. (Author; Ansys fluent)

## 5.2.6 Limitations and considerations for Ansys Fluent-fluid flow

### 1. Temperature change in fluid:

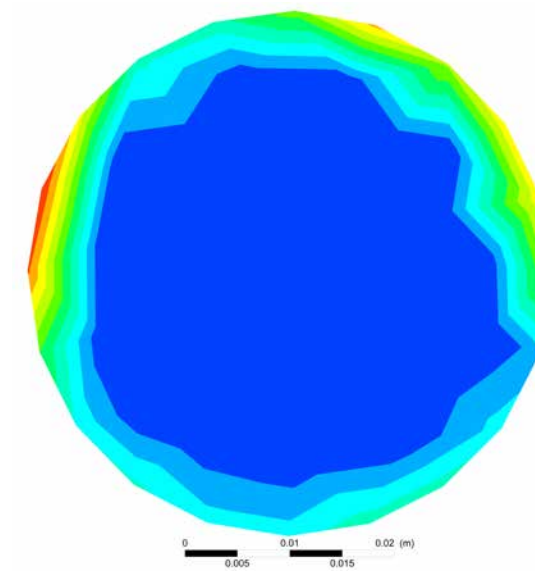
The heating of the fluid over time and the change in pressure due to expansion is neglected in the design. This expansion has been accommodated by the pressure management tube at the top of each networks that is used to regulate and maintain a steady pressure in the network and has been kept out of the scope of this thesis.

### 2. Deviation in result due to meshing quality:

In response to the limitation by license of Ansys, the meshing quality had to be compromised to the minimum possible requirement for the solvers to initiate and thus minor deviations in the result should be expected. For example, the pressure drop contours of the outlet tubes of the initial tubular void network with simple

geometry was smooth and comparatively precise as the meshing consisted of smaller node sizes. In contrast the final tubular void network with complex geometry had to accommodate the total number of allowed nodes with compromises for higher node size. As a result the pressure contour of the outlet for the final geometry is of a coarse nature as compared to the initial simple geometry, while all the other specifications and methods used in meshing are unchanged. The comparison of this limitation is shown in figure 5.8a for the initial geometry and figure 5.8b for the final geometry.

Since the variation in the result was very minimal ( with a maximum of  $\pm 3\text{-}5\%$  ) and negligible, the mesh size limitation was accommodated in the design methodology and carried forward.



Meshing no. of elements: **330529**

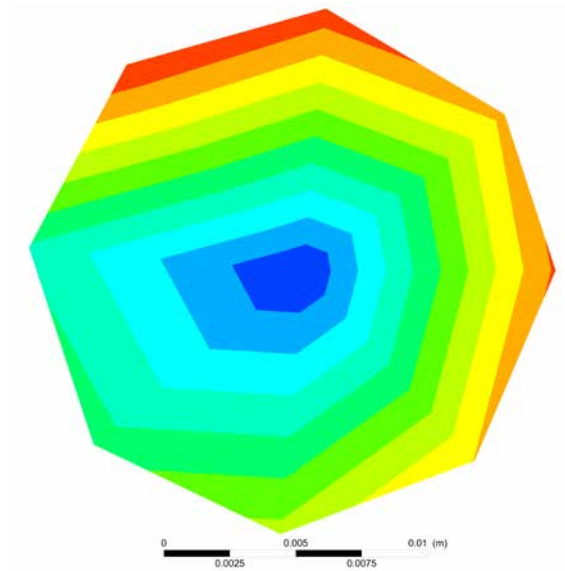
Meshing types: Automatic

Quality: Medium

Min size: 7.0 mm

Max size: 700.00 mm

Figure 5.8a. Pressure contour of outlet tube for the initial tubular void network geometry. (Author; Ansys fluent)



Meshing no. of elements: **383902**

Meshing types: Automatic

Quality: Medium

Min size: 7.0 mm

Max size: 700.00 mm

Figure 5.8b. Pressure contour of outlet tube for the final tubular void network geometry. (Author; Ansys fluent)

### 3. Long simulation times and inconsistent results for adjoint solver:

While the adjoint solver is a powerful tool to modify geometry based on the set targets, the result do vary largely for the various types of objectives set under the design tool. A minor change in the value for different calculation runs do result in the desired goal, but needs constant monitoring. Moreover the very long run times for simulations, which mostly results in undesired mesh results renders this as a cumbersome method.

In response to the same, the 3D simulation was compared to that of the behaviour and result of the 2D simulation and further modifications were assisted with 2D simulations with adjoint solver to overcome the problems. This method has been detailed out in section 7.6.2.

## 5.3 DESIGN STRATEGY 02 | TARGET 02

**Target geometry:** The solid mass of the facade panel

**Design strategy:** Maximise heat entrapment in the mass

**Simulation software:** Autodesk fusion 360 for topology optimisation  
Autodesk ReCap Photo for quad-mesh conversion  
Octopus in Grasshopper for modifying the quad mesh geometry

The geometry development of the flat surfaced panels made of GFRC was subjected to a target of maximising the surface area of the panels, primarily the external panel. Since the idea of subtracting mass with the help of topology optimisation as discussed in section 7.7.

The method involving the use of digital tools to maximise the surface area in order to maximise the heat entrapment was then divided into two parts, the first dealt with topology optimisation of the panels that helps in minimising the mass as well as maximising the surface area. The second part deals with converting the mesh into quad nodes and altering vertices of these quad nodes in order to further maximise the surface relation while maintain the average solar radiation on the surface during winter and summer. A schematic flow diagram of the design strategy 02 is shown in figure 5.9.

The final consideration for the software for topology optimisation was selected to be Fusion 360. The mechanical counterpart of Ansys was primarily considered but the complexity of the geometry with the mass along with the tubular structure within was unable to cope with the limitations of the mesh nodes to 31,000. The details about the considerations for the software and the limitations faced are discussed in chapter 5.

### 5.3.1 Geometry and meshing in Fusion 360

The geometry selected as an input was a flat facade panel made up of two segment of concrete mass (Figure 4.7). Since the meshing control per part is of limited function in Fusion 360, the complexity of the geometry to be compatible to the meshing algorithm needed modifications to eliminate meshing failures. To do so, the tubular network geometry was modified into low poly squared sections manually. The dimension of these tubes did not include any margins needed for the concrete cover for the tubes. This made the geometry mesh faster and accurate. The geometry of these tubes do not affect the topology optimisation as the geometry was constrained with a boundary of exclusion while simulating, in order to cope up with the minimum concrete cover needed around the tubular network. The actual tubular model in comparison to that of the low poly converted tubular network is shown in figure 5.10 a&b.

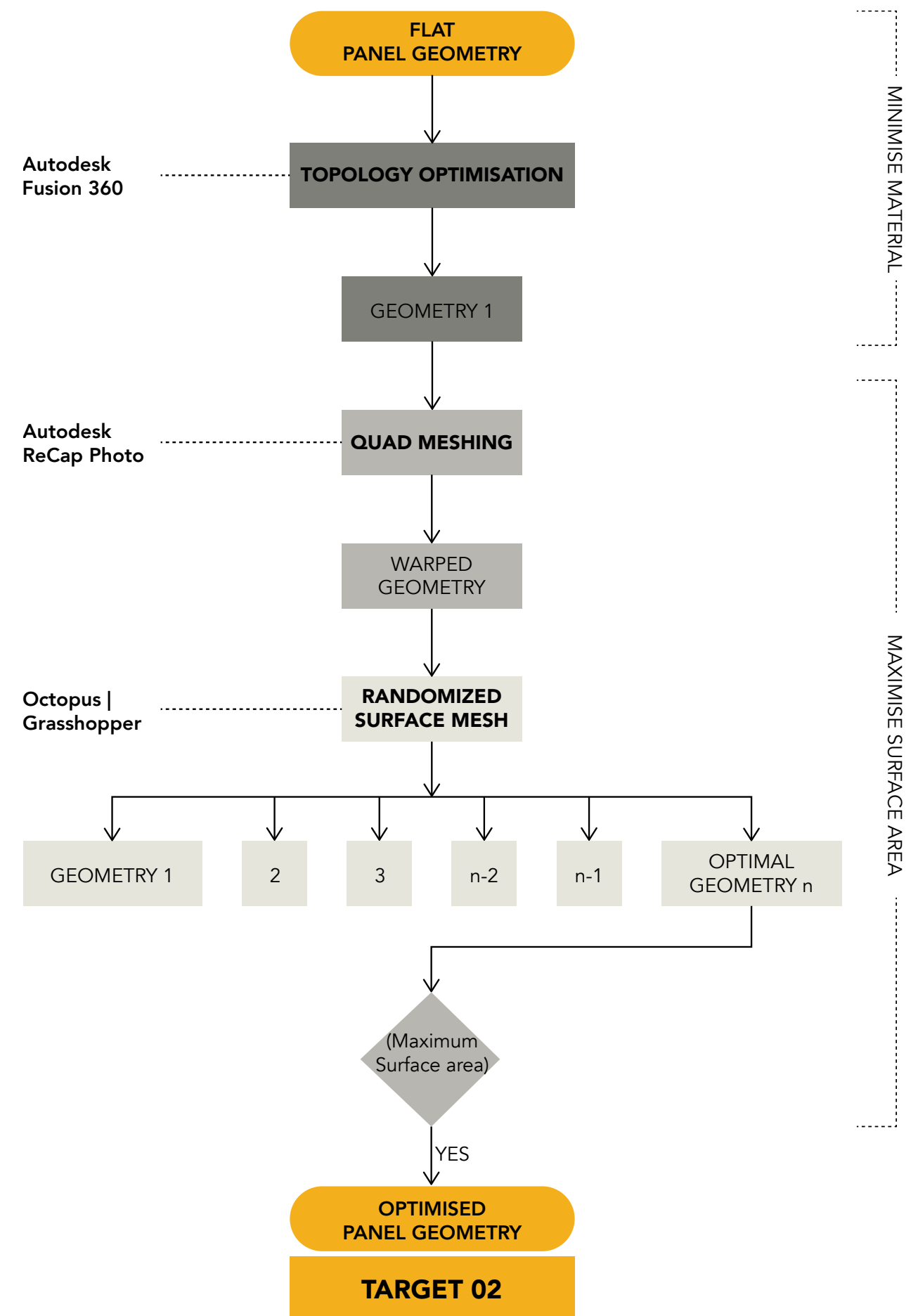


Figure 5.9. Flowchart showing the methodology used by design strategy 02 in order to achieve target 02. (Author)

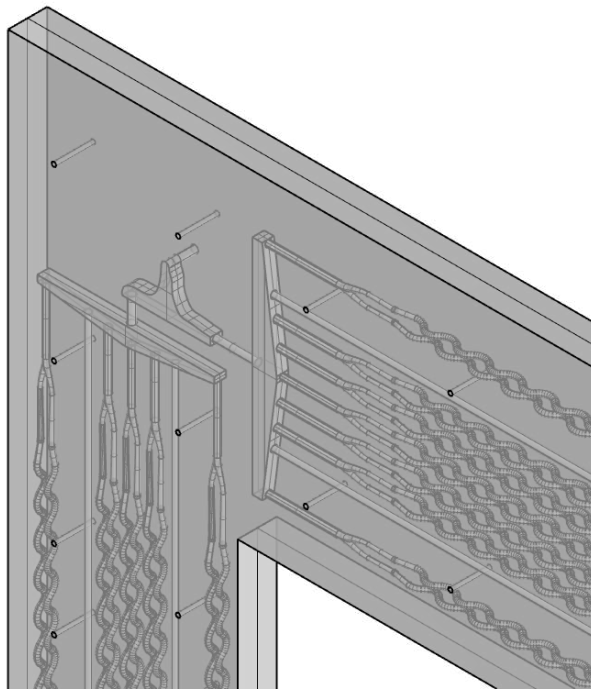


Figure 5.10a. Segment of original tubular network geometry with rounded surfaces resulting in high meshing complexity. (Author; Fusion360)

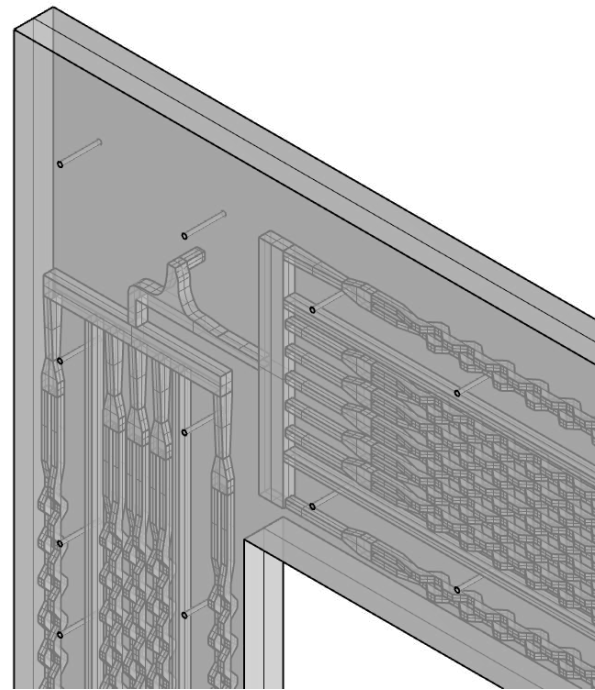


Figure 5.10b. Segment of modified tubular network geometry to low poly geometry to minimise meshing complexity. (Author; Fusion360)

### 5.3.2 Material and setup for Fusion 360

The digital setup for the topology optimisation in Fusion 360 considers only two materials, Concrete for the mass and glass fibre dowels as reinforced connection between the two facade panels. The default material library of Fusion 360 does not contain the specifics of the materials used in this project. While some properties of the used materials were referred and tested, some of the material properties were kept to default. For the specifics of the materials used and testing done please refer to section 6.1.1. Materials using these properties were then manually created in Fusion 360. The detail of the material setup of concrete and glass fiber is mentioned below.

The designed boundary conditions for the setup for topology optimisation is shown in figure 6.7 of section 6.1.3.

#### 1. Concrete (Gobain, 2019)

Non-linear  
 Thermal conductivity: 3.000E-01 W/(m·K)  
 Specific Heat: 0.750 J/(g·°C)  
 Thermal Expansion Coefficient: 5.000  $\mu\text{m}/(\text{m}\cdot^\circ\text{C})$   
 Young's modulus: 10.500 GPa  
 Poisson's ratio: 0.24

Shear modulus: 6510.000 MPa  
 Density: 2.026 g/cm<sup>3</sup> (lab test by author, 2019)  
 Damping coefficient: 0.00  
 Concrete compression: 20.000 MPa  
 Shear strength modification: 1.00  
 Yield strength: 2.9 0 MPa  
 Tensile strength: 1.50 MPa

#### 2. Glass fiber dowels (Schöck, Schoeck Combar, 2016)

Non-linear  
 Thermal conductivity: 0.7 W/mK axial, 0.5 W/mK radial  
 Thermal Expansion Coefficient: 0.8 - 1.2 x 10<sup>-5</sup> 1/K  
 Young's modulus: 50,000 N/mm<sup>2</sup>  
 Shear modulus: 150 N/mm<sup>2</sup>  
 Density: 2.2 g/cm<sup>3</sup>  
 Tensile strength: 580 N/mm<sup>2</sup>

The shape optimisation target was selected to be the mass of the facade panel to be optimised. To eliminate the high meshing complexity, the topology optimisation of the external and the internal facade panel was divided into two cases. The first being the external panels with the points of dowels acting as fixed points while for the internal panel the optimised first panel was added to the twin-wall setup geometry and simulated. A typical setup used for the topology optimisation in Fusion 360 is shown below in figure 5.11.

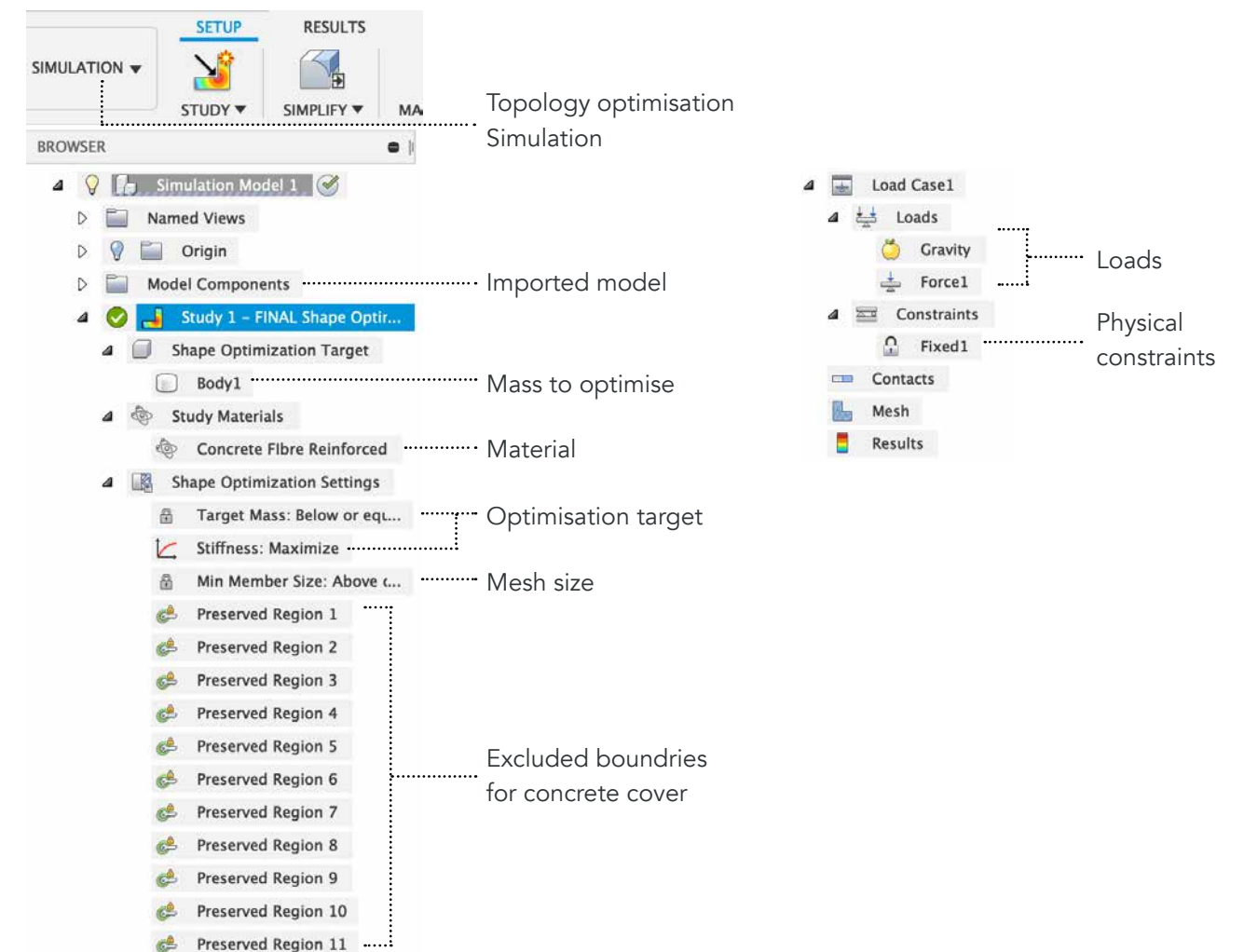


Figure 5.11. Image showing the setup used in Fusion 360 topology optimisation. (Author; Fusion360)

### 5.3.3 Validation for topology optimisation

The validation for the topology optimisation to verify the engine/ algorithm used and that the input parameters used in the software do provide reliable results and simulation visualisations, the standard Michell cantilever was analysed (Querin, Victoria, Alonso, Ansola, & Marti, 2017). The behaviour of the topology optimisation use by Fusion 360 and its Nastran solver is compared and analysed in terms of meshing and static stress (FEM) analysis to similar setup used in other reliable software. A schematic diagram of the setup used for Michell cantilever in Fusion 360 is shown in figure 5.12. It is to be considered that, since 3D topology optimisation is considered in this thesis, the geometry for the michell cantilever as depicted by Querin et al. (2017).

The values considered for the geometry of michell cantilever used in Fusion 360 are as following,

**Length:** 1.82196 m

**Height:** 1.0 m

**Thickness:** 0.005 m

**Load:** 1.0 N

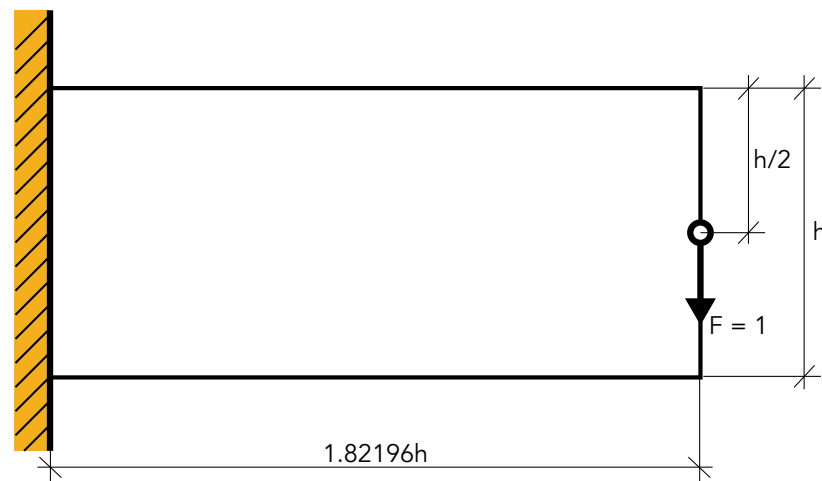


Figure 5.12. Michell cantilever of aspect ratio  $L = 1.82196$ . Source: Querin et al. (2017).

The parameters considered for topology optimisation of the above geometry in Fusion 360 are as following,

**Mesh size**  $\approx 25$  mm

**Goal:** Target mass  $\leq 30$  %

Maximise stiffness

**Boundary conditions:** Preserve entities with loads and constraints

**Material:** Steel

The simulated topology optimisation of the geometry is shown below. The derived geometry does follow the principal stress lines as have been analysed in other software or method to verify the effectiveness of the algorithm used for optimisation.

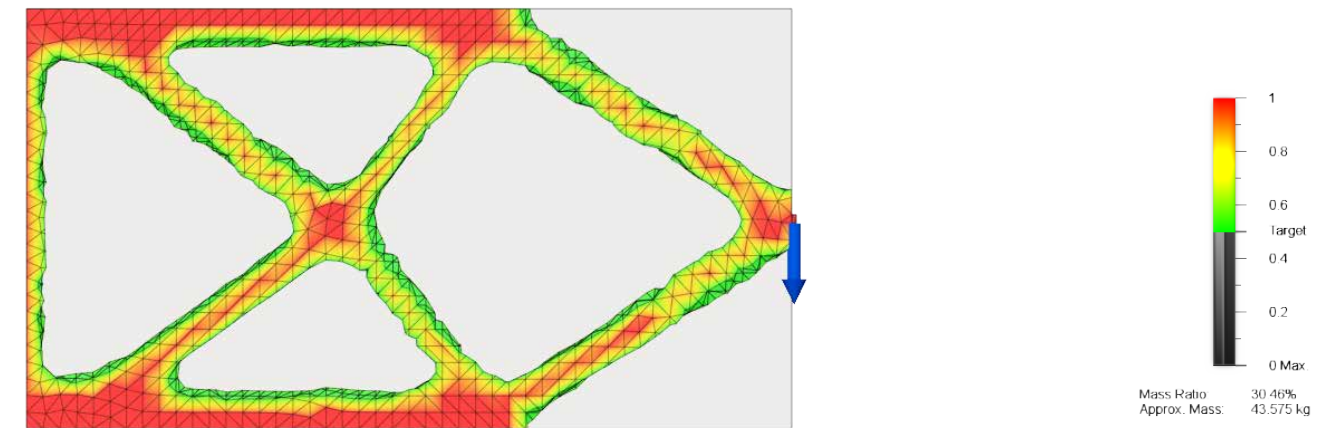


Figure 5.13. Topology optimisation of Michell cantilever geometry of aspect ratio  $L = 1.82196$ . (Author; Fusion360)

### 5.3.4 Limitations and considerations for Fusion 360

#### 1. Boundary conditions and constraints

The limited ability of the software to allocate a pre defined geometry to preserve boundaries along it to define the needed minimum cover for the material integrity does render zoned surface treatment for topology.

To overcome this limit, combined rectangular boundaries over the different segments of tubular networks and nodes are generated in the software and approximated for the optimisation process. A detail of these preserve boundaries are shown in figure 7.48 of section 7.7.1.

#### 2. Limited or no control over the mesh dimensions and behaviour for topology optimisation

The inability to define the node behaviour, mesh geometry type, meshing per part with a limited control only over the size of the mesh developed by the Nastran solver.

The default meshing type with fine mesh size was used for the solver to result in the most accurate form of the optimisation. The geometry of the mesh was although could not be modified and hence the default result by optimisation through Nastran solver was used for the project.

### 3. Highly complex resulting mesh

The resulting mesh of the topology optimisation is highly complex and heavy on the computer processing power to be used any further. The lack of post processing the mesh to further simplify the complexity or exporting to simplified surface geometry in any other format rather than for native Fusion 360 format to be used in any other digital programs.

The mesh was exported to another post processing software for further simplification as explained in the next section of this chapter.

### 4. Processing time

While the simulation of the topology optimisation is low than compared to any other programs for such complex geometries, the very high processing time to export the optimised geometry to a mesh is cumbersome which may at time may account to 12-14 hours.

## 5.3.5 Remeshing

The complex triangulated mesh geometry derived from the topology optimisation of the mass of the facade panels using Fusion 360 was then converted to quad meshes using Autodesk ReCap photo. While this is a simple method of importing the mesh, checking for possible errors, correcting them and exporting them to a new mesh, there is a limitation of 20,000 mesh faces only. To extract the most fine possible result, only the optimised surfaces of the panels were imported and exported back. The rest of the facade panels being restricted to the optimisation process were manually merged with the primary geometry.

A comparative analysis between the complex triangulated mesh resulted from Fusion 360 to that of the quad re-meshed has been shown in figure 5.14 below.

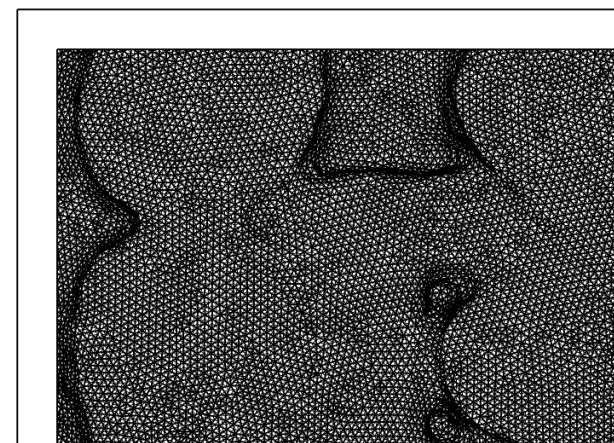


Figure 5.14a. Optimised geometry complex mesh from Fusion 360. (Author; Fusion360)

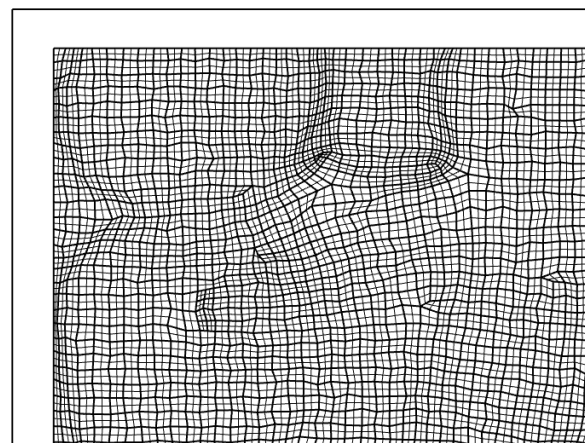


Figure 5.14b. Simplified quad mesh using Autodesk ReCap Photo. (Author; ReCap Photo)

## 5.3.6 Modifying surface mesh

While the target O2 to maximise the surface area has been achieved by doing the topology optimisation, to maximise the surface area further while keeping the summer and winter radiation unchanged to that of the optimised surface. This process was done using Ladybug+Honeybee for analysing the radiation and Octopus multi-objective evolutionary optimisation for the surface modification.

To derive the needed surface geometry, the nodes of the quad mesh were identified and the overlapping nodes were eliminated. These nodes were then arranged in an euclidean order and a new mesh was generated. The winter and summer day radiation facing north were calculated only for the front optimised surface and not the other surfaces of the mass of external panel. The surface area was also calculated for the front optimised surface of the external panel. A view of the script is shown below in figure 5.15 and the detailed version in the appendix.

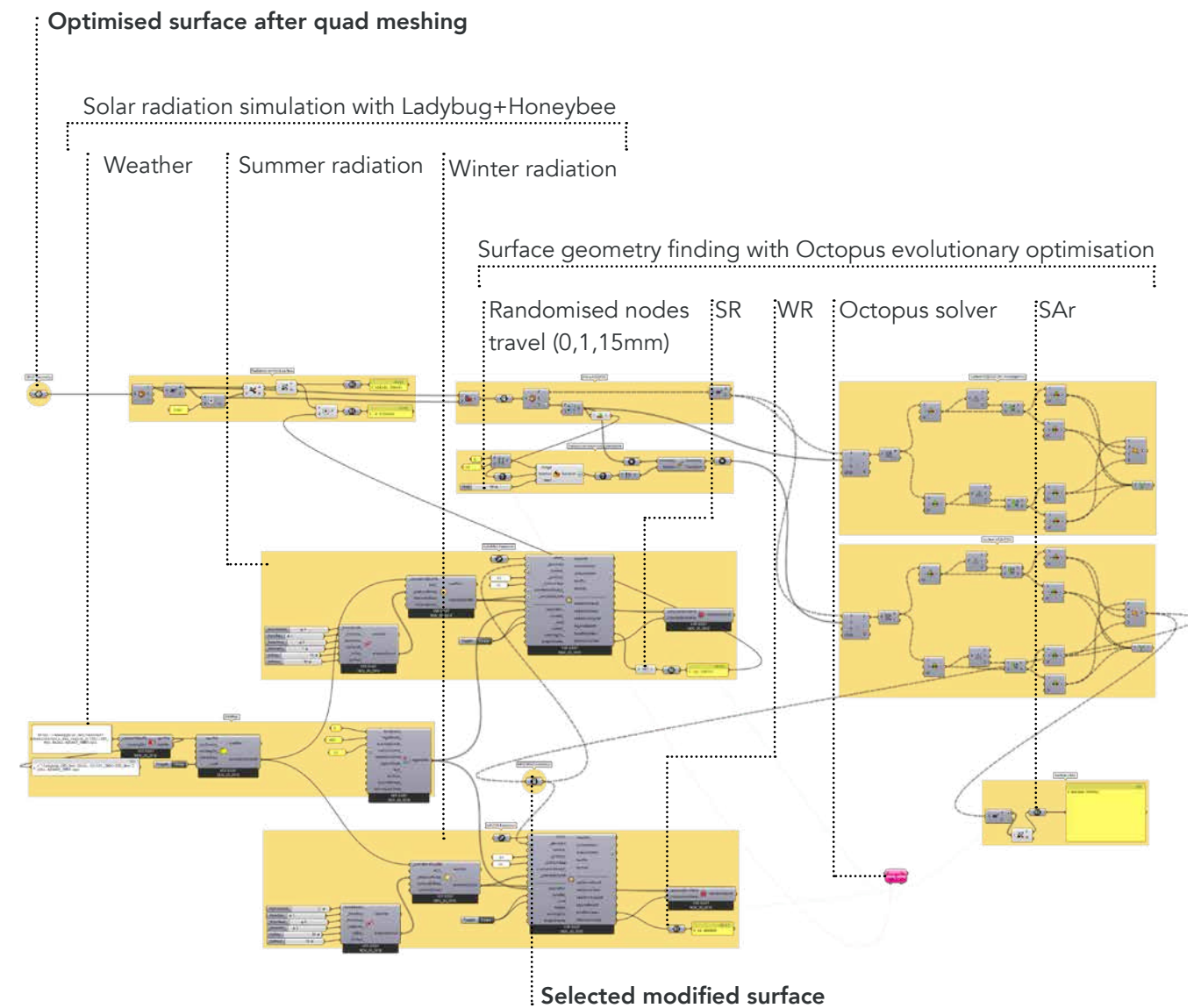


Figure 5.15. Scripting for modifying the surface mesh to maximise surface area.

**1. Weather:** New Delhi, India

**2. Orientation:** South

**3. Period**

Hours: 0800 to 1800 hours

Days: 1 to 30

Summer: April to July

Winter: November to February

**4. Phenotypes**

WR: Total winter radiation on optimised surface

SR: Total summer radiation on optimised surface

SAr: Surface area of optimised surface

**5. Genomes**

Randomised movement of nodes in a domain of 0 to 15 mm with 1mm steps.

Since the solver running and initiating radiation for each surface for summer and winter consumes a huge amount of time and the high number of nodes resulting from the fine mesh would result in infinite number of possibilities to shift the nodes. The setup used for Octopus solver is shown below in figure 5.16, while others were set to default. Amongst the pool of results, the maximum with the surface area while keeping the radiating almost similar was chosen that completes the target 02.

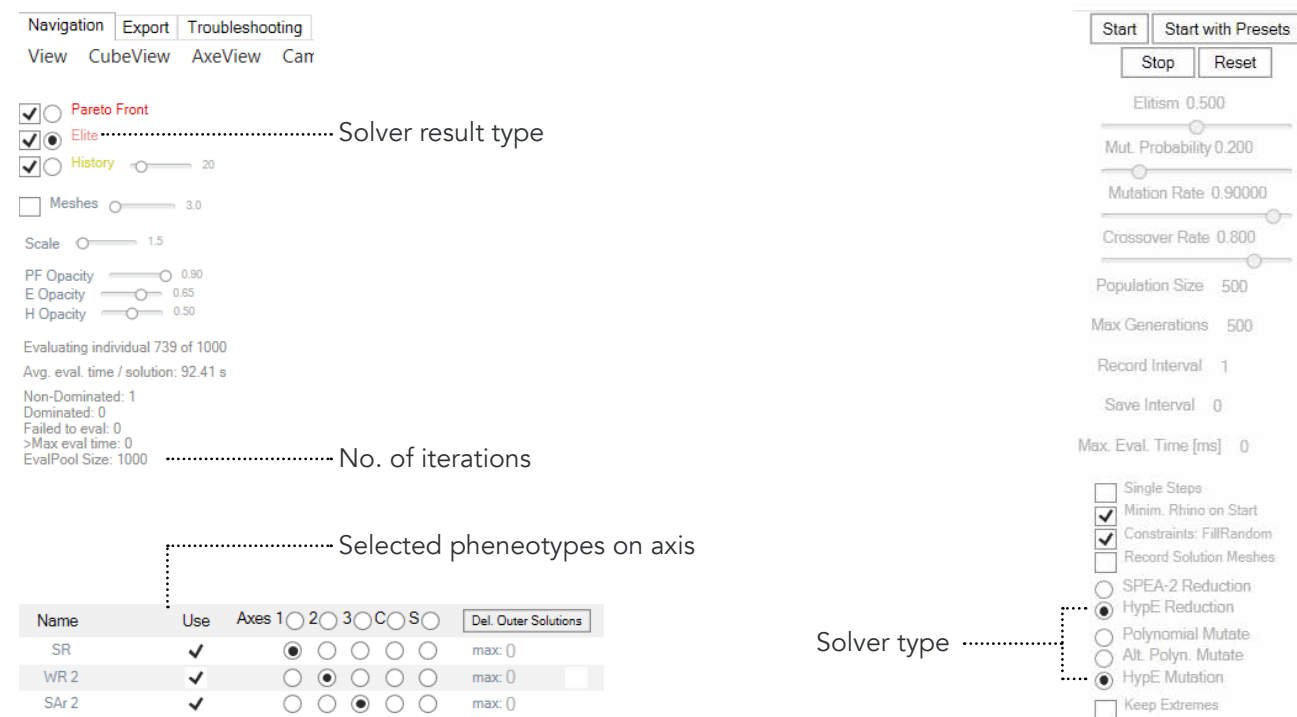


Figure 5.16. Image showing the setup used in Octopus for geometry analysis (Author; Octopus)

## 5.4 PERFORMANCE

**Target geometry:** The mass of facade panel + the void tubular network within the panel

**Analysis strategy:** Analyse heat transfer

**Simulation software:** COMSOL Multiphysics

With the followed design strategies and the design methodology to derive the needed geometry, the goal to achieve the maximum possible efficiency. With the goal achieved, the performance of the designed facade unit is to be checked in response to verify the effectiveness of the two basic goals:

**1. Maximised volume of the void tubular networks**

**2. Maximised surface area of the external facade panel**

To perform the check a basic heat exchange simulation was done using Comsol multiphysics. Since the water within the panels are kept stagnant to absorb the heat and flow between the panels within a time frame of only 11 minutes, the flow of the fluid is neglected in this simulation and the domain of fluid is considered as a mass with properties of water. The method of performing this check was divided into 2 instances of heat transfer and performance evaluation:

**Instance 01: From external environment to void tubular network of water within the external panel**

**Instance 02. From void tubular network of water within the internal panel to the indoor space.**

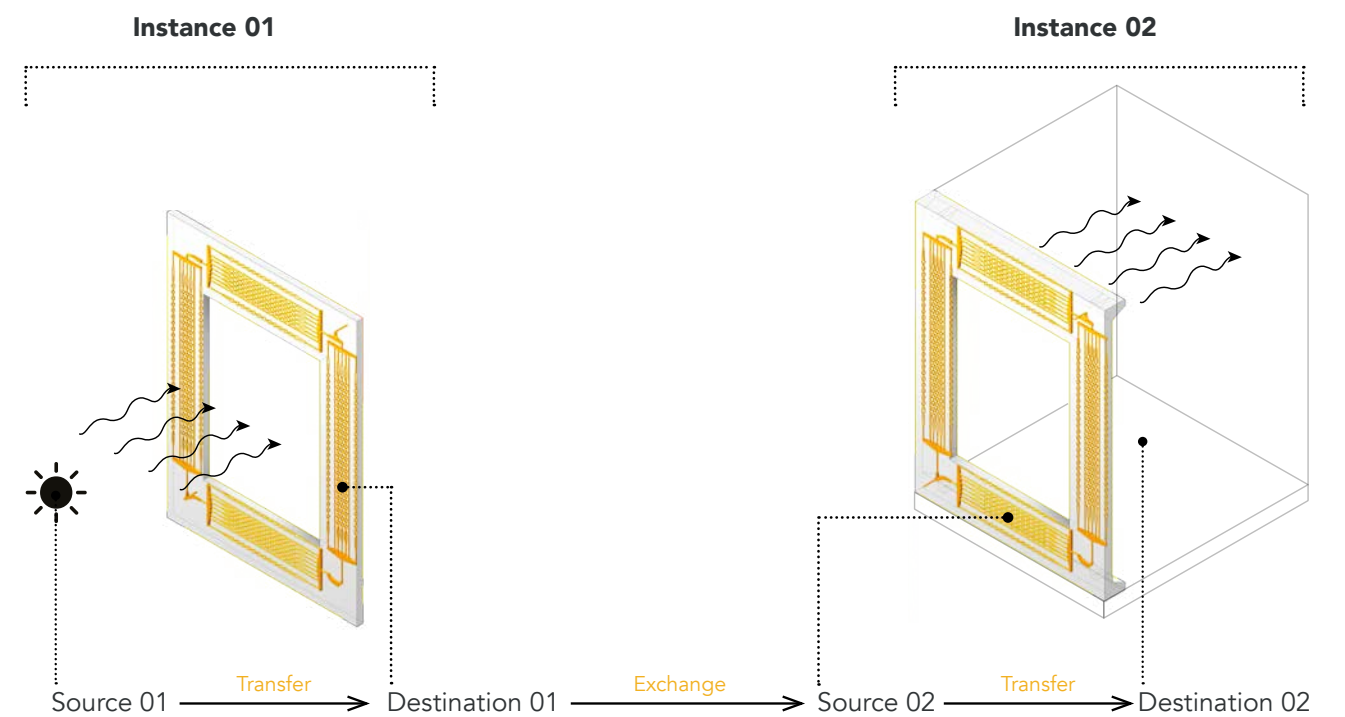


Figure 5.17. Diagram showing the two different instances to analyse heat transfer efficiency of the facade panels. (Author)

### 5.3.1 Geometry and meshing

The geometry used for the simulation was divided into two types. The first one with the designed and optimised tubular network geometry within the mass of the facade panels (see network geometry 06 in section 8.1.6) and the second one the same as the first with an exception that the tubular network is that of the one without any design optimisation with the straight tubes (see network geometry 01 in section 6.3).

To analyse the heat transfer difference in sense of the increased surface area after topology optimisation and geometry modification using Octopus, the final geometry (see final facade panel geometry in section 8.1.10) of the mass of the facade panel is supposed to be compared to that of a flat facade panel. But due to the very high processing time by COMSOL that could exceed 2 days of computing, a equivalent geometry with triangulated slit geometry was developed manually. The comparison between these different facade surfaces is shown below in figure 5.18. Since the geometries do consist of small segments of surfaces developing the internal void tubes, a fine mesh setting was used to develop the meshing while all the other settings were kept to default.

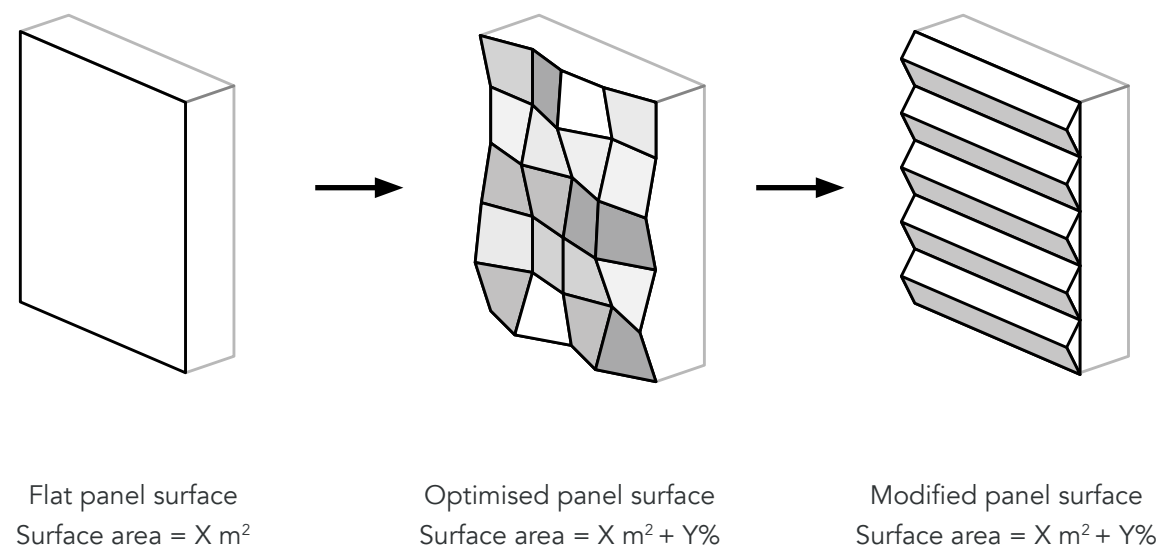


Figure 5.18. Diagram showing the consideration of geometry modification to simplify meshing. (Author)

### 5.3.5 Domains and materials for COMSOL

The design domain for COMSOL is primarily grouped by the type of material (figure 5.19). Depending on the type and location within the imported geometry, the material of the domain is applied. While the default material library is applied to the domains, the thermal conductivity of the materials are in primary concern for the heat exchange simulation. Depending on the materials selected in this project and minor modifications made to the geometry to simplify the calculation, the thermal conductivity of the materials are changed manually.

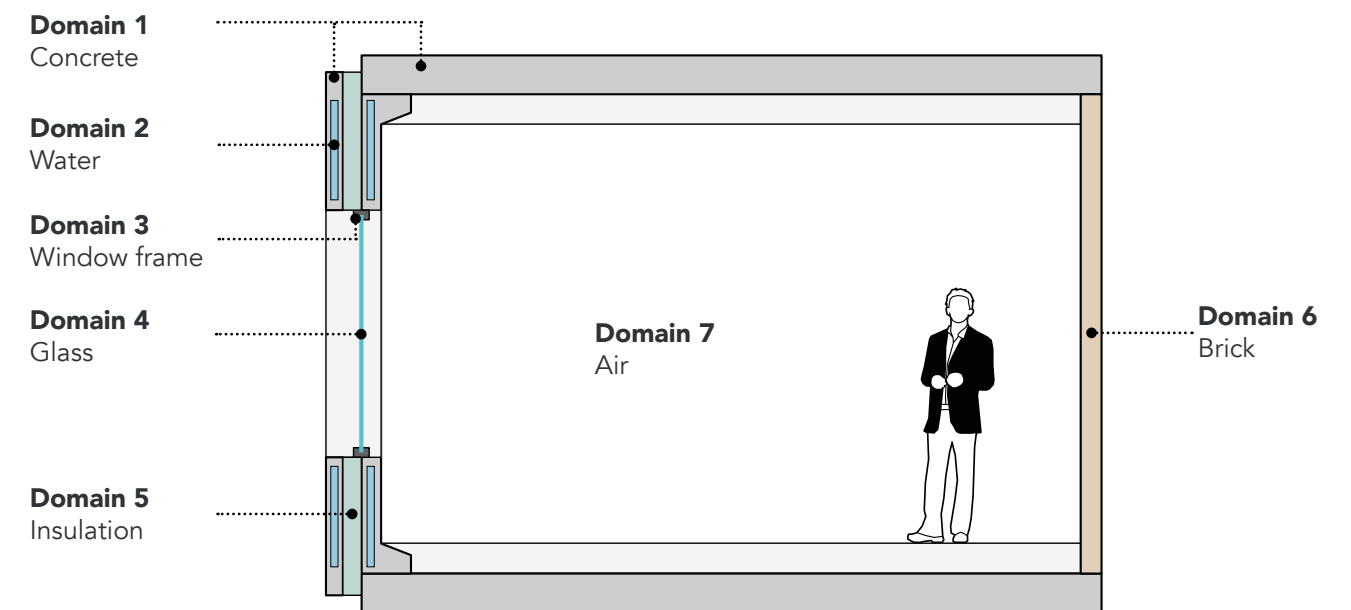


Figure 5.19. Section of the 3D geometry showing the domains set-up in COMSOL. (Author)

#### Thermal conductivity of materials used for COMSOL heat transfer simulation

Concrete:  $1.3 \text{ W}/(\text{m}^2\text{K})$  (Gobain, 2019)

Window section:  $0.144 \text{ W}/(\text{m}^2\text{K})$  (see section 7.8.3)

Glass:  $0.043 \text{ W}/(\text{m}^2\text{K})$  (see section 7.8.4)

Insulation:  $0.05 \text{ W}/(\text{m}^2\text{K})$  (see section 7.8.6)

Brick:  $0.5 \text{ W}/(\text{m}^2\text{K})$  (COMSOL default)

### 5.3.5 Set-up for COMSOL

The simulation for the heat transfer in the designed heat exchanging facade panel, is carried out for the winter scenario on the winter solstice for critical evaluation of the design. This was considered primarily as the heat source during the winter is the environment with solar radiation. This case does reverse during the summer as the heat source is the environment along with the users inside, the appliances and other mechanical heat sources. Since this project was not based upon an existing case, the accurate relevant efficiency of the facade would have been vaguely measured.

**Weather:** Delhi, India

**Day:** 22nd of December (Winter Solstice)

**Start time:** 0800 hrs

**Simulation period:** 1440 hrs with 1 minute interval.

**Simulation type:** Time dependent

Depending on the instance of the simulation, the flux and the probes vary. Since the water flow within the designed facade system is not considered in the thermal simulation, the values are manually abstracted and fed to simulate the heat transfer cycle. The flux and probes and flux allocations for both the instances are shown below in figure 5.20. The individual set-up for the different instances are discussed in section 7.9.

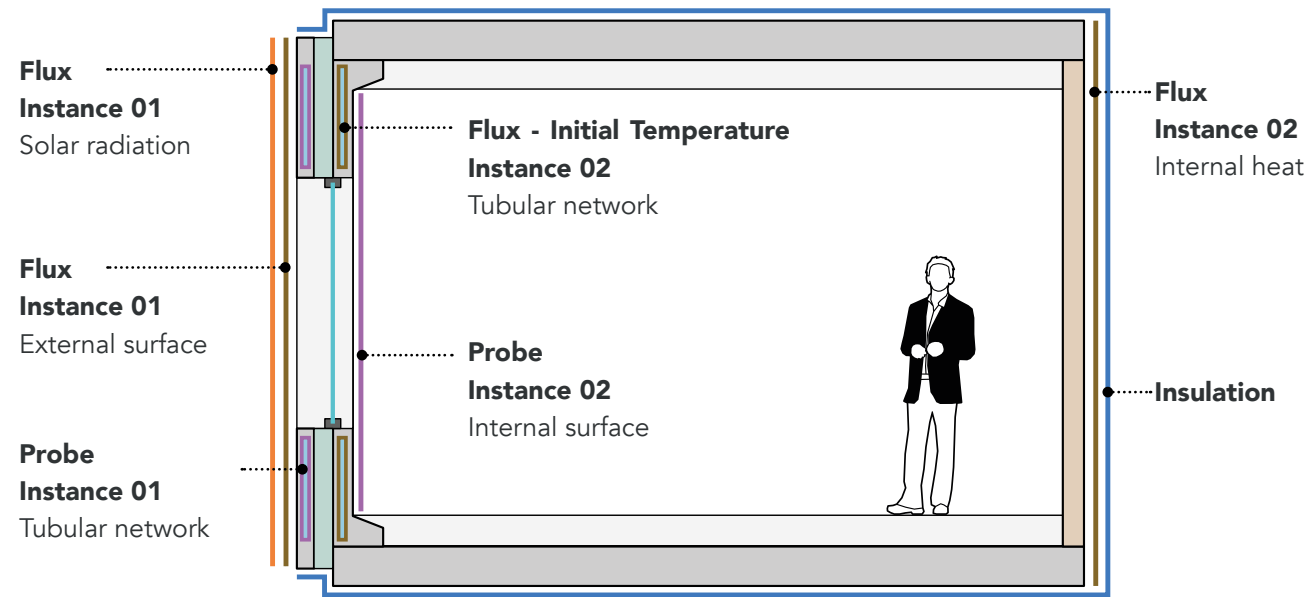


Figure 5.20. Section of the 3D geometry showing the flux and probe for set-up in COMSOL. (Author)

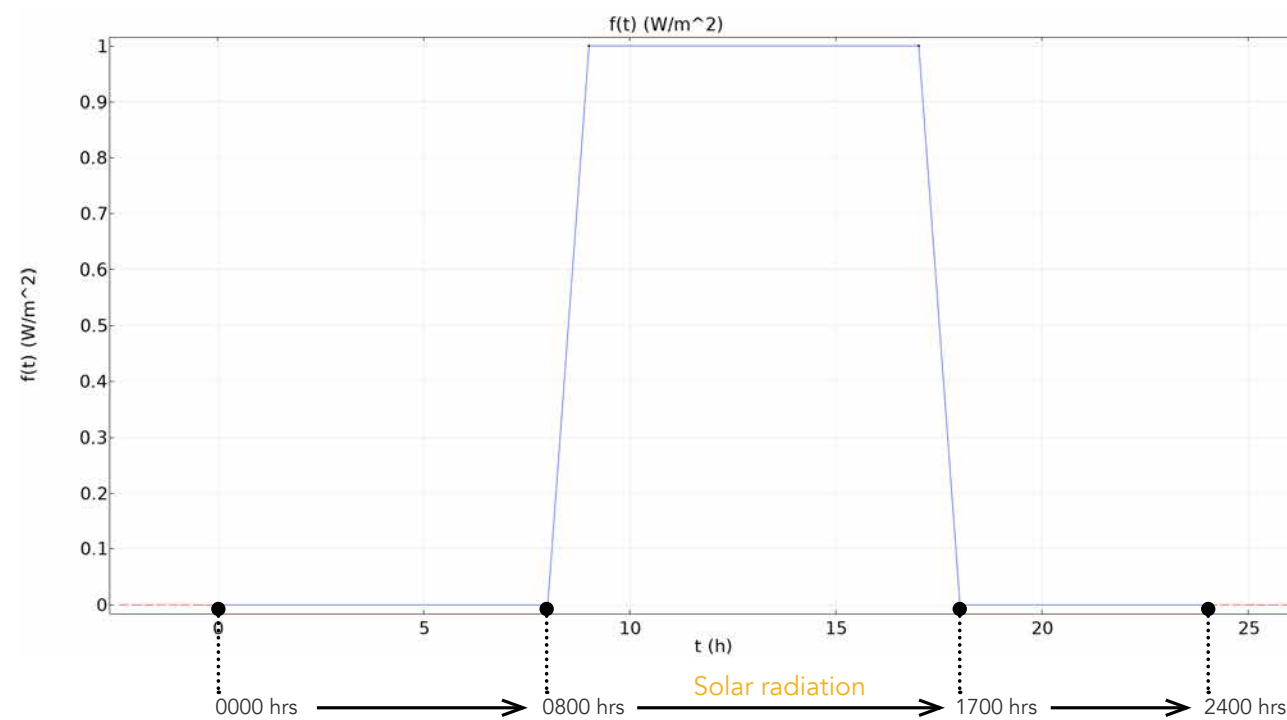


Figure 5.21. Solar radiation time function applied to Flux 1 for instance 01 set-up in COMSOL. (Author; Comsol)

The external temperature is provided by the weather file but due to the complex nature of the 3D geometry and the setup, solar radiation was unable to be simulated. To tackle the problem, the average solar radiation on the surface was calculated using Ladybug + Honeybee in grasshopper and fed manually with a time function for the simulated day as shown in figure 5.21. The derived surface radiation is stated below.

**Weather:** Delhi, India

**Day:** 22nd of December (Winter Solstice)

**Time of radiation:** 0800 hrs to 1800 hrs

**Surface area of the external panel:** 18.04 m<sup>2</sup>

**Surface radiation per day or per shift:** 2.97 kWh/m<sup>2</sup> ≈ 300 Wh/m<sup>2</sup>

Figure 5.22. Set up used in COMSOL multiphysics with inputs on the left column and output with 3D visualization of the imported geometry with applied materials.

The scripting for calculating the solar radiation on the external facade surface is shown in appendix 12.7. The other conditioned temperature set as the initial temperature for the heat transfer simulation were applied to the Common model inputs and initial values of the common domains while rest others were set to ambient temperature to respond the weather input set for the simulation. A typical setup used for this project along with the 3D model with different probes are shown in figure 5.22 below.

### 5.3.5 Constraints and considerations for heat transfer simulation

**1. Geometry meshing:** Since the meshing of the optimised geometry was not possible and as a response an approximated surface was used to analyse the heat transfer, there might be a variance in the calculated result.

**2. Solar radiation:** The inability of the solver to process the solar to surface radiation because of the complex 3D geometry does neglect the solar angles even though a manual flux was setup to replace.

**3. Indoor temperature.:** The simulation does not take into consideration the heat generated in the indoor space nor the heat transmitted through convection or radiation due to time constraints. The very high computation time for the convection and radiation through the CFD counterpart in COMSOL was left out of the scope of this thesis. The average value of heat transfer through the inner surface was compared to that of the typical requirement of a office space and the efficiency of the facade system was speculated.

**4. Water flow and heat loss:** In order to simplify the heat transfer simulation, the continuous flow of water between the internal and external panel was not simulated. By doing so, the heat losses during the movement and transfer time of the water between the panels in neglected.

## 5.5 CONCLUSION

The method followed in the digital work-flow of this project was described along with the specific targets set to be achieved at the end of this thesis. The specifics of the two target set along with the evaluation done at the end were described and the needed support for various different digital tools were mentioned. With this method followed, the number of different possible options that could have resulted from the single boundary condition and the constraints leading to the final geometry was made evident.

The use of different digital tools do imply specific constraints which then shape the final geometry. These constraints specific to various digital tools are mentioned along with the possible workarounds and considerations made to overcome. The needed modifications made which correspond to the final geometry to make it compatible with minimum work load were done and has been stated in this chapter. This modified geometry is further simulated and referred but does not carry forward its mention any further in the chapter. To verify the nature of the simulations carried out in this project, validation of each digital tool was made and compared either to analytical calculations or standard models and the outputs were compared. The settings of these parameters set were then carried forward to perform similar simulations ahead in this project.

This page is intentionally left blank.

# 6. FABRICATION CRITERIAS

## *CHAPTER OVERVIEW*

This chapter elaborates the fabrication criteria discussed in chapter 4. It details out the structural system used in the design of the facade panel and the related materials and fixtures considered to attain the boundary condition laid. The concrete cover for the geometry with respect to the structural system and fabrication is also determined with experiments. The method of fabrication and the limitations related to the materials used in the process and the method itself were derived and informed to the network geometry which forms the basic network geometry of the tubes at the end of the chapter.

The conceptual network geometry designed in consideration of the basic parameters are in context to the layout of the facade panel, but do need to comply with constraints by the structural system and the method of fabrication. The constraints thus needed by the mentioned entities need to be calculated, simulated and tested before the implementation of the same into the design criteria. To make a clear understanding of these two mentioned factors, this chapter is broadly classified into the calculation / simulation and designing under structural systems and the method of fabrication, with materials, fixtures and equipments considered over-lining them.

## 6.1 STRUCTURAL SYSTEM

The structural system is dependent on the materials used along with the reinforcement members and their behaviour in collaboration to the fixing constraints and the loading conditions. The following mentioned materials and fixtures were studied and analysed for their behaviour over the designed panel.

### 6.1.1 Materials and reinforcement

#### 1. Concrete

The mixture of concrete preferred to be used for this thesis was assumed to be that of an High performance concrete with compressive strength greater than 60 MPa or an Ultra high performance concrete with compressive strength ranging over 140 MPa. One such example is the Lafarge Ductal JS1000 UHPC with steel fibres which can range upto 150 MPa in compressive strength performance (figure 6.1a). Depending on the limitation of sourcing such special made concrete in small quantities to perform the designed facade panel, locally available fibre reinforced concrete with a compressive strength of 20 MPa, usually used for abrasion resistant flooring was used and experimented with. The concrete used for experimentation was Weber Beamix with fibres by Saint Gobain (figure 6.1c).

To perform the density test of this concrete mixture in order to perform tests for reinforcement cover, a cube of dimension 50 x 50 x 50 mm was cast and weighed. This along with the properties documented by the manufacturer are mentioned below (Gobain, 2019):

Density: 2026 kg / m<sup>3</sup> (lab test by author, 2019)

Compressive strength > 20 N/mm<sup>2</sup>

Bending tensile strength > 6 N / mm<sup>2</sup>

Tensile strength > 1.5 N / mm<sup>2</sup>

Shrinkage < 0.03%



Figure 6.1a. Weber Beamix with fibres by Saint Gobain, concrete cube of 100 x 100 x 100 mm. (Author)

In contrary to simulate the performance of the concrete in combination to the restricted boundary conditions for that of the topology optimisation in section of the facade, the Ductal concrete by Lafarge was used with the following properties. (Ductal, 2019)

Density: 2,400 – 2,565 kg/m<sup>3</sup>

Flow: 7 to 10 in. (175 to 250 mm) diameter without visible sign of fibre segregation

Compressive Strength > 100 MPa at 4 days

Compressive Strength > 150 MPa at 28 days

Tensile Strength > 5 MPa at 28 days

Modulus of Elasticity > 45 GPa at 28 days

Long-term Shrinkage < 800 microstrain at 28 day



Figure 6.1b. A bag of Lafarcge Ductal JS1000 with steel fibres. (Ductal, 2019)



Figure 6.1c. A bag of Weber Beamix with fibres by Saint Gobain. (Gobain, 2019)

These values may differ in terms of local curing in Delhi, India with an average curing temperature higher than 23°C and low relative humidity.

The composition of the concrete mix used for the physical testing and prototyping in this thesis was the one directly from the manufacturer of the product and no alteration whatsoever was made. Some of the contents of the mixture are mentioned below.

Limestone flour :	25 -50 %	Fibre type: Glass fibre
Calcium sulphate (natural) :	5-10%	Fibre thickness: 50 microns
Grey cement :	2-5%	Fibre length: 6mm
Aluminium silicate hydrate :	0.1- 1%	

## 2. Reinforcement mesh

the reinforcement mesh used for the design of the facade panel is selected to be Solidian Grid Q142/142-CCE-25 mesh which is comprised of Carbon fibre and epoxy resin (Solidian\_A, 2019) made for special built high performance loading systems like flyover bridges etc. The availability of the selected sample was the reason for the selection. By performance the Solidian GRID Q121/121-AAE-38 could perform well for the designed facade panel for this thesis.

### Type and number of reinforcement mesh

The verification for the strength and performance validation of the reinforcement mesh in accordance to the technical approval by Deutsches Institut für Bautechnik (DIBt, 2017), was performed using a setup of a twin wall system of 250 mm thick internal load bearing panel and 140 mm thick external panel with an insulation layer >140mm of thickness. The specific mesh used for this test was Solidian GRID Q121/121-AAE-38 made up of AR-Glass and epoxy resin (Solidian\_A, 2019). The property of this specific mesh used to that of the proposed mesh for this thesis has been compared in table 6.1, and it is evident that while the prior mesh configuration is sufficient enough for the design facade panel, the later delivers a performance of 2 to 3 time that envisaged for the design as the tests does consider only the self weight of the system and not the loads by the fixtures and that of the load by the high wind pressure and a much ticker configuration of the twin wall panel. By this it was concluded that a single mesh along the span of each facade panels i.e internal and external, should perform beyond the limit state of the design. Specific analytical solution per mesh configuration was let out of the framework of this thesis as it does not affect the design of the facade panel except the consideration for the maximum size and layout of the mesh along with the minimum cover needed to limit the design criteria, which have been successfully derived from the referred test.

	solidian GRID Q121/121-AAE-38	solidian GRID Q142/142-CCE-25
<b>Fiber material</b>	AR-Glass	Carbon
<b>Impregnation</b>	Epoxy Resin	Epoxy Resin
<b>Tensile strength (Longitudinal)</b>	1.480 N/mm <sup>2</sup>	3.100 N/mm <sup>2</sup>
<b>Tensile strength (Transversal)</b>	1.560 N/mm <sup>2</sup>	3.300 N/mm <sup>2</sup>
<b>Resisting force (Longitudinal)</b>	179 kN/m	440 kN/m
<b>Resisting force (Transversal)</b>	188 kN/m	468 kN/m
<b>Modulus of elasticity (Longitudinal)</b>	>72.000 N/mm <sup>2</sup>	>220.000 N/mm <sup>2</sup>
<b>Modulus of elasticity (Transversal)</b>	>72.000 N/mm <sup>2</sup>	>205.000 N/mm <sup>2</sup>

Table 6.1. Comparison of properties of Solidian GRID Q121/121-AAE-38 and Solidian Grid Q142/142-CCE-25; (Solidian\_A, 2019; Solidian\_B, 2019)

### Concrete cover of reinforcement mesh

The mesh are available in a maximum size of 2,500 mm x 6,000 mm and needs to be considered for designing the panel with an mesh overlap of at least 15 mm (DIBt, 2017).

As prescribed by the test, the minimum recommended concrete cover for these reinforcement meshes need to be at least 15 mm on all sides (DIBt, 2017). This concrete cover limitation needs to be addressed while designing the location of the tubes and other fixtures in the facade panel.

## 3. Reinforcement dowels

The other critical member to be designed was the reinforcement dowel that connect the resting internal panel to that of the hung external panel upon the prior. The criteria of selecting the specific material for this design was to rule out the use of metal based solutions and consider a material with very low thermal conductivity to increase the insulating behaviour of the facade panel by eliminating the aspect of thermal bridges, which is a primary concern with steel connection dowels. In reference to the above concerns, the Schöck Combar Isolink TA-H (for horizontal reinforcement) and TA-D (for diagonal reinforcement) comprised of glass fibre reinforced polymer (GFRC) was selected.

### Type and number of reinforcement dowels

The designing of the dowels to determine the number of such entities needed and determining their location on the designed facade panel was highly critical to inform and manipulate the design constrains for the arrangement and minimum cover needed around the hollow tubular network to be cast within the mass of the concrete facade panels.

The physical properties of this material are mentioned below:

Length of a bar, TA-H/ TA-D: 300 mm

Diameter: 12 mm (14 mm with grooves)

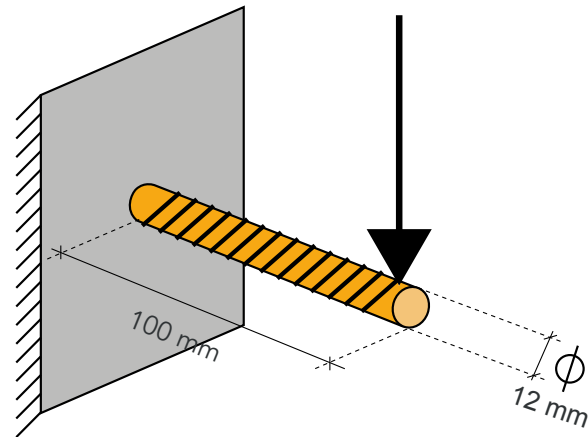


Figure 6.2. Diagram showing the setup to determine the cross section of the dowel needed. (Author)

The design of the reinforcement was calculated analytically and verified by a structural simulation using karamba 3D plug-in of Rhinoceros' grasshopper. This was then tallied with that of the design guidelines enlisted by the company Schöck. To calculate the number of bars needed for the design, the total amount of cross section of the bar needed was calculated with a setup as shown in the figure 6.2, where the bar is considered to be loaded as a cantilever. The length of the overhang is 100 mm equal to the width of the insulation. The load applied is the total mass of the concrete of the external panel.

Width of the insulation layer = Length of overhang =  $L = 100$  mm

Volume of the external panel =  $0.932$  m<sup>3</sup>

Density of concrete =  $2,400$  kg/m<sup>3</sup>

Total weight of the external panel =  $F = 2,203$  kg =  $21.6$  kN

The properties of the material of the reinforcement bar used are mentioned below (Schöck, Schoeck Combar, 2016),

$E$  = Tension modulus of elasticity =  $60,000$  N/ mm<sup>2</sup>

$I$  = Moment of inertia =  $(\pi r^4)/4 = 1017.87$  mm<sup>4</sup>

$\sigma_{\text{limit}}$  = Limit stress =  $20$  N/mm<sup>2</sup>

Firstly, the deflection of the material at to validate the setup done in Karamba 3D was determined as following analytically:

$$\delta = \frac{F L^3}{3E I}$$

$$\delta = 117 \text{ mm}$$

The above mentioned setup was analysed to be that in Karamba 3D and found to be,  $\delta = 118.7$  mm, which is almost similar to the analytical calculation and the properties of material and performed simulation is validated.

Secondly, considering the previous deflection is very high, the design was limited to the maximum allowable deflection of  $L/360$  (BIS, 2016) and determine the needed cross section diameter for the reinforcement.

To determine the radius the following equation was set up.

$$\delta = 0.27 \text{ mm} = \frac{F L^3}{3E I}$$

$$\Rightarrow r = 27.4 \text{ mm}$$

This under simulation in Karamba 3D, did result in an almost similar result of  $r = 28.5$  mm.

It was also noticed from the simulation that with 57 mm diameter of the reinforcement cross section, the shear stress value did account to  $11.9$  KN/cm<sup>2</sup> or  $119$  N/mm<sup>2</sup>, which is well above the allowable limit stress of the material at  $20$  N/mm<sup>2</sup>.

It is to be noted that, the material of Schoeck Combar may crack under such loading condition as stated in Schöck (2016), and fail eventually even if the considered deflection is really small. The material of schoeck combar does not show any yielding behaviour and hence fails at a sudden. The value of  $\sigma_{\text{limit}} = 20$  N/mm<sup>2</sup>, is highly limited to the actual property of the material which is around  $\sigma_{\text{limit}} = \text{Limit stress} = 150$  N/mm<sup>2</sup> limited for safety measures which is or else considered to be a factor of 1.3 for normal design considerations.

Therefore, the radius of the cross section of reinforcement needed was calculated from the shear limit of the material as equated below,

$$\sigma_{\text{limit}} = \frac{M \times y}{I}$$

where,  $y$  = radius of the cross section required

$$\Rightarrow r = 103.2 \text{ mm}$$

The same by analysis of Karamba 3D does analyse a value of  $103$  mm, with no deviation from the analytical solution.

Hence, the total cross sectional area of schoeck combar reinforcement needed = 8364.6 mm<sup>2</sup>

Cross section of a single 12 mm schoeck combar reinforcement = 113.09 mm<sup>2</sup>

Hence total number of schoeck combar reinforcement bars needed = 73.9 ≈ 74 bars.

The above derived design for the reinforcement using 74 schoeck combar dowels are then cross checked to that of the guidelines provided to design by the company (Schöck, 2018).

As discussed in the example (Schöck, 2018) of designing a sandwich wall freely suspended cover layer as is the case considered in this thesis, the different loading cases were undertaken and analysed for the number of bars needed for each type of TA-H and TA-D.

Cover layer:  $h_v = 100$  mm

Insulation thickness :  $h_o = 100$  mm

Structural layer:  $h_r = 140$  mm

Bond length of the isolink in the concrete :  $h_{norm} = 60$  mm

Wall area :  $A = 4 \times 3 = 12$  m<sup>2</sup>

Selected concrete type class ≥ C30/37

Load case 1 : Wind pressure,  $W^k =$  Wind load : 1 kN/m<sup>2</sup>

Load case 2 : Temperature gradient over the thickness of the cover layer according to the approval,  $\Delta T = 5$  K

Load case 3 : Fresh concrete pressure, not applicable

Load case 4 : Self weight of cover layer

Load case 5 : Temperature difference between cover layer and structural according to  $\Delta\theta = 40$  K

Verification in the ultimate limit state for the Schöck Isolink type TA-H,

Combination of load cases 1 + 2,

Required quantity per cover layer = 5.3 pieces / m<sup>2</sup> (Schöck, 2018, Table 13)

= 40.3 ≈ **40 pieces of TA-H** for an area of 7.6 m<sup>2</sup>

Verification in the ultimate limit state for the Schöck Isolink type TA-D,

Under load case 4: Self weight of the cover layer,

Required quantity per cover layer = 0.68 pieces / m<sup>2</sup> (Schöck, 2018, Table 13)

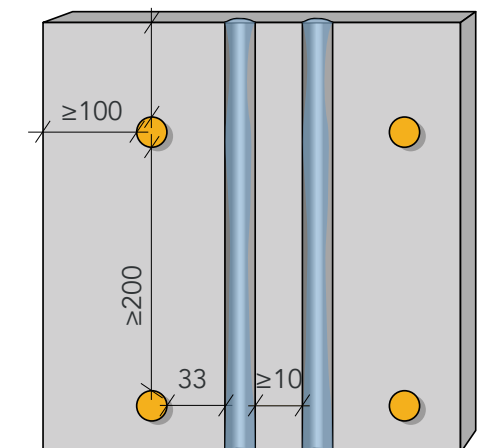
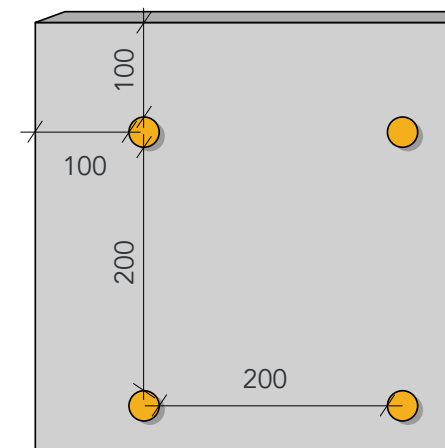
= 4.89 ≈ **5 pieces of TA-D** for an area of 7.6 m<sup>2</sup>

### Concrete cover of reinforcement dowels

By the above guidelines there has been a discrepancy with the design guidelines provided by the company which accounts for 45 number of combars in combination to that of the one calculated analytically and through structural simulation that accounts for 74 number of combars.

On the other hand, the concrete cover as mentioned by the guidelines of the company (Schöck, 2016) and the national technical approval (DfT, 2016) has been depicted below to be as 100 mm from the edge to that of 200 mm between two dowels. These constraints of the concrete cover needed around the dowels was analysed with the combined design of void tubular network and mass of the facade panel and was figured out that the interference in the design to comply with the mentioned concrete cover will render the design not to be a viable solution as it demands the complete space over the tubular network geometry. While the above mentioned concrete cover was based on the guidelines of C 30/35 concrete, the proposal of using a high strength fibre reinforced concrete would suffice the minimum needed cover.

While the needed cover between the edge of the reinforcement dowel and that of the tubes as recommended needs to be of 100 mm while that in the design is limited to a minimum of 33 mm, a test for the integrity of the concrete cover to that of the maximum experienced over a single dowel was tested. The details of the same are outlined in section 6.1.4 after the structural analysis of the same was made.



Note: All dimensions in mm

Figure 6.3a. Prescribed concrete cover for the reinforcement dowels. (Author)

Figure 6.3b. Designed concrete cover for the reinforcement dowels. (Author)

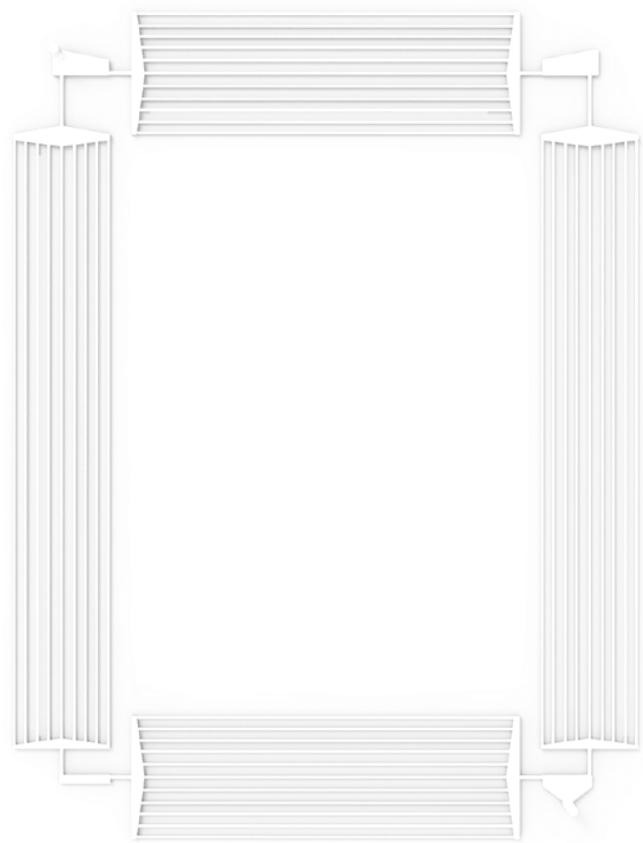
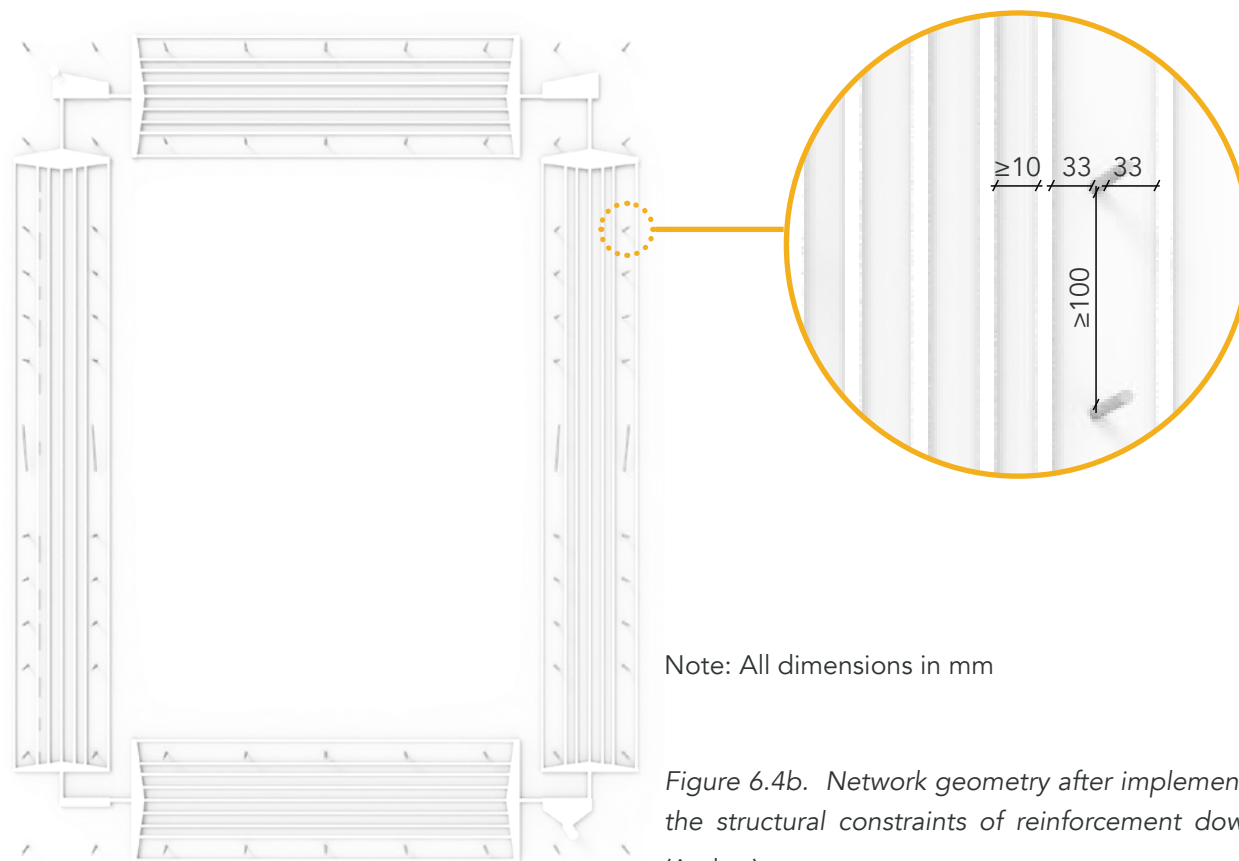


Figure 6.4a. Network geometry before implementing the structural constraints of reinforcement dowels. (Author)



Note: All dimensions in mm

Figure 6.4b. Network geometry after implementing the structural constraints of reinforcement dowels. (Author)

## 6.1.2 Fixtures

With the core composition of the facade comprised of the material and the reinforcements there are additional fixtures that are used to design a complete facade panel. The specific details and the behaviour of them on the design has been discussed herewith.

### 1. Window

The window section used for the design of the facade panel was selected to be Schüco AWS 75 SI+ due to various different reasons mentioned below.

The ability to accommodate double or triple glazing by choice

The ability to fix form the inner space

Wind load resistance of C5/B4 with capacity of 2000 Pa and 1000 Pa for repeated pressure under 50 cycles (NSAI\_standards, 2016). This confirms the ability to resist the high speed winds of 39 m/sec of the designed locality of Delhi , India

Low thermal conductivity of 0.9 W/m<sup>2</sup>K for higher performance of facade to

Density of the cross section:

Total weight of the window section: 8.8 m x (1.16 + 1.5 kg/m) = 23.5 kg

More details about the selection purpose, performance and details are discussed in section 7.8.

### 2. Glass

The glass selected for the design configuration is Saint Gobain Planitherm PLT T- Argon in a configuration of 6-12-6 mm. Although the glass selected is a double pane glass, the structural calculations are based on the loading for a triple glass pane for designing the panel as future proof.

Total surface area of the fenestration = 4.79 m<sup>2</sup>

Total thickness of glass = 12 mm

Total weight by the glass panel = 460 kg

More details about the selection purpose, performance and details are discussed in section 7.8.

### 6.1.3 Structural behaviour

The behaviour of the designed facade panel with the tubular network geometry inlay subjected to the defined boundary conditions in the previous sections of this thesis. A summary of the boundary conditions applied to the facade panel for static structure analysis is mentioned below..

Wind load @39 m/sec = 7681 N

Window load (483.5 kg) = 4741 N (include weight of aluminium section as shown in figure 6.5)

Two point loads (2 x 75 kg human resting) = 735.5 N

The setup to analyse the static structural behaviour of the designed panel was considered to be done with Karamab 3D as first, but as the combined geometry of the mass of the twin panel system along with the embedded tubular network geometry within these mass was not possible to be analysed by Karamab 3D, as it could not be simplified to be considered as a shell while neglecting the mass of the panel within, which or else if done would vary the volume of the panel by a huge margin and deviate the results. The second consideration was to analyse with Ansys static structural component, but as described in section 5.2, the

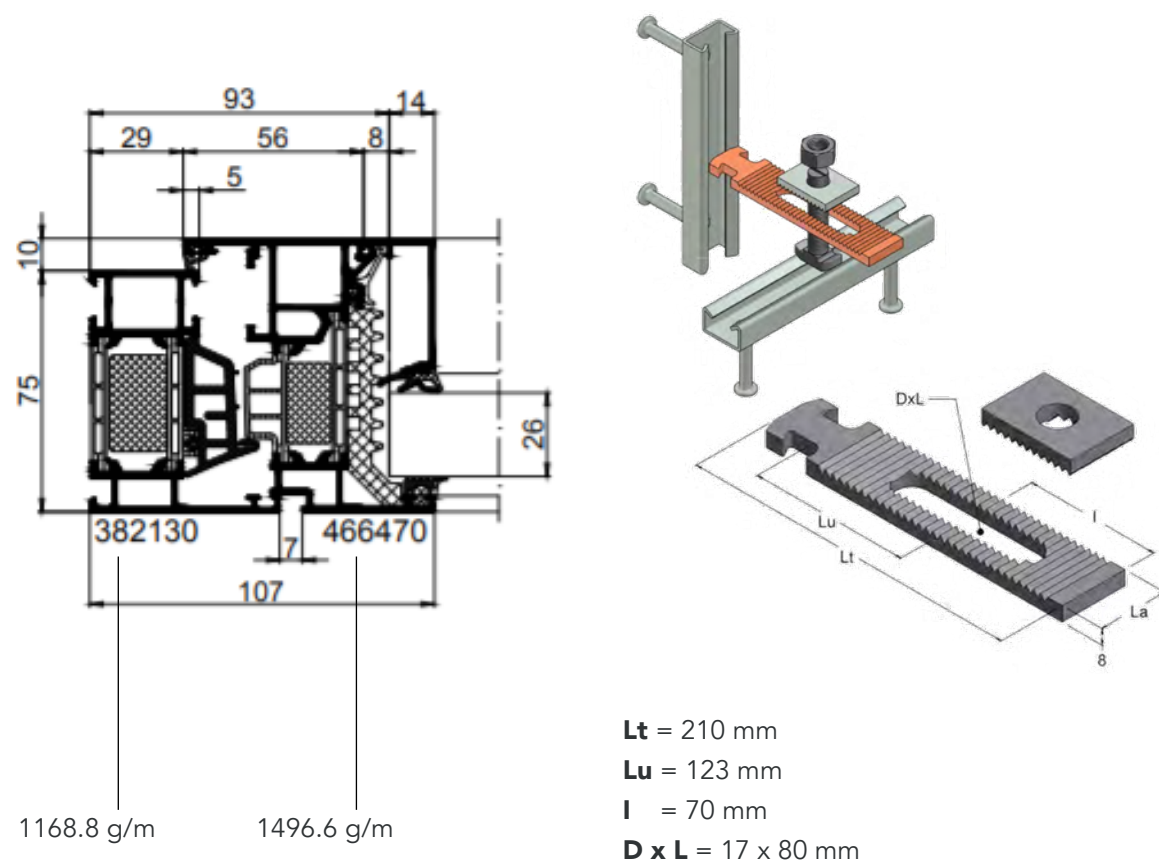


Figure 6.5. Sections used in Schüco AWS 75 SI+. Figure 6.6. Exploded view of the facade bracket with dimensions. (Technogrip, 2015)

### 3. Facade bracket

The facade bracket needed for the fixture of the designed panel is to mount it at four corners, two at the top and two at the bottom. By design, the facade bracket needs to hold the heavy weight of the panel only in the XY plane of moment and not be loaded over vertically in the Z axis and hence the selected bracket for the designed facade panel is the Hook-head toothed straps by Damilano group's Technogrip designed for prefabricated facade panels with a configuration as shown below. The profile of 40/22/2.5 has a allowable load carrying capacity of 8.5 kN (safety factor=3) and 11.5 kN (safety factor=2), per bracket which is well beyond the design load and is safe to be used.

Lt = 210 mm

Lu = 123 mm

l = 70 mm

D X L = 17 x 80 mm

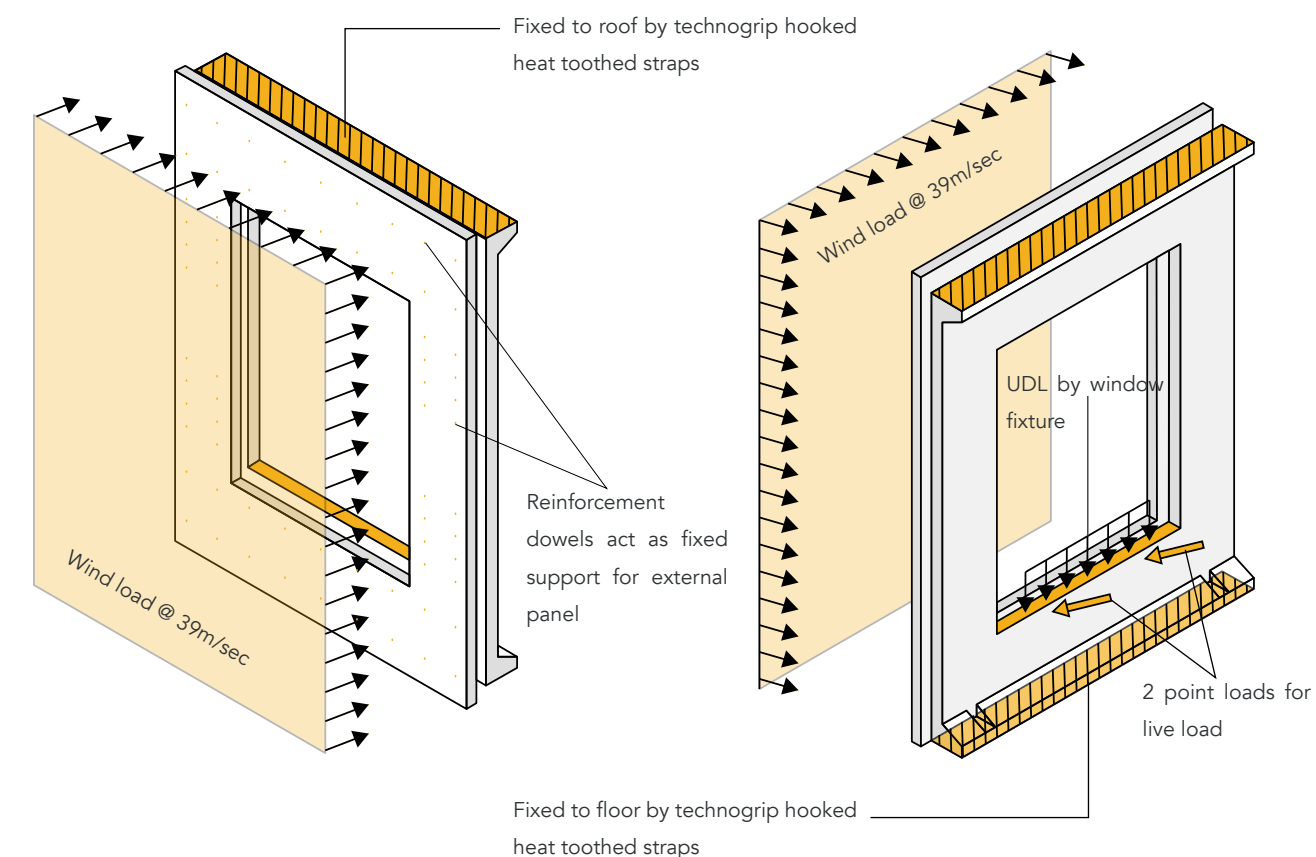


Figure 6.7a Boundary conditions implied on the design for static structural analysis, view from external panel. (Author)

Figure 6.7b. Boundary conditions implied on the design for static structural analysis, view from internal panel. (Author)

limitation of 31,000 elements or nodes did limit the meshing of the combined geometry even if analysed per panel. To overcome these limitations the multi-physics analysis software Fusion 360 was used, through which a very fine mesh could be generated resulting in accurate results of the setup within the boundary conditions.

The setup of the above mentioned boundary conditions in Fusion 360 is shown in figure 6.7.

The static structural analysis (figure 6.8) upon the defined boundary conditions does signify that the maximum displacement is that of 0.1741 mm which is negligible at the critical nodes of the facade panel. The image of this simulation is shown in image x and has been exaggerated to imply the behaviour of the deflection. It is to be noted that the insulation material and fluid within the facade panel has not been considered in this analysis.

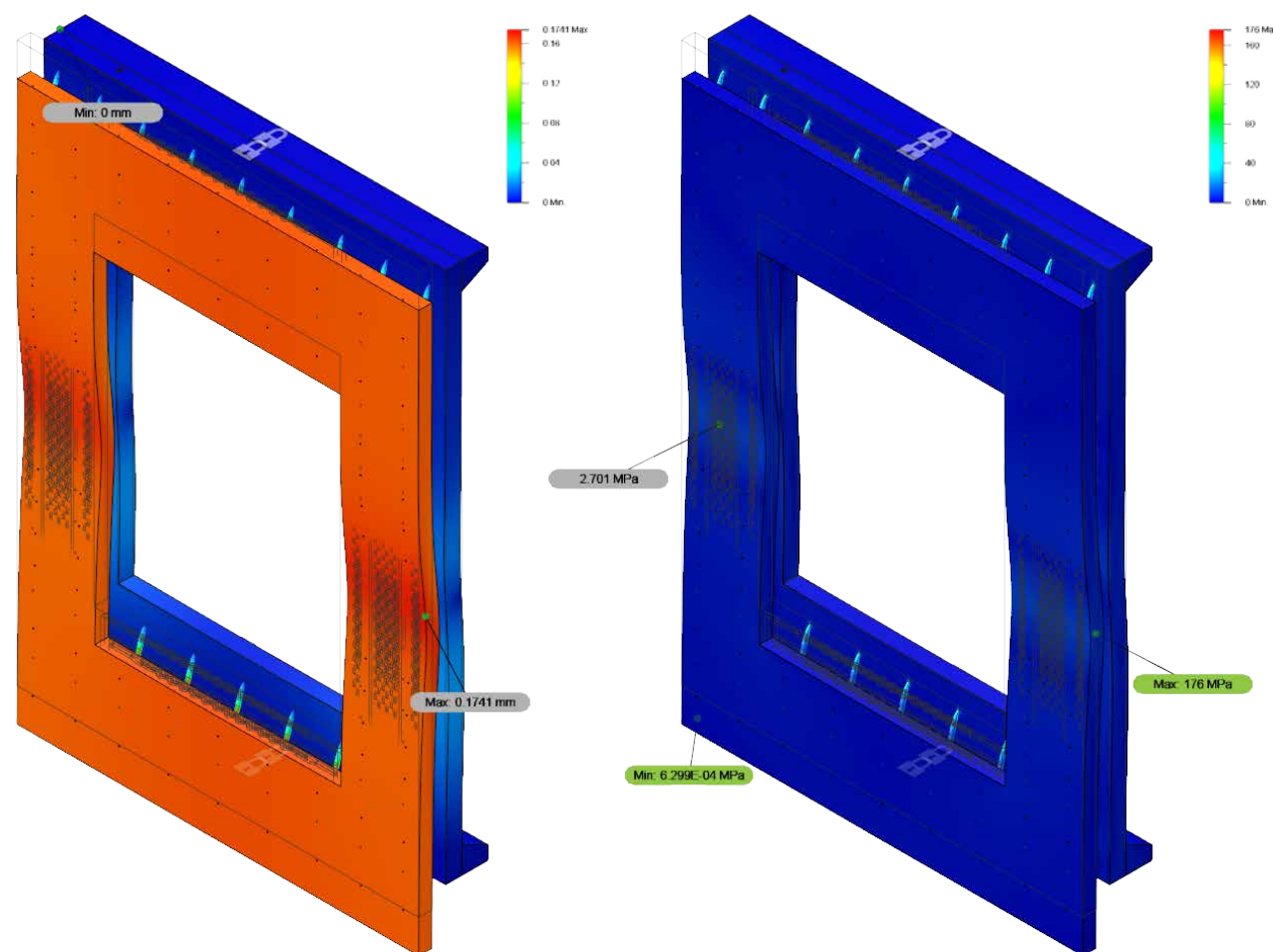


Figure 6.8a. Static structural analysis of the twin panel facade system showing the deflections. (Author; Fusion 360)

Figure 6.8b. Static structural analysis of the twin panel facade system showing the von mises stress. (Author; Fusion 360)

## 6.1.4 Handling and installation

The facade panel is now analysed for its structural stability and performance upon installation on site, where it is loaded to the external boundary conditions and loaded with different fixture. But in combination to the above scenario, the handling and installation also does pose the facade panel to a very different loading condition. The typical method used to install prefabricated panels are tilt-up crane installation system (figure 6.9), where the panel is lifted using 3 point anchors at an angle of 15 degrees to the main structure. This method is preferred over others because these panels are intended to be installed only after the structure is complete or may be simulatanelously and also in the case of replacement or facade upgradation. These anchors could either be prefabricated within the panel, or held with on frame belts. Since the designed panel consists of a void tubular network within and to be of higher effectiveness ,the later method of lifting was used.

After lifting the installation of the panel takes place by first tipping out the top section into place with anchors and then rotating the panel into place with the top half acting as a hinge. This allows for the workers for easy handling and minimum risks of failure. But to accommodate this movement a minimum installation tolerance of 40 mm between the twin-wall facade support and the structure of the building.

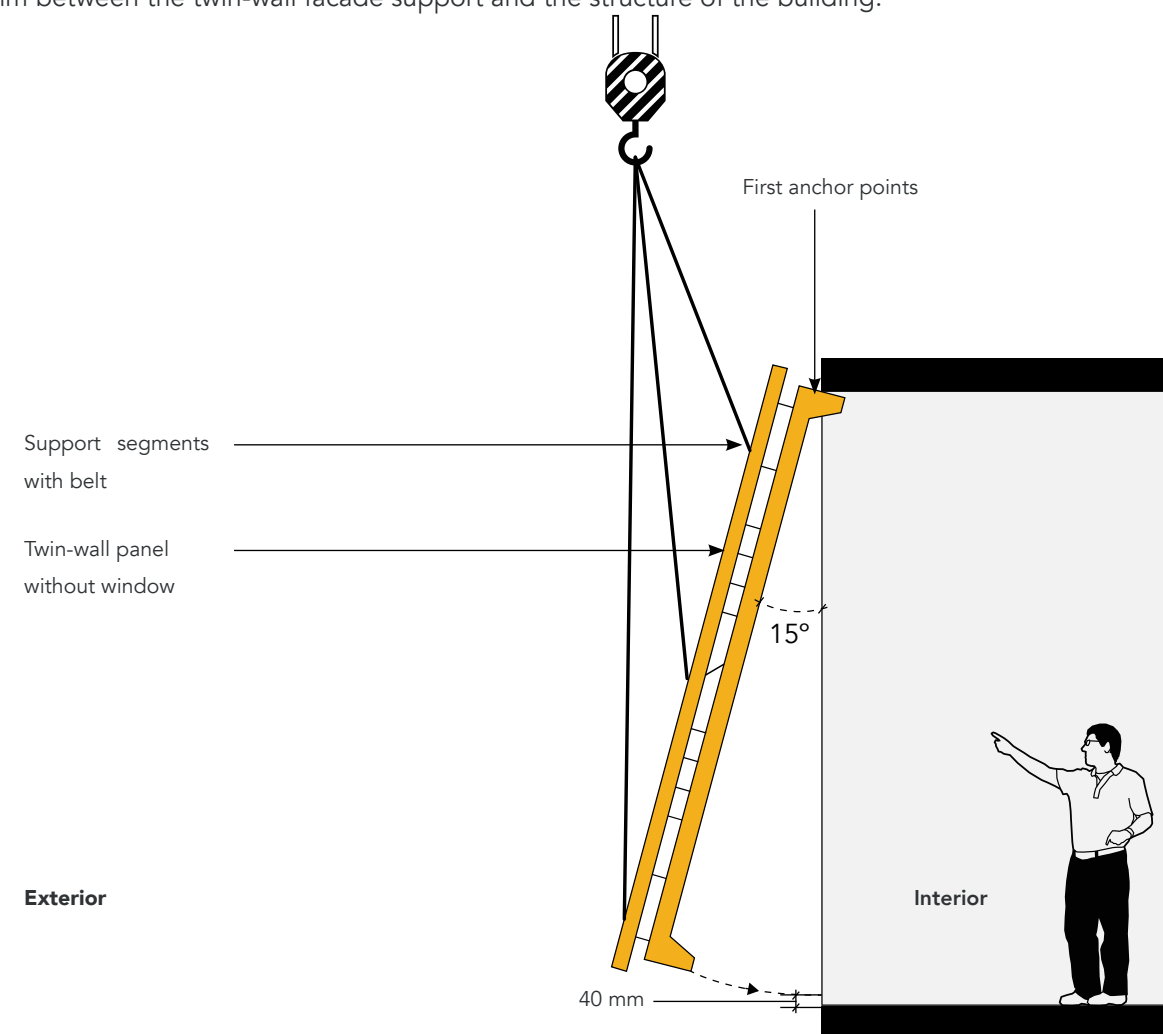


Figure 6.9. Installation of the prefabricated twin-wall facade panel using 3-point tilt-up system by crane. (Author)

### 6.1.4 Concrete cover

The concrete cover matters per type of reinforcement. As derived from the previous sections, the concrete cover stated for reinforcement mesh was considered to be 15 mm on all sides and was implemented in the design to limit the geometry as shown in the section in figure 6.10. The reinforcement dowels on the other hand were a hindrance upon the assessment of the location of the calculated number of dowels to that of the concrete cover needed by them from the inlaid cast tubular network geometry which made the possibility of implementing the envisaged design within the facade panel, which would or else eliminate the design purpose of implementing the heat exchange tubes within the facade and hence the complete functional purpose of the system. While the number of reinforcement bars calculated analytically and by static structural simulation using Karamba 3D was considered over the design guidelines provided by the company as discussed in section 6.1.1, a physical test was performed in the lab to check the amount of load a single reinforcement dowel could carry, with the fibre reinforced concrete used for this project (figure 6.12).

To analyse the maximum loading on the design twin wall facade panel, a Karamba 3D set up was made, where the internal tubes were neglected and the maximum possible loading was considered as the mass of the panel. The 72 dowels were considered as fixed points upon which the load of the front panel was applied and restricted to translation and rotation in all axis.

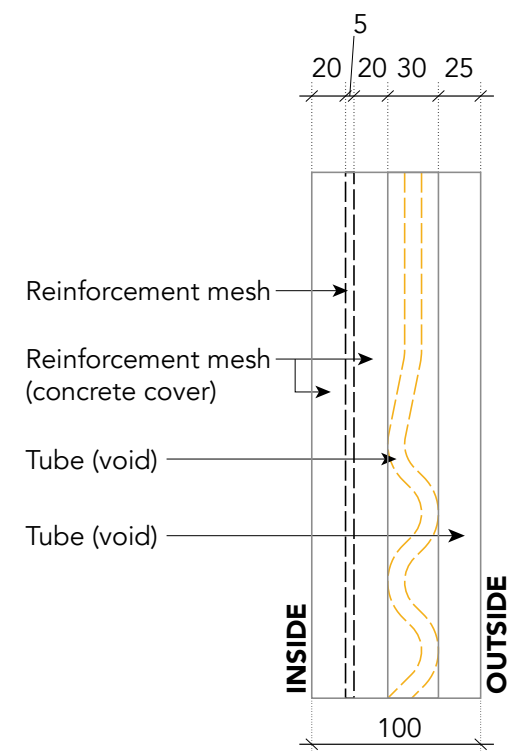


Figure 6.10. Section showing the design constraint zones for the reinforcement mesh and the design. (Author)

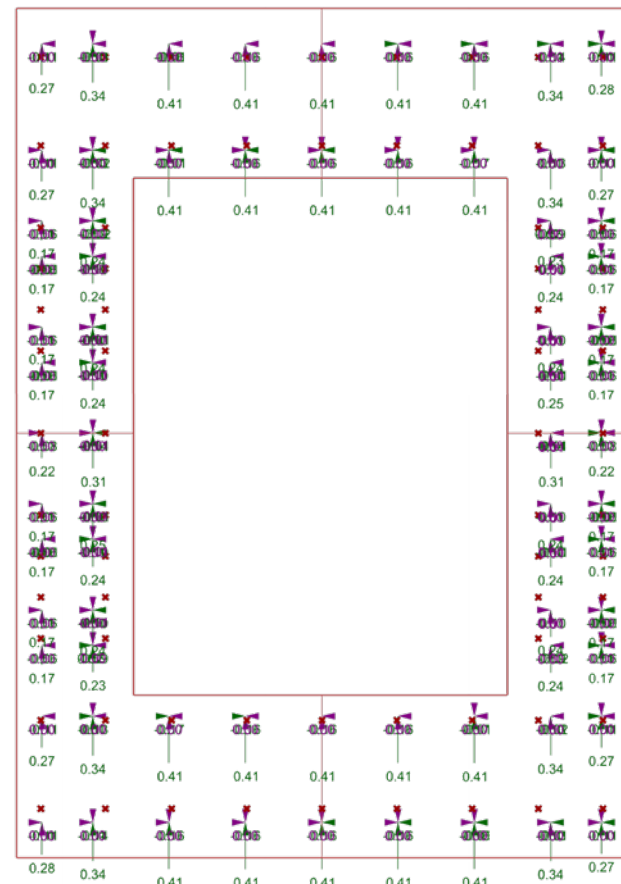


Figure 6.11. Reaction forces on each dowel analysed in Karamba 3D. (Author; Grasshopper)

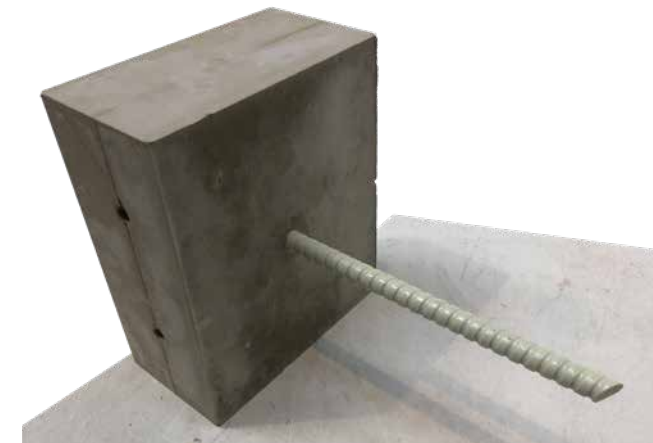


Figure 6.12a. Prototype of the concrete mass with 2 x 10 mm diameter tubes and the reinforcement dowel with 33 mm concrete cover from both of their edges. (Author)



Figure 6.12b. Laboratory setup of the concrete mass with 2 x 10 mm diameter tubes and the reinforcement dowel with 33 mm concrete cover from both of their edges. (Author)

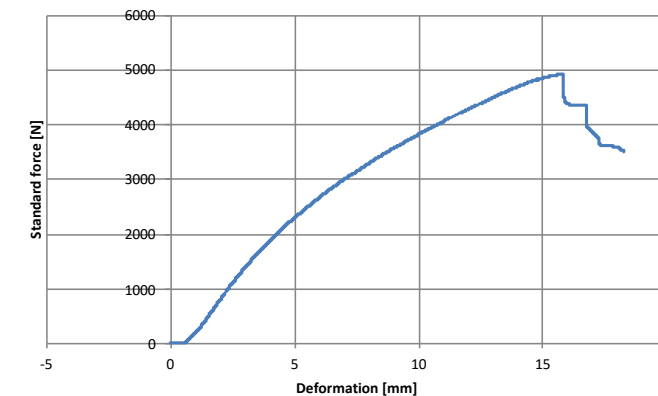


Figure 6.12c. Graph of the loading test showing the force applied (N) to that of the displacement (mm). (Author)

This setup did result in a deflection of 2.04 mm on loading of 840 N. The trend in the graph of the tests shown in figure 6.12c does show that the deflection increased gradually until just below 5000 N before it did start splitting the cover around the concrete, but there had been no deformation that would affect the small concrete cover. This test does comply the design consideration with the information that the designed location of the tubes and the reinforcement dowels with the concrete cover would suffice the boundary conditions it is subjected to. Figure 6.13 shows the splitting of concrete cover after the test.

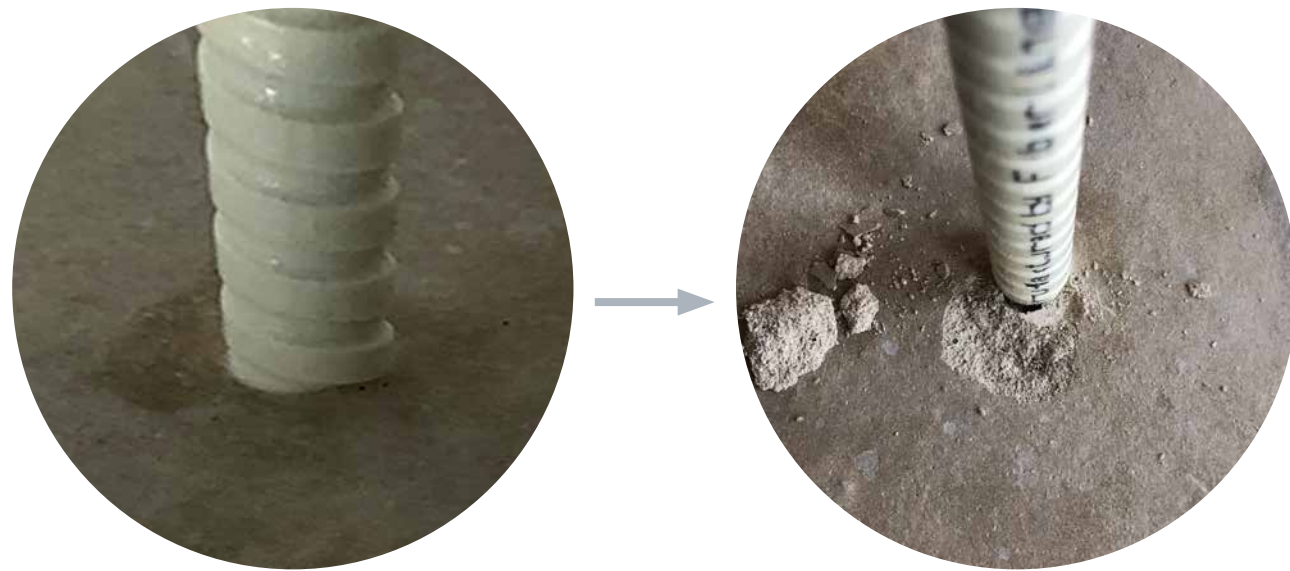


Figure 6.13. Condition of the concrete cover before (left) and after (right) the loading test. (Author)

## 6.2 FABRICATION

More above the constraints derived from the structural analysis of the designed facade panel, the constraints by the method of fabrication used and the materials used by thus are of higher priority to ensure that the designed geometry could be brought to life. The geometry of the network is complex to be embedded within a concrete mass and these complexities do keep multiplying as will be discussed in the further chapters. To comply with the design a method of inverse investment casting was selected. Inverse investment casting is similar to the method of investment casting, with the difference that the lost was mould is inside the cast mass rather than the mass being casted inside the lost wax mould. More of this method is discussed in the literature reasearch section 2.4.

### 6.2.1 Material

The concern of developing the mould in the form of the complex tubular network geometry, made up of wax was a challenge, as casting would not be a feasible solution for such small segments of the geometry. The wax used for or else casting would have a fragile property upon which the casting of concrete would be complicated. To address this concern, the method of additive manufacturing of wax was considered.

The filament used was Print2Cast 3D Filament Wax by an US based company named Machinablewax Inc. who have developed a wax filament to be commercially use to print 3D objects (figure 6.14). This material is usually use to print moulds to cast intricate jewelleryes using the lost wax casting method. The use of such material and technique was chosen to be experimented in a large scale architectural application. The physical properties of the wax filament are mentioned below (MachinableWax, 2016):

Specific Density: 0.91238 grams / cubic cm  
 Flash Point (COC): 575 degrees F  
 Melt Point (Ring & Ball Method): 242 degrees F (117C)  
 Viscosity 270 degrees F = 34,400cP  
 Volumetric Shrinkage (from melting point to room temp): 5% typical  
 Ash content for lost wax casting applications is low (.004%)  
 Coefficient of Thermal Expansion (in./in. °F):  $9.5 \times 10^{-5}$   
 Colouring: blue dye, permanent, oil base



Figure 6.14. A roll of wax filament (Machinablewax.com)

The workaround using this material to derive design constraints by the method of 3D printing the wax filament as well as the constraints by the behaviour of the material itself is discussed further. While this material is high;y recyclable back to the filament, it is to be noted that the fumes over melting the wax filament for extrusion could be harmful and mandatory precaution must be taken while over exposing to the printing must be avoided (MachinableWax, 2016).

### 6.2.2 Geometry

The geometry of the tubular network is limited to the ability and performance of 3D printing the wax filament. The following for considerations in favour of the fabrication of the wax printed network do outline the possible design outcome.

#### 1. Support free

The design of the network was designed in such a manner so as the geometry of the tubes could be printed without the need of support members. The reason behind this was to eliminate the extra printing time as well as material used. The extra supports would also result in uneven surface of the printer geometry which would be then reflected onto the hollow geometry cast within the concrete.

## 2. Overhang

In order to eliminate the supports for printing, the geometry need to be considered for the overhang it could be printed without the supports. To analyse the same, the wax filament was printed for various angles of inclination to verify the possible inclination that could be achieved without the support while extrusion. The tests performed are shown in figure 6.15. These test geometries were tested for single outer layer with an spiral extrusion for smooth geometry without layer breaks. It was evident that the geometry of 0 to 35° do satisfy the criteria of a support-less print while the 40° fails. Although the test of the overhang would be critical based on the final geometry of the tubes in response to various different design parameters explored ahead in the chapter. The final geometry to comply with this criteria is explained in section 7.4.3.

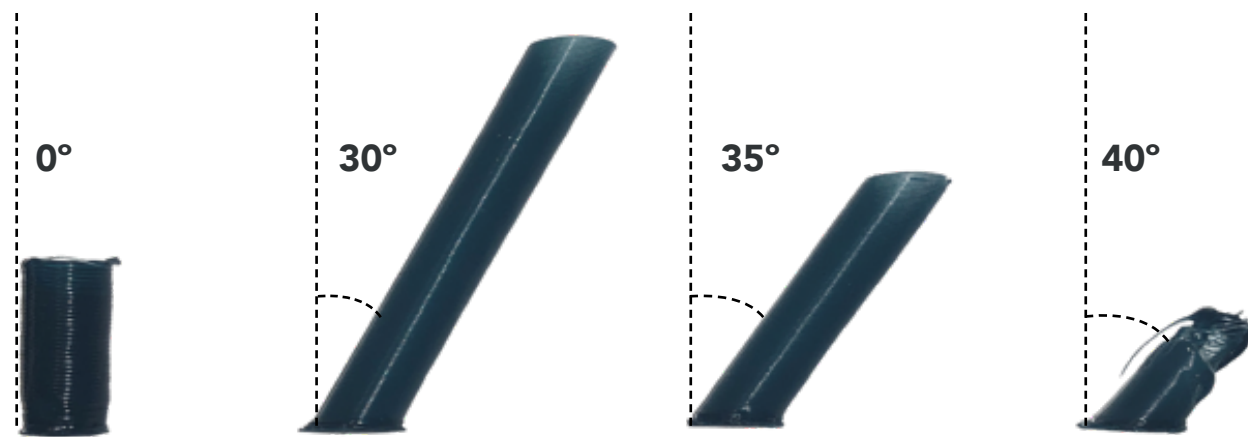


Figure 6.15. Test for overhang of 3D printing wax with single outer layer and spiral extrusion. (Author)

## 3. Infill

Solid print would make high use of material, increase time and also be problematic for the purpose of melting the wax out to develop the void of tubular geometry within the mass of concrete. The amount of infill used in the geometry is to be analysed so as the heat to melt could penetrate throughout equally. The amount of infill in combination to the geometry should be able to with stand the load of the concrete poured upon. To analyse the same, tubular geometries of 15 mm diameter and with 2 outer layers were cast with concrete used for the prototype of this thesis (figure 6.17). With this test it was found that the tubular geometry with 15% infill was the one which did show no signs of deformation under the concrete load of 100 mm high and is considered for printing the geometry with this infill configuration. The geometries used for the infill is shown in figure 6.16.



Figure 6.16. Infill geometry used for printing tubes with varying percentage for loading test. (Author)

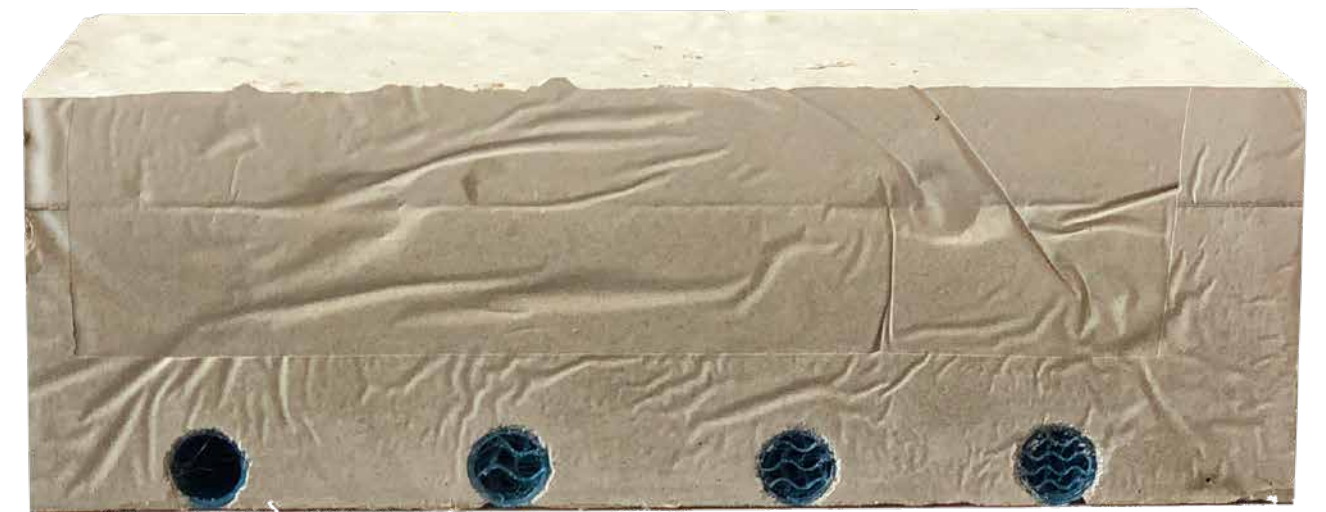


Figure 6.17. Section showing the loading test for tubes with different infill percentage. (Author)

## 4. Exit points

With the applied constraints by the material and method of fabricating the geometry using additive manufacturing process, the network geometry will be informed to a defined limit of design exploration. Along with these constraints, the method of inverse investment casting does demand for melting the wax out to form the shape of tubular network within the concrete facade panel. Because the geometry is too complex and spanned all across the facade panel which has only one physical input and output, the geometry needs to be facilitated with extra flow out points, especially at junctions where there are chances of clogging the wax because of unavailability of direct exit points. The tubular geometry was hence added with tubes at multiple junction as shown in figure 6.27 in section 7.3.3. These exit points would be then sealed using water proof sealant except the ones needed to be accessed for maintenance.

## 6.2.3 Method

The method of fabricating the designed facade panel with the method of inverse investment casting, needs to follow three different steps viz., printing the inner mould, casting the concrete with the inner and the outer mould, melting the inner mould out to derive the designed casting.

### 1. Printing

The printing of the inner mould was done with a wax filament using a commercial grade 3D printer. Various different configured settings were used to print the tubular network geometry using the wax filament. While the specifications to be used for the extrusion as mentioned by the filament manufacturer are as following.

Extrusion temperature = 140°C-150°C

Bed temperature = 80°-90°C

Shells = 2-3

Print speed = 20 to 70 mm/s

The printer used for the purpose of the extrusion printing is the Creality 3D X-CR 2 Color, dual colour printer capable with a single nozzle, capable of printing a maximum size of 300 x 300 x 400 mm, courtesy of Aaron Bislip.

The usual problems experienced while printing the wax filament are mentioned herewith:

**Lumping / extrusion speed:** The slow extrusion speed of the filament does result in lumping the material while forming small bubbles in the extrusion rather than a smooth continuous geometry. The solution was to eliminate the lower limit of temperature for extrusion of the filament to develop a smooth extrusion of the filament even at temperatures as low as 140°C. This problem is shown in figure 6.18.



Figure 6.18. Problems in extrusion printing due to lumping of material



Figure 6.19. Problems in extrusion printing due to shifting of layer by vibrating bed

**Slow cooling:** While this factor largely depends on the geometry size to that of the time taken to extrude each layer. Smaller geometries like the tubes with a diameter of 10 to 15 mm are fast enough to be printed a single layer. Due to this the temperature of the printed layer does not tend to cool down before the next layer is printed, resulting in deformation of the geometry gradually. The heat from the nozzle could sometimes also be a problem if not cooled rapidly as the wax has a melting temperature as low as 117°C. The solution to this was to either print the layers slowly or to imply external cooling methods using fans to ensure that the printed layer is cooled fast enough before the next layer is extruded. The other solution was to implement a cooling tower. This problem is shown in figure 6.20.

**Splitting of layers:** The layers if not stuck properly, which could also be a side effect of rapid cooling, does not stick well to each other and result in splitting of the layers. This is also an result of loose adhesion of the geometry to the bed, which if detaches forms uneven tension around the geometry while splitting the layer. To find an optimum extrusion temperature and cooling required. An image of the same is shown in figure 6.21.



Figure 6.20. Problems in extrusion printing slow cooling of layers

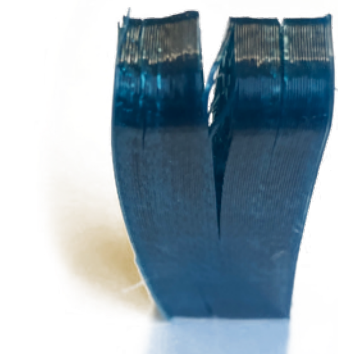


Figure 6.21. Problems in extrusion with splitting of layers

**Warping:** The warping of the geometry does tend to occur due to the detachment of the geometry or the brim off the heated bed. This usually happens to a geometry with a larger surface area printed in contact to the bed. A very high temperature of the printing bed and a small brim around the geometry may lead to this problem. This could be overcome by implementing a layer of double sided film over the heating bed to print as well as a wider brim for proper adhesion. This problem is shown in figure 6.22.

**Adhesion to bed:** The adhesion of geometry to the bed as discussed for the warping is also needed to be eliminated for the shift in layers. If the geometry does tend to loose partially, even if not detached from the bed could lead in a geometry with shifted layers. This problem is shown in figure 6.23.



Figure 6.22. Problems in extrusion printing due to geometry warping



Figure 6.23. Problems in extrusion printing due to improper adhesion to bed

**Instability/ printing speed:** Higher printing speed with slim and tall geometries as is the case for the printing of the small diameter tubes, do tend to buckle over the self weight and that of the movement of the bed, due to the speed of vibration caused by moving the bed for printing. The solution to this is either slowing down the extrusion print or printing in small segments or using a printed with a fixed bed system. This problem is shown in figure 6.24.

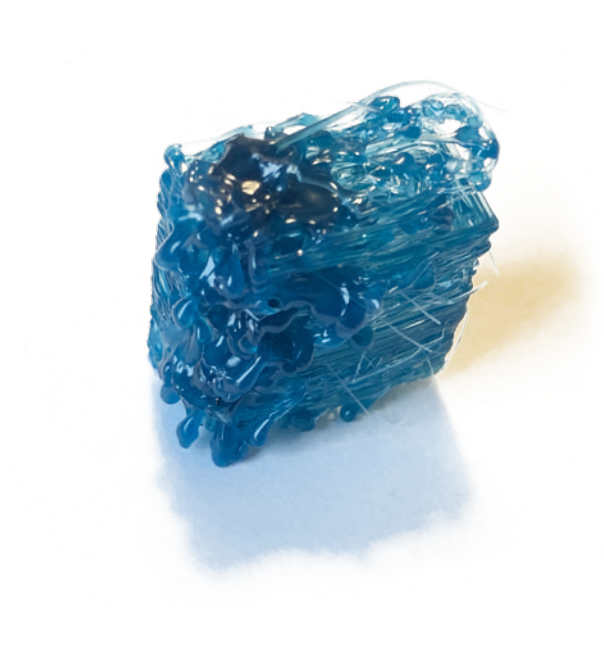


Figure 6.24. Problems in extrusion printing due to printing speed



Figure 6.25. A good quality of extrusion printing

In lieu to overcome the above mentioned problems, the final settings for successful printing of the geometry using a wax filament are as following:

Extrusion temperature = 165°C

Bed temperature = 70°C

Shells = 2

Print speed = 7 mm/s

Brim width = 10 mm

Nozzle width 0.4 mm

The details of the complete setting used are mentioned in appendix 12.8.

## 2. Casting

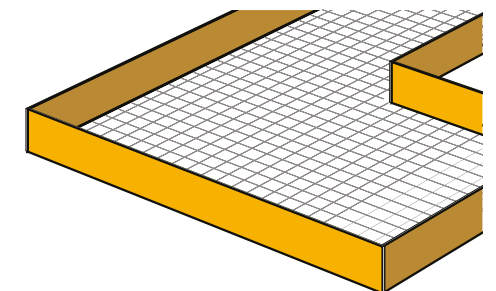
The next process is to cast the concrete with the printed wax form work in place. This process of casting does involve the implementation of the reinforcement mesh along with the reinforcement dowels in place and taken place in two parts. The insulation layer is placed in between these two layers.

As the geometry of the final panel as derived in section 8.1.7 is a complex shape, the method of gravity casting depends on the elimination of the undercuts of the geometry which would render release of the form work impossible after the curing. The method of eliminating the undercuts from the final geometry is discussed in section 7.7.1.

The method of casting has been explained with a series of diagram explaining the steps taken below with the help of diagrams by the author..

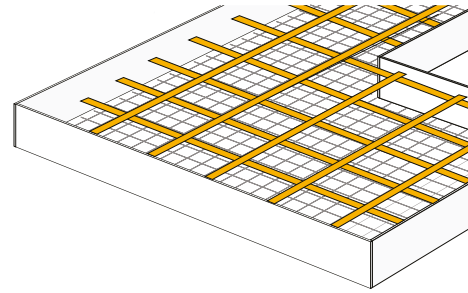
### Step 01:

The concrete facade panel is assumed to be cast along the surface rather than the depth for minimised load of the concrete on the inner 3D printed wax form work. Prior to the form work for the side walls, the CNC milled panel for the topology optimised facade surface is placed beneath. The flat surface of the facade panel faces up.

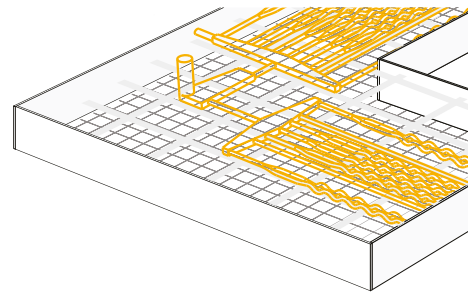


**Step 02:**

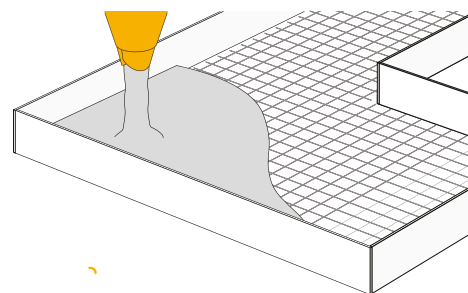
Depending on the type of facade panel viz., internal or external, the reinforcement mesh is laid. The mesh is managed for needed surface cover with the help of pin spacers as the carbon fibre mesh used in this project is of very light weight.

**Step 03:**

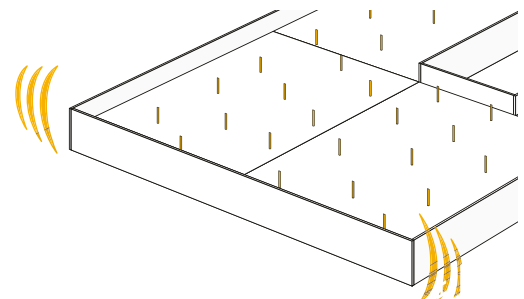
The internal form work for the inverse investment casting consisting of the tubular network is laid with pin supports to avoid leakage after cast. The inner surface of the form work is then lined with a release agent for smooth finish and easy removal of the concrete from the form work.

**Step 04:**

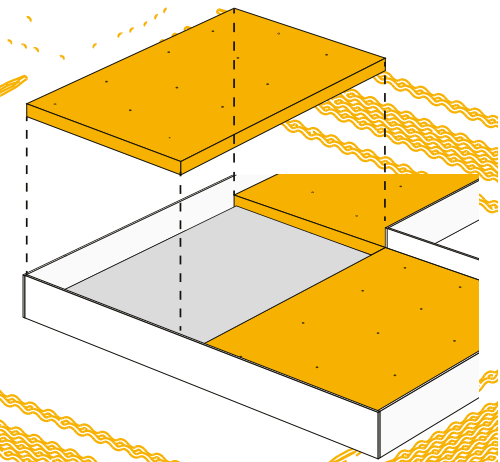
Reinforcement dowels are placed in place before the concrete is poured into the setup internal and external mould form work. Care needs to be taken for low height slow pouring from the edge of the form work to avoid pressure over the wax tubular network geometry which would or else may tend to break the mould and seep the fluid concrete inside the tubes.

**Step 05:**

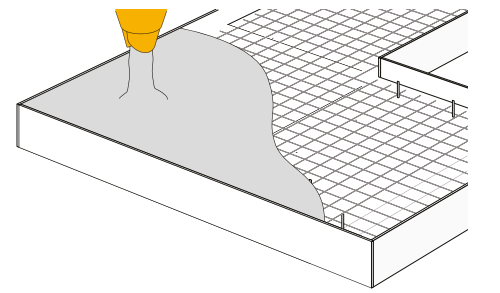
The cast panel is then vibrated to ensure the reach of the concrete at all the complex corners and to eliminate and trapped air while casting.

**Step 06:**

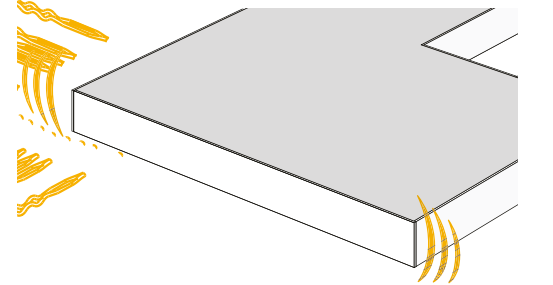
Only after the curing of the cast concrete for the first panel, the insulation panels, water tank and other needed fixtures within that is arranged between the external and internal facade panel is placed. Drills are made for the reinforcement dowels to be placed in location with the insulation panels.

**Step 07:**

The reinforcement mesh and the network geometry of the tubular structure is then placed as in step 02 and 03 for the second facade panel (internal/external) and poured with concrete.

**Step 08:**

The combination of the cast panel is then vibrated to ensure settlement of concrete and release trapped air and let to cure for 48 to 72 hours, for the prescribed concrete to harden before releasing the form work. It is then left to cure for 28 days before using installation.

**3. Melting**

The final step of the fabrication of the facade panel was that of melting the wax out of the cast mass. To do the same a mock-up was made with a wax tube cast within the concrete and melting it under high temperature oven of around 220°C. While the method performs as expected, some of the wax did melt and fill the pores of the concrete around the tubes which did develop a layering of water proof between the void and the concrete mass which did favour the design. In contrary the high energy used to melt the wax out as well as the effect of such high temperature on the reinforcement, the concrete as well as the bonding between the material would be compromised. To eliminate these problems an alternate efficient method was considered. Since the melting temperature of the wax is 117°C, the cast mass was subjected to be boiled under high pressure water which attains a temperature of 120°C. Since wax has a much low density than water, it would melt from the geometry within and float over the surface of water. To ensure the performance of the same, a small mock-up

was created. To be able to analyse the melting out of the wax from the mass within, a scaled down geometry of the design was printed with wax and cast within transparent epoxy resin. This cast mass was then pressure boiled in a pressure cooker used as a kitchen ware. The diameter of the pressure cooker at 220 mm was a limitation of the mock-up size. The image of the mock-up is shown in figure 6.26a. The final result of the melt wax from within the geometry of the mock-up does signify the possibility of using this method for the inverse investment casting and has been shown in figure 6.26b. The use of infill and not a solid geometry was in sense to make the water to be able to penetrate within these geometry and melt them out.

It is also to be considered that the water used in this process would be infected with hazardous composition from the wax filament and susceptible for highly polluting the water affecting the aquatic animals (MachinableWax, 2016). This water needs to be treated before releasing back to the environment and should be accounted for.

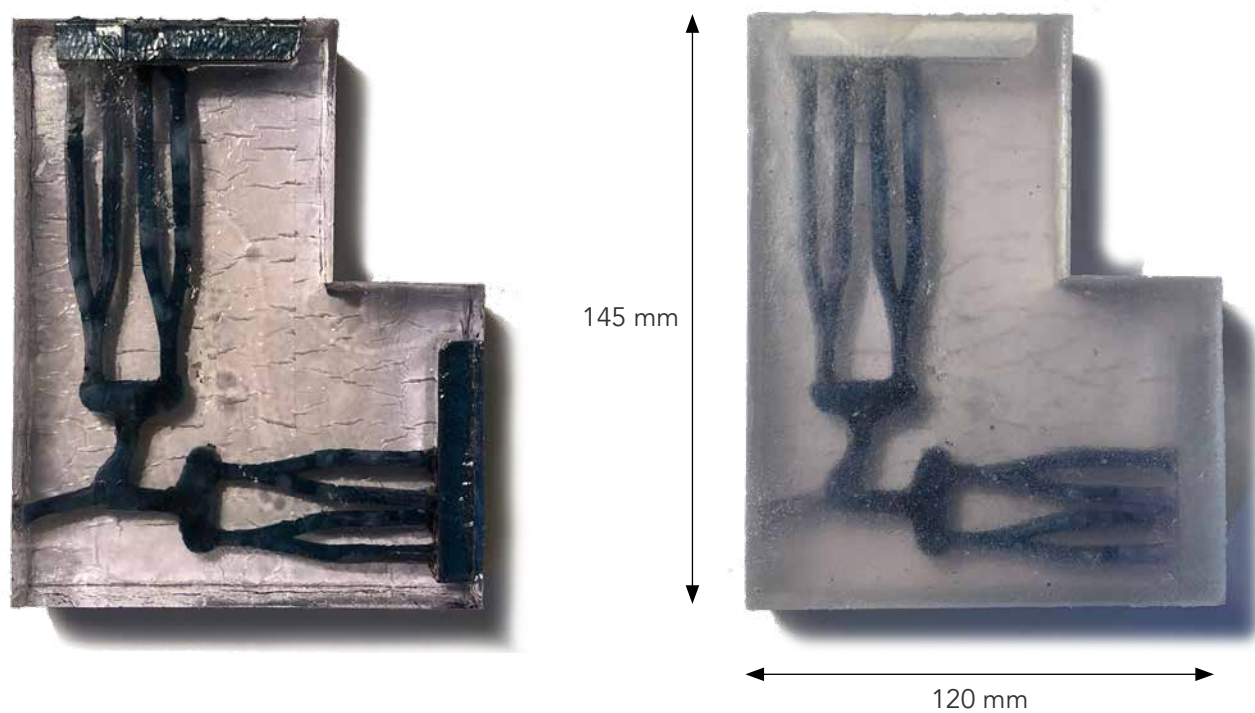


Figure 6.26a. Mock-up of the cast before melting the wax out. (Author)

Figure 6.26b. Mock-up of the cast after melting the wax out. (Author)

## 6.3 BASE NETWORK GEOMETRY

By considering all the above mentioned constraints and modifications by the structural analysis and the method of fabrication along with the materials used, the base geometry for further modification was designed. The network geometry one (figure 6.27) will serve as the benchmark for comparison to the modified geometries depending on enhancing the efficiency of the heat exchange system here on. This geometry does account to a fluid carrying capacity of 20.6 litre per panel and resulting to a pressure drop of 1071.8 Pa within the inlet to the outlet.

### 7.3.3 Network Geometry 01

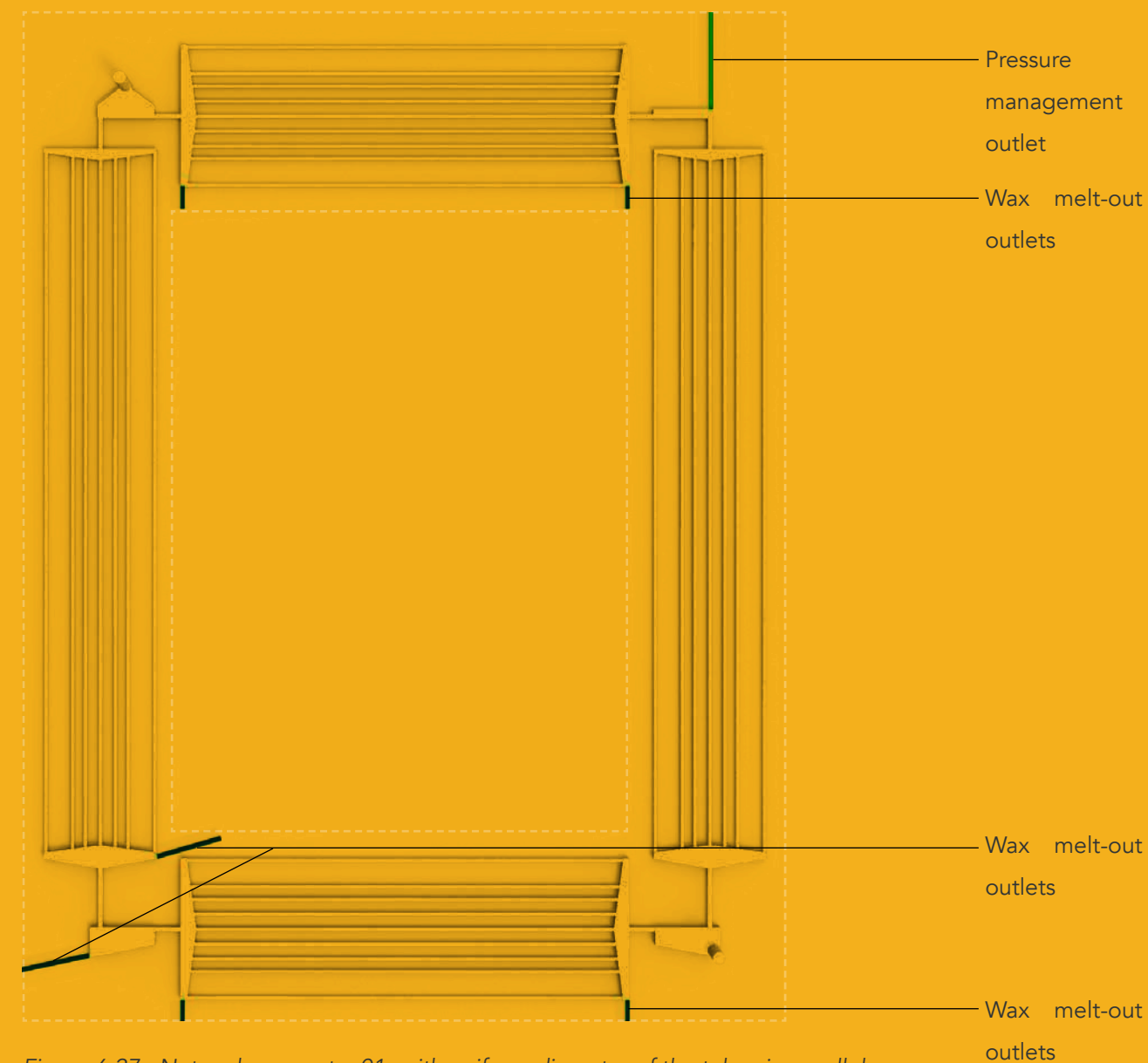


Figure 6.27. Network geometry 01- with uniform diameter of the tubes in parallel  
Source: author

Volume of network:	Pressure drop in network
<b>20.63 litres</b>	<b>1235.34 Pa</b>
Change in volume	Change in pressure drop
<b>± 0.0 %</b>	<b>± 0.0 %</b>

\*Change in volume and pressure drop are calculated to this network geometry as reference. The tubes for pressure management and wax meltout are leftout of the design further on.

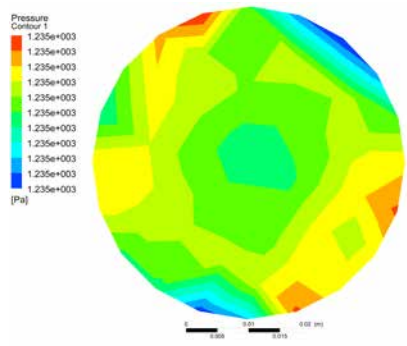


Figure 6.28a. Pressure contour inlet  
(Author; Ansys fluent)

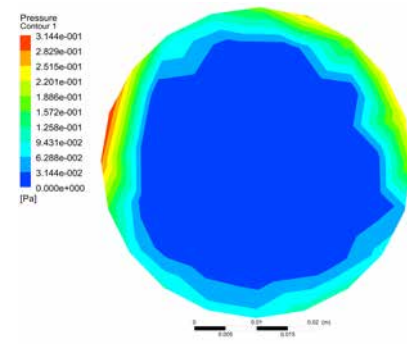


Figure 6.28b. Pressure contour outlet  
(Author; Ansys fluent)

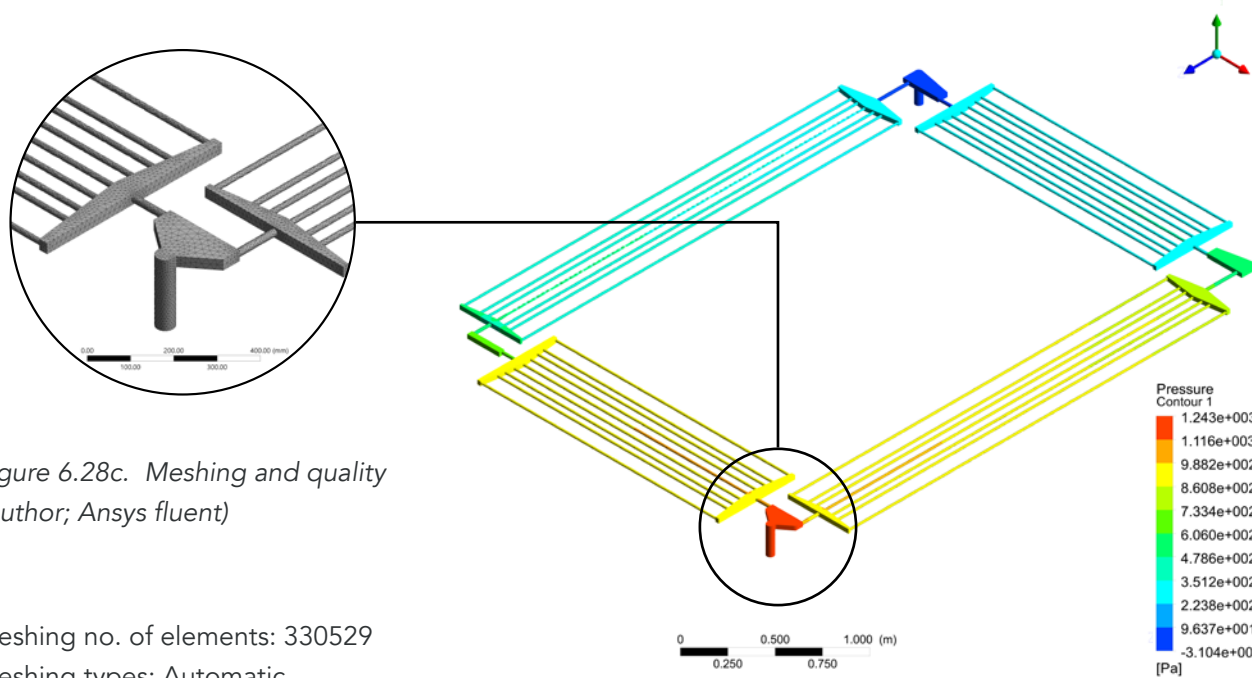


Figure 6.28c. Meshing and quality  
(Author; Ansys fluent)

Meshing no. of elements: 330529  
 Meshing types: Automatic  
 Quality: Medium  
 Min size: 7.0 mm  
 Max size: 700.00 mm

Viscous model: k-epsilon  
 Method: Spatial Discretization-  
 Least Squares Cell Based

No. of iterations: 200  
 $\Delta P$ : 1071.8 Pa  
 Convergence cycle: NA

No. of iterations: 2000  
 $\Delta P$ : 1235.34  
 Convergence iteration: NA  
 flat plate zone

Convergence exponential: e-03  
 Simulation time: 36 minutes

Figure 6.28d. Pressure of boundary domain (Author; Ansys  
 fluent)

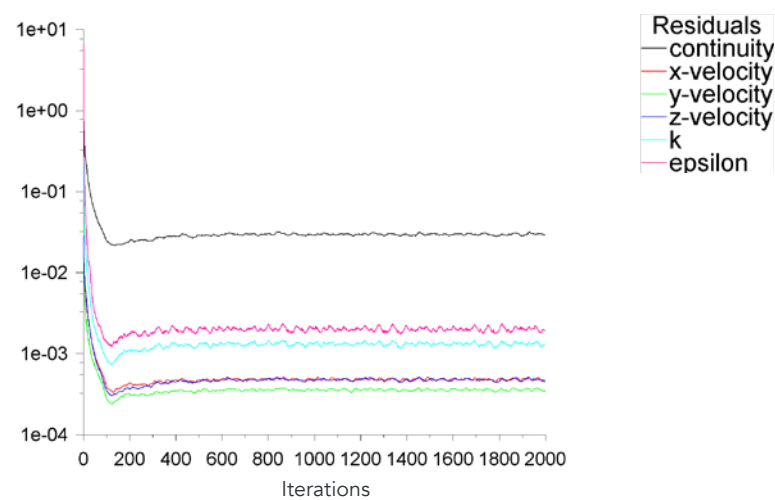


Figure 6.28e. Graph for 2000 iterations for CFD of geometry 01  
(Author; Ansys fluent)

## 6.4 CONCLUSION

The structural system for the designed facade panel did describe the various different material used, their purpose and properties along with their interaction with the designed facade panel with the tubular network geometry within. The discrepancy with the number of dowels to that of the analytically calculated and simulated to that of the company specification was verified and was concluded with the help of a physical test to ensure the stability of the concrete cover proposed in the design. The interference of the reinforcement mesh and the dowels did constrain the design exploration boundary as well as the geometry of the network to accommodate the reinforcements.

The second aspect analysed was for the fabrication of the designed system. The use of the special wax filament for 3D printing the network geometry was discussed and the final setting used for a successful print while discussing the problems faced and their solutions were detailed. The limitation of the wax filament and the method of fabrication used for the network geometry, 3D printing were analysed in combination with tests performed and these derived limitations were informed for the further geometry exploration. The method used to melt the wax out of the cast geometry was set to be done under a pressurised hot water tub and related experiments were performed with a scaled geometry as a proof of concept proposed.

Through this chapter various different constraints related to the fabrication and the related structure considerations were derived, through which the following sub-research question was proved to be true and answered.

### Sub research question answered:

*How does the constraint of the manufacturing process affect the method of design?*

This page is intentionally left blank.

# 7. DESIGN CRITERIAS

## *CHAPTER OVERVIEW*

While the previous chapter elaborates on the fabrication criteria, this chapters does elaborates the design criteria discussed in chapter 4. Each of the mentioned design criteria are analysed , modified, evolved and optimised, first for the tubular network geometry and then for the combination of the concrete mass with that of the inlaid void of tubular network for the maximum possible performance. This chapter concludes with the performance assessment of the designed facade panel.

## 7.1 MEDIUM OF FLUID

As discussed earlier the medium of fluid is considered to be water with the following state and properties.

Temperature of water = 20° C

Roughness factor = 4mm by the 3D printing of wax and 1mm of concrete = 5mm

$\rho$  = density of the fluid = 998.206 kg/m<sup>3</sup>

$\mu$  = dynamic viscosity of fluid = 1001.61 x 10<sup>-6</sup> kg/ms

## 7.2 TYPE OF FLOW

The fluid considered as a medium to transfer the heat within the tubes is considered to be water in this research and its related properties were considered to ensure the flow of water. The study for the flow was made to ensure that the water within the designed network follows a laminar flow and not a transitional or turbulent flow in order to eliminate huge pressure drops and blockages within the network as discussed in chapter 6.

To ensure laminar flow of the medium, the Reynolds Number was taken into account. Reynolds number is a dimensionless value which is applied in fluid mechanics to represent whether the fluid flow in a duct or past a body is steady or turbulent. To determine the type of flow the following criteria was considered. (engineeringtoolbox, 2013)

Laminar flow:  $Re < 2300$

Transitional flow:  $2300 < Re < 4000$

Turbulent flow:  $Re > 4000$

This value is obtained by comparing the inertial force with the viscous force.

The Reynolds number is denoted by Re.

Reynolds Number = Inertial Force / Viscous Force

The Reynolds number formula is expressed by,

$$Re = \frac{\rho v d}{\mu}$$

where,

$\rho$  = density of the fluid = 998.206 kg/m<sup>3</sup>

$v$  = velocity of the fluid = to be determined

$\mu$  = dynamic viscosity of fluid = 1001.61 x 10<sup>-6</sup> kg/ms

$d$  = diameter of the tube = 15 mm = 0.015 m



Figure 7.1a. Turbulent flow



Figure 7.1b. Laminar flow

As determined above, to calculate the Reynolds number the velocity of the fluid ( $v$ ) or the volumetric flow ( $Q$ ) through the geometry was needed to be determined. The velocity in return depends on the total volume of the geometry. Since the geometry is supposed to be evolving and hence the volume changing drastically, for initial simulations, the primary speculated geometry is considered after the modifications due to the fixtures, manufacturing and structural constraints as depicted in figure 6.3 & 6.4 of chapter 6.1.1.

$V$  = volume of geometry/ fluid = 20.6 litres

$t$  = cycle time for fluid between panels (assumed) = 30 minutes

$a$  = cross section area of the tube = 0.0001767 m<sup>2</sup>

$Q$  = Volumetric flow rate =  $V/t = 20.6/30 = 0.68$  l/min  
= 0.00068 m<sup>3</sup>/min

$v$  = velocity of water =  $Q/a = 0.00068 / 0.001767$   
= 0.38 m/min  
= 0.0063 m/sec

Hence  $Re = (998.206 \times 0.0063 \times 0.015) / 1001.61 \times 10^{-6}$   
= 941

Since the Re value for laminar flow ranges up till 2300, to minimize the cycle time for the fluid between panels, the Re was maximised and the relative velocity of fluid was calculated.

Hence for a value to be assumed over maximum possible fluid velocity and Re below 2300,

**$v$  = velocity of the fluid = 0.15 m/sec**

**$Re$  = Reynolds number = 2256**

**$Q$  = Volumetric flow rate = 1.6 l/min or 0.0016 m<sup>3</sup>/min or 2.732 x 10<sup>-5</sup> m<sup>3</sup>/sec**

**$d$  = diameter of the tube = 15 mm = 0.015 m**

The above mentioned values are used in the further stages of calculations and simulations in computation software.

## 7.3 FLOW RESISTANCE

The branched geometry of the tubes in the network are arranged in the sequence of a parallel connection, develops extra resistance in consideration to the intermediate geometry of the manifolds where the fluid travels before entering the tubes from the inlet. The flow resistance of the tube increases with the increase in the number of intermediate tubes connected in parallel sequence. The system's flow resistance could be compared to that of an electric circuit connected in parallel sequence. The increase in the flow resistance of the tubes ( $R_1, R_2, R_3, R_4, \dots$ ) does develop increased pressure drop as compared to increased voltage drop in that of an electric circuit. To ensure that all the tubes across the designed network have similar flow resistance, the radius of the tubes ( $r_1, r_2, r_3, r_4, \dots$ ) across the network needs to be varied in diameter. This study of deriving

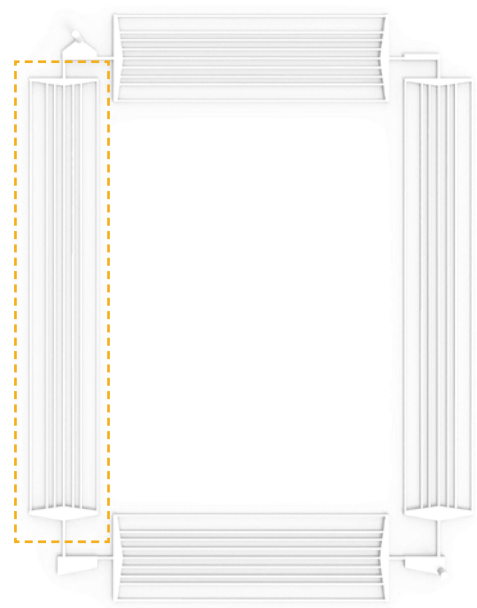


Figure 7.2a. Void tubular network (Author)

the diameters has been described by Alston & Barber (2016). The reference flow resistance (R0) would be considered to be that of the central tube of 7.5mm radius (r0) direct in line with the inlet and outlet of one network.

It is to be taken into account that the change in volumetric flow rate (Q), velocity (v) of the liquid or the Reynolds number does not affect the determination of the diameter to manipulate the flow resistances and hence can be constant even if the volume of the network is modified.

The diameters of the tubes of a network was divided into two types: vertical and horizontal. The varying factors in these two types of network were the length of the tubes and the widths of the manifold by design.

### 7.3.1 VERTICAL NETWORK/s

As shown in the diagram, the 2 vertical sections of the complete network was considered first with an elevational length of the central tube being 3.09 metres. The central tube (Tube 0) has a diameter (d<sub>0</sub>) of 15 mm.

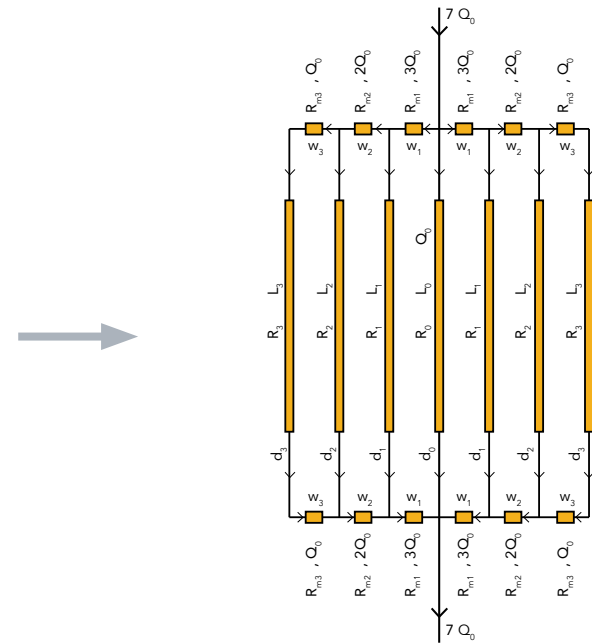


Figure 7.2b. Fluidic resistance of a sub-network (Author)

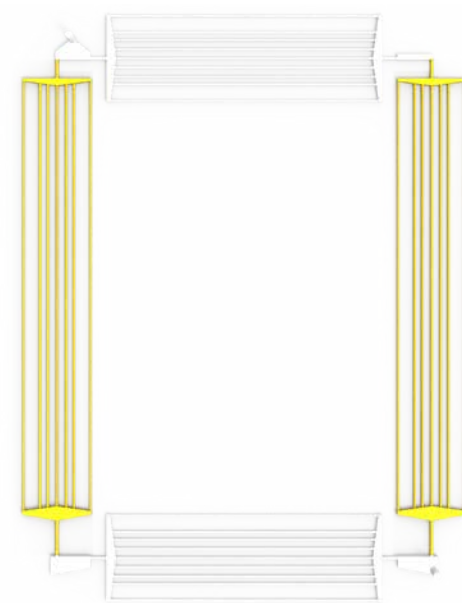


Figure 7.3a. Vertical sub-networks (Author)

### 1. Flow resistance of the central tube

To calculate the change in diameters needed for the equal flow resistances, at first the pressure drop ( $\Delta P_0$ ) in the central tube, Tube 0 was calculated. Pressure drop is the change in the pressure at the outlet as compared to that of the inlet this is denoted by  $\Delta P$  and calculated as below:

$$\Delta P = \lambda \times \frac{L}{D_h} \times \frac{\rho}{2} \times v^2$$

where,

$D_h$  = hydraulic diameter

$\lambda$  = friction factor

$L$  = Length of the tube

$v$  = velocity of the fluid

$\rho$  = density of the fluid

The Reynolds number is dependent on the type of geometry the fluid flows through and hence depends on the hydraulic diameter ( $D_h$ ) of the cross section geometry.

$$D_h = \frac{4a}{P}$$

where,

$a$  = cross sectional area of the tube

$P$  = wetted perimeter

$$\text{for a circular pipe, } D_h = \frac{4a}{P} = \frac{4(\pi d^2/4)}{\pi d} = d = 0.015\text{m}$$

The pipe friction factor ( $\lambda$ ) is a unit less factor which also does depends on the cross section geometry of the pipe and has been stated as  $64.00 / Re$  for a circular tube. Therefore, the frictional factor for the central tube is

$$\lambda_0 = 64.00 / Re = 0.028$$

Hence the pressure difference across the central tube is

$$\Delta P_0 = \lambda_0 \times \frac{L_0}{d_0} \times \frac{\rho}{2} \times v^2 = 0.028 \times (3.09/0.015) \times (997/2) \times (0.15)^2$$

$$\Delta P_0 = 69.65 \text{ Pa}$$

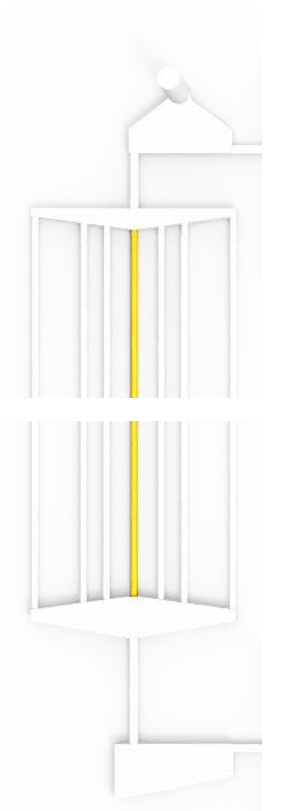


Figure 7.3b. Central tube of vertical network

The next is to determine the flow resistance ( $R_0$ ) of the central tube depending on the calculated pressure difference and the volumetric flow rate of the fluid determined in the previously.

The flow resistance of the tube is denoted by

$$R_0 = \frac{\Delta P_0}{Q} = \frac{69.65}{2.732 \times 10^{-5}}$$

$$R_0 = 0.255 \times 10^7 \text{ kg m}^{-4} \text{ s}^{-1}$$

The above calculated  $R_0$  will be the base reference for the other tubes to achieve the value similar to it by modifying the diameter of the inlets.

## 2. Flow resistance of the manifolds

As the fluid flow to through the manifolds and then to the other parallel tubes, the manifold also does generate a resistance of the segment between the two tubes. The resistance of these manifold segments keep adding up as the number of tubes are added in parallel to the central tube. The distance of the tubes or the widths of the manifold ( $w_0, w_1, w_2, w_3\dots$ ) are informed by the geometry and its design in concern to the limitations and constraints of the materials, fixtures and structural system (figure 7.4).

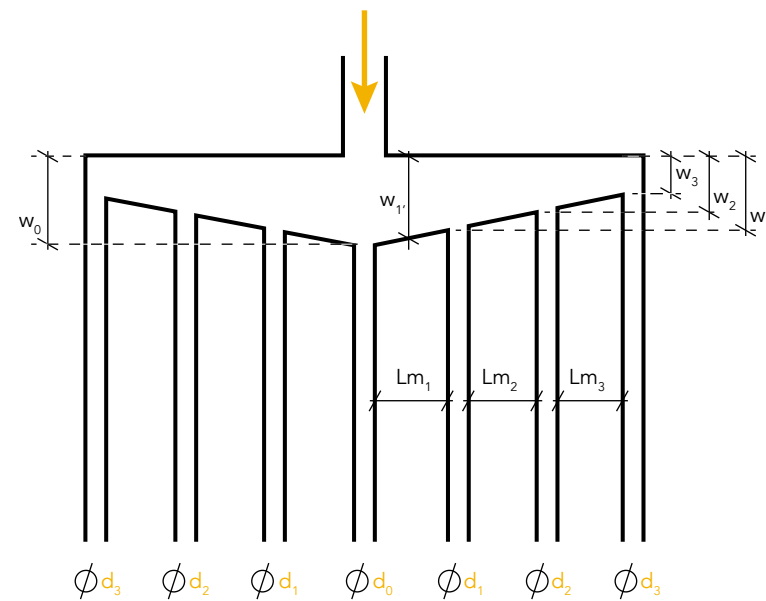


Figure 7.4. Annotations of different factors of the tubes of the vertical network. (Author)

From the designed geometry, the following values for the manifold m1 can be derived

$w_0$  = width of manifold over 1st tube = 0.045 m

$w_1$  = width of manifold over 2nd tube = 0.038 m

$w_1$  = average width of the manifold =  $(w_0 + w_1) / 2 = 0.042$  m

$Lm_1$  = length of the manifold (c/c between two tubes) = 0.06 m

$b$  = depth of the manifold =  $d = 0.015$  m

The pressure drop in the manifold is given by,

$$\Delta P_{m1} = \lambda_{m1} \times \frac{L_{m1}}{Dh_{m1}} \times \frac{\rho}{2} \times v^2$$

The manifolds are rectangular boxes into which the tubes are fused into. The tapered geometry does ensure a different The hydraulic diameter ( $Dh$ ) of a rectangular cross section geometry is calculated as following.

$$Dh_{m1} = \frac{4(w_1 \times b)}{2(w_1 + b)} = \frac{4(0.042 \times 0.015)}{2(0.042 + 0.015)} = 0.022 \text{ m}$$

The pipe friction factor ( $\lambda$ ) also does depend on the cross section geometry of the pipe and for a rectangular cross section has to be determined by the ration of its length over breadth. Therefore, the frictional factor for the central tube is referred from appendix 12.1 (Subramanian, 2019):

$$w_1 / b = 0.042 / 0.015 = 2.8 \approx 3$$

referring to the table 12.2,

$$\lambda_{m1} = 68.36 / Re = 0.030$$

Therefore calculating the pressure drop across the first manifold m1

$$\Delta P_{m1} = \lambda_{m1} \times \frac{L_{m1}}{Dh_{m1}} \times \frac{\rho}{2} \times v^2 = 0.030 \times (0.06/0.022) \times (997/2) \times (0.15)^2$$

$$\Delta P_{m1} = 0.98 \text{ Pa}$$

The resistance of the first manifold by referring the flow resistance network diagram x, is calculated as

$$R_{m1} = \Delta P_{m1} / (3Q) = 0.98 / (3 \times 2.732 \times 10^{-5})$$

$$R_{m1} = 0.00112 \times 10^7$$

From the flow resistance network geometry 02 it is evident that the resistance across the tube 1 within inlet and outlet of the network does add up with the resistance of the manifold at downstream and upstream nodes.

Hence, the effective pressure drop across tube 1 is calculated as

$$R_1 = R_0 - (6 \times R_{m1}) = 0.0255 \times 10^7 - (6 \times 0.00112 \times 10^7)$$

$$R_1 = 0.247 \times 10^7 \text{ kg m}^{-4} \text{ s}^{-1}$$

### 3. Determining the diameter of tubes in parallel

The final stage includes determining the diameter of the tube 1 with the same length as the tube 0 so as the flow resistance of tube 1 matches to that of  $R_0 = 0.255 \times 10^7 \text{ kg m}^{-4} \text{ s}^{-1}$ . This will ensure equal flow of water through all the tubes so as to minimise the possible pressure drop because of branching the tubes. To do this we equate  $R_1$  and  $R_0$  with  $d_1$  as the unknown variable in the equation.

$$\begin{aligned} R_1 &= R_0 \\ 0.247 \times 10^7 &= \lambda_0 \times \frac{L_0}{d_0} \times \frac{\rho}{2} \times v^2 \\ &= 0.028 \times \frac{3.09}{d} \times \frac{997}{2} \times (0.15)^2 \end{aligned}$$

Hence,  $d = 0.0165 \text{ m}$  or **16.5 mm**

In the similar manner, the diameter for the other tubes were also determined as shown in table 7.1. The diameters for the vertical network of tubes are as follows:

- $d_0 = 15 \text{ mm}$
- $d_1 = 16.5 \text{ mm}$
- $d_2 = 15.8 \text{ mm}$
- $d_3 = 14.8 \text{ mm}$

### 7.3.2 HORIZONTAL NETWORK/s

As shown in the diagram, the 2 horizontal sections of the complete network was considered first with an elevational length of the central tube being 1.89 metres. The central tube (Tube 0) has a diameter ( $d_0$ ) of 15 mm

In a manner similar to that used in calculating the diameter of the different tubes in the vertical network, the diameter for the tubes for the horizontal network were also determined as shown in table 7.2. The diameters for the horizontal network of tubes are as follows:

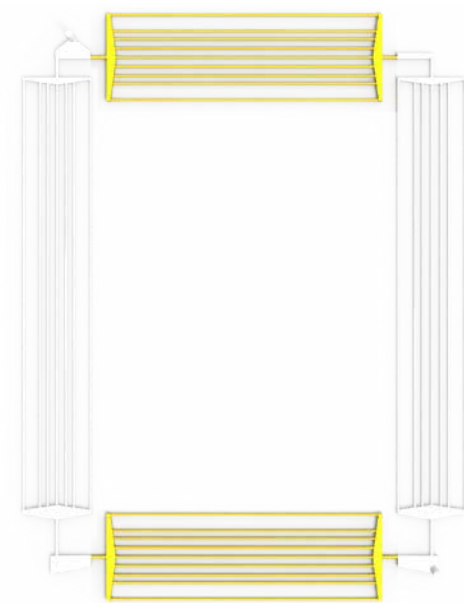


Figure 7.5. Horizontal sub-networks (Author)

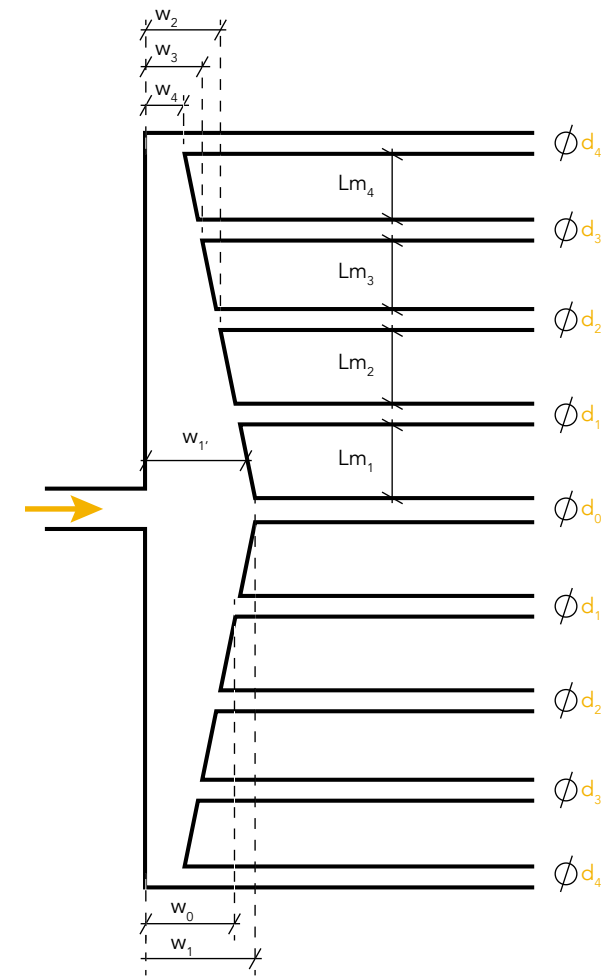


Figure 7.6. Annotations of different factors of the tubes of the horizontal network. (Author)

- $d_0 = 15 \text{ mm}$
- $d_1 = 16.7 \text{ mm}$
- $d_2 = 17.5 \text{ mm}$
- $d_3 = 17 \text{ mm}$
- $d_4 = 16.5 \text{ mm}$

The change in the volume and the pressure drop in comparison to the base network and the details of the CFD simulation are depicted with the network geometry 06 in section 8.1.

#### Assumptions:

The flow of water is assumed only to be at 20°C and for the whole period of heat exchange events. The change in temperature may have an effect on the viscosity of the water but the flow resistance in the tubes are devoid of the fact in analytical solving, while the real world scenarios may vary. The manifold of inlet and outlet are considered to be the same for the analytical calculations. The assumption of the fraction of sizes in diameter are expected to be replicated in the manufacturing.

	Length of tube (m)		Tube diameter/ Height of cross section (m)		Tube radius/ Width of cross section (m)		Dh (m), by design	f=pipe friction	ΔP = Pressure Difference (Pa)		R = Flow Resistance of tube (kg m-4 s-1)			d = Modified diameter (m)
	L0	Lm	d	h	r	b			ΔP0	ΔPm	R0	Rm	Rst	
For Central Tube			3.09		0.015		0.0075	f0	69.6548773			2549118.337	d0	0.015
For Manifold (General)		Lm	0.435	a	0.045	b	0.015	fm	6.982535141	Rm	255535.7078			
For Manifold 1		Lm1	0.06	w1'	0.04209	b	0.015	f1	0.979755035	Rm1	11951.83847	R1	2477407.306	d1
For Manifold 2		Lm2	0.0512	w2'	0.03452	b	0.015	f2	0.884229391	Rm2	16179.80996	R2	2412688.067	d2
For Manifold 3		Lm3	0.1075	w3'	0.02372	b	0.015	f3	1.759045617	Rm3	64374.75181	R3	2283938.563	d3
For Straight Tube		Lst	2.778	d	0.015	r	0.0075	f st	62.62176347			Rst	2412688.067	d st

Table 7.1. Excel table for vertical network tube diameters

	Length of tube (m)		Tube diameter/ Height of cross section (m)		Tube radius/ Width of cross section (m)		Dh (m), by design	f=pipe friction (Pa)	ΔP = Pressure Difference		R = Flow Resistance of tube (kg m-4 s-1)			d = Modified diameter (m)
	L0	Lm	d	h	r	b			ΔP0	ΔPm	R0	Rm	Rst	
For Central Tube			1.889		0.015		0.0075	f0	42.58189748			1558344.511		0.015
For Manifold (General)		Lm	0.435	a	0.045	b	0.015	fm	6.982535141	Rm	255535.7078			
For Manifold 1		Lm1	0.06	w1'	0.0583	b	0.015	f1	0.908179735	Rm1	8309.02912	R1	1491872.278	d1
For Manifold 2		Lm2	0.06	w2'	0.0513	b	0.015	f2	0.933539181	Rm2	11388.06038	R2	1423543.916	d2
For Manifold 3		Lm3	0.05	w3'	0.044	b	0.015	f3	0.672074339	Rm3	12297.75349	R3	1374352.902	d3
For Manifold 4		Lm4	0.1075	w4'	0.033	b	0.015	f3	1.567414051	Rm3	57361.72475	R4	1259629.452	d4
For Straight Tube		Lst	1.723	d	0.015	r	0.0075	f st	38.83992025			Rst	1374352.902	d st

Table 7.2. Excel table for horizontal network tube diameters

### 7.3.3 Network Geometry 02

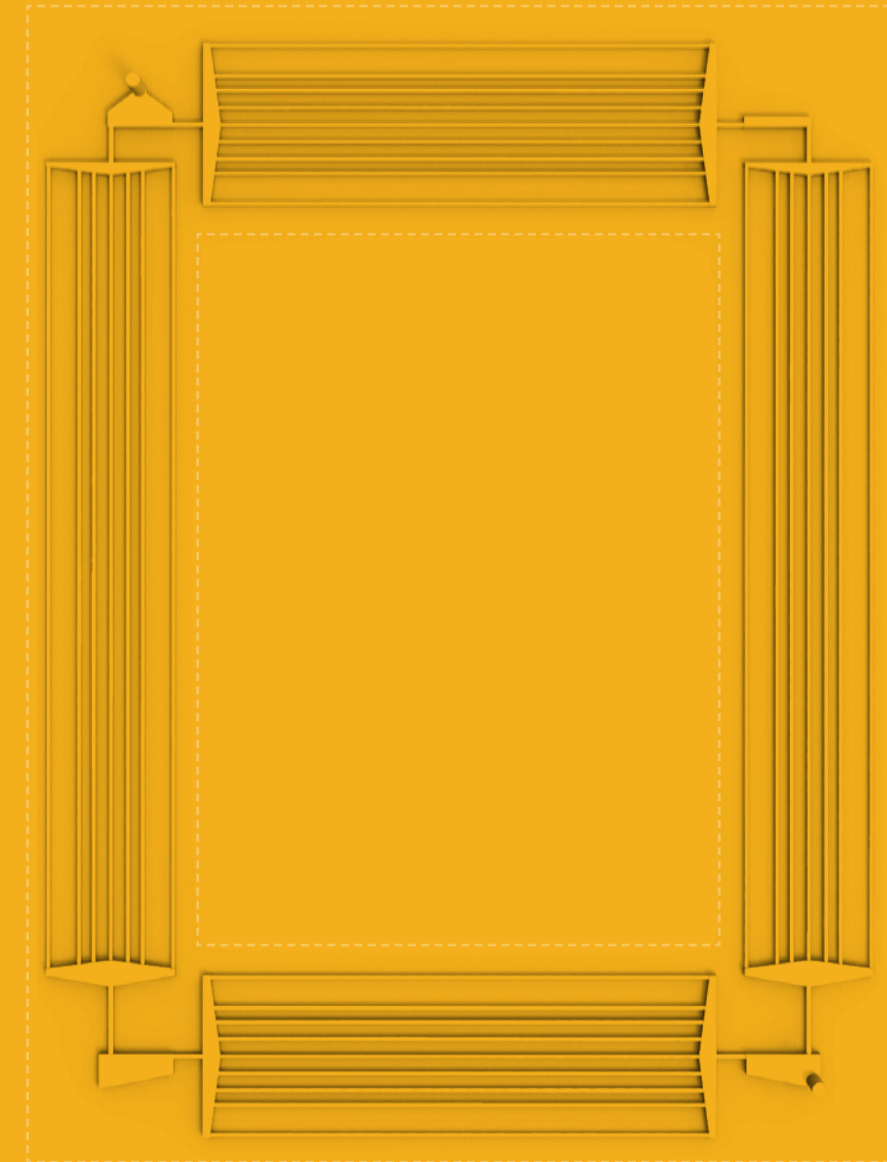


Figure 7.7. Network geometry 02- with variable diameter of the tubes in parallel (Author; Ansys)

Volume of network:	Pressure drop in network
<b>22.53 litres</b>	<b>1167.96 Pa</b>
Change in volume	Change in pressure drop
<b>+ 9.2 %</b>	<b>- 5 %</b>

Change in volume and pressure drop are calculated to network geometry 01 as reference.

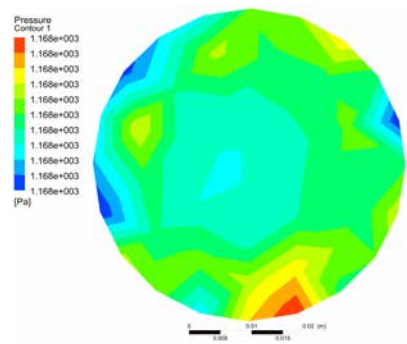


Figure 7.8a. Pressure contour inlet (Author; Ansys)

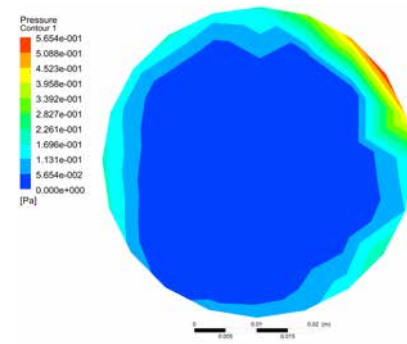


Figure 7.8b. Pressure contour outlet (Author; Ansys)

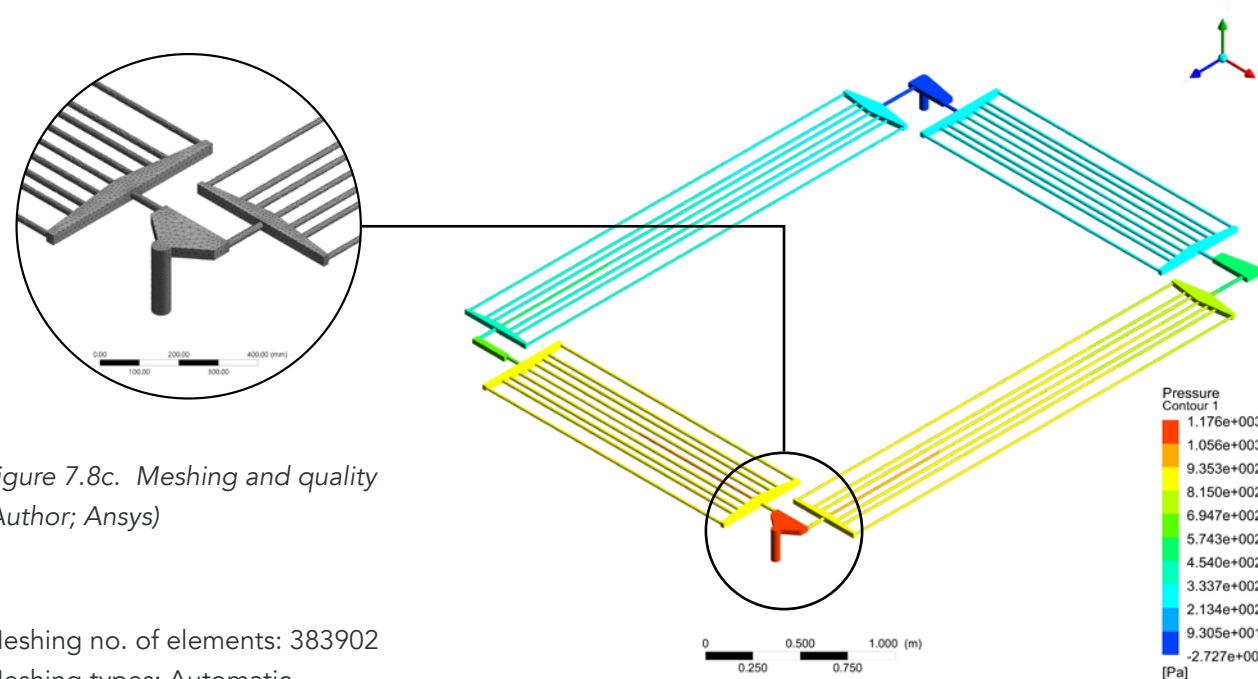


Figure 7.8c. Meshing and quality (Author; Ansys)

Meshing no. of elements: 383902  
 Meshing types: Automatic  
 Quality: Medium  
 Min size: 7.0 mm  
 Max size: 700.00 mm

Viscous model: k-epsilon  
 Method: Spatial Discretization-  
 Least Squares Cell Based

No. of iterations: 200  
 ΔP: 1022.7 Pa  
 Convergence cycle: NA

No. of iterations: 2000  
 ΔP: 1167.96  
 Convergence iteration: NA  
 flat plate zone  
 Convergence exponential: e-03  
 Simulation time: 49 minutes

Figure 7.8d. Pressure of boundary domain (Author; Ansys)

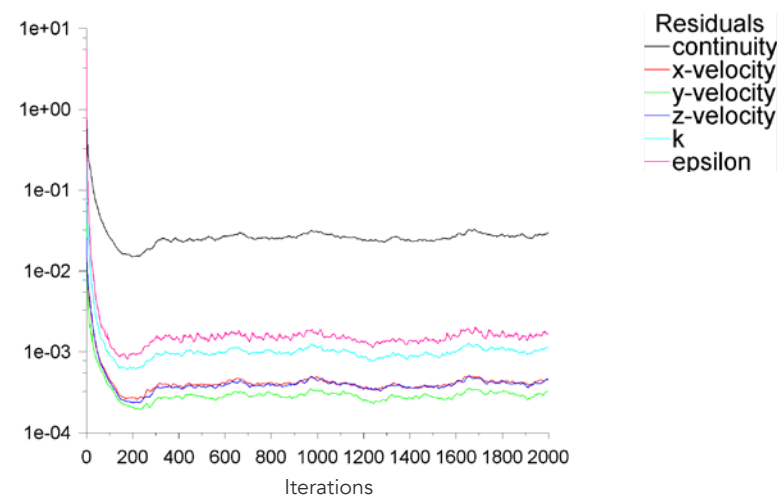


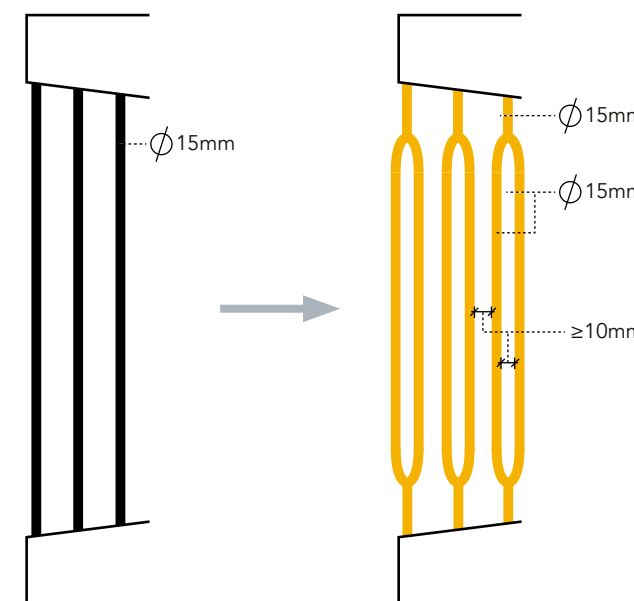
Figure 7.8e. Graph for 2000 iterations for CFD of geometry 02 (Author; Ansys)

## 7.4 VOLUME VARIANCE

The higher the amount of water concealed within the tubular network, higher is the capacity of thermal exchange within the outdoor and the indoor environment. To ensure the same a number of possibilities were considered and modified while the geometry was complied with the limitations of concrete as a material as well as allowing the facilitations of different facade and structural fixtures. The modification of the geometry was also informed by the limitations of the inverse investment casting manufacturing method. The limitation of the additive manufacturing method along with the printed material- wax was also taken into account.

### 7.4.1 Method 1: Splitting of tubes

The first method adopted to increase the volume of the network was by splitting each of the tubes into two with a limitation of at least 10 mm cover between the networks to ensure integrity of concrete as a material. Lower than this up-till 10 mm is possible if the reach of the complex geometries is upright and easy (Jipa et al., 2016). The flow of the concrete at these complex junction is dependent on the mixture of the concrete and the fibre size. The reason to split the tubes and branch into two and not choosing to have two tube starting from the manifold is to eliminate the extra pressure drops of the fluid travel within the manifold and have a considerable amount of gap between the inlets rather than crowding. The modified geometry after splitting the tubes is shown in figure 7.10.



**+ 85.5%**  
 increase in volume

Figure 7.9. Schematic diagram of single tube split into two with a consideration of minimum concrete cover of 10 mm

### 7.4.2 Network Geometry 03

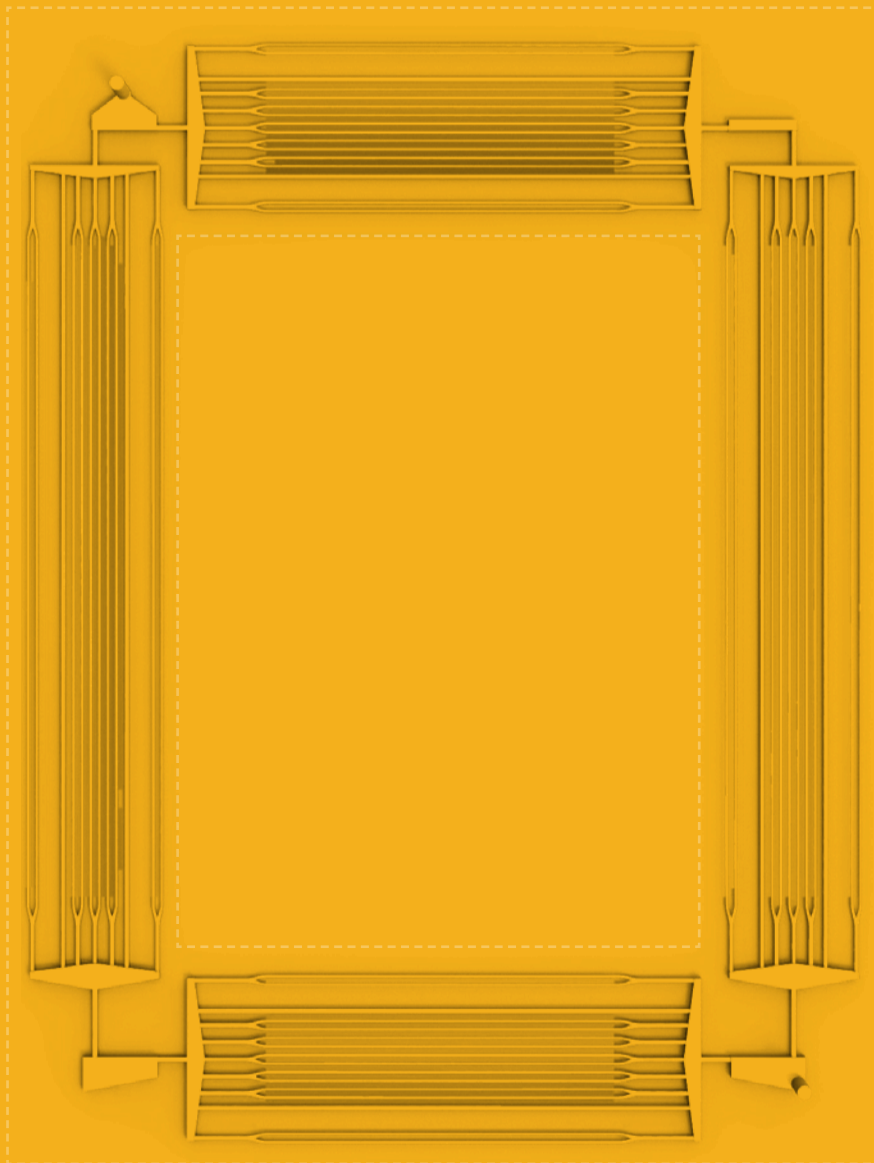


Figure 7.10. Network geometry 03- with individual tubes split into two

Volume of network:	Pressure drop in network
<b>30.1 litres</b>	<b>1332.34 Pa</b>
Change in volume	Change in pressure drop
<b>+ 46 %</b>	<b>+ 7.8 %</b>

Change in volume and pressure drop are calculated to network geometry 01 as reference.

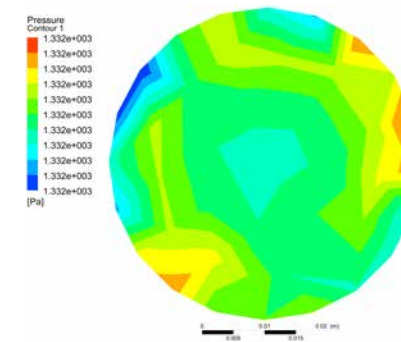


Figure 7.11a. Pressure contour inlet (Author; Ansys)

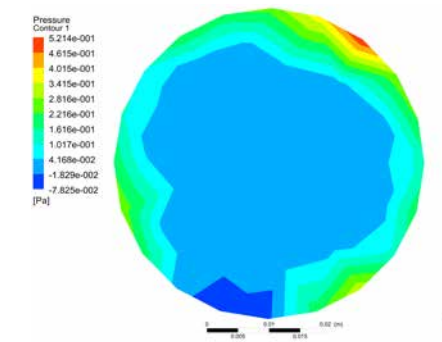


Figure 7.11b. Pressure contour outlet (Author; Ansys)

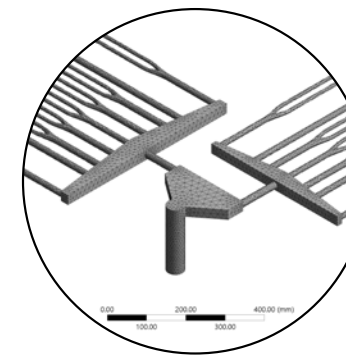


Figure 7.11c. Meshing and quality (Author; Ansys)

Meshing no. of elements: 386687  
 Meshing types: Automatic  
 Quality: Medium  
 Min size: 7.0 mm  
 Max size: 700.00 mm

Viscous model: k-epsilon  
 Method: Spatial Discretization-  
 Least Squares Cell Based

No.of iterations: 200  
 $\Delta P$ : 1166.63 Pa  
 Convergence cycle: NA

No.of iterations: 2000  
 $\Delta P$ : 1332.34  
 Convergence iteration: NA  
 flat plate zone  
 Convergence exponential: e-03  
 Simulation time: 45 minutes

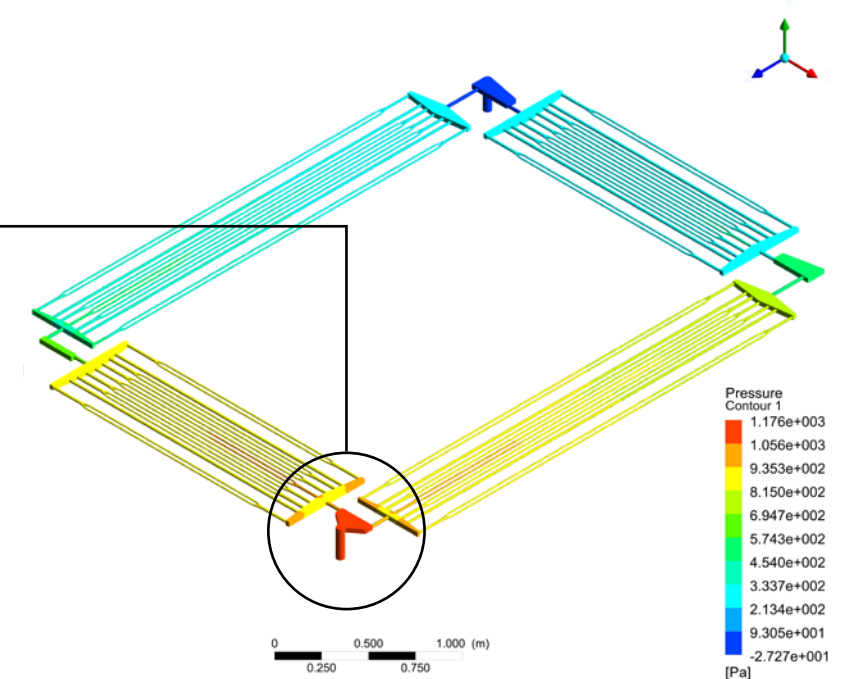


Figure 7.11d. Pressure of boundary domain (Author; Ansys)

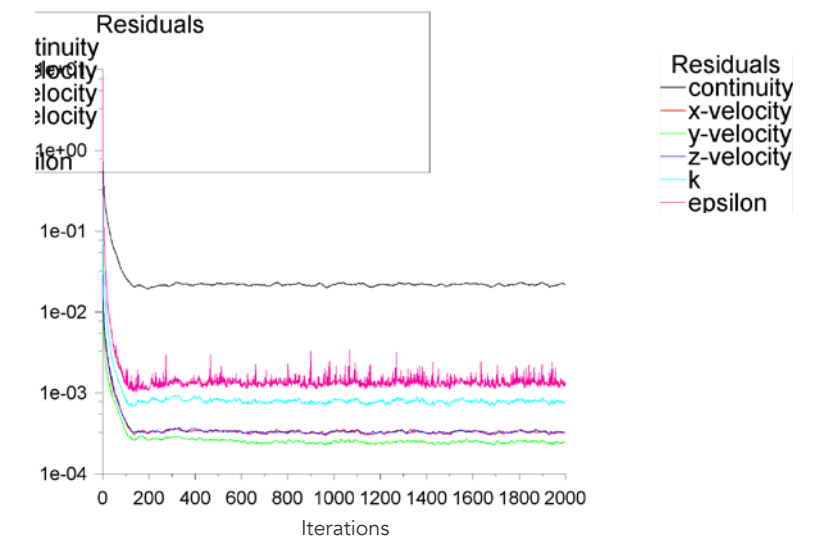


Figure 7.11e. Graph for 2000 iterations for CFD of geometry 03 (Author; Ansys)

### 7.4.3 Method 2: Curling of tubes

The second method involves increasing the length of the tube by curling it in along the thickness of the panel and hence increase the volume of the tubular network. The length and curvature of the arcs are governed by the thickness of the panel, the reinforcement layers and the required minimum concrete cover. The concrete cover needed here relates to the cover for the tubular network and the reinforcement layer and is not in concern with the corrosion of the reinforcement as all the materials used in the construction of the concerned facade panel are corrosion free materials as mentioned in section 7.8.1.

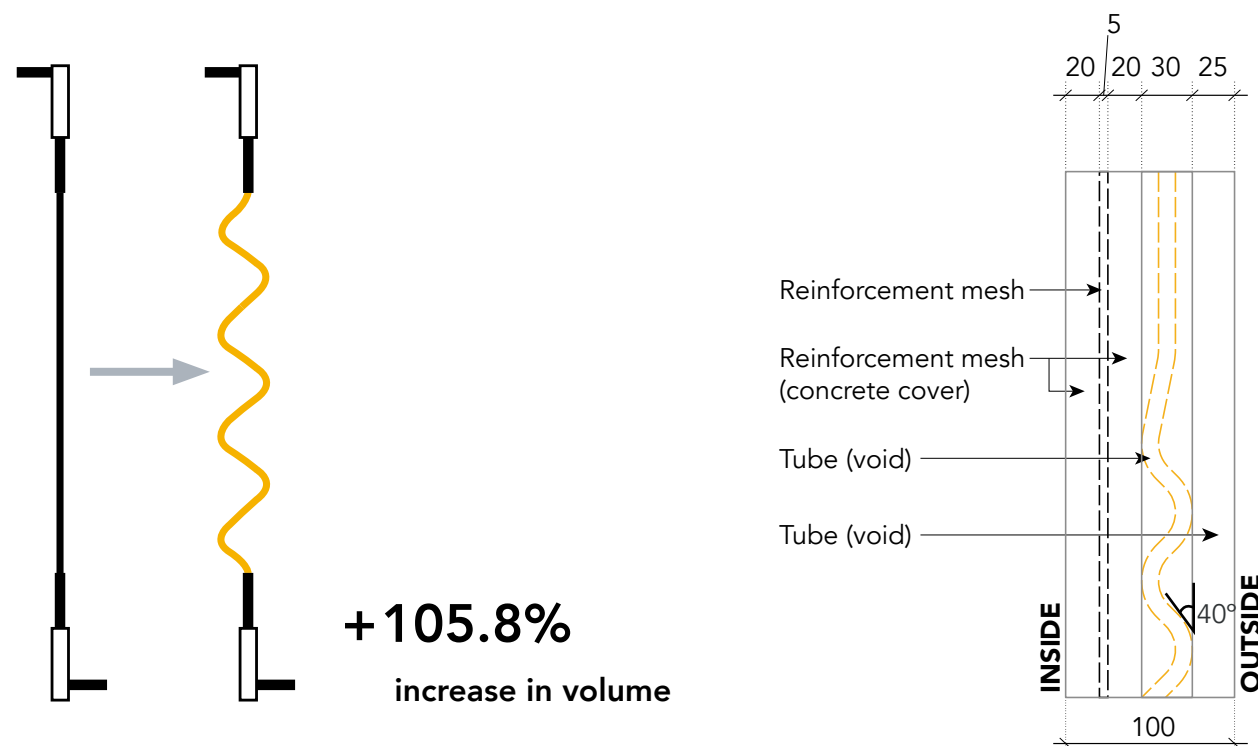


Figure 7.12. Section showing the allowable width for the curving of the tubes (Author).

Figure 7.13. Section of the external facade panel showing the allowable width for the curving the tubes (Author).

Depending on the developed complex geometry for the tubular network, the decided method of manufacturing was chosen as an inverse investment casting. This let the inner geometry to be fabricated in a loss mould material like wax and the possible method to manufacture the complex geometry with wax is chosen to be material extrusion additive manufacturing or commonly known as 3D printing of wax. Depending on the same, the other guiding factor for the inclination of the geometry was informed by the ability of free-form 3D printing wax and the maximum inclination the material in combination with the printing method could handle. Along with the tests performed for the inclination of the wax in normal geometry, tests for the modified curved tubular geometry were done to analyse the maximum possible inclination of the curved tube without any support with 15% infill geometry. The goal of printing at higher inclination without supports is preferred

as higher is the inclination higher are the number of curls and higher is the amount of volume of the tubular network. The printed geometries are shown in figure 7.15. The geometry with 30° to 40° do show smooth extrusion and geometry sustaining while three one at 45° starts to show signs of imperfection and does possess the risk of failure at certain point while 3D printing wax.

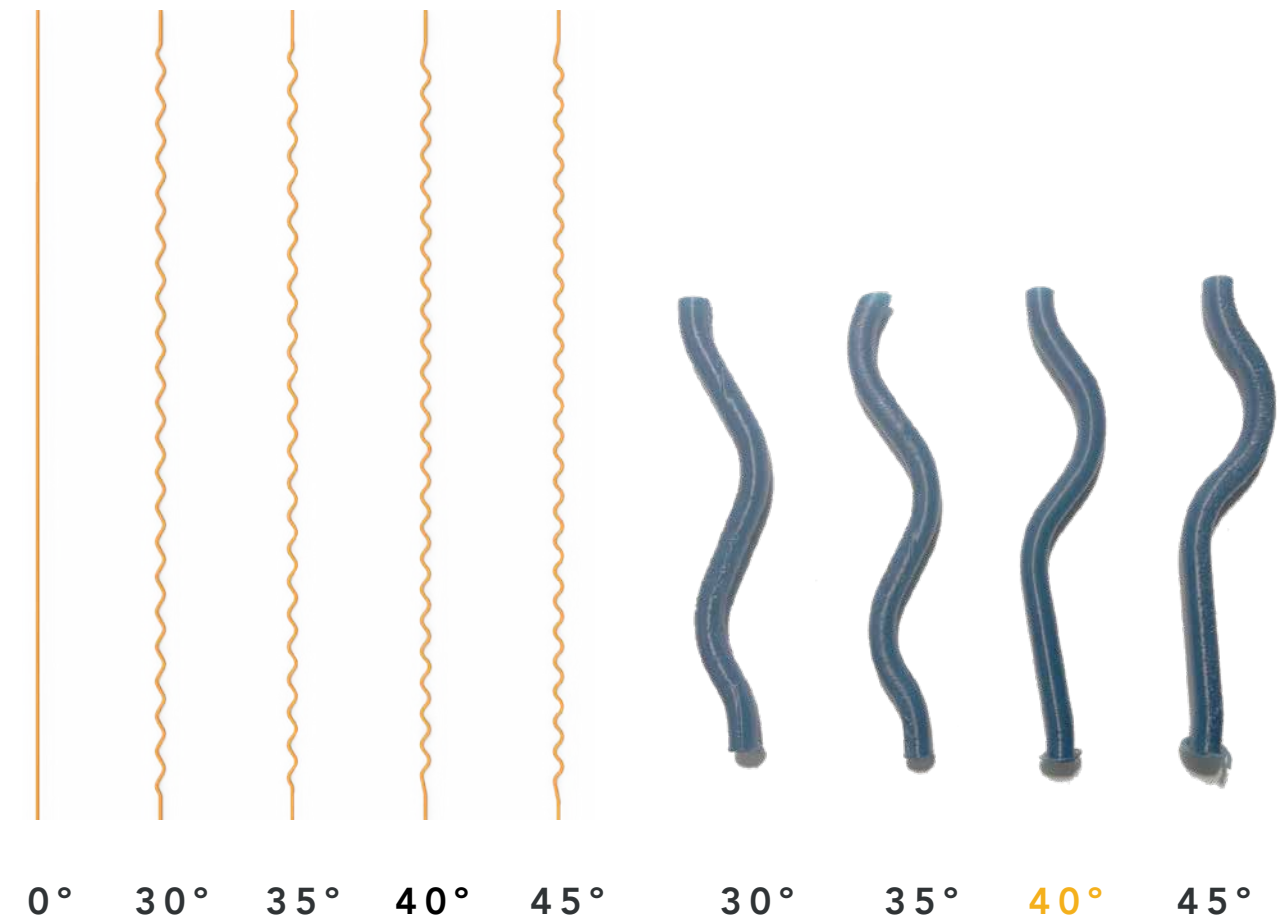


Figure 7.14. Tubes at different inclination degrees within the specified width and volume increment by %. (Author)

Figure 7.15. 3D printed curved tubes at different degrees (Author).

The curved networks were altered along the division of the single tube to ensure extra possible concrete cover at the bends of the tubes. The modified network geometry along with the change in volume and the pressure drop across the network and the details of the simulation has been depicted in the figure 7.16.

### 7.4.4 Network Geometry 04

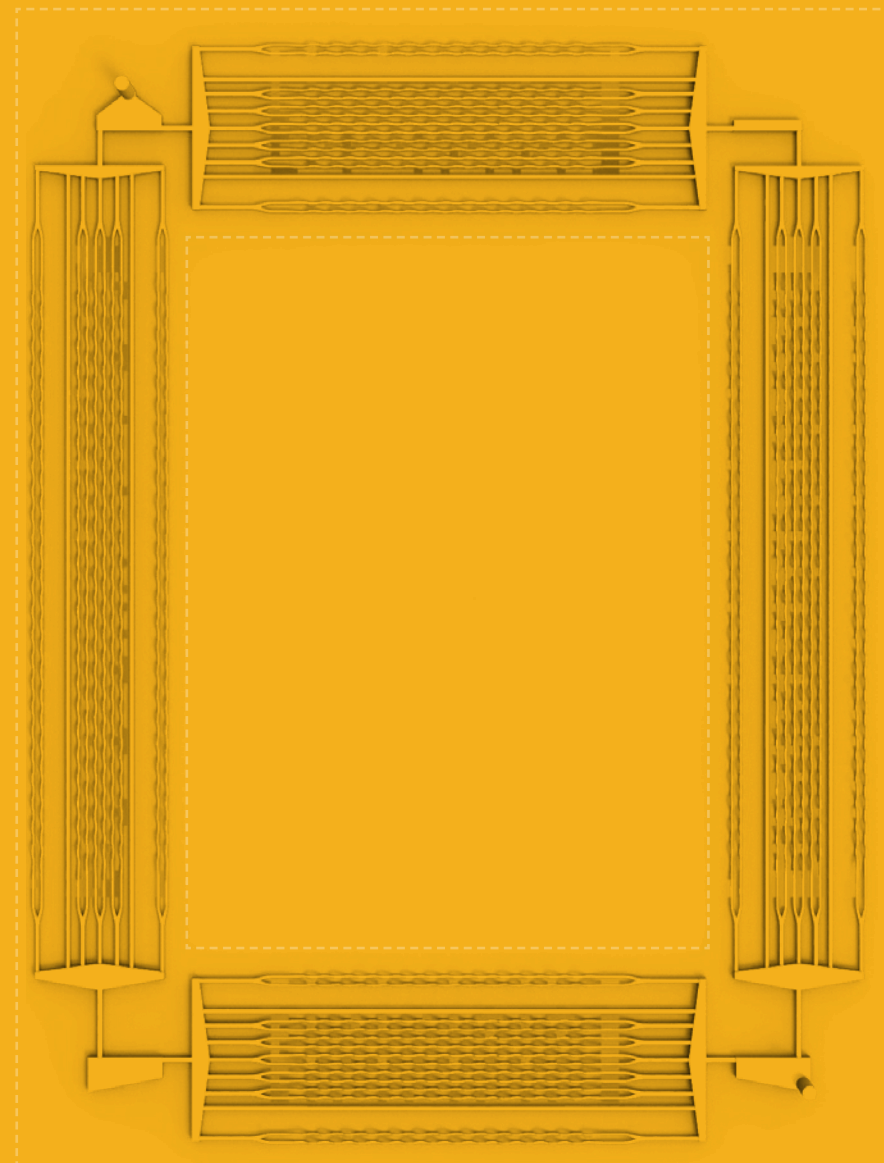


Figure 7.16. Network geometry 04- with curled split tubes in parallel

Volume of network:	Pressure drop in network
<b>31.2 litres</b>	<b>1463.10 Pa</b>
Change in volume	Change in pressure drop
<b>+ 51.4 %</b>	<b>+ 18.4 %</b>

Change in volume and pressure drop area calculated to network geometry 01 as reference.

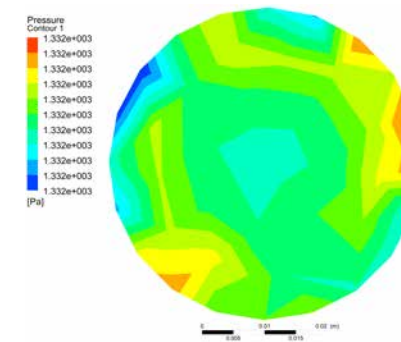


Figure 7.17a. Pressure contour inlet (Author, Ansys fluent)

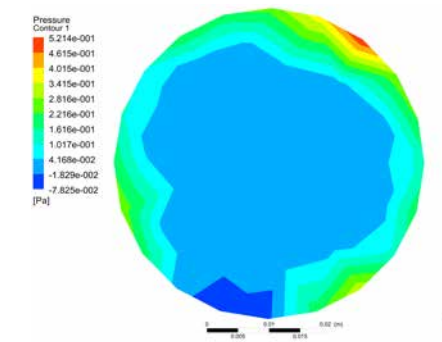


Figure 7.17b. Pressure contour outlet (Author, Ansys fluent)

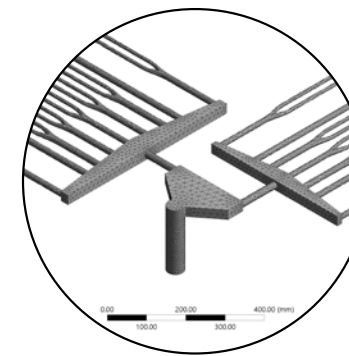


Figure 7.17c. Meshing and quality (Author; Ansys Meshing).

Meshing no. of elements: 434419  
 Meshing types: Automatic  
 Quality: Medium  
 Min size: 7.0 mm  
 Max size: 700.00 mm

Viscous model: k-epsilon  
 Method: Spatial Discretization-  
 Least Squares Cell Based

No.of iterations: 200  
 $\Delta P$ : 1273.31 Pa  
 Convergence cycle: NA

No.of iterations: 2000  
 $\Delta P$ : 1463.10  
 Convergence iteration: NA  
 flat plate zone  
 Convergence exponential: e-03  
 Simulation time: 45 minutes

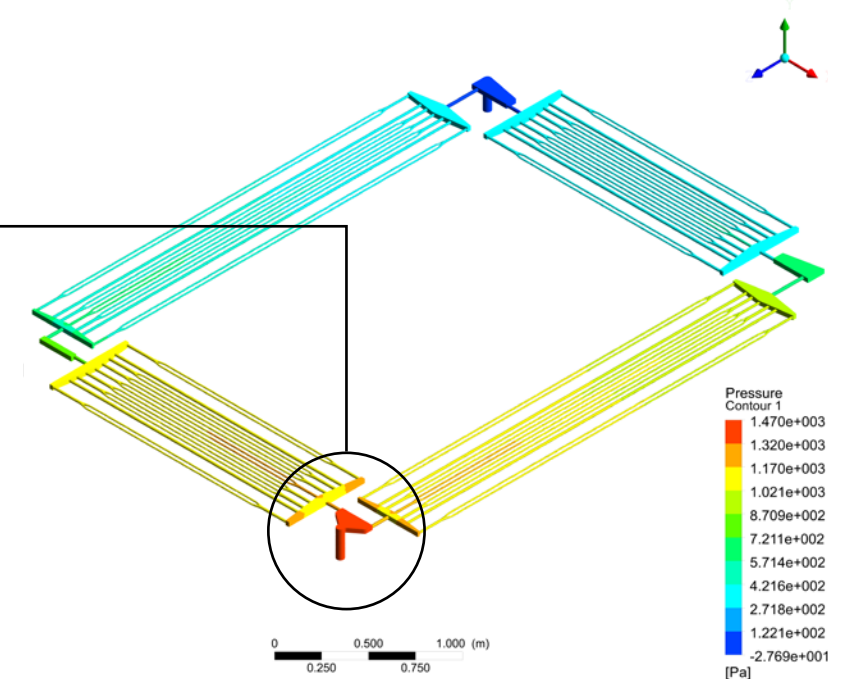


Figure 7.17d. Pressure of boundary domain (Author, Ansys fluent).

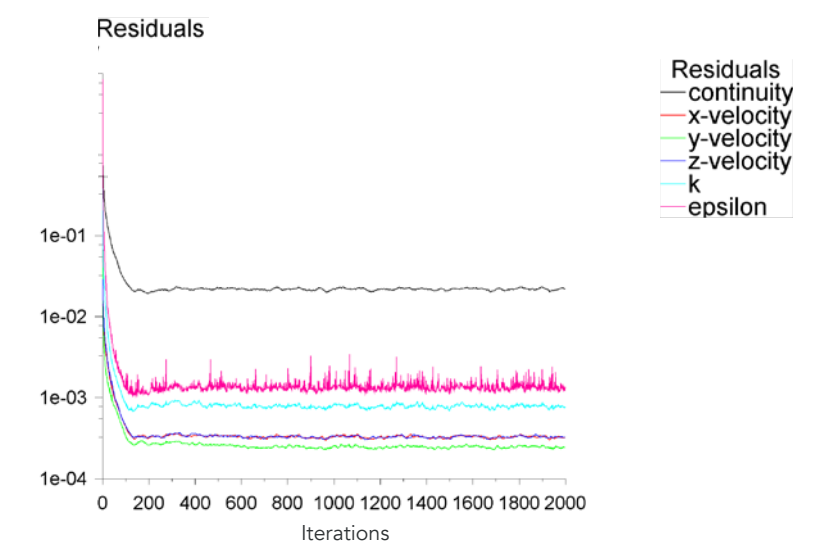


Figure 7.17e. Graph for 2000 iterations for CFD of geometry 04 (Author, Ansys Fluent)

## 7.5 PRESSURE DROP

With increasing the volume of the network and the increasing the length of the tubes with complex geometry, the pressure drop along the individual tubes will increase in comparison to that of a straight tube with 15 mm diameter. To analyse the same, pressure drop simulation of the primary tube was done using Ansys with its Fluent- Fluid flow counterpart. The pressure drop across this tube was set as a benchmark for the other developed geometries to be analysed and has been depicted below. To ensure a valid comparison between the different geometries the elevational length of the tube was derived from the network geometry 04. The

### 7.5.1 Tube type 01

Length: 2832 mm, projected  
Diameter: 15 mm, uniform

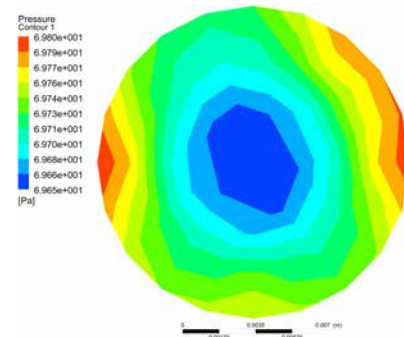


Figure 7.18a. Pressure contour inlet (Author; Ansys)

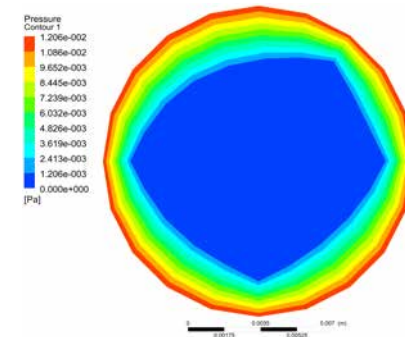


Figure 7.18b. Pressure contour outlet (Author; Ansys)

Meshing no. of elements: 51729  
Meshing types: Automatic  
Quality: Medium  
Min size: 1.40 mm  
Max size: 141.00 mm

Viscous model: Laminar  
Method: Spatial Discretization- Least Squares Cell Based

No. of iterations: 200  
 $\Delta P$ : 71.6 Pa  
Convergence cycle: NA

No. of iterations: 1000  
 $\Delta P$ : 69.8  
Convergence iteration: 900-950, flat plate zone  
Convergence exponential: e-07  
Simulation time: 8 minutes

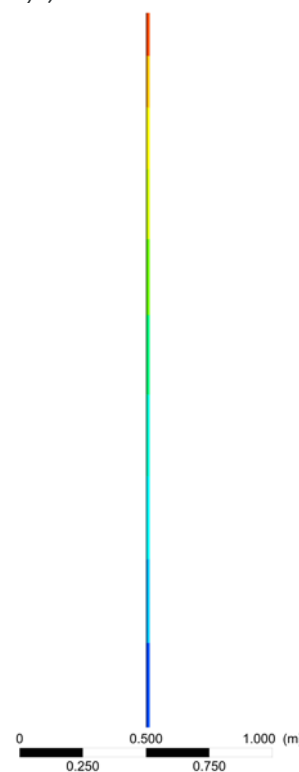


Figure 7.18c. Pressure contour boundary (Author; Ansys)

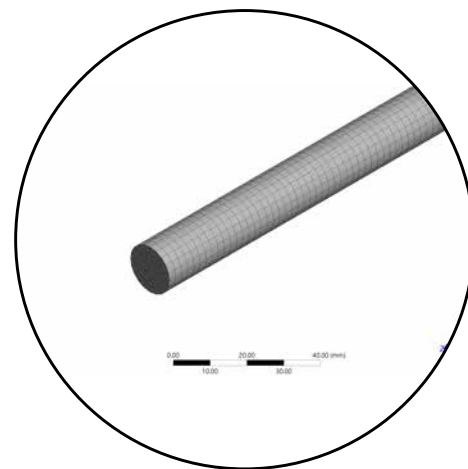


Figure 7.18d. Meshing and quality (Author; Ansys)

### 7.5.2 Tube type 02

Length: 2328mm, projected  
Diameter: 10 mm, uniform

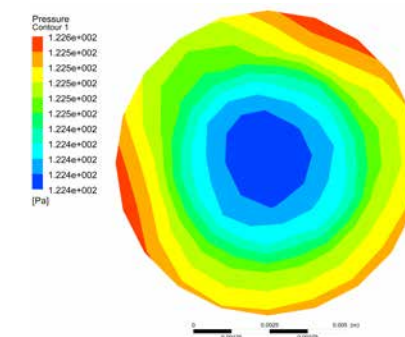


Figure 7.19a. Pressure contour inlet (Author; Ansys)

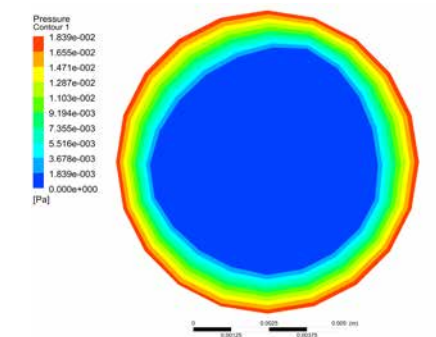


Figure 7.19b. Pressure contour outlet (Author; Ansys)

Meshing no. of elements: 88920  
Meshing types: Automatic  
Quality: Medium  
Min size: 1.40 mm  
Max size: 141.00 mm

Viscous model: Laminar  
Method: Spatial Discretization- Least Squares Cell Based

No. of iterations: 200  
 $\Delta P$ : 124.57 Pa  
Convergence cycle: NA

No. of iterations: 1000  
 $\Delta P$ : 122.57 Pa  
Convergence iteration: 850-900, flat plate zone  
Convergence exponential: e-07  
Simulation time: 9-10 minutes

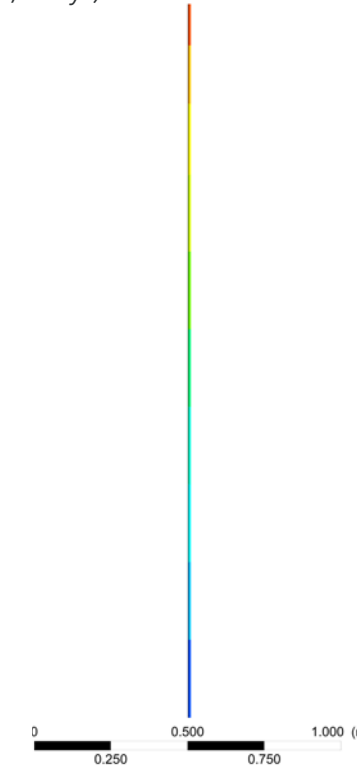


Figure 7.19c. Pressure contour boundary (Author; Ansys)

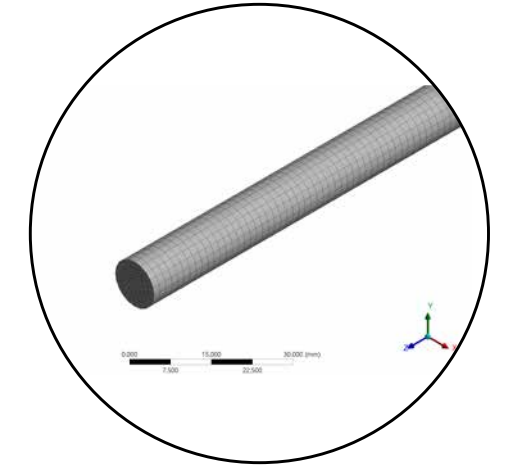


Figure 7.19d. Meshing and quality (Author; Ansys)

effective lengths and tube diameters per geometries are mentioned per simulations. The defined settings as per the validation of the tube in section 5.2.5 was used further.

The targeted pressure drop for the further modifications and their respective simulations would be that of the tube 01 at 69.8 Pa. With the division of the tube and splitting into two branches, the change of the diameter of the tube was needed to comply with the constraints by the material to allow for minimum concrete cover/ separation width of 20 - 10 mm and the diameter of the modified tube was reduced to 10 mm and the CFD simulations for the same were run to check the pressure drop. It is evident as discussed earlier that pressure drop is inversely proportional to the diameter of the tube and hence an increase in the pressure drop is

expected as compared to tube 01. It is to be considered that the length of the tubes with 10 mm diameter have been considered from the split tube of the network geometry 04. The results and the considered parameters are depicted below.

It was evident from the previous simulation that the decrease in the diameter of the tubes does significantly increase the pressure drop. As mentioned in the prior section of volume modification, the need to increase the volume did demand for the split tubes to be curled along the thickness of the panels and hence increases complexity as well as the effective length of the tube. With the increase in length the pressure drop increases as it is directly proportional to the length of the tube. To analyse the same, this complex geometry was simulated and analysed for the speculated change and depicted below.

### 7.5.3 Tube type 03

Length: 2832 mm, projected  
Diameter: 10 mm inlet;  
15 mm outlet

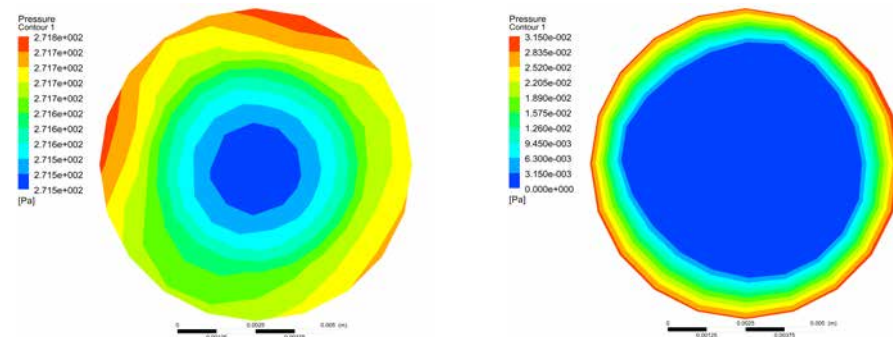


Figure 7.20a. Pressure contour inlet (Author; Ansys)

Figure 7.20b. Pressure contour outlet (Author; Ansys)

Meshing no. of elements: 118404  
Meshing types: Automatic  
Quality: Medium  
Min size: 1.40 mm  
Max size: 141.00 mm

Viscous model: Standard k-e,  
Standard wall Fn  
Method: Spatial Discretization- Least Squares Cell Based

No. of iterations: 200  
 $\Delta P$ : 303.95 Pa  
Convergence cycle: NA

No. of iterations: 1000  
 $\Delta P$ : 271.48 Pa

Convergence iteration: 572  
Convergence exponential: e-05  
Simulation time: 18 minutes

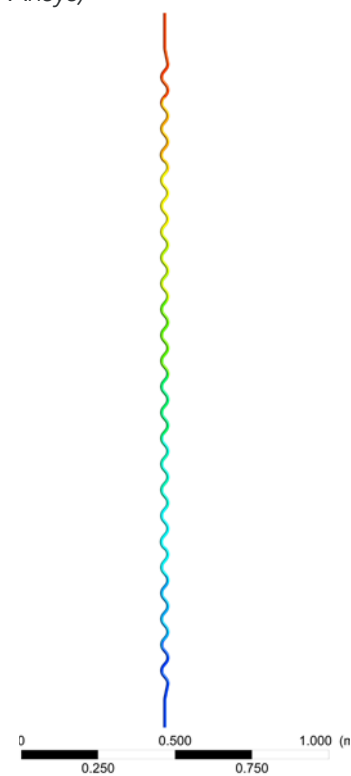


Figure 7.20c. Pressure contour boundary (Author; Ansys)

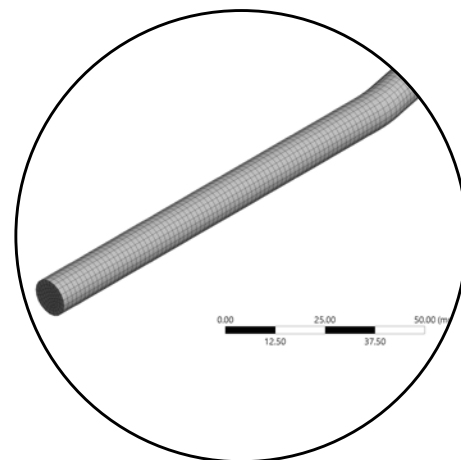


Figure 7.20d. Meshing and quality (Author; Ansys)

The pressure drop across a single tube has increased in manifold and to avoid the increased pressure drop and improve the one close to that of tube 01, measures and modification to the geometry was needed and to do the same the alterations in the geometry was considered. The varying of the tube with different possibilities were analysed to a maximum and minimum diameters set to 10 mm and 15 mm respectively. The one with a varying diameter of 10 mm at the inlet and 15 mm at the outlet was the one that shows drastic decrease in the pressure drop across the geometry. To be taken into consideration the sweeping of the inlet and the outlet geometry using the CAD software Rhino 6 was a key factor in achieving this change. The Sweep1 method was used with the smaller diameter of inlet first and the larger diameter of outlet next along with the path. Altering the method of selecting the curves may change the geometry achieved herewith and hence the pressure drop values.

### 7.5.4 Tube type 04

Length: 2832 mm, projected  
Diameter: 15 mm, uniform

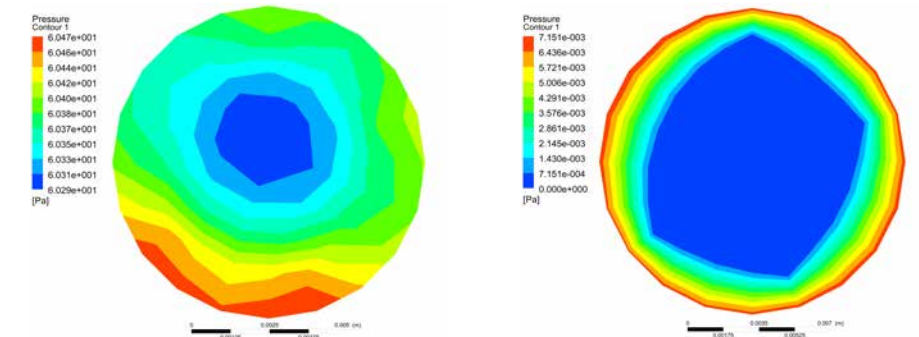


Figure 7.21a. Pressure contour inlet (Author; Ansys)

Figure 7.21b. Pressure contour outlet (Author; Ansys)

Meshing no. of elements: 57534  
Meshing types: Automatic  
Quality: Medium  
Min size: 1.40 mm  
Max size: 141.00 mm

Viscous model: Standard k-e,  
Standard wall Fn  
Method: Spatial Discretization- Least Squares Cell Based

No. of iterations: 200  
 $\Delta P$ : 60.42 Pa  
Convergence cycle: NA

No. of iterations: 1000  
 $\Delta P$ : 60.47 Pa

Convergence iteration: 269  
Convergence exponential: e-05  
Simulation time: 11 minutes

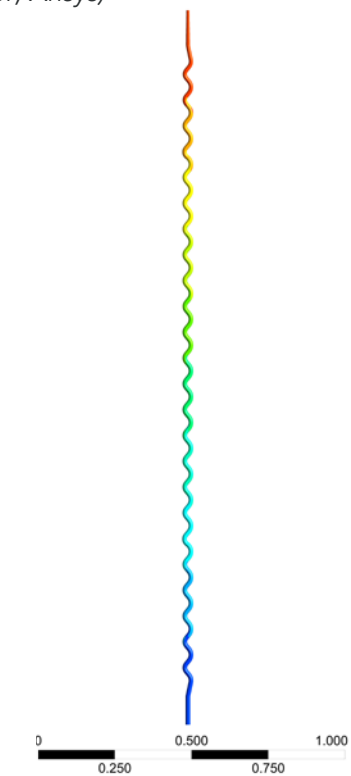


Figure 7.21c. Pressure contour boundary (Author; Ansys)

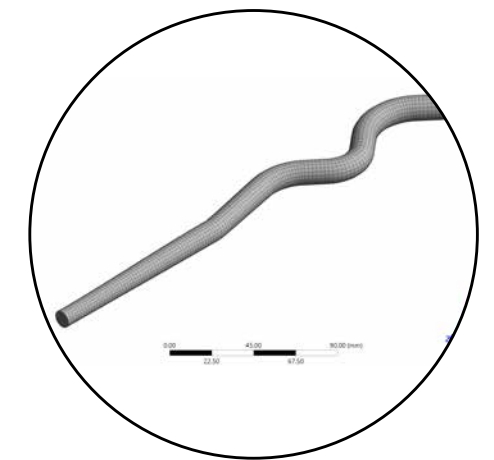


Figure 7.21d. Meshing and quality (Author; Ansys)

While the pressure drop in the tube 04 was significantly reduced with the modified geometry, the splitting of the tube 01 into two does tend towards high pressure drop and the setup of the tube 01 branched into two was further simulated for the pressure drop as depicted below to determine the pressure drop with two straight tubes of 10 mm diameter and converged back to the 15 mm tube. It is to be noted that the minimum size of the meshing in this simulation has been increased in comparison to the previous simulation to accommodate the limited number of elements allowed for analysis in a single geometry in the Ansys fluent student version which or else would have crossed the limit of allowed 512k elements only.

### 7.5.5 Tube type 05

Length: 2832 mm, projected  
Diameter: 10 mm inlet;  
10 mm outlet

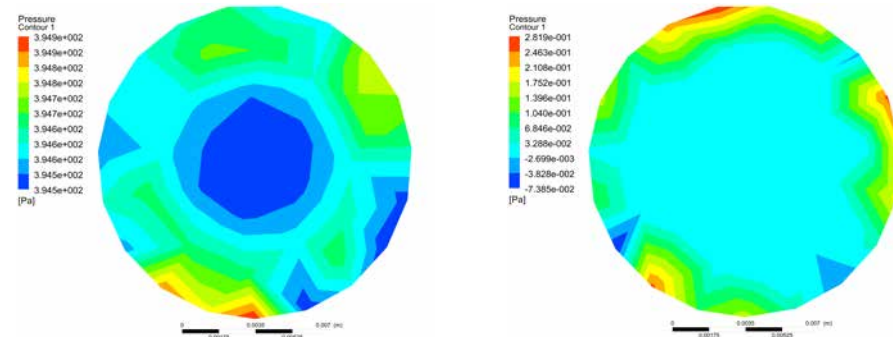


Figure 7.22a. Pressure contour inlet (Author; Ansys)

Figure 7.22b. Pressure contour outlet (Author; Ansys)

Meshing no. of elements: 255222  
Meshing types: Automatic  
Quality: Medium  
Min size: 2.50 mm  
Max size: 141.00 mm

Viscous model: Standard k-e,  
Standard wall Fn  
Method: Spatial Discretization- Least Squares Cell Based

No.of iterations: 200  
 $\Delta P$ : 390.88 Pa  
Convergence cycle: NA

No.of iterations: 2000  
 $\Delta P$ : 394.45 Pa

Convergence iteration: 1956  
Convergence exponential: e-05  
Simulation time: 18-20 minutes

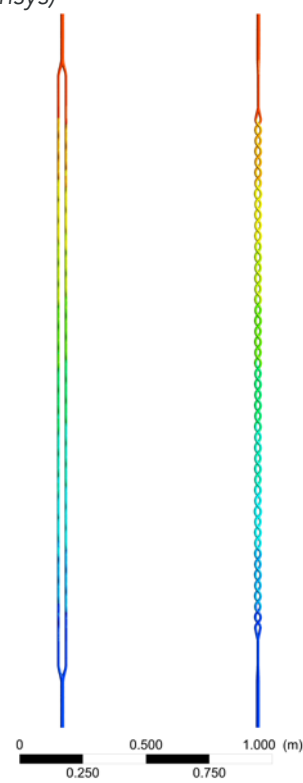


Figure 7.22c. Pressure contour boundary (Author; Ansys)

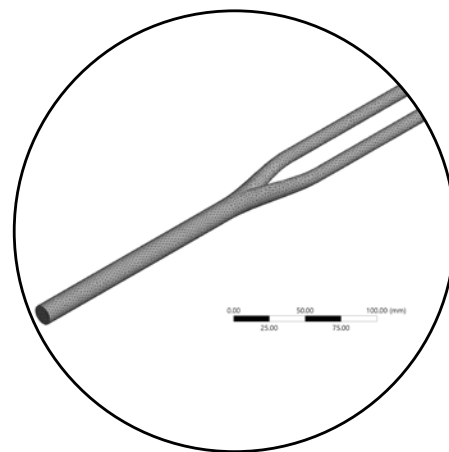


Figure 7.22d. Meshing and quality (Author; Ansys)

### 7.5.6 Tube type 06

Length: 2832 mm, projected  
Diameter: 10 mm inlet;  
15 mm outlet

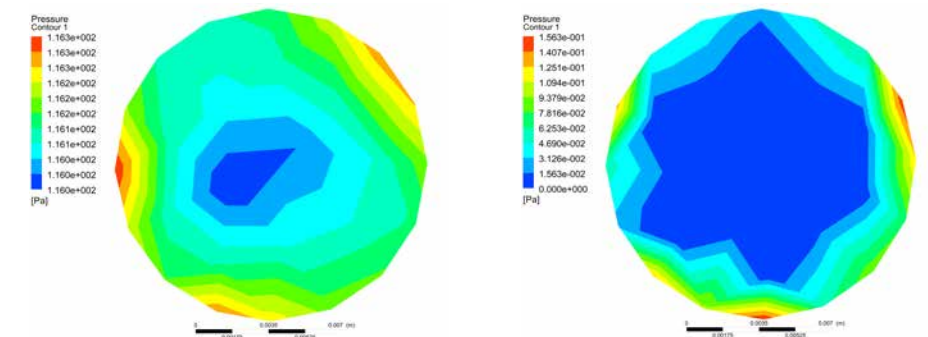


Figure 7.23a. Pressure contour inlet (Author; Ansys)

Figure 7.23b. Pressure contour outlet (Author; Ansys)

Meshing no. of elements: 274276  
Meshing types: Automatic  
Quality: Medium  
Min size: 3.00 mm  
Max size: 100.00 mm

Viscous model: Standard k-e,  
Standard wall Fn  
Method: Spatial Discretization- Least Squares Cell Based

No.of iterations: 200  
 $\Delta P$ : 116.42 Pa  
Convergence cycle: NA

No.of iterations: 1000  
 $\Delta P$ : 116.34 Pa

Convergence iteration: 747  
Convergence exponential: e-05  
Simulation time: 22 minutes

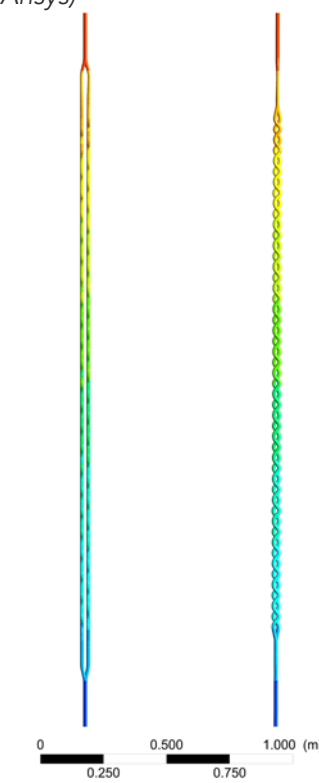


Figure 7.23c. Pressure contour boundary (Author; Ansys)

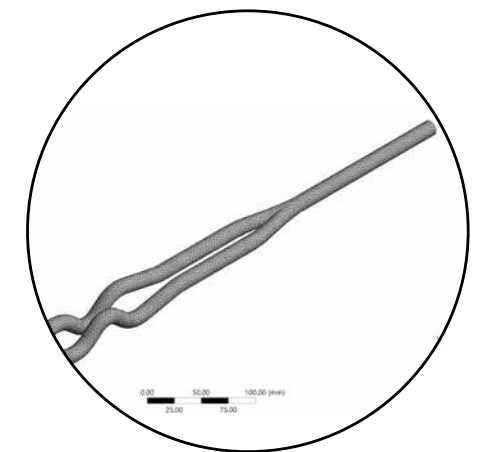


Figure 7.23d. Meshing and quality (Author; Ansys)

Now that it is evident that the pressure drop in a single tube is much higher with the uniform radii, the one with the varying radius at inlet and outlet was carried out and analysed for the speculated decrease in pressure drop. The study and used setup and details are depicted below. As mentioned earlier, due to the limitation of the allowable elements for the analysis, the minimum size for the mesh is increased and its effect can be seen in the rather polygonal shapes of the inlet and outlets which was rather designed as circular cross section. The contour mapping of the pressure of these geometries would have been less distorted with a smoother meshing unlike the current mapping. This may differ the actual simulation results by a fraction, and with a comparable mesh size setup made for the simulations from the large to small size, it does hold a valid stance for comparison, the fluid flow behaviour and state the change in pressure drop.

It was evident from the above made simulations that the pressure drop in a single straight uniform radii tube of 15mm has increased from 69.8 Pa to 116.4 Pa and that the change in geometry with strategies to maximise volume while minimising the pressure drop has been proven to significantly in favour of the goal. A comparative analysis of the six different types of tubes analysed has been outlined below and the change is noticeable and is compared in the table 7.3.

Geometry	$\phi 15$	$\phi 10$	$\phi 10$	$\phi 10$	$\phi 15$	$\phi 15$
Properties	$\phi 15$	$\phi 10$	$\phi 10$	$\phi 15$	$\phi 15$	$\phi 15$
Method	Laminar	Laminar	k-epsilon	k-epsilon	k-epsilon	k-epsilon
Converged iteration	N.A (assumed flat plate zone)	N.A (assumed flat plate zone)	572	269	1956	747
Volume (litre)	0.5	0.18	0.20	0.43	0.50	0.96
Change in volume	N.A	- 64 %	- 60 %	- 14 %	$\pm 0$ %	+92 %
Pressure drop (Pa)	69.8	122.57	271.48	60.47	394.45	116.34
Change in pressure drop	N.A	+ 75.6 %	+ 288.9 %	- 9.33 %	+ 465.1 %	+ 66.6 %
Simulation time (minutes)	08	09-10	18	11	18-20	22

Table 7.3. Comparison of different tubes typology evolved by design. (Author)

The finalised geometry of the single tube was coupled up with others and arranged in the network geometry with modifications from network geometry 04 and analysed for the pressure drop across the inlet and outlet of the complete network geometry. The network geometry 05 should perform better than that of network geometry 04 in terms of pressure drop across the network while marginally increasing the volume due to the modified geometry of the individual tubes. The details of the simulation used for CFD and the details are depicted next along with the results.

## 7.5.7 Network Geometry 05

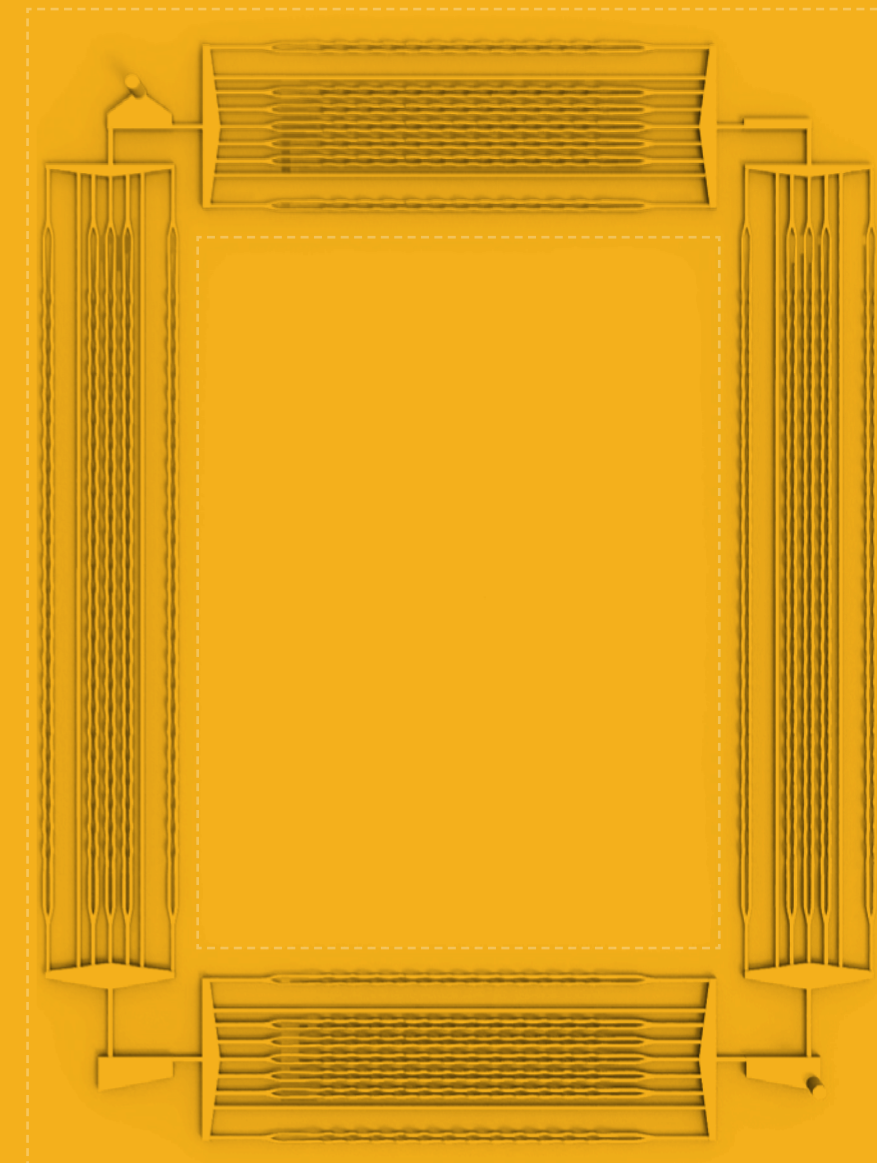


Figure 7.24. Network geometry 05- with variable diameter of the split tubes in parallel. (Author)

Volume of network:

**29.41 litres**

Change in volume

**+ 42.7 %**

Pressure drop in network

**1319.67 Pa**

Change in pressure drop

**+ 6.8 %**

\*Change in volume and pressure drop are calculated to network geometry 01 as reference.

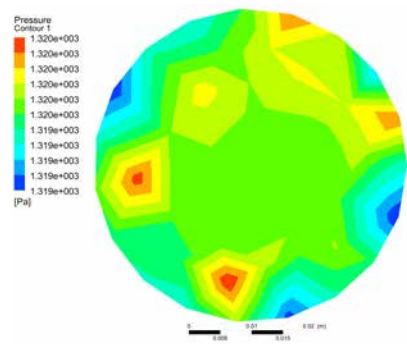


Figure 7.25a. Pressure contour inlet (Author)

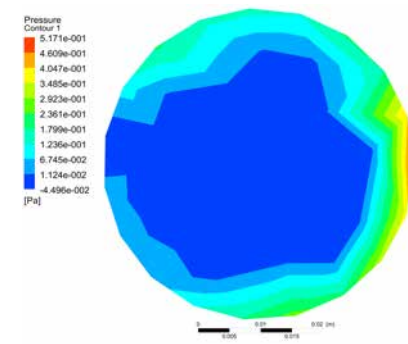


Figure 7.25b. Pressure contour outlet (Author)

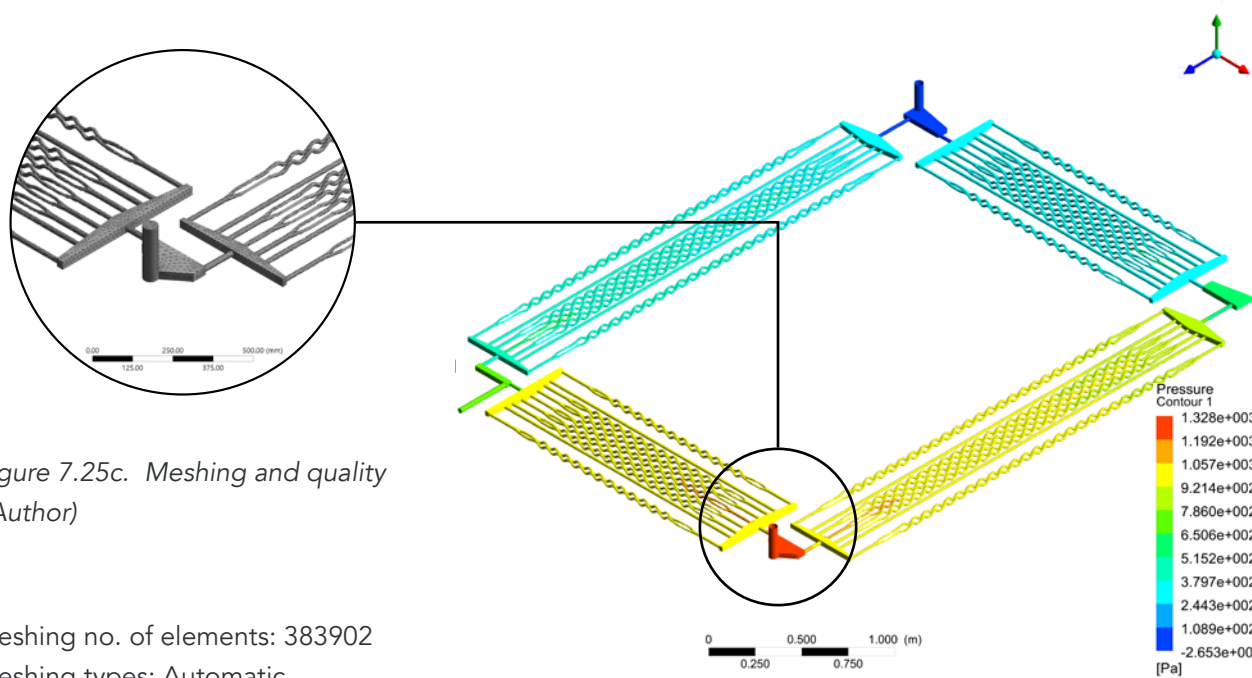


Figure 7.25c. Meshing and quality (Author)

Meshing no. of elements: 383902  
 Meshing types: Automatic  
 Quality: Medium  
 Min size: 7.0 mm  
 Max size: 700.00 mm

Viscous model: k-epsilon  
 Method: Spatial Discretization-  
 Least Squares Cell Based

No. of iterations: 200  
 $\Delta P$ : 1154.25 Pa  
 Convergence cycle: NA

No. of iterations: 2000  
 $\Delta P$ : 1319.67  
 Convergence iteration: NA  
 flat plate zone

Convergence exponential: e-03  
 Simulation time: 1hr 2 minutes

Figure 7.25d. Pressure of boundary domain (Author)

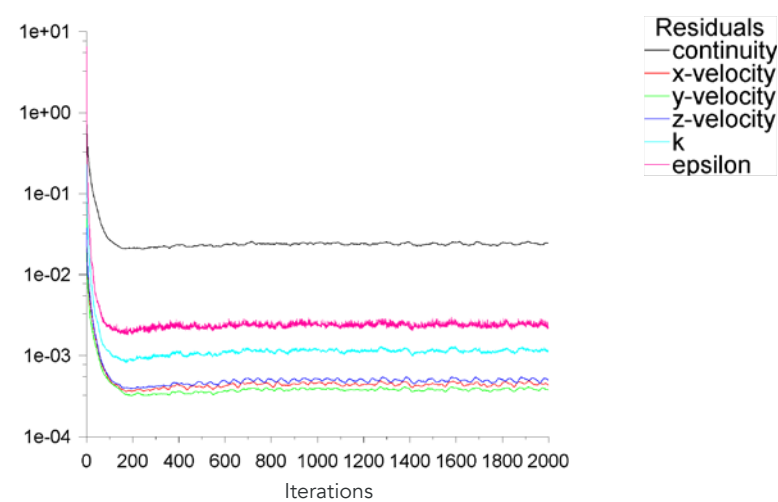


Figure 7.25e. Graph for 2000 iterations for CFD of geometry 05 (Author)

The results of the pressure drop from the CFD simulations does show that the decrease in the pressure drop across the geometry has been decreased with a huge margin and that the geometry derived for tube 06 does help in achieving the goal. But as the overall pressure drop has been multiplied into a huge factor than required for a smooth flow of the fluid in this complex geometry. The simulation conducted in this geometry was considered to be turbulent because of the marginal Reynolds number of 2256 considered depending on the flow velocity of the panel. To make room for the same in simulation and derive results of robust nature, a viscous model with standard k-epsilon method and standard wall functions were selected as the other simulations done and the method selected was Spatial Discretization with Least Squares Cell Based meshing method. While the other simple geometries do show a nature of converging result within a run of 2000 iterations, the complex network geometry does have a fluctuating result and does not converge. By the results of the 200 and 2000 iterations, it was noted that the variance was very marginal and limited to 1 to 5 Pa in difference and hence a flat plate zone was considered and the values were analysed. It is also to be noted that the coarse meshing done due to the limitation of the Ansys fluent student version may be a reason enough to why the iterations don't converge within 2000 iterations. It is assumed that the solver would converge beyond the simulated iterations but it would consume a huge amount and time as well as computing power as was terminated by choice.

## 7.6 SHAPE MODIFICATION

The possibilities of geometric modifications to maximise the volume while minimising the pressure drop across the network were adopted but limited to the scope of a single tube only. The multiplication of the tubes forming into a complex geometry across the facade panel, which has been constrained by different parameters, fixtures, material and fabrication methods. The next method was to computationally modify the geometry of the network with a single combined goal of minimising the pressure drop and unifying the velocity across the network. It was already noted that the limitation of maximum allowable elements by the software did result in a coarse geometry mesh with results not being so robust as they fluctuated without merging, although at a very low error level. On behalf of the previous simulation result, it was obvious that shape optimisation of the complete network was not possible to be carried out and had to be managed smartly for efficient results and to comply to the same, the four corner junctions that merged the two parallel networks into a series were considered and selected for the shape optimisation of the node.

### 7.6.1 3D- Shape optimization

The method of shape optimisation for a CFD based pressure reduction was simulated first in Ansys fluent and modified using its adjoint solver, that can optimise shapes by multi objective combined equations. The viscous model used for these simulations were limited to the laminar flow of water as if allowed for turbulence

would generate results in the small geometry where the change in volume occurs from the inlet to the node and from the node to the outlet. The convergence exp. energy is set to e-06 for robust results but may not converge the result because of the nature of flow. This was overcome by maximising the number of iterations done to expand the domain of the solver to evolve. The result of the high iteration values should reflect the response of the result desired with minimum possible deflection to the real world scenario. As a first stance one of the four nodes was selected in the criteria of being the one that connects two parallel networks into a series between the inlet and the outlet. It was simulated for the pressure drop with parameters and methods mentioned below. It is to be noted that the velocity of the water at the inlet is still considered to be 0.15 m/sec for the purpose of simulation and the comparative check of the result, while the velocity at these nodes would have been much higher and the difference in pressure for these nodes combined with the complete

### Node type 01 (Non-optimised)

Diameter: 15 mm inlet; 15 mm outlet  
Volume: 0.00085 m<sup>3</sup> or 0.85 litre

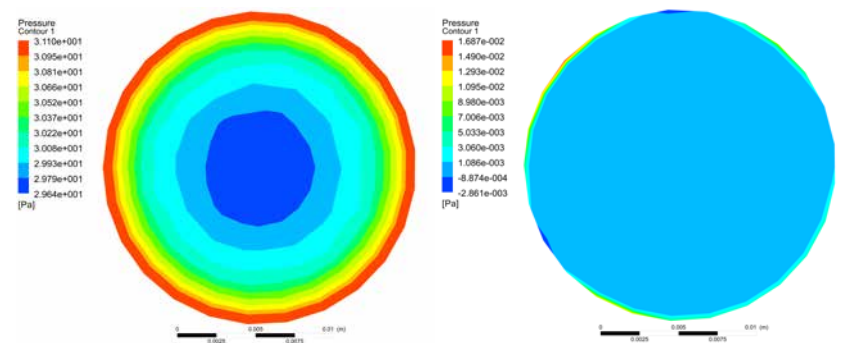


Figure 7.26a. Pressure contour inlet (Author)

Figure 7.26b. Pressure contour outlet (Author)

Meshing no. of elements: 281992  
Meshing types: Inflation, patch conforming method, Face Meshing  
Quality: Medium  
Min size: 2.5 e-002 mm  
Max size: 2.5 mm

Viscous model: Standard k-e,  
Standard wall Fn  
Method: Spatial Discretization- Green Gauss Cell Based

No. of iterations: 200  
 $\Delta P$ : 30.5 Pa  
Convergence cycle: NA

No. of iterations: 2000  
 $\Delta P$ : 31.09 Pa  
Convergence iteration: 1545  
Convergence exponential: e-05  
Simulation time: 19 minutes

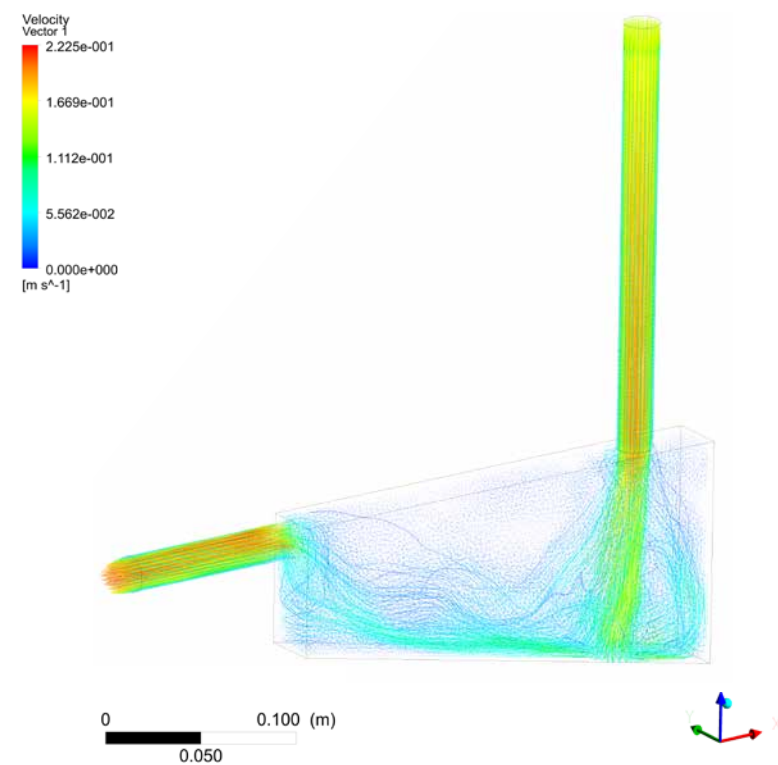


Figure 7.26c. Velocity flow lines of boundary (Author)

network would be of a higher difference. Also the method used here has been changed to Green Gauss cell based as the adjoint solver does not comply with the least square cell based solver mesh. Because the geometry is small for the mention speed, there might be cases with reverse flow, but as the iterations increase it may be eliminated and the solver may converge.

The next step was that of optimising the shape in the adjoint solver and modify the geometry with the parameters mentioned below. The desired change in result were set to a decrease in the steps of -10 % at first and multiple iterations of the same were made while increasing the goal of the difference for desired change in pressure drop. The adjoint solver was designed for calculating the pressure drop and velocity in combination, that can monitor pressure drop while unifying the velocity of the outlet between the inlet and the outlet. To do the same, a boundary of the desired zone of the geometry to be modified was set in the solver (figure 7.27). As the inlet and outlet were not needed to be modified and had to be in line connected to the geometry network of the panel, only the node of volume was selected with manually adjusted extra spaces to allow for needed deformation but within the limits of the concrete cover constraints. Various different progressive iterations of the same are shown below. It was to be considered that the mentioned goal at times did not achieve the desired change and modified the geometry abruptly which drastically increased the pressure drop. In such situations the geometry was reverted back and tried with a lower expected change in the pressure drop. This was done by a combination of target change in value for -ve percentage or decrease value.

The desired shape with a highly reduced pressure drop was generated after 4 repeated steps of shape optimisation. In spite of the results achieved, the method of shape optimisation as shown above was a highly time consuming process and unreliable results were generated after an iteration which are not shown in the design flow. In fact a total of 11-12 optimisation runs were made and 4 of them were successfully modified by changing the change in target.

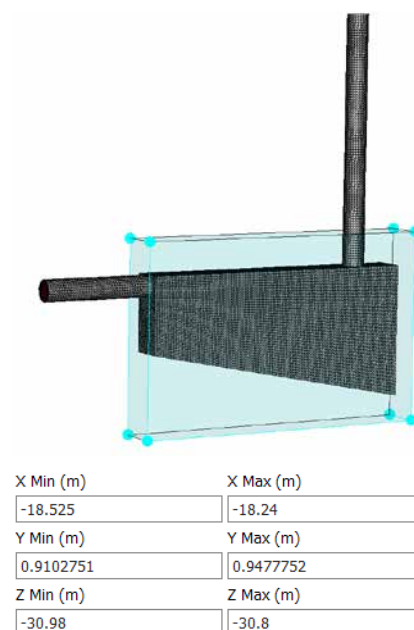
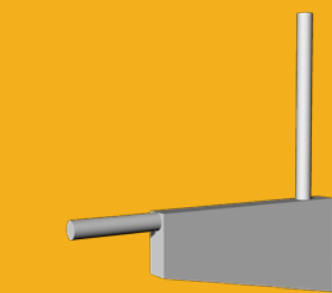


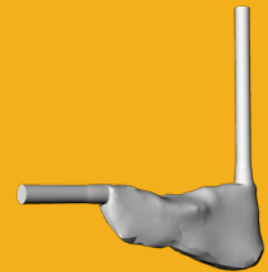
Figure 7.27. Setup of boundary zone for modification (Author)

### Adjoint solver setup parameters

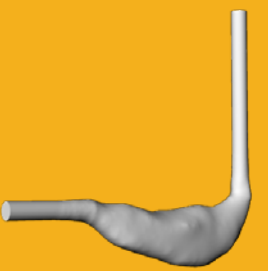
Observables: Pressure drop + Volume integral (x, y, z axis)  
Observable goal: Minimise  
No of iterations: 1000  
Zones of integration: as shown in figure 7.27  
Zones to be modified: Boundary  
Convergence iteration: N.A  
Convergence exponential: e-05  
Simulation time: 55 minutes



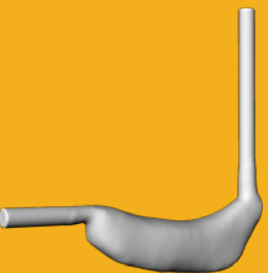
Base shape



Optimised shape 01



Optimised shape 02



Optimised shape Final



Simplified shape

Target set	Change in pressure drop	Change in volume	Time taken
NA	31.09 Pa	0.85 litres	NA
-15 % pressure change and volume variance	20.78 Pa	0.80 litres	65 minutes
-30 % pressure change and volume variance	19.2 Pa	0.40 litres	190 minutes
-15 % pressure change and volume variance	12.5 Pa	0.45 litres	190-200 minutes
Smoothen	13.31 Pa	0.47 litres	NA

Table 7.4. Comparison of stages in shape optimisation of node 01. Source: author, Ansys fluent.

**Node type 01 (Optimised + Simplified)**

Diameter: 15 mm inlet; 15 mm outlet  
 Volume: 0.00085 m<sup>3</sup> or 0.85 litre

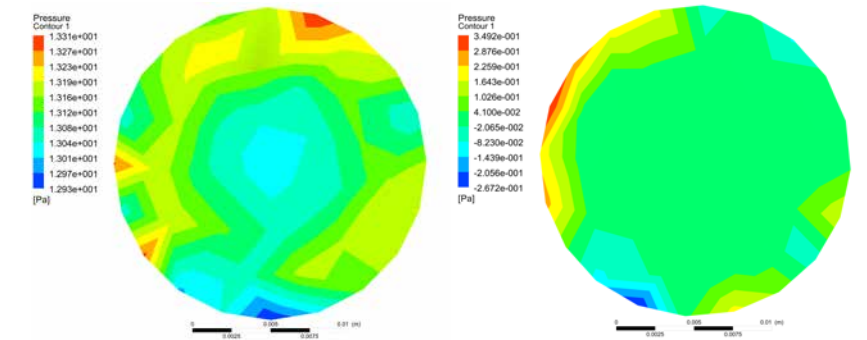


Figure 7.28a. Pressure contour inlet (Author)

Figure 7.28b. Pressure contour outlet (Author)

Meshing no. of elements: 39576  
 Meshing types: Automatic  
 Quality: Medium  
 Min size: 5.0 e-002 mm  
 Max size: 5.0 mm

Viscous model: Standard k-e,  
 Standard wall Fn.  
 Method: Spatial Discretization- Green  
 Gauss Cell Based

No. of iterations: 200  
 ΔP: 15.5 Pa  
 Convergence cycle: NA

No. of iterations: 2000  
 ΔP: 13.30 Pa  
 Convergence iteration: 1018  
 Convergence exponential: e-05  
 Simulation time: 73 minutes

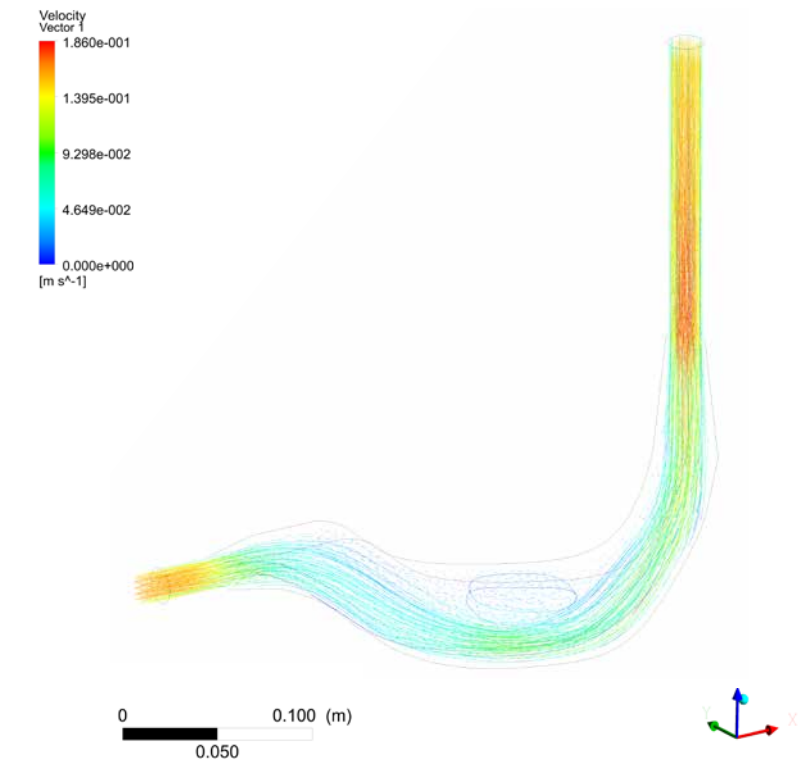


Figure 7.28c. Velocity flow lines of boundary (Author)

**7.6.2 2D- Shape optimization**

To understand the logic behind the same, the velocity flow of the fluid within these geometries were analysed. A comparative understanding was derived from the fluid flow behaviour in the primary shape compared to that of the final simplified shape. As shown below in figure 7.31 for the base shape and figure 7.32 for the final simplified shape, there were micro turbulent flows generated within the volume of the shape as there was enough room than required for the fluid flow transition from one network to another while changing the orientation. It was evident that the shape was optimised depending on the velocity flow pattern of the liquid within the inlet and outlet of the shape, and that the adjoint solver was trying to achieve the same by skewing the geometry iteration by iteration.

If this was supposed to be the case, it would have been more efficient to analyse the flow pattern of the fluid in the network and simplify the geometry manually and eliminate the turbulent sectors. The velocity flow of the liquid was needed to be visualised in the sectional view as it is not possible to map it on the surface mesh while slicing the whole complex network was not a feasible solution because of the complex geometry. Also the low resolution meshing done for the 3D network geometry 05 was not enough to accurately analyse the flow at the junction. Considering these factors a 2D fluent flow analysis of a network geometry equivalent to the network geometry 05 was made and analysed for water as a fluid in it as shown in figure 7.29.

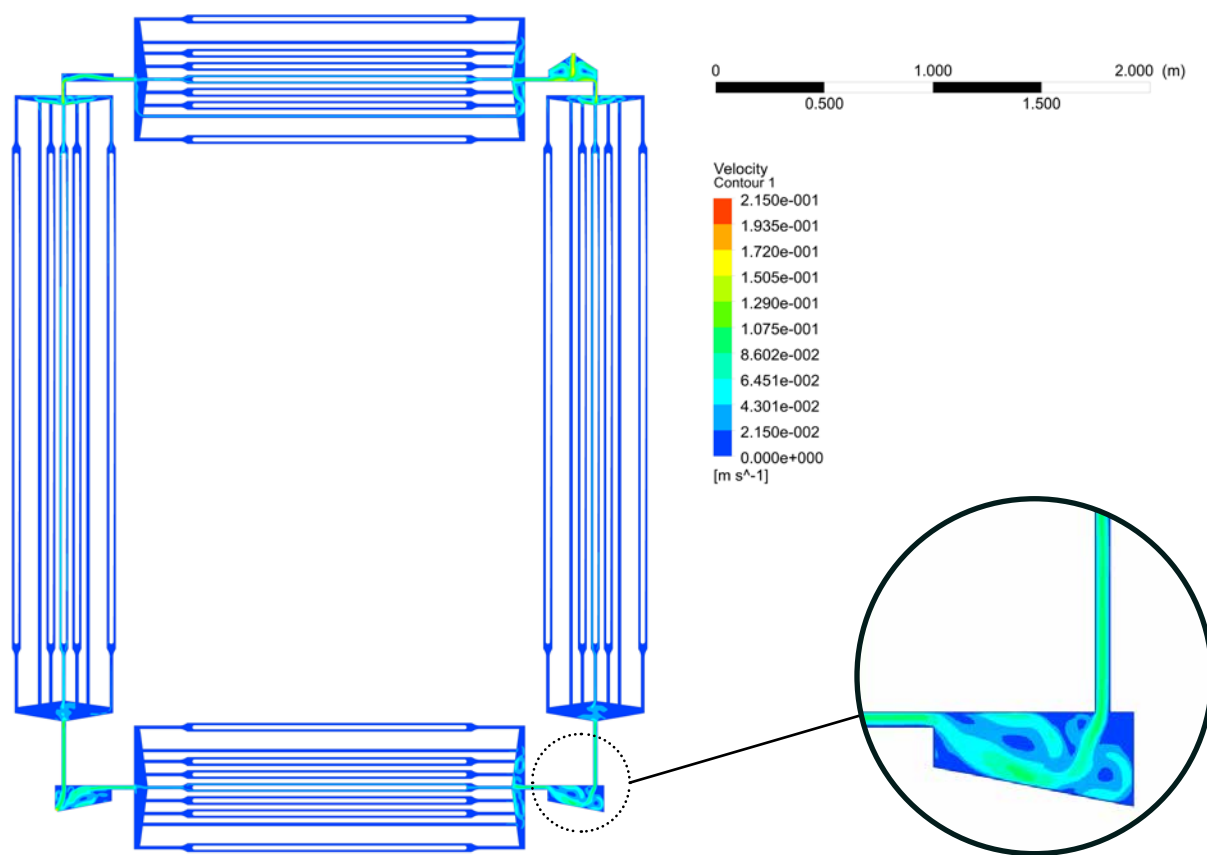


Figure 7.29a. 2D simulation of water flow in network geometry 05. (Author; Ansys fluent)

Figure 7.29b. Node 01 zoomed in (Author; Ansys fluent)

From the above simulation, it is evident that the flow of the liquid at node 01 was as speculated from the 3D flow of the fluid in the node. The flow in the 2D flow mapping would be more accurate than the part simulation done for the shape of only Node 01 separately as the velocity of the inlet would differ and the meshing in the 2D mapping was much sharper than those in the network geometry 05. In similar manner, the behaviour of the fluid flow is also analysed for the other three nodes.

For the fluid flow in the 2D network geometry as shown above, water is considered as the medium of fluid within it. But in the lieu of consideration for the fabrication of the complex geometry, the method considered is inverse investment casting using 3D printed wax network geometry which is needed to be melted out. For the same, the flow of the melted wax within the network is also supposed to be considered along with the water, but separately. Figure 7.3 shows the diagram of the 2D flow of the melted wax at 120°C boiled with water. This simulation could have been advanced to be considered as a dual medium flow of water with wax and was left out of the scope of this thesis.

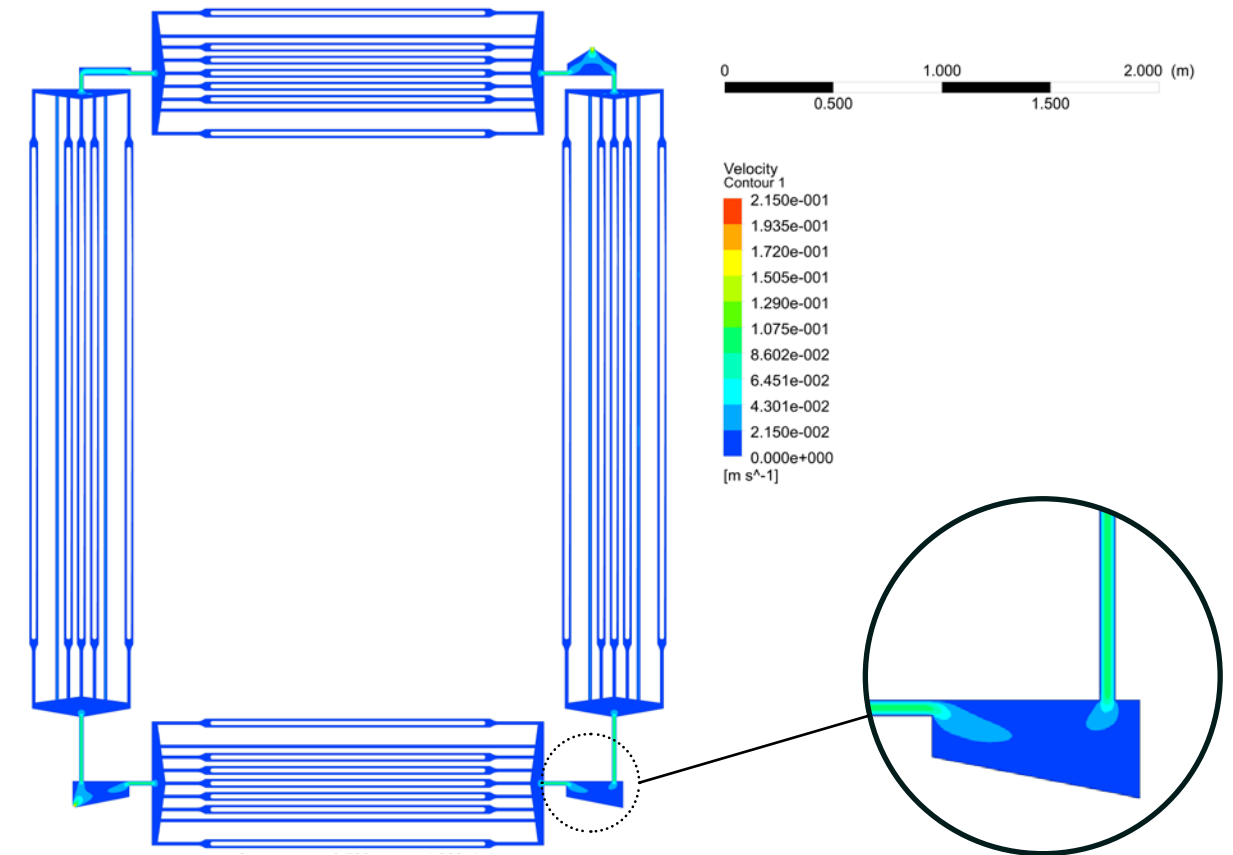


Figure 7.30a. 2D simulation of molten wax flow in network geometry 05. (Author; Ansys fluent)

Figure 7.30b. Node 01 zoomed in (Author; Ansys fluent)

It is notable that the pattern of fluid flow of the two different mediums are varying slightly because of their viscosity. These two different 2D simulated fluid flow simulated mapping for water and wax were considered in combination and simulated with modifications done manually according to the flow path of the fluids in the nodes and trimmed the volumes where the flow was diverted to form turbulences or stagnant to allow for a smooth flow path for the fluid to flow through the shape.

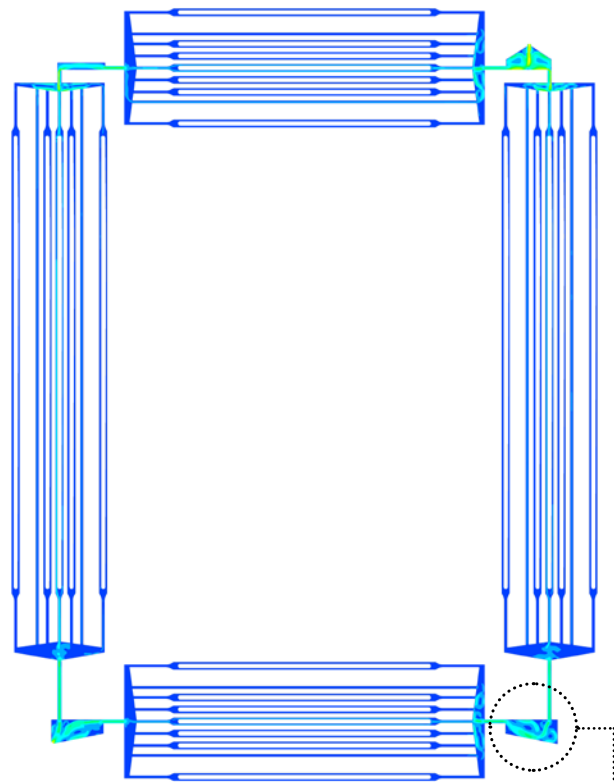


Figure 7.31a. 2D simulation merged for water and wax flow in network geometry 05. (Author; Ansys fluent)

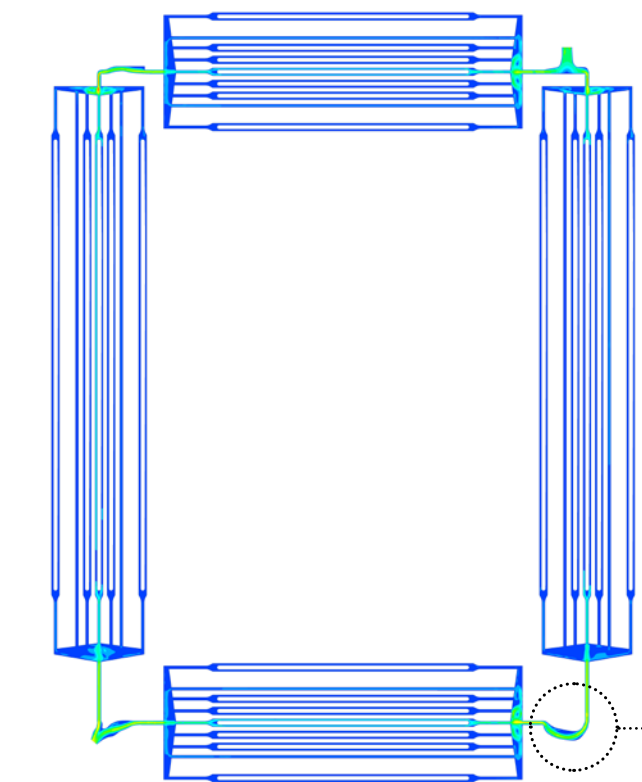


Figure 7.32a. 2D simulation of water flow with trimmed nodes to eliminate turbulent zones (Author; Ansys fluent)

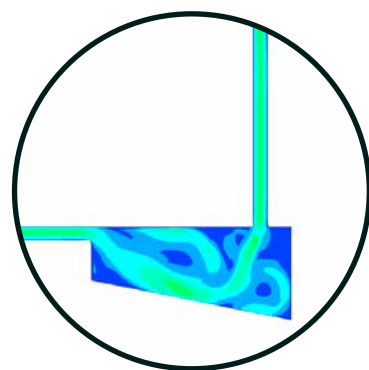


Figure 7.31b. Node 01 zoomed in primary (Author; Ansys fluent)

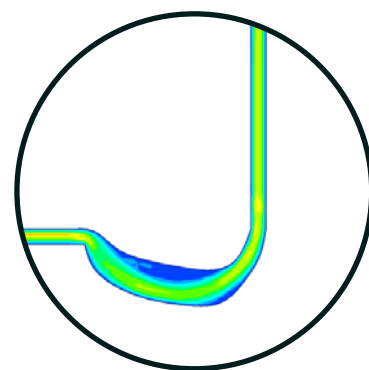


Figure 7.32b. Node 01 zoomed in optimised (Author; Ansys fluent)

Pressure drop: **1319.69 Pa**

Pressure drop: **62.51 Pa**

**- 94.9 %**

**change in pressure drop**

Note: Pressure drop calculated to equivalent 3D network geometry (05 & 06) simulations.

As seen in the 2D geometry transformation, the pressure drop as per the 2D geometry has been dropped by a huge margin of **94.9 %** and proves the viability of the solution in optimising the geometry for much reduced pressure drop in its 3D counterpart.

## 7.7 HEAT TRANSFER - GEOMETRY

The primary purpose of the designed facade system's function is to cater the transfer of heat from the outer panel to the inner panel and vice-versa depending on the climatic condition with the help of the water in the tubes within the facade panel as the heat exchange medium. To transfer the heat, the thermal energy is needed to be captured within the mass of concrete of the facade panel and transfer it to the water within the tubes of the network embedded within the mass of concrete.

The procedure of transferring of thermal energy from the outer layer of air (environment) to the second mass of water through the medium of concrete is occurred by the method conduction. The expression for the generic occurrence of conduction is stated below:

$$\frac{Q}{t} = \frac{k A (T_2 - T_1)}{d}$$

where,

Q/t = rate of heat transfer

k = thermal conductivity of the material

T<sub>2</sub> - T<sub>1</sub> = temperature difference between the two materials

d = thickness of the material

Through the expression, it is evident that the transfer of heat over time is directly proportional to the surface area of the object in contact and inversely to that of the thickness of the material. If the surface area of the front panel facing the outer environment is increased, the heat transfer through the panel to the water will also increase in the similar amount of fractions. To modify the facade panel for the same this the outer surface of the facade panel needs to be modified at a micro level to allow for undulated geometries to increase the surface area while the elevational footprint remains unchanged. This is the exact same principle used by heat sink channels to capture heat by maximising the possible surface area and transferring them through a medium to another zone. While the exact method used by heat sink elements could not be adopted for a large scale concrete facade, the proposed modification does call for two specific changes along with increasing the surface area. Firstly, due to the geometry undulations, there would be self shading of the geometry which would reduce the sun radiation on the surface. This criteria is suitable to welcome micro shading zones during the summer to avoid excess heating of the panel, that would or else minimise the efficiency of it, but during the winter it may affect the performance as compared to that of a flat panel.



Figure 7.33. Increasing surface area by adding fins in a regular electronic heat sink. (Accel thermal)

## 7.7.1 Topology optimisation

To accomplish the above mentioned criteria, there are two possible methods. Firstly, the obvious idea is to add a specific designed geometry onto the surface that is designed in response to that of the sun radiation to maximise during the winter in order to maximise heat trap and to minimise in summers to eliminate the excess heat. By doing so, it is also obvious that the weight of the panel will also increase in response to the added material. The other possibility is an approach exactly inverse to the aforementioned, by subtracting the material from the surface of the panel in a manner that complies to both the situations mentioned. By doing so, there may be a huge compromise with the structural stability of the material that may promote non-calculated stresses and behaviour across the panel. To make a stance as a middle ground with a beneficiary stance of increasing the surface area to increase the heat conduction and minimising the summer radiation by undulating the surface to promote self shading while complying with the structural behaviour of the panel, the method of topology optimisation of the concrete facade panels was adopted.

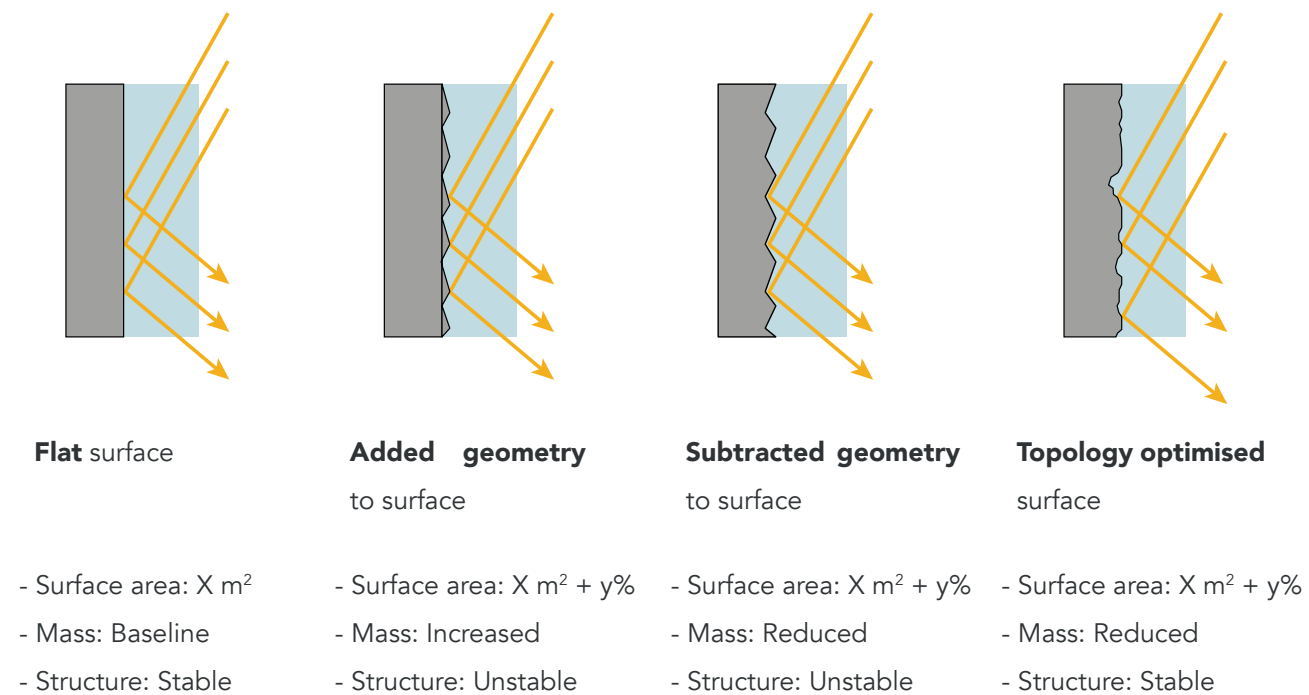


Figure 7.44. Different possible methods to maximise surface area. (Author)

### 1. Goals

The method of topology optimising in this context was set to a goal of minimising the volume of material needed while maximising the stiffness of the panel. The amount of weight reduction was set in response to the behaviour of/ algorithm used by the software, the thickness or the location of the panel: internal or external and the type of concrete mixture used. It was also considered for the surface geometry to be not smoothed and left in a raw triangulated facets/ quad faces that results in a rough surface with self shading capability as discussed above.

### 2. Considerations and limitations

The designed concrete facade panels if allowed for unbounded order of topology optimisation for volume reduction, the algorithms may tend to scoop out material along the thickness of the panels and gap through the sections where there are no need of volume in regards to the supports and the loading condition as shown in figure 7.45. In case of such occurrences, the network geometry of the tubes that are cast in within the concrete panel would be exposed or tend to lose the minimum cover required by concrete as a material.

The same was experimented with different methods of topology optimisation methods using different software. At first plug-in for Rhinoceros 3d were used. The first one amongst them was Ameba, which is based on BESO method. The results analysed by this method was a very basic form of topology optimisation which did scoop out all possible zones to minimise the mass of the geometry as there are no control over the allowable percentage and region of optimisation, as shown in the figure 7.45. While this method is not robust enough for the purpose needed by this thesis, it was scrapped.

The next method tried was by millipede 2D and 3D, which is a reliable method in the field of topology optimisation that uses a proprietary algorithm. At first the 2D model was tested in place for the behaviour and expression it provides in relation to the panel with the network geometry of the tubes as shown in figure 7.46.



Without boundary constraint  
With window load  
Target: 50% volume reduction  
172 iterations, 25 minutes

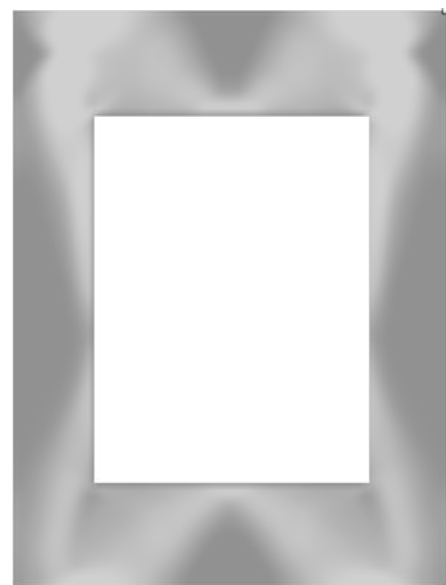
With boundary constraint  
No window load  
Target: 50% volume reduction  
58 iterations, 20 minutes

With boundary constraint  
With window load  
Target: 50% volume reduction  
58 iterations, 28 minutes

Figure 7.45. Different iterations of topology optimisation with Ameba in grasshopper. (Author; Ameba)

This even though holds true for the back panel alone, the complex 3D geometry of tubes along with the multiple support systems could not be simulated for optimisation in 2D. The downside was that the size and the complexity of the system with small elements for the reinforcement dowels does result in a very complex meshing and was unable to be loaded onto the script to be handle by grasshopper and the possibility of using this software had to be overseen.

The next possible mode to make a check on the capability of the software that can handle complex geometries for the topology optimisation, were the ones commercially used multi-physics software. The first choice for the same was static solver along with the topology optimisation in the Ansys Workbench as already considered for the previous CFD optimisation, but because the software was a student version only, the limitation for static structural analysis in Ansys is very much limited to only 31,000 nodes / elements unlike the 512,000 for fluent solver. Such similar meshing limitations also did hold true for the Simulia Abaqus. In lieu of the complex geometry system and small parts to be match meshed for the designed panel combination, the choice of using a multi-physics was switched to Autodesk Fusion 360, which has absolutely no limitations in their student license, except generative algorithm based optimisations and holds the capability of solving topology optimisation in a commercial grade robust manner. The Fusion 360 uses the Nastran solver engine and uses the widely preferred SIMP and Level-set method.



Cell size: 75  
Iterations: 4  
Penalization: 2  
Min. Density: 0.2  
Target density: 0.5



Cell size: 200  
Iterations: 200  
Penalization: 3  
Min. Density: 0.2  
Target density: 0.5

Figure 7.46. Different iterations of topology optimisation with Millipede 2D in grasshopper. (Author; Millpede)

### 3. Constraints

To perform a well designed simulation that falls within the domain of result expected while complying with the integrity of the geometry and the fixtures, constraints were needed to be applied in the model. Without the application of constraints, the optimisation solver would find the best possible method of eliminating material through the panel thickness creating voids which are totally not desired in the final design of the facade panel. An example of such has been shown in figure 7.47. While the overall dimensions of the system is set along with the structural detailing of the reinforcements to be placed and fixtures to be mounted on the panels, the basic boundary outlines has been shown in the figure 7.48 & 7.49. The secondary boundary condition is that from the tubular network geometry which is embedded within the concrete facade panel along with the minimum cover needed for concrete as a material to perform. These mentioned boundary conditions were limited in the simulation for the geometry to be optimised with a minimal scope of material reduction possible at critical places only.

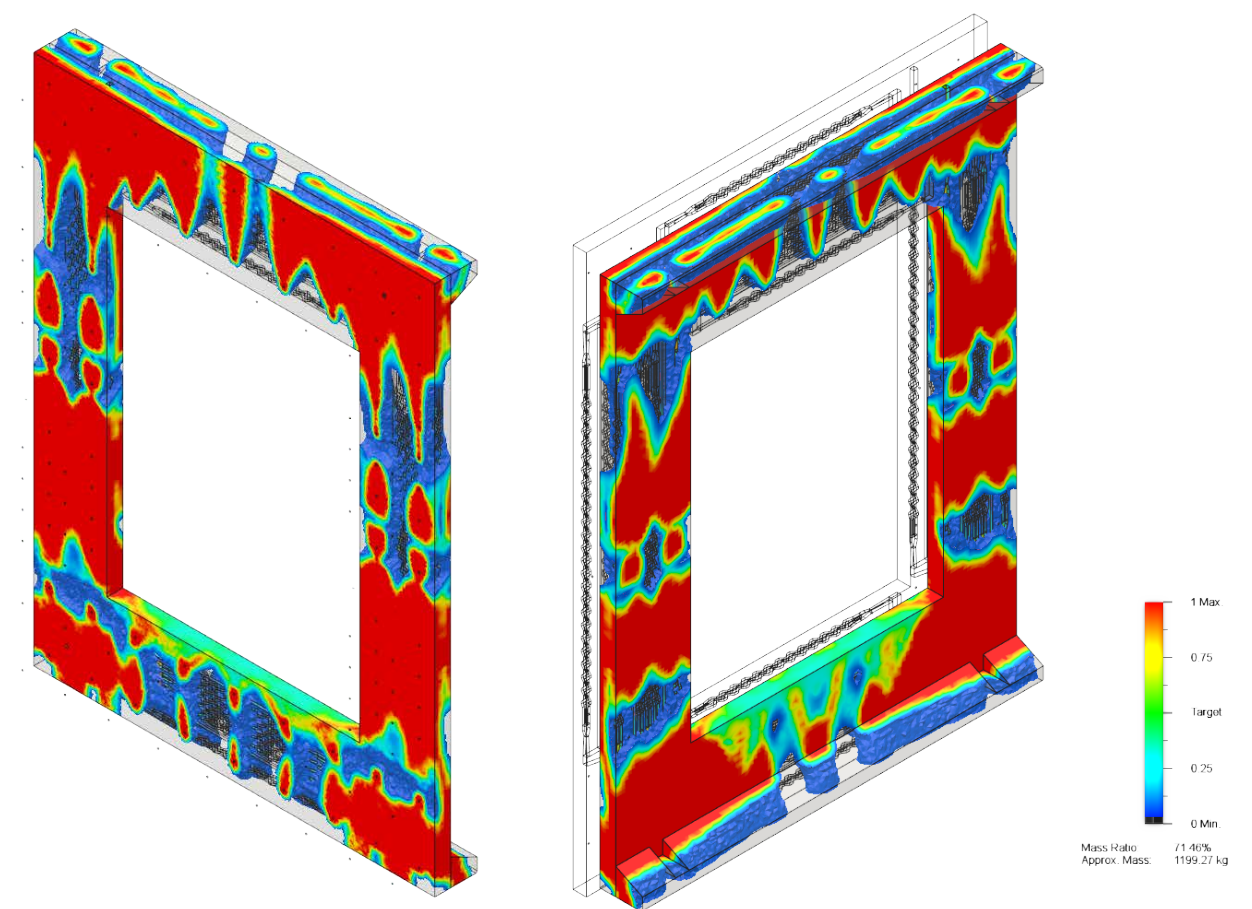


Figure 7.47. Topology optimisation of external (left) and internal (right) facade panels without applying constraints to maintain minimum concrete cover. (Author; Fusion 360)

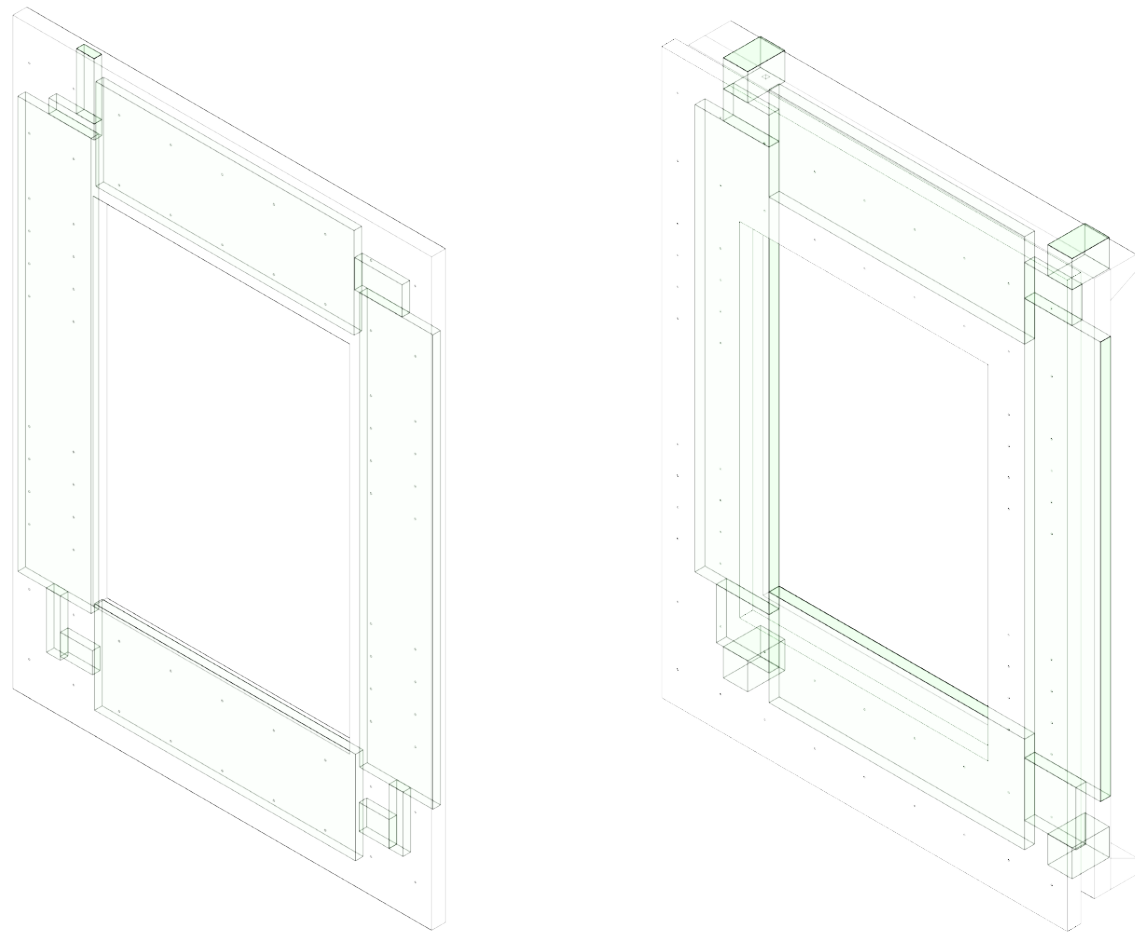


Figure 7.48a. View of constrained boundaries for topology optimisation of the external facade panel. (Author; Fusion 360)

Figure 7.49a. View of constrained boundaries for topology optimisation of the internal facade panel. (Author; Fusion 360)



Figure 7.48a. Plan of constrained boundaries for topology optimisation of the external facade panel. (Author; Fusion 360)



Figure 7.49b. Plan of constrained boundaries for topology optimisation of the internal facade panel. (Author; Fusion 360)

#### 4. Boundary conditions

The boundary conditions were set to be limited and simple within the setup for the topology optimisation in Fusion 360. The meshing done for the geometry was minimised to 10 mm in order to the minimal material performing of concrete, so as the pixel size for the SIMP solver is minimised. The loading conditions were as following:

Wind load @ 39 m/sec for 10 m above ground level for 7.86 m<sup>2</sup> of surface area of opaque section: 7173 N

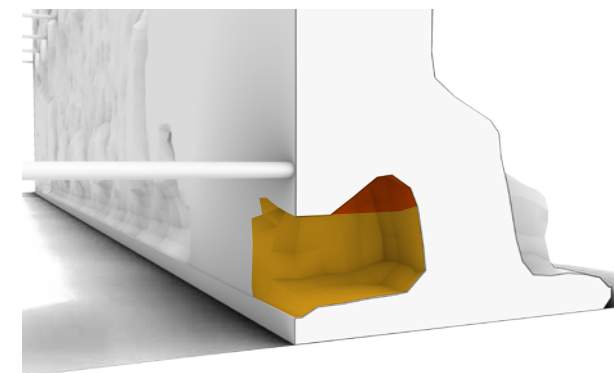
Window load: 2000 N

Live load of 2 people: 735 N X 2

The fixations of the panels are dependent on the location of the fixed points on them depending whether it is the exterior panel or interior. While the fixed geometries for the interior panel are specified in the design as shown in figure 4.6 in section 4.1.2, the reinforcement dowels connecting the interior panel to that of the exterior panel act as multiple fixed point for the exterior panel alone. To do the same, connections between different parts of the combined panel were made with a marginally small 1mm overlap which is automatically computed and modified in Fusion 360.

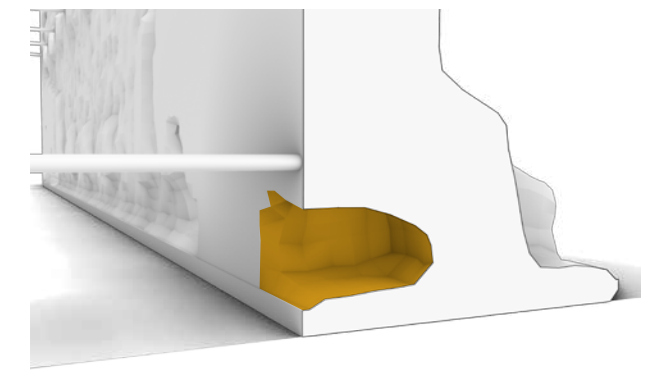
#### 5. Fabrication constraints

With the implied constraints, the method of topology optimisation was limited to specific zones that it can monitor for reaching the goal of volume reduction. But also above that, there was another constraint that is governed by the method of fabrication of the panel. Excluding the inner form-work of 3D printing wax for the inverse investment casting process, the surface geometry developed by the topology optimisation of the facade panel needs to be fabricated, and the most suitable method to do the same would be to develop a form-work upon which the concrete would be cast and formed into the desired shape. To make the geometry comply with the casting within a mould with its negative geometry of the surface topology, the method of



■ Inaccessible zone for removable cast form work

Figure 7.50a. Zoomed segment with undercut. (Author; Meshmixer)



■ Accessible zone for removable cast form work

Figure 7.50b. Zoomed segment without undercut. (Author; Meshmixer)

topology optimisation has to eliminate any form of undercut so as to ensure possible un-moulding of the form-work. This also ensures multiple use of the form-work for batch production rather than being limited to only a specific panel casting. While topology optimisation with fabrication constraints are possible in Ansys and Abaqus, there is no such measure available in Fusion 360 yet, but the To ensure that the final optimised geometry does comply with the method of fabrication without any undercuts, the optimised geometry was shrinkwrapped using the shrinkwrap meshing tool in Ansys Space Claim modelling counterpart and modified using Autodesk Meshmixer. This ensures that the possible undercuts in the geometry are eliminated by wrapping a mesh over the geometry. It is also to be considered that the sizing of the mesh for shrinkwrap in Ansys also does depend on the comparative mesh size of the possible undercuts to that of the mesh size used for shrinkwrap to eliminate underlining meshes of the tube network. The other minor segments which did contain undercuts were eliminated and cleaned manually using Autodesk Meshmixer.

Using these above mentioned conditions and constraints, the two different facade panels were optimised in different iterations as target geometries. A desired percentage in decrease of the volume was set and by using the slider the percentage was checked through the most satisfied geometries that do not compromise the geometry of the panel and concrete cover around the reinforcement dowels. The different iterations of the two different panels along with the selected iterations are depicted below.

Original mass : **2935.73 kg**  
 Reduced mass : **2431.43 kg**

**- 17.7 %**  
**decrease in volume**

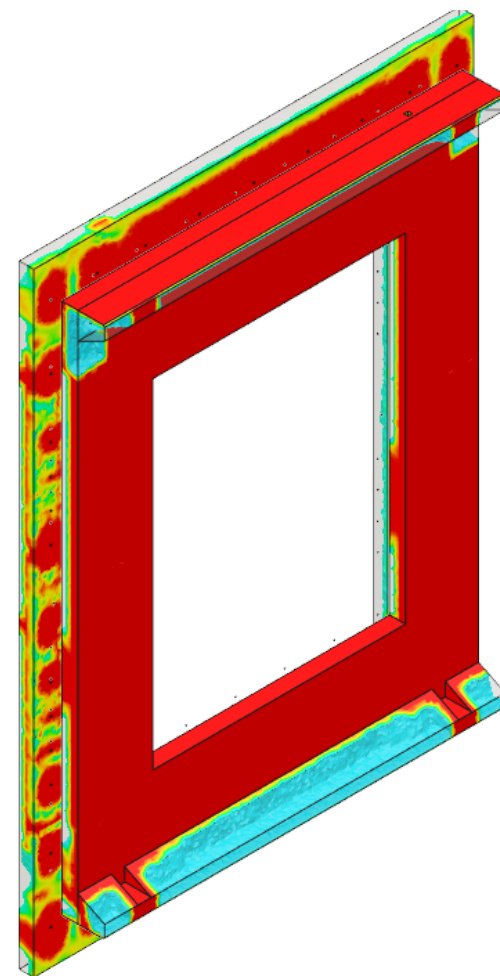
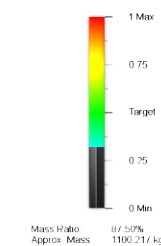
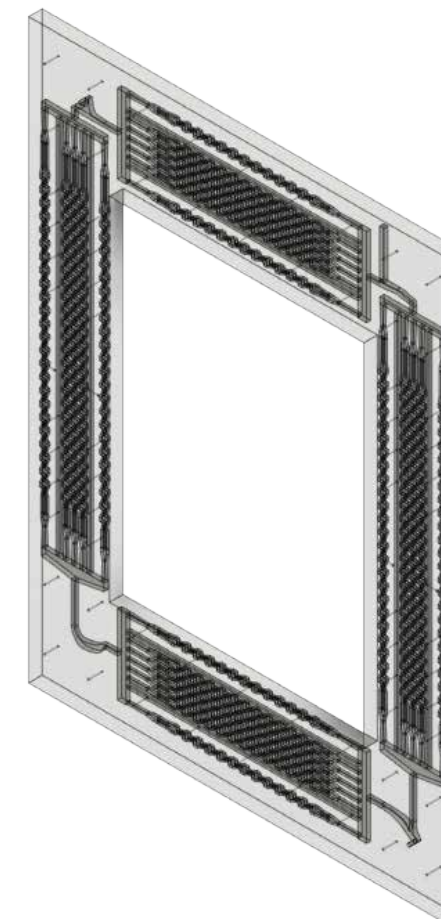
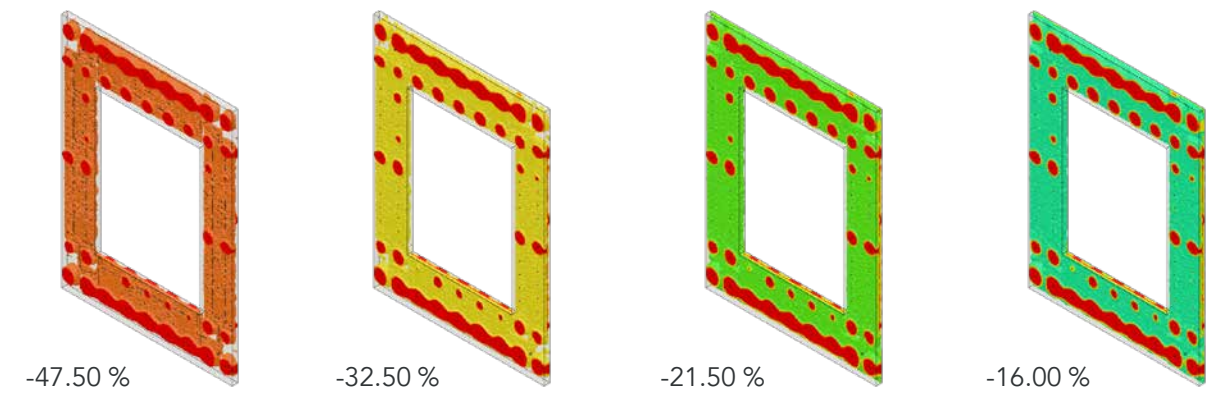


Figure 7.51. Optimised facade twin panel (Author; Fusion 360)



**- 12.5 %**  
**decrease in volume**

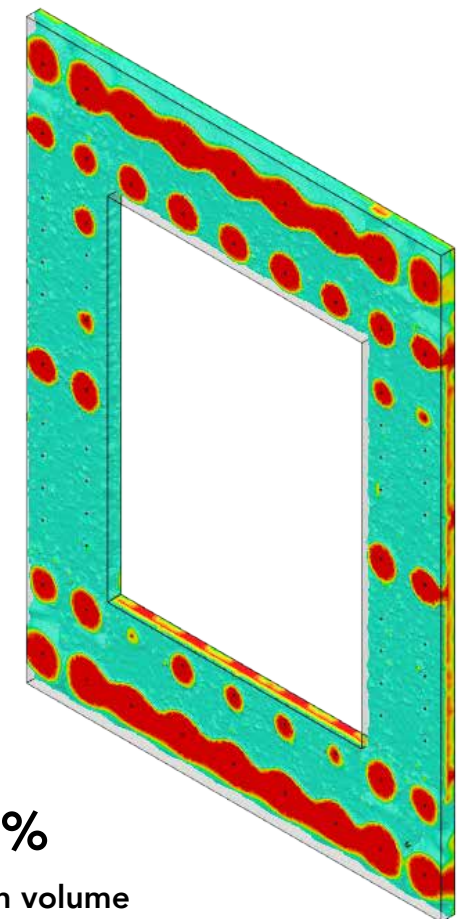
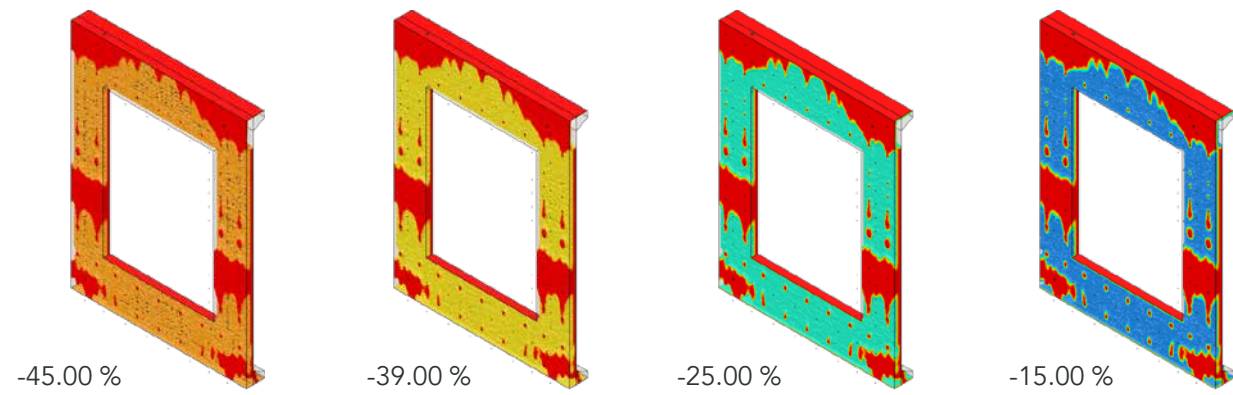


Figure 7.52. External panel used for the process of topology optimisation (Author)

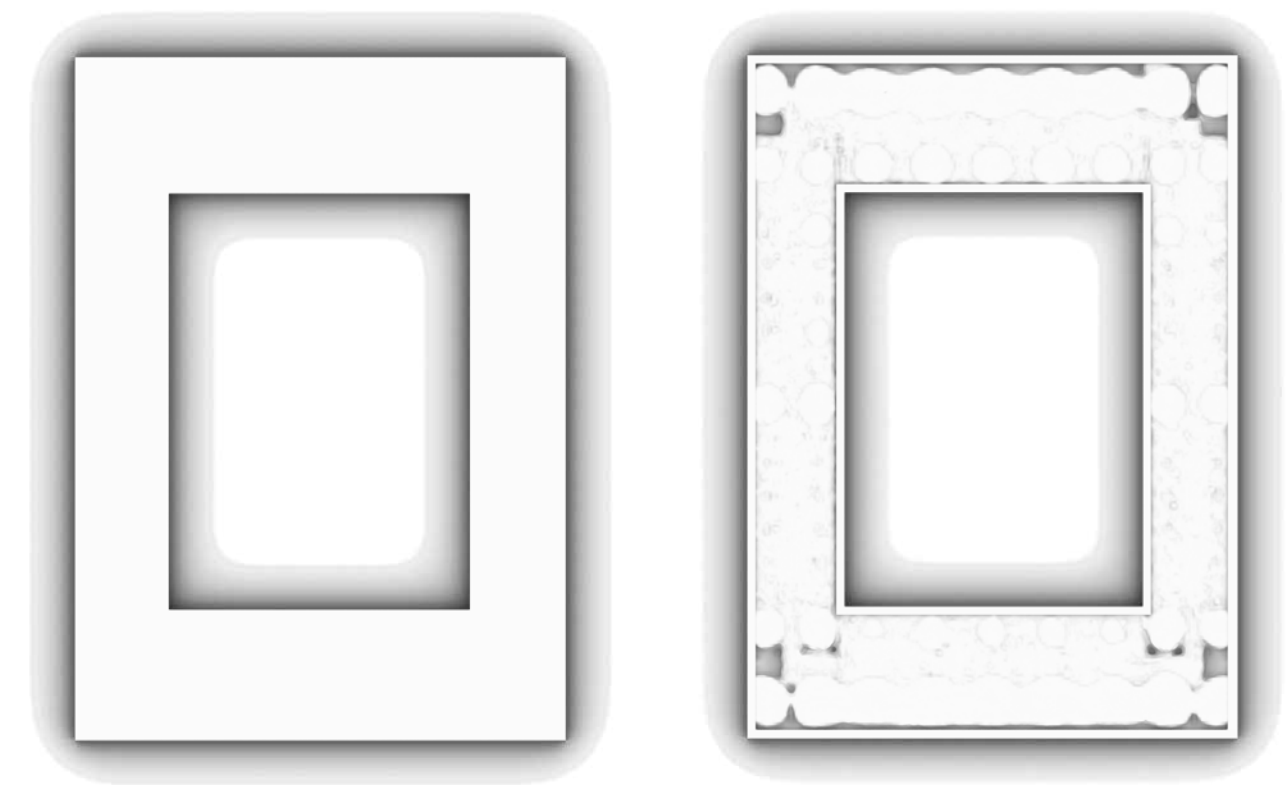
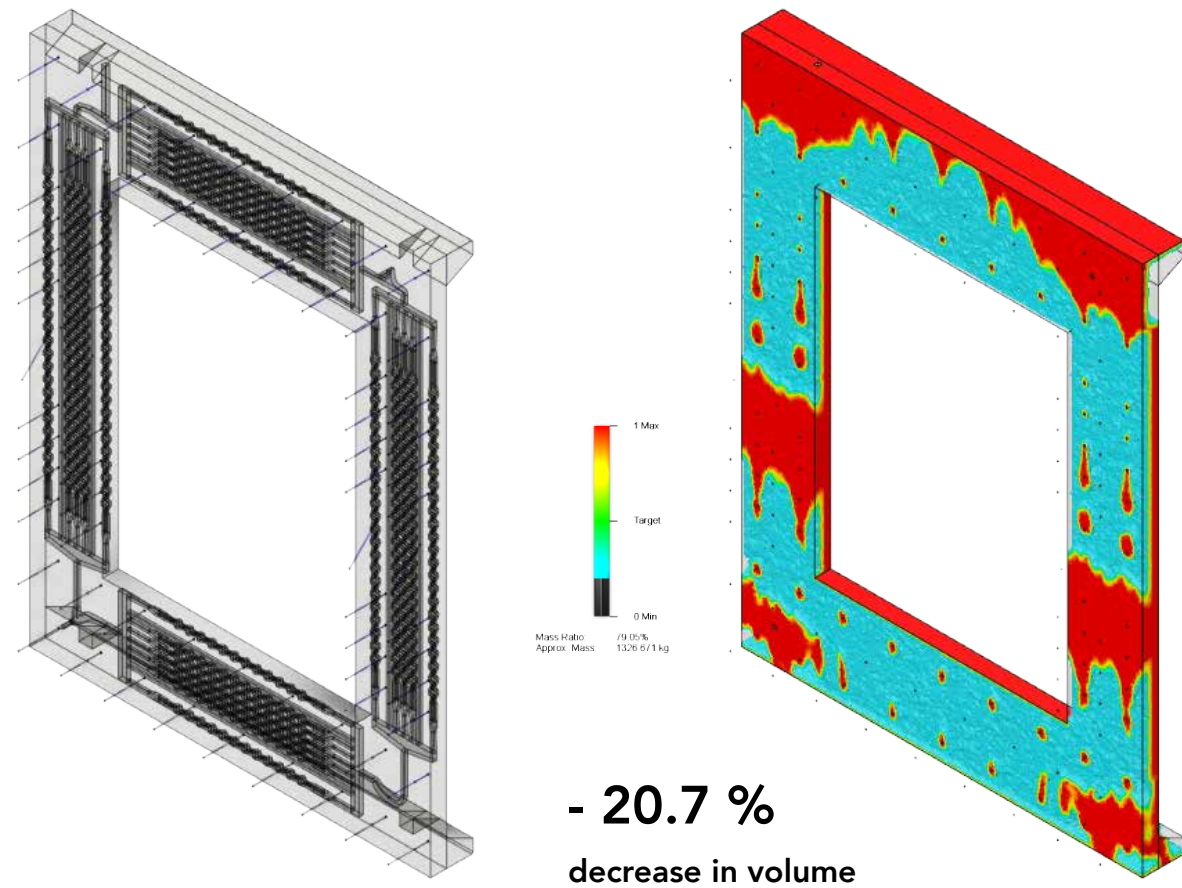
Figure 7.53. Optimised external panel selected with 87.5 % of volume to the input geometry.

With a variable ranging between 100% massing to that of the value set for target change in volume, 80% in this case for the external panel, the possible options were monitored for the compliance with the reinforcement and minimum cover needed for the material integrity and the one with 87.5% of the total volume was chosen to be the optimum choice in the range.

For the internal panel, the value set for change in value for the topology optimisation was at 70% and the range to monitor the optimal design was ranged between 100 to 70% . the one in compliance with the



Now that by processing the topology optimisation of the panels and deriving the final geometries in compliance with the fabrication method, fixtures, material behaviours and reinforcements, the possible performance of the optimised facade panels are needed to be analysed. The change in fraction of the surface area of the outer surface of the external panel would correspond to direct translation in the change in thermal conduction rate of the panel. While there is a considerable amount in the increase in the surface area, there is a trade-off in respect to the undulated surface developed that would have self shading and the change in solar radiation on the surface is simulated in the next section.



Surface area of opaque region: 7.86 m2

Surface area of opaque region: 8.77 m2

**+ 12.5 %  
increase in surface area**

Figure 7.54. Internal panel used for the process of topology optimisation (Author)

Figure 7.55. Optimised internal panel selected with 79.3% of volume to the input geometry. (Author; Fusion 360)

Figure 7.56. Flat panel exterior ELEVATION (Author)

Figure 7.57. Optimised panel exterior ELEVATION (Author)

reinforcement and minimum cover needed for the material integrity and the one with 79.3% of the total volume was chosen to be the optimum choice in the range. The constrained zone for the internal facade panel was continued to enclose the inner facet in lieu of the consideration for the maintenance of the surface in interior and also to be made complaint for casting of the panel with moulds only on one side of the form work a and hence only the outer facet of the internal facade panel was let to be considered for the topology optimisation.

\* The calculated surface area of the facade panels does consider the common trim around the edges of the panel and the window.

### 7.7.3 Solar Radiation

With the increase in the surface area by 5.5% , the conduction rate of the external panel is increased by 5.5% too. The next step was to check the performance and effect of the solar radiation on the outer flat surface of the external panel to that of the outer topologically optimised surface of the external panel oriented towards south in the different months of the year in the climate of Delhi, India. As mentioned earlier, with the need to increase the surface area, the surface was chosen to be modified with the method of topology optimisation and is speculated to increase the performance of the exterior facade panel and the system in combination by increasing or maintaining the solar radiation in comparison to that of the flat panel and decrease the amount of solar radiation by mutual shading of the undulated geometries developed by optimisation during the summer.

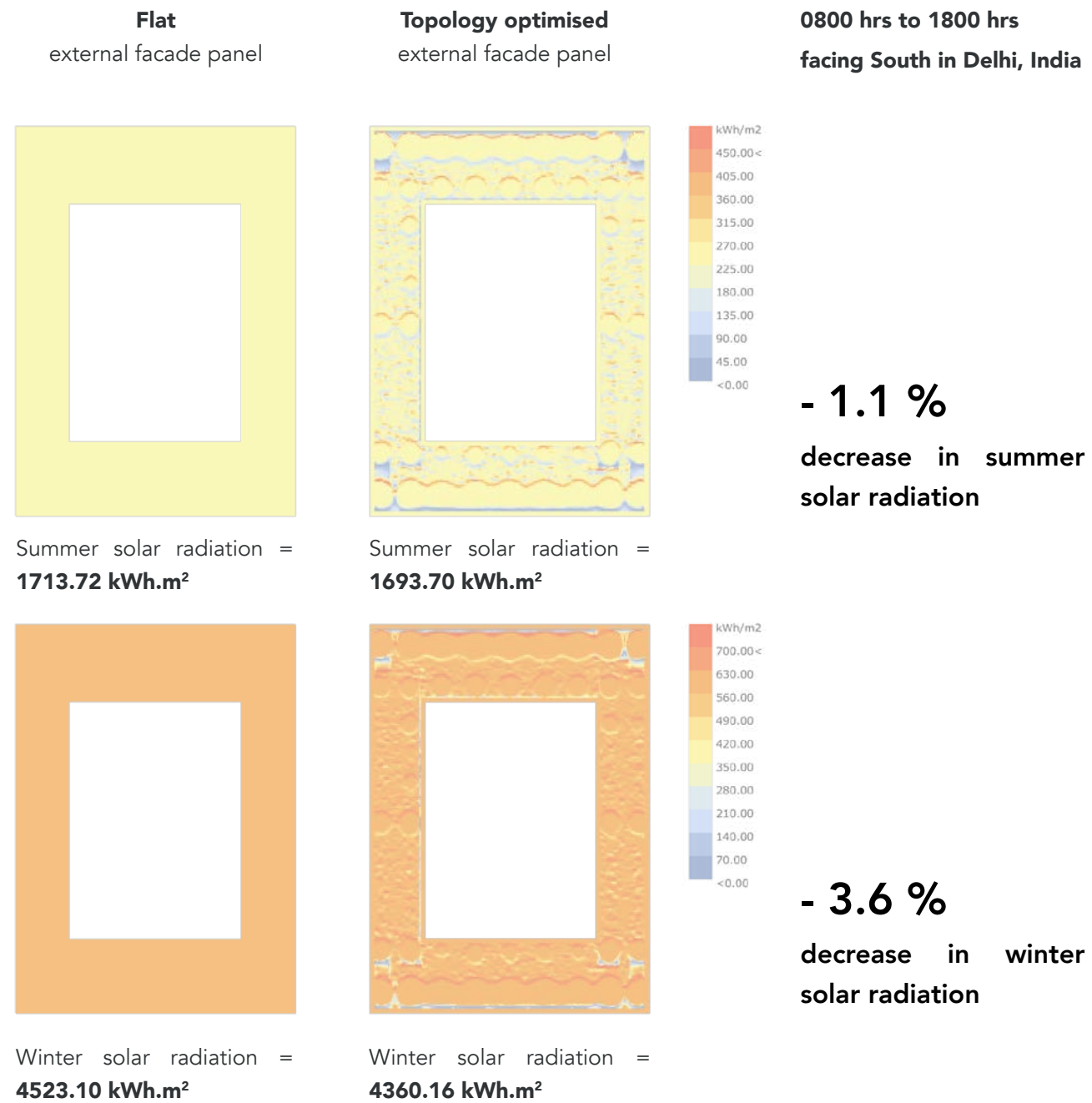


Figure 7.58. Comparison of solar radiation over the flat and modified surface (Author; Ladybug)

The images above show the solar radiation on the flat and the optimised geometry of the facade panel during the summers and during the winters in Delhi, India. To understand better about the behaviour of the panels in the different seasons, the solar radiation analysis was fragmented per month and studied. A comparative analysis of the performance of the geometry of the facade under solar radiation was analysed. To do so the two different configurations of the flat panel to that of the optimised and modified facade panel were simulated and compared. The graph below shows the solar radiations only on the front facade of the panels for simulated per month of the year for a general operating timing of 0800 hrs to 1800 hrs of the day all round the month for a location of the building facing South in Delhi, India.

The facade design is considered to have a 40% WWR as suggested by Diwania, Garg, & Mathur (2011) for an north oriented facade in Delhi . The research done was based on a comparatively low U-value of the fenestration of 3.3 W/m<sup>2</sup>K for a double glazed unit. Since the designed performance of the fenestration as discussed in the next section is much higher than that of the refereed research, the orientation for the facade was considered to be simulated and checked for its efficiency in the south orientation. The real world scenario could have a lesser than 40% WWR for a souther oriented facade with much higher radiation and efficiency than speculated in this thesis.

From the graph shown (figure 7.59), it is evident that while the solar radiation for the optimised panel is marginally lower than that of the flat panel during winter and other cooler months, during summer the performance of the optimised facade gains over the flat panel by minimising the solar radiation significantly so as to prevent the over heating of the panel. It is also to be taken into account that although the solar radiation on the optimised surface is low during the winters, the increased surface area over the flat panel can compensate on that for the effect of conduction of heat from the external environment to the mass of the facade.

It is to be noted that in all of the above simulations for solar radiations, the context of the surrounded building the facade is use don is considered to be not obstructing direct solar radiation throughout the year.

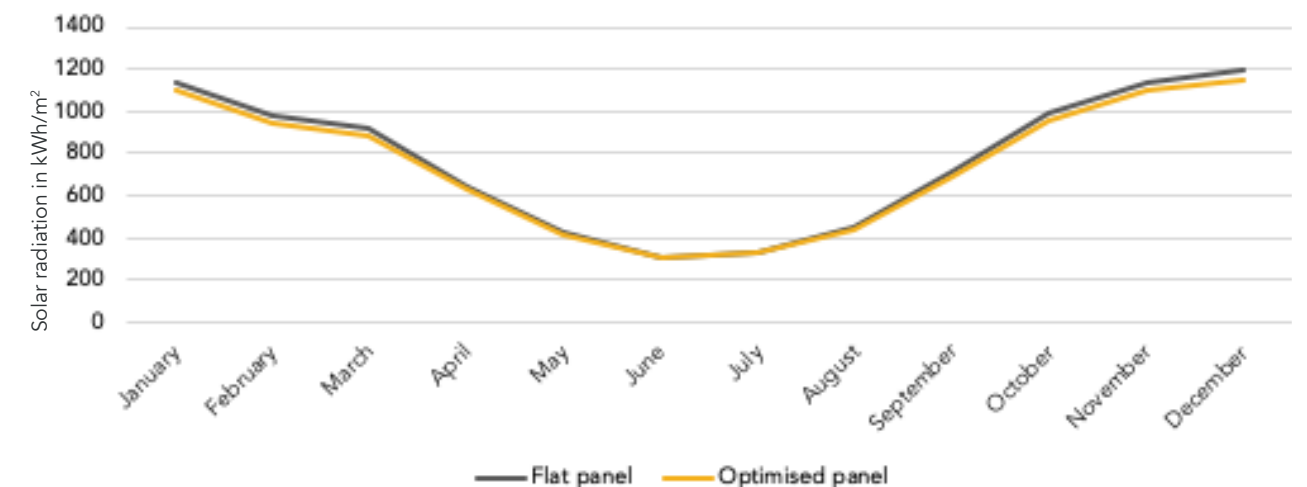


Figure 7.59. Table showing solar radiation per month from 0800 to 1800 hrs per month in New Delhi, India facing south (Author; Ladybug)

## 7.7.2 Surface modification

Although the increase in the surface area was resulted from the topology optimisation of the flat surface of the facade panels, the further modification to increase the surface area of the optimised outer surface of the external panel was carried out. This was done by using Octopus plug-in for grasshopper. The methodology of doing the same is explained in chapter 5 and a summary of the process involved to modify the topology optimised geometry is depicted in figure 7.60.

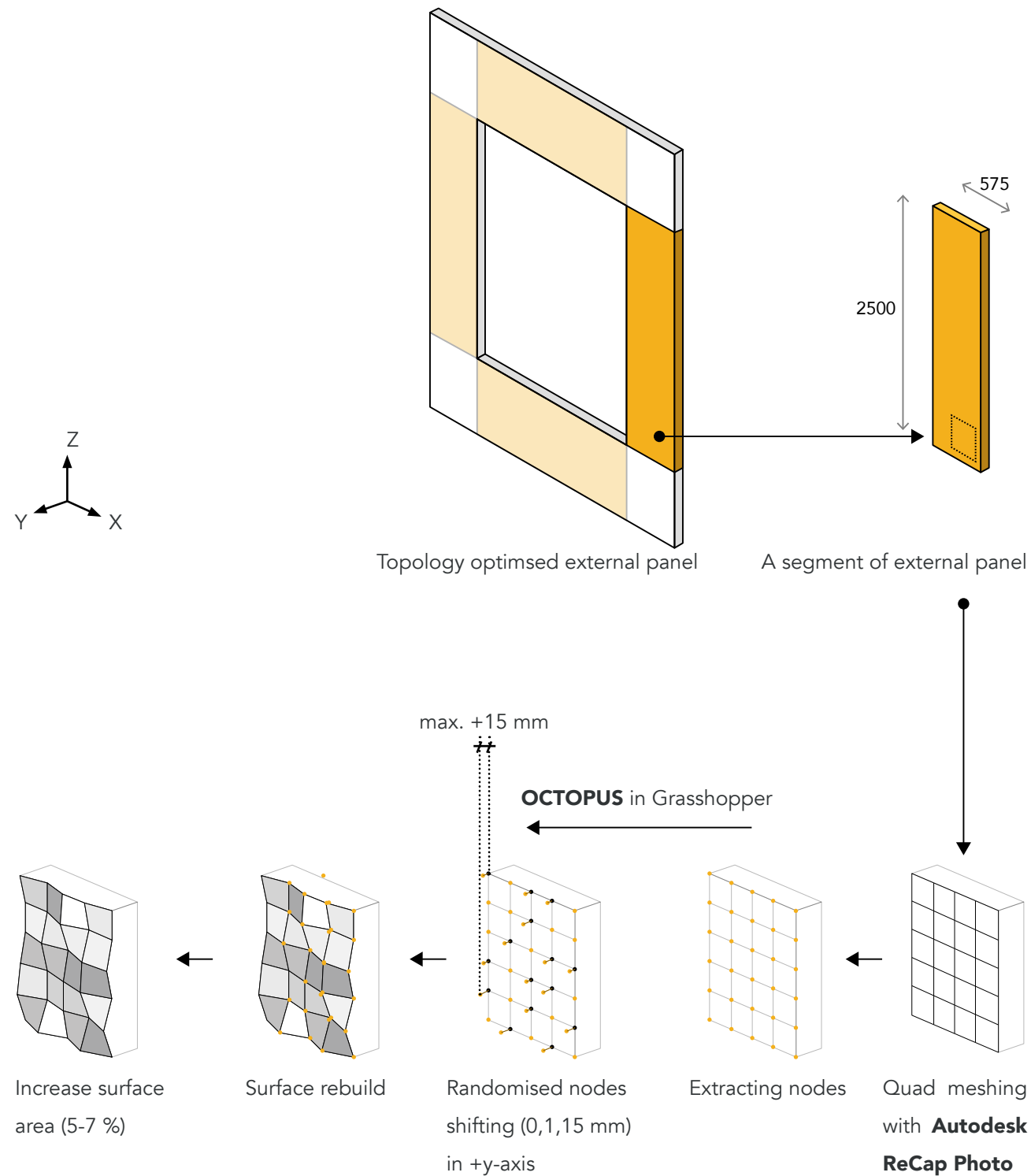


Figure 7.60. Method used to modify geometry for maximum surface area with similar solar radiation. (Author)

The method of doing the same was to convert the optimised geometry to quad mesh using Autodesk ReCap Photo and then re-meshing the surface while extracting the nodes. These nodes are then subjected to a randomised translation of 15 mm maximum with 1mm of incrementation in the +y-axis. The modified geometries are then subjected to radiation analysis of the surface during winter and summer. To accommodate the high resolution of the meshing and endless possibilities of geometries, the optimised surface of the panel was divided into 4 segments as shown in figure 7.6 and one of the segment was subjected to analyse the possible increment in the surface area using this method.

To find out the best possible solution from the evaluation done by Octopus, a 3D graph (figure 7.61) with Surface area (SA) against the winter radiation (WR) and summer radiation (SR) was plotted. It was noted that while the radiation follow a trend of linear graph being proportional to each other, the highest possible surface area amongst the evaluated option was chosen. By doing so it was found that a further increment of 5-7 % in the total surface area could be achieved that should account for higher heat transfer between the environment and the external surface.

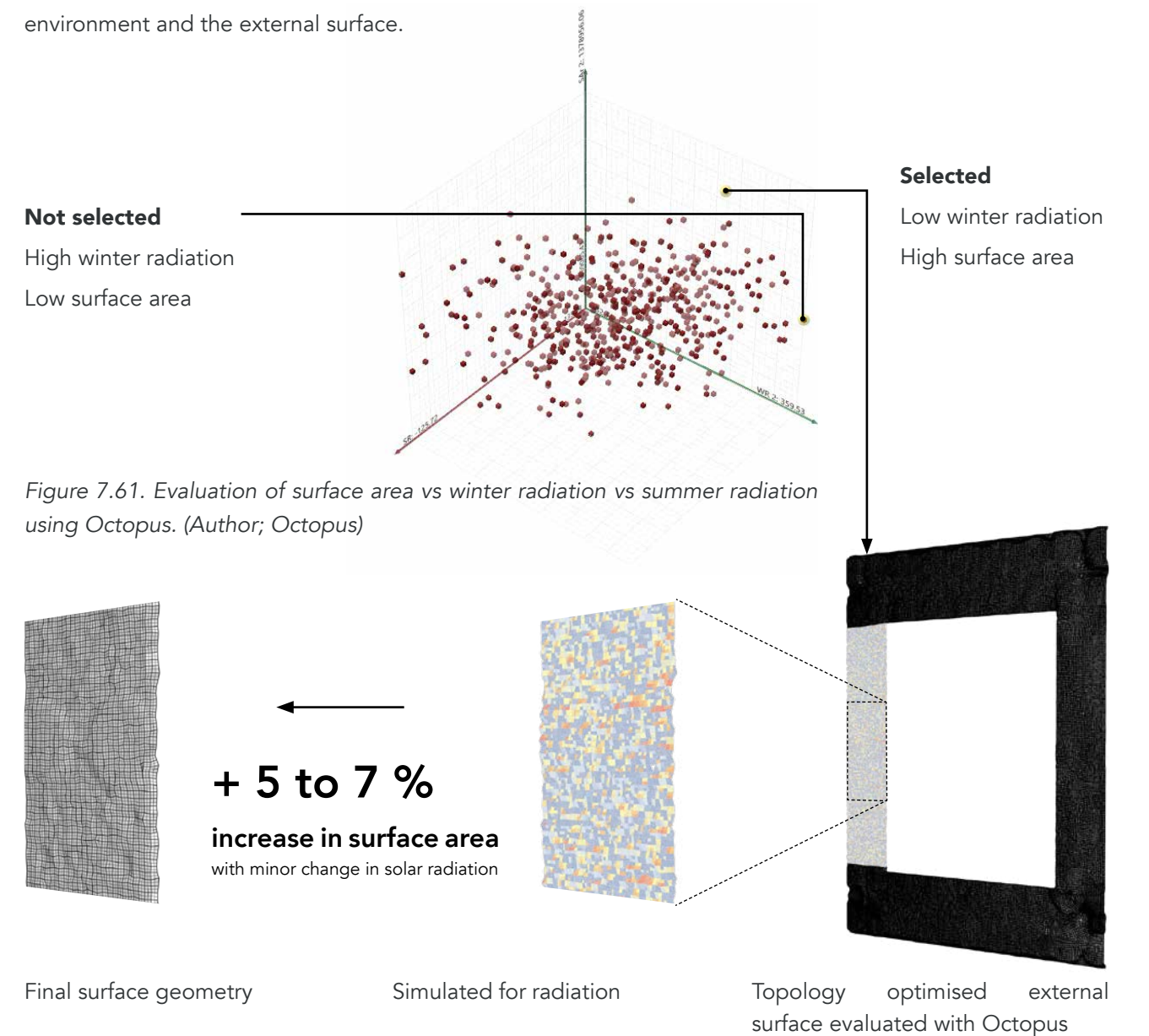


Figure 7.61. Evaluation of surface area vs winter radiation vs summer radiation using Octopus. (Author; Octopus)

Figure 7.62. Surface modification using Octopus to develop and evaluate surface with maximum surface area with similar solar radiation in summer and winter. (Author; Octopus)

## 7.8 HEAT TRANSFER- INSULATION

The performance of a facade does depend on the its insulating value. The use of a twin wall facade panel is primary designed to solve the purpose of thermal bridging occurring at the structural beams or slabs of the building being exposed to the environment, decreasing the performance index of the building. With the implementation of a twin wall facade panel, it is essential to make sure that the performance of a building is supposed to be of higher value, and this thesis does extend that by finding measures to even widen this gap by further improving the performance of the facade panel.

As stated by the Energy Conservation Building Code of India for the Delhi city, the maximum U-factor requirement of an opaque assembly for Business building types with less than 10,000 m<sup>2</sup> AGA is 0.63 W/m<sup>2</sup>K and 0.40 W/m<sup>2</sup>K for other building types. For the building to be complaint for ECBC+, the maximum U-value requirement further reduces to 0.44 W/m<sup>2</sup>K for business typology and 0.34 W/m<sup>2</sup>K for all other building typologies.

To ensure that the panel is ECBC complaint and future proof, the reinforcements of the panel was shifted from a steel mesh to that of an carbon fibre composite mesh and from the steel dowels that hold the two panels together from steel to that of glass fibre composites. With the replacement of the steel members for all the possible reinforcement sectors of the designed facade panel, not only that it will help in improving the insulation of the facade panel by decreasing or eliminating the usually occurring thermal bridges between the external and internal panel, but also decreases the possibilities corrosion and the environmental footprint by a huge margin.

The materials selected for the combination of the panel are listed below

### 7.8.1 Materials considered to improve insulation

#### 1. Reinforcement dowels

The reinforcement dowels selected for the replacement of traditionally used steel dowels to minimise the thermal bridge between the external and internal facade panel was chosen to be Schöck Combar Isolink which is a non metallic composite re-bar solution made up of glass fibre reinforced polymer (GFRC). The polymer composition of the material makes this reinforcement bar solution very low on thermal conductivity which helps in increasing the insulation value of the panel. The specific models selected for the designed panels is the Isolink TA\_H and TA-D of 12mm in diameter. Some of the properties of the material to determine of insulating value of the panel has been outlined below:

Density (g/cm<sup>3</sup>): 2.2

Thermal conductivity (W/mK): 0.7 (axial); 0.5 (radial)

Thickness/ diameter: 12 mm



Figure 7.63a. Schöck Combar Isolink TA-H for horizontal reinforcement. (Schöck, 2016)



Figure 7.63b. Schöck Combar Isolink TA-D for diagonal reinforcement. (Schöck, 2016)

#### 2. Reinforcement mesh

The reinforcement mesh selected for the facade panels were also filtered on the basis of non metallic solution and the Solidian flat reinforcement mesh solutions were considered for this system. The possibility of this mesh to be used in any form of shape open up its possibility of sustainable and efficient means of reinforcement. The specific model used for the panels in this thesis is the Solidian Grid Q142/142-CCE-25 which has a grid gap of 142mm and a wider mesh strand size of 25 mm. Some of the properties of the material to determine of insulating value of the panel has been outlined below:

Density (g/cm<sup>3</sup>): 2

Thermal conductivity (W/mK): 24

Thickness (m): 0.0025

Since the thickness of the reinforcement mesh is relatively small in comparison to that of the panel, it has not been considered in the sections for analytical or computed simulations.

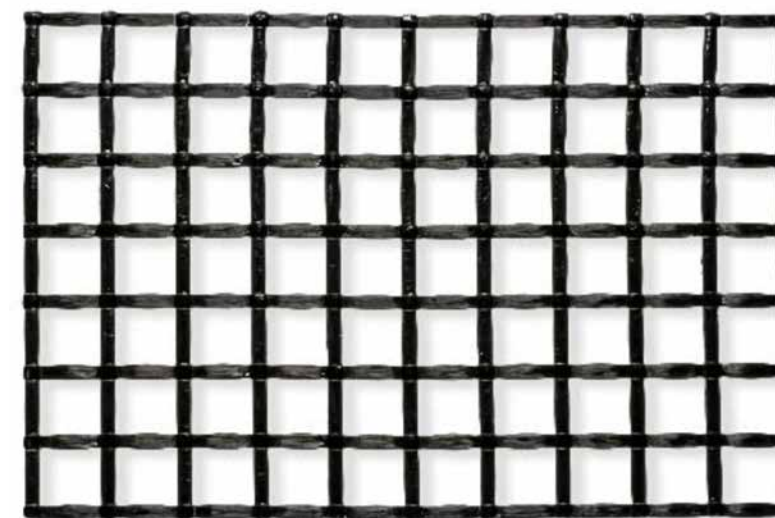


Figure 7.64. Solidian Grid Q142/142-CCE-25. (Solidian\_B ,2019)

### 3. Window section

To design the window for the office space behind the facade panel, tilt and turn type of module was determined and the Schüco AWS75 SI+ was selected which provides the possibility of installation of the window from inner space eliminating the need for building maintenance form-work while offering a very low U-value which is achieved by the implementation of high number of thermal breaks within the section. This section also holds the modular ability of fixing double or triple panel glass by choice. Some of the properties of the material to determine of insulating value of the panel has been outlined below:

U-value ( $W/m^2K$ ): 1.2

Total elevational area of window frame ( $m^2$ ): 0.876

Total edge length of the window frame (m): 8.62



Figure 7.65. Schüco AWS75 SI+. (Schüco, 2019)

### 4. Glass panel

The glass panel desired for this selection was supposed to be a triple pane glass for obvious reasons of high insulating value with low heat transmittance but the unavailability or scare availability only by cross country import in India, the design was selected to be comprised and limited only to a double pane glass. The filler for the gaps between the glass panes were through stringent to be that of an argon fill. To comprise a glass with these configuration a glass by Saint gobain Argon filled double glass with a configuration set of 6-12-6 mm. The glass selected was Saint Gobain Planitherm PLT T- Argon having a neutral colour shade. The reason behind choosing this glass was that this glass although having a very low U-value does allow 74% of visual light transmittance, which is suitable for a office space and is sustainable in saving artificial lighting during

the daytime. Some of the properties of the material to determine of insulating value of the panel has been outlined below:

U-value ( $W/m^2K$ ): 1.5

Total elevational area of glass ( $m^2$ ): 3.66

Total edge length of the glass (m): 7.76

The edge spacer used within the glass was chosen to be the Ultimate Swiss spacer by Saint gobain with a psi value of 0.036  $W/mK$

The analytical determination of the U-value of the configuration was needed and was done on basis of the elevation and section of the panels. A schematic diagram of the effective facade panel elevation has been shown in figure 7.66.

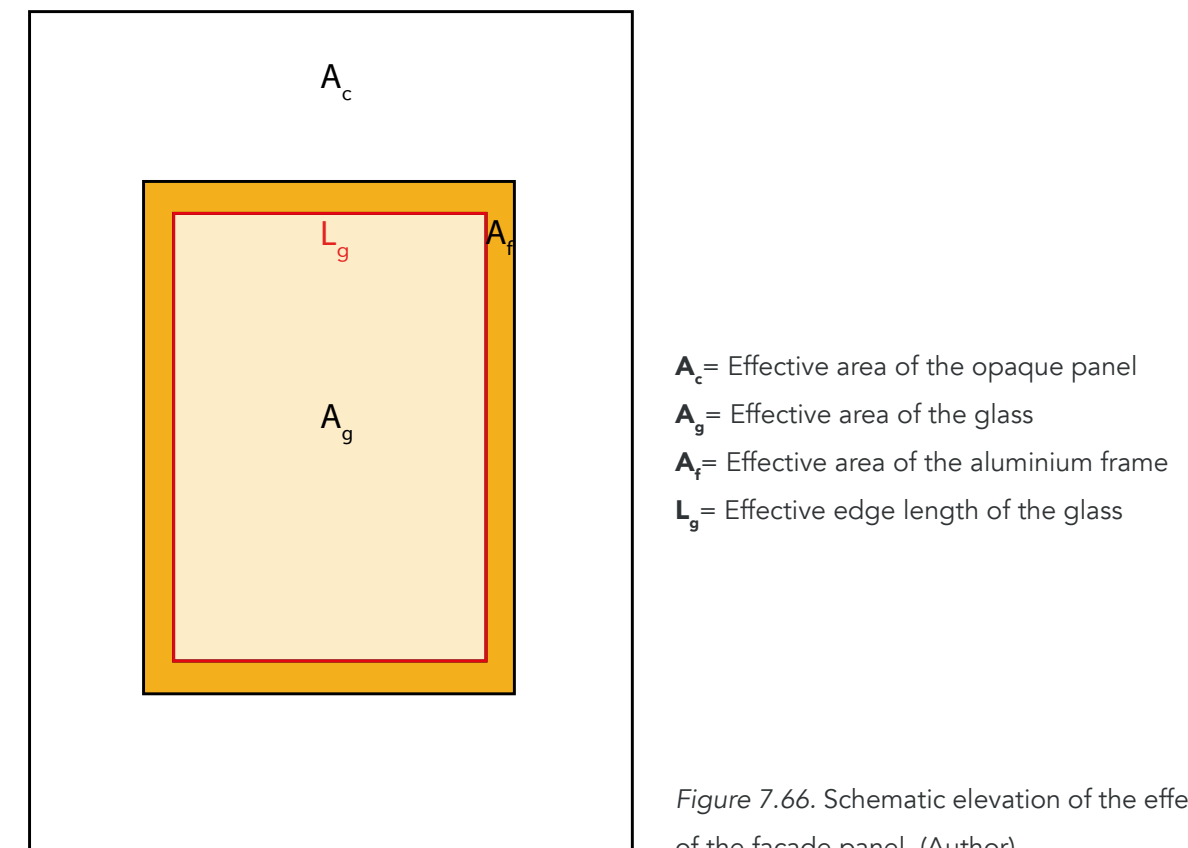


Figure 7.66. Schematic elevation of the effective areas of the facade panel. (Author)

## 7.8.2 U-value of the fenestration

To start with the U-value of the fenestration of the facade was considered first and calculated analytically while simulating the same to verify the authenticity of the setup and results, which could then be applied onto the other similar simulation models

The values needed for the areas and effective edge length for the window frame and that of the glass are referred to figure 7.66.

The U-value of the fenestration is determined by the following expression (CIT & Stephenson College, 2019):

$$U_{\text{fenestration}} = \frac{(\sum U_g \times A_g) + (\sum U_f \times A_f) + (\sum L_g \times \Psi_g)}{\sum A_g + \sum A_f}$$

where,

$U_g$  = U-value of the glass combination

$U_f$  = U-value of the aluminium window section

$A_g$  = Effective area of the glass

$A_f$  = Effective area of the aluminium frame

$L_g$  = Effective edge length of the glass

$\Psi_g$  = Thermal bridging coefficient

Hence,

$$U_{\text{fenestration}} = \frac{(1.6 \times 3.66) + (1.2 \times 0.876) + (7.76 \times 0.036)}{(3.66 + 0.876)}$$

$$= 1.58 \text{ W/ m}^2\text{K}$$

The above analytically analysed model was simulated using Therm and Ladybug with properties of material specific to the setup and materials used. It is to be noted that some values of the materials used by the Aluminium window section were unknown and were hence considered as default by the ladybug material library. The depiction of the simulation is shown below with the help of the section of fenestration setup.

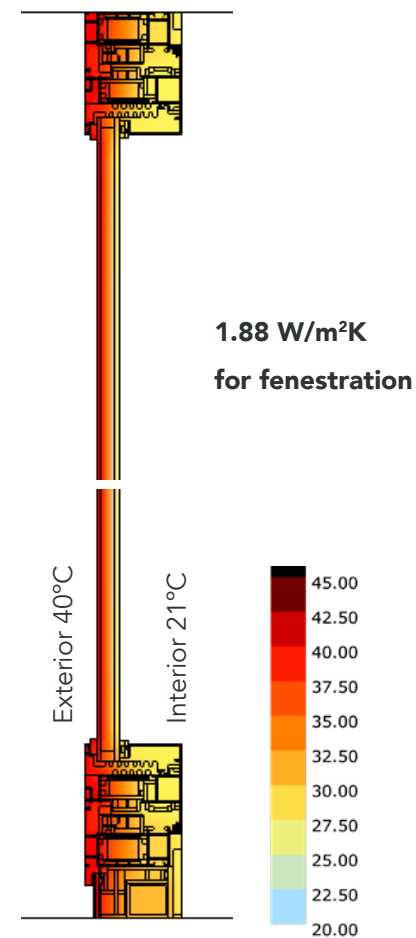
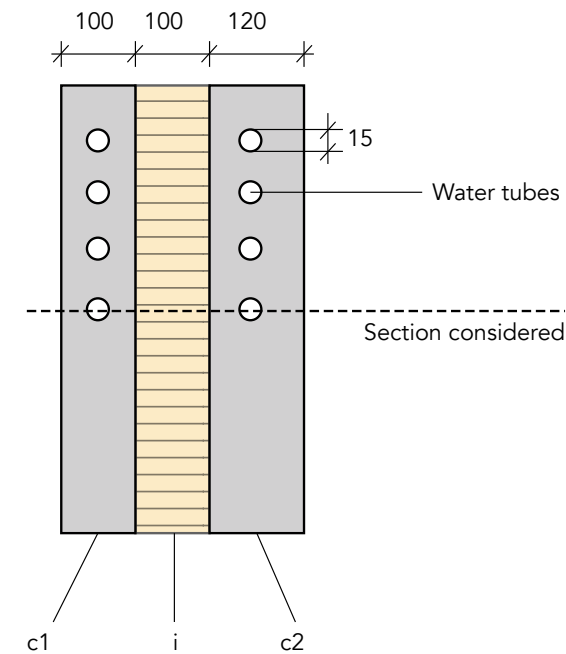


Figure 7.67. Therm analysis of the section of fenestration. (Author; Therm)

### 7.8.3 U-value of the opaque segments

In order to analyse the insulating behaviour of the opaque segment of the wall, the method of analytical calculation is divided into two different parts, the homogenised method of arrangement of the insulation and the inhomogeneous method of arrangement of the insulation in the twin panel system to accommodate

the distribution of the materials with different properties arranged in parallel to each other. The schematic diagram of the section and the segment of the section considered for the calculation has been depicted in figure 7.68. To perform the calculation, the depth of each material of the section are stated along with their thermal coefficient values as mentioned below (CIT & Stephenson College, 2019):



$d_{c1}$  = depth of external concrete panel  
 $d_{c2}$  = depth of internal concrete panel  
 $d_i$  = depth of layer of insulation  
 $d_w$  = depth/ diameter of water tube  
 $\lambda_c$  = Thermal heat coefficient of concrete  
 $\lambda_i$  = Thermal heat coefficient of insulating material  
 $\lambda_w$  = Thermal heat coefficient of water

Figure 7.68. Schematic diagram of homogeneous arrangement of the opaque section

With the above mentioned values, the total R-value of the combination, is calculated which is expressed as following:

$$R_{\text{opaque-1}} = r_{c1} + r_i + r_{c2} + 2(r_w)$$

$$= \frac{d_{c1}}{\lambda_{c1}} + \frac{d_i}{\lambda_i} + \frac{d_{c2}}{\lambda_{c2}} + \frac{2(d_w)}{\lambda_w} = \frac{0.1}{1.3} + \frac{0.1}{0.035} + \frac{0.12}{1.3} + \frac{2(0.015)}{0.6}$$

$$R_{\text{opaque-1}} = 3.076 \text{ m}^2\text{k/W}$$

Now since R-value is inverse to that of the U-value,

$$U_{\text{opaque-1}} = 1/R_{\text{opaque-1}} = 0.325 \text{ W/m}^2\text{k}$$

The second part is to analyse the inhomogeneous arrangement of the material in combination to the air films next to the internal and external facade panels to consider the convection behaviour of the panels. To do the same a schematic diagram of the arrangement was made as depicted in figure 7.69. The considered

segment for the analytical calculation is highlighted in the diagram. It is to be noted that the inhomogeneous arrangement of the insulation in the panel does affect in a minute fraction to the overall U-value.

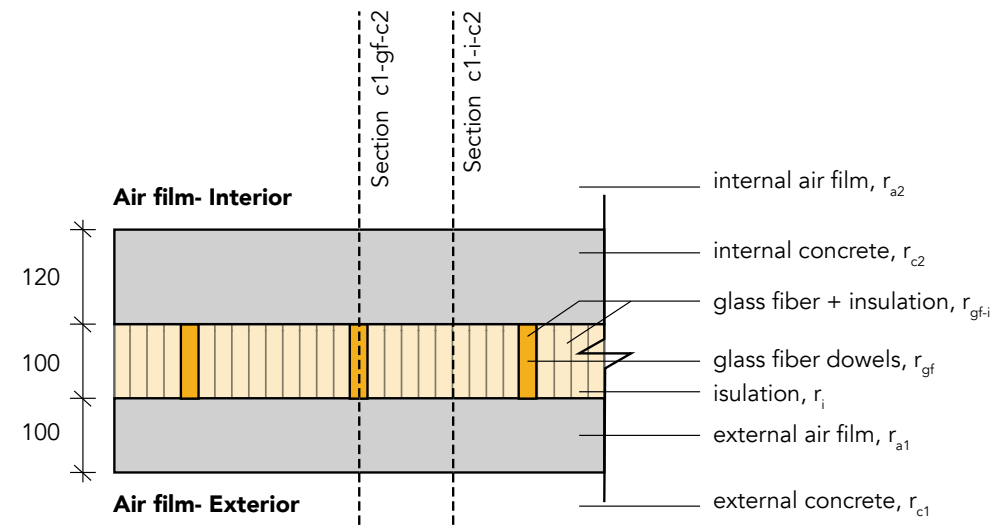


Figure 7.69. Schematic diagram of inhomogeneous arrangement of the opaque section

The length ratios of the different materials in the cross sections are calculated. The water tubes are excluded in the analytical calculation, which would or else improve the performance the cross section.

$L_{tot}$  = Total length of facade panel in plan = 3.00 m

$L_{gf}$  = Total cross sectional length of glass fibre dowels = 0.12 m x 9 nos. = 0.108 m

$L_i$  = Total cross sectional length of insulation = 3 - 0.108 = 2.892 m

Length ratios

$L'_{gf} = 0.108/3 = 0.036$

$L'_i = 2.892/3 = 0.964$

To calculate R-value ( $R_A$ ) of the longitudinal arrangement of the materials, we need to determine the r-values of the materials in combination

$r_{gf} = r\text{-value of the glass fibre} = d_{total} / \lambda_{gf} = 0.1/0.7 = 0.14 \text{ m}^2\text{K/W}$

$r_i = r\text{-value of the insulation} = d_{total} / \lambda_{gf} = 0.1/0.05 = 2.0 \text{ m}^2\text{K/W}$

where ,  $d_{total} = d_{c1} + d_i + d_{c2}$

Now, calculating the r-value for the combination of glass fibre and insulation

$1/r_{gf-i} = (L'_{gf}/r_{gf}) / (L'_i/r_i) = 0.739 \text{ W/m}^2\text{k}$

Hence,  $r_{gf-i} = 1.35 \text{ m}^2\text{K/W}$

Calculating the R-value ( $R_A$ ) of the longitudinal arrangement of the materials,

$$\begin{aligned} R_B &= r_{c1} + r_{gf-i} + r_{c2} + r_{a1} + r_{a2} \\ &= 0.0769 + 1.35 + 0.0923 + 0.127 + 0.039 \\ &= 1.6852 \text{ m}^2\text{K/W} \end{aligned}$$

To calculate R-value ( $R_B$ ) of the linear arrangement of the materials

Considering the segments c1-gf-c2 and c1-i-c2 as shown in figure 7.69,

$$\begin{aligned} r_{c1-gf-c2} &= r_{c1} + r_{gf} + r_{c2} + r_{a1} + r_{a2} \\ &= 0.0769 + 0.143 + 0.0923 + 0.127 + 0.039 \\ &= 0.4782 \text{ m}^2\text{K/W} \end{aligned}$$

$$\begin{aligned} r_{c1-i-c2} &= r_{c1} + r_i + r_{c2} + r_{a1} + r_{a2} \\ &= 0.0769 + 2 + 0.0923 + 0.127 + 0.039 \\ &= 2.3352 \text{ m}^2\text{K/W} \end{aligned}$$

Now,  $1/R_B = (L_{gf} / r_{c1-gf-c2}) + (L_i / r_{c1-i-c2}) = 0.488 \text{ W/m}^2\text{k}$

Hence,  $R_B = 2.05 \text{ m}^2\text{k/W}$

Calculating the total R-value of the inhomogeneous combination, is calculated which is expressed as following:

$$\begin{aligned} R_{opaque-2} &= (R_A + R_B) / 2 \\ &= 2.19 \text{ m}^2\text{k/W} \end{aligned}$$

Now since R-value is inverse to that of the U-value,

$$U_{opaque-2} = 1/R_{opaque-2} = 0.456 \text{ W/m}^2\text{k}$$

To analyse the opaque cross sections of the facade segments and determine the U-value of the configuration, simulations were carried out for the opaque segment in plan and the combined performance of the panel in section. The illustrations of the same are depicted herewith.

With a value within desired range to be compliant by the ECBC norms, the panel after optimisation and modified topology of the surface the U-value of the panel was re-simulated. The effective depth of the panel has been minimised at certain zones of the panel after optimisation to minimise the volume of the panel. A critical section of the opaque zone of the optimised panel was selected and the simulation for the same has been depicted below.

It was evident from the simulation that the U-value of the panel has reduced by a huge margin and that the U-value of the designed panel surpasses the ECBC+ complaint requirement. This suggests that the optimised panel proves to be highly efficient in the provided scenario in comparison to that of a regular concrete twin wall facade panel. The reason behind increased R-value of the facade panel can be pointed towards the insets developed by topology optimisation which insets air niches and self shading developed by the geometry.

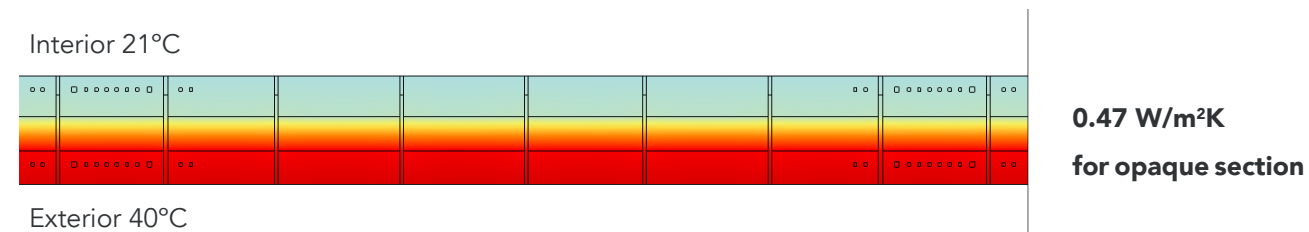


Figure 7.70. Thermal transmission simulation of the flat facade panel. (Author; Therm)

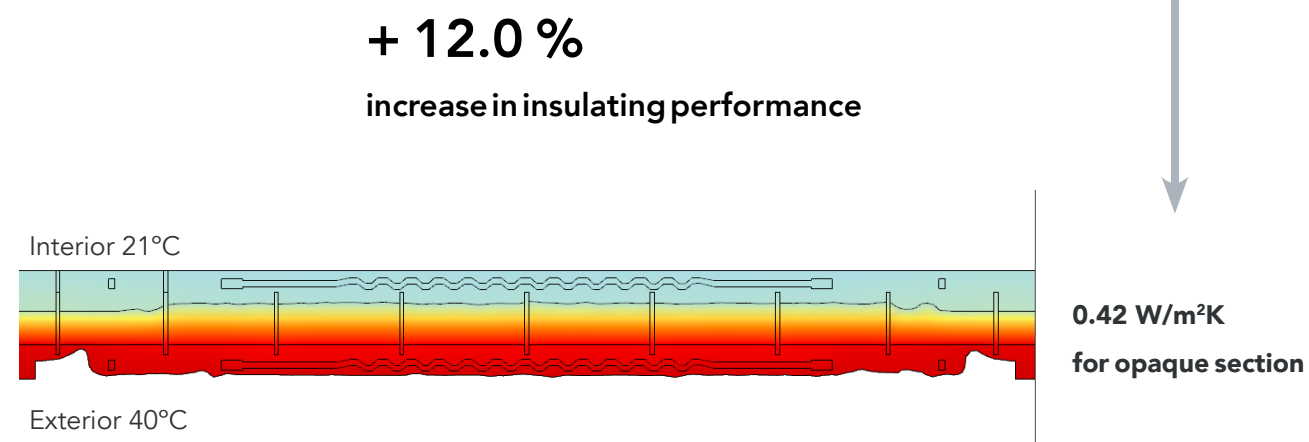


Figure 7.71. Thermal transmission simulation of the topology optimised facade panel. (Author; Therm)

Now, to calculate the U-value of the whole facade panel in combination we considered the higher value of the opaque section ( $U_{\text{opaque-2}}$ ) in consideration along with the  $U_{\text{fenestration}}$ .

$$U_{\text{facade}} = \frac{(U_{\text{opaque-2}} \times A_{\text{opaque-2}}) + (U_{\text{fenestration}} \times A_{\text{fenestration}})}{A_{\text{opaque-2}} + A_{\text{fenestration}}}$$

where,  $A_{\text{opaque}} = 7.862 \text{ m}^2$  and  $A_{\text{fenestration}} = 4.678 \text{ m}^2$

$$U_{\text{facade}} = 0.87 \text{ W/m}^2\text{K}$$

## 7.9 HEAT TRANSFER - PERFORMANCE

To analyse the amount of heat captured by the water within the tubes inside the external facade panel and the amount of heat transmitted to the indoor space from the heated water after exchange with the internal panel, COMSOL multiphysics was used to simulate the scenario. To analyse the thermal performance for the designed geometry, the method of simulation was split into two instances and have been described further with the help of a section of the setup and the different boundary conditions implied specific to the instances.

It is to be noted that the aspect of the heat transfer for performance determination of the panel is carried out in a broad manner in order to cope up with the limited time for this project.

### 7.9.1 Instance 1: From external environment to void tubular network of water within the external panel

The first stage of heat transfer is happens between the environment to the water within the external panel with the mass of concrete acting as the heat transfer medium. The water inside the external panel is selected as the domain probe to record the average temperature within it. The external temperature is provided by the weather file and the solar radiation is input manually in order to cope up with the large solving time for the complex geometry as explained in section 5.3.4.

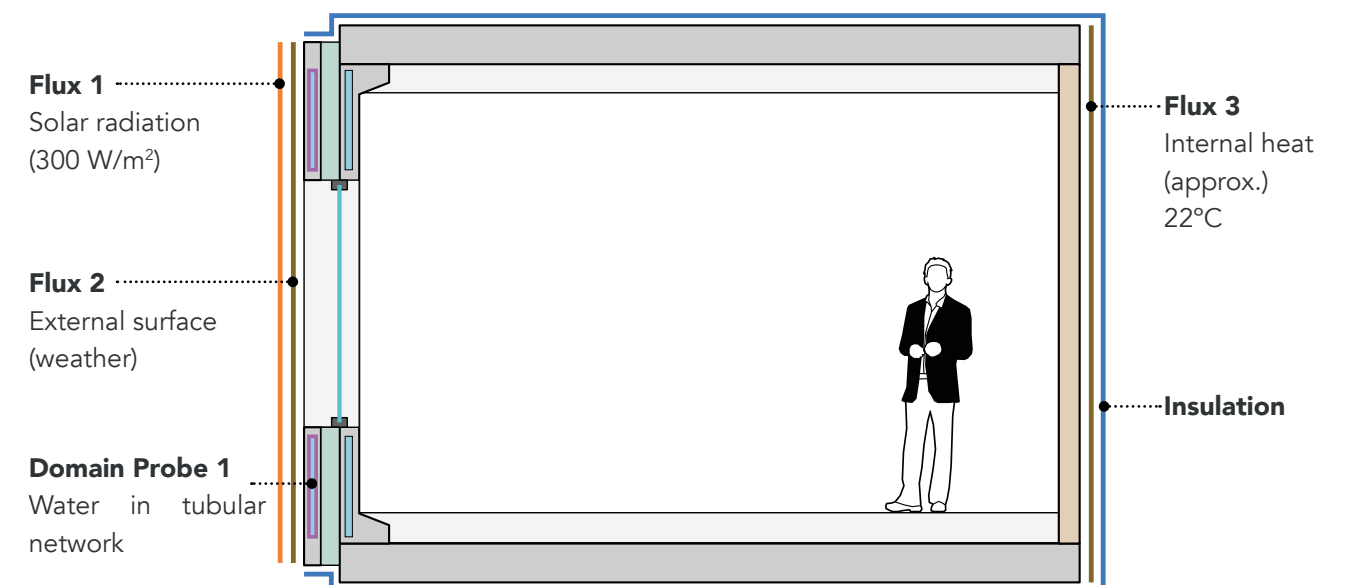


Figure 7.72. Section of the 3D geometry showing the flux and probe for instance 01 set-up in COMSOL. (Author)

The designed element that acts as an interface for the heat transfer between the environment and the external panel is the outer surface area of the external panel. To make a comparative analysis of a flat facade panel to that of the geometrically modified facade panel with increased surface area, the above shown setup was used for the two different 3D geometries of external panel. The change in average temperature of the water within the tubular network inside the external panel was recorded onto a graph for the same time period, external environment and boundary conditions.

### 1. Flat panel

The simulation starts at 0800 hrs and is recorded for 24 hours with steps per minute. As shown in the graph (figure 7.73), the water inside the flat panel does maximise just below 34°C attained at around midnight. This then slowly cools down over the night and reaches a temperature of 23.8°C by the next morning. The initial value of the temperature was set to the ambient value and was not influenced by any such phenomena before. The initial temperature for the adjacent does start with a temperature of 23.8°C.

### 2. Modified panel for increased surface area

As for the prior geometry, the simulation starts at 0800 hrs and is recorded for 24 hours with steps per minute. But in this case it is noted that the water inside the flat panel does attain a temperature of 36.8°C by 0030 hrs. While the attained temperature is higher than the flat surface panel, the cooling of the surface modified geometry tends to a 1°C lower temperature than the flat panel because of the decrease in the thermal mass by subtracting mass through topology optimisation. This difference in the initial temperature doesn't matter much to the heat absorption at the peak and is compensated by the extra energy gained by the surface modified panel. This comparative analysis does justify the added benefits of modifying the geometry of the external facade panel to maximise the surface area.

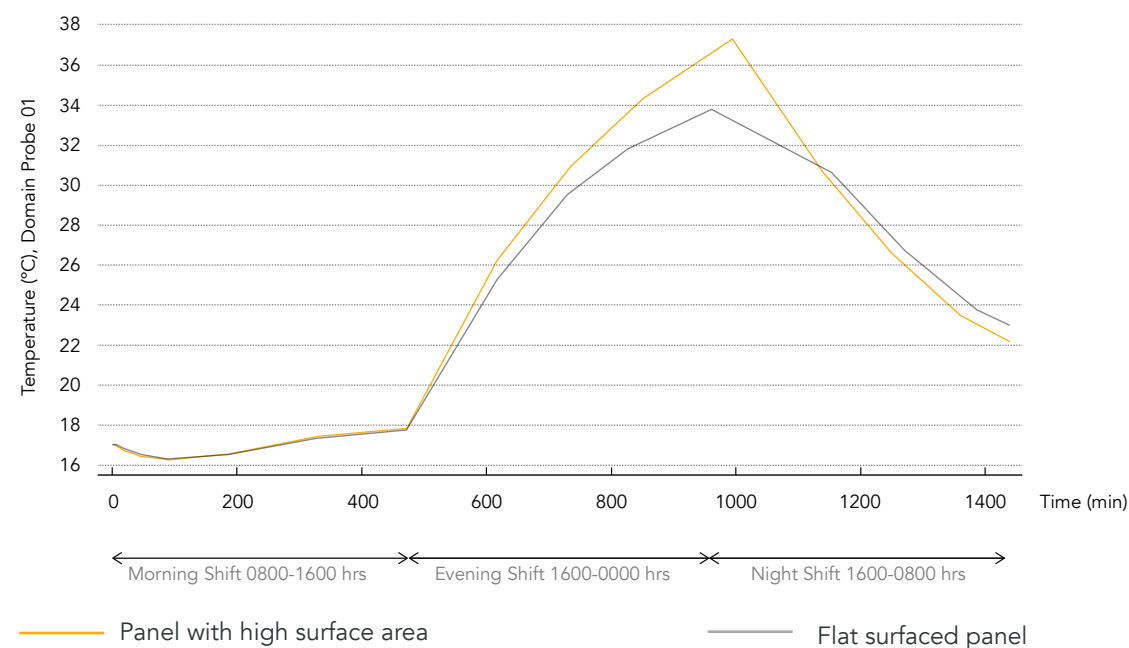


Figure 7.73. Graph showing average temperature change in the water inside the external panel over 24 hours starting from 0800 hrs. (Author; Comsol)

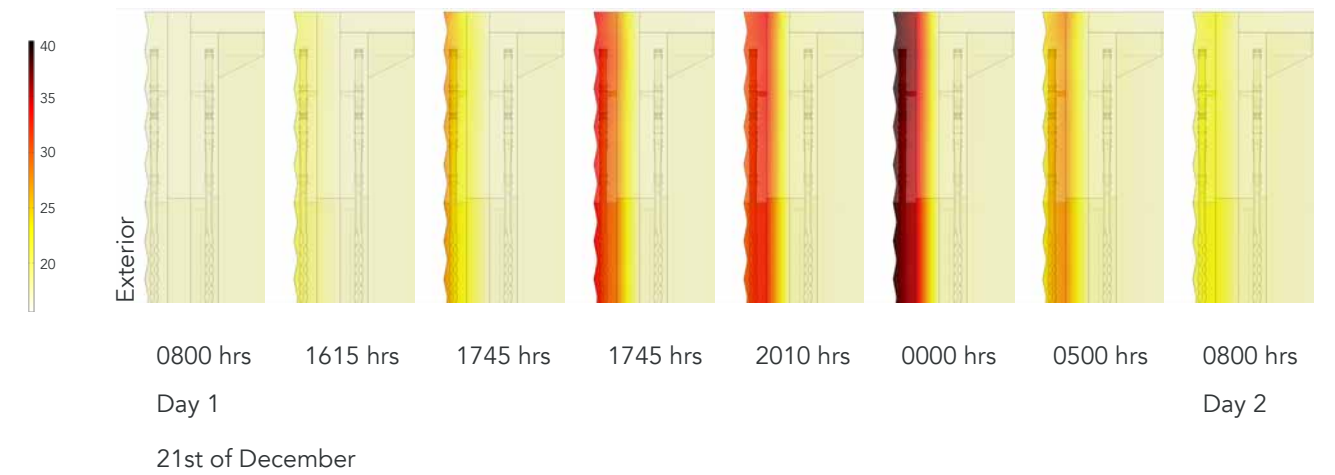


Figure 7.74. Section of a segment of the external facade panel with modified surface area exposed to the environment (Delhi) absorbing heat and transferring it to the fluid (water) within. (Author; Comsol)

## 7.9.2 Instance 2. From void tubular network of water within the internal panel to the indoor space.

The second stage of heat transfer is happens between the water inside the internal panel to the indoor space while the mass of concrete of the internal panel acts as the medium. The temperature from the domain probe of instance 01 was set as the initial temperature to the domain of the water inside the internal panel, which does act as a flux. The surface inside of the internal was set as the domain probe for this instance to analyse the energy transferred from the environment to the inside completing one cycle. This method of calculation was set to approximate the energy transfer capability or the performance of the facade.

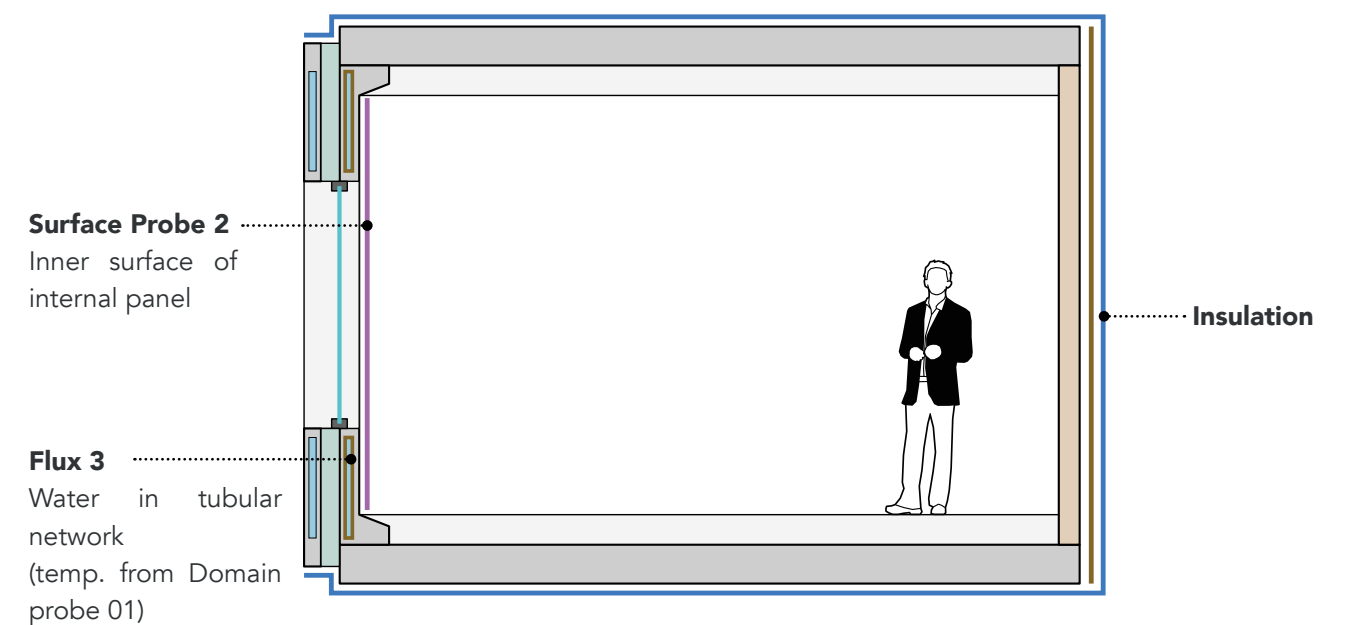


Figure 7.75. Section of the 3D geometry showing the flux and probe for instance 02 set-up in COMSOL. (Author)

The water inside the internal panel was setup with a manually defined initial value to act as Flux 1 which was referred from domain 01 at 1800hrs. The internal temperature was set to 17°C assuming that it was unconditioned for the day. For instance with the initial temperature of the flux 1 at 26°C, the energy dissipated to the indoor space is approx 95 W/m<sup>2</sup>. To put into reference an average office building in India for a 8 hour shift does require 550 W/m<sup>2</sup> per shift for a total 10 hours of which maximum of 60% account for HVAC (Singh, Sartor, & Ghatikar, 2013) or only 16.6 W/m<sup>2</sup> in 30 minutes. Hence, with proper thermal management of water exchange between the external and internal facade panels, the amount of thermal energy captured within the water can cater 6 hours approx. This could also be catered by circulating slow continuous flow of water after the required temperature of the fluid within external panel is achieved. It is to be noted that this heat exchange does not take into account the possible heat loss during the exchange of the water between the external and internal facade panels. The graph below shows that the energy dissipated to the indoor space is approx 95 W/m<sup>2</sup> by the tubular network geometry 06 with 28.11 litre capacity and 68 W/m<sup>2</sup> by network geometry 01 with 20.6 litre capacity within 30 minutes. The staggered nature of the graph is seen due to fact of the higher degree of steps selected for the simulation. The flattening of the graph after 30 minutes occurs due to the state of equilibrium.

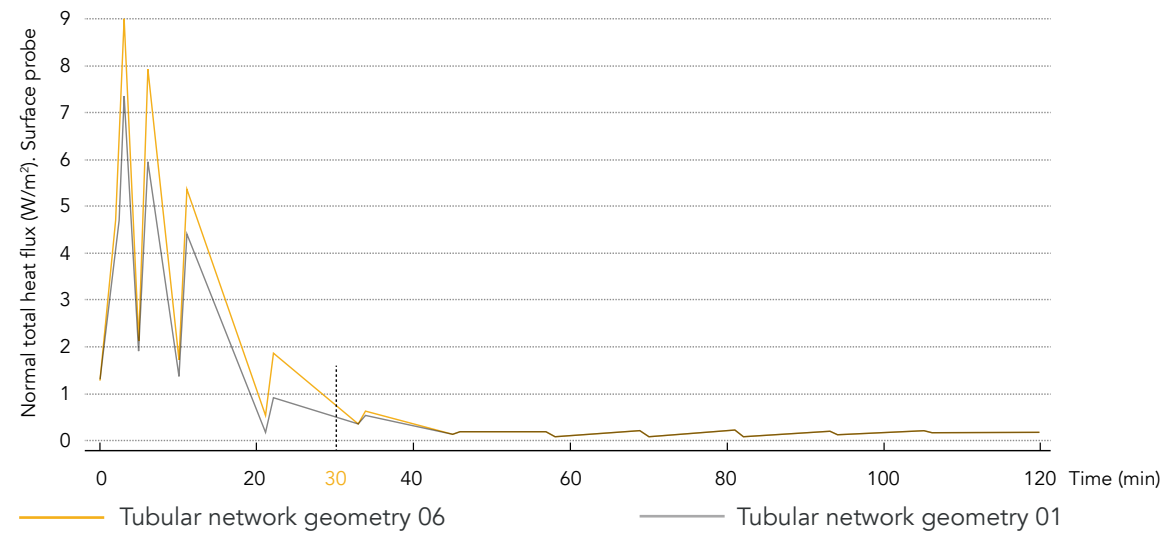


Figure 7.76. Graph showing average normal heat flux emitted by the water flux 3 (26°C) over the inner surface of the internal panel with an internal temperature of 17°C after 60 minutes. (Author; Comsol)

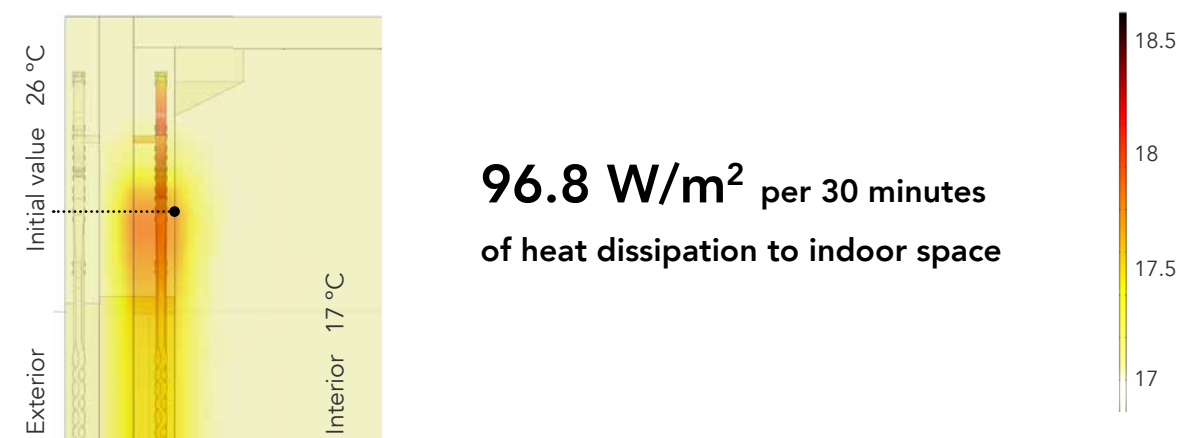


Figure 7.77. Image of section segment showing average normal heat emitted by water flux 3 (26°C) over the inner surface of the internal panel with an internal temperature of 17°C after 60 minutes. (Author; Comsol)

### 7.9.3. Work cycle

With the system designed and the heat exchange simulated, the work cycle needed to make the efficient use of this project is explained below. The process was analysed for a scenario with sunny days and cooler nights for a period of 24 hours, and has been broadly classified into 4 cycle types referring to the 3 different working shifts.

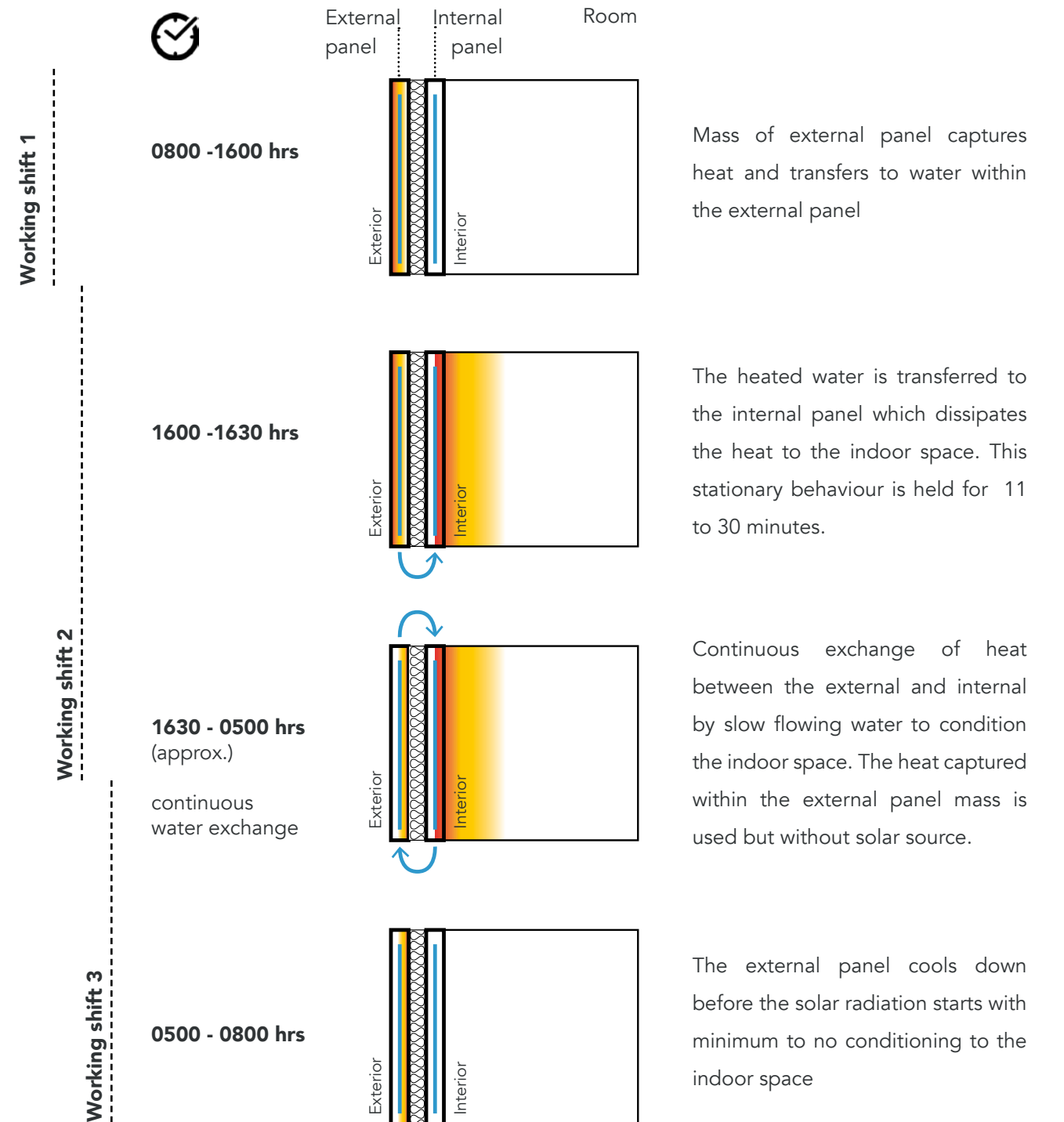


Figure 7.78. Diagram showing the heat exchange cycle between the internal and external panel to condition the internal space for a cycle of 24 hours. (Author)

## 7.10 CONCLUSION

The basic design criteria needed to design the network geometry was discussed in detail, with results of the evolved geometry analysed per step of modification done to derive a comparative analysis of the effect of the modification and considered criteria in determining either the change in volume or the pressure drop. The design modification did start at the level of a single tube, and manual shape optimisations were carried out to achieve the goal of minimum pressure drop and maximum increase in volume. After the tubes, the four different nodes of the network geometry for a single panel was computed and optimised for the optimum shape that minimises the pressure drop across the complete network. The change in the pressure drop and volume are simulated per step in Ansys fluent and documented for comparison. By this process of optimisation, various different constraints considered and limitation of the software were discussed.

The second half of this chapter deals with maximising the performance of the combination of the void tubular geometry within the mass of the facade in respect to various different criteria. The criteria of maximising the surface area to increase the heat conductivity to the concrete mass and transfer to the fluid in the void tubular network was selected to be achieved through topology optimisation, that served as a trade-off between the desired result without compromising the structural system rather improving it by decreasing the overall volume and thus the weight of the facade panels.

Through this chapter the tools used for optimisation, the various different parameters set to achieve the desired result and the methodology used to derive the final geometry was summarised, through which the following sub-research question was successfully answered.

### **Sub research question answered:**

*What method, tool and parameters of optimisation needs to be considered for deriving the geometry and maximising the efficiency of the heat exchange system ?*

# 8. RESULTS

## CHAPTER OVERVIEW

This chapter amalgamates the results derived from the previous stages of design derivation and a comparative analysis has been established to determine the final change in the performance of the design system with respect to change in volume, pressure drop across the tubular network in a single facade panel and the improvement in surface area, surface radiation and insulation behaviour of the combined geometry. This chapter also summarises the various different material used in this project.

## 8.1 FINAL RESULTS

The steps discussed in the previous section of this chapter helped in deriving the geometry for the external and internal panels while improving the performance of the heat exchange system by drastically minimising the pressure drop of the fluid cascaded within the small diameter tubes of the panels and the thermal exchange through geometry modification of the surface. All these modifications and simulations were accompanied by many different tests and simulations and have been stated in detailed in the above sections. The modification of the designs were also highly constrained by the method of fabrication, the varying properties of different materials, the structural system, the fixtures on the facade and the simulation limitations by the software. The final results hence derived from all the above steps procured have been amalgamated and stated in this section of the chapter to have a comparative brief review of the final geometry.

### 8.1.1 Medium of fluid

The medium of fluid chosen for the system of heat exchange was selected as water and simulations were carried for water at 20°C. In lieu of the method of fabrication, analysis for molten wax at 120°C was also considered for simulation of the CFD and a common ground of both were chosen.

### 8.1.2 Type of flow and parameters attained

In consideration to the behaviour of the fluid within the primary designed network geometry and referred projects as mentioned in section 7.2, the flow type of the was limited to a laminar flow only. The maximum possible Reynold's number to contain the nature of fluid to be laminar, depended upon the volume and the minimum possible time to drain the specified volume of water from one network geometry to other. The parameters thus decided for flow of fluid are as follows:

$v$  = velocity of the fluid = 0.15 m/sec

$Re$  = Reynolds number = 2256

$Q$  = Volumetric flow rate = 1.6 l/min or 0.0016 m<sup>3</sup>/min or  $2.732 \times 10^{-5}$  m<sup>3</sup>/sec

$d$  = diameter of the tube = 15 mm = 0.015 m

### 8.1.3 Decreasing flow resistance in tubes

It was realised that the decrease in diameter, increasing length and multiplying the number of tubes in parallel connection between an inlet and outlet, the pressure drop increases and varies largely per tube. To decrease the pressure drop across the network and unify the flow of fluid in a uniform pattern in all tubes, the resistance

of the tubes in parallel connection were needed to be modified for their diameters as suggested by Alston & Barber (2016). In reference to the same, the diameters for the vertical and horizontal networks were sorted separately and calculated and the results are as following:

#### Vertical network :

$d_0 = 15$  mm

$d_1 = 16.5$  mm

$d_2 = 15.8$  mm

$d_3 = 14.8$  mm

#### Horizontal network:

$d_0 = 15$  mm

$d_1 = 16.7$  mm

$d_2 = 17.5$  mm

$d_3 = 17$  mm

$d_4 = 16.5$  mm

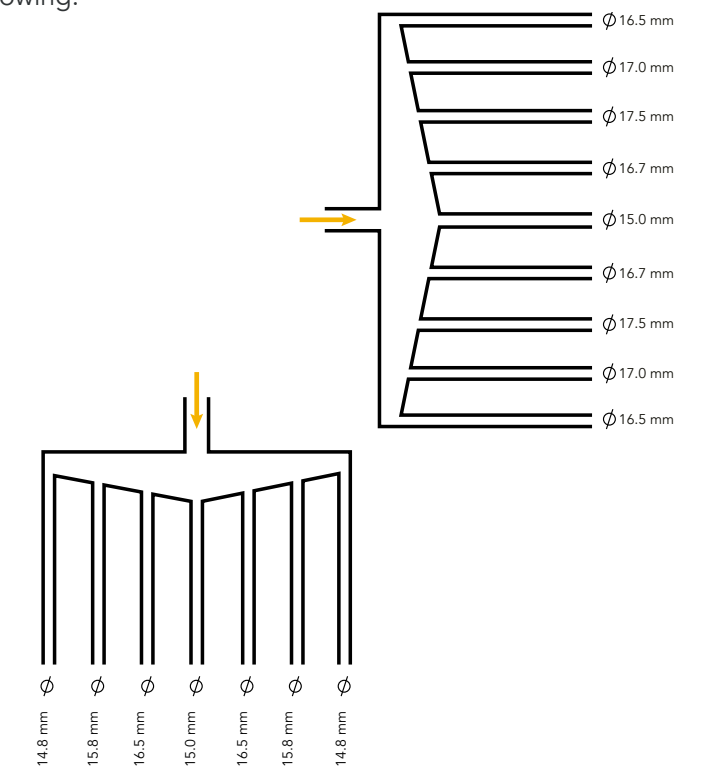


Figure 8.1. Vertical + Horizontal network zoomed in diameters

### 8.1.4 Volume variation of the tubes

To increase the performance of the heat exchange system and maximise the fluid transfer cycle between the external and internal facade panel per day, higher thermal mass was needed and this needed the design to deviate from regular geometry of tube's configuration. To increase the thermal mass of the fluid within the panels, the volume of the individual tubes and thus the network was prescribed to be increased significantly and various different options were considered. With the modification of geometry, the length and the volume of the tubes increased while leading towards significant drop in pressure across the tubes. To minimise the pressure drop after modifying the tubes for maximum possible increase in volume, the two following configurations were selected.

First method: Splitting the 15 mm diameter tube into two branched tubes of 10 mm diameter in concern to the maximum possible after allowing concrete cover for the material integrity. The change in volume was by 92 %.

Second Method: By manipulating the 10 mm diameter split tubes to be manipulated to form curls along the depth of the facade panel. This geometry is limited in depth in consideration to accommodate concrete cover needed and the reinforcement of the carbon fibre mesh. The angle of degree of curvature of the tube was constrained by the method of inverse investment casting method chose for casting the tubes cascaded within

the concrete facade panel. The same is done by 3D printing of wax tubes and casting the same with concrete and melting the printed wax within by pressure boiling of water. The limitation of 3D printing the wax at a maximum possible 40° angle without any support did limit the angle in degree of curling the design of tubes along the depth of the facade panel to 40°.

The depiction for implementation of the two methods above are show in figure 8.2.

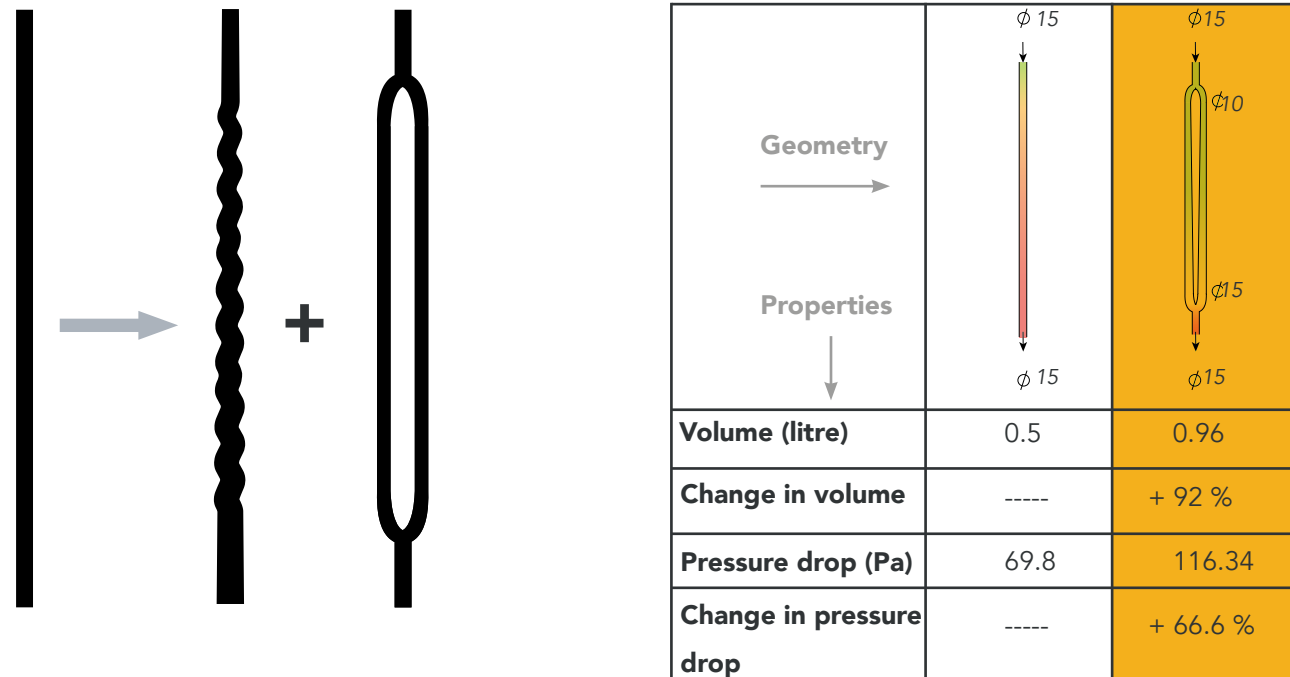


Figure 8.2. Schematic diagram showing the two steps used to modify the geometry. (Author)

Table 8.1. Comparison of the primary tube geometry to that of the modified. (Author)

### 8.1.5 Pressure drop in individual tubes

The increased complexity of the tubes from a single straight tube of 15 mm diameter to that of a branched and curled tube, did increase the effective length of complexity of a single tube per decision taken towards modifying the geometry and hence has significantly increased the pressure drop along the tube. In order to minimise the pressure drop across the modified tube to that of the original straight 15 mm diameter tube, different comparative analysis were done and settled up with a branched tubes with varying diameters from 10 mm at inlet to 15 mm at outlet, which was limited by the minimum required concrete cover of 10 mm between the geometries. This method also did contribute towards increasing the volume of the network geometry. The orientation of the branched tubes were altered to make room for more concrete at the curved junctions and increased strength.

A depiction of the change in volume and pressure drop from a single unified diameter tube to a modified tube has been stated in figure 8.3.

**+105.8%**  
increase in volume

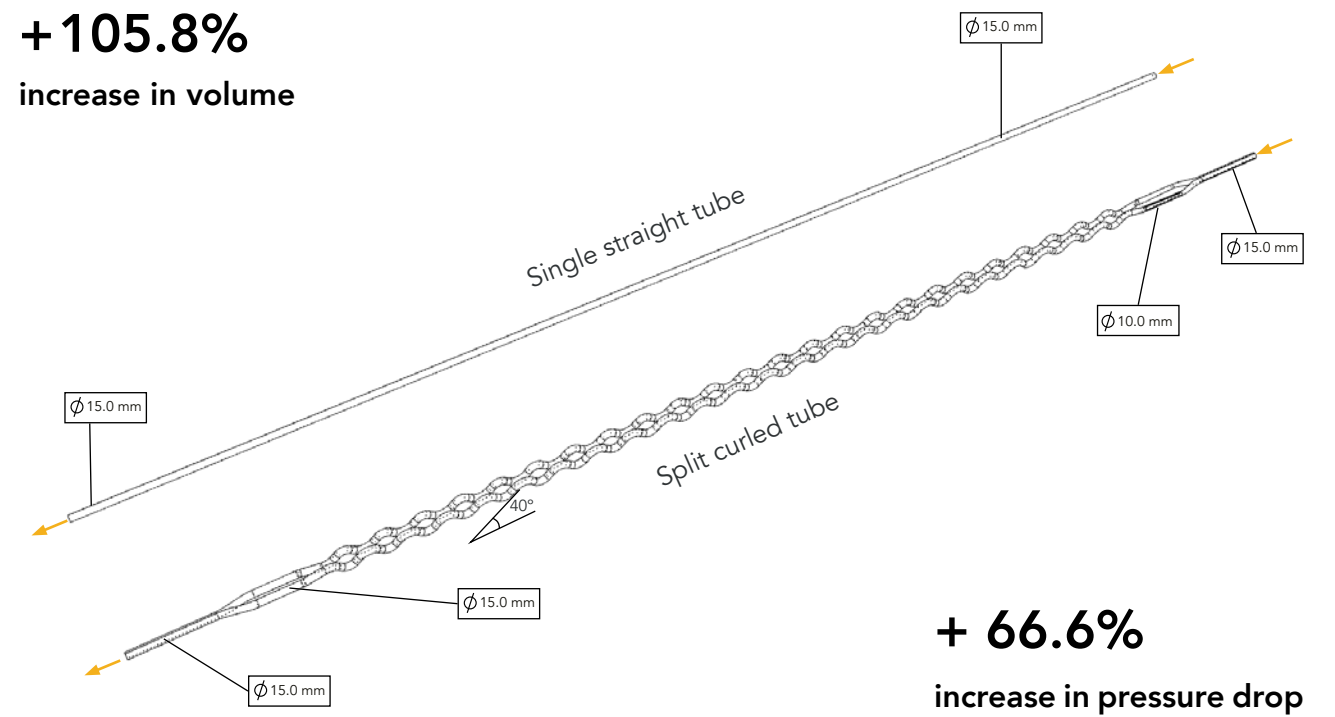


Figure 8.3. Transition of single 15 mm diameter tube of length 2832 mm to a split tube with varying diameter of 10-15mm and curled along the depth of the panel at 40° inclination. (Author)

### 8.1.6 Shape optimisation of nodes

While the modification of tubes to minimise the pressure drop did prove promising, but was limited only to the segment of individual tubes, the combination of these tubes in the complete network did maintain a high pressure drop. To minimise the pressure drop across the whole network geometry, the vision was diverted towards the four corner nodes of the network where the individual parallel network setup did merge. This was done by shape optimisation of these nodes in response to the pressure drop and unifying volume flow at the outlet. The result of one corner junction has been depicted below in comparison to that of the primary geometry of the node.

The behaviour of the flow of water within the network geometry and nodes were analysed in a 2D simulation of the network. Since the inner geometry has to be fabricated by 3D printing of wax and to be melted out by high pressure of boiling water, the simulation of the fluid flow for molten wax was also analysed and combined with that of the water flow analysis. A comparative study of the shape optimisation to that of the fluid flow analysis in the nodes reflects the behaviour of the flow as speculated in the 2D simulation of the fluid flows. Hence the nodes were optimised on basis of the combined 2D flow mapping of water and molten wax as fluid and eliminate the zones where flow path of the fluid does not interact with and micro turbulence formed in

these zones. This was preferred over the time consuming and unreliable method of 3D shape optimisation, which delivers the same geometry modification with improved results.

The primary and the final modified geometry of the nodes are shown in table 8.2 and the final void tubular network geometry in figure 8.4.

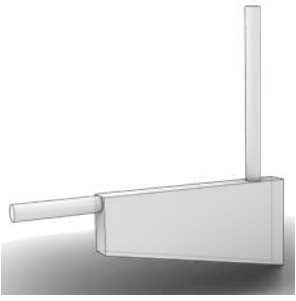
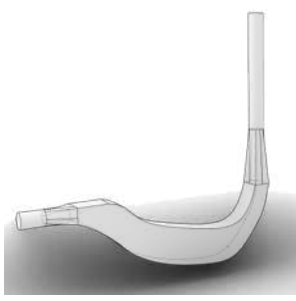
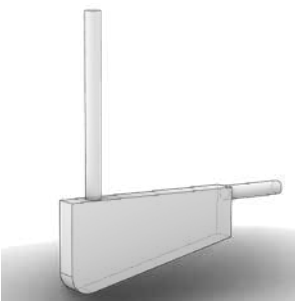
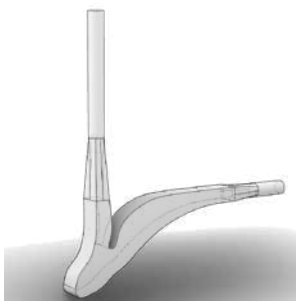
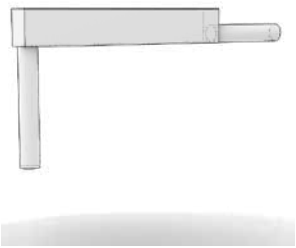
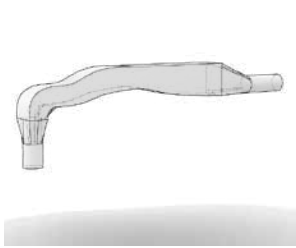
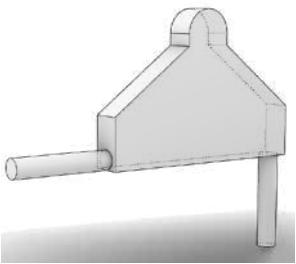
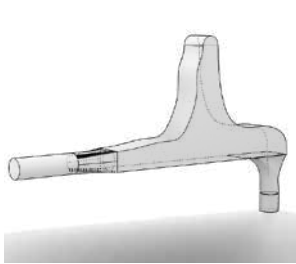
	Primary geometry	Modified geometry	Change in volume	Change in pressure drop
Node 1			- 44 %	- 57 %
Node 2			- 44 %	- 57 %
Node 3			- 44 %	- 57 %
Node 4			- 44 %	- 57 %

Table 8.2. Change in pressure drop of primary geometry and modified geometries of different nodes

### 8.1.7 Network Geometry 06

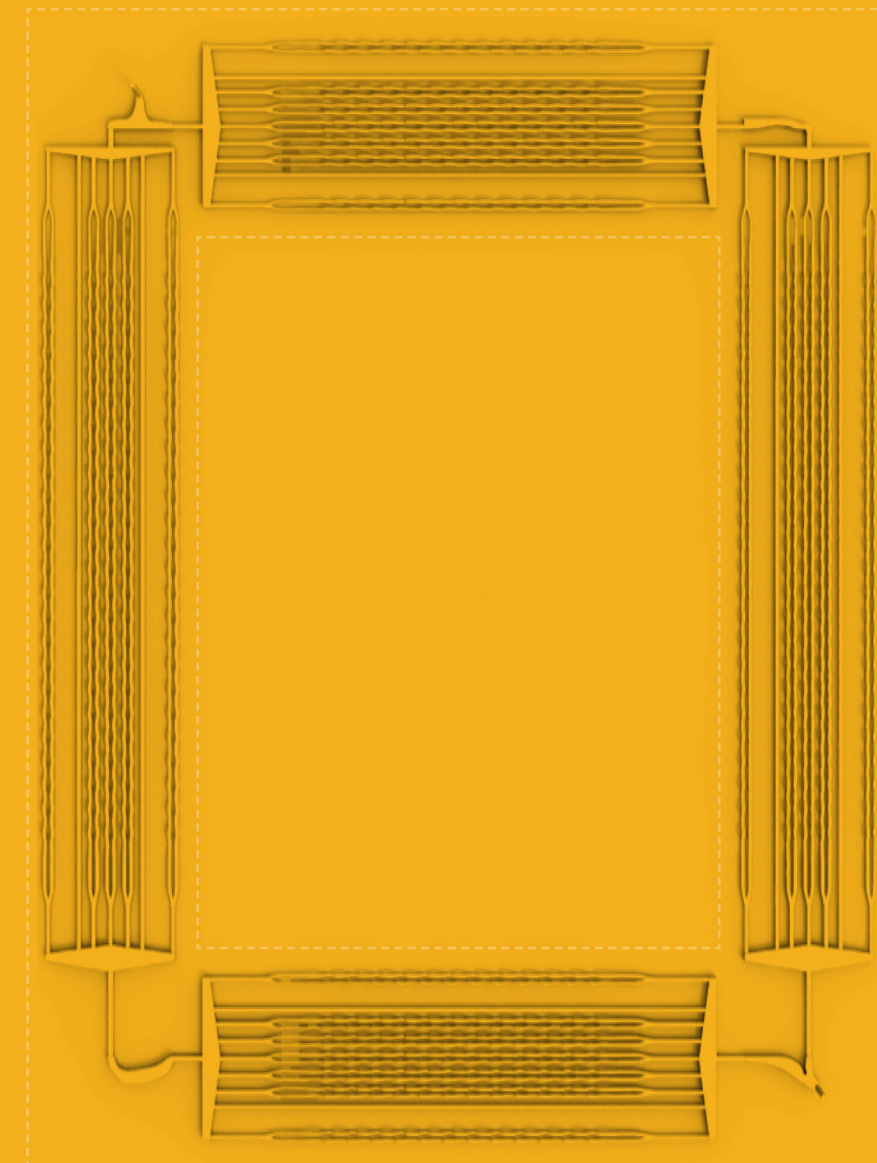


Figure 8.4. Network geometry 06- with optimised corner nodes  
Source: author

Volume of network:	Pressure drop in network
<b>28.11 litres</b>	<b>62.51 Pa</b>
Change in volume	Change in pressure drop
<b>+ 36.4 %</b>	<b>-94.9 %</b>

\*Change in volume and pressure drop are calculated to network geometry 01 as reference.

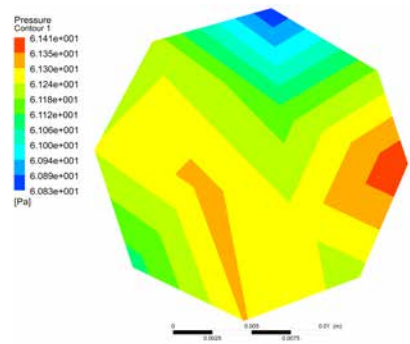


Figure 8.5a. Pressure contour inlet (Author; Ansys fluent)

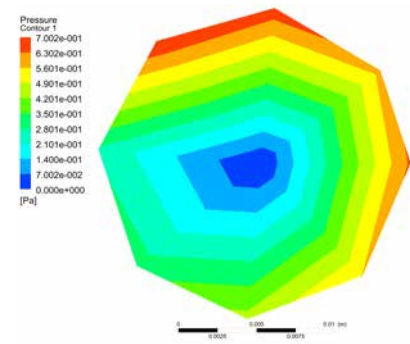


Figure 8.5b. Pressure contour outlet (Author; Ansys fluent)

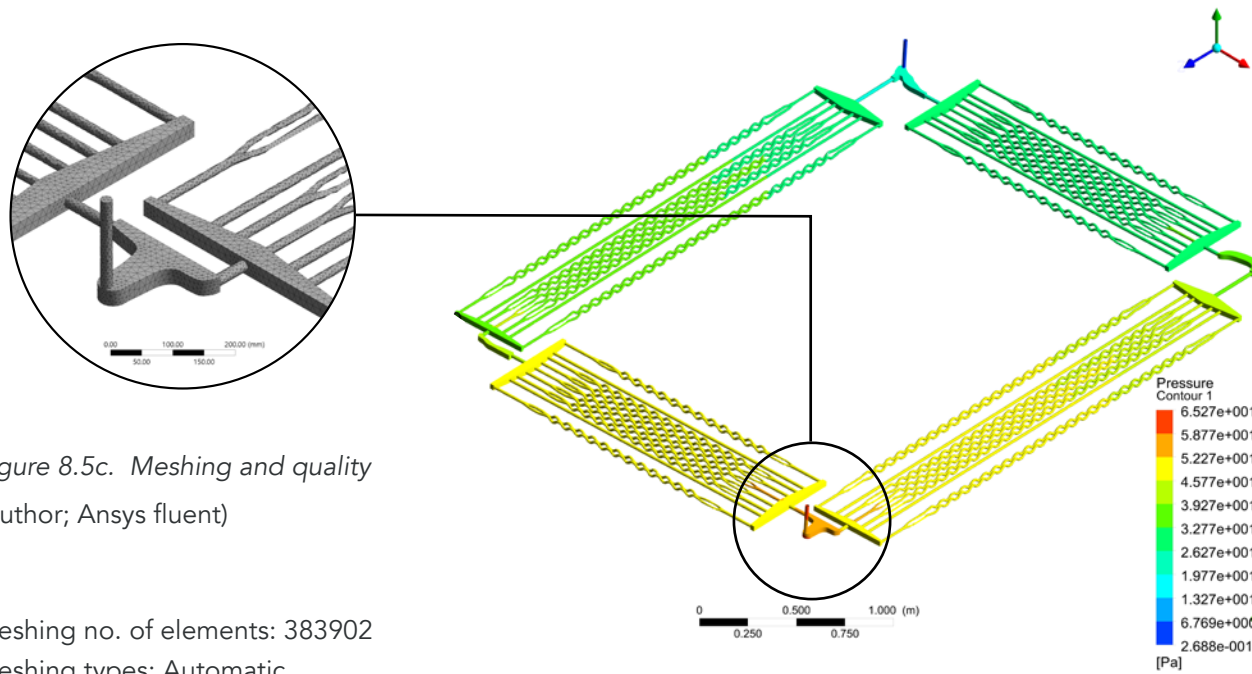


Figure 8.5c. Meshing and quality (Author; Ansys fluent)

Meshing no. of elements: 383902  
 Meshing types: Automatic  
 Quality: Medium  
 Min size: 7.0 mm  
 Max size: 700.00 mm

Viscous model: k-epsilon  
 Method: Spatial Discretization-  
 Least Squares Cell Based

No. of iterations: 200  
 $\Delta P$ : 1154.25 Pa  
 Convergence cycle: NA

No. of iterations: 2000  
 $\Delta P$ : 1319.67  
 Convergence iteration: NA

flat plate zone

Convergence exponential: e-03  
 Simulation time: 1hr 2 minutes

Figure 8.5d. Pressure of boundary domain (Author; Ansys fluent)

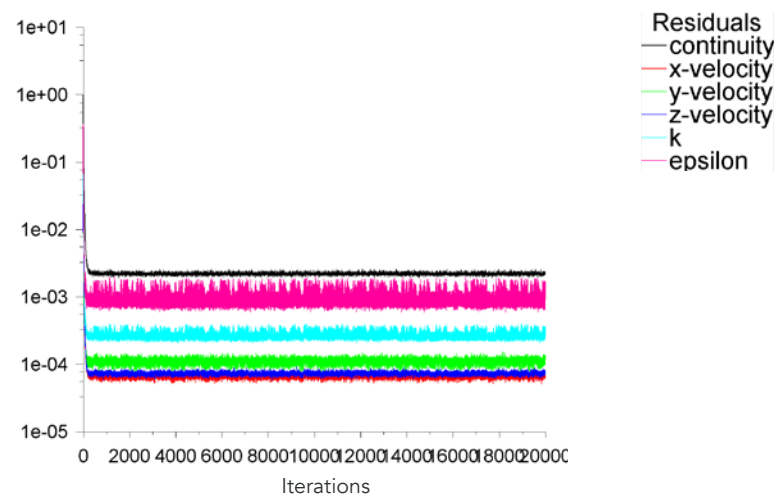
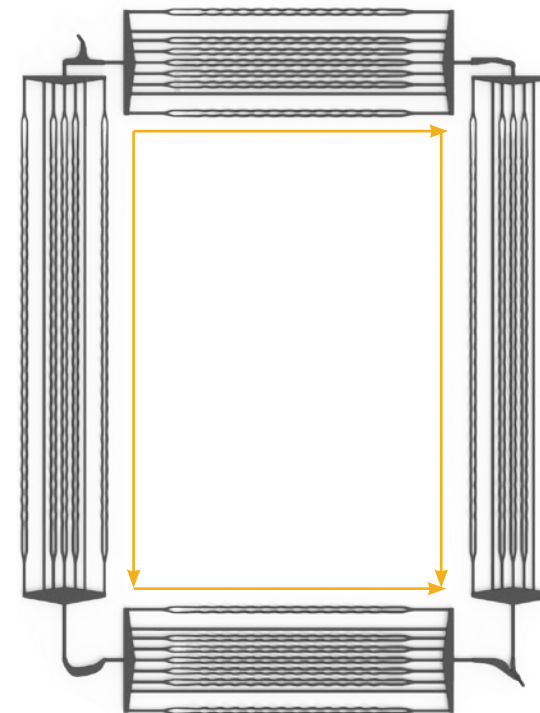


Figure 8.5e. Graph for 2000 iterations for CFD of geometry 06 (Author; Ansys fluent)

## 8.1.8 Downstream and upstream of network

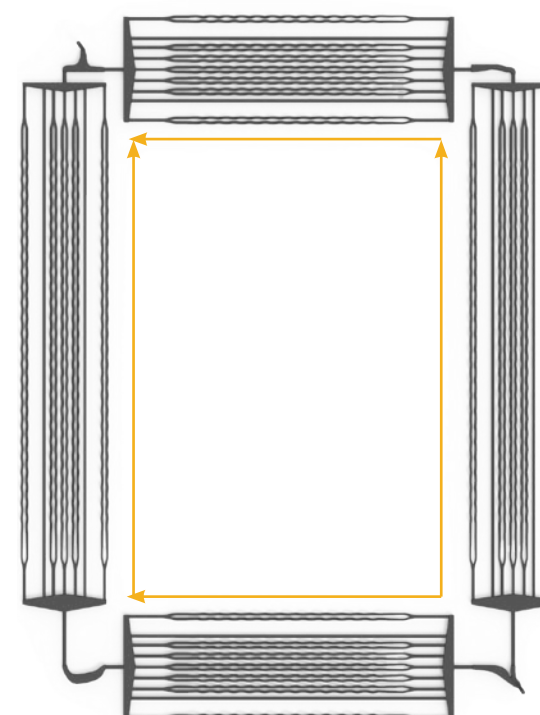
As the design depicted by the tubular network geometry 06 terminates the process of design of the downstream network within the external panel, the design of the tubular network geometry of the internal panel has been modified in accordance to the direction of the upstream water flow. The comparison of the difference in the geometry of the downstream and upstream network is shown below. The pressure drop along the inlet and outlet of these two different geometries vary marginally and can be overseen.



### Downstream network

The downstream network is embedded within the external panel. The fluid in this network flows from top to bottom in the direction shown in the figure. The diameter of the split tubes increase from left to right and top to bottom form 10-15mm in accordance to the direction of the fluid flow to minimise pressure drop

Figure 8.6a. Downstream geometry showing direction of fluid flow. (Author)



### Upstream network

The upstream network is embedded within the internal panel. The fluid in this network flows from bottom to top against gravity in the direction shown in the figure. The diameter of the split tubes increase from right to left and bottom to top form 10-15mm in accordance to the direction of the fluid flow to minimise pressure drop. The pressure drop difference between the optimised downstream and upstream tubular network is very minimal.

Figure 8.6b. Upstream geometry showing direction of fluid flow. (Author)

### 8.1.9 Comparison of Network geometries

The amalgamation of all the different methods adopted to increase the volume while minimising the pressure drop across the geometry has been summarised in a comparative chart in table 8.3. The standard network geometry here is considered to be the one after being constrained by the dimensions and boundary conditions of the facade panel, fabrication method, fixture and structural considerations.

Network Geometry	Change in diameter	Chanel network	Tube profile	Node optimisation	Total Network volume	Change in volume	Total pressure drop	Change in pressure drop
1	○○○	⊥		×	20.6 litres	NA	1235.34 Pa	Na
2	○○○	⊥		×	22.53 litres	+ 9.2 %	1167.96 Pa	+ 5 %
3	○○○	⊥		×	30.13 litres	+ 46 %	1332.34 Pa	+ 7.8 %
4	○○○	⊥	~	×	31.25 litres	+ 51.4 %	1463.10 Pa	+ 18.4 %
5	○○○	⊥	~	×	29.41 litres	+ 42.7 %	1319.69 Pa	+ 6.8 %
6	○○○	⊥	~	✓	28.11 litres	+ 36.4 %	62.51 Pa	- 94.9 %

Note: Change in pressure drop and volume is in reference to network geometry 01.

Table 8.3. Change in configuration, pressure drop and volume of different network geometries. (Author)

### 8.1.10 Improving heat transfer by optimisation & modification

With the inner geometry of the tubular network in place, the improvement of the heat transfer conducted between the panels was considered and to do the same topology optimisation of the combined geometry of the external internal panel along with the tubes were carried out. By doing so, the surface area of the outer facet of the external panel was increased which being directly proportion to the conduction of heat was also increased by the same fraction. It was found that while the winter solar radiation on the outer facet of the flat external facade panels was higher than that of the optimised panel due to mutual shading of the micro geometries, it favoured the flat panel in receiving the direct sunlight. But due to the similar reason the summer solar radiation for the optimised facade panel was lower than that of the flat panel bringing an advantage to the former panel in resting overheat of the panel under summer sun. The radiation analysis and the surface area of the flat panel to that of the topologically optimised external facade panel are shown in figure 8.7:

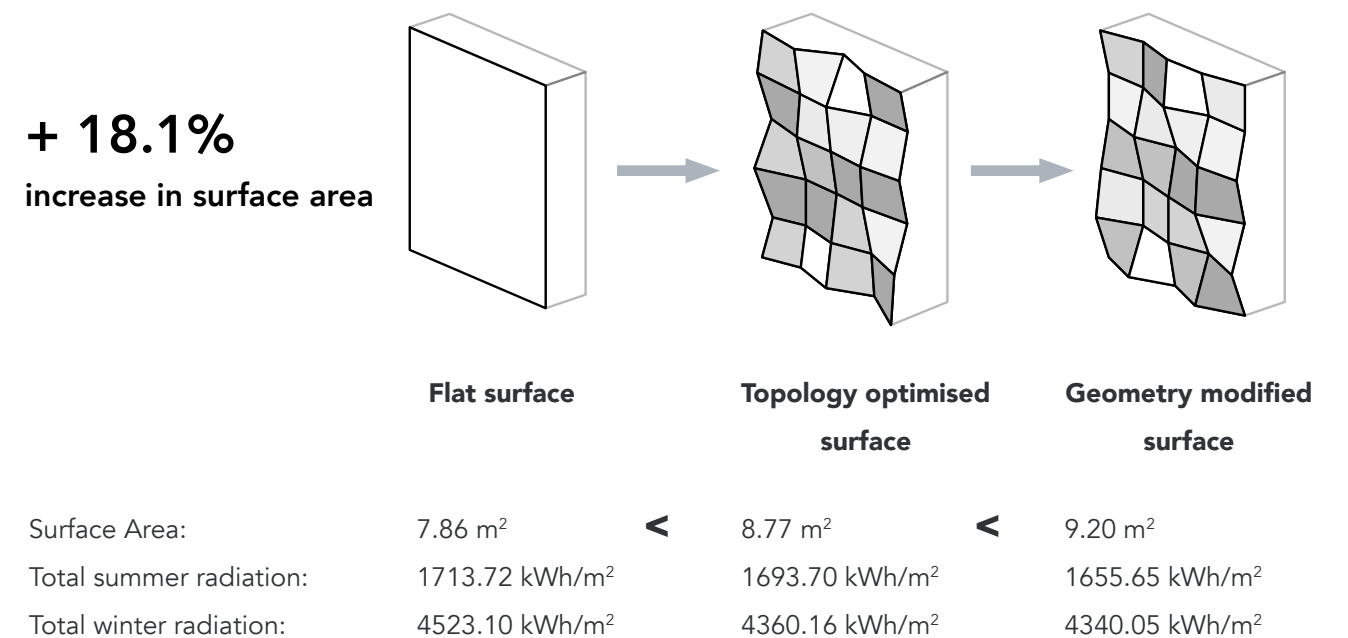


Figure 8.7. Change in surface area and radiation from a flat surface to the final surface geometry of the external facade panel to enable higher solar heat entrapment. (Author)

The constraint for the external panel for topology optimisation was limited to only the external facet and other constraints to be able to be cast in a form work for the modified geometry. The internal panel by other means was also limited to be optimised only for the external facet to eliminate daily internal maintenance and to be complied with form work for fabrication. In contradiction, the footing volumes of the internal panel was allowed to be optimised as they would be covered under the flooring and the ceiling boards and need not be considered for daily maintenance. The final geometries of the optimised external and internal facade panel are depicted herewith.



Figure 8.8. Front view of optimised external panel. (Author)

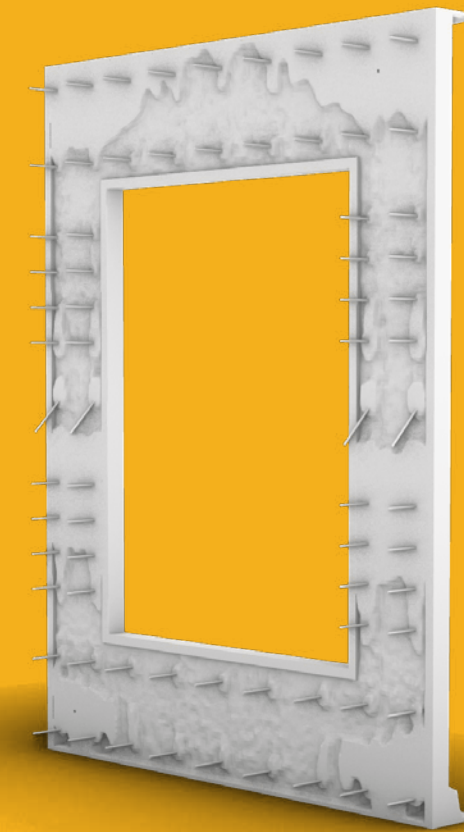


Figure 8.10. Front view of optimised internal panel. (Author)

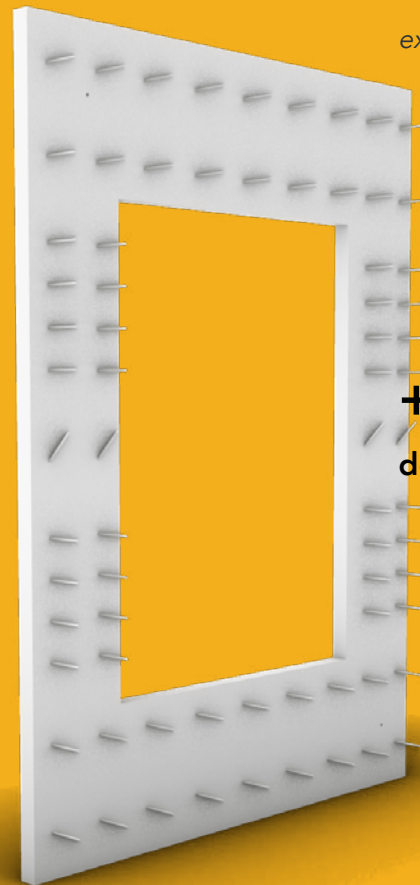
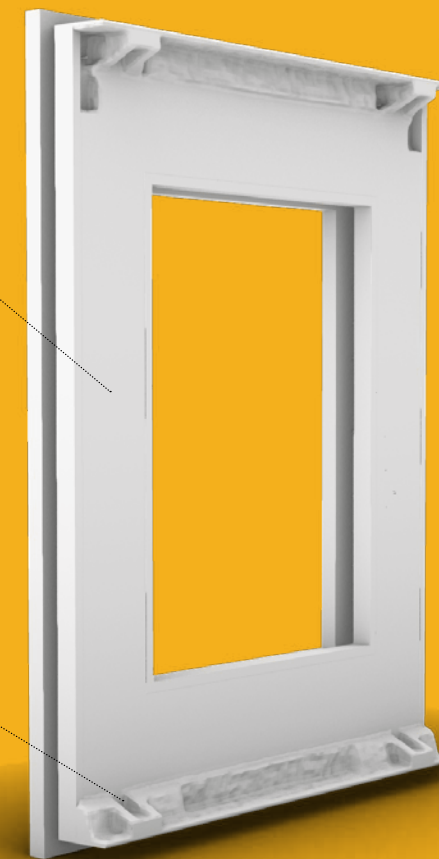


Figure 8.9. Back view of optimised external panel. (Author)

Constrained for flat inner surface



+ 20.7 % decrease in volume

Figure 8.11. Back view of optimised internal panel. (Author)

### 8.1.11 Improving insulation of the panel

While the increase in surface area as a result of the modified geometry of the panels does effect the conduction and the solar radiation behaviour of the topologically optimised panel to that of a flat panel, another aspect that matters a most was that of the insulating behaviour of the panel as that of the flat counterpart and hence were put to comparison in critical sections of the modified geometry. From the different simulations run in Therm and ladybug was evident that the optimised panel has an edge over the flat panel in terms of high insulating value in combination for the opaque sections. While the flat panel did have a value of  $0.47 \text{ W/m}^2\text{K}$  which was complaint with the ECBC norms of India, the optimised panel at a value of  $0.42 \text{ W/m}^2\text{K}$  is complaint with the ECBC+ norms. The fenestration part of the facade delivers an U- value of  $1.88 \text{ W/m}^2\text{K}$  and the combined value of a single facade panel accounts for an U-value of  $1.118 \text{ W/m}^2\text{K}$ . A comparative analysis of the therm simulations of a regular facade section to that of a topologically optimised facade section with  $0.95 \text{ W/m}^2\text{K}$  are depicted below.

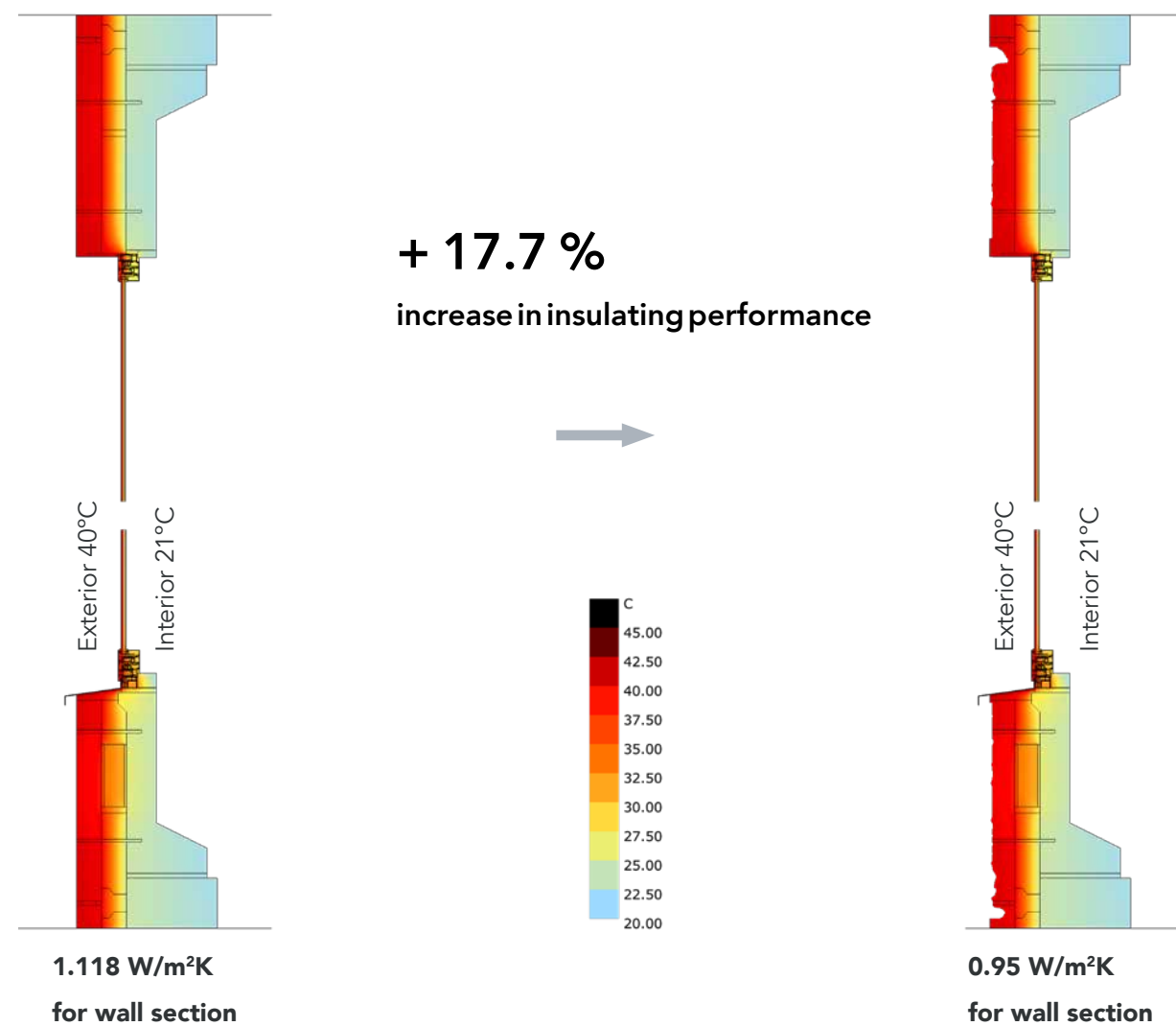


Figure 8.12a. Thermal transmission simulation of a section of flat facade panel. (Author; Therm 2D)

Figure 8.12b. Thermal transmission simulation of a section of topology optimised facade panel. (Author; Therm 2D)

### 8.1.12 Heat transfer and efficiency

With the first target set to maximise the volume of the water inside which increases the thermal entrapment within in order to maximise the transfer of heat between the internal and external panel. According to the simulations done, it was evident that the increase in the volume of water by 36.4%, the energy transfer increases by 39.7%.

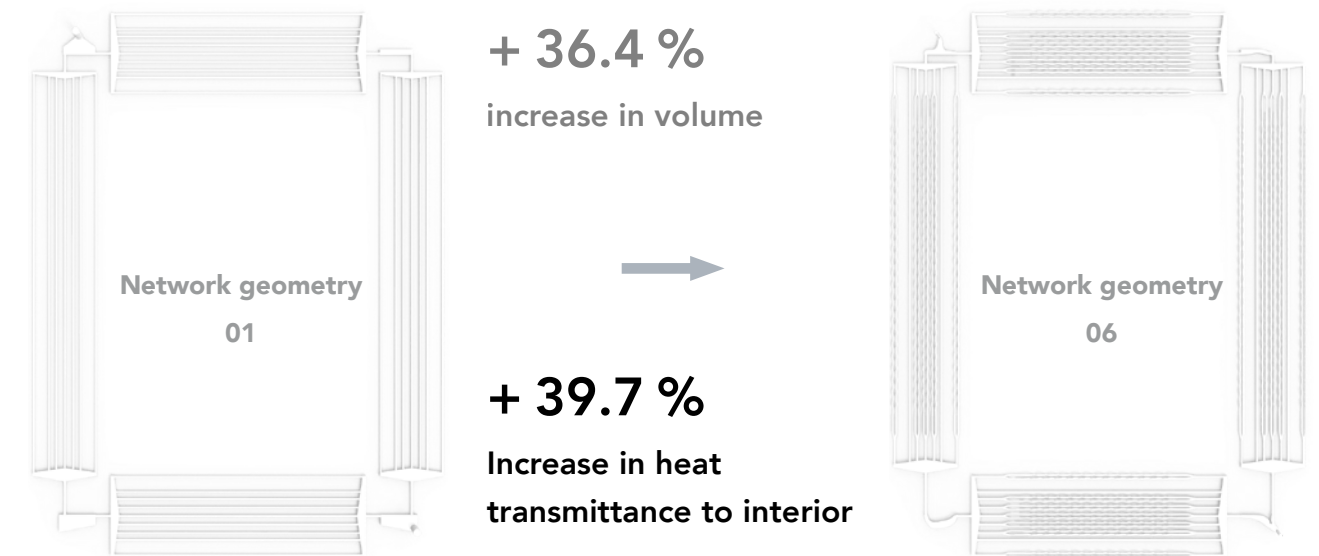


Figure 8.13. Increase in heat transmittance due to increased volume of void tubular network. (Author)

The second target to increase the surface area of the outer surface of the external panel, it was analysed that the increase in surface area corresponds to an increase in the heat captured by 3°C. This signifies that by an improvement of surface area by 18.1% an increment of around 9% in temperature of the water inside the external panel could be achieved.

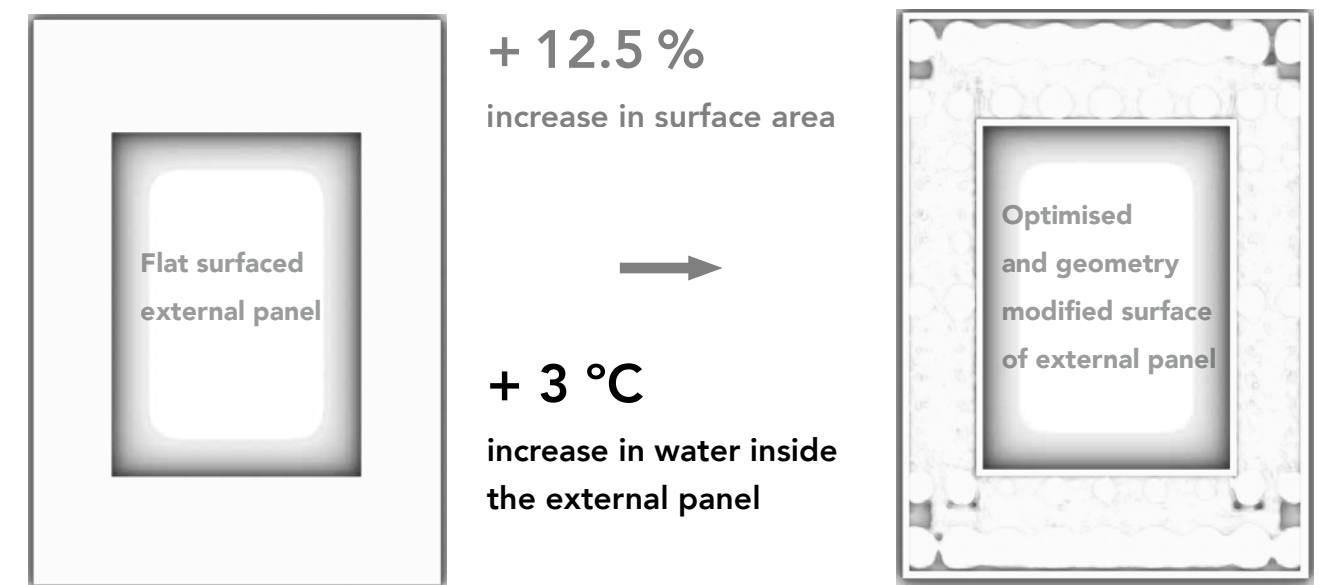
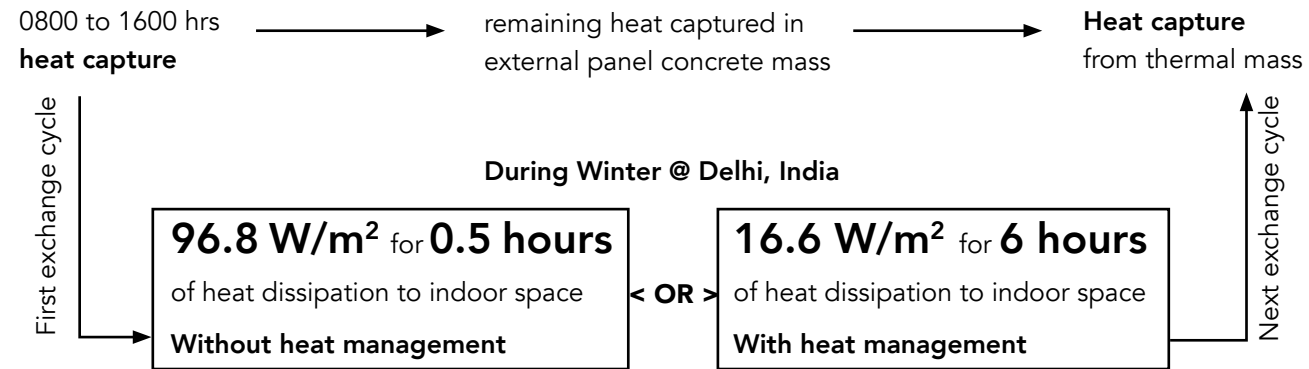


Figure 8.14. Increase in water temperature within external panel due to increase in surface area of outer surface of external facade panel. (Author)

The capacity of the heat exchange captured by the water inside the tubular network can be simplified to the following instances:



### 8.1.13 Materials and fixtures selected

In order to accomplish the above mention insulating value of the facade panel, considerations in terms of material were made with a goal of eliminating the need of high embodied energy materials such as steel and adopt more sustainable materials viz., fibre based reinforcements etc. A summarised list of the materials and fixtures sorted for the design of the facade panel along with their reason of selection are listed below, while more detailed specifications of these materials and their use are already discussed in sections 6.1 and 7.8.

#### 1. Reinforcement dowels

Product: Schöck Isolink TA\_H and TA-D

Specification: 12mm diameter

Material: Glass fibre reinforced polymer (GFRC)

Reason of selection: Non metallic based with very high thermal resistance which eliminated the thermal bridge, corrosion free, slimmer concrete cover, sustainable alternative.

#### 2. Reinforcement mesh

Product: Solidian Grid Q142/142-CCE-25

Specification: 142 x 142 grid, 25 mm wide, 2.5 mm thick

Material: Carbon fibre composite

Reason of selection: Low thermal conductivity than steel mesh reinforcement, eliminates corrosion, slimmer concrete cover, thin profile allows higher degree of freedom for topology optimisation, sustainable alternative.

#### 3. Window section

Product: Schüco AWS75 SI+

Specification: 75 mm front profile

Material: Aluminium

Reason for selection: Tilt and turn window suitable for office typology, for double or triple glass accommodation, highly insulated performance with thermal breaks in comparison to other sections, able to be serviced from

the inner floor space of building that eliminated need for building maintenance scaffolding.

#### 4. Glass panel

Product: Saint Gobain Planitherm PLT T

Configuration: 6-12-6 mm configuration with Argon filling, neutral colour shade

Reason for selection: Scarce or unavailability of triple pane glass in India, highest possible insulating value for double pane glass with maximum visible light transmittance of 74%, adequate performance and cheaper in comparison to triple pane glass.

#### 5. Concrete

Product: Weber Beamix with fibres by Saint Gobain

Configuration: Concrete mix with glass fibre of thickness 50 microns and length 6mm

Reason for selection: Availability, very high fracture resistance, high compressive strength with smooth finish and relatively low density than regular concrete.

#### 6. Facade brackets

Product: Hook-head toothed straps by Damilano group's Technogrip

Configuration: 40/22/2.5 (refer section 6.1.2)

Reason for selection: Very high load carrying capacity of 8.5 kN (safety factor=3) and 11.5 kN (safety factor=2) satisfying the load to carry for the designed facade panel.

#### 7. Fabrication material (inner formwork)

Product: Print2Cast 3D Filament Wax by Machinablewax Inc.

Configuration: 3D Printable wax @ extrusion temp 150-160°C

Reason for selection: Printable for complex shape, melt out from concrete resulting in voids within mass, recyclable (by melting and re-stranding).

## 8.2 PATH DEPENDENCY ANALYSIS

Starting from the phase of decision making of the materials to be chosen from the literature review, to the understanding of the fabrication method, availability of desired materials, selection for prototyping while deciding for real world application, behaviour of materials, behaviour of the design, understanding of physics and simulations to design-optimize-upgrade and analyse the efficiency of the final design done to achieve the maximum of its capacity. The involvement of the various different simulation methods to verify the cohesive behaviour of the designed system within the facade panels was a crucial path undertaken which relates to respective physics and methods of deriving the final design of the project.

To summarise all the results derived and the path considered in this process of designing and optimising the concrete facade panels has been depicted with the help of a table 8.4.

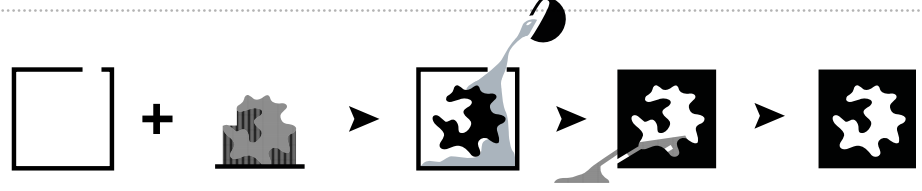
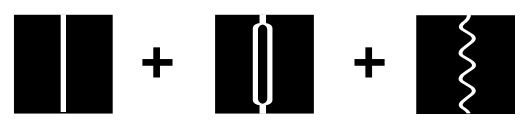
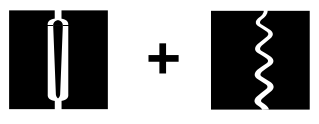
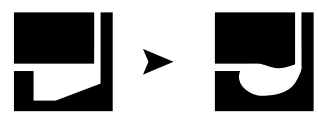
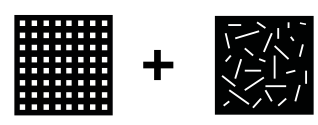
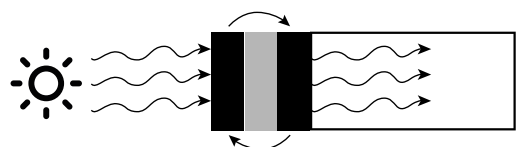
<p><b>Criteria 1</b></p> <p>Material selected: CONCRETE, WATER &amp; WAX</p>		<p>Basic built materials chosen were concrete for the panel mass, water as the fluid for heat exchange within the void tubular network concealed in the mass of concrete. Printable wax filament was chosen for developing the form-work inside the concrete.</p>
<p><b>Criteria 2</b></p> <p>Type of facade panel: TWIN WALL- NON LOAD BEARING</p>		<p>Non load bearing facade with twin panels and insulation fixed by 4 points was chosen to maximise the insulation performance as well not to act as the structural system of the building to enable future facade maintenance and upgradation, increasing life span of the building.</p>
<p><b>Criteria 3</b></p> <p>Fabrication method INVERSE INVESTMENT CASTING</p>		<p>Inverse investment casting with two form-work: the internal for the void of the tubular network and the external to cast the mass of concrete. The internal form-work was 3D printed with wax and melted out by boiling the combined mass inside pressurised water at temperature &lt; 120°C.</p>
<p><b>Criteria 4</b></p> <p>Maximising volume SPLITTING + CURLING</p>		<p>Volume of void tubular network was maximised by splitting single tube into two and curling tubes along the section allowing higher volume of water resulting in higher amount of heat exchange between the two panels. The final volume of water inside the panels is about 28 litres with an increase of 36.4 % to basic geometry.</p>
<p><b>Criteria 5</b></p> <p>Minimise pressure drop MODIFY TUBE DIAMETER</p>		<p>Maximising the volume increases pressure drop in the tubular network. To minimise the pressure drop the individual tubes were modified with varying diameters depending on their parallel layout, varying the diameter from 10 to 15 mm along the length of single tubes.</p>
<p><b>Criteria 6</b></p> <p>SHAPE OPTIMISATION</p>		<p>The nodes of network were also optimised for their shape using ANSYS fluent to optimise the shape for minimum pressure drop only across the nodes. The optimisation was done for water and molten wax combined as the fluid. Final pressure drop is 62.51 Pa with a decrease of 94.9% to the base geometry.</p>
<p><b>Criteria 6</b></p> <p>Increase efficiency IMPROVE INSULATION</p>		<p>Materials without metal content viz, glass fiber dowels &amp; carbon fibre mesh were used to reinforce the panels and fixtures of high thermal insulating value were used for higher performance. Topology optimised opaque surface with mutual shading, achieved ECBC+ norms and final facade U-value of 1.12 W/m<sup>2</sup>K by THERM 2D.</p>
<p><b>Criteria 6</b></p> <p>TOPOLOGY OPTIMISATION</p>		<p>Maximising heat entrapment within external facade panel by increasing surface area, maximised by performing topology optimisation of the surface using FUSION 360 and modifying the geometry to further maximise surface area with similar solar radiation using OCTOPUS. Final surface has 18.5% increase over flat surface.</p>
<p><b>Criteria 7</b></p> <p>Evaluation HEAT EXCHANGE</p>		<p>Heat transfer from environment to water inside external panel achieves a peak temperature of 37°C and heat transfer from water (26°C) to indoor (17°C) transmits 98 W//m<sup>2</sup> in 30 minutes. If water flow is conditioned and slow-pace exchanged between panels, energy need of 300W/m<sup>2</sup> could be met for two working shifts per day.</p>

Table 8.4. Details showing the path chosen for this project. Source: author.

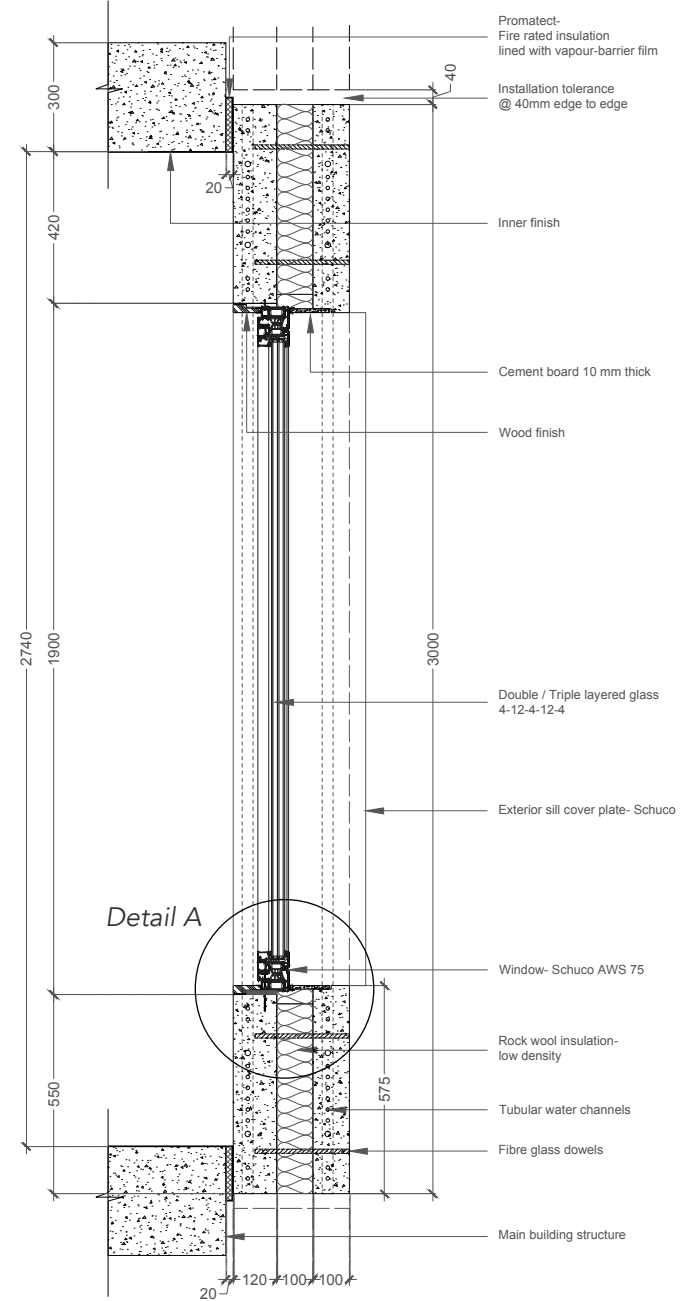
This page is intentionally left blank.

# 9. DETAILS & PROTOTYPE

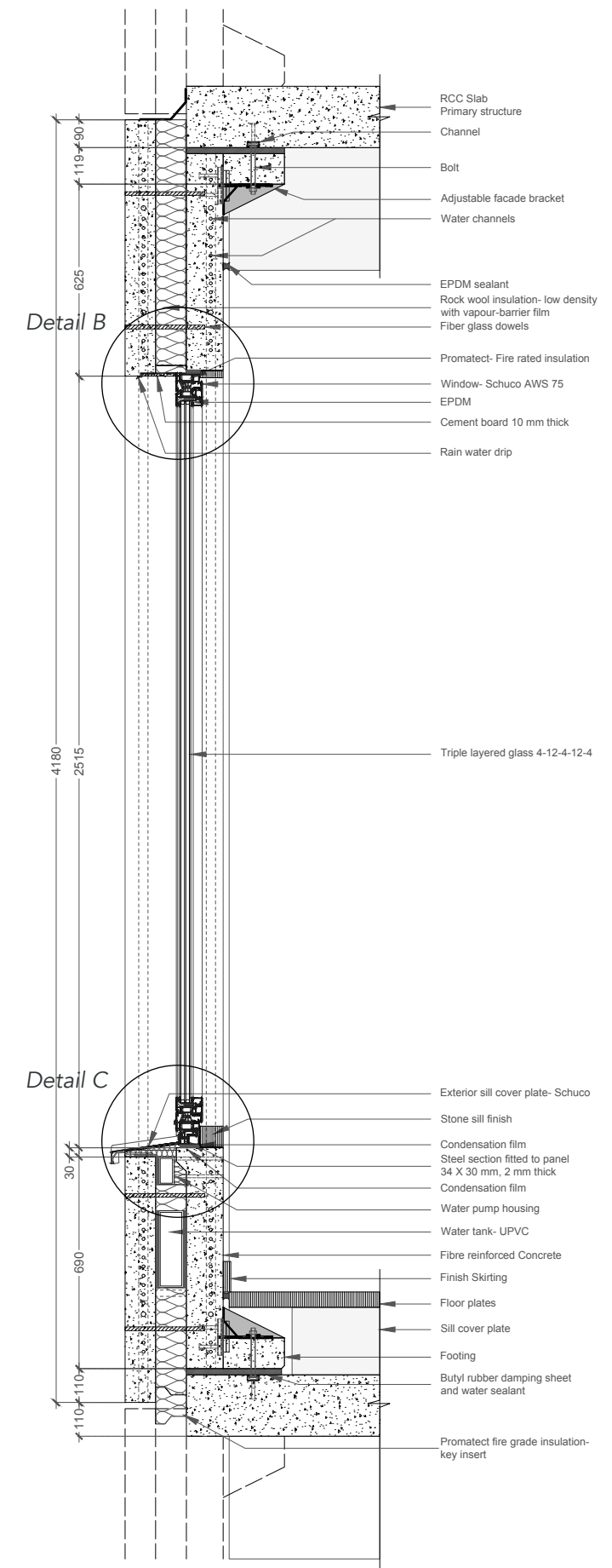
## *CHAPTER OVERVIEW*

This chapter is to reflect the details of the facade design and the method of fixing the facade panel. This chapter also depicts the prototypes made for the analysis of the final proposed design.

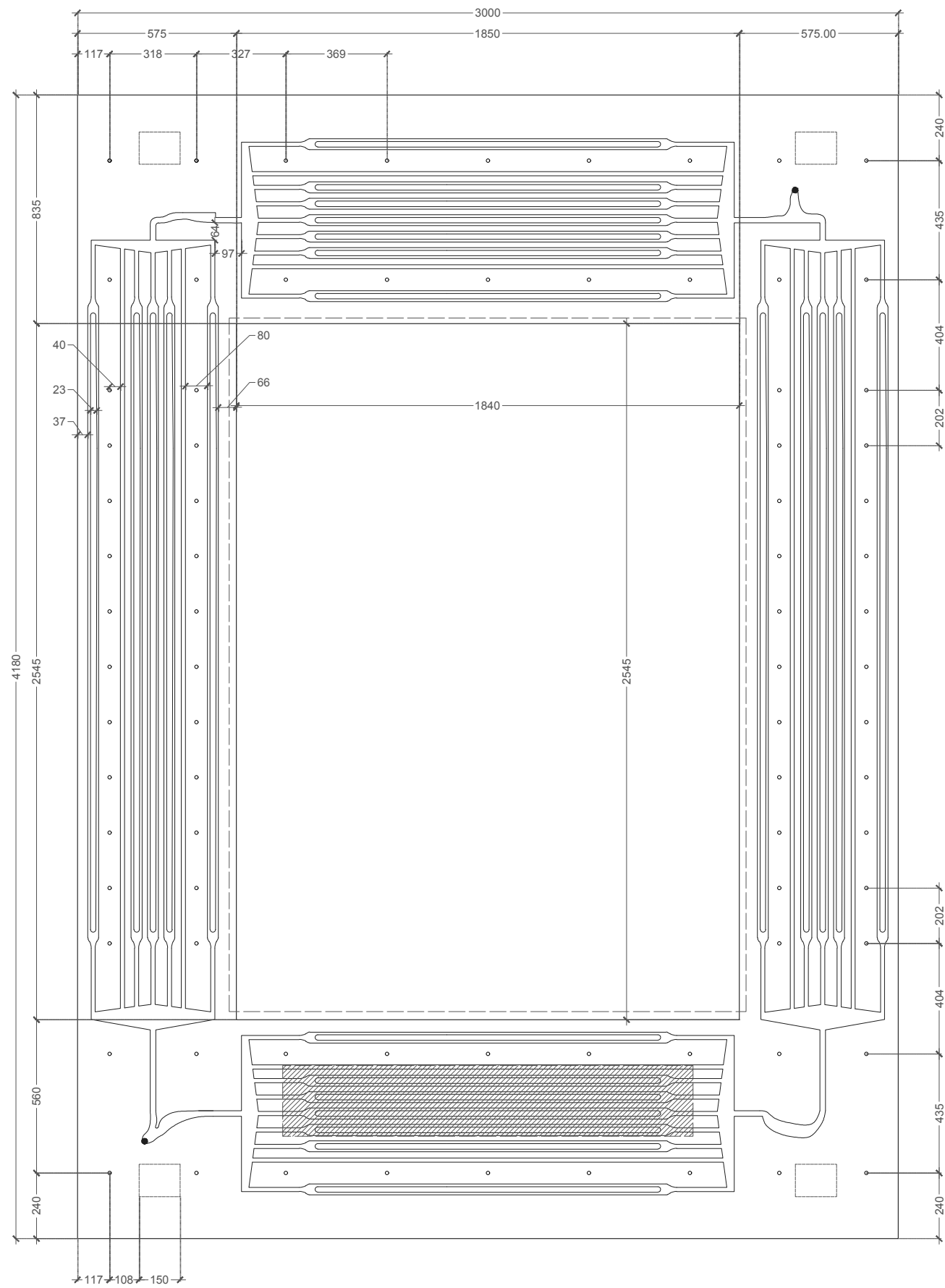
# 9.1 SCHEMATIC DRAWINGS



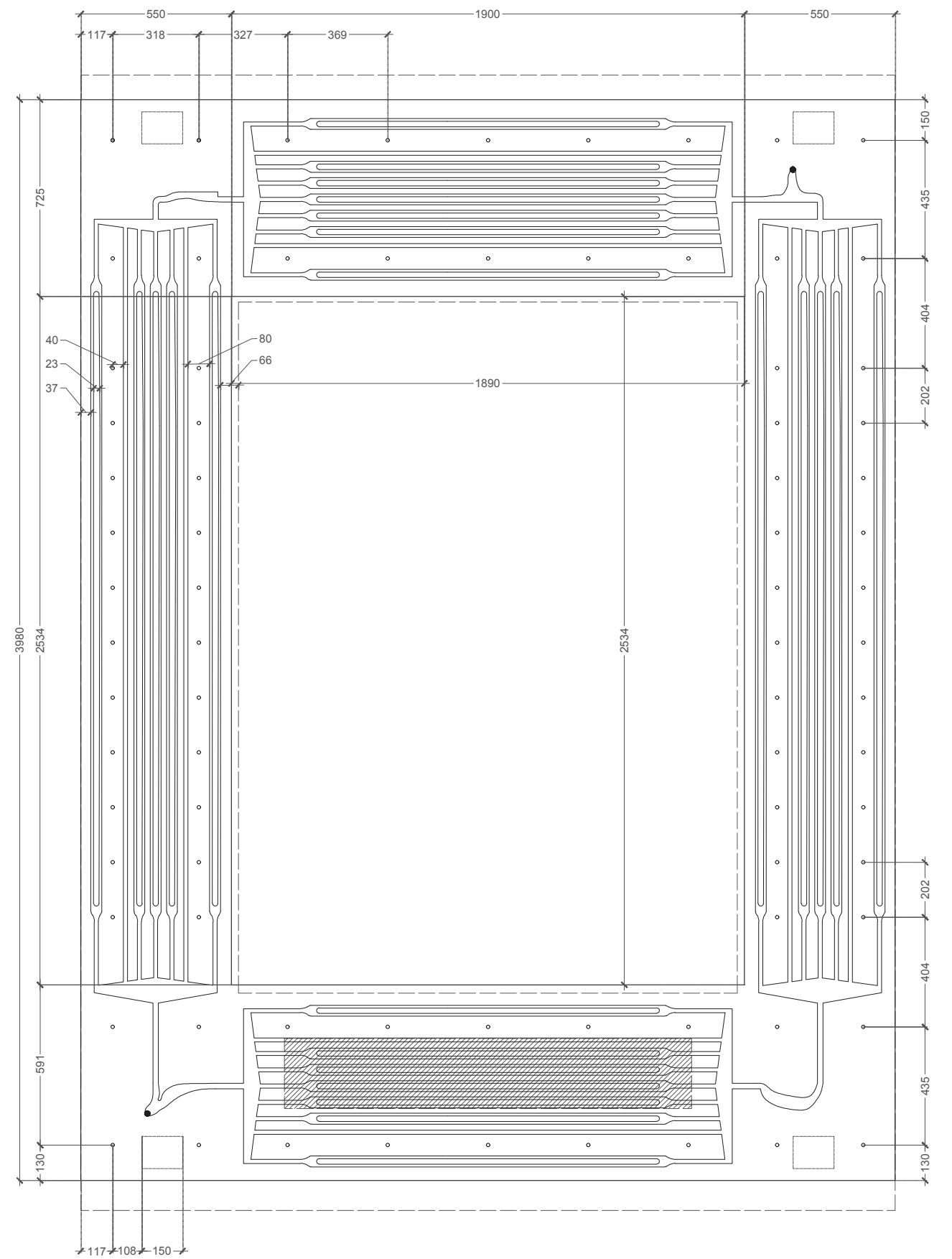
PLAN | 1:20



SECTION AA | 1:20

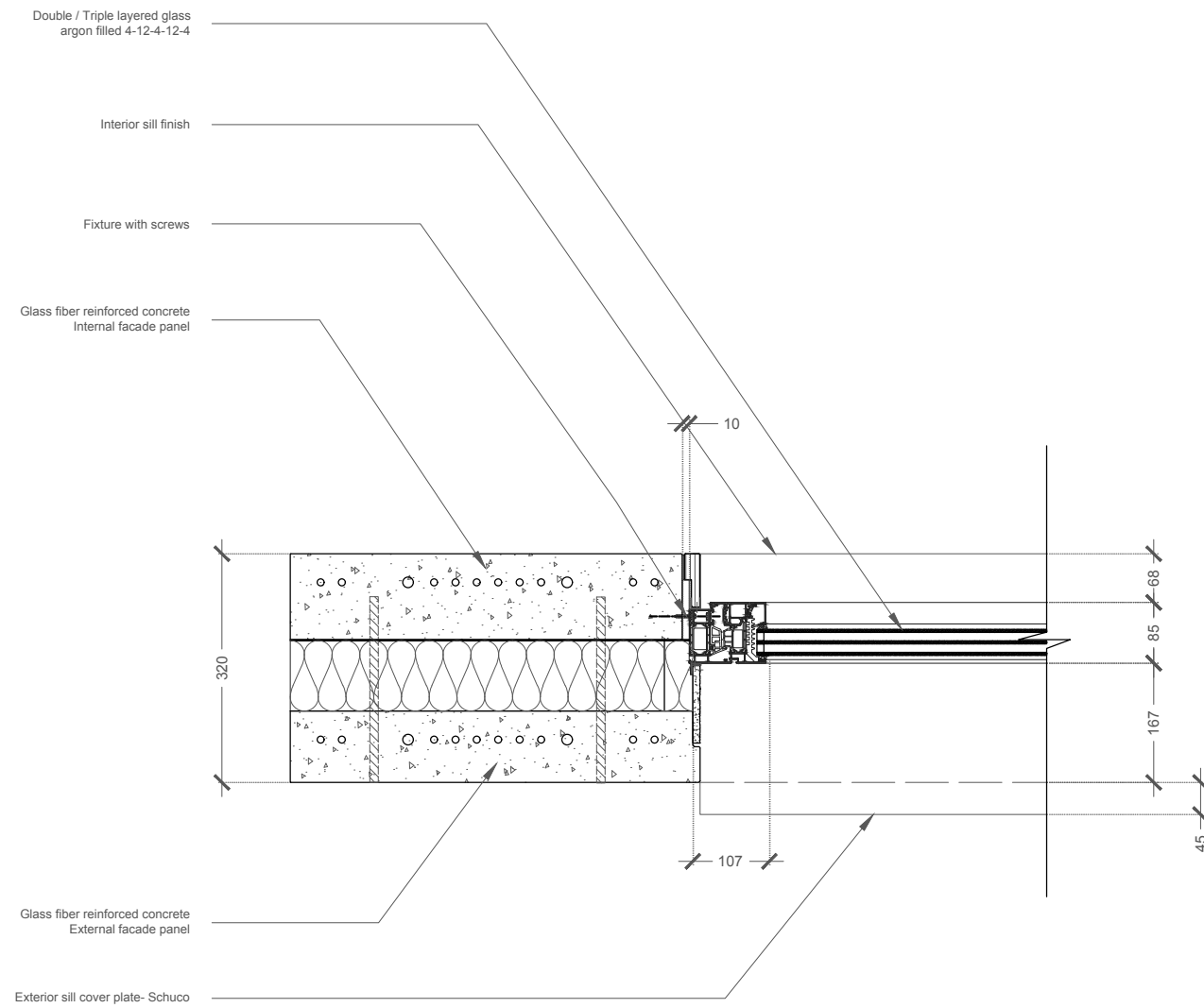


ELEVATION\_EXTERNAL PANEL | 1:20

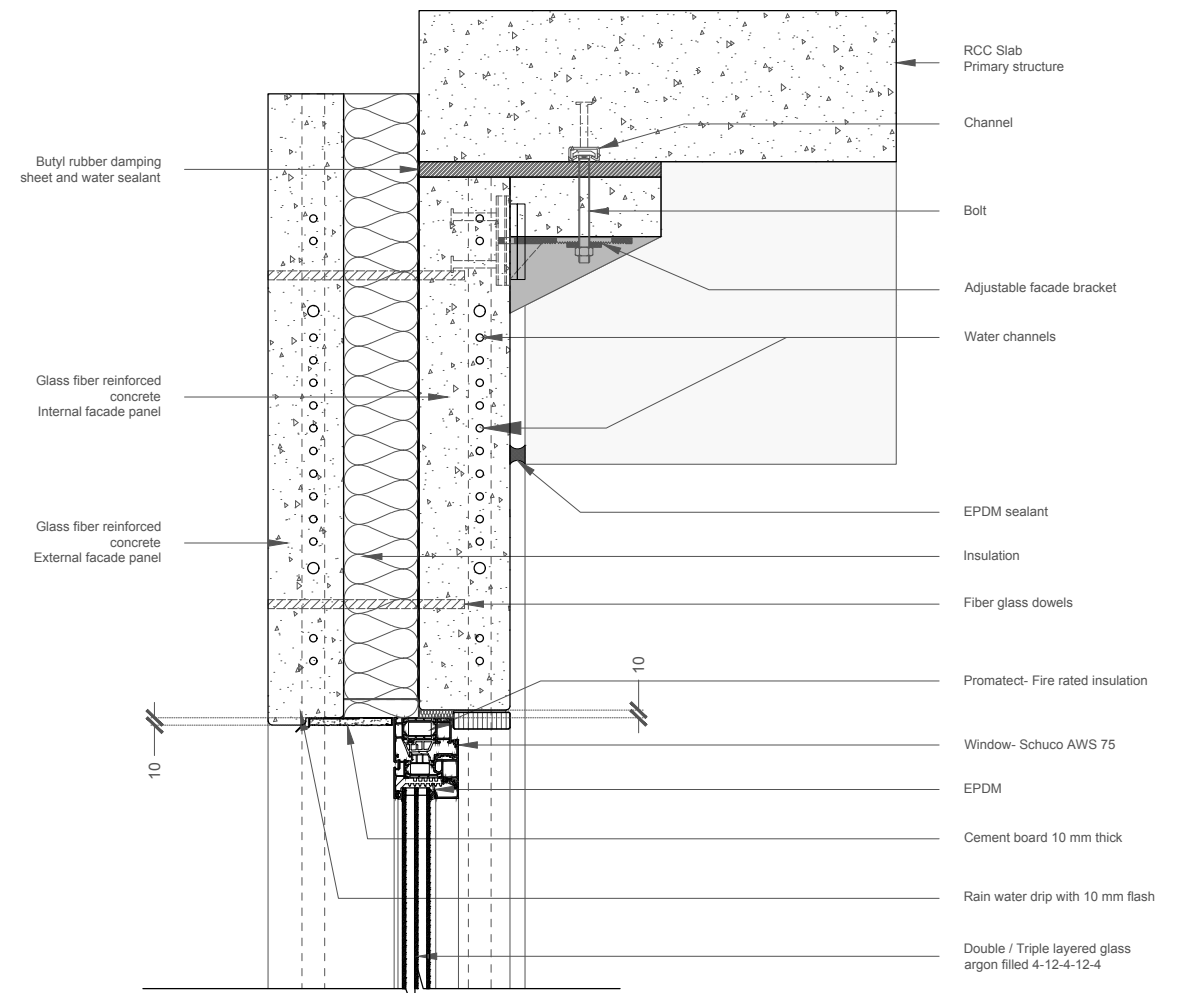


ELEVATION\_INTERNAL PANEL | 1:20

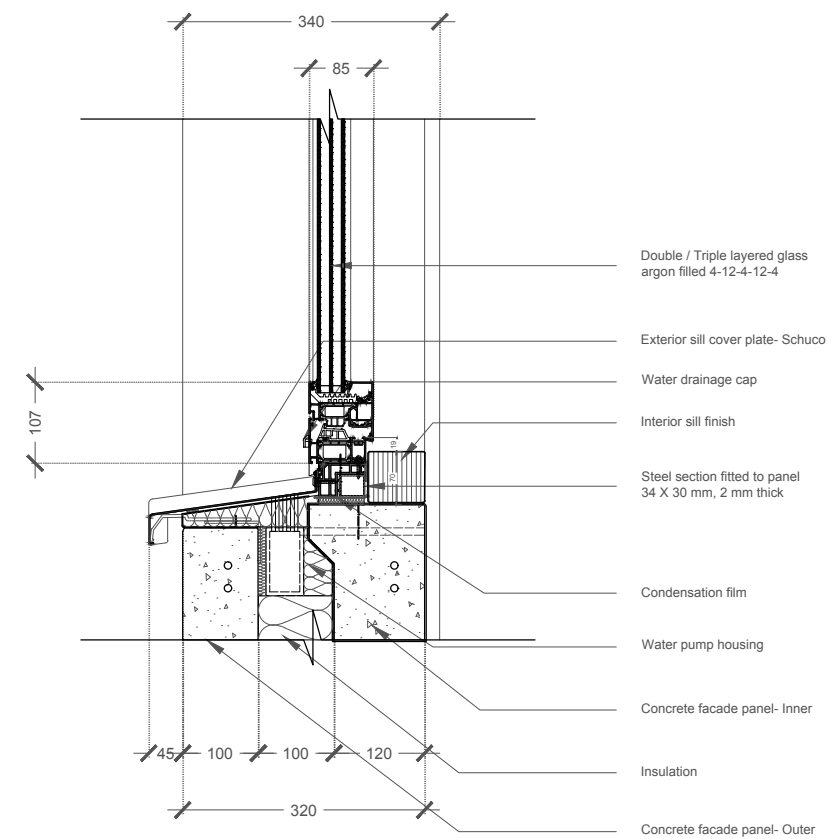
# 9.2 DETAILS



DETAIL A | 1:10

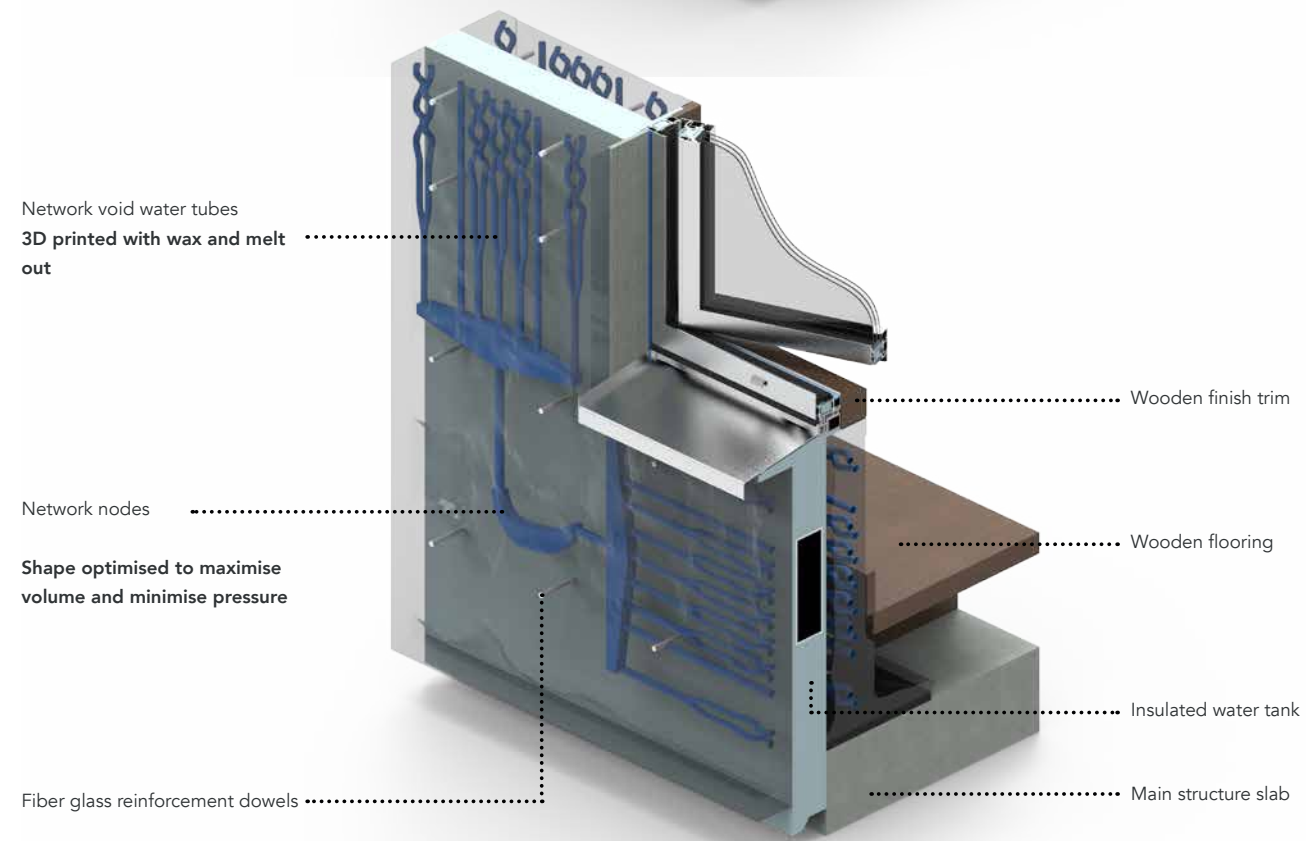
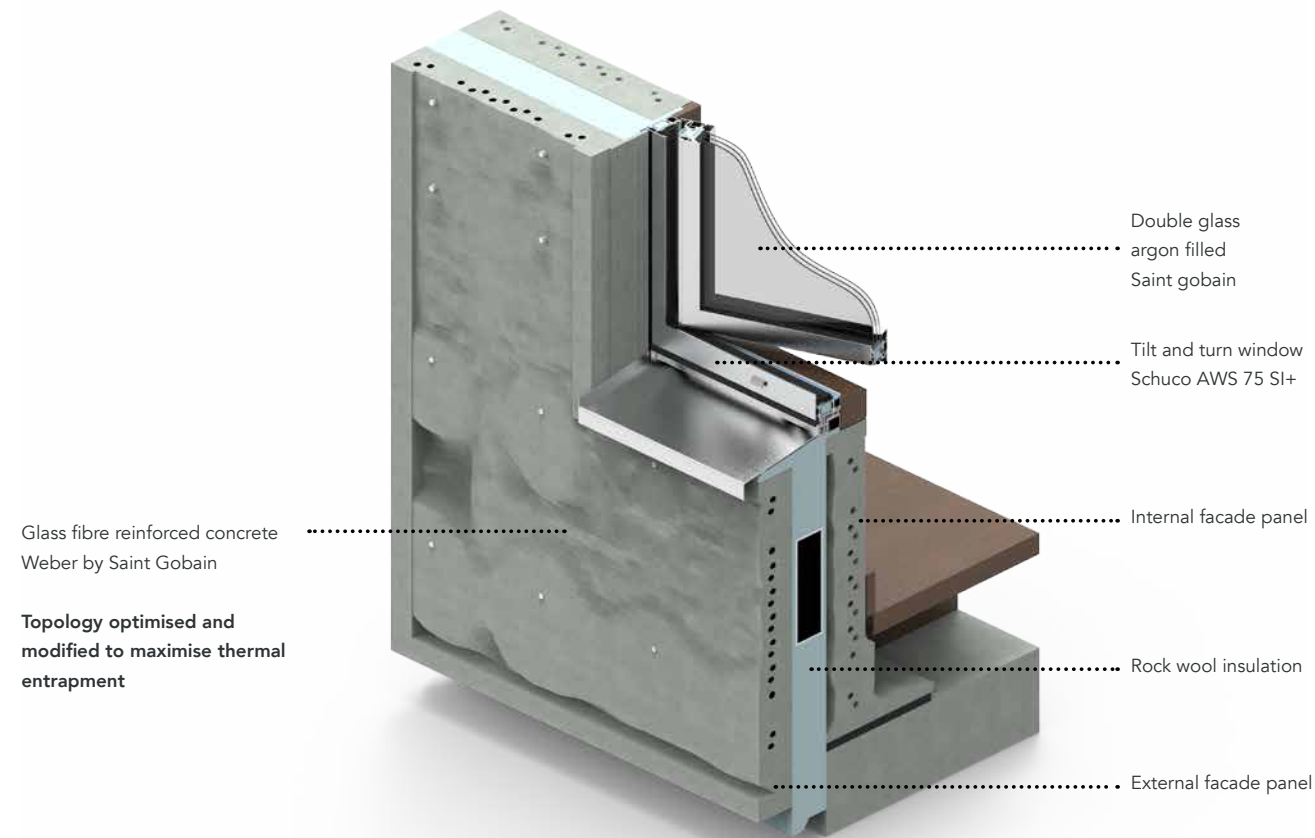


DETAIL B | 1:10



DETAIL C | 1:10

### 9.3 PHYSICAL PROTOTYPES



EXTERNAL PANEL WITH VOID TUBULAR NETWORK



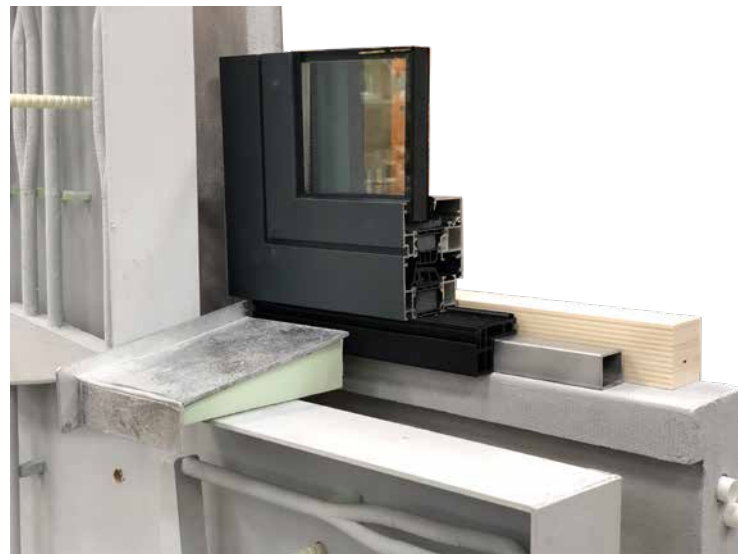
INTERNAL PANEL WITH OPTIMISED SURFACE



INTERIOR FACE OF INTERNAL PANEL WITH OPTIMISED SURFACE

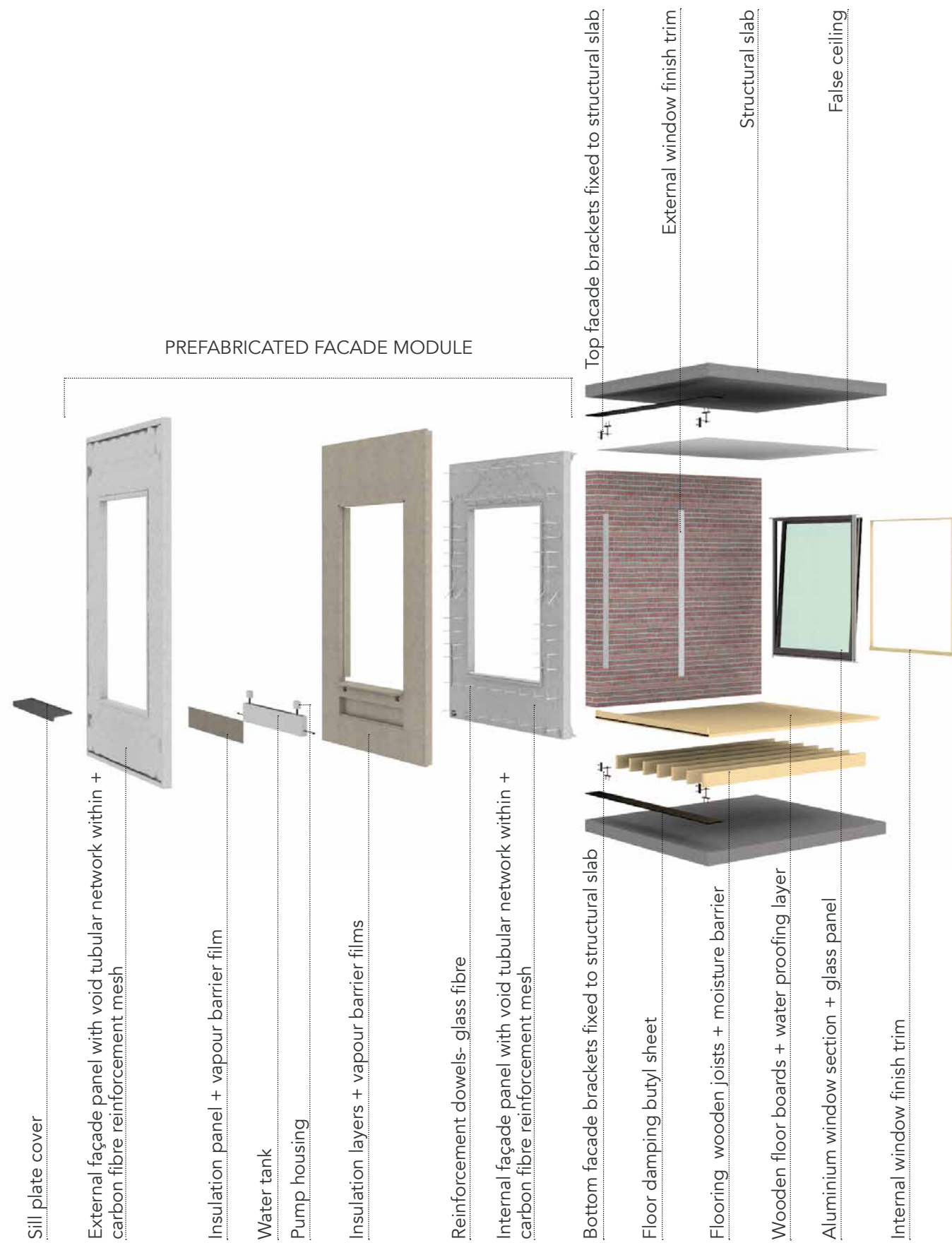


CAST CONCRETE FOR OPTIMISED SURFACE PATTERN



WINDOW FIXTURE

## 9.4 EXPLODED VIEW



## 9.5 ASSEMBLY SEQUENCE



The façade panel is pre-fabricated and transported to the built site. It is lifted to position by a crane using 3-point tilt-up system.

The upper section of the panel is put into place at 15° and fixed with a temporary bracket system to the top brackets cast within the panel.

The panel is then released from the crane and the bottom and the top sections are lined with butyl sheets and fixed permanently with brackets at 4 points.

The window, interior + exterior window trims and the inner finishes are laid out.

## 9.6 OPTIONS PER USE TYPE



FACADE PANEL WITH CENTRED WINDOW



FACADE PANEL IN HORIZONTAL RIBBON PATTERN



FACADE PANEL IN VERTICAL STRIPS PATTERN



INTERIOR OF THE FACADE WITH OPTIMISED SURFACE

This page is intentionally left blank.

# 10. CLOSURE

## *CHAPTER OVERVIEW*

This chapter concludes and discusses the end result of the research and development accomplished through this thesis. It also reflects upon the study made to approach the thesis as well as critics the hindrances faced during the project. The possible future aspects of this thesis concludes this chapter.

## 9.1 CONCLUSION

With the study made through this project, the selection of concrete as a material for developing countries like India and the function as a facade panel was made evident. The method of optimisation as a design tool is stated feasible for this project by studying the reliability of this tool in the infrastructure industry and implication. The result of such computation tools in manipulating the efficiency of functioning and reducing energy demand of a building while developing a language of architectural ornamentation in-sync to the current trend of technology in architecture is embraced. The development of the design language is developed in a cohesive manner and experimented depending on the studied constraints and availability of tools, materials and services. The possibilities of modern digital tools and the fabrication method have been studied, and its influence on the final design has been made evident with the referred projects and the approach with non-traditional way of manufacturing with existing technologies.

The realised projects in architecture and various different technological fields similar to the design and research ideology of the proposal have been studied, and inferences were derived. These inferences were extended to follow the demand by design and experimented, before applying the same or analysing for changes needed further for the research. The mentioned design inferences provide a framework for the initiation of the project research, tool selection and design of the final prototype that delivers the author's visualisation. The literature study does build a clear framework and design intent with selection of the scope for this thesis.

An elaborate study about the different aspects of a topic has been dealt prior to the shift in focus for the designing of the integrated function in the panel down the lane. The process of design was developed while exploring a large variety of possibilities in designing the same project while considering the aspects of applicability in further research of the design for advanced applications, viz., complex panel shapes or non linear facade panels. The design did consider the possible state-of-the-art technology and materials available by resources to explore the design while being constrained by the same technologies and materials to avoid unnecessary complexities and developing the design sustainably.

Various different software and design methods were experimented in order to simulate the behaviour of the integrated function in the design and the behaviour of the combination of the inlaid network geometry void to that of the mass of the panel, before the same could be considered for fabrication. While this method did introduce hindrances, in terms of capability of the software (along with the type of available license), the integration of them, justification of use of specific terms of these software, experimentation with materials and the method of fabrication and equipments, the path considered to analyse and approach the envisaged design for fabrication was successfully laid out. The final section of this thesis does discuss and compare the output of the various different stages of designing the facade with the integrated function to establish a comprehensive lookout of the project.

It was evident from the designing process of this thesis that with the help of computational tools the

behaviour of various different functions, in this case the flow of the fluid and the behaviour of the stresses along the facade panel, could provide effective solutions. These computation tools can help in maximising the efficiency of the function by analysing the possible pressure drops and micro turbulences in the designed tubular network by the help of CFD simulations and minimise the use of material while maximising efficiency by modifying the surface geometry through simulation for topology optimisation of a mass. With this design process it was also made evident that the use of software alone for simulation for specific purpose do not always solve the problem. Mitigating the behaviour and proper analysis could save time and resources which could rather be solved in a rather simple manner. This was the case with analysing the fluid flow in the junction in 3D which was simplified and analysed through a 2D simulation and the end result did perform as effective as that through the time consuming shape optimisation through 3D simulation, while this statement may not hold true for all events and design considerations.

While the designed facade panel was needed to be verified for fabrication, various methods and materials were explored and derived from the fields not related to architecture. The combination of various different experiments performed for the validation of the proposed method of inverse investment casting with an inlay for 3D printed wax and the concrete in combination, did result in a rather contemplating decision of proposing this method for commercial use. While this method and idea could be limited to the prototyping and proof making of the proposal, various different commercial methods could also be applied to the same while driving similar results and design concept.

The overall effectiveness of the designed project was evaluated by performing a heat exchange simulation in a broad manner and did provide a rather convincing result of energy transfer processed by the proposal. This energy exchange system for opaque facade segments can surely help in conditioning spaces around the globe (except extreme climates) and highly reduce the energy demands that takes a step forward for a more sustainable future.

## 9.2 CRITICAL REFLECTION

The designed facade panel with integrated heat exchange system does project ambitious results to be realised upon implementation but also does include some considerations to be made.

While the fluid flow within the panel is minimised for pressure drop and maximised for volume, the real world considerations of thermal effect on the behaviour of the fluid within may vary the envisaged results. Additional measures to manage the pressure and the thermal energy to develop an active heat exchange scenario between the panels is to be considered for a marketable commercial product.

Simulations verified the method of increasing the surface area to maximise the solar gain within the thermal mass of concrete. But this does contradict to the purpose of subtracting the material from the concrete mass

by topology optimising to achieve the surface with increased surface area, which in turn minimises the thermal mass used to capture the heat. The simulations did imply the same when the heat released by the optimised panel was faster than the standard panel.

The methodology followed in this project was dependent on various computation tools to derive the desired design target but was limited by the inter-compatibility within the flow of design derivation. Possible venture to combine the workflow into a simplified method could have been a coherent approach.

Limitation by the variables, algorithm and constrained domain selection in Fusion 360 for topology optimisation delivers a specific result in terms of aesthetic, limiting the choices and control for the aesthetics. It could be overcome by using custom algorithms for topology optimisation and/or defining boundary constraints to desired geometries. On the bright side, exploration and implementation of the digital work-flow involving different computation programs did evolve my skills and understanding of the various aspects to be considered and tackle the design.

With the limited knowledge and skills with thermal management of a building, the capacity calculation for the facade could be carried out only for a winter situation in an approximated manner. Moreover, the heat exchange simulation was performed to evaluate the design decisions, methodologies undertaken and verification of the capacity of the designed panel, which was never a target for this project conducted for a period of only 8 to 9 months. This simulation was even limited to the energy reading on the inner surface of the internal panel and not the air space, without considering convection, radiation, indoor occupancy, equipment and mechanical sources. Had there been an extended time-frame or the term of this thesis, in-depth evaluation and modification in respect to the thermal management would have been detailed out. The design and assessment made could establish a start point for a detail investigation of a similar project and carry forward.

## 9.3 FUTURE SCOPE

The ideology and the design intent of this may be further researched and made evident to be applied to different aspects viz., refurbishing the facade of an existing building if permissible by the structural configuration, use of industrial grade optimisation tools etc. The framework of the study has been specific to the scope and research framework specified at the start which may or may not be relatable to other location, typology, function element, material, design and fabrication tool. While this thesis does provide the overview of the considerations and experimentations made to design a similar facade panel with specific integrated function in the facade, further explorations may drive the way for further simplification of the approached method.

This thesis did not consider the exploration of the efficiency of the facade in terms of real-time heat exchange

from the exterior to the indoor environment and the exact reduction in the energy consumption of space while the required comfort level is achieved. While the designed facade aims at maximising the intended integrated function for heat exchange, the constraints and considerations related to the working efficiency of the system in terms of heat exchange per climate was not taken into account in this thesis and could be experimented further.

Some of the considerable factors for further research are mentioned below.

1. Possibility of fabricating a hollow geometry for the complex shape of the inlaid tubular network geometry developed to maximise volume and minimise pressured drop, to keep the fabricated hollow geometry without the need to print wax and flow out.
2. A possible way of coating the inlay of the tubular network, either by applying it on the wax print or by applying after the wax is flown out. The properties of the coating needed for the inlay applied to the printed wax needs to be of high melting or burning temp of 150°C to withstand the temperature while melting the wax out. It also needs to be thermally conductive for letting the heat transfer between the concrete mass and water within the tube and waterproof to avoid possible seepage of water into the concrete mass.
3. A similar study could be applied to a complex, non-planar, non-traditional facade panel and design a network structure on the basis of different parameters for the same to be applicable on a wide range of facade panels.
3. Overlooking the constraints by the software, some results could be prototyped by fabrication in 1:1 scale and studied the effect of the geometry for water flow
4. A similar study could be made for a prototype with a controlled internal and external temperature to analyse the exchange of heat and efficiency of the designed facade panel.
5. The method of simulation made could be analysed in a parametric manner and combine the different physics for a coherent design solution.
6. In-depth analysis of the thermal efficiency in different climatic conditions could be performed and necessary design inputs be derived for manipulating certain aspects of the design proposed.
7. Analysis for return of investment over time of the designed facade could be made that would access the energy saved for the conditioning space, reduction in maintenance cost and long term service of concrete over other low life cycle materials typically used for facade construction.

This page is intentionally left blank.

# 11. BIBLIOGRAPHY

- Ahmed, F., Deb, K., & Bhattacharya, B. (2018). Structural Topology Optimization using Multi-objective Genetic Algorithm with Constructive Solid Geometry Representation. Kanpur: IIT Kanpur.
- Alsamsam, I., P.E. Ph.D., Lemay, L., P.E., & VanGeem, M., P.E. (2008). Structures congress 2008 crossing borders. In Sustainable high performance concrete buildings (pp. 1-11). Reston, VA; American Society of Civil Engineers; 2008. doi:10.1061/41016(314)168
- Alston, M. E., & Barber, R. (2016, August 24). Leaf venation, as a resistor, to optimize a switchable IR absorber. Daresbury, United Kingdom: Scientific Reports.
- Altair OptiStruct™ Overview. (n.d.). Retrieved December 2018, from Altair Hyperworks: [altairhyperworks.com/optistruct](http://altairhyperworks.com/optistruct)
- Ameba. (2018). Topology Optimization Modeling- Ameba- User Manual. XIE Archi-Structure Design.
- Amelar, S. (2015). The Broad Museum by Diller Scofidio + Renfro. Retrieved from Architectural Record: <https://www.architecturalrecord.com/articles/7532-the-broad-museum-by-diller-scofidio-renfro>
- Andrews, P. (2006, March 4). York Minster façade. Retrieved from Flickr: <https://www.flickr.com/photos/mortimer/143388390>
- Archello. (2013). archello. Retrieved from Graphic concrete characterises apartment block tähytjää: <https://archello.com/project/ulappatori>
- Archiseb. (2018, December 5). food4rhino. Retrieved from Topos: <https://www.food4rhino.com/app/topos>
- Association, P. C. (2018, December 10). Ultra-High Performance Concrete. Retrieved from Cement.org: <https://www.cement.org/learn/concrete-technology/concrete-design-production/ultra-high-performance-concrete>
- Astbury, J. (2017, November 10). Feature: Just how sustainable is cross-laminated timber? Retrieved from The Architects' Journal: <https://www.architectsjournal.co.uk/buildings/feature-just-how-sustainable-is-cross-laminated-timber/10024485.article>
- Auburn. (2018). Retrieved from Historical timeline of concrete: <http://www.auburn.edu/academic/architecture/bsc/classes/bsc314/timeline/timeline.htm>
- Azmeem, N., & Shafiq, N. (2018). Ultra-high performance concrete: From fundamental to applications. Perak: Elsevier.
- Basulto, D. (2008, November 19). In Progress: 290 Mulberry / SHoP Architects. Retrieved from ArchDaily: <https://www.archdaily.com/9028/in-progress-290-mulberry-shop-architects>
- Beghini, L., Beghini, A., Katz, N., Baker, W., & Paulino, G. (2014). Connecting architecture and engineering through structural topology optimization. Chicago: Elsevier.
- Bendsoe, M., & Sigmund, O. (2003). Topology Optimization- Theory, Methods and Applications. Lyngby:

Springer.

- Bianchini, R. (2016, August 13). L.A. | Art wears a lace veil: The Broad Museum. Retrieved from Inexhibit: <https://www.inexhibit.com/case-studies/los-angeles-broad-museum-diller-scofidio-renfro/>
- BIS, B. o. (2016). National Building Code of India 2016. India: Bureau of Indian Standards.
- Boswell, C., Sarkisian, M., Clark, R., & Ball, A. (2006). St. Regis Hotel & Residences A Vibrant Gem in San Francisco's Fine Arts Center. PCI Journal.
- Bradley, D. (2010, April 20). TR10: Green Concrete. Retrieved from MIT Technology Review: [http://www2.technologyreview.com/news/418542/tr10-green-concrete/?\\_ga=2.107064641.2141111095.1546452753-979502326.1546452753](http://www2.technologyreview.com/news/418542/tr10-green-concrete/?_ga=2.107064641.2141111095.1546452753-979502326.1546452753)
- Bristogianni, T., Oikonomopoulou, F., Veer, F., Snijder, A., & Nijse, R. (2017). Production and Testing of Kiln-cast Glass Components for an Interlocking, Dryassembled Transparent Bridge. Delft: TU Delft.
- CCI. (2018, December 12). Introduction to GFRC (Glass Fiber Reinforced Concrete). Retrieved from concretecourtinstitute: <https://concretecourtinstitute.com/free-training/introduction-to-gfrc-glass-fiber-reinforced-concrete/>
- Chapman, C., Saitou, K., & Jakiela, M. (1994). Genetic Algorithms as an Approach to Configuration and Topology Design in Transactions of ASME, Journal of Mechanical Design 116(4): 1005-1012. Massachusetts Institute of Technology.
- Chen, T., & Chiou, Y. (2013). Structural Topology Optimization Using Genetic Algorithms in roceedings of the World Congress on Engineering 2013 Vol III. London.
- Chockalingam, S., Sethunayanan, R., & Ramanathanan, R. (1989). Natural Fiber Reinforced Concrete. Annamalainagar: Annamalai University.
- Choi, W.-h., Huang, C.-g., Kim, J.-m., & Park, G.-J. (2015). Comparison of some commercial software systems for structural optimization in 11th World Congress on Structural and Multidisciplinary Optimisation. Sydney.
- Choi, W.-h., Kim, J.-m., & Park, G.-J. (2016). Comparison study of some commercial structural optimization software systems. Heidelberg: Springer.
- Christensen, P., & Klarbring, A. (2009). An Introduction to Structural Optimization. Linköping: Springer.
- Concrete Recycling. (2009, July). Retrieved from World Business Council for Sustainable Development: <http://www.wbcdcement.org/index.php/key-issues/sustainability-with-concrete/concrete-recycling>
- Condit, C. (1968). The First Reinforced-Concrete Skyscraper: The Ingalls Building in Cincinnati and Its Place in Structural History in Technology and Culture, Vol. 9, No. 1 (Jan., 1968), pp. 1-33. The Johns Hopkins University Press.
- Cork Institute of Technology CIT, & Stephenson College. (2019, May 04). [tippenergy.ie](http://tippenergy.ie). Retrieved from <https://>

tippenergy.ie/wp-content/uploads/2011/09/Module-3.4-Caulation-of-U-value-thermal-bridging.pdf

Crow, J. M. (2008, February 27). The concrete conundrum. Retrieved December 2018, from <https://www.chemistryworld.com/features/the-concrete-conundrum/3004823.article>

Das, P., & Karakoti, I. (2014). Intercomparability of Isotropic and Anisotropic Solar Radiation Models for Different Climatic Zones of India. AICHE.

DBIt, D. I. (2016, Novemeber 3). National technical approval for Schöck Combar. Berlin, Germany: Deutsches Institut für Bautechnik.

DBIt, D. I. (2017, May 22). National technical approval for solidian sandwich panel. Berlin: Deutsches Institut für Bautechnik.

(1975). Design Considerations for a Precast Prestressed Apartment Building. Chicago: Prestressed Concrete Institute.

DESIGN, m. A. (2012). The case for tall wood buildings .

Didwania, S., Garg, V., & Mathur, J. (2011). Optimization of window-wall ratio for different building types. ResearchGate.

DN-32 Connections for Architectural Precast Concrete. (n.d.). Precast/ Prestressed Concrete Institute.

Dominguez, A., Claver, J., & Sebastian, M. (2017). Study for the selection of design software for 3D printing topological optimization in Manufacturing Engineering Society International Conference 2017, MESIC 2017, 28-30. Elsevier.

Ductal, L. (2019, May 05). Ductal JS1000. Retrieved from [www.ductal.com](http://www.ductal.com): [https://www.ductal.com/sites/ductal/files/atoms/files/2\\_ductal\\_js1000.pdf](https://www.ductal.com/sites/ductal/files/atoms/files/2_ductal_js1000.pdf)

engineeringproductdesign. (2018). What is Additive Manufacturing? Retrieved from [engineeringproductdesign.com](http://engineeringproductdesign.com): <https://engineeringproductdesign.com/knowledge-base/additive-manufacturing-processes/>

engineeringtoolbox. (2013). Reynolds number: Introduction and definition of the dimensionless Reynolds Number - online calculators. Retrieved from [www.engineeringtoolbox.com](http://www.engineeringtoolbox.com): [https://www.engineeringtoolbox.com/reynolds-number-d\\_237.html](https://www.engineeringtoolbox.com/reynolds-number-d_237.html)

Fraser, M. (2019, May 16). Sir Banister Fletcher's Global History of Architecture. Bloomsbury Visual Arts.

Friedbert , B. K., Kauhsen, B., Polonyi, S., & Brandt, J. (2013). Concrete construction manual. Munich: Birkhauser.

Gagg, C. R. (2014). Cement and concrete as an engineering material: An historic appraisal and case study analysis. Elsevier.

Gaudilliere, N. (2015, August 19). First prototypes: 3D printed concrete wall 2. Retrieved from [xtreeE](http://xtreeE): <https://www.xtreee.eu/2015/08/19/first-prototypes-3d-printed-concrete-wall-2/>

[www.xtreee.eu/2015/08/19/first-prototypes-3d-printed-concrete-wall-2/](https://www.xtreee.eu/2015/08/19/first-prototypes-3d-printed-concrete-wall-2/)

Gebisa, A., & Lemu, H. (2017). A case study on topology optimized design for additive manufacturing. Stavanger: IOP Publishing Ltd.

Geleff, J. (2018, 12 10). Glass Towers Are So Passé. What Will Replace Them? Retrieved from [architizer.com](http://architizer.com): [https://architizer.com/blog/practice/materials/glass-skyscrapers-passe/?fbclid=IwAR1OuJu17ut76vtzXN8iehVnSFsUdg19DKvf2Go6KTMb8JVkr\\_TW6T3Lg](https://architizer.com/blog/practice/materials/glass-skyscrapers-passe/?fbclid=IwAR1OuJu17ut76vtzXN8iehVnSFsUdg19DKvf2Go6KTMb8JVkr_TW6T3Lg)

Gensler. (2015). Gensler. Retrieved from The Broad: <https://www.gensler.com/projects/the-broad>

Gerns, E., & Freedland, J. (2006). Understanding terra-cotta distress: Evaluation and repair approaches. Palgrave Macmillan Ltd.

Gobain, W. S. (2019, April 04). Weber Vezelversterkte egalisatie. Retrieved from Weber beamix: [https://www.nl.weber/search-document/content\\_type/product?products%5B%5D=309](https://www.nl.weber/search-document/content_type/product?products%5B%5D=309)

Hafez, A. H. (2016, June 6). Integrating Building Functions into Massive External Walls. Architecture and the Built environment. Delft: Delft University of Technology,.

Henriksen, T. (2017). Advancing the manufacture of complex geometry GFRC for today's building envelopes. Delft: [abe.tudelft.nl](http://abe.tudelft.nl).

History of Insulation with Masonry. (n.d). Retrieved from masonry advisory council: [masonryadvisorycouncil.org](http://masonryadvisorycouncil.org)

Hoces, A. P. (2018, Month 21). Coolfacade Architectural Integration of Solar Cooling Technologies in the Building Envelope . Architecture and the Buuilt environment. Delft, The Netherlands: Delft University of Technology.

Horsley, F. (2001). Recommended Practice for Glass Fiber Reinforced Concrete Panels. Precast / Prestressed Concrete Institute.

Howarth, D. (2017, May 11). First apartment in Tadao Ando's 152 Elizabeth Street revealed. Retrieved from Dezeen: <https://www.dezeen.com/2017/05/11/apartment-interior-michael-gabellini-tadao-ando-152-elizabeth-street-residential-building-nolita-new-york/>

ianVisits. (2017, September 28). How Crossrail is using 3D-printing to build its stations. Retrieved from [ianVisits](http://ianvisits.co.uk): <https://www.ianvisits.co.uk/blog/2017/09/28/how-crossrail-is-using-3d-printing-in-its-stations/>

Iskender, M., & Karasu, B. (2018). Glass Fibre Reinforced Concrete (GFRC). Eskişehir: ECJSE.

Jipa, A., Bernhard, M., Meibodi, M., & Dillenburger, B. (2016). 3D-Printed Stay-in-Place Formwork for Topologically Optimized Concrete Slabs. Proceedings of the 2016 TxA Emerging Design + Technology Conference (pp. 97-107). Zurich: ETH Zurich.

Kabel, M. (2008, February 17). Wikipedia. Retrieved from [commons.wikimedia](http://commons.wikimedia.org): <https://commons.wikimedia.org/wiki/File:Kabel.jpg>

org/wiki/Pantheon#/media/File:Pantheon\_cupola.jpg

Katifori, E., & Szollosi, G. J. (2010, January). Damage and Fluctuations Induce Loops in Optimal Transport Networks. *Physical Review Letters*. ResearchGate.

Kiranyaz, S., Ince, T., & Gabbouj, M. (2013). Optimization Techniques: An Overview In: *Multidimensional Particle Swarm Optimization for Machine Learning and Pattern Recognition*. Adaptation, Learning, and Optimization, vol 15. Springer.

Kjcerbye, P., & Sai, L. H. (2001). *STRUCTURAL PRECAST CONCRETE HAND BOOK*. Building and Construction Authority.

Klijn-Chevalerias, M. d., Loonen, R., Zarzycka, A., Witte, D., Sarakinoti, M., & Hensen, J. (2017, May 01). Assisting the development of innovative responsive façade elements using building performance simulation. *Symposium on Simulation for Architecture and Urban Design* (pp. 243-250). Eindhoven University of Technology.

Koskiahde, A. (2004). An experiential petrographic classification scheme for the condition assessment of concrete in facade panels and balconies. Elsevier.

Kumar, K., Cini, C., & Sifton, V. (2012). Assessment of design wind speeds for metro cities of India. *International Association for Wind Engineering*.

Leary, M., Merli, L., Torti, F., Mazur, M., & Brandt, M. (2014). Optimal topology for additive manufacture: A method for enabling additive manufacture of support-free optimal structures. Elsevier.

Liu, J., Gaynor, A., Chen, S., Kang, Z., Suresh, K., Takezawa, A., . . . Kato, J. (2018). Current and future trends in topology optimization for additive manufacturing. Springer.

Liu, K., & Tovar, A. (2014). An efficient 3D topology optimization code written in Matlab. Springer.

Lubell, S. (2014). Broad Collection Sues Seele over Problematic Los Angeles Museum Facade. Retrieved from *The Architects Newspaper*: <https://archpaper.com/2014/06/broad-collection-sues-seele-over-problematic-los-angeles-museum-facade/>

Lyrenmann, M. (2018, August 12). Smart Slab. Retrieved from *Digital Building Technologies*: <http://dbt.arch.ethz.ch/project/smart-slab/>

Müller, W., & Vogel, G. (1982). *DTV Atlas zur Baukunst*, Volume I. 4th edition. p.15. Munich.

MachinableWax. (2016, June 12). Technical info\_Safety Data Sheet. Retrieved from *Machinablewax*: [https://www.machinablewax.com/docs/SDS-MachinableWax\\_F99\\_O+\\_P2Cast.pdf](https://www.machinablewax.com/docs/SDS-MachinableWax_F99_O+_P2Cast.pdf)

Magan, C. (2016). *Topology Optimization of a Concrete Floor Slab Guided by Vacuumatic Formwork Constraints*. Delft: TU Delft.

Malaga, K., Flansbjer, M., Blanksvärd, T., & Petersson, Ö. (2012). Textile reinforced concrete sandwich panels.

Millipede. (2014). Retrieved from sawapan.eu: [http://www.sawapan.eu/sections/section88\\_Millipede/files/MillipedeMarch2014.pdf](http://www.sawapan.eu/sections/section88_Millipede/files/MillipedeMarch2014.pdf)

Mlot, S. (2018, December 7). People Who Live in 3D-Printed Houses Should Definitely Throw Shade. Retrieved from *Geek*: <https://www.geek.com/tech/people-who-live-in-3d-printed-houses-should-definitely-throw-shade-1745829/>

Novotná, M., Kostecká, M., Hodková, J., & Vokáč, M. (2014). *Use of textile reinforced concrete – especially for façade panels*. Prague: Trans Tech Publications.

Novotná, M., Kostecká, M., Hodková, J., & Vokáč, M. (2014). *Use of textile reinforced concrete – especially for façade panels*. Prague: Trans Tech Publications.

NSAI\_standards. (2016). I.S. EN 12210:2016. Windows and doors - Resistance to wind load - Classification. Brussels: European committee for standardization.

NYA. (2015). *MUSEUM Broad Museum*. Retrieved from *Nabih Youssef Associates*: <http://www.nyase.com/broad-museum.php>

Oh, J.-K., Lee, J.-J., & Hong, J.-P. (2014). *Prediction of compressive strength of cross-laminated timber panel*. Japan: Springer.

O'Hegarty, R., Kinnane, O., & McCormack, S. (2016, October). *Review and analysis of solar thermal facades*. Dublin: Elsevier.

Omebere-Iyari, N. K., & Azzopardi, B. (2007). *A study of flow patterns for gas/ liquid flow in small diameter tubes*. Nottingham, United Kingdom: IChemE, The University of Nottingham.

Panda, S. (2017). *Dealing with reuse of concrete in India's circular economy*. Delft: TU Delft.

Parameswaran, V. S. (1991). *Fibre-reinforced Concrete: a Versatile Construction Material*. *Building and Environment*, Vol. 26, No. 3 (pp. 301-305). Great Britain: Pergamon Press.

Paulino, G. (2013, 1 23). Topology optimization connects architecture and engineering. Retrieved from *ILLINOIS Grainger College of Engineering*: <https://grainger.illinois.edu/news/2013-01-23-topology-optimization-connects-architecture-and-engineering>

Paulino, G. (2013, January 23). Topology optimization connects architecture and engineering. Retrieved from *University of Illinois*: <https://cee.illinois.edu/news/topology-optimization-connects-architecture-and-engineering>

Pearce, A., & Ahn, Y. (2013). *Green luxury: A case study of two green hotels*. ResearchGate.

Peña, J. M. (2006). *Heuristic Optimization*. Universidad Politécnica de Madrid.

Phaidon. (2018). *SANAA's most impressive creations*. Retrieved from *Phaidon*: <https://de.phaidon.com/agenda/architecture/picture-galleries/2010/april/08/pritzker-prize-laureate-2010-sanaa/>

Plummer, A., Aburas, S., Nikas, G., Santi, M., & Velasquez, M. P. (2016). Perkins + Will- Research Journal 2016 / VOL 08.02. Perkins + Will.

Practical aspects of structural optimisation- A study guide. (2018). Altair University.

Querin, O., Victoria, M., Alonso, C., Ansoła, R., & Marti, P. (2017). Topology Design Methods for Structural Optimization. Chennai: Elsevier- Academic press.

Richard, P., & Cheyrezy, M. (1995). Composition of Reactive Powder Concretes. St Quentin en Yvelines: Pergamon.

Sarakinioti, V., Turrin, M., Teeling, M., De Ruiter, P., Van Erk, M., Tenpierik, M., ... Vlasblom, D. (2017). Spong3d : 3D printed facade system enabling movable fluid heat storage. *Spool*, 4(2), 57-60. DOI: 10.7480/spool.2017.2.1929

Sarakinioti, M. V., Turrin, M., Konstantinou, T., & Tenpierik, M. (2018, March 03). Developing an integrated 3D-printed façade with complex geometries for active temperature control. Delft: Elsevier.

SBCI. (2009). Buildings and Climate Change: Summary for Decision Makers. UNEP Sustainable Building and Climate Initiative.

Schöck. (2016, April). Schoeck Combar. Retrieved from Schoeck UK: [www.schoeck.co.uk/en-gb/combar](http://www.schoeck.co.uk/en-gb/combar)

Schöck. (2018). Schoeck Combar. Retrieved from Schoeck UK: [www.schoeck.co.uk/en-gb/combar](http://www.schoeck.co.uk/en-gb/combar)

Schüco. (2019, May 04). Schüco Window AWS 75.SI+. Retrieved from Scheuco: [https://www.schueco.com/web2/in/architects/products/windows/aluminium/schueco\\_aws\\_75\\_si\\_plus/](https://www.schueco.com/web2/in/architects/products/windows/aluminium/schueco_aws_75_si_plus/)

Schittich, C. (2008). In detail- Building Skins. Birkhauser.

Serbia, T. B. (2018, December 12). bis.org.rs. Retrieved from Classification of concrete: <http://www.bis.org.rs/en/about-concrete/classification-of-concrete>

Sigmund, O. (2001). A 99 line topology optimization code written in Matlab. Springer.

Simulia, 3. (2018). 3ds. Retrieved from Abaqus Overview: Abaqus Overview

Singh, R., Sartor, D., & Ghatikar, G. (2013, April). Best Practices Guide for High- Performance Indian Office Buildings. Berkeley Lab, Lawrence Berkeley National Laboratory.

Slobbe, G. (2015). Optimisation of Reinforced Concrete Structures. Delft: TU Delft.

Smyth, M. (2018). A Study of the Viability of Cross Laminated Timber for Residential Construction. Stockholm: KTH School of Architecture and the Built Environment.

Solidian\_A. (2019, May 05). Technical DataSheet solidian GRID Q121/121-AAE-38. Retrieved from Solidian: [https://www.solidian.com/fileadmin/user\\_upload/pdf/TDS/solidian\\_GRID\\_Q121.121-AAE-38.pdf](https://www.solidian.com/fileadmin/user_upload/pdf/TDS/solidian_GRID_Q121.121-AAE-38.pdf)

Solidian\_B. (2019, May 05). Solidian. Retrieved from Technical data sheet solidian GRID Q142/142-CCE-25:

[https://www.solidian.com/fileadmin/user\\_upload/pdf/TDS/solidian\\_GRID\\_Q142.142-CCE-25.pdf](https://www.solidian.com/fileadmin/user_upload/pdf/TDS/solidian_GRID_Q142.142-CCE-25.pdf)

Stamkot, S. (2016, April 21). harpersbazaar. Retrieved from Chanel heeft nieuws!: <https://www.harpersbazaar.com/nl/mode-juwelen/news/a2364/chanel-heeft-nieuws/>

Statista. (2018). Major countries in worldwide cement production from 2012 to 2017. Retrieved from Statista: <https://www.statista.com/statistics/267364/world-cement-production-by-country/>

Stephens, H. (2016). THE PAPER CITY. Retrieved from tumblr: <http://thepapercity.tumblr.com/post/130258645764/diller-scofidio-renfro-seele-inc-broad-museum>

Studinka, & Joseph. (1986). Fibrated cement without asbestos. London: Civil engineering London.

StudioInternational. (2004, June 7). White femininity - Dior Omotesando. Retrieved from Studio international: <https://www.studiointernational.com/index.php/dior-omotesando>

Subramanian, R. S. (2019, 01 08). Pipe Flow Calculations. Retrieved from clarkson.edu: <https://web2.clarkson.edu/projects/subramanian/ch330/notes/Pipe%20Flow%20Calculations.pdf>

Technogrip, D. G. (2015). Sistemi costruttivi per la prefabbricazione. Italy: Damilano Group.

TheBroad. (2015). The Building. Retrieved from The Broad: <https://www.thebroad.org/about/building>

Torregrosa, E. C. (2013). Dosage optimization and bolted connections for UHPFRC ties. Valencia: Universitat PolitècnicaDe valència .

Utle, E. (2017, June 12). Solidworks. Retrieved from An Introduction to Designing for Metal 3D Printing: <https://blogs.solidworks.com/solidworksblog/2017/06/introduction-designing-metal-3d-printing.html>

Vahidi, E., & Malekabi, M. (2011). GRC and Sustainable Building Design in GRC 2011.

Wang, M. Y., & Wang, X. (2004). "Color" level sets: a multi-phase method for structural topology optimization with multiple materials. Elsevier.

Wang, M., Chen, S., Wang, X., & Mei, Y. (2005). Design of Multimaterial Compliant Mechanisms Using Level-Set Methods. American Society of Mechanical Engineers.

Wang, S., Wang, M., & Tai, K. (2005). An Enhanced Genetic Algorithm for Structural Topology Optimization. Shatin: The Chinese University of Hong Kong.

Watts, A. (2013). Modern Construction Handbook. Ambra.

WillisConstruction. (2015). Article from: PCI National Award Submittal. Retrieved from pre-cast.org: <http://www.pre-cast.org/broadmuseum.asp>

Zimmerman, W. (2015, June 25). MULBERRY HOUSE. Retrieved from archilovers: <https://www.archilovers.com/projects/159316/mulberry-house.html>

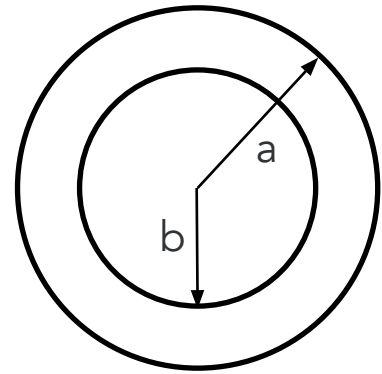
Zingg, D., Nemec, M., & Pulliam, T. (2008). A comparative evaluation of genetic and gradient-based algorithms applied to aerodynamic optimization in REMN – 17/2008. Shape design in aerodynamics, pages 103 to 126. Toronto: University of Toronto Institute of Aerospace Studies.

# 12. APPENDIX

## 12.1 WETTED PERIMETER

Wetted perimeter (C) ratios for different shapes, used in calculation of flow of fluids through tubes (Subramanian, 2019).

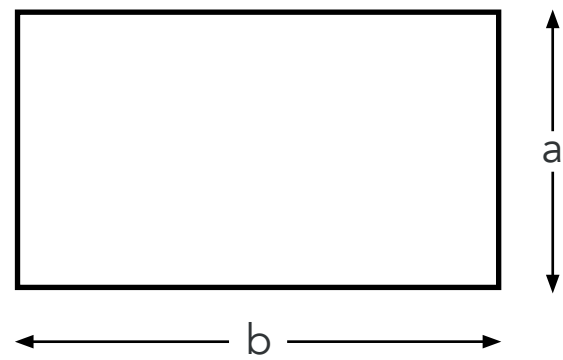
### 1. For circular tube sections



$a/b$	$C$	$a/b$	$C$
1.0	24.00	10,0	22.34
1.25	23.98	20.0	21.57
1.67	23.90	100	20.03
2.5	23.68	1000	18.67
5.0	23.09	$\infty$	16.00

Table 12.1. Wetted perimeters for circular tubes

### 2. For rectangular tube sections



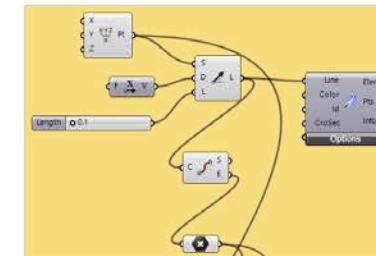
$a/b$	$C$	$a/b$	$C$
1.0	14.23	6.0	19.70
1.33	14.47	8.0	20.59
2.0	15.55	10.0	21.17
2.5	16.37	20.0	22.48
4.0	18.23	$\infty$	24.00

Table 12.2. Wetted perimeters for rectangular tubes

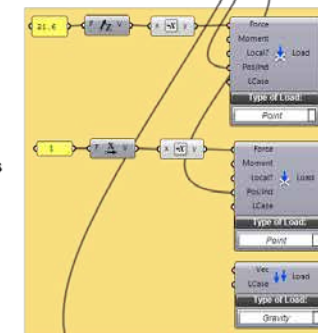
## 12.2 CALCULATE NO.OF DOWELS

Plugins used: Karamba 3D

Define geometry for a single reinforcement dowel



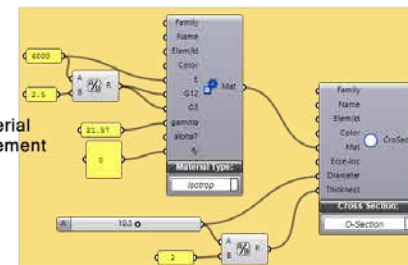
Define loads



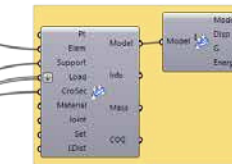
Define supports



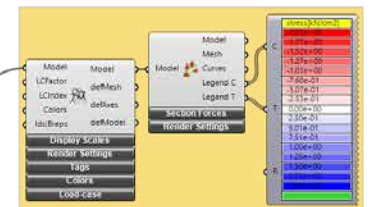
Define material for reinforcement dowels



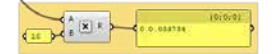
Compute



Visualise

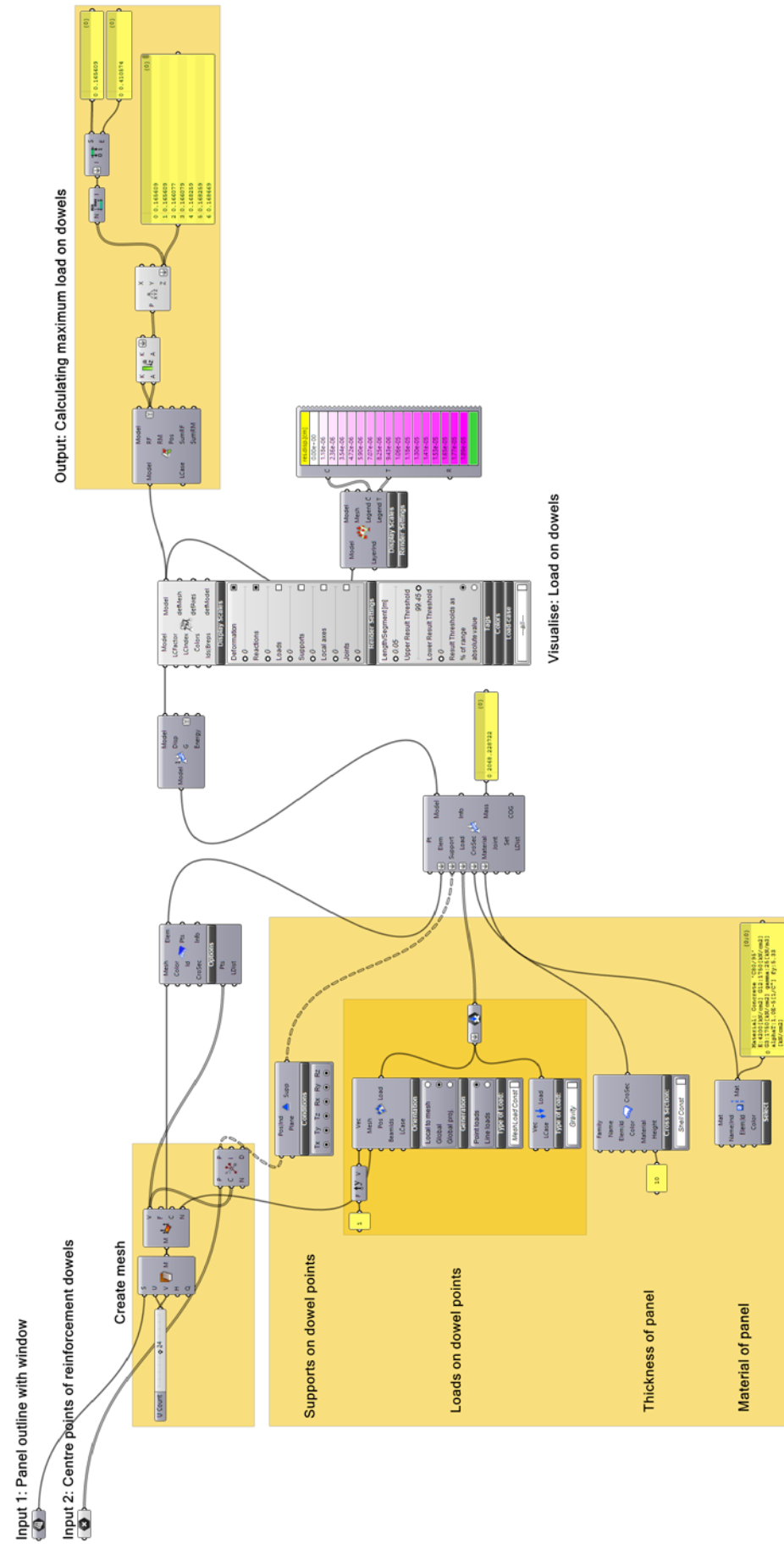


Output: Displacement



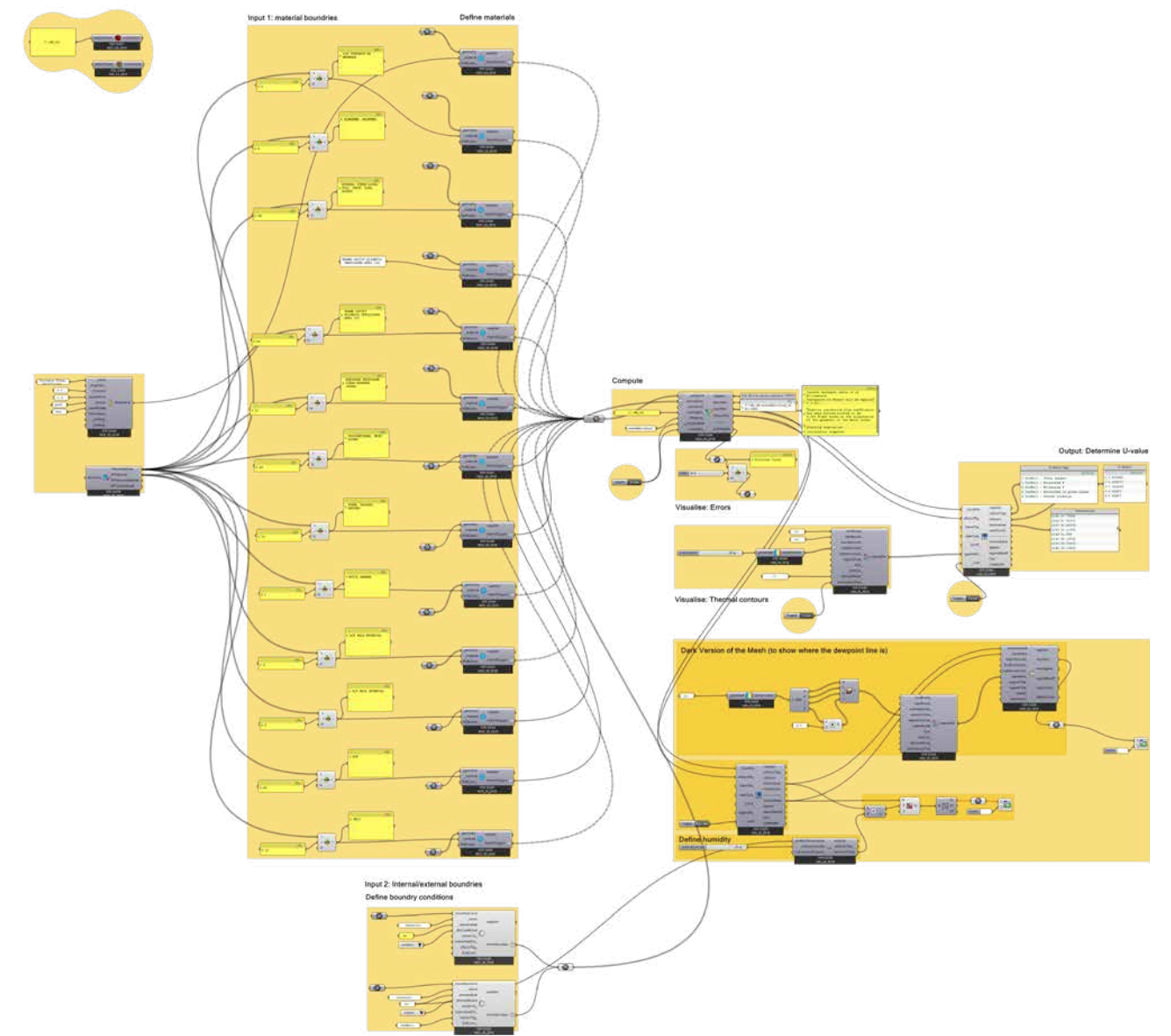
# 12.3 CALCULATE LOADS ON DOWELS

Plugins used: Karamba 3D



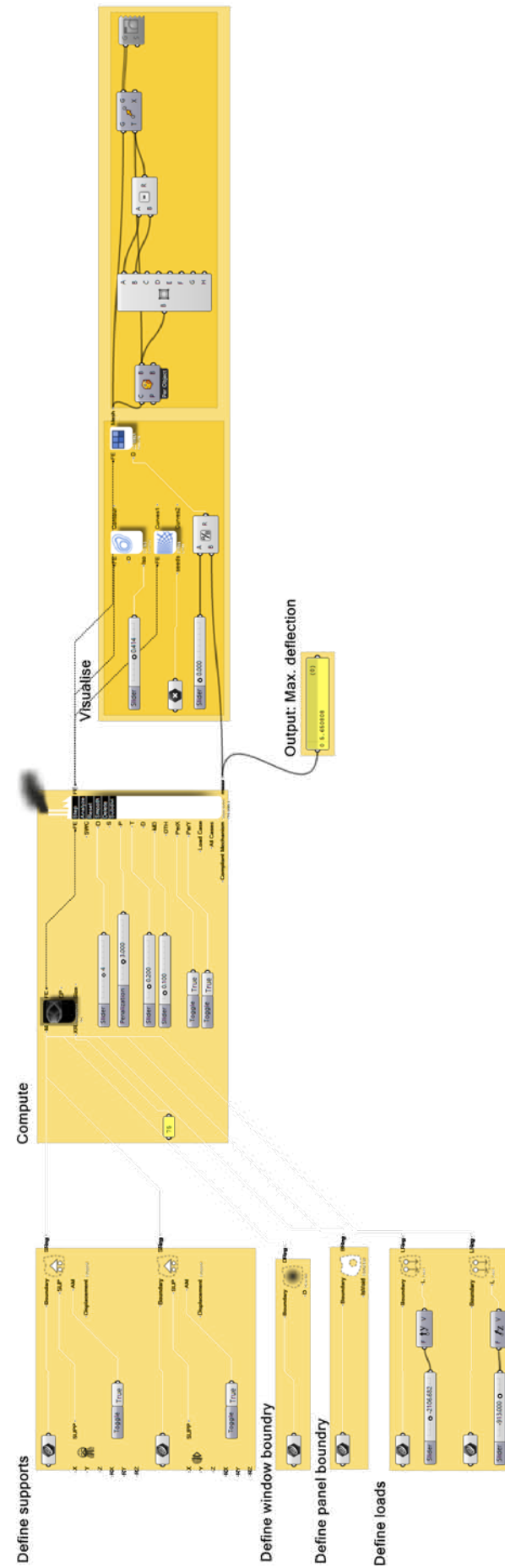
# 12.4 CALCULATE U-VALUE

Plugins used: THERM 2D + Honeybee + Ladybug



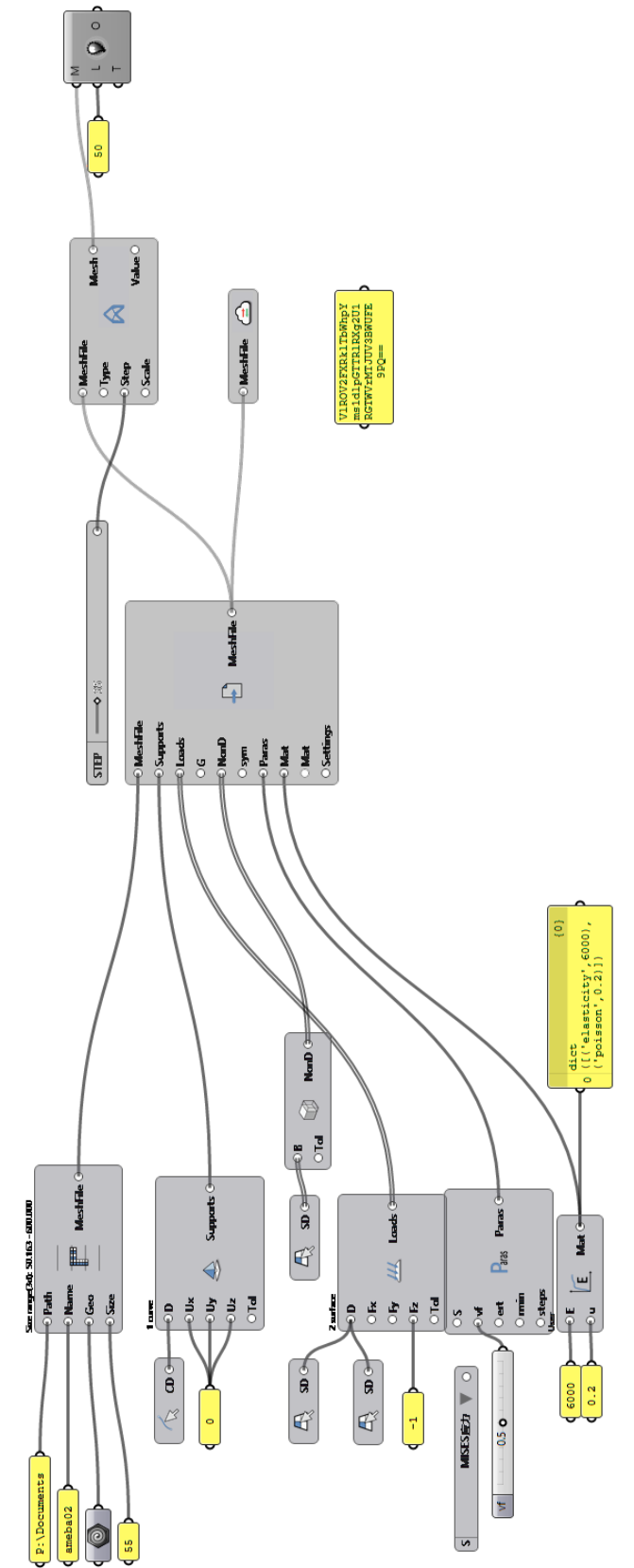
# 12.5 TOPOLOGY OPTIMISATION

Plugins used: Millipede



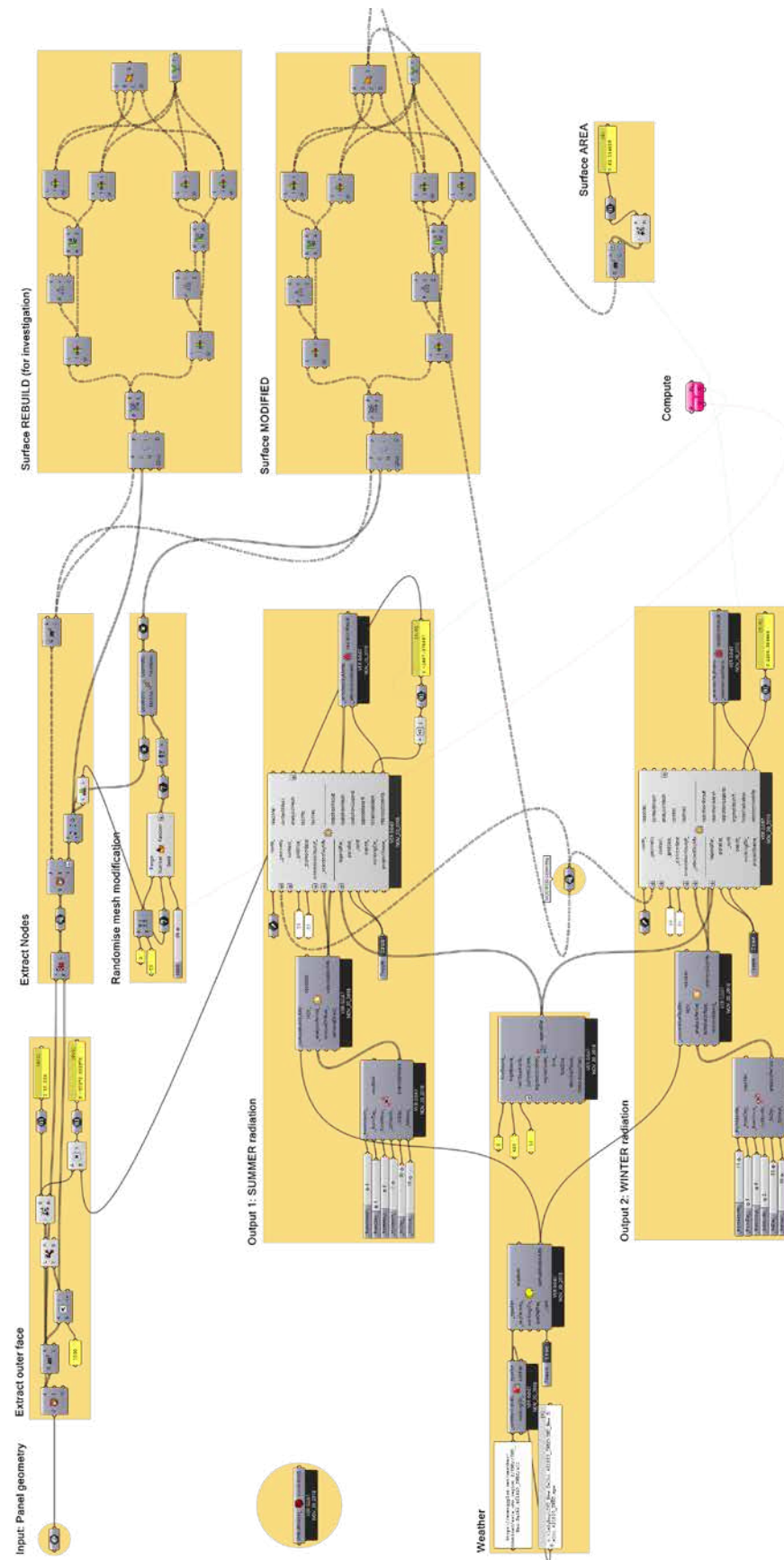
# 12.6 TOPOLOGY OPTIMISATION

Plugins used: AMEBA



## 12.7 SURFACE MODIFICATION

Plugins used: Octpous + Honeybee + Ladybug



## 12.8 m-CODE FOR 3D PRINTING WAX

```
PK<?> creality_cr_x_crx_wax[general]
```

```
version = 4
```

```
name = CRX WAX
```

```
definition = fdmprinter
```

```
[metadata]
```

```
quality_type = draft
```

```
setting_version = 6
```

```
type = quality_changes
```

```
[values]
```

```
adhesion_type = skirt
```

```
layer_height = 0.3
```

```
layer_height_0 = 0.3
```

```
material_bed_temperature = 60
```

```
prime_tower_enable = False
```

```
prime_tower_position_x = 30
```

```
prime_tower_position_y = 10
```

```
retraction_combing = off
```

```
PK<?> !@/7 | creality_cr_x_0_#2_crx_wax[general]
```

```
version = 4
```

```
name = CRX WAX
```

```
definition = fdmprinter
```

```
[metadata]
```

```
quality_type = draft
```

```
setting_version = 6
```

```
type = quality_changes
```

```
position = 0
```

```
[values]
```

```
brim_width = 10
```

```
infill_sparse_density = 0
```

```
material_flow = 98.5
```

```
material_print_temperature = 215
```

```
prime_tower_min_volume = 30
```

```
retraction_amount = 4
```

```
retraction_speed = 35
```

```
speed_infill = 50
```

```
speed_layer_0 = 30
```

```
speed_print = 40
```

```
speed_topbottom = 30
```

```
speed_travel = 90
```

```
speed_travel_layer_0 = 80
```

```
speed_wall = 40
```

```
speed_wall_0 = 30
```

```
speed_wall_x = 40
```

```
top_bottom_pattern = lines
```

```
top_bottom_thickness = 0.9
```

```
top_thickness = 0.9
```

```
wall_0_wipe_dist = 0
```

```
wall_line_count = 3
```

```
wall_thickness = 0.8
```

```
PK<?> !Éif # # □ creality_cr_x_1_#2_crx_wax[general]
```

```
version = 4
```

```
name = CRX WAX
```

```
definition = fdmprinter
```

```
[metadata]
```

```
quality_type = draft
```

```
setting_version = 6
```

```
type = quality_changes
```

```
position = 1
```

```
[values]
```

```
infill_sparse_density = 10
```

```
material_flow = 120
```

```
material_print_temperature = 210
```

```
prime_tower_min_volume = 30
```

```
retraction_speed = 30
```

This page is intentionally left blank.

This page is intentionally left blank.

